Discrete Dynamics in Nature and Society

Discrete Optimisation for Complex and Smart Transportation Systems

Lead Guest Editor: Tingsong Wang
Guest Editors: Lu Zhen, Wen Yi, and Abraham Zhang

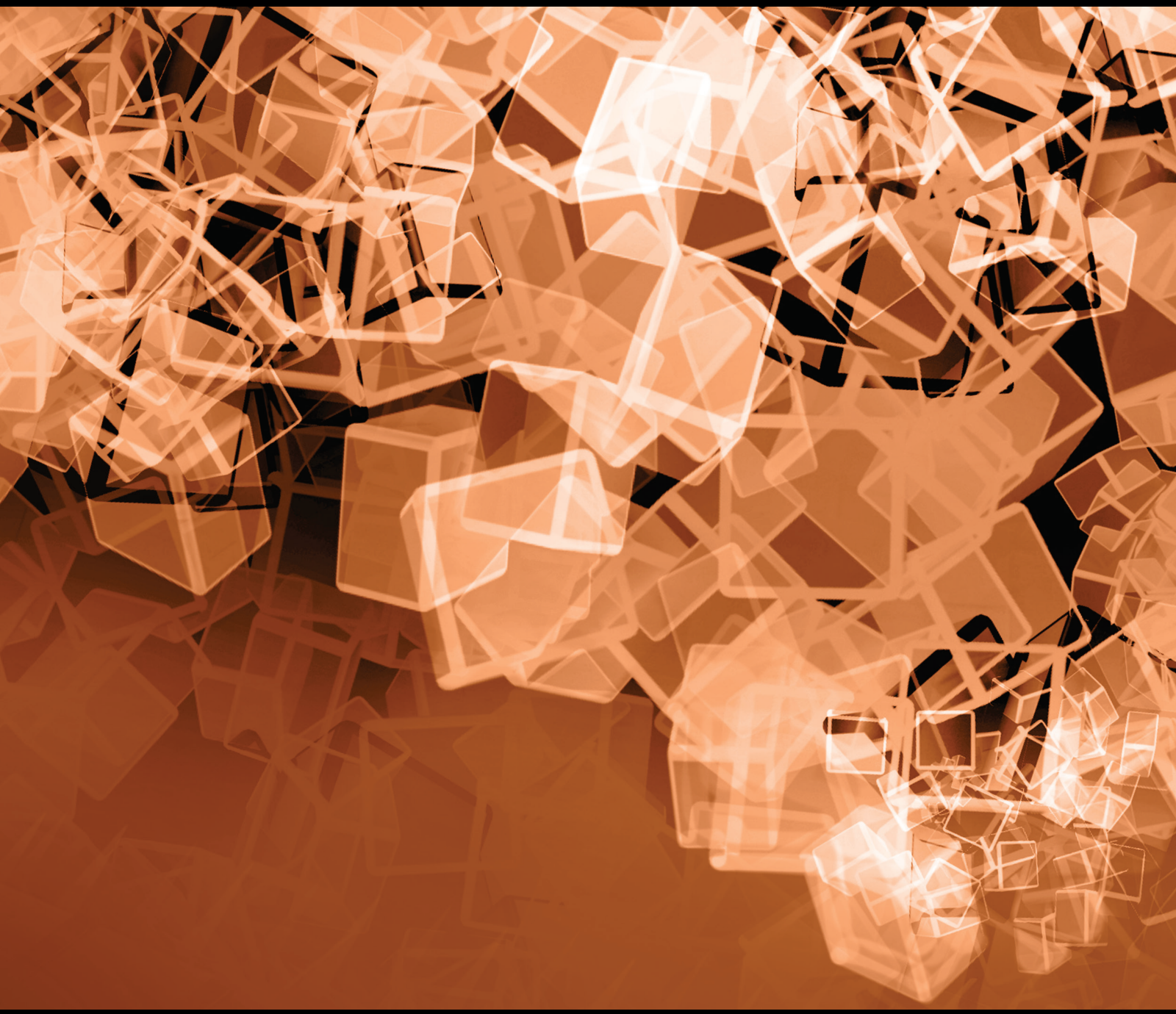

Discrete Optimisation for Complex and Smart Transportation Systems

Discrete Dynamics in Nature and Society

Discrete Optimisation for Complex and Smart Transportation Systems

Lead Guest Editor: Tingsong Wang
Guest Editors: Lu Zhen, Wen Yi, and Abraham Zhang

Contents

Hindawi
Discrete Dynamics in Nature and Society
Volume 2021, Article ID 6623563, 10 pages
https://doi.org/10.1155/2021/6623563

Research Article

Research on Cold Chain Logistics Distribution Route Based on Ant Colony Optimization Algorithm

Haiou Xiong

College of Port and Shipping Management, Guangzhou Maritime University, Guangzhou 510725, China

Correspondence should be addressed to Haiou Xiong; xionghaiou@gzmtu.edu.cn

Received 19 November 2020; Revised 2 March 2021; Accepted 24 March 2021; Published 17 May 2021

Academic Editor: Tingsong Wang

The cold chain logistics distribution industry not only demands all goods can be timely distribution but also requires to reduce the entire logistics transportation cost as far as possible, and distribution vehicle route optimization is the key problem of cold chain logistics transportation cost calculation. The traditional optimization method spends a lot of time to search so that it is tough to find the globally optimal path approach, which results in higher distribution costs and lower efficiency. To solve the above-mentioned problems, a cold logistics distribution path optimization solution, ground on an improved ant colony optimization algorithm (IACO) is formulated. Specially, other constraints, e.g., the transport time factor, transport cooling factor, and mean road patency factor, can be added to the unified IACO. Meanwhile, the updating mode of traditional pheromone is improved to limit the maximum and minimum pheromone concentration on the road and change the path selection transfer probability. The simulation results and experiment make clear that the IACO algorithm is lower than the chaotic-simulated annealing ant colony algorithm (CSAACO) and the traditional ACO algorithm in terms of convergence speed, logistics transportation distance, and logistics delivery time. At the same time, we have successfully obtained the optimal logistics distribution path, which can provide valuable reference information for improving the economic benefits of cold chain logistics enterprises.

1. Introduction

With the increasing exploitation of the modern economy, advanced science, and information technology, the existing online shopping paradigm has gradually become an indispensable way of life for people. This shopping mode not only greatly facilitates people's life but also drives the mushroom growth of the emerging logistics industry paradigm. As the "third benefit source," logistics has an increasingly obvious impact on economic development, and more and more enterprises have joined logistics, which has gradually become one of the industries with fierce competition [1–3]. Logistics distribution broadly refers to the logistics campaigns of selecting, processing, casing, partitive, and gathering materials within a certain area according to the needs of users and delivers them to the places designated by users on time [4, 5]. In the process of logistics and transportation, the research objectives of scholars are to reduce the logistics cost of enterprises, shorten transportation time, further enhance the character of transportation service, and obtain the optimal route of transportation. How to realize scientific logistics distribution is a very complicated and crucial problem that every logistics enterprise must face [6]. Logistics enterprises need to realize the goal of low cost and high efficiency in the transportation process.

As a result of the late start disadvantages of domestic logistics in the current situation, the research time of emerging logistics distribution path design is relatively short. At first, the driver mainly plans the optimal logistics distribution path with his own experience. Due to the lack of scientific guidance, the obtained logistics distribution path is not the optimal one, with low logistics distribution efficiency and high logistics distribution cost.

The key issue to the vehicle routing problem (VRP) lies in the optimization of the whole logistics system [7, 8]. Meanwhile, the problem mentioned above is NP-hard problem [8]. With the increase of quantity distribution of goods, the traditional path planning algorithm is not in a

relatively short period to get access to the first-rank solution through the system to choose the high-point conveying path distribution vehicle. Optimizing the vehicle scheduling and arranging delivery vehicle distribution order can reduce the distance of the vehicle and the rate of empty. Only when the number of customer nodes and lines is smaller, can the exact solution be obtained. However, when the scale of the problem increases, the exact solution will take a long time and have a low effect. On the other hand, the man-machine interaction method requires managers to have enough professional knowledge of logistics distribution and will increase the randomness of vehicle distribution route selection. Generally, heuristic algorithm should be adopted to solve this kind of problems. This algorithm, referring to the continuous induction, analysis, and reasoning of the experience, has been solved for specific problems, and the method to solve this kind of problems is generated. The goal is to get the satisfactory solution or optimal solution of the global problem with an appropriate cost, which not only saves time but also meets the actual requirements of users. Because of the advantages of high efficiency and simple implementation, heuristic algorithms, e.g., grey wolf optimization (GWO) algorithm [9], chaos particle swarm optimization (CPSO) [10], genetic algorithm (GA) [11], firefly algorithm (FA) [12], and ant colony optimization (ACO) [13], have attracted wide attention in the field of optimization research and developed very fast in the recent years.

It can be seen from the existing studies, considering the ACO algorithm, that there are two problems in the cold chain logistics path scheduling and optimization. On the one hand, there are few studies on the specific application requirements of the ACO algorithm in the cold chain logistics path optimization, ignoring the influence of the algorithm itself on the optimization accuracy and convergence speed. On the other hand, the constraint conditions of path optimal scheduling are too simple to meet the requirements of optimization accuracy under the current complex road conditions. Aiming at the existing problems in the current research, this paper proposes an improved ant colony optimization (IACO) algorithm-based cold chain logistics distribution scheduling and optimization method to reduce cold chain logistics transportation cost and improve transportation efficiency from the perspective of the transport time factor, transport cooling factor, and mean road patency factor.

2. Related Works

The ACO is a population intelligent optimization algorithm, which can acquire the typical shortest path between demand nest and food via using the parallel mechanism of positive feedback and the cooperation between ants. This algorithm not only has the advantages of good parallelism and fast solving speed but also has an excellent performance in path optimization and task assignment. Therefore, the ACO algorithm has attracted extensive attention in the field of optimization research and developed very fast in the recent years, from the perspective of medical logistics distribution, agricultural products logistics distribution, port logistics ship transportation path, and supermarket logistics distribution, as well as cold chain logistics distribution.

Based on analyzing the characteristics of medical logistics distribution, the literature [14] put forward reasonable assumptions and constraints of the mathematical model of pharmaceutical logistics and constructed the objective function of optimizing the distribution path. Because of the strong ability to acquire better solutions, the ACO paradigm is utilized to reoptimize the objective function. Simulation results demonstrate the higher efficacy of the proposed scheduling algorithm. With the gradual improvement of residents' requirements for food quality, the literature [15] optimized fresh agricultural products logistics distribution routes, which can save costs and build up the operating potency of relevant enterprises. The first study of fresh agricultural products distribution route optimization model presented VRP and vehicle routing problem with time windows (VRPTW) paradigm then completed the fresh agricultural products logistics distribution path clustering GA optimization design and finally given optimization clustering GA implementation steps. MATLAB was used to complete the experimental design, study the external similarity of fresh agricultural products transportation, analyze the clustering results of logistics distribution and obtaining the path within the group, and conduct the performance test. The results show that this method can scientifically configure the logistics route, step up the number of fresh transport vehicles, and improve the full load rate. After the traditional port logistics ship transportation path optimization, the ship transportation cost is very high and the transportation time is too long. Aiming at the abovementioned problems, a new method of port ship transport path optimization was studied in the literature [16] by using artificial intelligence (AI) algorithm, and the optimization problem was solved through two stages of ship distribution and customer management. The results show that the method based on an AI algorithm can effectively reduce transportation costs and shorten transportation time. Distribution is an important link in logistics, build up the potency of distribution, dramatically reduce logistics costs, and improve the quality of service (QoS). Therefore, it is necessary to choose line optimization. Combined with the characteristics of supermarket logistics distribution, the total transport distance minimum model was established in the literature [17], and simulated annealing (SA) algorithm was used to solve the scheduling problem. The achieved results show that the path scheme was shortened from 131.29 km of the initial random scheme to 71.294 km of the optimal solution via the SA algorithm. The path scheme was conducive to reducing the logistics distribution cost and has reference significance for the path selection of supermarket logistics distribution. Aiming at the distribution efficiency and cost of fresh products cold chain logistics distribution, an ACO-based optimization scheduling method for the distribution planning of low carbon cold chain logistics is proposed in the literature [18]. The cold chain logistics model was constructed by adding carbon emission cost and goods damage cost, which considered transportation cost, fixed cost, cold preservation cost, and time scheduling cost. The simulation

results show that the integration of the GA paradigm and the standard ACO algorithm, the optimization algorithm, has faster convergence speed and higher solution accuracy.

Based on the existing researches, there are two problems in the intelligent logistics path scheduling optimization, considering ACO algorithm: (1) there are few types of research on the specific application requirements of ant colony algorithm taking into the intelligent logistics path optimization consideration, ignoring the clear influence of the scheduling algorithm itself on the optimization accuracy and convergence speed; (2) the constraint conditions for path optimization are too simple to meet the requirements of optimization accuracy under the current complex road conditions. Aiming at the existing problems in the present research, this paper proposes an intelligent logistics distribution path optimization method based on an improved ant colony algorithm.

Aiming at the problems of low solving efficiency and high solving error rate in the current cold chain logistics distribution path scheduling and design methods, to build up the success rate of logistics distribution path formulation as shown in Figure 1, an optimal logistics distribution path design method based on IACO algorithm was proposed. The effectiveness of the IACO algorithm in optimal logistics distribution path design is analyzed through a concrete example, which considers constraints based on transport time, transport cost, refrigeration cost, and average road patency degree.

3. VRP Problem and Modeling

VRP is an important research object in the process of cold chain logistics distribution optimization. The vehicle path optimization problem is clearly defined as an NP-hard problem [7, 8]. With the increasing number of goods distributions, the traditional exact optimization scheduling algorithm and heuristic optimization scheduling algorithm cannot get the optimal yet achievable solution in such a short time. Therefore, the bionic optimization algorithm, regarded as a fast-developing direction in solving combinatorial optimization problems in recent years, is needed to deal with this category of combinatorial optimization paradigm. For example, ACO algorithm is a computer simulation algorithm for biological foraging behavior in nature, which has the features of parallelism, robustness emergence, and evolution, and will become an important method to solve the distribution path problem. Most logistics distribution path scheduling optimization can achieve a certain goal, e.g., the shortest delivery time, the shortest delivery path length, or the lowest delivery cost, and meet some constraints, e.g., the maximum vehicle load, and the end of delivery time. For customers with different distribution points, finding the most scientific and reasonable logistics distribution path includes many key reasons, e.g., distribution center, distribution vehicles, and customer points.

Logistics distribution VRP paradigm can be depicted as follows: considering that a certain number of customer points N each with a different number of goods demand g_i, a distribution center to provide customers the goods, a vehicle team M, is responsible for the goods distribution, capacity of distribution vehicle group q is the appropriate route scheduling, intending to achieve satisfied customers, and certain constraints, e.g., the shortest distance, the smallest cost, and the least time-consuming. VRP involves many elements, the most important of which are target and constraint. The main goals of VRP are to minimize the total transportation cost, decrease the total distribution mileage of distributed vehicles, and minimize the number of distributed vehicles, maximize the level of customer service and other goals. Meanwhile, the constraints of VRP mainly include vehicle capacity constraints, delivery mileage constraints, task time window constraints, vehicle departure time constraints, distribution sequence constraints, the total number of vehicle constraints, vehicle type constraints, return vehicle yard constraints, set delivery type constraints, and customer cargo type constraints. The following assumptions are made in the construction of the mathematical model: distribution center, the location is fixed; there is only one distribution center, which is responsible for all the distributions of vehicle scheduling. Distribution vehicles, onboard capacity, driving speed, and maximum driving distance are the same, and onboard capacity is greater than the customer demand for goods. The distribution vehicles start and end at the same distribution center, and the routes passed by the distribution vehicles cannot be repeated. Customer points, the location coordinates of all customer points, service time, priority, and quantity demanded are known. Therefore, the required number of distribution vehicles is represented as follows:

$$M = \left[\frac{\sum_{i=1}^{N} g_i}{\sigma \cdot q}\right] + 1, \tag{1}$$

where σ is a constant depending on constraint condition such as the complexity of goods loading and unloading and varying in the interval of $(0, 1)$. In general, the parameter $\sigma = 0.85$ is applied in this paper. In the whole model, based on the symbol definition in Table 1, the costs mathematical model of cold chain logistics distribution path selection is established.

$$\begin{aligned}
&\min C = \sum_i \sum_j \sum_k C_{ij} \cdot Y_{ijk};\\
&s.\text{t.} \quad \sum_i G_i \cdot X_{ki} \le g_i, \quad i = 1, 2, \ldots, M,\\
&\sum_i Y_{ki} = 1, \quad i = 1, 2, \ldots, M,\\
&\sum_j X_{kijk} = Y_{ki}, \quad i = 0, 1, \ldots, M,\\
&\sum_i Y_{kijk} = Y_{kj}, \quad j = 0, 1, \ldots, M,\\
&X = X_{ijk} \in S, X_{ijk} \in \{0, 1\}, Y_{ki} \in \{0, 1\},
\end{aligned} \tag{2}$$

where i and j represent the index of the customer point, and k denotes the index of the delivery vehicle. The vehicle k visits the customer i only once, the cargo demand volume of the customer point i is g_i, and the total amount of customer

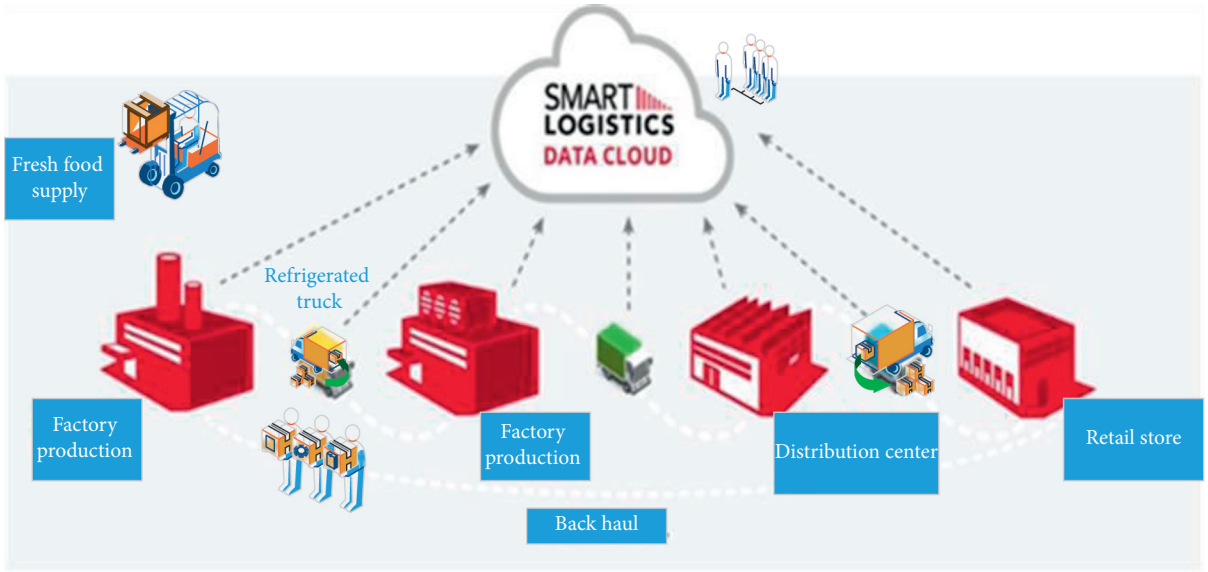

Figure 1: Framework of the proposed action quality assessment.

Table 1: Symbol definition.

Symbol	Description
X_{ik}	The delivery of customer point i is completed by the delivery vehicle k
Y_{ijk}	Distribution vehicle k travels from customer point i to customer point j
C_{ij}	All shipping costs from customer point i to customer point j
g_i	Customer point i demand capacity
G_i	Customer point actual volume of traffic

demand cannot exceed the maximum capacity of all vehicles in the distribution center. In conclusion, the logistics distribution scheduling and route optimization problem are a typical set of combined optimization paradigm. ACO algorithm is a category of the problem, which can be resolved by the positive feedback and distributed collaborative heuristic search algorithm, and always looks for a source from the food to the nest of the short circuit. This process is quite similar to the logistics distribution route optimization problem. Therefore, to introduce change into the ACO algorithm, resolve it.

4. Improved Ant Colony Algorithm-Based Optimal Logistics Distribution

4.1. Traditional Ant Colony Algorithm. The ACO algorithm is regarded as an AI optimization model that simulates the behavior of natural ant colonies in their search for food, which shows that the ant can choose the route according to the pheromone secreted by the preceding ant, and the probability of the route to the food source is proportional to the pheromone intensity secreted on the route. Therefore, a feedback phenomenon of information will be formed in the path of ants, i.e., the more the ants choose a certain path, the more the pheromones are left on the path, and the more likely the subsequent ants will choose this path to find the shortest path.

Through experts researching for years, the application of ACO algorithm has made great research advance and extensive role in various engineering fields. The algorithm with slower speed of convergence is tending to split up into local optimal solution, and other shortcomings can be resolved via the improvement of local pheromone updating rule, dynamic adjustment of related parameters and optimum combination, and global update strategy implementation algorithm optimization to improve the convergence speed of ant colony algorithm, enhance the global search randomness, and significantly inhibit the algorithm appear premature phenomenon.

Suppose in the moment of t, the total amount of ants arriving at the node i is $B_i(t)$, then the total amount of ants for n nodes (i.e., customer point number) is $m = \sum_{i=1}^{n} B_i(t)$. Also, the distance between node i and node j is d_{ij}. Initially, all the routes have no ant crawling, and the initial pheromone is the same, namely, $\mu_{ij} = C$, where $\mu_{ij}(t)$ refers to the pheromone concentration on the scheduling route between node i and node j at any time t, and $\eta_{ij}(t)$ is the heuristic information function corresponding to the distribution route R_{ij}. Then, at the time t, the path transition probability of ant k on a node i to the node j is

$$P_{ij}^{k}(t) = \begin{cases} \dfrac{\left[\mu_{ij}(t)\right]^{\alpha} \cdot \left[\eta_{ij}(t)\right]^{\beta}}{\sum_{s \in \text{allowed}(k)} \left[\mu_{is}(t)\right]^{\alpha} \cdot \left[\eta_{is}(t)\right]^{\beta}}, & j \in \text{allowed}(k), \\ 0, & \text{other.} \end{cases} \tag{3}$$

4.2. Improved Ant Colony Algorithm. The prior yet promising ACO paradigm has many advantages, e.g., strong robustness, positive feedback algorithm, and ease to combine with other algorithms. However, the traditional ACO approach also inevitably takes possession of some defects, e.g., it is easy to split up into the local optimal solution, which leads to the phenomenon of search stops, and it needs to search for a long time, when resolving the prior problem of NP-hard, traditional ACO approach for the optimal solution, considering faster speed and higher efficiency, which will be relatively low in the application of traditional ACO paradigm for an optimal path in the process of logistics transportation, and a common method is to solve the cold chain logistics transportation, the shortest distance between the starting point to finish path length is used to measure the merits of the solution. However, in the process of logistics scheduling, it will be an urge to consider the selected road of the average degree of free distribution, e.g., the cost of transportation and shipping time. Therefore, the choice of the road is more than one constraint conditions for the optimal solution of the problem, which considers the standard ACO algorithm, jointly considering multiple constraint conditions of the optimal path selection of IACO, the existing ACO based on heuristic function, and pheromone update methods while using the one node to the endpoint of the IACO inspired by the distance function.

The improved ant colony algorithm enhances the pheromone updating mode by using the constraint function model, which consisted of the material flow transport time factor, the logistics transport cost factor, and the road average mobility factor, so that the logistics transport time is shorter, the transport route is shorter, and the transport efficiency is higher. Heuristic function in traditional ACO algorithm is $\eta_{ij}(t)$, which ignores the ant traverse direction guidance; its value is only considering the reciprocal of the distance between two nodes $1/d_{ij}$. Because of the ignorance of direction for the inspiration function, it is easily leading to traverse the ants tending to step in the process of the optimization of the shortest and deviate from the direction of the whole optimization, which is limited to the local optimal shortest path rather than the whole. Toward this end, this paper takes into full consideration the distance relationship between the ant's current position, historical position, and future traversal position and improves the heuristic function as follows:

$$\eta_{ij}(t) = \frac{1}{L_i + d_{ij} + d_{jp}}, \tag{4}$$

where L_i presents the total length of the path that the ant has traveled to the node i. The ant leaves behind pheromones throughout the journey, and when all the ants have completed a round, the ant releases pheromones around the route, depending on the length of the path it has constructed. Therefore, after each round of movement, relevant information brought by ants should be updated. The pheromone update rule of each path can be defined as follows:

$$\mu_{ij}(t+1) = (1-\rho)\mu_{ij}(t) + \Delta\mu_{ij}, \tag{5}$$

where $\Delta\mu_{ij} = \sum_{k=1}^{m} \Delta\mu_{ij}(k)$ defines the pheromone enhancement located on the scheduling path during this iteration and $\Delta\mu_{ij}(k)$ further defines the pheromone quantity left on the path by the ant k in this iteration. The volatile coefficient ρ is used to describe the persistence of pheromone quantity [13]. Since the fixed value method cannot reflect the characteristics of the ACO algorithm, the adaptive variable value method is adopted in this paper to accelerate the convergence speed and reduce the probability of premature convergence, specifically as follows, where $\text{Iteration}_{\text{cur}}$ denotes the number of current iterations and $\text{Iteration}_{\max}$ represents the number of maximum iterations:

$$\rho = \begin{cases} 0.2, & \text{Iteration}_{\text{cur}} \in [0,\ 0.25 \cdot \text{Iteration}_{\max}], \\ 0.4, & \text{Iteration}_{\text{cur}} \in [0.25 \cdot \text{Iteration}_{\max},\ 0.75 \cdot \text{Iteration}_{\max}], \\ 0.6, & \text{Iteration}_{\text{cur}} \in [0.75 \cdot \text{Iteration}_{\max},\ \text{Iteration}_{\max}]. \end{cases} \tag{6}$$

The optimal solution obtained by the classical optimization algorithm is the local minimum near the given initial value, which is not the minimum from the global point of view. Naturally, it is easy to remind of finding the local minimum through multiple initial points and then finding the global minimum among multiple local minimum values. Based on the process proposed in [13], the optimal path considers the selection of several key factors, e.g., road transport time costs an average of the unobstructed degree to quickly obtain the optimal solution, transport cost factor average road unobstructed degree factor, and then transform the model into the standard ant colony algorithm, and finally achieve the path of the constraint conditions based on real-time updates and dynamic selection, guide choice of logistics transportation toward the optimal path, and get the optimal solution more precisely.

In the analysis of the basic ACO approach, it is found that there are two pheromone updating strategies, i.e., real-time updating and global updating. The former means that the ant renovates the pheromone of the scheduling path immediately after it gets from one node to another. The latter means that the ant updates pheromones along the path only after it has traversed all the nodes. Compared with these two methods, a global updating strategy can accelerate the convergence speed rapidly. At present, many studies have shown that global update has a good effect. Meanwhile, there are some defects. For example, global update in this method usually converges too early, and many ants will quickly converge on the same path so that a better solution cannot be found and obtained, i.e., it falls into the local optimal solution situation. During

pheromone updating, the system usually only updates the pheromone of the ants that finds the optimal path. The ant pheromone update usually can use the following two ways, one is to find the best performing in the process of circulation of ants; this way is usually slow convergence speed, not too early lead to rapid convergence to a certain path. The ant will continue to find a new path, and it is easier to find a better path. The other way is to find the ants with the best performance in the whole operation. This updating method can rapidly improve the convergence speed and obtain a better solution, but it also prevents the ant colony from searching for a better solution, which makes the entire ant colony easily trapped in a relatively poor path. Therefore, this paper proposes a new hybrid update pheromone strategy, which is in the process of searching previous cycle, using the iterative optimal method of pheromone update in time. This pheromone update is to find out the best in the circle of ants; this method is usually easy to find many more optimal solutions, which can effectively avoid premature of an ant colony in the poor solution. After multiple cycles (in this case, ten cycles) are completed, the updates are then performed using the global optimal solution, i.e., pheromone updates are performed using the ants that have the best performance of the entire operation. After mixing pheromone update rule was adopted, the algorithm will converge to the optimal solution concentration, thus can also find a more feasible solution, and can continue to search for other, more optimal solution and keep the fast convergence speed and can be used effectively to overcome a single global update which is easy to appear prematurely into a locally optimal solution.

4.2.1. Logistics Transport Time Factor, $F_{time}(j)$. The penalty cost of delivery time is related to the paradigm that whether the delivery vehicle meets the time window of the distribution point. Part of the penalty cost is the loss cost of an early arrival and waiting when the delivery vehicle arrives before the time window required by the distribution point. The other part is when the delivery vehicle arrives after the required time window at the distribution point, resulting in the penalty cost of delay. Then, the time penalty cost is

$$F_{\text{time}}(j) = \begin{cases} \dfrac{T(j)}{T_{\max}(j)}, & T(j) < T_{\max}(j); \\ 0, & \text{otherwise}, \end{cases} \tag{7}$$

where $T_{\max}(j)$ represents the upper limit of the maximum estimated time allowed for logistics in road transportation, and $T(j)$ represents the actual time required for logistics transportation. $F_{\text{time}}(j)$ is the factor of logistics transportation time and represents the ratio between the actual transportation time of logistics to the node j and the estimated maximum time. The larger the ratio is, the longer the actual transport time is.

4.2.2. Logistics Transport Cooling Factor, $F_{cool}(j)$. The main purpose of refrigeration is to maintain a constant temperature to ensure the freshness of fresh products. Suppose that the refrigeration cost mainly includes the cost of keeping the carriage temperature constant in the transportation process of distribution vehicles, the cost of an early arrival and waiting of distribution vehicles, and the cost of the lateness of distribution vehicles. For simplicity, transportation cost is usually related to the price of the product and fuel consumption caused by the multivehicles. Importantly, the longer the vehicle travels, the higher the distribution cost will be. Let the cooling cost be formulated by the ratio of the actual cooling cost $C(j)$ and maximum estimated cooling cost $C_{\max}(j)$ as follows:

$$F_{\text{cool}}(j) = \begin{cases} \dfrac{C(j)}{C_{\max}(j)}, & C(j) < C_{\max}(j); \\ 0, & \text{otherwise}. \end{cases} \tag{8}$$

4.2.3. Mean Road Patency Factor, $F_{patency}(j)$. Traffic performance index (TPD) is an index that comprehensively reflects the unblocked conditions of regional traffic roads [19, 20]. This index was proposed in the urban road traffic operation evaluation index system, and the ratio between the actual speed and the standard speed is used to reflect the traffic congestion level. The driving speed of the vehicle will be divided according to the TPI standard and the average speed when the road is clear will be the benchmark to calculate the driving speed range of the vehicle. When calculating the driving time of a vehicle, it can be divided into two situations: considering and ignoring the smooth condition of the road. If the smooth condition of the road is not taken into account, it is assumed that the vehicle can keep the standard speed at a constant speed without hindrance, and the driving time can be obtained by comparing the driving distance with the speed. If the road condition is considered, the traveling speed of the vehicle needs to be calculated by TPD to calculate the traveling time. The mean road patency factor $F_{\text{patency}}(j)$ can be represented as follows:

$$F_{\text{patency}}(j) = \begin{cases} \dfrac{P(j)}{P_{\max}(j)}, & P(j) < P_{\max}(j); \\ 0, & \text{otherwise}, \end{cases} \tag{9}$$

where $F_{\text{patency}}(j)$ represents the ratio between the patency degree of the route from logistics to the node j and the lowest tolerance of patency degree of vehicle driving road. The larger the ratio in equation (9), the larger probability the distribution vehicle chooses this route. $P(j)$ represents the patency degree of the route to the node j, and $P_{\max}(j)$ is the minimum tolerance for road patency of a vehicle. In all, the logistics transport cost factor $F_{\text{cost}}(j)$ can be defined as follows:

$$F_{\text{cost}}(j) = \omega \cdot F_{\text{time}}(j) + \xi \cdot F_{\text{cool}}(j) + \psi \cdot F_{\text{patency}}(j), \tag{10}$$

where ω, ξ, and ψ define the weight coefficients of time, cooling, and average road patency in the process of logistics transportation to the node j, respectively. To increase the

speed of convergence for the algorithm, the worst path of the mass path is weakened, a penalty factor is added to reduce the probability of its being selected, and pheromone concentration on the better-quality path is enhanced to make the ant choose the better-quality path. The pheromone updating formula in the standard ACO algorithm based on equation (5) formulation is improved as follows:

$$\mu_{ij}^{*}(t+1) = \frac{(1-\rho)\mu_{ij}(t) + \Delta\mu_{ij}}{F_{\text{cost}}(j)}. \tag{11}$$

To build up the convergence speed of this algorithm, the quality path-based worst path is weakened, and the penalty factor is added to reduce the probability of its being selected and increase the pheromone concentration on the stronger and better-quality path leads the ant to choose the better-quality path. The pheromone renovation in standard ant colony algorithm occurs locally. Substituting equations (4) and (11) into equation (3), the path transition probability of ant k on node i to node j for the IACO approach is defined as

$$\mathrm{P}_{ij}^{k}(t) = \begin{cases} \dfrac{\left[(1-\rho)\mu_{ij}(t) + \Delta\mu_{ij}/F_{\text{cost}}(j)\right]^{\alpha} \cdot \left[1/L_i + d_{ij} + d_{jp}\right]^{\beta}}{\sum_{s\in\text{allowed}(k)}\left[(1-\rho)\mu_{ij}(t) + \Delta\mu_{ij}/F_{\text{cost}}(j)\right]^{\alpha} \cdot \left[1/L_i + d_{ij} + d_{jp}\right]^{\beta}}, & j \in \text{allowed}(k), \\ 0, & \text{other}. \end{cases} \tag{12}$$

The steps to solve the optimal logistics distribution path of IACO algorithm are represented in Algorithm 1.

5. Results and Discussion

Through the above introduction of algorithm improvement and detailed process, this experiment will use test data to simulate the IACO scheduling paradigm and analyze the test results to evaluate the quality of the improved algorithm for cold chain logistics.

5.1. Environmental Setting. The operating platform of the simulation system is characterized by a CPU capacity of 2.6GMHz, a memory size of 4 GB and OS mode of Windows 7. To analyze the performance of the optimal cold chain logistics distribution path design method based on the proposed IACO algorithm, considering transport time factor, transport cooling factor, and mean road patency factor, MATLAB software is used to realize the simulation test. The key parameter settings of IACO are interpreted in Table 2.

It is known that a logistics company, only one distribution center, has 8 distribution vehicles, the maximum load resource of each vehicle is 10 T, and the maximum driving distance of each vehicle is 500 km, and it needs to provide resource services for 30 customer points at the same time. The basic information and location of the logistics distribution center and customers are shown in Figure 2.

5.2. Results and Analysis. The proposed IACO algorithm, existing CSAACO algorithm, and traditional ACO algorithm are diffusely used to solve the optimal path of logistics vehicles. Five simulation experiments were conducted to calculate the optimal logistics distribution path length for each experiment, and the results are shown in Figure 3. Each experiment can be conducted under different situations. More specially, the number varying from 1 to 5 represents the customer points varying from 8 to 12. Besides, it can be seen from Figure 3 that the average length of the optimal logistics distribution path of IACO is 111 km. The ACO algorithm's average length of optimal logistics distribution scheduling path is 114.7 km. Meanwhile, the average length of the optimal logistics distribution path of the CSAACO algorithm is 114.5 km. In addition, the IACO algorithm can obtain a better logistics distribution path, improve logistics distribution speed, reduce the time transmission cost of logistics distribution, and have higher practical application value. As shown in Figure 3, the optimal path length of the IACO algorithm is reduced by 3.7 km and 3.5 km compared with ACO and CSAACO, respectively. Importantly, the total number of iterations for each experiment to find the optimal logistics distribution path is represented as follows: IACO: 60, 58, 52, 54, 57; CSAACO: 74, 75, 74, 79, 73; ACO: 77, 79, 76, 78, 76.

Compared with the ACO algorithm and the CSAACO scheduling paradigm, the average optimal path time of the IACO paradigm is shortened by 258000 s and 15000 s, respectively. When customer scale in 100~200, task time of the algorithm for the conventional ACO algorithm, CSAACO algorithm, and the proposed IACO in this paper are not so obvious, with increasing customer scale, under the condition of the scale of performing the same task, the time of the IACO algorithm is far lower than the CSAACO and ACO algorithms. This algorithm can make up for the CSAACO algorithm and the ACO algorithm optimization time longer due to faster speed. Compared with ACO and CSAACO, the path distance of the IACO algorithm is reduced by 25000 m and 5800 m, respectively. When the customer task scale is 100, the distance of the proposed algorithm is about 2650 m shorter than that of the CSAACO algorithm. Compared with the prior ACO algorithm, the scheduling distance of the reformative algorithm is shortened by about 5 km. Moreover, with the increase in scale, the gap is gradually widening. The envisioned IACO algorithm shows more obvious advantages and has better path optimization ability.

The above experimental results make clear that the IACO scheduling paradigm has obvious improvement in optimization efficiency and quality compared with the CSAACO

Initialize the ant colony, place all ants on the node respectively, and the initial pheromones on all paths are the same;
Iteration times NC = 0;
Calculate the probability of each ant choosing the next crawling node, and crawl to the next node according to the calculation results;
Update the pheromone on the path between adjacent nodes;
Update the pheromone on the entire path after all ants crawl the entire path;
Iteration times NC = NC + 1;
$\text{Iteration}_{\max}$: then, output the optimal logistics distribution path;

Algorithm 1: Establishing the optimal logistics distribution path optimization problem corresponding to the directed graph.

Table 2: Parameters setting of the IACO approach.

Symbol	Description	Value
α	1	Pheromone factor
β	3	Expected heuristic factor
ρ	0.4	Pheromone volatility
ω	0.33	Weight coefficient of transport time
ξ	0.33	Weight coefficient of transport cooling
ψ	0.33	Weight coefficient of mean road patency
$\text{Iteration}_{\max}$	300	Maximization iterations
N	21	Total number of customer points
M	8	Total number of distribution vehicles
q	125	Total distribution vehicle capacity

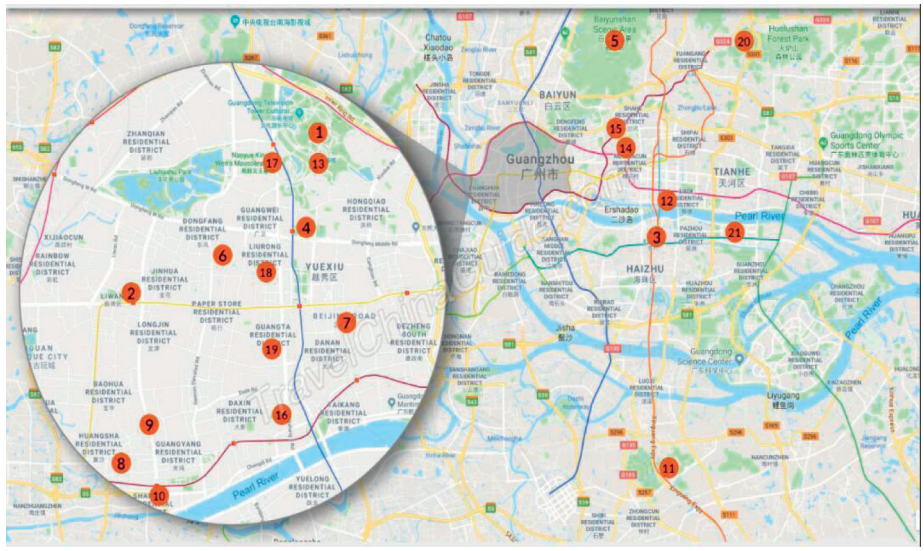

Figure 2: Customer location information map in Guangzhou (brown points).

algorithm and ACO method. Especially as the service customer scale expands unceasingly, the proposed algorithm can more effectively deal with the scheduling problem of logistics distribution time-consuming and poor quality, the advantages are better reflected, the IACO scheduling paradigm is presented in this paper under the condition of the same customer scale task, shorten the time of the distribution tasks effectively, reduce the transportation path distance, accelerate the algorithm convergence speed, and maximize the enhanced efficiency of the logistics industry as a whole and distribution.

As can be seen from Figure 4, the total amount of iterations for the IACO algorithm to find the optimal logistics distribution path was significantly less than that for traditional ACO and CSAACO, which accelerated the solving efficiency of the optimal logistics distribution path. Therefore, the IACO algorithm can be applied to the solution of large-scale logistics distribution path design problems, and its practical application scope is more extensive. Moreover, the convergence speed is much faster, so the path scheduling algorithm in this paper is exceeded by the basic ACO from both convergence speed and the comparison of the results.

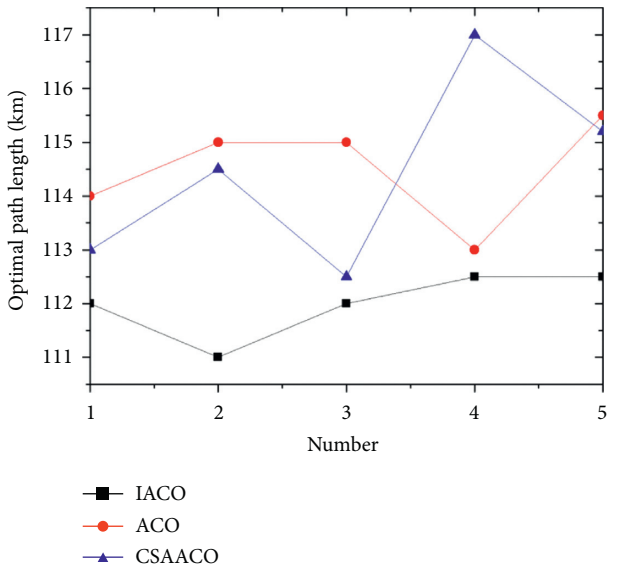

Figure 3: The optimal logistics distribution path length comparison.

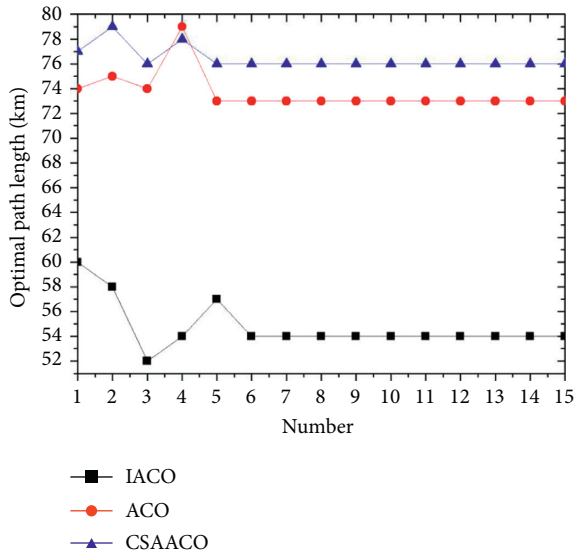

Figure 4: Comparison of iteration times of optimal logistics distribution path.

The problem that the basic ACO is easy to stop at the locally optimal solution is effectively solved in the improved algorithm.

It can be seen in Figure 4 that the IACO scheduling paradigm presented in this paper has great advantages and proves the correctness and effectiveness of the IACO algorithm. This example is solved in the simple case of a single logistics distribution center. If there are multiple logistics distribution centers, it is only necessary to divide the distribution centers into different regions through the decomposition method and then solve them independently. The resulting solution may not be the global optimal solution, but it is still very effective and feasible.

Besides, the total amount of iterations for the IACO scheduling paradigm to find the optimal logistics distribution path is significantly less than that for the CSAACO and ACO algorithm as seen in Figure 4, which speeds up the solving efficiency of the optimal logistics distribution path and can be applied to deal with the design scheduling problem of large-scale logistics distribution path, so the practical application scope is more extensive.

Through the analysis of Figure 5, the appropriate combination of selected parameter values is conducive to obtaining the optimal solution. Therefore, in practical problems, appropriate parameters should be selected according to the actual deployment situation for different problems. To sum up, the optimal search effect was best when $\alpha = 1$, $\beta = 3$, $\rho = 0.4$, and the optimal path distance was 880 km.

It can be seen from Figure 5 that the optimal path length IACO algorithm lies in an 880 km, and convergence speed is fast, so both form the convergence speed and carry on the comparison to the final result; this IACO scheduling paradigm is better than the basic ant colony algorithm, which is easy to stall on the local optimal solution of the problem in

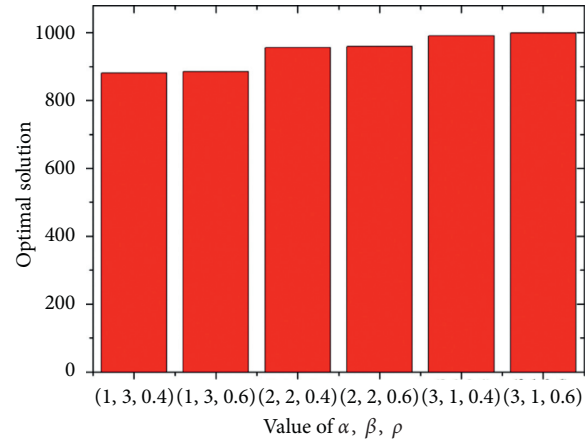

Figure 5: Effect of α, β, ρ on path planning.

the improved algorithm which has been effectively solved. As seen from Figure 5, the IACO scheduling paradigm in this paper has great advantages and also proves the correctness and effectiveness of the improved ant colony algorithm.

6. Conclusions

The problem of route choice of logistics transportation is crucial to the transportation cost, time, and efficiency of logistics enterprises, and it is a difficult problem faced by all logistics industries. It is of great practical value to analyze the optimal logistics distribution path. To solve some problems existing in the current logistics distribution path, design method is proposed in this paper based on the IACO algorithm of the optimal design method of logistics distribution path, at the same time, to join based on the transport time factor, transport cooling factor, and mean road patency factor, improved pheromone update methods, which

changed the logistics path transition probability, and compared with the traditional ACO scheduling approach and CSAACO scheduling approach, the outstanding results show that the IACO algorithm can obtain the ideal logistics distribution path, and the search efficiency is high and has a very wide application prospect. Its superior performance is embodied in that it increases the global optimization ability, shortens the distribution path, reduces the cost of distribution for logistics enterprises, improves distribution efficiency, and promotes the rapid development of the logistics industry.

Data Availability

The data used to support the findings of this study are available from the corresponding authors upon request.

Conflicts of Interest

The author declares no conflicts of interest.

Authors' Contributions

H. X. conceptualized the study, developed methodology, utilized software, validated the study, did formal analysis, investigated the study, provided resources, curated the data, wrote the original draft, reviewed and edited the article, visualized and supervised the study, did project administration, and was responsible for funding acquisition. The author read and agreed to the published version of the manuscript.

Acknowledgments

This work was supported Guangzhou Education Science Planning Project in 2019, "CDIO-Based Research on Innovative and Applied Talent Training Mode" (201912027); Guangzhou Maritime University Innovation and Strength Project in 2018, Logistics Engineering Key Major Construction (F410608); Guangzhou Maritime University Innovation and Strength Project in 2017, Logistics Engineering Key Major Construction (E320103); and Education and Scientific Research Project of Education Department of Guangdong Province in 2020 (2020GXJK403).

References

[1] S. Winkelhaus and E. H. Grosse, "Logistics 4.0: a systematic review towards a new logistics system," *International Journal of Production Research*, vol. 58, pp. 18–43, 2020.

[2] L. Rosenbaum, "Facing covid-19 in Italy - ethics, logistics, and therapeutics on the epidemic's front line," *New England Journal of Medicine*, vol. 382, no. 20, pp. 1873–1875, 2020.

[3] T. P. Vu, D. B. Grant, and D. A. Menachof, "Exploring logistics service quality in hai phong, Vietnam," *The Asian Journal of Shipping and Logistics*, vol. 36, pp. 54–64, 2020.

[4] K. Zheng, Z. Zhang, and B. Song, "E-commerce logistics distribution mode in big-data context: a case analysis of JD.COM," *Industrial Marketing Management*, vol. 86, pp. 154–162, 2020.

[5] J. Wang, M. K. Lim, M.-L. Tseng, and Y. Yang, "Promoting low carbon agenda in the urban logistics network distribution system," *Journal of Cleaner Production*, vol. 211, pp. 146–160, 2019.

[6] X. Cui and C. Xie, "Design and implementation of logistics management system based on SSH technology," *Journal of Physics: Conference Series*, vol. 1533, p. 042057, 2020.

[7] Z. Wang and J.-B. Sheu, "Vehicle routing problem with drones," *Transportation Research Part B: Methodological*, vol. 122, pp. 350–364, 2019.

[8] S. Pelletier, O. Jabali, and G. Laporte, "The electric vehicle routing problem with energy consumption uncertainty," *Transportation Research Part B: Methodological*, vol. 126, pp. 225–255, 2019.

[9] L. Xiao, M. Xu, Y. Chen, and Y. Chen, "Hybrid grey wolf optimization nonlinear model predictive control for aircraft engines based on an elastic BP neural network," *Applied Sciences*, vol. 9, no. 6, p. 1254, 2019.

[10] Q. Zhang, S. Liu, D. Gong, H. Zhang, and Q. Tu, "An improved multi-objective quantum-behaved particle swarm optimization for railway freight transportation routing design," *IEEE Access*, vol. 7, pp. 157353–157362, 2019.

[11] Y. Liu, S. Ji, Z. Su et al., "Multi-objective AGV scheduling in an automatic sorting system of an unmanned (intelligent) warehouse by using two adaptive genetic algorithms and a multi-adaptive genetic algorithm," *PloS One*, vol. 14, p. e0226161, 2019.

[12] X. Zhou, "Path planning of coastal tourism based on the improved firefly algorithm," *Journal of Coastal Research*, vol. 106, no. sp1, pp. 263–266, 2020.

[13] M. Wang, T. Ma, G. Li, X. Zhai, and S. Qiao, "Ant colony optimization with an improved pheromone model for solving MTSP with capacity and time window constraint," *IEEE Access*, vol. 8, pp. 106872–106879, 2020.

[14] Z. Liu, Z. Li, W. Chen, Y. Zhao, H. Yue, and Z. Wu, "Path optimization of medical waste transport routes in the emergent public health event of COVID-19: a hybrid optimization algorithm based on the immune-ant colony algorithm," *International Journal of Environmental Research and Public Health*, vol. 17, no. 16, p. 5831, 2020.

[15] L. Liu, H. Wang, and S. Xing, "Optimization of distribution planning for agricultural products in logistics based on degree of maturity," *Computers and Electronics in Agriculture*, vol. 160, pp. 1–7, 2019.

[16] L. Kang, "Research on marine port logistics transportation system based on ant colony algorithm," *Journal of Coastal Research*, vol. 115, no. sp1, pp. 64–67, 2020.

[17] B.-H. Zhou and F. Tan, "A self-adaptive estimation of distribution algorithm with differential evolution strategy for supermarket location problem," *Neural Computing and Applications*, vol. 32, no. 10, pp. 5791–5804, 2020.

[18] B. Zhao, H. Gui, H. Li, and J. Xue, "Cold chain logistics path optimization via improved multi-objective ant colony algorithm," *IEEE Access*, vol. 8, pp. 142977–142995, 2020.

[19] R. F. M. Neto, L. E. Paris, F. A. Junior et al., "Environmental performance index for Brazilian public airports: the Infraero experience," *Environmental Science & Policy*, vol. 112, pp. 164–171, 2020.

[20] L. Wang, J. Yang, N. Zhang et al., "A spatial-temporal estimation model of residual energy for pure electric buses based on traffic performance index," *Tehnicki Vjesnik*, vol. 24, pp. 1803–1811, 2017.

Hindawi
Discrete Dynamics in Nature and Society
Volume 2021, Article ID 5599512, 12 pages
https://doi.org/10.1155/2021/5599512

Research Article

Incorporating Space-Time Correlation of Population Densities into the Design of a Candidate Rail Transit Line over Years

Liu Ding[1,2], **Kunpeng Zhang**[1,3] **and Binglei Xie**[1]

[1]*Shenzhen Key Laboratory of Urban Planning and Decision Making Simulation, Shenzhen Graduate School, Harbin Institute of Technology, Shenzhen 518055, China*
[2]*College of Transport and Communications, Shanghai Maritime University, Shanghai 201306, China*
[3]*Shenzhen Transportation Design & Research Institute LTD., Shenzhen 518003, China*

Correspondence should be addressed to Liu Ding; stunker@126.com

Received 5 February 2021; Revised 28 March 2021; Accepted 10 April 2021; Published 28 April 2021

Academic Editor: Tingsong Wang

In contrast to private cars, rail transit systems are a more effective way to deal with the emerging challenges in cities with high population densities, such as congestion, air pollution, and traffic emissions. Rail transit systems, however, are commonly costly, due to substantial investments in construction and maintenance. It is thus necessary to design the candidate rail transit systems carefully to ensure public transport accessibility and sustainability, with consideration of the space-time correlation of population densities. In this paper, the space-time correlations of population densities are incorporated into the design of a candidate rail transit line over years. A closed-formed mathematical programming model is proposed, with an optimisation objective of social welfare budget maximisation. The social welfare budget is defined as the summation of the expected social welfare and social welfare margins. The model decision variables include rail line length, rail station number, and project start time of the candidate rail transit line. The analytical solutions for the proposed rail design model are given explicitly for different scenarios with various constraints.

1. Introduction

1.1. Motivation and Literature Review. The preferred travel mode in areas with low population density is a private car, such as the United States. The preferred travel mode in areas with high population density is rail transit, such as Hong Kong. One possible reason is that high congestion and long delay may occur on highways, during morning peak hours on working days in highly populated areas. The generalised travel cost of a private car may be higher than rail transit in such areas.

The travel mode choices were commonly examined, with the assumptions of given and fixed population densities (see, e.g., [1–3]). These assumptions were reasonable in their models because the travel mode choices were analysed for short-term operation optimisation. Under these assumptions, the effects of population densities on travel mode choices, however, were not explicitly investigated. The effects of population densities are of some importance and significance, for the design optimisation of a candidate rail transit line over years.

In the transportation corridor of a candidate rail transit line, the population densities in each residential location vary year by year. If the increase of population density in the first year leads to an increase in the second year, positive temporal correlations then exist between population densities in the first year and the second year, and vice versa. Similarly, if the increase of population density in one residential location leads to the increase of population density in another residential location, positive spatial-temporal correlations then exist between population densities in these two residential locations.

The space-time correlation of population densities can be considered, with the nested logit model (e.g., [4–6]) and the C-logit model (e.g., [6–9]). In these nested logit models and C-logit models, spatial-temporal correlation of population densities was considered in the residential locations and/or travel choice behaviours of households. In contrast with the nested logit model, the C-logit model had a simple closed-form probability expression and was simpler for calibration [7,8].

In these nested logit and C-logit models, the space-time correlations between alternatives were investigated to calculate the choice probabilities for the residential locations and/or travel choice behaviours of households. In other words, the space-time correlations of population densities cannot explore explicitly with the nested logit and C-logit models. The possible effects of the space-temporal correlation of population densities on the design of a candidate rail transit line cannot be examined explicitly by nested logit or C-logit models.

The space-time correlations of population densities can be taken into account explicitly by the space-time correlation coefficient of population densities [2, 3, 7, 8, 10–12] proposed a bilevel optimisation model to estimate the space-time correlation of OD demands during the same peak hour periods due to day-to-day fluctuations over the whole year. Liu [2] investigated the effects of spatial and temporal correlation of population densities on system disutility in a railway transportation corridor. It concluded that the spatial and temporal correlation of population densities had a significant influence on the results of population densities and the system performance measured in system disutility, consumer surplus, and social welfare of railway system.

Zhang et al. [3] explored the implementation flexibility of multiperiod rail line design with consideration of uncertainties in population distribution. The space-time correlation of population densities was taken into account, but the proposed model was not analytical. Yang et al. [8] proposed an estimation framework based on the Generalized Method of Moment to infer the probability function of origin-destination (OD) demand variables using sets of traffic counts over a network. Sun et al. [7] conducted the stochastic OD traffic demand estimation with a biobjective optimisation model for the traffic count location problem.

It was noted that the space-time correlations of population densities were mainly considered for road traffic origin-destination estimation in these previous studies. In this paper, we will incorporate the space-time correlations of population densities by the space-time correlation coefficient of population densities for the design optimisation of a candidate rail transit line.

Based on the space-time correlation coefficient of population densities, a closed-form programming model is introduced to examine the effects of space-time correlation of population densities on the design of a rail transit line in this paper. The optimisation objective of the proposed model is budget social welfare maximisation. The budget social welfare is defined as a summation of expected social welfare and social welfare margin. The model decision variables include rail line length, rail station number, and the project start time.

1.2. Problem Statement and Contributions. As shown in Figure 1, a linear transportation corridor is separated into n residential locations from the Central Business District (CBD) to the city boundary, and the planning time horizon is divided into m equal time periods. n and m are positive integers. $L(t_1)$ and $L(t_2)$ are the lengths of candidate rail transit line with respect to project start time in years t_1 and t_2, which can be determined endogenously with the use of the proposed model. $\widetilde{P}(x_1, t_1)$ and $\widetilde{P}(x_2, t_2)$ are the population densities in residential locations x_1 and $x_2$in years t_1 and t_2, respectively, with $\forall x_1, x_2 \in [0, B]$ and $\forall t_1, t_2 \in [0, m]$. Spatial correlation exists between population densities $\widetilde{P}(x_1, t_1)$ and $\widetilde{P}(x_2, t_1)$, and $\widetilde{P}(x_1, t_2)$ and $\widetilde{P}(x_2, t_2)$, while temporal correlation exists between population densities of $\widetilde{P}(x_1, t_1)$ and $\widetilde{P}(x_1, t_2)$, and $\widetilde{P}(x_2, t_1)$ and $\widetilde{P}(x_2, t_2)$.

Two major extensions to the related literature are made in this paper: (i) the effects of space-time correlation of population densities on the design of a candidate rail transit line over years are investigated by a closed-form mathematical programming model; (ii) the analytical optimal solutions of design variables of the candidate rail transit line over years are obtained with the proposed model.

The remainder of this paper is organised as follows: in the next section, some basic considerations are given. A rail design model is proposed in Section 3, taking account of the space-time correlation of population densities along a linear transportation corridor. Section 4 gives illustrative numerical examples to show the application and contributions of the proposed model. A summary of this paper is given in Section 5.

2. Basic Considerations

2.1. Assumptions. To facilitate the presentation of the essential ideas, some basic assumptions are made, listed as follows:

A1. The candidate rail transit line is assumed to be linear and start from the CBD and then be built along a linear transportation corridor [1, 13]. The candidate rail transit line project in each period is assumed to finish on time and the rail service is expected to be supplied at the end of each design period [14].

A2. The standard deviation (SD) of the population density is assumed to be an increasing function with respect to its mean value. This function is referred to as the stochastic population density function. In addition, the stochastic population density function is assumed to be a nondecreasing function with respect to its mean value. [15].

A3. Households' responses to the quality of the rail service provided are measured by a generalised travel cost that is a weighted combination of in-vehicle time, access time, waiting time, and the fare [16]. Households

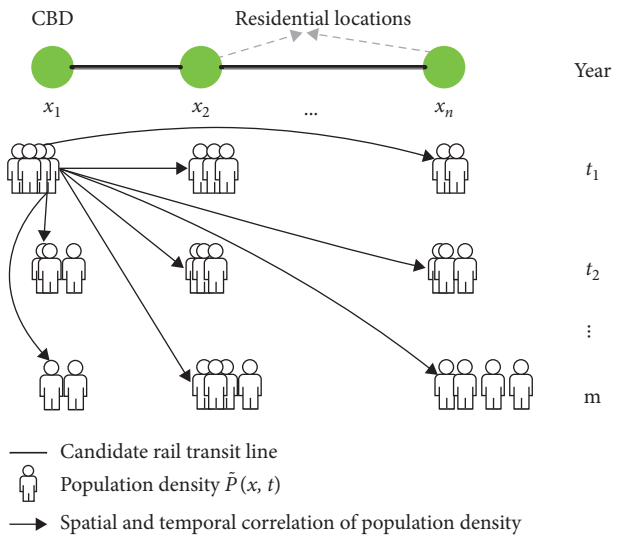

FIGURE 1: Spatial and temporal correlation of population densities in a candidate rail transit line over years.

are assumed to be homogeneous and have the same preferred arrival time at the workplace located in the CBD. This study focuses mainly on households' home-based work trips, which are compulsory activities. The number of trips is, thus the number of trips is not affected by other factors, such as income level [17].

A4. The study period is assumed to be a peak hour, for instance, the morning peak hour, which is usually the most critical period in the day [19].

A5. Rail station number depends on rail line length and rail station spacings. To obtain the analytical solutions, an even rail station spacing is assumed. In other words, with the assumption of constant rail station spacing, once rail line length is determined, the rail station number is also determined. This assumption is also used in the works of Li et al. [17] and Liu [2].

2.2. Space-Time Correlation of Population Densities. To take into account the space-time correlation of population densities, it is assumed that there exists a perturbation in the population density. The yearly perturbed population density $\tilde{P}(x,t)$ is given by the following equation [12]:

$$\tilde{P}(x,t) = P(x,t) + \varepsilon, \tag{1}$$

where $P(x,t)$ is the expected population density at location x in year t, $E[\tilde{P}(x,t)] = P(x,t)$; ε is a random term, with $E[\varepsilon] = 0$. It is noted that the expected population density $P(x,t)$ is a deterministic value. In terms of A2, the SD of population density can be expressed as [15]

$$\sigma[\tilde{P}(x,t)] = \sqrt{\mathrm{var}[\tilde{P}(x,t)]} = \varphi(P(x,t)), \tag{2}$$

where $\varphi(\bullet)$ is defined as the stochastic population density function, which represents the functional relationship between the mean value and the standard deviation of the stochastic population density. Specifically, a coefficient of variation of population density CV_P is defined as

$$\mathrm{CV}_P = \frac{\varphi(P(x,t))}{P(x,t)}, \tag{3}$$

where CV_P is a standardised measure of the dispersion of the probability distribution or frequency distribution of the population density.

To take spatial and temporal correlations between population densities into account, the following spatial and temporal covariance is defined as [10]

$$\sigma_P(x_1,t_1;x_2,t_2) = \mathrm{cov}[\tilde{P}(x_1,t_1),\tilde{P}(x_2,t_2)] = \rho_{x_1,t_1}^{x_2,t_2}\varphi(P(x_1,t_1))\varphi(P(x_2,t_2)), \tag{4}$$

where $\rho_{x_1,t_1}^{x_2,t_2}(-1 \le \rho_{x_1,t_1}^{x_2,t_2} \le 1)$ is the correlation coefficient, which is an important measurement reflecting the statistical correlation between $\tilde{P}(x_1,t_1)$ and $\tilde{P}(x_2,t_2)$. There are three correlation coefficient cases: negative, positive, or zero, representing negative, positive statistical dependence or statistical independence of population densities. Specifically, with $x_1 = x_2$ and $t_1 = t_2$, the spatial and temporal covariance becomes the standard deviation value.

2.3. Households' Residential Locations Choice Behaviours. Households are assumed to choose the residential locations to maximise their own utilities subject to budget constraint. A Cobb–Douglas form of the utility function is adopted, shown as follows [17]:

$$U(g(x,t),h(x,t)) = \alpha \log g(x,t) + \beta \log h(x,t), \tag{5}$$

where $U(g(x,t),h(x,t))$ represents the daily household utility function for residential location x in year t; $g(x,t)$ is the daily consumption of nonhousing goods for households in a residential location x in year t, of which the price is normalised to 1; $h(x,t)$ is the consumption of housing in a residential location x in year t, measured in square meters of floor space; α and β are positive constraints, and $\alpha + \beta = 1$.

The budget constraints for households are expressed as follows:

$$g(x,t) + r(x,t)h(x,t) = I - \pi(x,t), \tag{6}$$

where $r(x,t)$ is the daily housing rent per unit of housing in residential location x in year t, I is the average daily household income, and $\pi(x,t)$ is the daily generalised travel cost from residential location x to the CBD in year t.

Under user equilibrium condition, no households can increase his/her utility by unilaterally changing their

location choices. Mathematically, the utility maximisation for households can be expressed as

$$\max U(g(x,t),h(x,t)) = \alpha \log g(x,t) + \beta \log h(x,t). \tag{7}$$

A similar mathematical formulation has been formulated in Li et al. [17]. According to the equilibrium condition proposed in their study, the equilibrium household utility is shown as follows:

$$U_{\text{equilibrium}} = \alpha \log\left(\frac{I\alpha}{\alpha+\beta}\right) + \beta \log\left(\frac{I\beta}{r(0,t)(\alpha+\beta)}\right), \tag{8}$$

with

$$r(x,t) = r(0,t)\left(1 - \frac{\pi(x,t)}{I}\right)^{(1/\beta)}, \tag{9}$$

$$h(x,t) = \frac{I\beta}{r(0,t)}\left(1 - \frac{\pi(x,t)}{I}\right)^{-(\alpha/\beta)}, \tag{10}$$

where $U_{\text{equilibrium}}$ is the equilibrium household utility in year t and $r(0,t)$ is the housing rent in the CBD in year t. $r(x,t)$ in equation (9) is the daily housing rent function per unit of housing in residential location x in year t, and $h(x,t)$ in equation (10) is the daily consumption function of housing for households in residential location x in year t. It can be seen that both $r(x,t)$ and $h(x,t)$ are functions of daily generalised travel cost from residential location x to the CBD in year t.

To keep the balance of the supply and demand of housing, it requires that

$$h(x,t)P(x,t) = Y(x,t). \tag{11}$$

Substituting equations (10) in (11), we have

$$P(x,t) = \frac{r(0,t)}{I\beta}\left(1 - \frac{\pi(x,t)}{I}\right)^{(\alpha/\beta)} Y(x,t), \tag{12}$$

where $h(x,t)$ represents the consumption of housing in residential location x in year t, measured in square meters of floor space, and $P(x,t)$ is the expected population density of households in residential location x in year t at equilibrium.

The population conservation equation can be expressed as

$$\int_0^B P(w,t)\mathrm{d}w = P^t, \tag{13}$$

whereP^t is the total population along the candidate rail transit line in year t and B is the length of the rail transportation corridor. To describe the year-by-year variation of the total population, a yearly growth factor is assumed and shown as follows [14]:

$$P^t = (1+\gamma(t))P^0, \tag{14}$$

where $\gamma(t)$ is a compound-account factor to measure the growth of the total population compared with the based year and P^0 is the total population in the base year. As $\gamma(t)$ is positive, the implication is that the total population along the candidate rail transit line increases and vice versa. $(1+\gamma(t))$ is the multiplier of the total population to measure the variation of the total population in year t compared with the total population in the base year.

2.4. Social Welfare Budget. The government or the rail operator will build a rail transit line to meet the increasing travel demand of households and eases highway traffic congestion. Social welfare is commonly used to assess the performance of a candidate rail transit line. Due to the yearly uncertainty associated with rail travel demand, the social welfare of the candidate rail transit line is also not a deterministic value. Because of the uncertainty of social welfare, an extra safety margin is assigned to ensure a higher probability of gaining a certain level of social welfare. In view of this, the concept of social welfare budget is proposed as follows:

$$\phi(\text{SW}) = E[\text{SW}] + \lambda\sigma[\text{SW}], \tag{15}$$

where $\phi(\text{SW})$ is the social welfare budget, $E[\text{SW}]$ is expected social welfare, λ is a negative parameter, $\sigma[\text{SW}]$ is the standard deviation of social welfare, and $\lambda\sigma[\text{SW}]$ is the social welfare margin.

λ relates to the requirement on ensuring a certain social welfare gain. A high value of λ implies a relatively high $\phi(\text{SW})$ and a higher probability of social welfare gain. Formally, λ can be related mathematically to the probability that there is a gain in the budget social welfare, namely,

$$p(\text{SW} \geq \phi(\text{SW}) = E[\text{SW}] + \lambda\sigma[\text{SW}]) = \delta, \tag{16}$$

where δ is the probability of a gain in the social welfare budget. Rearranging terms in equation (16), then

$$p\left(\frac{\text{SW} - E[\text{SW}]}{\sigma[\text{SW}]} \geq \lambda\right) = \delta. \tag{17}$$

From equation (16), we can obtain

$$p\left(\frac{\text{SW} - E[\text{SW}]}{\sigma[\text{SW}]} < \lambda\right) = 1 - \delta. \tag{18}$$

Let $\Phi(\bullet)$ be the standard cumulative distribution function. Equation (18) can be rewritten as follows:

$$\Phi(\lambda) = 1 - \delta. \tag{19}$$

As $1 - \Phi(\lambda) = \Phi(-\lambda)$, equation (19) can be transformed as

$$\Phi(-\lambda) = \delta, \tag{20}$$

and, with equation (20), $\lambda = -\Phi^{-1}(\delta)$ can be obtained. Thus, the social welfare budget defined in equation (15) can be rewritten as

$$\phi(\text{SW}) = E[\text{SW}] - \Phi^{-1}(\delta)\sigma[\text{SW}]. \tag{21}$$

The value of δ represents the government's or rail operator's attitudes toward social welfare gain. A larger δ

implies a larger negative safety margin and a higher probability of a gain in social welfare budget.

Social welfare of the candidate rail transit line consists of the consumer surplus of households and the profit of the rail operator. Mathematically, expected social welfare $E[\mathrm{SW}]$ can be expressed as follows:

$$E[\mathrm{SW}] = E[\mathrm{CS}] + E[\mathrm{PR}], \tag{22}$$

where $E[\mathrm{CS}]$ is expected consumer surplus of households and $E[\mathrm{PR}]$ is the expected profit of the rail operator.

The expected consumer surplus of households $E[\mathrm{CS}]$ is given by

$$E\,[\mathrm{CS}] = 365\left(\sum_{t=1}^{m}\int_0^B\int_0^{q(x,t)} (q(x,t))^{-1}(w)\mathrm{d}w - q(x,t)\pi(x,t)\right), \tag{23}$$

where 365 is a parameter converting daily consumer surplus into yearly consumer surplus, $q(x,t) = E[\widetilde{q}(x,t)]$ is the expected travel demand of rail service from residential location x in year t, $\pi(x,t) = E[\widetilde{\pi}(x,t)]$ is the expected generalised travel cost from residential location x to the CBD in year t by rail, m is planning time horizon in years, and B is the length of the rail transportation corridor.

The expected profit of rail operator $E[\mathrm{PR}]$ is given by

$$E[\mathrm{PR}] = 365\left(\sum_{t=1}^{m}\int_0^B (q(x,t))(f(x,t)-c)\mathrm{d}x - L(t)C_r - n_s^t C_s\right)\kappa(t), \tag{24}$$

where 365 is a parameter converting daily profit into yearly profit, $f(x,t)$ is rail fare, c is a variable cost to supply rail service for each passenger, $L(t)$ is rail length in year t, C_r is yearly unit fixed maintenance cost of rail line, n_s^t is rail station number in year t, and C_s is yearly fixed operation cost of each rail station.

In terms of A3, the travel demand function of rail service from residential location x in year t, $\widetilde{q}(x,t)$ is assumed to be given by an exponential function shown as follows [18]:

$$\widetilde{q}(x,t) = \widetilde{P}(x,t)\exp\left(-\theta\left(\pi(x,t) + \varepsilon_q\right)\right), \tag{25}$$

whereθ is a positive constant, which responds to the households' sensitivity to the rail service level, and ε_q is a random term, with $E[\varepsilon_q] = 0$. The inverse function of travel demand can be obtained as follows:

$$(\widetilde{q}(x,t))^{-1}(\widetilde{q}(x,t)) = \pi(x,t) + \varepsilon_q = \frac{1}{\theta}\ln\frac{\widetilde{P}(x,t)}{\widetilde{q}(x,t)}. \tag{26}$$

Substituting it into equation (23), the following equation is obtained:

$$E[\mathrm{CS}] = 365\sum_{t=1}^{m}\int_0^B \frac{q(x,t)}{\theta}\mathrm{d}x. \tag{27}$$

The expected generalised travel cost consists of fare, access cost from residential locations to rail stations, waiting for cost for rail service at stations, and in-vehicle cost from rail stations to the CBD, shown as follows [20]:

$$\pi(x,t) = f(x,t)\kappa(t) + \mu_c t_c(t) + \mu_w t_w(t) + \mu_i t_i(t), \tag{28}$$

where $(\mu_c/\mu_w/\mu_i)$ are values of access time, waiting time, and in-vehicle time, respectively; $f(x,t)$ is distance-based fare for rail service, $\kappa(t)$ is a compound-account factor to convert future values to present values, $t_c(t)$ is average access time from residential locations to the rail station, with $(\partial t_c(t)/\partial n_s^t) < 0$,$t_w(t)$ is average waiting time for rail service at stations, and $t_i(t)$ is average in-vehicle cost from rail stations to CBD. The distanced-based fare $f(x,t)$ is given by

$$f(x,t) = f_0 + f_1 x, \tag{29}$$

where f_0 is the fixed fare component and f_1 is the variable fare component per kilometre. Waiting time $t_w(t)$ is closely concerned with travel demand and supply of the rail service. For long-term planning, this value can be estimated using the following function:

$$t_w(t) = 0.5h(t), \tag{30}$$

where 0.5 is a reasonable parameter for short train headway and passengers arrival time and $h(t)$ is the average headway in year t [21].

The average headway in year t is closely concerned with cycle time of train operation $T(t)$ and fleet size of trains $F(t)$:

$$h(t) = \frac{T(t)}{F(t)}. \tag{31}$$

The cycle time of train operation can be calculated by [22]

$$T(t) = \frac{2L(t)}{v(t)} + 2\varsigma, \tag{32}$$

where $L(t)$ is the rail line length in year t, $v(t)$ is the average train speed in year t, and ς is average constant terminal time. The average in-vehicle travel time from rail station i to the CBD, $t_i(t)$, is given by the distance between rail station i and the CBD $D_i(t)$, divided by the average train speed in year t, $v(t)$, namely,

$$t_i(t) = \frac{D_i(t)}{v(t)}, \tag{33}$$

where $D_i(t)$ can be calculated as follows if a constant station spacing is assumed:

$$D_i(t) = \frac{L(t)}{n_s^t}, \tag{34}$$

with $i \in [1, n_s^t]$.

In terms of equations (1), (2), (24)–(32), we obtain the expected budget social welfare shown as follows:

$$E[\mathrm{SW}] = 365\left(\sum_{t=1}^{m}\int_0^B (q(x,t))\left(f(x,t)+\frac{1}{\theta\kappa(t)}-c\right)\mathrm{d}x - L(t)C_r - n_s^t C_s\right)\kappa(t). \tag{35}$$

The standard deviation of travel demand for rail service $\sigma[\widetilde{q}(x,t)]$ is

$$\sigma[\widetilde{q}(x,t)] = \varphi(P(x,t))\exp\left(-\theta\left(\pi(x,t)+\varepsilon_q\right)\right), \tag{36}$$

and the standard deviation of budget social welfare can be calculated as follows:

$$\sigma[\mathrm{SW}] = 365\left(\sum_{t=1}^{m}\int_0^B CV_P\rho_{x_1,t_1}^{x_2,t_2}q(x,t)\left(f(x,t)+\frac{1}{\theta}-c\kappa(t)\right)\right)\mathrm{d}x. \tag{37}$$

3. Model Formulation and Properties

As stated above, the government or rail operator aims to maximise the social welfare budget of the candidate rail transit line by determining the optimum rail line length, rail station number, and project start time of the candidate rail transit line.

3.1. Model Formulation. In terms of equations (21), (22), and (37), the social welfare budget maximisation model is formulated as follows:

$$\max_{L(t),n_s^t,\widehat{t}} \phi(\mathrm{SW}) = 365\sum_{t=1}^{m}\left(\int_0^B q(x,t)\left(f(x,t)+\frac{1}{\theta\kappa(t)}-c\right)\left(1-\Phi^{-1}(\alpha)CV_P\rho_{x_1,t_1}^{x_2,t_2}\right)\mathrm{d}x - L(t)C_r - n_s^t C_s\right)\kappa(t), \tag{38}$$

where $\phi(\mathrm{SW})$ is the social welfare budget, $L(t)$ is rail line length, n_s^t is rail station number, and $\widehat{t}$ is the project start time of the candidate rail transit line.

3.2. Model Properties

Proposition 1. *For the budget social welfare maximisation problem (38), the social welfare budget $\phi(SW)$ is a decreasing function of the spatial and temporal correlation coefficient $\rho_{x_1,t_1}^{x_2,t_2}$.*

Proof. In terms of equation (38), it can be found that the variation of budget social welfare $\phi(SW)$ with respect to spatial and temporal correlation coefficient $\rho_{x_1,t_1}^{x_2,t_2}$ depends on the variation of $(1-\Phi^{-1}(\alpha)CV_P\rho_{x_1,t_1}^{x_2,t_2})$ with respect to $\rho_{x_1,t_1}^{x_2,t_2}$. It is easy to find that $(1-\Phi^{-1}(\alpha)\mathrm{CV}_P\rho_{x_1,t_1}^{x_2,t_2})$ is a decreasing function of $\rho_{x_1,t_1}^{x_2,t_2}$.

Proposition 2. *For the social welfare budget maximisation problem (38), at the equilibrium of equations (8)–(10), the optimal rail length $L(t)$, rail stations number n_s^t, and project start time $\widehat{t}$ can be obtained by the following equations:*

$$\begin{aligned}
L(t) &= \frac{\int_0^B q(x,t)\left(f(x,t)+(1/\theta\kappa(t))-c\right)\left(1-\Phi^{-1}(\alpha)\mathrm{CV}_P\rho_{x_1,t_1}^{x_2,t_2}\right)\mathrm{d}x}{C_r},\\
n_s^t &= \frac{\int_0^B q(x,t)\left(f(x,t)+(1/\theta\kappa(t))-c\right)\left(1-\Phi^{-1}(\alpha)CV_P\rho_{x_1,t_1}^{x_2,t_2}\right)dx}{C_s},\\
\widehat{t} &= \log_{1+k}\left|\frac{(C_r+C_s)(1+\kappa)}{1-\Phi^{-1}(\alpha)CV_P\rho_{x_1,t_1}^{x_2,t_2}} - \sum_{t=1}^{m}\int_0^B\left(\frac{1}{\theta}\frac{\partial q(x,t)}{\partial t}+q(x,t)\left(f(x,t)-c\right)\right)\mathrm{d}x\right| - \sum_{t=1}^{m}\log_{1+\kappa}\left|\int_0^B\left(\frac{\partial q(x,t)}{\partial t}\left(f(x,t)-c\right)\right)\mathrm{d}x\right|,
\end{aligned} \tag{39}$$

with

$$\frac{\partial q(x,t)}{\partial t} = P(x,t)f(x,t)(1+\kappa)\left(\frac{1}{\beta(I-\pi(x,t))}-\theta\right). \tag{40}$$

Proof. To obtain the optimal solution of the rail line length, the partial derivative of objective function equation (38) with respect to $L(t)$ was set to zero. Then,

$$\frac{\partial\phi(\mathrm{SW})}{\partial L(t)} = 365\sum_{t=1}^{m}\left(\int_0^B\frac{\partial q(x,t)}{\partial L(t)}\left(f(x,t)+\frac{1}{\theta\kappa(t)}-c\right)\left(1-\Phi^{-1}(\alpha)\mathrm{CV}_P\rho_{x_1,t_1}^{x_2,t_2}\right)\mathrm{d}x - C_r\right)\kappa(t) = 0, \tag{41}$$

where

$$\begin{aligned}
\frac{\partial q(x,t)}{\partial L(t)} &= \exp\left(-\theta\left(\pi(x,t)+\varepsilon_q\right)\right)\left(\frac{\partial P(x,t)}{\partial L(t)} - \theta P(x,t)\frac{\partial \pi(x,t)}{\partial L(t)}\right),\\
\frac{\partial P(x,t)}{\partial L(t)} &= \frac{\alpha r_0^t}{I^2\beta^2}\left(1-\frac{\pi(x,t)}{I}\right)^{(\alpha-\beta/\beta)} Y(x,t)\frac{\partial \pi(x,t)}{\partial L(t)},\\
\frac{\partial \pi(x,t)}{\partial L(t)} &= \mu_w \eta \frac{\partial h(x,t)}{\partial L(t)},\\
\frac{\partial h(x,t)}{\partial L(t)} &= \frac{2}{v(t)F(t)} > 0,
\end{aligned} \tag{42}$$

and, then, the optimal rail line length can be obtained as follows:

$$L(t) = \frac{\int_0^B q(x,t)\left(f(x,t)+(1/\theta\kappa(t))-c\right)\left(1-\Phi^{-1}(\alpha)\mathrm{CV}_P\rho_{x_1,t_1}^{x_2,t_2}\right)\mathrm{d}x}{C_r}. \tag{43}$$

Similarly, to obtain the optimal solution of the rail station number, the partial derivative of objective function equation (38) with respect to n_s^t was set to zero, namely,

$$\frac{\partial \phi(\mathrm{SW})}{\partial n_s^t} = 365\sum_{t=1}^{m}\left(\int_0^B \frac{\partial q(x,t)}{\partial n_s^t}\left(f(x,t)+\frac{1}{\theta\kappa(t)}-c\right)\left(1-\Phi^{-1}(\alpha)\mathrm{CV}_P\rho_{x_1,t_1}^{x_2,t_2}\right)\mathrm{d}x - C_s\right)\kappa(t) = 0, \tag{44}$$

and, then, the optimal rail station number can be obtained as follows:

$$n_s^t = \frac{\int_0^B q(x,t)\left(f(x,t)+(1/\theta\kappa(t))-c\right)\left(1-\Phi^{-1}(\alpha)\mathrm{CV}_P\rho_{x_1,t_1}^{x_2,t_2}\right)\mathrm{d}x}{C_s}. \tag{45}$$

To obtain the optimal solution of the project start time of the candidate rail transit line, the partial derivative of objective function equation (38) with respect to t was set to zero, namely,

$$\frac{\partial \phi(\mathrm{SW})}{\partial t} = 365\sum_{t=1}^{m}\left(\begin{array}{c}\int_0^B \frac{\partial q(x,t)}{\partial t}\left(f(x,t)\kappa(t)+\frac{1}{\theta}-c\kappa(t)\right)\left(1-\Phi^{-1}(\alpha)\mathrm{CV}_P\rho_{x_1,t_1}^{x_2,t_2}\right)+q(x,t)\left(f(x,t)-c\right)\left(1-\Phi^{-1}(\alpha)\mathrm{CV}_P\rho_{x_1,t_1}^{x_2,t_2}\right)\frac{\partial \kappa(t)}{\partial t}\mathrm{d}x\\ -C_r\frac{\partial \kappa(t)}{\partial t} - C_s\frac{\partial \kappa(t)}{\partial t}\end{array}\right) = 0, \tag{46}$$

where

$$\begin{aligned}
\frac{\partial q(x,t)}{\partial t} &= \exp\left(-\theta\left(\pi(x,t)+\varepsilon_q\right)\right)\left(\frac{\partial P(x,t)}{\partial t} - P(x,t)\frac{\partial \pi(x,t)}{\partial t}\right),\\
\frac{\partial P(x,t)}{\partial L(t)} &= -\frac{\alpha r_0^t}{I^2\beta^2}\left(1-\frac{\pi(x,t)}{I}\right)^{(\alpha-\beta/\beta)} Y(x,t)\frac{\partial \pi(x,t)}{\partial t},\\
\frac{\partial \pi(x,t)}{\partial t} &= f(x,t)\frac{\partial \kappa(t)}{\partial t},\\
\frac{\partial \kappa(t)}{\partial t} &= 1+\kappa,
\end{aligned} \tag{47}$$

and, then, the optimal project start time of the candidate rail transit line can be obtained as follows:

$$\widehat{t} = \log_{1+k}\left|\frac{(C_r+C_s)(1+\kappa)}{1-\Phi^{-1}(\alpha)CV_P\rho_{x_1,t_1}^{x_2,t_2}} - \sum_{t=1}^{m}\int_0^B\left(\frac{1}{\theta}\frac{\partial q(x,t)}{\partial t}+q(x,t)\left(f(x,t)-c\right)\right)\mathrm{d}x\right| - \sum_{t=1}^{m}\log_{1+\kappa}\left|\int_0^B\left(\frac{\partial q(x,t)}{\partial t}\left(f(x,t)-c\right)\right)\mathrm{d}x\right|, \tag{48}$$

with

$$\frac{\partial q(x,t)}{\partial t} = P(x,t) f(x,t)(1+\kappa)\left(\frac{1}{\beta(I-\pi(x,t))} - \theta\right). \tag{49}$$

4. Numerical Examples

To facilitate the presentation of the essential ideas and contributions of this study, two illustrative examples are given below.

4.1. Example 1. The input parameters are summarised in Table 1.

Figure 2 plots the contour of optimal social welfare budget in the space of spatial and temporal correlation coefficient (cc) with the objective of social welfare budget maximisation. It can be seen that, for a particular spatial cc, as temporal cc increases, the optimal social welfare budget of the candidate rail transit line decreases. For instance, for spatial cc 0, as temporal cc increases from −1 to 1, the optimal social welfare budget decreases from level of 1.071×10^{10} HK$ to 7.750×10^{9} HK$.

For a given total population, positive temporal cc means that the increase of population density in the first year leads to the increase of population density in the next year. As a result, households are distributed to limited residential locations and the total population has a centralised distribution.

In summary, as temporal cc increases, the total population has a more centralised distribution, and the social welfare budget of the candidate rail transit line decreases. More centralised population distribution can lead to a lower social welfare budget of the candidate rail transit line. Decentralised population distribution takes a high social welfare budget of the candidate rail transit line.

Similarly, for given temporal cc, as spatial cc increases, the optimal social welfare budget decreases. For instance, for temporal cc 0.8, as spatial cc increases from −1 to 1, the optimal social welfare budget decreases from 7.822×10^{9} HK$ to 7.526×10^{9} HK$.

Positive spatial cc implies the increase in population density in a residential location and leads to the increase of population density in another residential location. A type of cooperation relationship may exist between these two adjacent residential locations. For instance, the population growth in a new town can lead to an increase in population density in residential locations of the adjacent suburban city.

In summary, as spatial cc increases, the residential locations are more correlated with each other, and the optimal budget social welfare decreases. More correlated residential locations can lead to lower budget social welfare for the candidate rail transit line. Conversely, a competitive relationship between residential locations leads to the availability of a high budget social welfare for the candidate rail transit line.

It is also noted that the effects of temporal cc on the optimal social welfare budget are more significant than spatial. For instance, as temporal cc increases from −1 to 1, the optimal social welfare budget decreases from level of 1.071×10^{10} HK$ to 7.750×10^{9}. As spatial cc increases from −1 to 1 and temporal cc of 0.8, the optimal social welfare budget decreases from 7.822×10^{9} HK$ to 7.526×10^{9} HK$.

Compared with traditional studies assuming a spatial and temporal cc of 0, the optimal social welfare is overestimated in parts of (a) and (b) in Figure 2 and underestimated in parts of (c) and (d). For instance, in part of (b), the results in traditional studies are overestimated from 7.154×10^{9} HK$ to 9.137×10^{9} HK$ with spatial and temporal cc of 1. In part (c), the results in traditional studies are underestimated from 1.130×10^{10} HK$ to 9.137×10^{9} HK$ with spatial and temporal cc of −1.

Table 2 shows numerical results of optimal rail line length $L(t)$, optimal rail station number n_s^t, and optimal project start time of the candidate rail transit line in terms of the base year with respect to temporal correlation coefficient (cc) of −1 and 1 and spatial cc from −1 to 1. It can be seen that with temporal cc of -1 the optimal rail line length $L(t)$ in each year is longer than that of a temporal cc of 1. For instance, with temporal and spatial cc of −1, the optimal rail line length is 30.98 km in year 1, 17.49 km in year 2, and 9.59 km in year 3, while the optimal rail line length is 22.09 km in year 1, 14.36 km in year 2, and 9.21 in year 3 with temporal cc of 1 and spatial cc of −1. It implies that the optimal rail line length is longer with decentralised population distribution than that with centralised population distribution.

It can also be seen that the optimal rail line length $L(t)$ in each year decreases as spatial cc increases from −1 to 1. For instance, with temporal cc of −1 and spatial cc increasing from −1 to 1, the optimal rail line length in year 1 decreases from 30.98 km to 20.74 km. It implies that as cooperation between residential locations becomes strong and competition between residential locations becomes week, the optimal rail line length in year 1 decreases.

From Table 2, it can be found that the optimal project start time of the candidate rail transit line $\hat{t}$ is fast-tracked when temporal cc increases from −1 to 1. For instance, with temporal and spatial cc of −1, the optimal project start time of the candidate rail transit line is year 11.19 in terms of the base year, while the optimal project start time of the candidate rail transit line, with temporal cc of 1 and spatial cc of −1 is 8.60. It implies that the optimal project start time of the candidate rail transit line is earlier under centralised population distribution than that under decentralised population distribution.

4.2. Example 2. Figure 3 gives the housing unit prices map around MTR stations for Hong Kong in the first half-year of 2015. The housing unit prices, within the range of two hundred meters at each MTR station, are the transaction prices of representing housing estates. The representing housing estates are in residential locations, which have the largest transaction numbers of housing estates in the past six months. The housing unit prices are measured in HK$/

Table 1: Parameters.

Symbol	Definition	Value
c (HK)	Variable cost for rail service	3
C_r (HK/km)	Daily unit fixed maintenance cost of rail line	10^6
C_s (HK)	Daily fixed operation cost of each rail station	1.1×10^6
CV_P	Coefficient of variation of population density	0.3
f_0 (HK)	Fixed component of fare for using the rail service	4
f_r (HK/km)	Variable component of fare per unit distance	0.1
$F(0)$	Fleet size of trains in base year 0	5
I (HK)	Average daily household income	400
$L(0)$ (Km)	Initial value of rail length in year 0	20
m (Years)	The planning and operation time horizon	3
n_s^0	Initial value of rail station number in year 0	20
θ	Sensitivity parameter in travel demand function	0.02
P^0	Initial value of total population in year 0	100000
α/β	Parameters of households' utility function	0.2/0.8
r_0 (HK	Average daily housing rent in the CBD	300
t_t (Hour)	Average access time	400
$v(0)$ (Km/hour)	Average train speed in year 0	60
$Y(x, 0)$ (Unit)	Housing supply in year 0	(P^0/B)
κ	Interest rate	0.01
γ	Growth rate of the total population along the transportation corridor	0.1
δ (%)	Probability of gaining budget social welfare	95
ς (Hour)	Constant terminal time	5/60
η	Parameter of waiting time function	0.5
$(\mu_c/\mu_w/\mu_i)$	Parameters for travel cost function	80/100/60

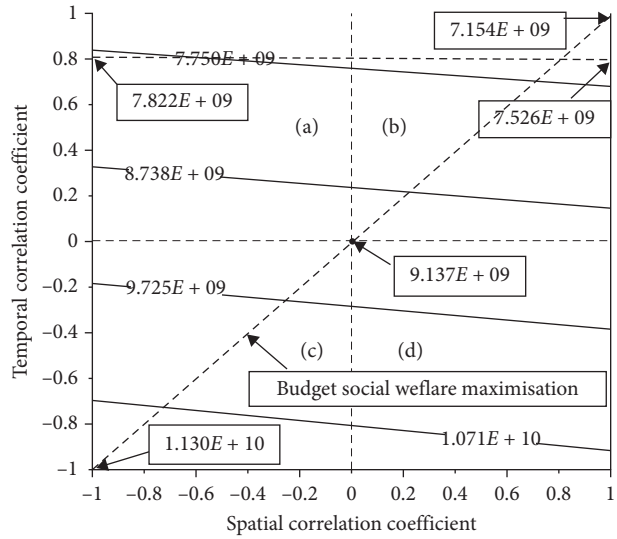

Figure 2: The effects of space-time correlation of population densities on social welfare budget.

square feet (Sqft). The data come from Centra data, linked by hk.centranet.com/eng/ehome.htm.

Table 3 gives the housing rent list of representing housing estates at each rail station of the West Island Line in first half-year of 2015. The housing rent price ratio is around 3% in Hong Kong at year 2015. This data comes from Chiefgroup of Hong Kong (www.chiefgroup.com.hk). The average flat size is 36.5 sqft, according to Housing Authority Annual Report 2014–2015 (www.housing.wa.gov.au/housingDocuments). The daily housing rents around rail stations of Western Island Line are calculated based on the housing prices, housing rent price ratio, the average flat size, and a constant parameter. For instance, in this example, daily housing rent = (36.5*7*housing price*3%)/(12*30), and 676.34 = (31864*3%*36.5*7)/(12*30).

Figure 4 shows the effects of space-time correlation of population densities on social welfare budget for the Western Island Line. It can be found that, with a given spatial correlation coefficient (cc) of population densities, as temporal cc increases from −1 to 1, the social welfare budget for the Western Island Line decreases. It also can be found that the effect of temporal cc of population densities is more

Table 2: Numerical results.

Temporal cc	Spatial cc	$L(t)$ (km)			n_s^t			$\hat{t}$
		$t = 1$	$t = 2$	$t = 3$	$t = 1$	$t = 2$	$t = 3$	
−1	−1	30.98	17.49	9.59	28	16	9	11.19
−1	−0.8	29.95	16.91	9.27	27	15	8	11.20
−1	−0.6	28.93	16.34	8.95	26	15	8	11.21
−1	−0.4	17.91	15.76	8.64	25	14	8	11.22
−1	−0.2	26.88	15.18	8.32	24	14	8	11.22
−1	0	15.86	14.60	8.00	24	13	7	11.23
−1	0.2	14.84	14.02	7.68	23	13	7	11.24
−1	0.4	13.81	13.45	7.37	22	12	7	11.25
−1	0.6	22.79	12.87	7.05	21	12	6	11.26
−1	0.8	22.77	12.29	6.73	20	11	6	11.27
−1	1	20.74	11.71	6.42	19	11	6	11.29
1	−1	22.09	14.36	9.21	20	13	8	8.60
1	−0.8	21.36	13.88	8.90	19	13	8	8.60
1	−0.6	20.63	13.41	8.60	19	12	8	8.61
1	−0.4	19.90	12.93	8.29	18	12	8	8.61
1	−0.2	19.17	12.46	7.99	17	11	7	8.62
1	0	18.44	11.99	7.68	17	11	7	8.62
1	0.2	17.71	11.51	7.38	16	10	7	8.63
1	0.4	16.98	11.04	7.08	15	10	6	8.64
1	0.6	16.25	10.56	6.77	15	10	6	8.65
1	0.8	15.52	10.09	6.47	14	9	6	8.66
1	1	14.79	9.61	6.16	13	9	6	8.67

Note: "cc" represents covariance coefficient. $L(t)$ represents optimal rail length in year t $t \in \{1, 2, 3\}$), n_s^t represents optimal rail station number in year t, and $\hat{t}$ represents the optimal project start time of the candidate rail transit line with respect to the base year.

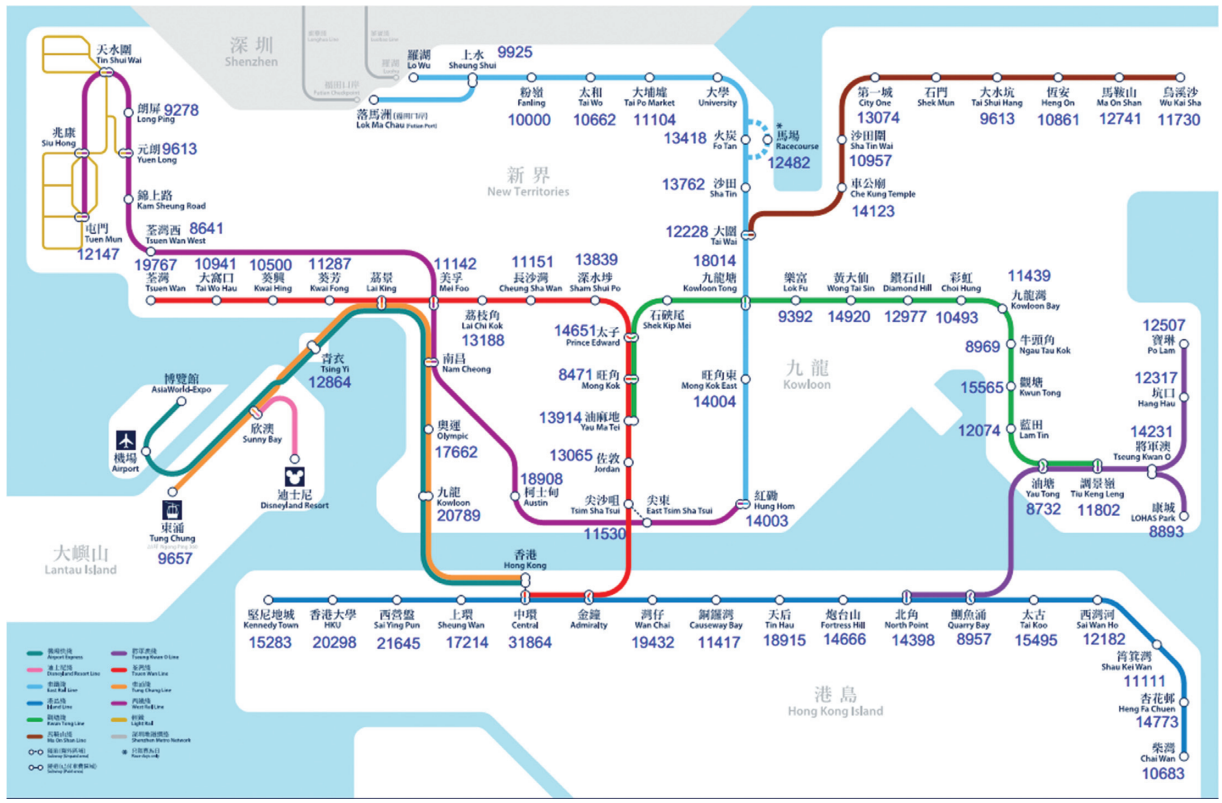

Figure 3: The housing unit prices map around MTR stations for Hong Kong in the first half-year of 2015.

Table 3: The housing rent list along the Western Island Line.

Station	Representing housing estates	Housing price (HK$/Sqft)	Daily housing rent (HK$)
(1) Central (CBD)	Winner Building	31864	676.34
(2) Sheung Wan	Hollywood Terrace	17214	366.52
(3) Sai Ying Pun	Island Grest	21645	460.88
(4) HKU	The Belcher's	20298	432.88
(5) Kennedy Town	Smithfield Terrace	15283	325.43

Note. The housing rent price ratio is around 3% in Hong Kong at year 2015. The housing rent price ratio is a measure of the relative affordability of renting and buying in a given housing market. It is calculated as the ratio of home prices to annual rental rates. This data comes from Chiefgroup of Hong Kong, linked by www.chiefgroup.com.hk_upload/pdf1_20140226170953_BJ_20131230.pdf. The average flat size is 36.5 sqft, according to Housing Authority Annual Report 2014–2015 (www.housing.wa.gov.au/housingDocuments). Daily housing rent = (36.5*7*housing price*3%)/(12*30). For instance, 676.34 = (31864*7*3%*36.5)/(12*30).

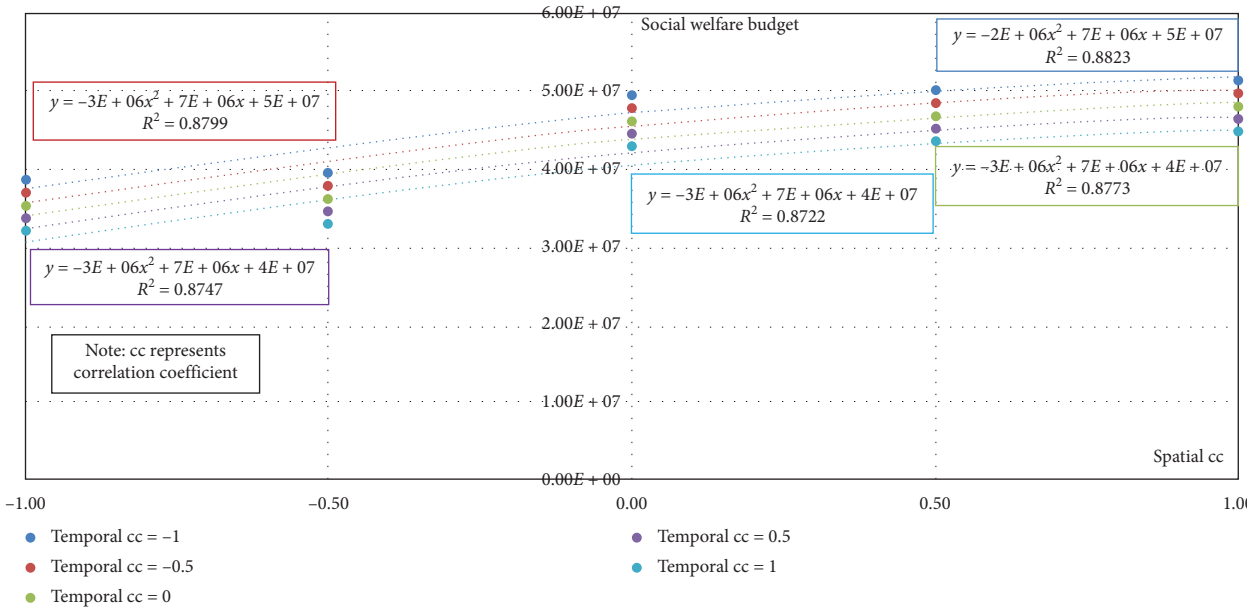

Figure 4: The effects of space-time correlation of population densities on social welfare budget for the Western Island Line.

significant than spatial cc of population densities on the social welfare budget. The results are in accord with the results of numerical example 1.

5. Conclusions

This paper proposes a closed-form model to investigate the effects of space-time correlation of population densities on the design of a candidate rail transit line over years. The traditional studies with an assumption of independence of irrelevant alternatives (IIA) population densities, namely, space-time correlation of population densities of 0, are special cases of the proposed model in this paper.

The proposed model offers several insights. For example, the decentralised population distribution takes the high social welfare budget of the candidate rail transit line. Competition between residential locations takes the high social welfare budget of the candidate rail transit line. The effects of the temporal correlation coefficient (cc) on the optimal social welfare budget are more significant than the spatial correlation coefficient. The optimal rail line length $L(t)$ in each year is longer compared to temporal cc of −1 with that with temporal cc of 1. The optimal project start time of the candidate rail transit line $\hat{t}$ is fast-tracked as temporal cc increases from −1 to 1.

The proposed model also offers some managerial implications. For instance, from Proposition 1, we know that the social welfare budget is a decreasing function of the spatial and temporal correlation coefficient. The rail transit line can strengthen the spatial and temporal correlation coefficient of population densities. The social welfare budget then can be eliminated by the construction of a candidate rail transit line. The optimal design value of a candidate rail transit line, namely, the optimal rail length, rail stations number, and project start time, can be determined explicitly by Proposition 2.

This paper provides a new avenue for the modelling and analysis of space-time correlation of population densities on the design of a candidate rail transit line over years.

In this paper, the population are assumed to be homogeneous with trips commuting only from residences to CBD. The proposed model can be extended to incorporate the effects of households' risk preference on early and late arrival to CBD on the design of a candidate rail transit line over years. [22].

The decision to extend a rail line involves consideration of technological, social, and economic factors. The prime reason could be social or in other words a desire to make life more convenient as regards manoeuvrability for a specific set of people, namely, those living in the vicinity of the line and new stations to be constructed. However, only pressing economic factor is considered in this paper. More detailed social factors can be taken into account in further studies, for instance, appreciation of land value along the rail line. [3].

Data Availability

The data used to support the findings of this study are available from the corresponding author upon request.

Conflicts of Interest

The authors declare that they have no conflicts of interest.

Acknowledgments

The work described in this paper was jointly supported by the National Natural Science Foundation of China (Grant no. 71473060), the Science and Technology Development Center, Ministry of Education of China (Grant no. 2018A01025), Humanities and Social Sciences Fund of the Ministry of Education (Grant no. 20YJCZH225), Shanghai "Science and Technology Innovation Action Plan" Soft Science Key Project (Grant no. 20692190900), and Shenzhen Philosophy and Social Sciences Planning Project of China (Grant no. SZ2019C004). The authors would like to thank Prof. W.H.K. Lam for his comments and suggestions and Mrs. Elaine Anson for her proofreading of this manuscript.

References

[1] T.-L. Liu, H.-J. Huang, H. Yang, and X. Zhang, "Continuum modeling of park-and-ride services in a linear monocentric city with deterministic mode choice," *Transportation Research Part B: Methodological*, vol. 43, no. 6, pp. 692–707, 2009.

[2] D. Liu, "Modelling the effects of spatial and temporal correlation of population densities in a rail transportation corridor," *European Journal of Transport & Infrastructure Research*, vol. 15, no. 2, pp. 243–123, 2015.

[3] K. Zhang, B. Xie, and D. Liu, "Implementation flexibility of multiperiod rail line design with consideration of uncertainties in population distribution," *Discrete Dynamics in Nature and Society*, vol. 2018, Article ID 5715304, 17 pages, 2018.

[4] C.-H. Wen and F. S. Koppelman, "The generalized nested logit model," *Transportation Research Part B: Methodological*, vol. 35, no. 7, pp. 627–641, 2001.

[5] G. Li and P. Rusmevichientong, "A greedy algorithm for the two-level nested logit model," *Operations Research Letters*, vol. 42, no. 5, pp. 319–324, 2014.

[6] B. Liu, Y. Zhang, and W. Du, "A simplified C-logit stochastic user equilibrium model on bimodal transportation network," *Mathematical Problems in Engineering*, vol. 2020, Article ID 3702965, 10 pages, 2020.

[7] W. Sun, H. Shao, L. Shen et al., "Bi-objective traffic count location model for mean and covariance of origin–destination estimation," *Expert Systems with Applications*, vol. 170, Article ID 114554, 2021.

[8] Y. Yang, Y. Fan, and J. O. Royset, "Estimating probability distributions of travel demand on a congested network," *Transportation Research Part B: Methodological*, vol. 122, pp. 265–286, 2019.

[9] Y. Yang, Y. Fan, and J. O. Royset, "Estimating probability distributions of travel demand on a congested network," *Transportation Research Part B: Methodological*, vol. 112, pp. 265–286, 2019.

[10] M. C. J. Bliemer, M. P. H. Raadsen, L. J. N. Brederode, M. G. H. Bell, L. J. J. Wismans, and M. J. Smith, "Genetics of traffic assignment models for strategic transport planning," *Transport Reviews*, vol. 37, no. 1, pp. 56–78, 2017.

[11] H. Shao, W. H. K. Lam, A. Sumalee, A. Chen, and M. L. Hazelton, "Estimation of mean and covariance of peak hour Origin-destination demands from day-to-day traffic counts," *Transportation Research Part B: Methodological*, vol. 68, pp. 52–75, 2014.

[12] H. Shao, W. H. K. Lam, A. Sumalee, and M. L. Hazelton, "Estimation of mean and covariance of stochastic multi-class OD demands from classified traffic counts," *Transportation Research Part C: Emerging Technologies*, vol. 59, no. 59, pp. 92–110, 2015.

[13] H.-S. J. Tsao, W. Wei, and A. Pratama, "Operational feasibility of one-dedicated-lane bus rapid transit/light rail systems," *Transportation Planning and Technology*, vol. 32, no. 3, pp. 239–260, 2009.

[14] H. K. Lo and W. Y. Szeto, "Time-dependent transport network design under cost-recovery," *Transportation Research Part B: Methodological*, vol. 43, no. 1, pp. 142–158, 2009.

[15] W. H. K. Lam, H. Shao, and A. Sumalee, "Modeling impacts of adverse weather conditions on a road network with uncertainties in demand and supply," *Transportation Research Part B: Methodological*, vol. 42, no. 10, pp. 890–910, 2008.

[16] Z. Qian and H. M. Zhang, "Modeling multi-modal morning commute in a one-to-one corridor network," *Transportation Research Part C*, vol. 19, no. 2, pp. 254–269, 2011.

[17] Z.-C. Li, W. H. K. Lam, S. C. Wong, and K. Choi, "Modeling the effects of integrated rail and property development on the design of rail line services in a linear monocentric city," *Transportation Research Part B: Methodological*, vol. 46, no. 6, pp. 710–728, 2012.

[18] Z.-C. Li, W. H. K. Lam, S. C. Wong, and A. Sumalee, "Environmentally sustainable toll design for congested road networks with uncertain demand," *International Journal of Sustainable Transportation*, vol. 6, no. 3, pp. 127–155, 2012.

[19] Y. Yin, S. M. Madanat, and X.-Y. Lu, "Robust improvement schemes for road networks under demand uncertainty," *European Journal of Operational Research*, vol. 198, no. 2, pp. 470–479, 2009.

[20] Z.-C. Li, W. H. K. Lam, S. C. Wong, and A. Sumalee, "Design of a rail transit line for profit maximization in a linear transportation corridor," *Transportation Research Part E: Logistics and Transportation Review*, vol. 48, no. 1, pp. 50–70, 2012.

[21] S. Guo, L. Yu, X. Chen, and Y. Zhang, "Modelling waiting time for passengers transferring from rail to buses," *Transportation Planning and Technology*, vol. 34, no. 8, pp. 795–809, 2011.

[22] D. Liu and W. H. K. Lam, "Modeling the effects of population density on prospect theory-based travel mode-choice equilibrium," *Journal of Intelligent Transportation Systems*, vol. 18, no. 4, pp. 379–392, 2014.

Hindawi
Discrete Dynamics in Nature and Society
Volume 2021, Article ID 6673555, 13 pages
https://doi.org/10.1155/2021/6673555

Research Article

Integrated Thermal Insulation Packing and Vehicle Routing for Perishable Products in Community Group Purchase

Wenbing Shui, Huimin Zhao, and Mengxia Li

Kunming University of Science and Technology, Kunming 650500, China

Correspondence should be addressed to Huimin Zhao; 20192206017@stu.kust.edu.cn

Received 19 November 2020; Revised 18 March 2021; Accepted 26 March 2021; Published 15 April 2021

Academic Editor: Tingsong Wang

Two transportation modes have been used to solve the "last kilometer" delivery problem of perishable products in China. One mode involves the use of refrigerated vehicles, and the other involves transportation with nonrefrigerated vehicles but with thermal insulation packaging and phase-change refrigerants. In this paper, we studied the distribution of fresh products using nonrefrigerated vehicles under the community group purchase model. A new integrated model that can simultaneously select insulation packaging methods and vehicle paths was developed. We designed a heuristic algorithm based on genetic algorithm to solve larger-scale problems. We found that nonrefrigerated vehicle delivery was better than refrigerated vehicle delivery when neither the cost of the phase-change refrigerant nor the cost of packaging accounts for more than 50% of the total cost. There was an optimal balance between insulation packaging cost and shipping cost. The combination of thin and light packaging materials and high-efficiency cold storage materials could achieve the goals of ensuring the quality of fresh products and reducing transportation costs simultaneously.

1. Introduction

As a new mode of social e-commerce, community group purchases are developing rapidly with the help of social software and other social traffic portals. Most users use community group purchase to buy perishable products such as vegetables and fruits. Temperature is the most important environmental factor affecting products' deterioration rate and postharvest life for these products, with higher temperatures providing an environment for bacterial growth and resulting in a shortened shelf life. To ensure the delivery quality and freshness of fresh agricultural products, ensuring complete cold chain transportation is key.

At present, two transportation modes are usually used to solve the "last kilometer" delivery problem. One mode involves the use of refrigerated vehicles to transport fresh agricultural products, and the other involves transportation with conventional nonrefrigerated vehicles but with thermal insulation packaging and phase-change refrigerants. There are high operating costs for the use of refrigerated vehicles. Besides, nonrefrigerated vehicles can cost less than refrigerated vehicles, and logistics companies have more choices in selecting different vehicle types. This allows greater flexibility in delivery, for example, the mixing of perishable products with other categories. Therefore, this transportation model is more appropriate than the refrigerated vehicle mode for filling the various and small product orders demanded by individual consumers.

Thermal insulation packaging plays an important role when we consider the nonrefrigerated vehicle transportation mode. The complex interaction between package selection and vehicle route optimization is reflected in the following two aspects. On the one hand, the phase transition temperature of the refrigerant determines the temperature boundary of product delivery in transit. The maximum allowable delivery temperature is codetermined by the initial quality, delivery time, and final quality requirement. Therefore, we focus on the quality of the phase-change refrigerant, which guarantees that the phase transition temperature is lower than the maximum allowable delivery temperature. On the other hand, the insulation packaging material determines the thermal resistance, which in turn

determines the insulation duration. At the same time, the insulation duration is also affected by vehicle routing. In summary, coordination between packaging selection and vehicle routing optimization is important.

Most published research on collaborative optimization has focused on common research topics such as the location-routing problem (LRP), production routing problem (PRP), production-distribution problem (PDP), and inventory routing problem (IRP). However, studies in this field on joint optimization of packaging systems and vehicle route planning are lacking because many package-dependent costs are frequently overlooked in logistics activities.

Compared with the existing works, our main contributions of this study are summarized as follows. This work studied the distribution of fresh agricultural products from a new perspective. It integrated the multitype thermal insulation packaging selection problem of nonrefrigerated vehicles into the vehicle routing problem (VRP). Another main contribution was that this paper designed a heuristic algorithm that can quickly solve large-scale problems. On the basis of the above research, this paper analyzed the benefits of this nonrefrigerated vehicle mode but with thermal insulation packaging and phase-change refrigerants. We aimed to reduce the logistics cost while guaranteeing the delivery quality of fresh food. This paper provides a theoretical basis for the incorporation of multiple packaging selection into the VRP.

The remainder of this paper is organized as follows: Section 2 introduces the related research review. Section 3 introduces the descriptions and assumptions of the problem and establishes relevant models and design algorithms. Section 4 presents some examples to verify the model and algorithm. Meanwhile, we analyze the interaction effect among the main parameters. Finally, we summarize the major conclusions of our study and provide several suggestions for further research.

2. Related Works

In this section, we introduce previous research on community group purchases, thermal insulation packaging, and distribution of perishable products.

2.1. Literature about Community Group Purchases. Community group purchases are a new business model, and research on them is scarce. Proper pricing mechanisms are conducive to higher profits under community group purchase models. Li et al. [1] developed two-stage pricing mechanisms to evaluate the impact of competition and waiting costs on the profitability and efficiency of community-based group purchases.

The intention to participate in community group purchases has received some attention among researchers, particularly in recent years. Li et al. [2] constructed a theoretical model and questionnaire on community group purchase consumer participation behavior based on the theory of stimulus-organism-response (SOR) and commitment trust theory.

In addition, some researchers have addressed the distribution of perishable products in the context of CGPs. Liu et al. [3] proposed a balanced scorecard to construct an index system to evaluate and select suitable distribution modes based on the analysis of community group purchase distribution of fresh agricultural products. Wang and Qiu [4] improved the VRP model by incorporating the minimum total cost, including fixed costs, transportation costs, and penalty costs, under the constraint function of the distribution time window for community group purchases. They concluded that the suggested approach is computationally very efficient and provides a reference for decision-making in fresh community group purchase enterprises.

2.2. Literature about Thermal Insulation Packaging and Phase-Change Refrigerants. Thermal insulation packaging is critical to maintaining low temperatures for the perishable products. Lee and Yoo [5] discovered that the higher the thermal insulation capacity of packaging was, the longer the changes in the physical properties of frozen cooked rice were delayed. Fang et al. [6] also indicated that the thermal insulation effect was influenced by packaging material. Li et al. [7] presented that different choices between more expensive and less expensive packaging lead to different sales, cost, and waste levels, and these different choices require different inventory control policies.

Simultaneously, the use of refrigerants during transportation by nonrefrigerated vehicles is another important research topic. Oró et al. [8] found that frozen product temperatures remained at lower values much longer when phase-change materials were employed. Singh [9] presented that the temperature control for perishable products during shipping can be improved with the use of phase-change materials. These studies can provide a theoretical basis for the transport of perishable products with nonrefrigerated vehicles.

2.3. Literature about Perishable Product Distribution. Perishable products require complete cold chain transportation for the best retention of product value and appearance. At present, most research covers refrigerated modes of perishable food product delivery. Amorim and Almada-Lobo [10] proposed a model that decouples minimization of distribution costs from maximization of the freshness state of the delivered products. Hsu et al. [11] considered the randomness of the perishable food delivery process with time windows to obtain optimal delivery routes, loads, fleet dispatching, and departure times for the delivery of perishable food products. Rabbani et al. [12] established a VRP model that considered minimization of transportation costs and a minimum freshness level to improve profit in the context of different numbers of depots. They considered different scenarios and described the routing problem based on the traditional transportation method.

However, this area of study lacks research on the use of nonrefrigerated vehicles for transportation of fresh products. Many enterprises have started to use nonrefrigerated

vehicles to transport fresh products because they allow greater flexibility in delivery. Byung and Young [13] presented a VRP that encompasses both refrigerated and general vehicles for multicommodity perishable food product delivery. This aim was to confirm the performance and availability of the refrigerated transport mode for perishable food product delivery in comparison with the general mode. However, the paper focused on specific vehicle routing, and packaging was not considered. Dieckmann et al. [14] designed new thermal insulation packaging materials made from feathers for nonrefrigerated vehicle transport. They concluded that feather materials have the potential to replace the materials currently used for delivery of perishable food products.

To the best of the authors' knowledge, Li et al. [15] offered the only study analyzing multiple types of packaging in the perishable food PRP. They pointed out that different packaging selections lead to different product shelf lives and influence the selling price. However, they used a pattern that is not applicable to community group purchases, while considering the complex relationships among quality of phase-change refrigerants, the types of packaging, and vehicle routing.

The current paper provides a new research perspective compared with the work of Shui and Li [16], which are the most recent literature relevant to the topic of our interest. The paper by Shui and Li [16] constructed a pricing model for community group purchase and a distribution cost-optimal model based on refrigerated vehicles. Meanwhile, they proposed a collaborative optimization mechanism of the pricing model and distribution model based on bilevel programming theory. Refrigeration cost, fuel cost, and fixed cost were taken into consideration in the refrigerated vehicle distribution model, while in this paper, we propose a nonrefrigerated vehicle distribution model based on the VRP problem, considering the choice of insulation packaging mode. In this model, the costs include fixed cost, fuel, packaging material, and coolant cost. In terms of algorithms, we extend initial work by designing a heuristic algorithm based on a genetic algorithm to obtain the optimal solution and solve by MATLAB, while the model in the other paper is solved by the exact algorithm and tested by LINGO. In terms of conclusion, Shui and Li [16] found that collaborative optimization mechanism of pricing and distribution can improve the profit level of community group purchase, while we found the specific conditions when nonrefrigerated vehicle distribution cost is lower than refrigerated vehicles.

In this study, we focus on multitype packaging selection in the context of transport of perishable produce in nonrefrigerated vehicles. To address the freshness issue, we consider the maintenance of low temperatures with thermal insulation packaging and phase-change refrigerants. Because community group purchases can aggregate customer demand, we assume that the delivery service at each point uses only one type of integrated packaging and establish a profit maximization model. In other contexts, the use of such a model may lead to packaging cost larger than distribution cost.

3. Materials and Methods

3.1. Problem Description and Assumption. Reducing logistics costs and optimizing distribution networks are essential for community group purchase enterprises, and perishable product quality continuously changes after the production stage. Thermal insulation packaging and phase-change refrigerants are needed to maintain a certain temperature when conventional nonrefrigerated vehicles are used to deliver perishable food products. The choice of packaging type and refrigerant quality influence the delivery quality of perishable food products, which is related to customer satisfaction. Therefore, insulation package selection is directly related to the profit level of community group purchase enterprises. The problem that we focus on is that when community group purchase enterprises receive orders, the distribution center begins to choose the appropriate package for each demand point to meet the insulation requirement based on different arrival times for each conventional nonrefrigerated vehicle. Each vehicle services the demand points in turn and delivers the perishable products to the head of the community group.

The integration of multipackage selection into the VRP is defined on a complete digraph $G = \{N, A\}$. The set N of nodes is comprised of the subset $N = \{i | i = 0, 1, 2, \ldots, L\}$, which indicates that there are L demand nodes and one distribution center "0." Let $A = (i, j)$ denote the set of arcs that link all nodes from i to j. In this paper, we establish the following assumptions:

(1) There is only one distribution center with different types of conventional nonrefrigerated vehicles.

(2) Because different types of fresh agricultural products have different distribution requirements, this paper considers only distribution of a single product.

(3) The location coordinates of the distribution center and the demand nodes are known.

(4) Each order quantity of each demand node is known, and each node can be visited once by one vehicle.

(5) There is no time limit on the service time of each demand point.

(6) Only one packaging type can be chosen for each demand point.

(7) The remaining perishable products must be sent to the head of the community group before phase change occurs in the refrigerant.

3.2. Objective Function and Constraints. We propose a mathematical model integrating package selection into the VRP, whereby a fresh community group purchase enterprise chooses the type of thermal insulation packaging as well as the optimal vehicle route to deliver the products to the demand points. We first derive formulations (6) and (9) before establishing the model.

Formula (6) derivation process is as follows.

Fourier [17] discovered that there is a linear relationship between the amount of thermal conductivity λ, the area of

thermal conductivity A, the temperature difference between the two sides of the wall ΔT, and the thickness of the wall δ.

$$Q = \lambda A \frac{\Delta T}{\delta}. \tag{1}$$

In equation (1), λ is the heat conductivity coefficient of the material, which reflects the strength of the material's thermal conductivity; the greater the coefficient of thermal conductivity is, the better the thermal conductivity of the material is. At the same time, the different thermal resistances R correspond to different conductivities λ for multiple types of packaging. The relationship between the two is shown as follows:

$$R = \frac{\delta}{\lambda}. \tag{2}$$

The temperature of the latent heat accumulator changes little in the process of phase change, so the temperature in the incubator can be regarded as approximately constant. According to equations (1) and (2), we can obtain equation (3), which is the heat transfer from the thermal insulation packaging b in transit:

$$Q = \frac{3600 t_i \left(T_s - T_b^0\right)}{R}, \quad \forall i \in N, b \in B. \tag{3}$$

In equation (3), T_S is the environmental temperature, T_b^0 is the temperature of insulation packaging b before the complete phase change of the refrigerant accumulator, and t_i is the time when the delivery service arrives at point i. It is calculated by equation (4):

$$t_j = \sum_{k=1}^{V} \sum_{i=0}^{L} \left(t_i^k + \frac{d_{ij}}{v_{ij}} + \frac{q_i}{v_0} \right) y_{ij}^k, \quad j \geq 1. \tag{4}$$

In equation (4), t_i^k is the time when vehicle k arrives at customer node i, and t_0^k denotes that vehicle k departs from the distribution center. Here, d_{ij} is the distance between customer node i and customer node j. v_{ij} is the average speed from customer node i to customer node j. v_0 denotes the loading and unloading speed at customer node i. q_i is the demand at node i.

$$Q = 1000\,\text{ml}. \tag{5}$$

Equation (5) denotes the amount of heat absorbed by a refrigerant during phase change, m is the quality of the refrigerant, and l is the phase-change latent heat of the refrigerant. We can derive equation (6) when equation (3) is equal to equation (5).

$$Q_i^b = \frac{3600\left(T_s - T_b^0\right) t_i A_i^b}{1000 L_b R_b}, \quad t_i = t_j, \forall i \in N, b \in B. \tag{6}$$

Equation (6) represents the quality of refrigerant Q_i^b by the refrigerant accumulator during a phase change to maintain a low temperature during transit to customer node i with packaging type b, L_b is the phase-change latent heat of the refrigerant with packaging type b, and R_b is the thermal resistances with packaging type b, while A_i^b denotes the total package area of package b at customer node i, and it is calculated by equation (7).

$$A_i^b = q_i \beta_b, \quad \forall i \in N, b \in B. \tag{7}$$

In equation (7), β_b is the area of category q_i packaging covered by product per unit volume.

Formula (9) derivation process is as follows.

Arrhenius [18] proposed the Arrhenius equation (8), which reflects the changes in the relationship between the chemical reaction rate constant and temperature.

$$K = A \cdot e^{(-Ea/rT)}, \tag{8}$$

$$M_k = M_0 - Kt. \tag{9}$$

In equation (8), A refers to the prefactor or rate constant. Here, Ea denotes activation energy. r represents the gas constant. T denotes the thermodynamic temperature. Equation (9) represents that the initial quality M_0 varies linearly with time t. Combining formulas (8) and (9), we can deduce formula (10) to ensure the maximum temperature limits T_i of fresh agricultural delivery quality.

$$T_i = \frac{E_a}{R \ln\left(At_i/\left(M_0 - M_k\right)\right)} - 273.15, \quad \forall i \in N, i \geq 1. \tag{10}$$

On the above basis, the model is as follows:

$$\text{Max}\, p \sum_{i=1}^{L} q_i z_i - \sum_{k=1}^{V} \sum_{i=0}^{L} \sum_{j=1}^{L} c_{ij}^k y_{ij}^k - \sum_{b=1}^{BN} s_b - \sum_{k=1}^{V} f_k O_k. \tag{11}$$

Formula (11) is the objective function, which aims to maximize profit, considering the total cost including transportation costs, the fixed cost of dispatching vehicles, and thermal insulation packaging and phase-change refrigerant costs. p is the given price of a single product. The binary variable Z_i is equal to 1 when community node i is delivered, and binary variable y_{ij}^k is equal to 1 when vehicle k visits node j immediately after node i. Binary variable O_k is equal to 1 when vehicle k is used. s_b represents the total packaging and refrigerant costs, which is calculated by equation (12). c_{ij}^k denotes the fuel cost of transportation from i to j by vehicle k, and it is calculated by equation (13). f_k denotes the fixed cost of vehicle k.

$$s_b = c_b^1 + c_b^2, \quad b \in B, \tag{12}$$

$$c_{ij}^k = a_0^k \times \left(b_0^k + c_0^k . w_i^k\right) d_{ij} f, \quad \forall i, j \in N, j \neq 0, k \in K. \tag{13}$$

In equation (12), let c_b^1 denote the packaging cost of using package b, which is the relative packing area and is calculated by equation (14). c_b^2 denotes the refrigerant costs of using package b, which is relative to the quality of the refrigerant and is calculated by equation (15). In equation (13), c_{ij}^k is relative to w_i^k, which is the weight of vehicle k leaving customer i, and w_i^k is shown in equation (16), where a_0^k, b_0^k,

and c_0^k are conversion parameters for vehicle k and f represents the unit fuel rate.

$$c_b^1 = \sum_{i=1}^{L} q_i \beta_b z_i U_i^b g_b, \quad \forall i \in N, b \in B. \tag{14}$$

In equation (14), β_b denotes the conversion parameter between the area of b and unit product quality. The binary variable U_i^b is equal to 1 if packaging type b is used in customer node i. g_b denotes the per unit area cost of packaging type b.

$$c_b^2 = \sum_{i=1}^{L} Q_i^b U_i^b h_b, \quad \forall i \in N, b \in B. \tag{15}$$

In equation (15), h_b denotes the unit cost of the refrigerant.

$$w_i^k = w_k + \sum_{i=1}^{L} q_i x_i^k = w_k + \sum_{i=1}^{L} \sum_{j=1}^{L} q_i y_{ij}^k, \quad \forall k \in K. \tag{16}$$

In equation (16), w_k denotes the weight of vehicle k, and binary variable x_i^k is equal to 1 when vehicle k visits customer node i.

Constraints (17) to (21) are used to represent the routing flow. Constraint (17) ensures that there is only one delivery service for each demand node. Constraint (18) indicates that each route starts and ends at the same demand node. Constraints (19) to (20) are used to ensure that if a vehicle is used, it must depart from and end up at the depot. Constraint (21) is designed to eliminate the subloop. Constraint (22) ensures that no route has total community demand exceeding the capacity of vehicle k. Constraint (23) is used to represent the relationship between x_{ij} and y_i^k. Constraint (24) aims to ensure that only one type of packaging can be selected for each demand node. Constraint (25) represents the relationship between Q_i^b and U_i^b that ensure that the value of quality of refrigerant is reasonable. Constraint (26) provides the maximum boundary of the product temperature when the delivery service arrives at demand node i. Constraint (27) aims to ensure that the temperature of the thermal insulation cannot exceed the temperature limits for delivery.

$$z_i - \sum_{k=1}^{V} x_i^k = 0, \quad \forall i \in N, i \geq 1, \tag{17}$$

$$\sum_{i=0}^{L} y_{ip}^k - \sum_{j=0}^{L} y_{pj}^k = 0, \quad \forall k \in K, p \in N, y_{ij}^k = 0, \forall i, j \in N, i = j, k \in K, \tag{18}$$

$$O_k - \sum_{p=1}^{L} y_{0p}^k = 0, \quad \forall k \in K, \tag{19}$$

$$O_k - \sum_{p=1}^{L} y_{p0}^k = 0, \quad \forall k \in K, \tag{20}$$

$$u_i - u_j + L y_{ij}^k \leq L - 1, \quad u_i, u_j \geq 0, i, j \in N, i \neq j, j \geq 2, \tag{21}$$

$$\sum_{i=1}^{L} \sum_{j=1}^{L} q_i y_{ij}^k \leq G_k O_k, \quad \forall k \in K, \tag{22}$$

$$\sum_{i=1}^{L} q_i x_i^k = \sum_{i=0}^{L} \sum_{j=1}^{L} q_j y_{ij}^k, \quad \forall k \in K, \tag{23}$$

$$\sum_{b=1}^{BN} U_i^b = Z_i, \quad \forall i \in N, i \geq 1, \tag{24}$$

$$Q_i^b \leq \text{Big} \cdot U_i^b, \quad \forall i \in N, i \geq 1, b \in B, \tag{25}$$

$$T_i = \frac{E_a}{R \ln\left(A t_i / \left(M_0 - M_k\right)\right)} - 273.15, \quad \forall i \in N, i \geq 1, \tag{26}$$

$$T_i \geq T_b^0 Z_i, \quad i \in N, i \geq 1, b \in B. \tag{27}$$

3.3. Algorithm Design. The VRP problem has been proven to be an NP-hard problem, with many constraints and a complex objective function. There are two common methods for solving this problem: heuristic methods and exact procedures. Exact procedures always have a limited range of applications in practice, so heuristic algorithms are most often used to solve routing problems. In the heuristic algorithm, the best-known result for VRPs has been obtained using Tabu search or simulated annealing. Genetic algorithms (GAs) have seen widespread application to various combinatorial optimization problems, such as certain types of VRPs. The heuristic algorithm base on GA is adopted in this paper because this paper considers the choice of packaging mode in traditional VRP.

The distribution schedule in our problem has to satisfy both the temperature constraints and load-capacity constraints for vehicles arriving at the demand nodes. However, it is difficult to construct a method of solving the above two constraints simultaneously. In this paper, we use a heuristic algorithm based on the genetic algorithm to obtain the solution to this problem. First, we use the natural numbers for encoding. For each of these chromosomes, we can calculate the corresponding delivery time and temperature requirement, and through decoding, we can obtain the vehicle selection. Furthermore, we choose different packaging types under the constraints of fresh product delivery time, initial quality, and requirements. Based on the packaging selected as above, we can calculate the quality of the refrigerant and the refrigerant and packaging costs. Finally, in these populations, we choose the individuals with the lowest cost—including fixed cost, packaging cost, and transportation cost—to carry out crossover, mutation, and selection until the optimal solution is found. The specific flowchart is shown in Figure 1.

The detailed contents of the heuristic algorithm base on GA are as follows.

3.3.1. Chromosome Structure. The solution to our problem includes vehicle route planning, vehicle type selection, and packaging selection. Therefore, we use natural numbers to encode the decision variables in the model, which represents the service order of demand nodes. The vehicle starts from the depot and provides delivery service for demand nodes when the total weight of the perishable goods at these distribution points is within the capacity limit of the vehicle. If this weight exceeds the capacity limit of the vehicle, the vehicle returns to the depot, and the next vehicle starts to distribute from point j until all demand points are serviced. To derive the highest profit in this process, we choose to forgo provision of delivery services when the distribution cost is higher than the cost of abandoning the delivery. This option is coded as "0." To express the relationship between route and vehicle choice, we use the structure of the chromosome shown in Figure 2 and the chromosome shown in Figure 2(b). Figure 2(a) shows the delivery schedule.

3.3.2. Initial Population Generation. Choosing an appropriate population size helps obtain the optimal calculation speed and most accurate solution. Therefore, this paper uses random rules to generate a set of initial populations with a size of 50.

3.3.3. Fitness Function. The fitness function is a standard for measuring individuals in the population. In this model, those individuals that satisfy the constraints and the objective function are retained, and others are eliminated. The goal of this paper is to maximize the profit of community group purchase enterprises. To help solve this problem, this paper uses the negative value of the objective function as the fitness function. Therefore, the fitness function of this paper is as follows:

$$f_1' = -\text{maxobjective function}. \tag{28}$$

3.3.4. Crossover. Crossover plays an important role in GA. The principle of the crossover operator is to simulate the process of chromosome repair and gene recombination in biological genetic evolution. It enables the algorithm to obtain a larger gene space, as is shown in Figure 2. We randomly select the gene values of 3 genes in parent 1 and copy them to the same gene of the offspring. Then, the genes in parent 2 with the same gene value as the selected gene from parent 1 are removed. Finally, the formation offspring are obtained by combining parent 1 and parent 2 (see Figure 3).

3.3.5. Mutation. To obtain a global solution, we destroy part of the route so that the individuals in the new group have diversity. We randomly select genes on two loci from the parent and then swap the genes on these two loci to obtain the offspring (see Figure 4).

4. Results and Discussion

In this section, this paper assumes that a strawberry planting enterprise in Kunming sells on a community group purchase website. At the same time, the community group purchase enterprise provides delivery services for communities. To investigate the relationship between these objectives, we carry out numerical experiments on randomly generated instances to evaluate the performance of the established model. All experiments are conducted on a computer with an Intel Core i5 2.5 GHz processor and 8 GB of memory.

In the first part, we first detail the parameter settings and base instance generation by taking reality into account. Then, accurate algorithm by LINGO and heuristic algorithm based on GA by MATLAB are used to solve these generated instances and compare running times in the next part. In part three, we compare two modes of transportation: refrigerated vehicles and nonrefrigerated vehicles. Parts four and five are devoted to examining the impact of packaging parameters on the overarching goal and exploring how to further reduce distribution costs.

4.1. Parameter Settings and Base Instance Generation

4.1.1. Vehicle-Related Parameter Setting. In the practical application at hand, the vehicle type is often different for refrigerated vehicles and nonrefrigerated vehicles. This leads to different load and dead-weight values for the vehicle and different coefficients of calculating fuel costs. The relevant parameter settings are shown in Tables 1 and 2. The same parameters independent of vehicle type are set as follows: $T_s = 22$, $V_0 = 600$, $f = 0.7$, and $p = 60$.

4.1.2. Package-Related Parameter Setting. At present, the thermal insulation packages used in the market are mostly divided into four different types: cartons, foam cartons, combined carton-and-foam packaging, and composite cartons. Generally, cartons are the cheapest and have the lowest insulation effect, and the combined carton-and-foam packaging type is expensive but has the best insulation effect. The packaging types b are set to $\{1, 2, 3, 4\}$. The value of the unit packaging cost g_b, the packaging thermal resistance R_b, and the temperature inside the packaging T_b^0 correspond to the packaging type b. Table 3 presents the detailed parameter generation for the packaging.

4.1.3. Base Instance Generation. A base instance is generated based on an investigation of a real enterprise setup. It includes a distribution center, 6 distribution points, and 3 different types of nonrefrigerated vehicles to meet different distribution requirements. We can obtain a great deal of information from the Internet. This information includes the location of the community, which can calculate the distance d_{ij} from node i to node j. The vehicle speed v_{ij} is randomly generated from $U[30, 80]$.

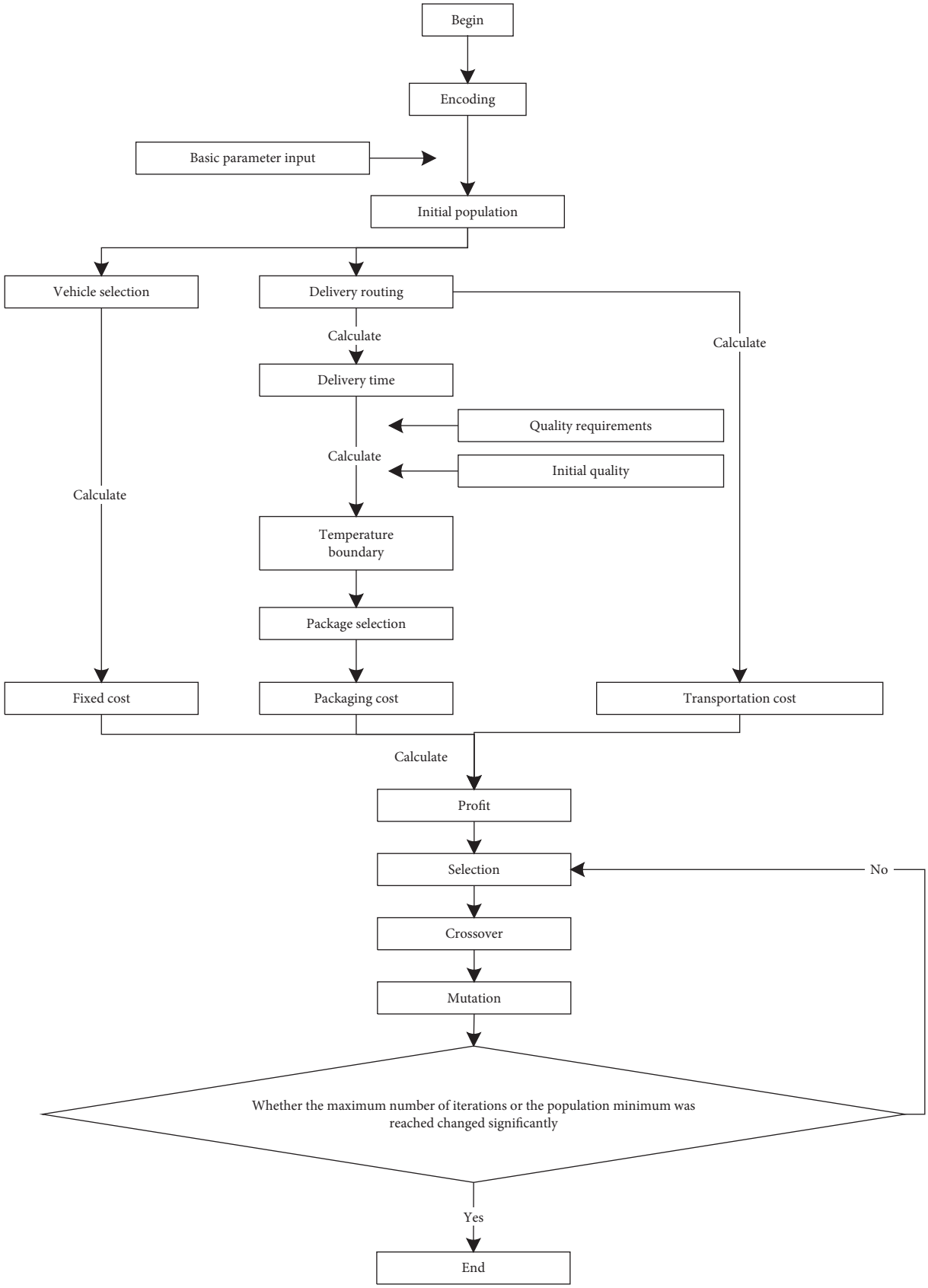

Figure 1: Flowchart of the heuristic algorithm based on the genetic algorithm.

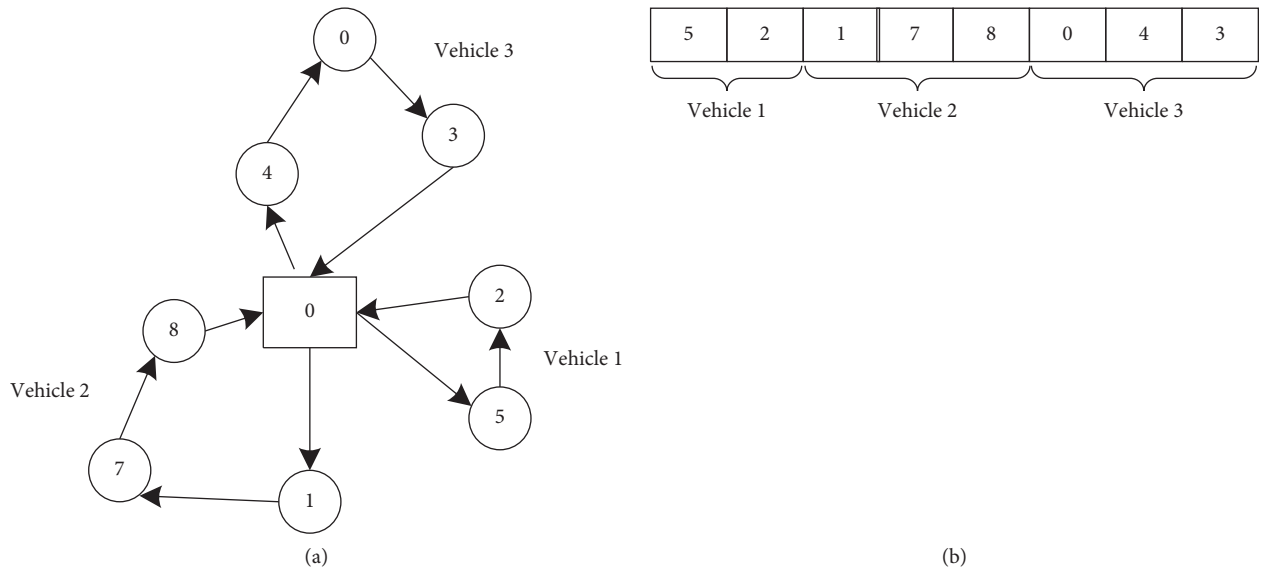

Figure 2: Delivery schedule and chromosome structure. (a) Delivery schedule. (b) Chromosome structure.

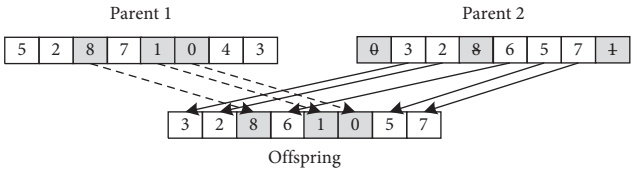

Figure 3: Map of crossover operator.

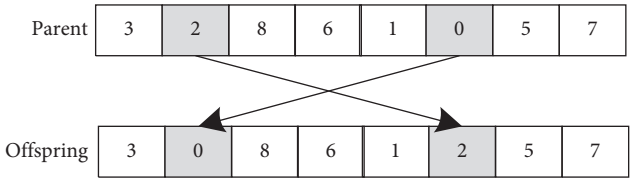

Figure 4: Map of mutation operator.

Table 1: Parameter setting for nonrefrigerated vehicles.

Parameter	Value		
k	1	2	3
f	218	258	458
G	1690	1615	4185
a_0	1.177	1.177	1.177
b_0	0.069	0.069	0.110
c_0	0.001	0.001	0.000
w	2250	2535	3825

4.2. Contrast Analysis between Accurate Algorithm and Heuristic Algorithm Based on GA. To show the effect of different algorithm on the model operation, we generally use LINGO to program the exact algorithm and use MATLAB to program the heuristic algorithm based on GA. We increase the distribution points from 6 to 10 and generate five data sets to compare the running times of the accurate algorithm and heuristic algorithm based on GA. These comparison results from accurate algorithm and heuristic algorithm based on GA appear in Table 4.

Table 2: Parameter setting for refrigerated vehicles.

Parameter	Value		
k	1	2	3
f	268	368	468
G	1485	3500	4380
a_0	0.012	1.369	1.749
b_0	0.061	0.061	0.061
c_0	0.014	0.014	0.014
w	2680	4580	4950

Table 3: Parameter settings for different types of packages.

Parameter	Value			
b	1	2	3	4
T_b^0	6.5	4.5	4	4.5
R_b	0.163	0.259	4.463	0.257
β_b	0.278	0.278	0.278	0.278
h_b	0.75	0.75	0.75	0.75
g_b	2.25	3.38	11.27	7.61
L_b	335	335	335	335

Table 4 shows that there is a significant difference in running time between accurate algorithm and heuristic algorithm based on GA in the calculation of these instances. Due to the NP-hard nature of our model, the solution run time for accurate algorithm by LINGO has an exponential pattern; therefore, accurate algorithm becomes unable to solve the model when there are more than 9 distribution points. In contrast, the running time in MATLAB is less than 2 seconds in the above instance because the problem can be combined with heuristic algorithm based on GA, which provides

Table 4: Parameter settings of different types of packages.

Data Number of distribution points	Accurate algorithm Time (s)	Heuristic algorithm based on GA Time (s)
6	823	0.126
7	1603	0.132
8	10825	1.286
9	86400+	0.525
10	86400+	1.043

convenience in the use of intelligent optimization algorithms. This indicates that it is possible to solve the problem with a large number of distribution points with the heuristic algorithm based on GA by MATLAB software; the results for the case with 10 distribution points are shown in Table 5.

Table 5 aggregates the results of the total profit and delivery route and the choice of packaging type. It can be seen that the final total profit is 38343. Vehicle 2 is chosen to provide delivery services for 10 community demand nodes. The route of the vehicle is 2-9-10-7-4-5-6-1-3-8, and the products delivered to all demand points are packed in cartons.

4.3. Contrast Analysis between Refrigerated and Nonrefrigerated Vehicles. To determine under what circumstances nonrefrigerated thermal insulation packaging is superior to refrigerated vehicles in terms of transporting fresh agricultural products, we set up two cases for the two types of vehicles. For refrigerated vehicles, we can obtain the calculation model for transporting fresh products in refrigerated vehicles from Shui and Li. In practical applications involving nonrefrigerated vehicles, we implicitly assume that the unit packaging cost and refrigerant costs are dependent on the purchase quantity and the manufacturer. We vary the cost of unit packaging and refrigerant in the case of nonrefrigerated packaging. We set up the following cases: Case 1 is identical to the base case with the only difference being that the unit packaging cost increases by 5%, and Case 2 is identical to the base case with the only difference that the unit packaging cost increases by 10%. Case 3 is identical to the base case with the only difference that the unit refrigerant cost increases by 5%. Case 4 is identical to the base case with the only difference that the unit refrigerant cost increases by 10%. The calculated results are shown in Table 6, and the contrast is shown in Figure 5.

We can observe from Figure 5 that the total profits are higher in Case 4, Case 1, and the base case than in Case 5. Nonrefrigerated thermal insulation packaging is superior to refrigerated vehicles under normal circumstances. Simultaneously, the opposite occurs when the unit packaging cost or refrigerant cost is relatively high in small-scale instances. To further investigate the relationship between these costs, we present Figure 6, which shows the percentage of the total cost of using an unrefrigerated vehicle according to Table 6. It clearly reflects which costs are predominant in the total cost.

We notice in Figure 6 that in Cases 1 and 3 and the base case, the cost of using nonrefrigerated vehicles is lower than that of using refrigerated vehicles. Neither the cost of the phase-change refrigerant nor the cost of packaging accounts for more than 50% of the total cost in these cases. A trade-off exists between the packaging cost and the refrigerant cost in the total cost. This consideration could make nonrefrigerated thermal insulation packaging superior to refrigerated vehicles in terms of transporting fresh agricultural products.

4.4. Trade-Off Cost between Packaging, Refrigerant, and Transportation. In this section, we analyze the impact of the trade-off between total profit and packaging parameters in the last-mile delivery problem. Two common situations arise when we consider the choice of packaging mode in reality. In the first situation, the distribution center selects the least expensive packaging to reduce the packaging cost. In the second situation, the distribution center chooses the best but more expensive packaging. To test the impact of these two situations on the total profit when nonrefrigerated vehicles with thermal insulation packaging are used to transport fresh produce, we set up seven scenarios involving a series of gradual conversions from the first situation to the second situation. By changing the thickness of the packaging, which increases 5 mm to 35 mm at intervals of 5 mm, we further change the packaging thermal resistance. Based on realistic factors, packaging with the same specifications has different unit packaging costs under different thicknesses. The relevant parameter settings are shown in Table 7.

From Figures 7 and 8, we have the following observations: (1) The cost of the phase-change refrigerant decreases gradually with increasing packaging thickness. (2) The packaging cost decreases at first and then continuously increases when the packaging thickness increases. (3) Transportation costs vary with the thickness of the packaging, and an overall downward trend is present. (4) Total profit increases at first and then starts to obviously decrease, and the profit reaches the optimal level when each packaging thickness is 10 mm. The above observations can be explained by the following: (1) There is an inverse relationship between the thickness of the packaging and the refrigerant quality, which is lower with thicker packaging. (2) The choice of providing multiple insulation methods with the same thickness is beneficial to businesses in terms of increased profits. (3) The choice among multiple packaging modes affects the choice of vehicle routing for distribution. Because the insulation effect increases with increasing thickness, there are more options when we consider the insulation effect in planning vehicle routing under this change. The

Table 5: The heuristic algorithm based on GA by MATLAB calculation results.

Time:	0.137 seconds									
Total profit	38343									
Candidate	1			2					3	
Delivery route	2-9-10-7-4-5-6-1-3-8									
z_i	1	2	3	4	5	6	7	8	9	10
b	1	1	1	1	1	1	1	1	1	1
Q_i^b	15.58	16.24	5.22	1.46	6.52	6.023	4.32	15.48	5.48	4.82

Table 6: Calculation results for each case.

	Instance of nonrefrigerated vehicle					Instance of refrigerated vehicle
	Base case	Case 1	Case 2	Case 3	Case 4	
Profit	25373.6	52542.1	24916.6	25217.7	25041.8	25172.11
	Percentage of the total cost of using an unrefrigerated vehicle					
	Base case (%)	Case 1 (%)	Case 2 (%)	Case 3 (%)		Case 4 (%)
Fixed cost	16.47	14.95	12.23	14.61		13.15
Packaging cost	21.00	37.91	51.24	18.68		16.81
Refrigerant cost	37.53	26.24	18.92	44.47		50.02
Fuel cost	25	20.91	17.84	22.25		20.02

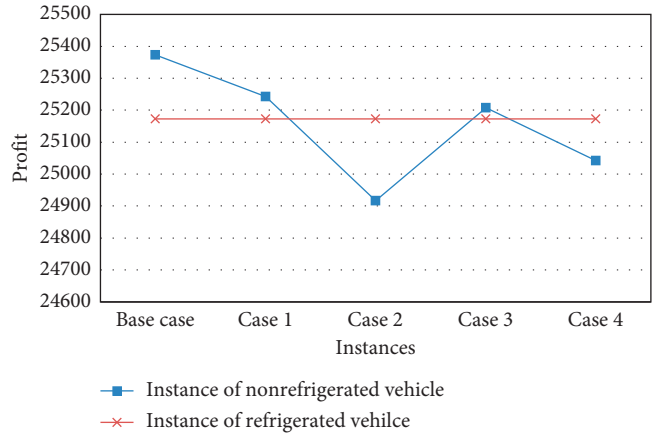

Figure 5: Comparison of nonrefrigerated and refrigerated vehicle cases.

distribution route with a lower distribution cost is selected to reduce the transportation cost after we consider the trade-off between the insulation effect and the distribution sequence. (4) We find that there is a trade-off between the objective value and the packaging thickness. On the one hand, this may be because packaging that is too thin is not conducive to maintaining the required distribution temperature, resulting in the need for more phase-change refrigerants to maintain it. This may result in an increase in the total cost of the insulation packaging. On the other hand, higher-priced, thicker packaging more often has a better thermal insulation effect, leading to a reduction in the required refrigerant quality. However, this may lead to an increase in the total packaging cost if the utility of increasing the thickness of packaging exceeds the utility of reducing the phase-change refrigerants. Therefore, the packaging for fresh food distribution should not be too thick or too thin; this choice is determined jointly by the cost of phase-change refrigerants and packaging and the latent heat of phase change of the refrigerants. In summary, the overall result shows that packaging thickness significantly impacts total profit, and the option to choose from multiple packaging modes is beneficial in terms of optimizing the distribution cost with nonrefrigerated vehicles.

4.5. Selection of Insulation Packaging Parameters. To further explore the impact of parameters on the multiple packaging choices, we generate a new class of cases including 3 scenarios. The first scenario is identical to the base case with the only difference being that the thickness of the selected packaging is set to 15 mm from 10 mm. The second scenario

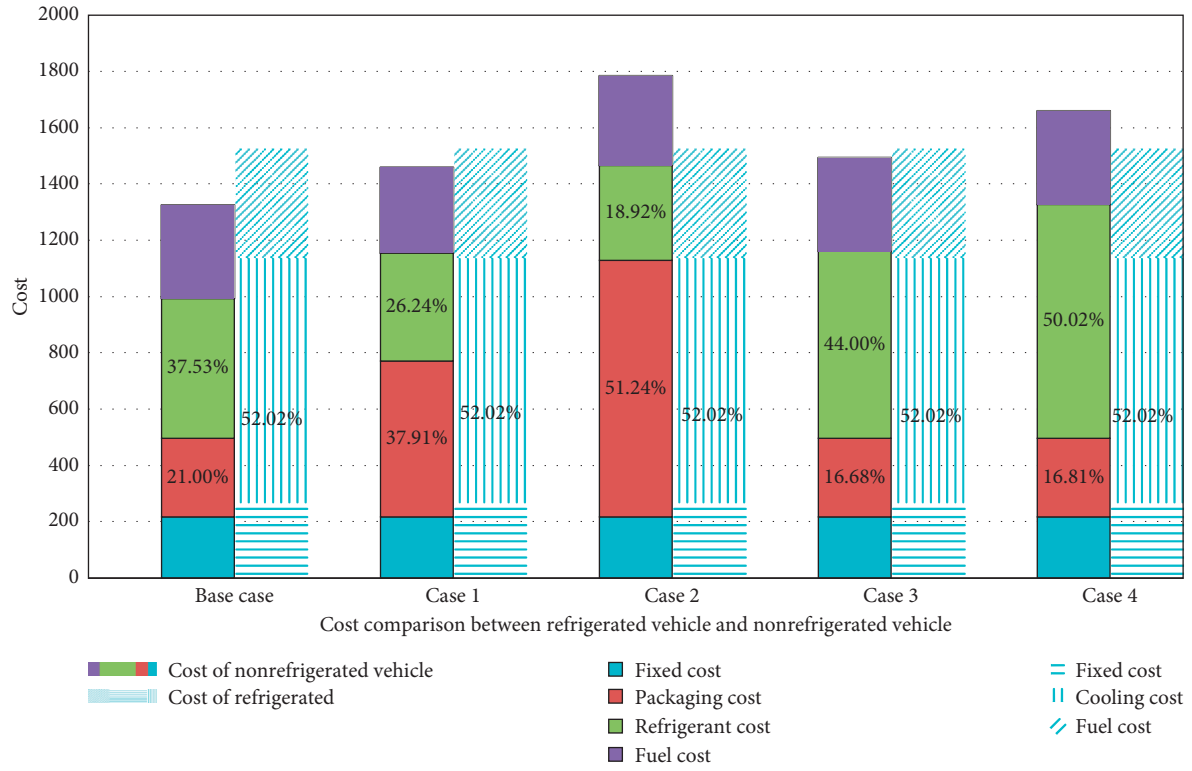

Figure 6: Cost comparison of refrigerated and nonrefrigerated vehicles.

Table 7: Parameter setting for unit packaging cost and packaging thermal resistance.

Scenarios	b	1	2	3	4
1	g_b	1.18	1.27	9.15	5.49
	R_b	0.082	0.130	4.020	0.131
2	g_b	2.25	3.38	11.27	7.61
	R_b	0.163	0.259	4.463	0.257
3	g_b	4.37	5.49	13.38	9.72
	R_b	0.246	0.390	4.901	0.412
4	g_b	6.48	7.16	15.49	11.83
	R_b	0.328	0.520	5.348	0.534
5	g_b	8.59	9.72	17.61	13.94
	R_b	0.409	0.649	5.790	0.655
6	g_b	10.7	11.83	19.72	16.06
	R_b	0.492	0.779	6.233	0.777
7	g_b	18.17	13.94	21.83	18.17
	R_b	0.574	0.901	6.676	0.923

is identical to the base case with the only difference that service quality requirements are set to 45 to 75. The third scenario is identical to the base case with only the difference that the latent heat of phase change is set to 335 to 200. The results of the calculation are shown in Table 8.

We can observe from Table 8 that packaging type 3 is not selected in any of the scenarios, which means that the distribution center usually uses cheaper packaging instead of using better, higher-priced packaging to save on distribution costs. Essentially, in choosing packaging, the community group purchase enterprise faces a trade-off between shelf life and cost, and as long as the less expensive packaging with the appropriate quality of phase-change refrigerant can ensure delivery quality requirements, the enterprise does not choose more expensive packaging that can extend shelf life of perishable products.

However, the distribution center chooses better, higher-priced packaging to prevent the food products from decaying when we have higher quality requirements or when the latent heat of the phase-change refrigerant is lower in scenario 1 and scenario 2. This conclusion has also been drawn by Li [15]. We can also see that the packing mode changes in scenario 1. The results indicate that the multiple packaging and thickness options have a significant impact

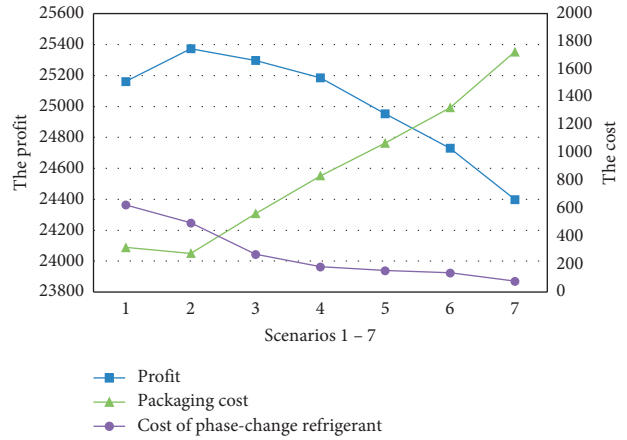

Figure 7: Cost and profit trends.

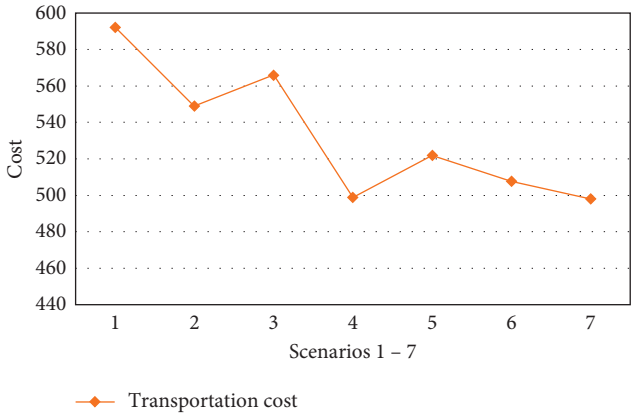

Figure 8: Transportation cost trend.

Table 8: Results of the calculation for each scenario.

	Profit	Community distribution points					
		1	2	3	4	5	6
		Selection of packing mode					
Base case	25373.61	1	1	1	1	1	1
Scenario 1	25480.18	1	1	2	2	1	1
Scenario 2	25384.71	2	2	2	2	2	4
Scenario 3	25252.47	1	2	2	2	2	4

on the final result and can further improve distribution costs and profits.

5. Conclusion

This paper proposes a collaborative optimization mechanism for different insulation package selections and cold chain logistics distribution paths under the community group purchase mode. For small-scale numerical examples, LINGO software is used to solve the problem. On this basis, a heuristic algorithm based on a genetic algorithm is proposed for large-scale numerical examples, and MATLAB is used to solve and prove its effectiveness.

Through parameter analysis, the following conclusions are drawn. First, the large-scale cases are more suitable for solution with the MATLAB software than with LINGO. Second, the use of nonrefrigerated thermal insulation packaging is superior to the use of refrigerated vehicles in terms of transporting fresh agricultural products when neither the cost of the phase-change refrigerant nor the cost of packaging accounts for more than 50% of the total cost. Third, the overall result shows that the option to use multiple packaging thicknesses is beneficial to improve the distribution cost of nonrefrigerated vehicles. Furthermore, choosing better packaging is beneficial in terms of reducing transportation costs. Finally, distribution centers usually use cheap packaging with high-quality refrigerants to ensure the quality of fresh produce and a low total cost.

In regard to future research, we will further consider multiproduct fresh food distribution in this way. In addition, the choice of refrigerant type should be taken into account. To further reduce the distribution cost, in the case of fewer fresh orders, the joint distribution of ordinary packages and fresh agricultural product packages by nonrefrigerated vehicles can be considered in the context of the community group purchase model.

Data Availability

The data used to support the findings of this study are available from the corresponding author upon request.

Conflicts of Interest

The authors declare that there are no conflicts of interest regarding the publication of this paper.

Acknowledgments

The authors acknowledge the National Natural Science Foundation of China (Grant no. 71462024).

References

[1] Y.-M. Li, J.-H. Jhang-Li, T.-K. Hwang, and P.-W. Chen, "Analysis of pricing strategies for community-based group buying: the impact of competition and waiting cost," *Information Systems Frontiers*, vol. 14, no. 3, pp. 633–645, 2012.

[2] Q. Li, X. Li, X. Xiu et al., "Study on consumers' community group purchase based on the integration of SOR and commitment-trust theory," *Journal of Xi'an Jiaotong University*, vol. 40, no. 2, pp. 25–35, 2020.

[3] Y. Liu, M. Jiang, L. Li et al., "Research on evaluation and selection of group purchase distribution mode in fresh Community1," *International Journal of Business and Social Science*, vol. 10, no. 9, pp. 101–109, 2019.

[4] Y. Wang and W. Qiu, "Optimization of distribution path for community group buying considering customer satisfaction," *IOP Conference Series: Materials Science and Engineering*, vol. 10, no. 1, Article ID 012008, 2020.

[5] H. G. Lee and S. Yoo, "Changes in the physical properties of frozen cooked rice depending on thermal insulation levels of packaging during freeze-thaw," *Journal of Food Science*, vol. 85, no. 12, pp. 4342–4350, 2020.

[6] W. Fang, H. Song, D. Wu et al., "Temperature field simulation of multi-temperature zone thermal insulation box based on fluent," *Packaging Engingeering*, vol. 41, no. 3, pp. 62–68, 2020.
[7] Q. Li, P. Yu, X. Wu et al., "Shelf life extending packaging, inventory control and grocery retailing," *Production and Operations Management*, vol. 26, no. 7, pp. 1369–1382, 2017.
[8] E. Oró, L. Miró, and L. F. Cabeza, "Thermal analysis of a low temperature storage unit using phase change materials without refrigeration system," *International Journal of Refrigeration*, vol. 35, no. 6, pp. 1709–1714, 2012.
[9] S. P. Singh, G. Burgess, J. Singh et al., "Performance comparison of thermal insulated packaging boxes, bags and refrigerants for single-parcel shipments," *Packaging Technology and Science*, vol. 21, no. 1, pp. 25–35, 2008.
[10] P. Amorim and B. Almada-Lobo, "The impact of food perishability issues in the vehicle routing problem," *Computers & Industrial Engineering*, vol. 67, pp. 223–233, 2014.
[11] C.-I. Hsu, S.-F. Hung, H.-C. Li et al., "Vehicle routing problem with time-windows for perishable food delivery," *Journal of Food Engineering*, vol. 80, no. 2, pp. 465–475, 2007.
[12] M. Rabbani, A. Farshbaf-Geranmayeh, N. Haghjoo et al., "Vehicle routing problem with considering multi-middle depots for perishable food delivery," *Uncertain Supply Chain Management*, vol. 4, no. 3, pp. 171–182, 2016.
[13] D. S. Byung and D. A. Young, "A vehicle routing problem of both refrigerated- and general-type vehicles for perishable food products delivery," *Journal of Food Engineering*, vol. 169, pp. 61–71, 2016.
[14] E. Dieckmann, B. Nagy, K. Yiakoumetti et al., "Thermal insulation packaging for cold-chain deliveries made from feathers," *Food Packaging and Shelf Life*, vol. 21, Article ID 100360, 2019.
[15] Y. Li, C. Feng, C. Jean-Francois et al., "The multi-plant perishable food production routing with packaging consideration," *International Journal of Production Economics*, vol. 221, p. 2020, Article ID 107472.
[16] W. Shui and M. Li, "Integrated pricing and distribution planning for community group purchase of fresh agricultural products," *Scientific Programming*, vol. 2020, Article ID 8839398, 15 pages, 2020.
[17] B. D. Coleman and J. Victor, "Thermodynamics and departures from Fourier's law of heat conduction," *Archive for Rational Mechanics and Analysis*, vol. 13, no. 1, pp. 245–261, 1963.
[18] M. Pinto and J. C Pinto, "Optimum reference temperature for reparameterization of the Arrhenius equation. Part 1: problems involving one kinetic constant," *Chemical Engineering Science*, vol. 62, no. 10, pp. 2750–2764, 2007.

Hindawi
Discrete Dynamics in Nature and Society
Volume 2021, Article ID 6654288, 11 pages
https://doi.org/10.1155/2021/6654288

Research Article

Forecasting the Number of the Wounded after an Earthquake Disaster Based on the Continuous Interval Grey Discrete Verhulst Model

Jun Zhang[1], **Tongyuan Wang**[2], **Jianpeng Chang**[1] **and Yan Gou**[3]

[1]*School of Management Science and Engineering, Chongqing Technology and Business University, Chongqing 400067, China*
[2]*School of Business, Henan University, Kaifeng 475001, China*
[3]*School of International Business, Chongqing Technology and Business University, Chongqing 400067, China*

Correspondence should be addressed to Tongyuan Wang; tongyuan_wang@163.com

Received 19 November 2020; Revised 30 January 2021; Accepted 22 March 2021; Published 5 April 2021

Academic Editor: Wen Yi

Earthquake disaster causes serious casualties, so the prediction of casualties is conducive to the reasonable and efficient allocation of emergency relief materials, which plays a significant role in emergency rescue. In this paper, a continuous interval grey discrete Verhulst model based on kernels and measures (CGDVM-KM), different from the previous forecasting methods, can help us to efficiently predict the number of the wounded in a very short time, that is, an "S-shape" curve for the numbers of the sick and wounded. That is, the continuous interval sequence is converted into the kernel and measure sequences with equal information quantity by the interval whitening method, and it is combined with the classical grey discrete Verhulst model, and then the grey discrete Verhulst models of the kernel and measure sequences are presented, respectively. Finally, CGDVM-KM is developed. It can effectively overcome the systematic errors caused by the discrete form equation for parameter estimation and continuous form equation for simulation and prediction in classical grey Verhulst model, so as to improve the prediction accuracy. At the same time, the rationality and validity of the model are verified by examples. A comparison with other forecasting models shows that the model has higher prediction accuracy and better simulation effect in forecasting the wounded in massive earthquake disasters.

1. Introduction

In recent years, frequent earthquake disasters have occurred frequently all over the world. Due to the uncertainty and destructiveness of earthquake, it has caused a great loss of people and property. For example, Haiti (7.3 magnitude on January 13th, 2010, killed 222500 people and injured 196000 people), Chile (8.8 magnitude on February 27th, 2010, killed more than 750 people), Japan (8.6 magnitude on March 11th, 2011, killed 19533 people and missed 2585 people), in China, Wenchuan (8.0 magnitude on May 12th, 2008, killed 69227 people, injured 374643 and missed 17923 people), and Yushu (7.1 magnitude on April 14th, 2010, killed 2698 people). These data are the official report of the massive earthquakes from China Seismological Bureau (https://www.cea.gov.cn/cea/dzpd/index.html). It can be seen that the occurrence of earthquake disasters has exerted a serious impact on people's production and life and also caused heavy casualties and economic losses. However, due to the sudden and fragility of earthquake disaster, it becomes difficult and challenging to prevent in advance. Measures can be taken to effectively deal with the disaster after it occurs, so as to reduce casualties and property losses [1, 2].

Massive earthquake disaster has the characteristics of strong suddenness and weak prediction, and its occurrence is often accompanied by road collapse, channel obstruction, and other problems, which cause inconvenience to rescue operations, so that emergency relief materials cannot be delivered timely and fully after the disaster. Therefore, it is necessary to accurately predict the emergency materials (such as medical materials needed to treat the wounded), and the premise of forecasting is to know the number of the wounded every day.

Through the forecasting of the number of the wounded, we can not only indirectly predict the demand for drugs in earthquake disaster emergency rescue but also play a guiding role in the allocation of relief materials.

Choosing a suitable mathematical model is key to achieving accurate prediction of the number of the wounded. After the occurrence of the massive earthquake disasters, only a small amount of information can be available for reference to the prediction of the number of the wounded in a short time. In view of this kind of information, the grey prediction model can play a very good prediction effect. Grey system prediction method is based on people's understanding of the uncertainty characteristics of system evolution, aiming at the problems of grey uncertainty prediction existing in reality, using a small amount of effective data, mining the inherent evolution law of the system, and then making a scientific prediction of the development trend of the system [3]. Therefore, we build a grey prediction model to forecast the number of the wounded after the massive earthquake disasters.

In this paper, we first analyze the previous data and find that the data of the wounded present the characteristics of "S-shape" and continuous interval dynamic change. According to the characteristics of data, interval grey number whitening method and grey discrete Verhulst method are selected to construct continuous interval grey number discrete Verhulst prediction model based on kernels and measures (CGDVM-KM), which is used to simulate and forecast the number of the wounded in Lushan earthquake of Sichuan Province in China, and good results are obtained. The grey prediction model proposed in this paper can provide a good support for the emergency rescue of massive earthquake disasters, so as to provide reference for the later material allocation of emergency rescue.

The main contributions of this paper are as follows. First, we use interval bleaching principle of converting continuous interval sequence information, such as nuclear and measure sequences, and then, it is combined with grey Verhulst model, and a nuclear sequence grey Verhulst model and measure is established. A continuous discrete Verhulst grey forecasting model is rebuilt which can effectively overcome errors done by the classical grey Verhulst model due to the parameter estimation using discrete simulation and prediction equation using continuous form equation of system error and improve the prediction precision. Second, due to the suddenness and persistence of major earthquakes, the number of diseases and injuries shows certain grey characteristics, such as the presence of known or unknown information, and the sample size is small and limited. Therefore, we will construct the CGDVM-KM to predict the number of illnesses and injuries in the early stage of an earthquake, as well as the need for emergency medicines. Through comparative analyses with several other grey prediction models, it is found that the model constructed in this paper can well fit the number of the wounded in the massive earthquake disasters, so as to accurately forecast the number of the wounded in a period of time in the future, and provide reference for emergency rescue and later material allocation.

The rest of this paper is organized as follows. Section 2 reviews the related literature. The data characteristics and methods used are introduced in Section 3. Section 4 presents the required forecast model. Section 5 forecasts the number of the wounded and makes comparative analysis. The conclusions are drawn in Section 6.

2. Literature Review

There are two aspects of literature related to this study: (1) the forecasting of the wounded in the massive earthquake disasters; (2) grey prediction model.

2.1. Forecasting the Wounded in Massive Earthquake Disasters. In the literature of the forecasting of the number of the wounded in the earthquake disasters, Wu and Gu used the modified exponential curve to fit the data and predict the number of death in Wenchuan earthquake in China [4]. Wang et al. established a BP neural network model to predict casualties in earthquakes. The model examined the key factors, such as earthquake magnitude, focal depth, epicenter intensity, disaster preparedness level, earthquake acceleration, population density, and disaster prediction, and used 37 severe earthquake disasters to train the network. The results show that the model is applicable to most earthquake situations [5]. Zhang et al. proposed to use the grey discrete Verhulst model to predict the drug supplies for emergency rescue of large-scale earthquake disasters [2]. Gul and Guneri established an artificial neural network (ANN) model for earthquake casualty prediction, which takes the time of earthquake occurrence, earthquake magnitude, and population density as the prediction factors, and use five earthquake disasters occurring in Turkey since 1975 as the network training sample [6]. Huang et al. introduced extreme learning machine (ELM) into earthquake casualty prediction. Through data training, the ELM network structure for earthquake casualty prediction was established, and the number of hidden layer nodes and excitation function was determined to ensure the reliability of ELM network prediction results [7]. Furthermore, Huang et al. proposed an adaptive chaotic particle swarm optimization (ACPSO) to optimize network parameters of traditional ELM to improve the stability and prediction accuracy of the network and apply the improved elm model to the prediction of casualties in earthquake disasters [8]. Firuzi et al. proposed an empirical model for mortality estimation in Iran based on vibration related parameters (PGA) [9].

As we all know, the neural network and extreme learning machine prediction methods need more original data for training and learning in advance. However, the emergency rescue of earthquake disaster is more urgent, requiring longer time and smaller sample size, so it is not applicable. However, the grey system model used in literature [2] only uses grey Verhulst model to predict the number of the wounded in real number, which does not fully reflect the characteristics of continuous interval of the number of patients. This paper not only takes into account the saturated "S" type change trend of the number of wounded and sick

people but also fully considers the characteristics of continuous interval of the number of wounded and sick people and uses the improved interval grey Verhulst model to predict the number of the wounded after the occurrence of earthquake disasters, so that the prediction accuracy can be improved.

2.2. Grey Prediction Models. Many scholars have studied the grey Verhulst prediction model. Zhang et al. introduced the grey Verhulst model into the field of load forecasting and the application of grey Verhulst model in medium and long-term load forecasting through typical examples [10]. Wang et al. proposed an unbiased grey Verhulst model for the inherent simulation error of grey Verhulst model [11]. Cui et al. proposed the grey discrete Verhulst model according to the incomplete adaptability of the traditional grey Verhulst model, referring to the idea of discretization, and through mutual generation of the original data [12]. Hashem-Nazari et al. proposed the direct basic form-focused nonequidistant grey Verhulst model and effectively predicted the socio-conomic time series focusing on the population of Iran [13]. Wang and Li built a derived non-equigap grey Verhulst model and explore the relationship between carbon dioxide emissions and economic growth. Empirical research shows that the relationship between carbon dioxide emissions and economic growth has an inverted U-shaped curve [14]. Rajesh used the grey Verhulst model to determine the driving factors of social and environmental risk management (SERM) in an elastic supply chain, so as to effectively improve the performance of enterprise SERM [15]. Wu and Xu used the grey Verhulst model to predict the comprehensive air quality index [16]. Zeng et al. used the improved grey Verhulst model to reasonably predict tight gas production [17]. Tian et al. used the Verhulst grey model to predict the value of ocean carrying capacity in the next five years (2017–2021) [18]. Zhao et al. predicted the number of patients with COVID-19 infection in China based on grey Verhulst model [19].

The traditional discrete GM (1,1) model does not always fit well, and sometimes the prediction error is large [20, 21], so some scholars began to study interval grey numbers. Zeng et al. developed a DGM (1,1) prediction model for interval grey number series [22]. According to the geometric characteristics of interval grey number sequence on two-dimensional coordinate plane, Zeng and Liu proposed a prediction model of interval grey number based on its geometrical characteristics through area transformation and coordinated transformation to transform interval grey number sequence into real number sequence without information loss. Thus, the interval grey number sequence with uncertain information is simulated and predicted [23]. Considering that some data are fuzzy or missing after earthquake disasters, which leads to difficulties in material demand prediction, Zhang et al. proposed using the fuzzy interval grey number for prediction to improve the prediction accuracy [24]. Li et al. proposed a new operation rule of grey interval number multiplication, which improved the accuracy of grey number division. Then, on the basis of the proposed calculation rules, combined with grey reduction preprocessing, the traditional grey heterogeneous data prediction modeling method is improved and applied to the inventory replenishment scheduling problem in emergency rescue scenarios [25]. Zeng et al. established a new interval grey number prediction model through the kernel function of grey number band and regional sequence [26]. Zeng et al. divided the interval grey numbers into two real number parts, namely, the "white" and "grey" parts. Then, grey Verhulst model and DGM (1,1) model are developed to simulate and predict the "white" and "grey" parts, respectively. Thus, the problem of expanding the range of interval grey number is solved to a certain extent [27]. Furthermore, according to the situation that the traditional grey correlation model cannot extract interval feature information from the interval grey number sequence, Ye et al. built a grey correlation analysis model (GRA) based on effective information transformation of interval grey number. Then, a multivariate GM (1, n) model is developed to predict the interval grey number series [28].

The aforementioned literature has optimized and applied the grey Verhulst model and interval grey number prediction model from various perspectives, but the scope of application of each model is not the same. None of the aforementioned models is appropriate for predicting the number of the wounded in the massive earthquake disasters. Considering that the number of wounded people after an earthquake is changing in a continuous interval, this paper will use the interval bleaching principle of converting continuous interval sequence information, such as nuclear sequence, and the measure which build nuclear sequence grey Verhulst model and measure, the final reduction build a continuous discrete Verhulst grey forecasting model. After the subsequent empirical test, the improved model is more effective and accurate in predicting the number of earthquake wounded.

3. Problem Descriptions

In this section, we analyzed the data of the number of the wounded after the massive earthquake disasters and then built a corresponding model to forecast according to the data characteristics.

3.1. Data Characteristics. In order to find the statistical law of the number of the wounded in the massive earthquake disasters, the statistical data of early earthquake disasters in Yushu, Qinghai Province, and Lushan, Sichuan Province, in China are selected. The statistical data curve is drawn and shown in Figure 1. These data are semidaily data, based on the official report of these two massive earthquakes from China Seismological Bureau (https://www.cea.gov.cn/cea/dzpd/index.html).

Through the statistical data analysis of the number of patients after the massive earthquake disaster, it can be concluded that there are two characteristics in the statistical data of the number of the wounded.

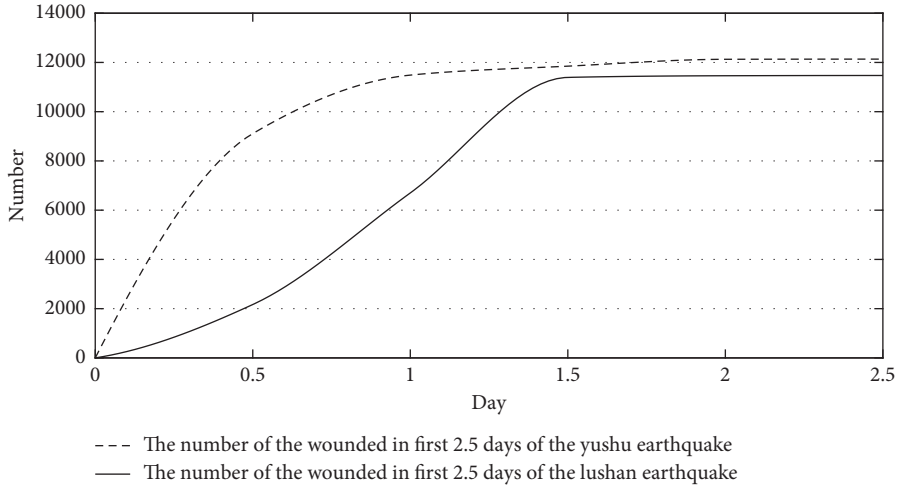

Figure 1: The number of the wounded in the early stage of earthquake.

3.1.1. Saturated "S-Shape" Characteristics. From Figure 1, we can see that, at the beginning of the rescue, the number of the wounded shows an exponential rapid growth (i.e., rapid growth period). With further development of the rescue operation, the number of newly discovered wounded people gradually decreased, and the growth rate gradually slowed down. Meanwhile, some wounded with minor injuries gradually recovered and withdrew from treatment, and some patients who were seriously injured would be sent to large hospitals to receive further treatment after simple treatment, so the number of the wounded gradually stabilized at a total amount and no longer increased (i.e., stationary period). As a whole, it shows a saturated "S-shape" change trend. At the same time, the real-time statistical data of the number of the wounded has been carried out at the beginning of the rescue operation, and it is easy to get along with the rescue operation.

3.1.2. Continuous Interval Dynamic Variability. The statistics of the number of the wounded can be divided into point data and interval data. The point data only reflects the number of the wounded found at the end of the recording time point of the day. In the golden rescue period, the search and rescue process is 24-hour without interruption. During and after the statistical process, wounded people were continuously found. The number is increasing every hour, which is a dynamic and continuous growth and changing process, and the number of the wounded has a continuous interval every hour and every day. Therefore, point data cannot accurately describe the real situation. The data of the wounded can be regarded as a continuous change interval, which can reflect the reality more truly and accurately.

3.2. Method. The construction of continuous interval grey number prediction model involves two problems. One is the whitening treatment of continuous interval grey number. That is, the continuous interval grey number sequence is transformed into real number sequence with equal amount of information. The other is to select the model aiming at the data characteristics of the real number. In the kernel and measure method, the midpoint of the lower bound of the interval is selected as the kernel sequence, and the interval length is selected as the measure sequence. The interval grey number is transformed into two real number sequences of kernels and measures, which can avoid the problems caused by the direct operation of interval grey number and make full use of all the information contained in the interval grey number. Therefore, it can well predict the interval grey number.

Verhulst model describes a dynamic development process, which initially shows an exponential rapid growth. As time goes by, the growth rate gradually slows down and finally decreases to zero due to the interference of some external factors, and the total amount is stable at a fixed value. That means the model is mainly used to describe the grey dynamic change process of the whole data with saturated "S-shape" feature. From the modeling process of the classical grey Verhulst model, we can see that there are some errors in the conversion process from the whitening equation to the final response formula, and the grey discrete Verhulst model can effectively reduce this error. Consequently, in view of the characteristics of saturated "S-shape" and continuous change interval in the number of the wounded in the massive earthquake disaster, this paper analyses the selection of prediction methods and interval whitening method and proposes the continuous interval grey discrete Verhulst model based on kernels and measures (CGDVM-KM) to simulate and predict the number of the wounded in Lushan earthquake, Sichuan Province, in China.

4. Construction of the Prediction Model

The basic idea of constructing continuous interval grey discrete Verhulst model based on kernels and measures is as follows. First, we whiten all the grey elements of continuous interval grey number sequence and then transform them into equal information of kernel sequence and measure sequence. Second, grey discrete Verhulst model of kernel and measure sequences is constructed to predict the kernels

and measures. Finally, we deduced and restored the upper and lower bounds of the continuous interval grey number, and then, the prediction of the continuous interval grey number is realized.

For the continuous interval grey number, the kernel is the center of the interval, reflecting the development trend of the continuous interval grey number sequence, which is expressed as half of the sum of the upper and lower bound interval data. The measure is the length of the continuous interval, reflecting the information mastering the continuous interval grey number sequence, and the numerical value is the difference between the upper and lower bounds. According to the literature of [12, 29], we have the following definitions.

Definition 1. Suppose a continuous interval $[a_k, b_k]$, and grey number $\otimes \in [a_k, b_k]$. We considered that $\widetilde{\otimes}_k = (a_k + b_k)/2$ is the kernel of the continuous interval, and $l(\otimes_k) = b_k - a_k$ is the measure of the continuous interval.

Definition 2. Suppose the original sequence as $X^{(0)} = (x^{(0)}(1), x^{(0)}(2), \ldots, x^{(0)}(k))$. Here, $X^{(0)}(k)$ indicates the data at time k. Suppose that $Y^{(0)} = (y^{(0)}(1), y^{(0)}(2), \ldots, y^{(0)}(n))$ is the reciprocal of $X^{(1)}$, where $X^{(1)}$ is the first aggregate generator operator (1-AGO) of $X^{(0)}$. Then, the following is obtained: $y^{(0)}(k) = 1/x^{(1)}(k)\,(k = 1, 2, \ldots, n)$. Suppose that $Y^{(1)} = (y^{(1)}(1), y^{(1)}(2), \ldots, y^{(1)}(n))$ is the 1-AGO of $Y^{(0)}$, and $y^{(1)}(k) = \sum_{i=1}^{k} y^{(0)}(i)$. Thus, the grey discrete Verhulst model is

$$y^{(1)}(k+1) = \beta_1 + \beta_2 k + \beta_3 y^{(1)}(k). \tag{1}$$

We can obtain the estimated parameters $\beta = (\beta_1, \beta_2, \beta_3)^T$ as follows:

$$\begin{cases}
\beta_1 = \dfrac{\sum_{k=1}^{n-1} y^{(1)}(k+1)}{n-1} - \dfrac{n}{2}\beta_2 - \dfrac{\sum_{k=1}^{n-1} y^{(1)}(k)}{n-1}\beta_3, \\
\beta_2 = \dfrac{6n\sum_{k=1}^{n-1} y^{(1)}(k+1) - \sum_{k=1}^{n-1}\left(k \cdot y^{(1)}(k+1)\right)}{n(n-1)(n-2)} - \dfrac{3n\sum_{k=1}^{n-1} y^{(1)}(k) - 6\sum_{k=1}^{n-1}\left(k \cdot y^{(1)}(k)\right)}{3n\sum_{k=1}^{n-1} y^{(1)}(k) - n(n-1)(2n-1)}\beta_3, \\
\beta_3 = \dfrac{n(n-1)(n-2)\sum_{k=1}^{n-1}\left(y^{(1)}(k+1) \cdot y^{(1)}(k)\right)}{12n\sum_{k=1}^{n-1} y^{(1)}(k) \cdot \sum_{k=1}^{n-1}\left(k \cdot y^{(1)}(k)\right) + n(n-1)(n-2)\sum_{k=1}^{n-1}\left(y^{(1)}(k)\right)^2 - 2n(2n-1)\left(\sum_{k=1}^{n-1} y^{(1)}(k)\right)^2 - 12\left(\sum_{k=1}^{n-1} k \cdot y^{(1)}(k)\right)^2} \\
\quad + \dfrac{+6n\sum_{k=1}^{n-1}\left(k \cdot y^{(1)}(k)\right) \cdot \sum_{k=1}^{n-1} y^{(1)}(k+1) + 6n\sum_{k=1}^{n-1} y^{(1)}(k) \cdot \sum_{k=1}^{n-1}\left(k \cdot y^{(1)}(k+1)\right)}{12n\sum_{k=1}^{n-1}\left(y^{(1)}(k)\right) \cdot \sum_{k=1}^{n-1}\left(k \cdot y^{(1)}(k)\right) + n(n-1)(n-2)\sum_{k=1}^{n-1}\left(y^{(1)}(k)\right)^2 - 2n(2n-1)\sum_{k=1}^{n-1}\left(y^{(1)}(k)\right)^2 - 12\left(\sum_{k=1}^{n-1} k \cdot y^{(1)}(k)\right)^2} \\
\quad \cdot 2n(2n-1)\sum_{k=1}^{n-1}\left(y^{(1)}(k)\right) \cdot \sum_{k=1}^{n-1}\left(y^{(1)}(k+1)\right) \\
\cdot 12n\sum_{k=1}^{n-1}\left(y^{(1)}(k)\right) \cdot \sum_{k=1}^{n-1}\left(k \cdot y^{(1)}(k)\right) + n(n-1)(n-2)\sum_{k=1}^{n-1}\left(y^{(1)}(k)\right)^2 - 2n(2n-1)\sum_{k=1}^{n-1}\left(y^{(1)}(k)\right)^2 - 12\left(\sum_{k=1}^{n-1} k \cdot y^{(1)}(k)\right)^2 \\
- \dfrac{12\left(\sum_{k=1}^{n-1} k \cdot y^{(1)}(k)\right) \cdot \left(\sum_{k=1}^{n-1} k \cdot y^{(1)}(k+1)\right)}{12n\sum_{k=1}^{n-1}\left(y^{(1)}(k)\right) \cdot \sum_{k=1}^{n-1}\left(k \cdot y^{(1)}(k)\right) + n(n-1)(n-2)\sum_{k=1}^{n-1}\left(y^{(1)}(k)\right)^2 - 2n(2n-1)\sum_{k=1}^{n-1}\left(y^{(1)}(k)\right)^2 - 12\left(\sum_{k=1}^{n-1} k \cdot y^{(1)}(k)\right)^2}.
\end{cases} \tag{2}$$

The time response function of the grey discrete Verhulst model is

$$\widehat{x}^{(1)}(k+1) = \frac{1}{\widehat{y}^{(0)}}(k+1) = \begin{cases} \left[k\beta_2 + \beta_1\right]^{-1}, & \beta_3 = 1, \\ \left[\beta_1\beta_3^{k-1} + \dfrac{\beta_2\left(1-\beta_3^k\right)}{1-\beta_3} - \beta_3^{k-1}\left(1-\beta_3\right)\dfrac{1}{x^{(0)}(1)}\right]^{-1}, & \beta_3 \neq 1. \end{cases} \tag{3}$$

Finally, the grey discrete Verhulst model based on kernels and measures is constructed as follows.

4.1. Prediction of the Kernels. From Definition 1, we can obtain the original sequence of kernel sequence:

$$X^{(0)}(\widetilde{\otimes}) = \left(\widetilde{\otimes}_1, \widetilde{\otimes}_2, \ldots, \widetilde{\otimes}_n\right). \tag{4}$$

The kernel sequence's time response function of the grey discrete Verhulst model is

$$\begin{aligned}\widehat{a}(k+1) &= \widehat{\widetilde{\otimes}}^{(1)}(k+1)\\ &= \left[\alpha_1\alpha_3^{k-1} + \frac{\alpha_2\left(1-\alpha_3^k\right)}{1-\alpha_3} - \alpha_3^{k-1}\left(1-\alpha_3\right)\frac{1}{\widetilde{\otimes}^{(0)}(1)}\right]^{-1}.\end{aligned} \tag{5}$$

According to (5), the kernel sequence at the corresponding time can be predicted by substituting a different time k.

4.2. Prediction of the Measures. From Definition 1, we can obtain the original sequence of measure sequence:

$$L^{(0)} = \left(l^{(0)}(1), l^{(0)}(2), \ldots, l^{(0)}(k)\right). \tag{6}$$

$L^{(0)}(k)$ indicates the number of the wounded at time k, and $L^{(1)}$ is the first aggregate generator operator (1–AGO) of $L^{(0)}$.

The measure sequence's time response function of the grey discrete Verhulst model is

$$\widehat{l}^{(1)}(k+1) = \left[\beta_1\beta_3^{k-1} + \frac{\beta_2\left(1-\beta_3^k\right)}{1-\beta_3} - \beta_3^{k-1}\left(1-\beta_3\right)\frac{1}{l^{(0)}(1)}\right]^{-1}. \tag{7}$$

It can be obtained by reduction:

$$\begin{aligned}\widehat{l}^{(0)}(k+1) &= \left[\beta_1\beta_3^{k-1} + \frac{\beta_2\left(1-\beta_3^k\right)}{1-\beta_3} - \beta_3^{k-1}\left(1-\beta_3\right)\frac{1}{l^{(0)}(1)}\right]^{-1}\\ &\quad - \left[\beta_1\beta_3^{k-2} + \frac{\beta_2\left(1-\beta_3^{k-1}\right)}{1-\beta_3} - \beta_3^{k-2}\left(1-\beta_3\right)\frac{1}{l^{(0)}(1)}\right]^{-1}.\end{aligned} \tag{8}$$

According to (8), the measure sequence at the corresponding time can be predicted by substituting a different time k.

4.3. Prediction Model of Upper and Lower Bounds of Continuous Interval Grey Number. The prediction values of kernels and measures sequences are solved by Definition 2.

$$\begin{cases}\widehat{a}(k+1) + \widehat{b}(k+1) = 2\widehat{\widetilde{\otimes}}(k+1),\\ \widehat{b}(k+1) - \widehat{a}(k+1) = \widehat{l}(k+1).\end{cases} \tag{9}$$

According to (5), the grey prediction model of upper and lower bounds of interval grey number $\widehat{\otimes}(k+1) \in [\widehat{a}(k), \widehat{b}(k)]$ can be obtained.

$$\begin{cases}\widehat{a}(k+1) = \widehat{\widetilde{\otimes}}(k+1) - \dfrac{1}{2}\widehat{l}(k+1),\\ \widehat{b}(k+1) = \widehat{\widetilde{\otimes}}(k+1) + \dfrac{1}{2}\widehat{l}(k+1),\end{cases} \tag{10}$$

$$\begin{cases}\widehat{a}(k+1) = \left[\alpha_1\alpha_3^{k-1} + \dfrac{\alpha_2\left(1-\alpha_3^k\right)}{1-\alpha_3} - \alpha_3^{k-1}\left(1-\alpha_3\right)\dfrac{1}{\widetilde{\otimes}^{(0)}(1)}\right]^{-1} - \dfrac{1}{2}\left(\left[\beta_1\beta_3^{k-1} + \dfrac{\beta_2\left(1-\beta_3^k\right)}{1-\beta_3} - \beta_3^{k-1}\left(1-\beta_3\right)\dfrac{1}{l^{(0)}(1)}\right]^{-1}\right.\\ \qquad\left. - \left[\beta_1\beta_3^{k-2} + \dfrac{\beta_2\left(1-\beta_3^{k-1}\right)}{1-\beta_3} - \beta_3^{k-2}\left(1-\beta_3\right)\dfrac{1}{l^{(0)}(1)}\right]^{-1}\right)\\ \widehat{b}(k+1) = \left[\alpha_1\alpha_3^{k-1} + \dfrac{\alpha_2\left(1-\alpha_3^k\right)}{1-\alpha_3} - \alpha_3^{k-1}\left(1-\alpha_3\right)\dfrac{1}{\widetilde{\otimes}^{(0)}(1)}\right]^{-1} - \dfrac{1}{2}\left(\left[\beta_1\beta_3^{k-1} + \dfrac{\beta_2\left(1-\beta_3^k\right)}{1-\beta_3} - \beta_3^{k-1}\left(1-\beta_3\right)\dfrac{1}{l^{(0)}(1)}\right]^{-1}\right.\\ \qquad\left. - \left[\beta_1\beta_3^{k-2} + \dfrac{\beta_2\left(1-\beta_3^{k-1}\right)}{1-\beta_3} - \beta_3^{k-2}\left(1-\beta_3\right)\dfrac{1}{l^{(0)}(1)}\right]^{-1}\right).\end{cases} \tag{11}$$

Equation (11) is the upper and lower bound prediction model of continuous interval grey number. The interval number of the wounded can be predicted by substituting it into different time intervals k. Finally, the average relative error and synthetic average relative simulation error can be obtained, respectively.

4.4. Error Test Standard. After using the prediction method to fit the curve, we need to use the relative error index to test the fitting degree.

Definition 3. Suppose that the sequence of the original continuous interval grey numbers is [30]

$$\begin{aligned} X^{(0)} &= \left(x^{(0)}(1), x^{(0)}(2), \ldots, x^{(0)}(n)\right) \\ &= \left([a_1, b_1], [a_2, b_2], \ldots, [a_n, b_n]\right). \end{aligned} \tag{12}$$

The simulated sequence of the model is as follows:

$$\begin{aligned} \widehat{X}^{(0)} &= \left(\widehat{x}^{(0)}(1), \widehat{x}^{(0)}(2), \ldots, \widehat{x}^{(0)}(n)\right) \\ &= \left(\left[\widehat{a}_1, \widehat{b}_1\right], \left[\widehat{a}_2, \widehat{b}_2\right], \ldots, \left[\widehat{a}_n, \widehat{b}_n\right]\right). \end{aligned} \tag{13}$$

The lower bound and upper bound residual sequences are

$$\begin{cases} \varepsilon_a = \left(\varepsilon_a(1), \varepsilon_a(2), \ldots, \varepsilon_a(n)\right) = \left(a_1 - \widehat{a}_1, a_2 - \widehat{a}_2, \ldots, a_n - \widehat{a}_n\right), \\ \varepsilon_b = \left(\varepsilon_b(1), \varepsilon_b(2), \ldots, \varepsilon_b(n)\right) = \left(b_1 - \widehat{b}_1, b_2 - \widehat{b}_2, \ldots, b_n - \widehat{b}_n\right). \end{cases} \tag{14}$$

Finally, we calculate the relative error sequence of the lower and upper bounds:

$$\begin{cases} \Delta_a = \left(\Delta_a(1), \Delta_a(2), \ldots, \Delta_a(n)\right) = \left(\left|\dfrac{\varepsilon_a(1)}{a_1}\right|, \left|\dfrac{\varepsilon_a(2)}{a_2}\right|, \ldots, \left|\dfrac{\varepsilon_a(n)}{a_n}\right|\right), \\ \Delta_b = \left(\Delta_b(1), \Delta_b(2), \ldots, \Delta_b(n)\right) = \left(\left|\dfrac{\varepsilon_b(1)}{b_1}\right|, \left|\dfrac{\varepsilon_b(2)}{b_2}\right|, \ldots, \left|\dfrac{\varepsilon_b(n)}{b_n}\right|\right). \end{cases} \tag{15}$$

(1) For $k \le n$, we considered that $\Delta_a(k) = |\varepsilon_a(k)/a_k|$ is the simulate the relative error at the point k of the lower bound sequence, and $\overline{\Delta}_a = (1/n)\sum_{k=1}^{n} \Delta_a(k)$is the average relative error of the lower bound sequence. The upper bound error calculation is omitted for similarity.

(2) $\overline{\Delta} = (1/2)(\overline{\Delta}_a + \overline{\Delta}_b)$ is called the comprehensive average model relative error.

(3) For α, when $\overline{\Delta} < \alpha$ and $\Delta_a(n) < \alpha, \Delta_b(n) < \alpha$ hold, the model is a residual qualified model.

The prediction results must overpass the accuracy test to judge whether the result is qualified and fits its accuracy level. Only the prediction model, which has overpassed the accuracy test, can ensure the rationality and accuracy of its prediction value. The lower the stage is, the better the prediction effect will be. By calculating the residual error and relative error of each point, the average simulation relative error of the upper and lower bounds and the comprehensive average simulation relative error of the model can be calculated. Then, the accuracy grade of the prediction model can be judged by referring to the continuous interval sequence error test table shown in Table 1.

Table 1: Continuous interval sequence error test table.

Accuracy classes	Average relative error α
Stage 1	0.01
Stage 2	0.05
Stage 3	0.10
Stage 4	0.20

Table 2: The number range of the wounded after the earthquake.

Time from earthquake occurrence (days)	The number range of the wounded
0.5–1	[2168, 6700]
1–1.5	[6700, 11393]
1.5–2	[11393, 11460]
2–2.5	[11460, 11470]

5. Prediction and Results Analysis

Taking the Lushan earthquake in Sichuan Province on April 20, 2013, as an example, we use the continuous interval grey discrete Verhulst model based on the kernels and measures (CGDVM-KM) to forecast the number of the wounded. The data in this paper come from the statistics of earthquake patients (with an interval of 0.5 days) released by China Seismological Bureau (http://www.cea.gov.cn). See more details in Table 2.

Step 1. The kernel sequence is as follows:

$$X^{(0)}(\widetilde{\otimes}) = (4434, 9046.5, 11426.5, 11465). \tag{16}$$

Step 2. The measure sequence is as follows:

$$L^{(0)} = (4532, 4693, 67, 10). \tag{17}$$

The first aggregate generator operator (1-AGO) of the measure sequence is

$$L^{(1)} = (4532, 9225, 9292, 9302). \tag{18}$$

Step 3. The simulation of the kernel sequence can be obtained as

$$\widehat{\widetilde{\otimes}} = (4434, 9046.49, 11425.96, 11465.26). \tag{19}$$

The simulation of the measure sequence's first aggregate generator operator (1-AGO) is

$$\widehat{l}^{(1)} = (4532, 9225.32, 9291.99, 9301.46). \tag{20}$$

The simulation sequence of the measure sequence can be obtained as

Table 3: Upper and lower bound errors.

	Time	Actual value $X(k)$	Prediction value $\hat{X}(k)$	Residual $\varepsilon(k) = X(k) - \hat{X}(k)$	Relative error (%) $\Delta_k = \lvert\varepsilon(k)/X(k)\rvert$
Lower bound	1	2168	2168	0	0.00000
	2	6700	6699.83	0.17	0.00254
	3	11393	11392.625	0.375	0.00329
	4	11460	11460.525	−0.525	0.00458
Average of relative error $\overline{\Delta}(1) = (\Delta_2 + \Delta_3 + \Delta_4)/3$					0.00347
Upper bound	1	6700	6700	0	0.00000
	2	11393	11393.15	−0.15	0.00132
	3	11460	11459.295	0.705	0.00615
	4	11470	11469.995	0.005	0.00004
Average of relative error $\overline{\Delta}(2) = (\Delta_2 + \Delta_3 + \Delta_4)/3$					0.00250
Comprehensive average relative error $\overline{\Delta}(3) = (\overline{\Delta}(1) + \overline{\Delta}(2))/2$					0.00299

Table 4: Simulation results.

Time from earthquake occurrence (days)	Original value	Prediction value
0.5–1	[2168, 6700]	[2168, 6700]
1–1.5	[6700, 11393]	[6699.83, 11393.15]
1.5–2	[11393, 11460]	[11392.625, 11459.295]
2–2.5	[11460, 11470]	[11460.525, 11469.995]
2.5–3	[11470, 11470]	[11465.100, 11466.440]
3–3.5	[11470, 11470]	[11465.685, 11465.875]
3.5–4	[11470, 11470]	[11465.765, 11465.795]
4–4.5	[11470, 11470]	[11465.780, 11465.780]
4.5–5	[11470, 11470]	[11465.780, 11465.780]

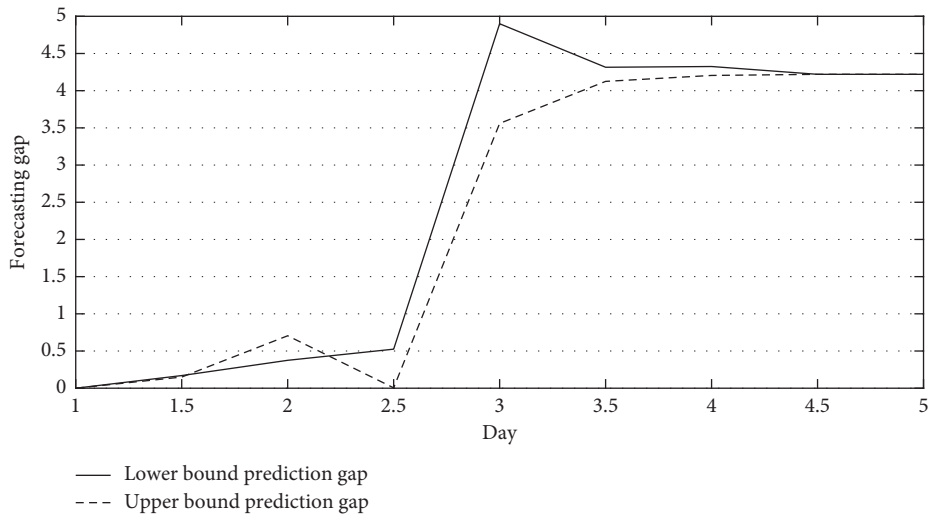

Figure 2: Prediction gap of the number of the wounded.

$$\hat{l}^{(0)} = (4532, 4693.32, 66.67, 9.47). \quad (21)$$

Step 4. The simulated values of the lower bound sequence of the interval are as follows:

$$\hat{a} = (2168, 6699.83, 11392.625, 11460.525). \quad (22)$$

The simulated values of the upper bound sequence of the interval are as follows:

$$\hat{b} = (6700, 11393.15, 11459.295, 11469.995). \quad (23)$$

Step 5. From $\overline{\Delta} = (1/n - 1)\sum_{i=2}^{n} \Delta_i$, it can be concluded that the average relative error of the lower bound is 0.00347% and the average relative error of the upper bound is 0.00250%. Thus, the average relative simulation error is 0.00299%. See more details in Table 3.

From Table 3, we can see that the residual error of each data is below 1, which shows good fitting. The final

Table 5: Comparison of prediction error between this model and other grey prediction models.

Model	GVM-R	GDVM-R	CGDVM-GA	CGDVM-ID	CGGM-KM	CGVM-KM	CGDVM-KM
Lower	3.270%	0.0218%	13.579%	0.0218%	5.599%	2.906%	0.00347%
Upper			13.532%	0.0153%	4.866%	1.841%	0.00250%
Average	3.270%	0.0218%	13.556%	0.0185%	5.233%	2.374%	0.00299%

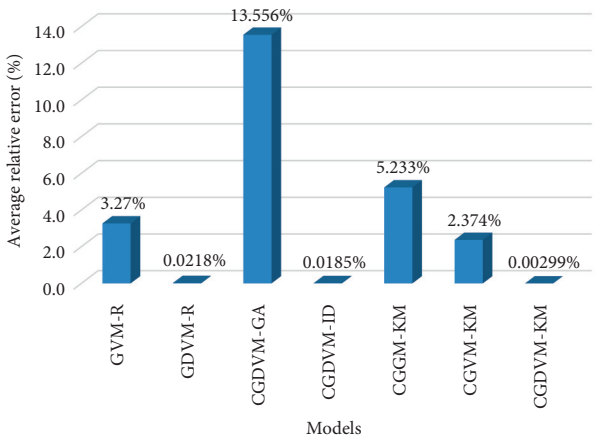

Figure 3: Prediction error of different models.

comprehensive average relative error is only 0.00299%, which belongs to the first-stage prediction accuracy (see Table 1). It is shown that the model can accurately simulate the number of the wounded in the massive earthquake disaster. Table 4 shows the whole simulation results.

In reality, we know that, with further development of rescue operations, some patients with minor injuries will gradually recover and withdraw from treatment, and some patients who are seriously injured will be sent to large hospitals with better medical conditions in safe areas for further treatment after simple treatment. Therefore, the overall number of the wounded will decrease slightly, and then the total number of patients will gradually maintain a relatively stable level. From the results of interval prediction, we can see that, after a period of time, the interval forecast data are stable at a value and no longer change, which is consistent with the actual situation.

From Table 4 and Figure 2, we can see that the model constructed in this paper has a good effect on forecasting the number of the wounded in the massive earthquake disasters. To further illustrate the effectiveness of this model, the prediction results of the model constructed in this paper are compared with the prediction results of other models. The following six models are selected for comparison: (1) the real number grey Verhulst model (GVM-R), (2) the real number grey discrete Verhulst model (GDVM-R), (3) the continuous interval grey discrete Verhulst dynamic model based on grey attributes (CGDVM-GA), (4) the continuous interval grey discrete Verhulst dynamic model based on information decomposition (CGDVM-ID), (5) the continuous interval grey GM (1,1) model based on kernels and measures (CGGM-KM), and (6) the continuous interval grey Verhulst model based on kernels and measures (CGVM-KM). Here, we divide the six models into three categories and compare them with the model constructed in this paper: the real number series models (i.e., model GVM-R and model GDVM-R), different interval whitening methods and the same prediction method models (i.e., model CGDVM-GA and model CGDVM-ID), and same interval whitening method and different prediction method models (i.e., model CGGM-KM and model CGVM-KM). The results are shown in Table 5 and Figure 3.

In the continuous interval grey prediction model, there are two key factors that affect the prediction accuracy: interval whitening method and grey prediction method. From Table 5, we can draw the following conclusions.

First, comparing with the real number grey prediction model, we find that the continuous interval grey prediction model has a higher prediction accuracy. This is because the whitening process of interval grey number can dig out more information from the data, and its prediction is more accurate. Second, under the same grey prediction method, we find that different whitening methods have a greater impact on the prediction results, and the whitening method based on kernels and measures has more advantages. This is because the whitening method is a way of interval data processing, and its purpose is to mine the information contained in interval data. The more the information is mined, the more accurate the prediction is. Finally, under the same whitening method, we find that different forecasting models have a great influence on the prediction results. The implied reason may be that the whitening method mines the interval data information, while the prediction method accurately and effectively fit the mined information, so as to predict the future trend. The grey discrete Verhulst model has more advantages than the grey GM (1,1) model and the grey Verhulst model. In summary, the continuous interval grey discrete Verhulst model based on kernels and measures (CGDVM-KM) constructed in this paper has the highest simulation accuracy.

6. Conclusions

The continuous interval grey number has a more complex data structure than the real number and discontinuous interval grey number, so it is more difficult to build a model with higher prediction accuracy. In this paper, through the analysis of the regularity and characteristics of the statistical data of the number of the wounded after the massive earthquake with saturated "S-shape" and its continuous interval dynamic change trend, we consider the kernels and measures whitening method and grey discrete Verhulst prediction model and construct a continuous interval grey discrete Verhulst dynamic prediction model based on kernels and measures to predict the number of the wounded after the massive earthquake disasters. Compared with other real number and interval prediction models, the results show

that the model constructed in this paper has higher prediction accuracy and better simulation effect and can more accurately and effectively simulate the number of the wounded after the massive earthquake disasters. Of course, the application of the prediction model is far more than the forecasting of the number of the wounded, and it has a good fitting for the data with saturated "S-shape" and continuous interval change trend.

At the same time, according to the research results of Feng et al. on the injury type and distribution data of the injured in Tangshan earthquake disaster and the medication data of the hospital for treating the injured in similar accidents, it can be seen that there is a linear correlation between the type and quantity of rescue drugs in earthquake disaster emergency rescue and the number of wounded people in an earthquake disaster [31]. Therefore, the continuous interval grey discrete Verhulst dynamic prediction model based on kernel sum measure can be used to predict the number of patients on the third day after the occurrence of Lushan earthquake disaster, and then, it is multiplied by the drug use coefficient of 40 kinds of conventional emergency relief drugs proposed in reference [31]. Finally, we can quickly and accurately calculate the type and quantity of emergency relief drugs on the third day after the Lushan earthquake disaster. Once the type and quantity of emergency relief drugs can be accurately and effectively, the headquarters and organizers of earthquake disaster relief will be able to timely and effectively allocate and supply the need for emergency relief medicines in earthquake-stricken areas, and the efficiency of earthquake disaster emergency relief can be improved.

Although we have constructed a model to effectively forecast the number of the wounded after massive earthquake disasters, the interval grey prediction model is a more complex model in the grey system theory, and there are many factors affecting its performance. Further optimization of the model is the direction of future research. In addition, the prediction of the number of the wounded is to better provide emergency relief materials, so how to more accurately correlate between the number of the wounded and materials needed is the focus of the next step.

Data Availability

The data used to support the findings of this study are included within the article.

Conflicts of Interest

The authors declare that there are no conflicts of interest.

Acknowledgments

This research was supported by the National Social Science Found of China (no. 10XGL013); Chongqing Social Sciences Planning Project (no. 2020TBWT09); Chongqing Municipal Education Commission Humanities and Social Sciences Research General Project (grant no. 18SKGH069); Scientific Research Start-up Foundation of Chongqing Technology and Business University (no. 1855016); Chongqing Doctoral Program of Social and Scientific Planning (no. 2018BS79); and Open Research Fund of Chongqing Key Laboratory of Electronic Commerce and Supply Chain System (1456026).

References

[1] S. Chen and C. Wang, "Incorporating a bayesian network into two-stage stochastic programming for blood bank location-inventory problem in case of disaster," *Discrete Dynamics in Nature and Society*, vol. 2019, Article ID 7214907, 2019.

[2] J. Zhang, C. S. Chen, and B. Zeng, "Demand forecasting of emergency medicines after the massive earthquake-a grey discrete Verhulst model approach," *Journal of Grey System*, vol. 27, no. 3, pp. 234–248, 2015.

[3] E. Kayacan, B. Ulutas, and O. Kaynak, "Grey system theory-based models in time series prediction," *Expert Systems with Applications*, vol. 37, no. 2, pp. 1784–1789, 2010.

[4] X. Wu and J. Gu, "A modified exponential model for reported death toll during earthquakes," *Earthquake Science*, vol. 22, no. 2, pp. 159–164, 2009.

[5] H. X. Wang, J. X. Niu, and J. F. Wu, "ANN model for the estimation of life casualties in earthquake Engineering," *Systems Engineering Procedia*, vol. 1, no. 1, pp. 55–60, 2011.

[6] M. Gul and A. F. Guneri, "An artificial neural network-based earthquake casualty estimation model for Istanbul city," *Natural Hazards*, vol. 84, no. 3, pp. 1–16, 2016.

[7] X. Huang, M. J. Luo, and H. D. Jin, "Application of improved ELM algorithm in the prediction of earthquake casualties," *Plos One*, vol. 15, no. 6, pp. 1–13, 2020.

[8] X. Huang, J. Y. Song, and H. D. Jin, "The casualty prediction of earthquake disaster based on extreme learning machine method," *Natural Hazards*, vol. 102, pp. 873–886, 2020.

[9] E. Firuzi, K. Amini Hosseini, A. Ansari, Y. O. Izadkhah, M. Rashidabadi, and M. Hosseini, "An empirical model for fatality estimation of earthquakes in Iran," *Natural Hazards*, vol. 103, no. 1, pp. 231–250, 2020.

[10] F. S. Zhang, F. Liu, and W. B. Zhao, "Application of grey Verhulst model in middle and long-term load forecasting," *Power System Technology*, vol. 5, pp. 37–40, 2003.

[11] Z.-X. Wang, Y.-G. Dang, and S.-F. Liu, "Unbiased grey verhulst model and its application," *Systems Engineering-Theory & Practice*, vol. 29, no. 10, pp. 138–144, 2009.

[12] L. Z. Cui, S. F. Liu, and Z. P. Li, "Grey discrete Verhulst model," *Systems Engineering and Electronics*, vol. 33, no. 3, pp. 590–593, 2011.

[13] M. Hashem-Nazari, A. Esfahanipour, and S. M. T. Fatemi Ghomi, "Non-equidistant "Basic Form"-focused grey verhulst models (Nbfgvms) for III-structured socio-economic forecasting problems," *Journal of Business Economics and Management*, vol. 18, no. 4, pp. 676–694, 2017.

[14] Z. X. Wang and Q. Li, "Modelling the nonlinear relationship between CO_2 emissions and economic growth using a PSO algorithm-based grey Verhulst model," *Journal of Cleaner Production*, vol. 207, pp. 214–224, 2018.

[15] R. Rajesh, "Social and environmental risk management in resilient supply chains: a periodical study by the Grey-Verhulst model," *International Journal of Production Research*, vol. 57, no. 11-12, pp. 3748–3765, 2019.

[16] L. Wu and Z. Xu, "Analyzing the air quality of Beijing, Tianjin, and Shijiazhuang using grey Verhulst model," *Air Quality Atmosphere and Health*, vol. 12, no. 8, pp. 1–8, 2019.

[17] B. Zeng, X. Ma, and M. Zhou, "A new-structure grey Verhulst model for China's tight gas production forecasting," *Applied Soft Computing*, vol. 96, 2020.
[18] R. Tian, Q. Shao, and F. Wu, "Four-dimensional evaluation and forecasting of marine carrying capacity in China: empirical analysis based on the entropy method and grey Verhulst model," *Marine Pollution Bulletin*, vol. 160, 2020.
[19] Y. F. Zhao, M. H. Shou, and Z. X. Wang, "Prediction of the number of patients infected with COVID-19 based on rolling grey Verhulst models," *International Journal of Environmental Research and Public Health*, vol. 17, no. 12, pp. 1–20, 2020.
[20] E. Liu, Q. Wang, X. Ge, and W. Zhou, "Dynamic discrete GM (1,1) model and its application in the prediction of urbanization conflict events," *Discrete Dynamics in Nature and Society*, vol. 2016, Article ID 3861825, 2016.
[21] W. Zhou and D. Zhang, "An improved metabolism grey model for predicting small samples with a singular datum and its application to sulfur dioxide emissions in China," *Discrete Dynamics in Nature and Society*, vol. 2016, Article ID 1045057, 2016.
[22] B. Zeng, S. Liu, and N. Xie, "Prediction model of interval grey number based on DGM (1, 1)," *Journal of Systems Engineering and Electronics*, vol. 21, no. 4, pp. 598–603, 2010.
[23] B. Zeng and S. F. Liu, "Prediction model of interval grey number based on its geometrical characteristics," *Journal of Systems Engineering*, vol. 26, no. 2, pp. 1654–1663, 2011.
[24] M. Zhang, H. Wu, Z. Qiu, Y. Zhang, and B. Li, "Demand prediction of emergency supplies under fuzzy and missing partial data," *Discrete Dynamics in Nature and Society*, vol. 2019, Article ID 6823921, 2019.
[25] C. Li, Y. Yang, and S. Liu, "A greyness reduction framework for prediction of grey heterogeneous data," *Soft Computing*, vol. 2, pp. 17913–17929, 2020.
[26] B. Zeng, G. Chen, and S.-f. Liu, "A novel interval grey prediction model considering uncertain information," *Journal of the Franklin Institute*, vol. 350, no. 10, pp. 3400–3416, 2013.
[27] B. Zeng, C. Li, G. Chen, and W. Zhang, "Verhulst model of interval grey number based on information decomposing and model combination," *Journal of Applied Mathematics*, vol. 2013, pp. 1–8, 2013.
[28] J. Ye, Y. Dang, and Y. Yang, "Forecasting the multifactorial interval grey number sequences using grey relational model and GM (1, *N*) model based on effective information transformation," *Soft Computing*, vol. 24, no. 7, pp. 5255–5269, 2020.
[29] L. Dang and L. I. Lin, "Prediction model of interval grey number based on kernels and measures," *Mathematics in Practice and Theory*, vol. 44, no. 8, 2014.
[30] B. Zeng, S. F. Liu, and J. Li, "An error inspection method for interval grey number prediction model based on kernel and interval length," in *Proceedings of the IEEE International Conference on Grey Systems and Intelligent Services*, Nanjing, China, October 2011.
[31] H. Feng, J. Li, S. Chen, M. Liu, and X. Sun, "Demand analysis of drugs for earthquake injury treatment," *Journal of Pharmaceutical Practice*, vol. 21, no. 2, pp. 100–102, 2003.

Hindawi
Discrete Dynamics in Nature and Society
Volume 2021, Article ID 6653051, 9 pages
https://doi.org/10.1155/2021/6653051

Research Article

A GD-PSO Algorithm for Smart Transportation Supply Chain ABS Portfolio Optimization

Yingjia Sun[1] **and Hongfeng Ren**[2]

[1]*University of Science and Technology of China, Hefei 230009, China*
[2]*Anhui Joyin Information Technology Co., Ltd., Hefei 230009, China*

Correspondence should be addressed to Yingjia Sun; sunyingjia@joyintech.com

Received 16 November 2020; Revised 2 March 2021; Accepted 22 March 2021; Published 1 April 2021

Academic Editor: Lu Zhen

Financial technology and smart transportation is key cross-field of transportation in the future. The demand for smart transportation investment is constantly released. As typical and efficient financial products, asset-backed securities (ABS) can greatly improve the turnover efficiency of funds between upstream suppliers and downstream buyers in the field of smart transportation and also help participants of the supply chain to maintain healthier financial situations. However, one of the most common problems of ABS is portfolio allocation, which needs portfolio optimization based on massive assets with multiple objectives and constraints. Especially, in the field of smart transportation, sources of underlying assets can always be complex, which may involve a variety of subdivision industries and regions. At the same time, due to the relationships between upstream and downstream entities in the supply chain, correlations among assets can be strong. So, during the optimization of smart transportation ABS portfolio allocation, it is necessary to identify and deal with those problems. Different from forward selection or linear optimization, which could have low efficiency for complicated problems with large sample size and multiple objectives, new methods and algorithms for NP-hard problems would be necessary to be investigated. In this article, a penalty function based on graph density (GD) was introduced to the particle swarm optimization algorithm (PSO), and a GD-PSO algorithm was proposed. Experiments also showed that the GD-PSO algorithm solved the problem of portfolio optimization in smart transportation supply chain ABS effectively.

1. Introduction

Smart transportation has been developed rapidly as a new field in China. The field of smart transportation involves a wide range of areas, including dozens of industries, such as transportation, construction, equipment manufacturing, information technology, leasing, and finance. Project operation often involves the flow of a huge volume of materials and funds between upstream and downstream entities. Supply chain financing is naturally a necessary mode of financial services in smart transportation. The application of asset-backed securities (ABSs) in this field is a good example with an innovative form, that is, based on a much better credit status of a downstream buyers entity or group, the accounts receivable held by the upstream suppliers can bring static expected cash flow in the future. By issuing ABS with those liabilities as underlying assets on the capital market, funds can be raised with lower interests and higher efficiency. Compared with traditional financing methods, another important advantage of supply chain ABS is that it usually has a credit guarantee from the core enterprises member with higher credit rating, which can greatly improve the ABS rating and control financial risks on the market.

Du and Zhou [1] studied the feasibility of supply chain ABS in China and got positive results about its application. Liang [2] also discussed the advantages of supply chain ABS of accounts receivable for small- and medium-sized enterprises in the transportation industry. Yang [3] found that it would be active and useful to employ financial leasing mode

for smart transportation projects, especially in the way of ABS. With rapid developments of smart transportation, the amount of ABS issued in this field was also increasing year by year (Figure 1).

However, the underlying assets of ABS usually have the following characteristics: small amount, high variation, and short term. After securitization, it is very likely to produce problems of mismatch between assets and the design of ABS, which can lead to short coverage of asset cash flow to securities payment, and the repayment risk of ABS can increase accordingly. Therefore, more and more ABS on the market are running with a circular purchase structure. The so-called circular purchase means that cash flow generated by underlying assets within a specific period of time is not fully used to pay to the investors. Instead, it is used to purchase new qualified underlying assets continuously.

At the same time, circular purchase in ABS is not a simple repeat purchase of underlying assets with funds in trust accounts accumulated by cash inflow of underlying assets purchased earlier, but a complicated transaction decision with multiple objects and constraints such as maximized amount, optimized structure, and controllable risks. For some smart transportation supply chain ABS, these decisions should be made every day. So, selecting assets from hundreds, thousands, or even millions of loans meeting those requirements has been a difficult problem because the amount of computation is huge and the objectives and constraints are complex and can contradict each other on some level.

What is more, in the field of smart transportation supply chain ABS, there are more difficulties raised from the relationships between upstream and downstream companies, entities with parallel positions, or other obligatory relationships in the supply chain. This means that the allocation of portfolio and control of granularity of assets will affect the risk exposures of portfolios directly.

As a result, in practice, only for ABS with a small number of assets, portfolios allocation could be made by setting simple screening rules to determine whether or not to select a single asset or sorting assets based on some dimensions and then dividing the whole parent pool. Although this method was useful for ABS with a few underlying assets, it would never meet all the requirements at the same time in complex situations, such as the total balance, amount of weighted average life, and diversification with a parent assets pool with a large number of samples. Another important drawback of this approach was the inability to optimize. For example, the size of the circular purchase package could be too small, the balance left in the trust special account could be too high, which would lead to excessive costs of deposition; or the final asset package might meet the requirements of weighted average age, maximum scale, and so on., but it did not reach the optimal diversification or reduce the risk of the portfolio to a level as low as it could be.

To solve the problems in portfolio selection and optimization in ABS with a circular purchase structure, researchers have conducted relatively few studies; a few studies about the ABS market in China are expected. Lei [3, 4] revealed that a circular purchase could face difficulties with

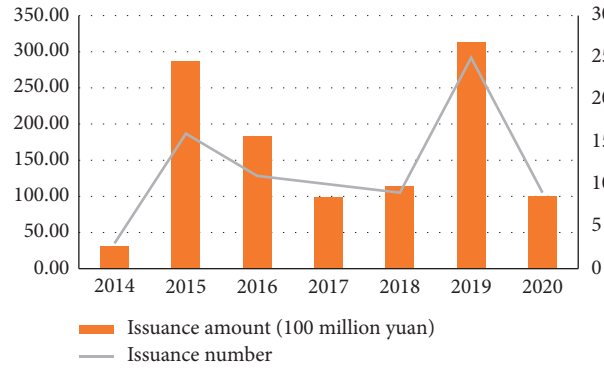

Figure 1: Supply chain ABS issuance (100 million yuan).

accounting. With more details, Lu Binbin [5, 6] discussed the motivation for circular purchase and potential problems during product design. At the same time, risks unique to the structure of circular purchase were analyzed, and the shortage of underlying assets supply as a primary problem was pointed out. Lu [7, 8] also provided suggestions on operations of circular purchase in ABS portfolio construction, focusing on building up an automatic and intelligent system; otherwise, the high-frequency circular purchase can not be realized.

About the optimization methods, with the introduction of genetic algorithms, tabu search, simulated annealing, neural networks, and a series of traditional or intelligent optimization algorithms, the efficiency and results of portfolio optimization had been improved greatly. For example, Chang et al. [9] developed heuristic algorithms based on genetic algorithms, tabu search, and simulated annealing and investigated the characteristics of the efficient frontiers. It was shown that problems could be harder with particular constraints but still could be solved even with discontinuous efficient frontiers. Fernández and Gómez [10] applied a neural network algorithm to the problem of portfolio selection with a given number of assets and limited capital amount. The algorithm performed well and showed some advantages compared with previous methods. The particle swarm optimization (PSO) algorithm was built up based on the principle of how bird swarms search in space [11] and could solve nonlinear optimization problems efficiently with fast convergence speed, especially in a high-dimensional space. Cura applied it to the optimization of venture capital portfolio and got positive results in efficiency and effectiveness [12]. However, although the PSO algorithm occupied some advantages for problems with a huge number of assets, it did not consider the relationships between dimensions, which could always be one of the most important facts for portfolio optimization of smart transportation supply chain ABS.

Considering those problems during the optimization of portfolios in smart transportation supply chain ABS, graph density (GD) was introduced to describe the correlations between assets and the objective function was rewritten by adding a penalty term based upon GD. Then, an algorithm based on PSO and Graph GD (GD-PSO) was proposed in

this article. The experiments showed that the NP-hard problem with large sample size in smart transportation supply chain ABS portfolio optimization had been solved efficiently with GD-PSO. Compared with simple PSO and forward selection algorithm, GD-PSO showed obvious advantages in convergence and efficiency. Thus, with the algorithm of GD-PSO, the multiple requirements, including high frequency, volume optimization, cost management, and risk control, in portfolio allocation for smart transportation supply chain ABS had been met, and better results were achieved.

In the following components of this article, the problem description, mathematical formulation, and algorithm design are provided in Section 2. In Section 3, a computational example and the comparison between GD-PSO and pure PSO method are discussed. Conclusions are shown in Section 4.

2. Model Design

2.1. Problem Description and Mathematical Model. Based on the analysis of smart transportation ABS issued in China, considering the characteristics of product form, issuing mechanism, debtor and creditor selection, cash flow collection and distribution, supplier subsidy, and so on, constraints and objects should be considered in the issuance and circular purchase of smart transportation supply chain ABS as discussed in this article.

2.1.1. Constraints in Smart Transportation Supply Chain ABS Portfolio Allocation

(1) Total Balance of Underlying Assets. For the issuance or circular purchase of supply chain ABS, there are often requirements of upper limits about total assets in the balance sheet of the portfolio. For ABS, which adopts a storage shelf mechanism as early as the time of applying for issuance, there has been a clear agreement on the total and circular purchase amount of underlying assets, meaning that the issued or circularly purchased assets can never exceed the upper limit of the agreed total or residual amount. Especially for products with circular purchase mechanism, funds for circular purchase often come from the balance of a special account held by a trust institution and usually get limits to keep the account still having funds after circular purchases, with a certain coverage rate to unpaid principal and interests of the ABS. An inequality for constraints in total amount was formed as follows:

$$\sum_{i=1}^{i=k} \mathrm{BAL}_i \le \mathrm{TBAL}_{\mathrm{ul}}, \tag{1}$$

where k was the number of accounts receivable included in the selected portfolio, BAL_i was the balance of a single asset i selected into the portfolio. $\mathrm{TBAL}_{\mathrm{ul}}$ was the upper limit of assets to be issued or circularly purchased due to the issuance declaration, trust account balance, and so on..

(2) Age of Accounts Payable. For entities located at the downstream stage of a supply chain, liabilities selected into the ABS portfolios should be repaid before the payment day of the ABS. Therefore, to extend the account period successfully, the number of days from issuance or circular purchase to the next payment day of ABS should be longer than the ages of liabilities involved in the ABS as underlying assets. Let $\mathrm{TERM}_{\mathrm{ul}}$ be the number of days to the payment day of ABS and TERM_i the age of assets i in the portfolio; then, the constraint about the age of accounts payable should be as follows:

$$\max\left(\mathrm{TERM}_i,\ 1 \le i \le k\right) \le \mathrm{TERM}_{\mathrm{ul}}. \tag{2}$$

At the same time, considering the cost of financing, the weighted average life was required not to exceed a certain value. Since there were generally no interest costs in the accounts payable itself, only age distribution needed to be discussed. Let the amount of weighted life of assets included in the portfolio be WTERM, the average interests rate of capital for the debtor during the period of ABS (T) be R, and, with the considering of excess subsidy to suppliers, the financing cost of ABS be RABS, while it was issued; then, financing costs savings of downstream buyers should be $R * \text{Portfolio size} * (T - \text{WTERM}) - \text{RABS} * (\text{Portfolio size}) * T$. If those savings were required to be greater than 0, or a certain value, while other variables in the formula were determined, WTERM would have an upper limit. That is to say, when the amount and costs of financing were fixed, only if the amount of weighted average life of those assets in the portfolio was below a certain threshold, aims of financing costs saving and liquidity pressure relieving could be achieved. The constraint condition in amount of weighted average life was shown in the following:

$$\frac{\sum_i^k \mathrm{TERM}_i \times \mathrm{BAL}_i}{\sum_i^k \mathrm{BAL}_i} \le \mathrm{WTERM}_{\mathrm{ul}}. \tag{3}$$

(3) Asset Diversification. For supply chain ABS, there was usually only one ultimate debtor that was qualified and with a large scale. However, the repayments generally came directly from different child companies or projects. In order to control risk concentration and meet regulatory requirements better, the ABS portfolio was usually required to be build up from underlying assets with diversification to a certain level. For example, according to the region or project type of the direct debtors, the percentage of accounts payable in each type could not exceed a critical value. This kind of constraint was expressed as follows:

$$\max\left(\frac{\sum_{m=1}^{m_j} \mathrm{BAL}_{mj}}{\sum_{i=1}^{k} \mathrm{BAL}_i},\ 1 \le j \le J\right) \le \mathrm{PAR}_{\mathrm{ul}}, \tag{4}$$

where J was the number of assets categories and BAL_{mj} was the balance of accounts payable m in category j of selected assets. $\mathrm{PAR}_{\mathrm{ul}}$ was the upper limit allowable for the proportion of accounts payable balances under each category.

2.1.2. Objects in Smart Transportation Supply Chain ABS Portfolio Allocation. Even if the requirements of those three basic constraints discussed above were met, it was still impossible to guarantee that the portfolio allocated was the best solution. For example, the size of the assets could be too small, which might lead to the lack of financing optimization effect. At the same time, it would not guarantee the optimization of asset diversification. Therefore, the following optimization objectives were added to the model.

(1) Maximized Asset Size. In order to improve the effect of financing optimization and alleviate the liquidity pressure of downstream entities in the supply chain, it was required to issue or circular purchase assets as large as possible to meet the upper limit of the scale. At the same time, the larger the purchase scale, the less the remaining funds in the special account and the lower the cost of keeping a balance with no interests in the trust account. The mathematical description of the optimization objective was shown as follows:

$$\begin{aligned} &\text{Let } A \in Z_0,\ B \in Z_0,\ A \neq B,\ a \in A,\ b \in B, \\ &\qquad \text{then sum}\left(\text{BAL}_a\right) \geq \text{sum}\left(\text{BAL}_b\right), \end{aligned} \tag{5}$$

where Z_0 was the collection of all accounts payable portfolios that meet the constraints with A and B as any two unique portfolio collections belong to it. Let A be the collections of optimal portfolios but B not, with a as any one optimal portfolio in A and b as any one portfolio in B which was not optimal; then, the total balance of portfolio a should always be larger than b.

(2) Maximized Asset Diversification. Portfolio risks usually involved a factor positively related to the correlation coefficient of individual assets. The higher the homogeneity of assets, the higher the degree of portfolio risk. Therefore, to get optimal portfolio allocation, it was necessary to minimize the correlation between assets, that was, to improve the diversification of assets. The optimization object of diversification was expressed as follows with the strength of assets correlation denoted as σ:

$$\begin{aligned} &\text{Let } A \in Z_0,\ B \in Z_0,\ A \neq B,\ (i,j) \subset A,\ (k,l) \subset B, \\ &\qquad \text{then sum}\left(\sigma_{ij}\right) \leq \text{sum}\left(\sigma_{kl}\right), \end{aligned} \tag{6}$$

where Z_0 was still a collection of all accounts payable portfolios that meet constraints, A was a collection of optimized accounts payable portfolio, B was a collection of nonoptimized portfolios different from A. (i, j), (k, l) are any pair of assets in A and B, respectively. Assets correlation strengths between (i, j), (k, l) were described as σ_{ij}, σ_{kl}.

Finally, the portfolio should be as close as possible to the optimization objects described in (5) and (6) and satisfy constraints in (1)–(4).

2.2. A GD-PSO Algorithm. For the asset portfolio optimization of smart transportation supply chain ABS, the degree of asset diversification should always be considered; that was, the relationships between assets should be introduced to the algorithm appropriately. A traditional method was to calculate the correlation coefficient between assets and to construct related terms in a function to quantify the relationships between assets. However, for accounts payable in supply chain finance, the relationships between them were difficult to quantify due to the lack of long-term, high-quality historical data. Another method was to calculate the Herfindahl–Hirschman Index (HHI), but the range of the coefficient was between $(1/P, 1)$, with P as the number of asset categories contained in the portfolio. Because the number of assets and the number of asset categories were likely to be different in different portfolios from every single iteration, there would be no strict comparability in HHI with the continuous adjustment of the portfolio during the process of optimization.

To solve those problems, we proposed an algorithm that integrated PSO and graph density theory (GD-PSO), which successfully solved the difficulty of measuring the relationships between underlying assets of smart transportation supply chain ABS. The two optimization objects of asset size and asset diversification were mixed into a single one, which could further improve the optimization results and the convergence speed of the PSO algorithm at the same time.

2.2.1. Objective Function with Density Penalty Term Based on an Incomplete Graph. The diagram in Figure 1 showed the relationships between liabilities belonging to the same or different categories (regions and debtors as examples), where the central nodes represent the debtor's regions, nodes in the middle layers represent the debtors, and outer nodes represent accounts payable (assets).

One type of debtor could correspond to one or more debtors, and one debtor could also correspond to one or more assets. In this incomplete graph, the number of edges connecting nodes could be used to define the GD of the nearby regions of those nodes. However, each asset has only one edge connected to the debtor to which it belongs and which was directly related to other assets. A debtor was also connected only to the region to which it belongs and which was directly connected to other debtors. In this situation, regions, debtors, and assets actually constituted a space of tree with three layers. The degree of association between assets could ultimately be traced back to the root node, that is, the similarities and differences between the debtor's region. Thus, the degrees of correlation between assets could be measured with the density of the region around the root node, that is, the sum of its edges. At the same time, because the number of liabilities under each debtor's name was different, these edges should have different weights, which could be quantified by the proportion of the number of assets under the debtor's name to the amount of the whole asset pool. After adjusting the density of the area around the root node to the weighted sum of the edges, the variable of density, which was recorded as D_{root}, was shown in the following function:

$$D_{\text{root}} = \frac{\sum_{c=1}^{C}\left(\sum_{i=1}^{I} a_{ci}\right) \times 1}{\sum_{i=1}^{N} a_i}, \tag{7}$$

where D_{root} was the relative weighted sum of the number of edges corresponding to the root node of asset category. Asset a, for example, was belonging to debtor c, and debtor c was belonging to region L, which was a node denoted as node_L. The number of edges connected to node_L was C, corresponding to the number of C debtors. The weight of each edge corresponded to the proportion of assets held by the debtor in the entire pool. The density of the surrounding area of the asset a was defined as the proportion of assets in a group formed by assets under the names of debtors in category L to all assets.

From the viewpoint of practical application, the density value was exactly equal to the proportion of the asset amount under the root node of its debtor's category to the whole parent pool, which was very intuitive and easy to understand. That was also meaningful because assets that belong to a category with a relatively large number and high balance of assets would be more likely to get the pooling of risk and in danger of having assets being default concurrently. For the optimal object of maximizing risk diversification, the degree of risk concentration should be punished in the process of iteration.

Considering the penalty term based on the GD defined above, the formula of the objective function with matrix operations was shown in the following:

$$\text{obj}(X_i) = wb \cdot \text{round}(X_i)' - (1-w)D_{\text{root}} \cdot \text{round}(X_i)', \tag{8}$$

where b was an N-dimensional vector with the balance of each asset in the parent pool as an element, X_i was the solution of portfolio allocation in ith iteration, w was the weight related to the priorities of the objects in maximizing portfolio balance or diversification, and D_{root} was an N-dimensional vector representing the density around each asset, which was described in formula (7). The notation "$\cdot$" represents the dot product of two vectors and round was the rounding function to round a number to the nearest integer.

Compared with the objective function of scale optimization in formula (5), the second term was added as the penalty term in formula (8), which would integrate the optimal object of scale and diversification and improve the convergence rate at the same time. Weight w was used to control the priority of objects in scale and diversification. The requirement of scale maximization was usually prior to diversification in portfolio allocation of smart transportation supply chain financial ABS, so w was usually set as a number close to 1. However, in order to ensure the significance of the penalty term, w should not be too large.

2.2.2. GD-PSO Optimization Algorithm for Smart Transportation Supply Chain ABS Portfolio Allocation. Based on the mathematical model and methods described above, the steps of the GD-PSO algorithm were as follows:

(a) Let the whole parent pool as the search space, a certain number (recorded as M) of portfolios were generated randomly as the starting position of the spatial search. With N as the number of assets in the parent pool, each portfolio was a vector of N dimensions. When a portfolio contained a certain asset, the corresponding element of the vector would be recorded as 1, else as 0. It should be noted that in order to improve the accuracy of the optimization algorithm, the integer programming problem was transformed into a noninteger problem, and the solution on each dimension was allowed to be numbers between 0 and 1 in the iterative process. When calculating the results of objective and constraint functions, numbers in the solution vector were rounded to the nearest integer; that is, if it was less than 0.5, the number was set to 0, else to 1. The initial portfolio was described as follows:

$$X_i = \left(x_i^1, x_i^2, \ldots, x_i^N\right), \quad i = 1, 2, \ldots, M, \tag{9}$$

where the solution of the portfolio allocation on asset n in the ith iteration was denoted as x_i^n and the vector of the solution in the ith iteration was X_i.

(b) The optimal objective function value of each portfolio was calculated, and the positions of the best portfolio and swarm, with constraints met and minimum objective function value obtained in an iteration, were denoted as X_{best} and G_{best}, respectively. If there was no portfolio meeting constraint conditions in an iteration, one or multiple portfolios closest to the constraint condition would be selected, and then one portfolio with the minimum objective function would be set as the best position. For two or more portfolios that obtain the minimum objective function value simultaneously, one of them would be selected as X_{best} randomly.

(c) With the best individual and swarm position at X_{best} and G_{best}, other portfolio vectors in the space as probe particles would "fly" to them at the speed described in formula (10) to form a number of M new points in the N-dimensional space, which was another set of portfolio vectors for the next iteration, as shown in formula (11). Then, step b is repeated to get the optimal portfolio location X_{best} and the optimal portfolio swarms location G_{best} again for the next iteration.

$$\begin{aligned} v_{i+1} = {} & w_{\text{pso}} v_i + c_1 * \text{rand}_1\left(p\text{best}_i - x_i\right) + c_2 \\ & * rand_2\left(g\text{best}_i - x_i\right). \end{aligned} \tag{10}$$

v_{i+1} was the velocity of particles in the $i+1$th iteration dependent on the velocity of last iteration with an inertial weight w_{pso}, on the distance to the best individual and swarm positions with learning weights c_1 and c_2. Two $u(0,1)$ distributed random variables were denoted as rand_1 and rand_2.

Then, the positions of the portfolios for the $i+1$th iteration should be as follows:

$$X_{i+1} = X_i + v_i. \tag{11}$$

(d) Repeat steps b and c, until the convergence condition or the upper limit of the number of iterations is

Figure 2: Asset relationships in parent asset pools.

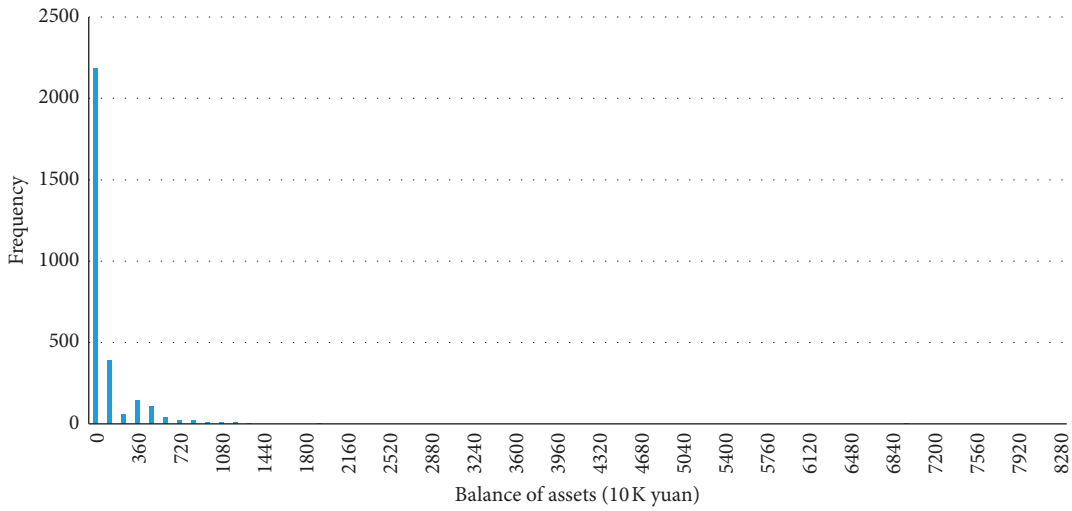

Figure 3: Distributions of assets in the parent pool: balance of assets.

reached. Then, the optimal portfolio allocation was obtained.

3. Computational Experiments

According to the data of issued ABS, the parent asset pool composed of 1000 accounts payable was built with a total balance at 1.61368 billion yuan, weighted average life of 160.20 days, maximum percentage of a region assets at 26.40, and the maximum life at 604 days. In Figures 2 and 3, it was shown that the balance, life, and region of individual assets could vary largely in the parent pool, which was according to the characteristics of real static pools of smart transportation ABS underlying assets on the market. For example, the average balance was 1.61 million yuan, but with a standard deviation of 2.87 million yuan and minimum and maximum values at 0.50 and 69.77 million yuan, respectively. As to the lives of assets, the average value was 147.57 days, while the standard deviation reached 109.92 days and minimum and maximum values spread from 1 to 604 days.

At the same time, those sample assets were also copied and added to the initial asset pool and another two parent pools with 2000 and 3000 samples were formed. Those parent pools had a larger sample size but had the same sample structure as the initial one. So, they were comparable to the initial one and could be used to test the performance of the algorithm in higher-dimensional spaces. The distribution of the parent pool was shown in Figures 2 and 3.

Formula (8) was applied as the objective function, while formulas (1), (3), (4) were as constraint functions. As to the life of the liabilities, because the legal period of supply chain ABS could be longer, for example, two years, all liabilities in the parent pool can meet the constraint requirement in (2) with the maximum life of 604 days. Therefore, the constraints in formula (2) are no longer added. Constraints and related thresholds were set as described in Table 1.

Set the number of points in the initial space N to be 50 and the minimum step of the objective function before search terminated to be $10\ e-8$. Since the elements in the final solution should be integers, the minimum step size of the best swarm's position could be appropriately amplified to 0.2. The inertial weight w was set to 0.5, while the learning factors of c_1 and c_2 were set to be 0.8. With those parameter settings, the steps of the GD-PSO algorithm described in 3 were followed and results were shown in Tables 2 and 3 and Figure 4.

Results in Table 2 show that, with the same samples, when objective and constraint functions were fixed, no

Table 1: Constraints and thresholds used in data validation.

Constraints	Variable name	Critical value		
		Sample size = 1000	Sample size = 2000	Sample size = 3000
Maximum amount of portfolio (10,000 yuan)	$WTERM_{ul}$	100000	200000	300000
Weighted average life limit (days)	$TBAL_{ul}$	150	150	150
Maximum percentage of a region (%)	$PAR(location)_{ul}$	30	30	30
Maximum percentage of a debtor (%)	$PAR(lender)_{ul}$	15	15	15

Table 2: Comparison of GD-PSO and PSO algorithm results.

Algorithm	Sample size	Maximum number of iterations	Optimal number of iterations	Total portfolio size (10,000 yuan)	Assets	Weighted average life (days)	The maximum percentage of a region	The maximum percentage of a debtor	Duration (s)
PSO	1000	100	No convergence	—	—	—	—	—	—
	1000	500	No convergence	—	—	—	—	—	—
	1000	2000	No convergence	—	—	—	—	—	—
	1000	19	No convergence	99998.79	563	141.80	28.05	5.50	9.61
GD-PSO	1000	100	19	99999.13	592	146.37	24.57	6.56	9.33

Table 3: GD-PSO performance testing of algorithms.

Algorithm	Sample size	Maximum number of iterations	Number of iterations to convergence	Total amount in portfolio (10,000 yuan)	Number of assets	Weighted average life of assets in the portfolio (days)	Maximum percentage of a region	Maximum percentage of a debtor	Time consumed to convergence (s)
GD-PSO	1000	100	19	99999.1303	592	146.37	24.57	6.56	9.337
	2000	100	22	193179.8014	1121	146.627	26.64	4.95	6.96
	3000	100	22	281108.8644	1618	148.777	26.40	3.05	7.44

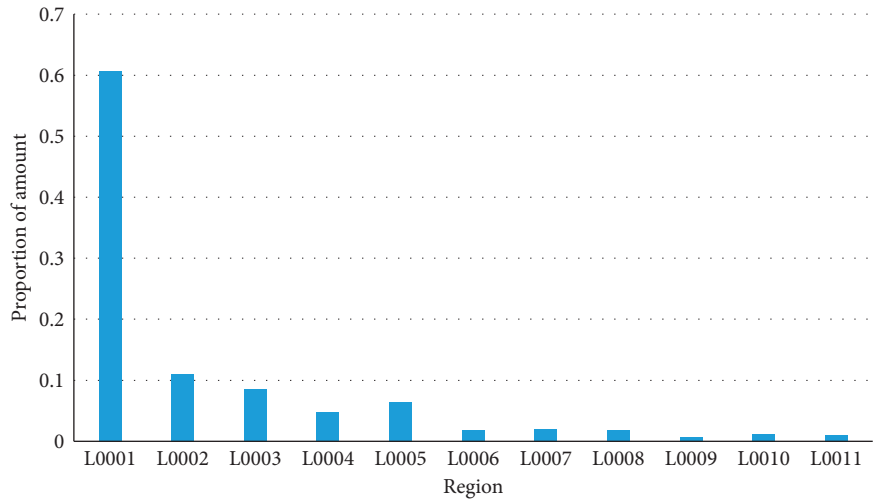

Figure 4: Distribution of assets among different regions.

convergence could be reached after 100 iterations in a 1000-dimensional space with a simple PSO algorithm, while the GD method was not introduced. Even if the number of iterations was increased to 2000, the convergence result still could not be obtained. However, when the GD-PSO algorithm was applied, only 19 iterations were

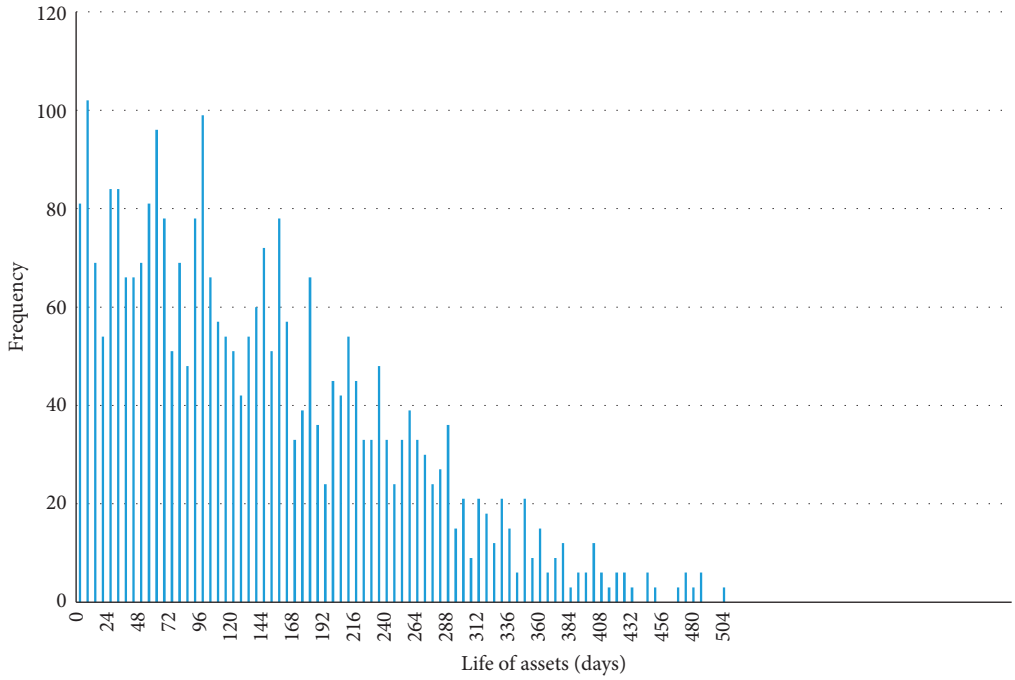

Figure 5: Distributions of assets in the parent pool: life of assets.

necessary to reach convergence. At the same time, when the number of iterations was kept the same, with the GD-PSO algorithm, the result of optimal portfolio balance (999,987,863 yuan, after 19 iterations) was better than that with the pure PSO algorithm (999,991,303 yuan, after 19 iterations). Regarding the degree of diversification, GD-PSO also showed advantages superior to PSO. It could also be found in Table 2 that with GD-PSO, the maximum percentage of assets in a region (24.57) was lower than the result of PSO (28.05). Moreover, in Figure 5, the result of pure PSO showed 9 visible root nodes, while the number for GD-PSO algorithm was 11. The number of assets connected to a single root node was increased in the diagram of GD-PSO (with an average number of 53.82 to 51.18 in PSO), which means that the degree of diversification in the optimal result of GD-PSO was improved. In terms of time performance, with the same number of iterations, GD-PSO algorithm still took less time than PSO. That could be related to the penalty term in the objective function of the GD-PSO algorithm, which could make the differences between portfolios more significant and then allocate the best solution of a nonlinear problem more efficiently.

As shown in Table 3, it was found that the performance of the GD-PSO algorithm was not significantly reduced by increasing the sample size of the parent asset pool from 1000 to 2000 or even 3000, while the sample structure, parameters, and constraint and objective functions were kept unchanged. Those results mean that in higher-dimensional spaces, the GD-PSO algorithm could still meet the requirements of supply chain ABS portfolio allocations and achieve optimal objects.

4. Conclusions

In this article, portfolio optimization of smart transportation asset-backed securities was modeled as a high-dimensional nonlinear optimization problem with multiple objects and constraints, and correlations between risky assets were considered. Based on particle swarm optimization algorithm, graph density measurement and penalty function were introduced and the GD-PSO algorithm was proposed. Compared with simple PSO, GD-PSO provided better optimal results with greatly improved computation efficiency. However, there were still some limitations with this method. For example, the graph density was calculated based on the whole parent asset pool and was a static measurement, while during the processes of spatial search and iteration, the vectors of portfolios were dynamic. To further improve the performance and accuracy of portfolio allocations for ABS in smart transportation ABS and other fields, in future studies, more investigation will be done regarding the density measurement in a dynamic space and its application in the optimization algorithm.

Data Availability

The data come from a supply chain financial technology company in China and cannot be made publicly available due to confidentiality requirements.

Conflicts of Interest

The authors declare that they have no conflicts of interest.

References

[1] J. Du and X. Zhou, "Discussion on the possibility of asset securitization under supply chain finance," *Economic Research Guide*, vol. 10, no. 7, pp. 159-160, 2014.

[2] L. Liang, "Actively promote supply chain innovation and application: analysis of supply chain asset securities," *Bonds*, vol. 7, no. 7, pp. 81–86, 2018.

[3] S. Yang, "Investment and financing analysis PPP urban smart transportation monitoring system," *Construction Transport and Transportation*, vol. 33, no. 1, pp. 66-67, 2017.
[4] X. Lei, "Discussion on accounting treatment of asset securitization," *China CPA*, vol. 5, pp. 91–95, 2017.
[5] B. J. Keys, A. Seru, and V. Vig, "Lender screening and the role of securitization: evidence from prime and subprime mortgage markets," *Review of Financial Studies*, vol. 25, no. 7, pp. 2071–2108, 2012.
[6] Lu, "Difficulties in design and operational countermeasures of circular purchase structure of asset securitization," *Shanghai Finance*, vol. 7, pp. 84–87, 2017.
[7] S. Malamud, H. Rui, and A. Whinston, "Optimal incentives and securitization of defaultable assets," *Journal of Financial Economics*, vol. 107, no. 1, pp. 111–135, 2013.
[8] Lu, "A practical application analysis of circular purchase structure of asset securitization," *Fujian Finance*, vol. 9, pp. 40–44, 2017.
[9] T.-J. Chang, N. Meade, J. E. Beasley, and Y. M. Sharaiha, "Heuristics for cardinality constrained portfolio optimisation," *Computers & Operations Research*, vol. 27, no. 13, pp. 1271–1302, 2000.
[10] A. Fernández and S. Gómez, "Portfolio selection using neural networks," *Computers & Operations Research*, vol. 34, no. 4, pp. 1177–1191, 2007.
[11] J. Kennedy and R. C. Eberhart, "Particle swarm optimization," in *Proceedings of the IEEE International Conference on Neural Networks*, Perth, Australia, 1995.
[12] T. Cura, "Particle swarm optimization approach to portfolio optimization," *Nonlinear Analysis: Real World Applications*, vol. 10, no. 4, pp. 2396–2406, 2009.

Hindawi
Discrete Dynamics in Nature and Society
Volume 2021, Article ID 6675785, 13 pages
https://doi.org/10.1155/2021/6675785

Research Article

Insights on Crash Injury Severity Control from Novice and Experienced Drivers: A Bivariate Random-Effects Probit Analysis

Daiquan Xiao,[1] Quan Yuan,[2] Shengyang Kang,[1] and Xuecai Xu [1]

[1]*School of Civil and Hydraulic Engineering, Huazhong University of Science and Technology, Wuhan, China*
[2]*State Key Laboratory of Automotive Safety and Energy, School of Vehicle and Mobility, Tsinghua University, Beijing, China*

Correspondence should be addressed to Xuecai Xu; xuecai_xu@hust.edu.cn

Received 3 November 2020; Revised 19 November 2020; Accepted 15 March 2021; Published 29 March 2021

Academic Editor: Tingsong Wang

This study intended to investigate the crash injury severity from the insights of the novice and experienced drivers. To achieve this objective, a bivariate panel data probit model was initially proposed to account for the correlation between both time-specific and individual-specific error terms. The geocrash data of Las Vegas metropolitan area from 2014 to 2017 were collected. In order to estimate two (seemingly unrelated) nonlinear processes and to control for interrelations between the unobservables, the bivariate random-effects probit model was built up, in which injury severity levels of novice and experienced drivers were addressed by bivariate (seemingly unrelated) probit simultaneously, and the interrelations between the unobservables (i.e., heterogeneity issue) were accommodated by bivariate random-effects model. Results revealed that crash types, vehicle types of minor responsibility, pedestrians, and motorcyclists were potentially significant factors of injury severity for novice drivers, while crash types, driver condition of minor responsibility, first harm, and highway factor were significant for experienced drivers. The findings provide useful insights for practitioners to improve traffic safety levels of novice and experienced drivers.

1. Introduction

According to the National Center for Statistics and Analysis (NCSA), each year, it is estimated that 25,000 people got killed in motor vehicle crashes, and the trend tends to cause a 9% increase. Among these crashes, novice drivers account for a large proportion, whose risk per mile driven is nearly 3 times greater than that of experienced drivers, especially in the first 6 months when licenses are issued [1]. Furthermore, novice drivers are easily influenced by a variety of factors, such as various distractions (e.g., neon lights and billboards) along the roadways, smartphones, and online chatting, which causes more severe injury than experienced drivers. A variety of factors affect the injury severity, including human (drivers, pedestrians, and bicyclists), vehicles, roadway, and environment, but novice and experienced drivers may cause different injury severity levels because of the personal features and factors. However, the identification and determinants of injury severity among novice and experienced drivers have not been uniformly recognized, although various scholars have explored different aspects of novice drivers, experienced drivers, or both. Moreover, for the injury severity levels, there may exist interrelations between their unobservables of both groups; thus, how to estimate the two (seemingly unrelated) injury severity levels simultaneously and to control for interrelations between their unobservables may be challenging. Therefore, it is necessary to investigate and determine the influencing factors of injury severity for novice and experienced drivers so that some general consensus can be reached, and the interrelations can be addressed.

From the beginning of this century, the crash analysis of novice drivers has been very active. Ferranteet et al. [2] explored the relationship among novice drink drivers, recidivism, and crash involvement using multivariate survival analysis. The results found that if a driver's first drink driving offense occurred at a younger age, he/she was significantly more likely to drink, drive, and crash again. After that, Simons-Morton et al. [3] described the effects of the Checkpoints Program on parent limits on novice teen

driving through six months after licensure. It was found that it was possible to foster modest increases in parental restrictions on teen driving limits during the first 6 months of licensure, but the level of restriction was not sufficient to protect against violations and crashes. Continued with the crashes of novice teenage drivers, Braitman et al. [4] identified the characteristics and contributing factors leading to crashes of novice 16-year-old drivers in Connecticut. The results revealed that three-fourths of the crash-involved teenagers were at fault, while more than half of the at-fault crashes of newly licensed novice drivers involved more than one contributing factor including speed, loss of control, and slippery roads. From the perspective of simulation, Ivers et al. [5] explored the risky behaviors and risk perceptions of young novice drivers and sought to determine the relation with crash risk. A detailed questionnaire was conducted and Poisson regression was employed to explore crash risk. The results reached that self-reported risky driving behaviors among novice drivers were associated with 50% increased risk of a crash and the types of novice driver policies need to be strengthened. A similar study by McDonaldet al. [6] developed simulator scenarios for assessing novice driver performance with crash data. Chapman et al. [7] evaluated crash and traffic violation rates before and after licensure for novice California drivers subject to different driver licensing requirements. Plots and Poisson regression were employed to compare overall rates and subtypes of crashes and traffic violations among novice drivers. It was found that novice 16- and 17-year-old drivers' highest crash rates occur almost immediately after they were licensed, and their peak traffic violation rates were delayed until around age of 18. A recent study by Curry et al. [8] employed the Poisson regression to compare crash rates of older and younger novice drivers. It was found that older novice drivers experienced much less steep crash reductions over the first year of licensure than younger novice drivers. Moreover, early night crash rates of novice drivers under age 21 declined rapidly while changes in late-night crashes were much smaller.

Compared to novice drivers, experienced drivers perform much better due to the personal status, driving experience, decision-making ability, and so on, so not many studies concentrate on experienced drivers individually. However, in order to verify this, a variety of studies have focused on the comparison between novice and experienced drivers. From the ergonomics aspect, Underwood et al. [9] performed the eye fixations, while novice and experienced drivers drove along different types of roadways. Differences in sequences of fixations were found between novice and experienced drivers on three types of roads, and experienced drivers showed greater sensitivity overall, while the novice drivers revealed some stereotypical transitions in the visual attention. From the perspective of driving skill, Craen et al. [10] questioned whether novice drivers overestimate their driving skills more than experienced drivers. Questionnaires were designed, and the results showed that when the novice drivers were compared themselves to the average and peer drivers, they were not as optimistic about their driving skills, but when comparing their self-assessment with actual behavior, they overestimated their driving skills. Mitchell et al. [11] compared the crash circumstances of common crash types for novices and experienced drivers in New South Wales, Australia. Correspondence analysis revealed that the crash characteristics between novice and experienced drivers were similar, but vehicle speed, fatigue, and alcohol were risky factors in novice driver crashes. Crundall [12] tested hazard prediction in isolation to assess discriminates between novice and experienced drivers. Based on the Situation Awareness Global Assessment Technique, the results suggested that experienced drivers found hazard prediction less effortful, while response time measures can discriminate between novice and experienced drivers.

Simulation plays an important role in the crash risk analysis of novice and experienced drivers. By simulating different scenarios, Lee et al. [13] detected the road hazards of novice teen and experienced adult drivers. The results indicated that a large portion of teen drivers failed to disengage from peripheral task engagement in the presence of hazards, while the adult drivers observed hazards and demonstrated overt recognition of hazards more frequently than the teen drivers did. A similar study by Smith et al. [14], from the perspective of the sleepiness effect, investigated hazard perception in novice and experienced drivers. Based on the video test, the results indicated that the hazard perception skills of the more experienced drivers were relatively unaffected by mild increases in sleepiness, but the novice drivers were significantly slowed. Ohlhauser et al. [15] compared the driving performance of novice teenage drivers and experienced drivers over the span of six monthly simulator sessions. It was found that novice drivers' perception response times (PRT) to the braking events were significantly longer than those of the experienced drivers. From the visual information search in simulated junction negotiation, Scott et al. [16] compared gaze transitions of novice and experienced drivers. The results revealed that when scanning the junction, young experienced drivers distributed their gaze more evenly across all areas, whereas older and novice drivers made more sweeping transitions, bypassing adjacent areas. A similar study by Alberti et al. [17] strengthened the impact of a restricted field of view on visual search and hazard perception, by comparing novice and experienced driver performance in a driving simulator. The results showed that all drivers were more likely to avoid the hazards when presented with a wide view, but gaze movement recording revealed that only experienced drivers made overt use of wider eccentricities. Seacrist et al. [1] made the comparison of crash rates and rear-end striking crashes among novice teens and experienced adults using a driving study. The results identified significantly more crashes and rear-end striking crashes among the teen group than the adult group, which conformed to the previous findings.

Another important approach to determining the influencing factors of crash rate/injury is econometric modeling. Simon-Morton et al. [18] compared rates of risky driving among novice adolescent drivers and adult drivers and elevated g-force event rates by Poisson regression with random effects. The findings revealed that elevated g-force events among novice drivers may have contributed to crash and near-crash rates that remained much higher than adult

levels after 18 months of driving. Chapman et al. [7] employed plots and Poisson regression to compare overall rates and subtypes of crashes and traffic violations among novice drivers.

During the last decade, there have been a variety of different approaches and perspectives [19–22] presented in safety evaluation, among which multivariate regression analysis has been considered as one critical method dealing with two or more dependent variables with correlation and heterogeneity issues. At an early stage, Yamamoto and Shankar [23] developed a bivariate ordered-response probit model of driver's and passenger's injury severities in collisions with fixed objects. The results revealed the driver's characteristics, vehicle attributes, types of objects, and environmental conditions had an effect on both driver and passenger injury severity. After that, Dong et al. [24] analyzed injury crashes and proposed a random-parameter bivariate zero-inflated negative binomial regression model. A Bayesian approach was employed as the estimation method, and the results showed that the proposed model outperformed other investigated ones. The model gained new sights into how crash occurrences were influenced by risk factors. Focused on temporary disability and permanent motor injuries, Ayuso et al. [25] introduced a bivariate copula-based regression model for the joint analysis. The findings illustrated that the conditional distribution function of injury severities may be estimated. A similar study by Wali et al. [26] applied copular-based bivariate ordinal models to investigate the degree of injury severity sustained by drivers involved in head-on collisions. Chen et al. [27] developed a random-parameter bivariate ordered probit model to examine influencing factors by two drivers involved in the same rear-end crash between passenger cars. Taken both within-crash correlation and unobserved heterogeneity into consideration, the proposed model outperformed the individual ordered probit models with fixed parameters, which provides the foundation for this study. A recent study by Besharati et al. [28] extended into a bivariate spatial negative binomial Bayesian model with random effects of traffic fatalities and injuries across Provinces of Iran. Unobserved heterogeneity and spatial correlation were addressed, and the results helped to prioritize area-wide safety initiatives and programs. Besides bivariate regression models, different multivariate regression models, for example, multivariate tobit analysis [29–32], Bayesian multivariate approach [33, 34], multivariate spatial or/and temporal models [35–39], and mixture of abovementioned models, have been presented to address correlation and unobserved heterogeneity among injury severities.

As summarized from the literature above, there have been various methods and comparisons about the crash risk analysis of novice and experienced drivers. However, most of the studies address the crash risk of novice and experienced drivers separately, and there may exist interrelations between the unobservables, which can be accommodated by multivariate regression models. Therefore, the purpose of this study is to estimate the two (seemingly unrelated) nonlinear injury severity levels and to control for interrelations between their unobservables with bivariate random-effects probit models, which can address the injury severity levels simultaneously and accommodate the interrelations between the unobservables (i.e., heterogeneity issue).

2. Methodology

This study attempts to jointly model the injury severity of novice drivers and experienced drivers. Since the injury severity levels could be interdependent, there may be an interrelation between the unobservable factors influencing the injury severity of novice drivers and experienced drivers. In order to address this issue, the bivariate probit model is proposed where the injury severity levels of novice and experienced drivers rely on the set of independent variables, and the interrelation between the two error terms is considered as an auxiliary parameter. The reason that the bivariate probit model is selected lies in that whether the interrelation is significantly different from zero or not, the selected model does not require exclusion restrictions to provide meaningful estimates, particularly of the interrelation coefficient ρ[40]. More importantly, the bivariate panel data probit model can estimate two (seemingly unrelated) nonlinear processes and control for interrelations between the unobservables, which can account for the correlation in both time-specific and individual-specific error terms.

Specifically, the model includes two equations, one for the binary injury severity of novice drivers (y_{1it}) with main responsibility, Property Damage Only (PDO) (0) or injured and fatality (1), and the other for the binary injury severity of experienced drivers (y_{2it}) with main responsibility, PDO (0) or injured and fatality (1). Therefore, the equations can be expressed as follows:

$$\begin{cases} y_{1it} = 1\left(x_{1it}^{'}\beta_1 + v_{1it} > 0\right), \\ y_{2it} = 1\left(x_{2it}^{'}\beta_2 + v_{2it} > 0\right), \end{cases} \tag{1}$$

where i represents the panel variable (here is referred to as individual observation) with $i = 1,\ldots N$, and t denotes the time point (here is referred to year) with $t = 1,\ldots T$. The dependent variables y_{1it} and y_{2it} are explained by the independent variables x_{1it} and x_{2it}, respectively. β_1 and β_2 are coefficients, and v_{jit} refers to the process-specific error terms with $j \in (1, 2)$. Here, v_{jit} includes two parts, an individual-specific time-invariant error term α_{ji} and a time-specific idiosyncratic shock u_{jit}; that is, $v_{jit} = \alpha_{ji} + \mu_{jit}$; thus, equation (1) can be described as

$$\begin{cases} y_{1it} = 1\left(x_{1it}^{'}\beta_1 + \alpha_{1i} + u_{1it} > 0\right), \\ y_{2it} = 1\left(x_{2it}^{'}\beta_2 + \alpha_{2i} + u_{2it} > 0\right). \end{cases} \tag{2}$$

Due to the normalization of the error terms, the two components are assumed that the error terms α_j are normally distributed, and the idiosyncratic shocks u_j are standard normally distributed. The ratio of the time-constant individual-specific error term and the composite error term is calculated as

$$\lambda_j = \operatorname{corr}\left(v_{jit}, v_{jis}\right) = \frac{\sigma_{\alpha_j}^2}{\sigma_{v_j}^2}, \tag{3}$$

where $t \neq s$; if $t = s$, the correlation of the error terms can be calculated as

$$\operatorname{corr}\left(v_{1it}, v_{2is}\right) = \begin{cases} \rho_\alpha \sigma_{\alpha 1} \sigma_{\alpha 2} + \rho_u, & if\ s = t, \\ \rho_\alpha \sigma_{\alpha 1} \sigma_{\alpha 2}, & if\ s \neq t, \end{cases} \tag{4}$$

where ρ refers to the correlation of the error terms.

The individual likelihood function Li can be obtained from the product of the joint probability of the observed binary outcome variable $\{P_i(\alpha_1, \alpha_2)\}$ and the joint density of the random-effects error terms $\{f_2(\alpha_1, \alpha_2; \mu_\alpha)\}$,

$$L_i = \int_{\alpha_1} \int_{\alpha_2} P_i(\alpha_1, \alpha_2) f_2(\alpha_1, \alpha_2; \mu_\alpha) \mathrm{d}\alpha_1 \mathrm{d}\alpha_2, \tag{5}$$

where μ_α refers to the covariance of the random-effects error terms ($\mu_\alpha = \rho_\alpha \sigma_{\alpha 1} \sigma_{\alpha 2}$). Since the joint density of the random-effects error terms is assumed to follow a bivariate normal distribution, the joint probability of the observed binary outcome variable is expressed as

$$P_{it}(\alpha_1, \alpha_2) = \Phi_2\left\{k_1\left(x_{1it}^{'}\beta_1 + \alpha_{1i}\right), k_2\left(x_{2it}^{'}\beta_2 + \alpha_{2i}\right), k_1 k_2 \rho_u\right\}, \tag{6}$$

where $\Phi_2[\cdot]$ refers to the bivariate normal cumulative distribution function and $k_j = \begin{cases} 1, & if\ y_j = 1, \\ -1, & \text{otherwise}, \end{cases}$.

According to Greene [41], the bivariate normal cumulative distribution function can be described as the following form:

$$\Phi_2(x_1, x_2, \rho_u) = \int_{-\infty}^{x_2} \int_{-\infty}^{x_1} \varnothing_2(z_1, z_2, \rho_u) \mathrm{d}z_1 \mathrm{d}z_2, \tag{7}$$

while the density takes the form as follows:

$$\varnothing_2(z_1, z_2, \rho_u) = \frac{e^{(-(1/2))\left(x_1^2 + x_2^2 - 2x_1 x_2 \rho_u\right)/\left(1-\rho_u^2\right)}}{2\pi\left(1 - \rho_u^2\right)^{1/2}}. \tag{8}$$

Thus, the likelihood of the sample can be expressed as follows:

$$L = \prod_{i=1}^{N} \int_{\alpha_1} \int_{\alpha_2} \left\{ \prod_{t=1}^{T} P_{it}(\alpha_1, \alpha_2) \right\} f_2(\alpha_1, \alpha_2; \mu_\alpha) \mathrm{d}\alpha_1 \mathrm{d}\alpha_2. \tag{9}$$

The estimation can make full use of quasirandom numbers (Halton draws) and maximum simulated likelihood to achieve the correlation between the error terms of both processes. For more details about the bivariate probit and random-effects probit models, refer to Yildirim et al. [40] and Plum [42].

3. Data Description

Similar to the dataset adopted by Xiao et al. [43], Arc GIS open data site maintained by Nevada Department of Transportation (NDOT) from 2014 to 2017 was considered as the data source. "Identical" dataset here denotes that both datasets are from the same open dataset by NDOT, but the variables and modeling employed in this study are different; that is, the dataset is a different subset from the Xiao et al. 27 major and minor arterials in the metropolitan Las Vegas area were the target population selected in this study, which included City of Las Vegas, City of North Las Vegas, City of Henderson, and Clark County. Four main aspects were collected and considered: the crash status, the vehicle features, roadway characteristics, and environment.

As shown in Figure 1, 27 arterials 1999 injuries including both novice drivers and experienced drivers were considered. Conformed to Seacrist et al. [1], here, the novice and experienced drivers are selected among 16–19-year-old and 35–54-year-old drivers correspondingly. In Nevada, PDO, injury, and fatality are classified as three injury severity types. Since the fatality only accounted for 0.5% and the injury was quite similar, the injury and fatality categories were merged as one type, which may not affect the inference potentially. Therefore, the dependent variables in the proposed model were considered as binary injury severity, in which PDO was regarded as one, while injury and fatality were treated as the contrast, finally forming a binary probit model.

In the form of the vehicle profiles, the explanatory variables include the total vehicle, vehicle types, vehicle direction, vehicle action (e.g., changing lanes, making U-turn, and passing other vehicles), vehicle conditions (e.g., hit and run, mechanical defects, and driving too fast), and vehicle driver's age and driver's conditions (e.g., normal, fatigue, physical impairment, and distracted), whereas pedestrian, pedal cyclist, and motorcyclist are also considered. In this study, according to the classification by NDOT, when the crash happens, if there are two or more vehicles involved, the vehicle with the main responsibility here is considered as vehicle 1, and the rest with minor responsibility is vehicle 2. After the dataset was cleaned, crashes involving two vehicles account for 87% of injuries, which verifies the classification reasonably. In this study, the selected injury severity involves both novice and experienced drivers, so that the same injury can be addressed simultaneously.

The roadway characteristics involve the number of vehicle lanes, roadway conditions (e.g., dry, wet, ice, and snow), and the crash environment extracts the weather, lighting conditions, and first harm (e.g., median, fence, and pedestrian).

In order to evaluate the proposed models in Stata software, the categorical variables are digitalized, and all the variables collected are summarized in Appendixes A and B for novice and experienced drivers, respectively.

4. Results

Based on the typical variables selected, the characteristics of the crashes and correlation among main factors could be examined. In this study, Stata software was used to analyze the data. The correlation test was conducted to avoid the colinearity among the independent variables. In this study, crash type is

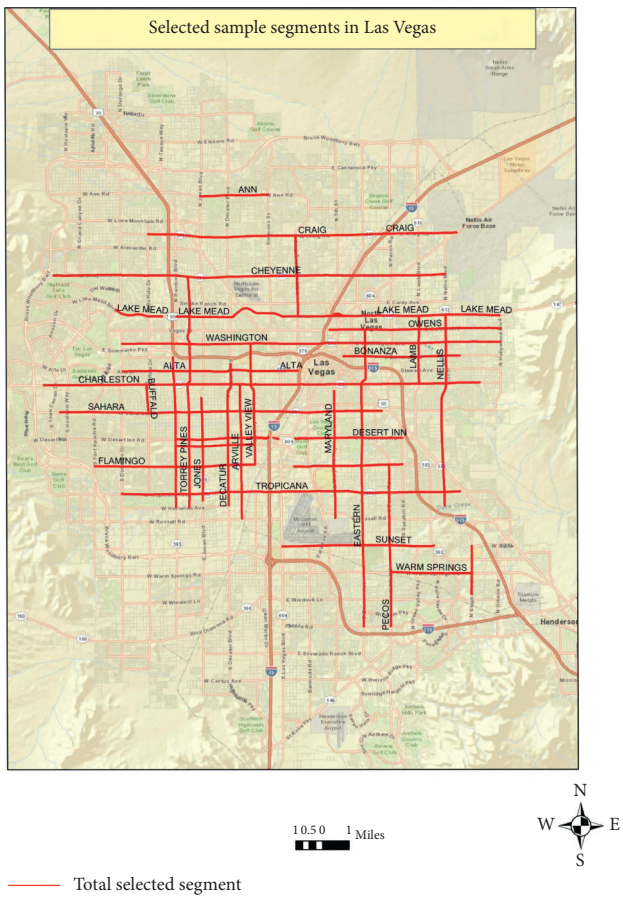

Figure 1: Selected arterials and crashes in Las Vegas.

highly related to total vehicle, while vehicle 2 action, vehicle 2 type, and vehicle 2 driver condition are highly correlated with each other; thus, in the final results, the variables with a high correlation may not occur at the same time.

The bivariate random-effects probit and bivariate probit models are proposed to assess the likelihood of novice and experienced drivers. The final results are presented in Table 1 with 50 Halton draws. In order to make the comparison, both numbers of observations are selected as the same.

As shown in Table 1, in the novice driver injury model, crash type, vehicle 2 type, pedestrian, and motorcyclist are significant for both bivariate probit model and bivariate random-effects probit model, while in the experienced driver injury model, crash type, vehicle 2 driver condition, first harm, and highway factor are significant. The covariances ρ of both models are not equal to 0, implying that correlation does exist between the injury severity levels of novice and experienced drivers, although the correlation is lower than 0.5. The log-likelihood values at convergence (−978.069) and zero (−1894.337) from the bivariate random-effects probit model are a little smaller than those (−925.747 and −1809.635) from the bivariate probit model, respectively. It can be found that the goodness of fit of the proposed bivariate random-effects probit model performs better than that of the bivariate probit model; thus, the following explanation would concentrate on the proposed model.

Table 1 demonstrates the effect on injury severity of novice and experienced drivers. For novice drivers, crash type and vehicle 2 type are negatively related to injury severity while pedestrian and motorcyclist notably increase the likelihood for injury severity levels. Compared to unknown crash types, the injury severity is reduced with the changing from angle to noncollision, which is understandable. Among all the crash types, angle and rear-end crashes frequently occur, accounting for about 85% and leading to different injury severities as verified by Xu et al. [44] and Hosseinpour et al. [45]. With the crash type from angle to noncollision, the injury severity of novice drivers is reduced about 110%.

Vehicle 2 type is negatively related to injury severity of novice drivers, indicating that the injury of cars and trucks is less than that of motorcycles, which is in line with the studies by Quddus et al. [46], Zmbon and Hasselberg [47], and Chang et al. [48]. Since motorcycles are exposed outside, even the drivers with minor responsibility (vehicle (2)) may still be suffered from severe injuries. Computed from the marginal effect, the injury severity of cars and trucks may be decreased about 4.9% compared to motorcycles.

Pedestrians play a positive significant role in the injury severity of novice drivers, meaning that the more the pedestrians, the more severe the injury of novice drivers. The study is uniform with Oh [49], and the possibility may go up to 139% if pedestrians are increased by onefold. The reason is that the driving skills of novice drivers are inadequate and they may become nervous when more pedestrians show up; thus, the possibility of running into injury is raised.

Similarly, motorcyclists have a positive association with the injury severity of novice drivers, implying that more motorcyclists may increase the injury severity. It can be calculated that the possibility may rise 167% if motorcyclists are increased by onefold, which is in agreement with common sense. More motorcyclists may produce the disordered traffic easily and cause more conflicts, especially for novice drivers, since they are not very skilled and may go on the rampage, thus leading to more chances of running into crashes.

For experienced drivers, crash type, first harm, and highway factor are negatively related to injury severity while vehicle 2 driver condition is positively concerned with injury severity. Similar to novice drivers, the injury severity is reduced with the crash type changing from angle to noncollision, compared to unknown crash types, and the possibility is reduced about 5.6%. It can be seen that the novice drivers or experienced drivers can be influenced by various crash types.

Different from the novice drivers, the driver conditions of vehicle 2 are positively significant to the injury severity of experienced drivers, indicating that, compared to the unknown, apparently normal condition causes less injury severity. This is in line with Weber et al. [50], and the possibility increases about 1.6% with the driver condition varying from the normal conditions to the unknown. Although most crashes happen under apparently normal conditions, the injury severity may be more severe under unknown conditions because the unknown makes the driving condition unpredictable.

Table 1: Results for bivariate probit and bivariate random-effects probit models.

Variable	Bivariate probit				Bivariate random-effects probit			
	Coef.	Std. Err.	z	$p>\|z\|$	Coef.	Std. Err.	z	$p>\|z\|$
Novice driver injury model								
Crash type	−0.109*	0.020	−5.49	0.000	−0.110*	0.019	−5.01	0.000
Vehicle 2 type	−0.050*	0.022	−2.25	0.024	−0.049*	0.024	−2.22	0.012
Pedestrian	1.329*	0.365	3.63	0.000	1.394*	0.384	3.61	0.000
Motorcyclist	1.513*	0.436	3.46	0.001	1.671*	0.490	3.44	0.001
Constant	0.887*	0.079	11.15	0.000	0.882*	0.080	11.17	0.000
Experienced driver injury model								
Crash type	−0.055*	0.021	−2.61	0.009	−0.056*	0.020	−2.61	0.005
Vehicle 2 driver condition	0.056*	0.016	3.52	0.000	0.057*	0.016	3.57	0.000
First harm	−0.106*	0.013	−7.81	0.000	−0.106*	0.014	−7.84	0.000
Highway factor	−0.616*	0.182	−3.37	0.001	−0.629*	0.174	−3.38	0.001
Constant	1.668*	0.195	8.52	0.000	1.681*	0.191	8.51	0.000
α_1	1.052	0.189	6.82	0.000	1.112	0.155	7.18	0.000
α_2	0.908	0.263	3.65	0.000	0.948	0.220	4.31	0.000
$\rho\alpha$	−0.256	0.087			−0.287	0.085		
$\rho\varepsilon$					0.416	0.086		
Goodness of fit								
No. of observations	1999				1999			
Log-likelihood at convergence	−925.747				−978.069			
Log-likelihood at zero	−1809.635				−1894.337			

Note. Coef. = coefficient; Std. Err. = standard error; ∗significant at the 5% level.

Variable	Description	Count (proportion)
(i) Dependent variables		
Injury severity	0-PDO	620 (31%)
	1-Injury and fatality	1379 (69%)
(ii) Categorical variables		
Crash type	1-Angle	868 (43.4%)
	2-Backing	15 (0.8%)
	3-Head-on	9 (0.5%)
	4-Rear-end	827 (41.3%)
	5-Sideswipe	100 (5.0%)
	6-Noncollision	176 (8.8%)
	7-Unknown base	4 (0.2%)
Vehicle 1 type	1-Car	1388 (69.4%)
	2-Truck/bus	284 (14.2%)
	3-Motorcycle base	43 (2.1%)
	4-Others	44 (2.2%)
	5-Pickup/van	240 (12.1%)
Vehicle 1 action	1-Backing up	11 (0.5%)
	2-Changing lanes	120 (6.0%)
	3-Going straight	1180 (59.0%)
	4-Making U-turn	20 (1.0%)
	5-Passing other vehicles/racing	5 (0.3%)
	6-Stopped	15 (0.8%)
	7-Turning left	370 (18.5%)
	8-Turning right	126 (6.3%)
	9-Other bases	7 (0.4%)
	10-Unreported	138 (7.0%)
	11-Unknown	7 (0.4%)

Table : Continued.

Variable	Description	Count (proportion)
Vehicle 1 driver condition	1-Apparently normal	1614 (80.7%)
	2-Driving under influence (DUI)	19 (1.0%)
	3-Drowsiness, fatigue, fainted, and so on	99 (5.0%)
	4-Illness/physical impairment	4 (0.2%)
	5-Inattention/distracted	113 (5.6%)
	6-Obstructed view	4 (0.2%)
	7-Other bases	63 (3.2%)
	8-Unknown	82 (4.1%)
Vehicle 1 condition	1-Disregarded traffic signs/signals/road markings	144 (7.2%)
	2-Driving too fast	168 (8.4%)
	3-Failed to yield right of way	499 (24.9%)
	4-Failure to keep in proper lane or running off road	140 (7.0%)
	5-Follwed too closely	324 (16.2%)
	6-Hit and run	62 (3.1%)
	7-Made an improper turn	48 (2.4%)
	8-Mechnical defects	8 (0.4%)
	9-Other types of improper driving	336 (16.8%)
	10-Unknown base	270 (13.5%)
Vehicle 2 type	1-Car	1033 (51.7%)
	2-Truck/bus	368 (18.4%)
	3-Motorcycle base	38 (1.9%)
	4-Others	262 (13.1%)
	5-Pickup/van	298 (14.9%)
Vehicle 2 driver age	0-Less than 16-year-old base	266 (13.3%)
	1-16–19 years old	96 (4.8%)
	2-20–34 years old	570 (28.5%)
	3-35–54 years old	725 (36.3%)
	3-More than 55 years old	382 (17.1%)
Vehicle 2 action	1-Backing up	0 (0.0%)
	2-Changing lanes	7 (0.4%)
	3-Going straight	955 (47.8%)
	4-Making U-turn	2 (0.1%)
	5-Passing other vehicles/racing	2 (0.1%)
	6-Stopped	674 (33.7%)
	7-Turning left	92 (4.6%)
	8-Turning right	38 (1.9%)
	9-Other bases	1 (0.01%)
	10-Unreported	6 (0.03%)
	11-Unknown	222 (11.1%)
Vehicle 2 driver condition	1-Apparently normal	1724 (86.2%)
	2-Driving under influence (DUI)	5 (0.2%)
	3-Drowsiness, fatigue, fainted, and so on	3 (0.1%)
	4-Illness/physical impairment	1 (0.05%)
	5-Inattention/distracted	2 (0.1%)
	6-Obstructed view	0 (0.0%)
	7-Others	1 (0.05%)
	8-Unknown base	263 (13.2%)
First harm	1-Cross median/centerline	9 (0.45%)
	2-Fence/wall	1 (0.05%)
	3-Light/luminary support	2 (0.1%)
	4-Motor vehicle in transport	435 (21.7%)
	5-Pedal cycle/pedestrian	10 (0.5%)
	6-Ran off road left/right	20 (1.0%)
	7-Slow/stopped vehicle	72 (3.6%)
	8-Other fixed/movable objects	6 (0.3%)
	9-Other noncollisions	7 (0.35%)
	10-No database	1437 (71.9%)

Table : Continued.

Variable	Description	Count (proportion)			
Road conditions	1-Dry	1942 (97.1%)			
	2-Wet	49 (2.5%)			
	3-Ice/snow	3 (0.1%)			
	4-Unknown base	5 (0.3%)			
Weather conditions	1-Clear	1707 (85.4%)			
	2-Cloudy	237 (11.9%)			
	3-Rain	44 (2.2%)			
	4-Blowing sand, soil, dirt, and snow	2 (0.1%)			
	5-Others	0 (0.0%)			
	6-Unknown base	9 (0.45%)			
Lighting conditions	1-Daylight	1334 (66.7%)			
	2-Dark	605 (30.3%)			
	3-Dawn	21 (1.0%)			
	4-Dusk	36 (1.8%)			
	5-Unknown base	3 (0.1%)			
Highway factor	1-Active work zone	17 (0.9%)			
	2-Inactive work zone	17 (0.9%)			
	3-Weather	540 (27%)			
	4-Others	26 (1.3%)			
	5-None base	1399 (69.2%)			
	Mean	S.D.	Min.	Max.	
(iii) Continuous variables					
Total vehicle	Total vehicles involved	2.06	0.59	1	6
Pedestrian	Pedestrian	0.04		0	1
Motorcyclist	Motor cyclist	0.02		0	1

Note. Unknown category in the dataset has no actual data.

The last two negatively significant variables are the first harm and highway factor. With the variation of first harm from cross median/centerline to "no data," the injury severity is decreased. Since first harm mainly includes motor vehicle in transport, slow/stopped vehicle, and "no data," the injury severity of motor vehicle in transport is the worst, which makes sense. Because the motor vehicles in transport have more chances of running into conflicts, the possibility of injury severity is reduced by 11% than the others.

Compared to none highway factor, injury severity in the active work zone is the worst, which reaches some consensus with Wong et al. [51] and Sze and Song [52]. In the active work zone, speeding happens frequently, as well as the stop-and-go traffic, thus causing more chances of running into conflicts and leading to injury severity.

5. Discussion

So far, there have been various approaches and comparisons about the crash injury analysis of novice and experienced drivers. However, most of the studies address the crash injury severity of novice and experienced drivers separately and there may exist interrelations between the unobservables. In this study, in order to estimate the two (seemingly unrelated) nonlinear injury severity levels and to control for interrelations between their unobservables, the bivariate random-effects probit models are proposed, which can address the injury severity levels simultaneously and accommodate the interrelations between the unobservables (i.e., heterogeneity issue).

As shown in Table 1, the closer examination of the estimated results reveals some similarities and differences between novice and experienced drivers. First, the similarity is that, among all the influencing variables, crash types are of significance for injury severity of both novice and experienced drivers. This indicates that certain crash type would lead to specific injury severity and need to be paid more attention whether for the novice or experienced drivers. Secondly, the difference is that significant variables for novice drivers may emphasize more on moving objects, especially the vulnerables, that is, pedestrians and motorcyclists, since their driving skills are not mature enough and still need more time to become accustomed to driving situation, while for experienced drivers, the injury severity is more derived from static facilities and environment. This implies that, after a certain driving period, experienced drivers have become used to the moving objects, while paying less attention to the static ones.

According to the results obtained, from an empirical point of view, for the novice drivers, more education and training hours are necessary before they are qualified to drive on the roadways safely, while the pedestrians and motorcyclists should be paid more attention with clear warning/crossing signs and helmets, respectively. As for the experienced drivers, more alternative facilities should be designed to avoid the first harm; the presence of active work zones increases the injury severity; thus, one way of improving the safety is to organize the traffic flow efficiently to avoid the conflicts between vehicles, so that the injury severity levels may be decreased.

Variable	Description	Count (proportion)
(i) Dependent variables		
Injury severity	0-PDO	2510 (31%)
	1-Injury and fatality	5594 (69%)
ii) Categorical variables		
Crash type	1-Angle	3452 (42.6%)
	2-Backing	50 (0.6%)
	3-Head-on	47 (0.5%)
	4-Rear-end	3290 (40.6%)
	5-Sideswipe	500 (6.2%)
	6-Noncollision	731 (9.0%)
	7-Unknown base	34 (0.4%)
Vehicle 1 type	1-Car	3950 (48.7%)
	2-Truck/bus	1872 (23.1%)
	3-Motorcycle base	168 (2.1%)
	4-Others	285 (3.5%)
	5-Pickup/van	1829 (22.5%)
Vehicle 1 action	1-Backing up	44 (0.5%)
	2-Changing lanes	495 (6.1%)
	3-Going straight	4787 (59.0%)
	4-Making U-turn	95 (1.1%)
	5-Passing other vehicles/racing	45 (0.5%)
	6-Stopped	91 (1.1%)
	7-Turning left	1327 (16.4%)
	8-Turning right	608 (7.5%)
	9-Other bases	63 (0.8%)
	10-Unreported	475 (5.8%)
	11-Unknown	74 (0.9%)
Vehicle 1 driver condition	1-Apparently normal	6197 (76.5%)
	2-Driving under influence (DUI)	803 (9.9%)
	3-Drowsiness, fatigue, fainted, and so on	70 (0.9%)
	4-Illness/physical impairment	90 (1.1%)
	5-Inattention/distracted	333 (4.1%)
	6-Obstructed view	25 (0.3%)
	7-Other bases	194 (2.4%)
	8-Unknown	392 (4.8%)
Vehicle 1 condition	1-Disregarded traffic signs/signals/road markings	698 (8.6%)
	2-Driving too fast	410 (5.0%)
	3-Failed to yield right of way	1686 (20.8%)
	4-Failure to keep in proper lane or running off road	523 (6.5%)
	5-Follwed too closely	1380 (17.0%)
	6-Hit and run	237 (2.9%)
	7-Made an improper turn	197 (2.4%)
	8-Mechnical defects	21 (0.3%)
	9-Other types of improper driving	1483 (18.3%)
	10-Unknown base	1469 (18.1%)
Vehicle 2 type	1-Car	4191 (51.7%)
	2-Truck/bus	1488 (18.4%)
	3-Motorcycle base	150 (1.8%)
	4-Others	1064 (13.1%)
	5-Pickup/van	1211 (14.9%)
Vehicle 2 driver age	0-Less than 16-year-old base	1078 (13.3%)
	1-16–19 years old	389 (4.8%)
	2-20–34 years old	2310 (28.5%)
	3-35–54 years old	2942 (36.3%)
	3-More than 55 years old	1385 (17.1%)

Table : Continued.

Variable	Description	Count (proportion)			
Vehicle 2 action	1-Backing up	2 (0.02%)			
	2-Changing lanes	34 (0.4%)			
	3-Going straight	3622 (47.8%)			
	4-Making U-turn	17 (0.2%)			
	5-Passing other vehicles/racing	9 (0.1%)			
	6-Stopped	2867 (35.3%)			
	7-Turning left	437 (5.4%)			
	8-Turning right	157 (1.9%)			
	9-Other bases	9 (0.1%)			
	10-Unreported	35 (0.4%)			
	11-Unknown	913 (11.2%)			
Vehicle 2 driver condition	1-Apparently normal	6994 (86.3%)			
	2-Driving under influence (DUI)	31 (0.3%)			
	3-Drowsiness, fatigue, fainted, and so on	38 (0.4%)			
	4-Illness/physical impairment	4 (0.04%)			
	5-Inattention/distracted	2 (0.02%)			
	6-Obstructed view	0 (0.0%)			
	7-Others	7 (0.07%)			
	8-Unknown base	1029 (12.7%)			
First harm	1-Cross median/centerline	9 (0.1%)			
	2-Fence/wall	4 (0.05%)			
	3-Light/luminary support	7 (0.08%)			
	4-Motor vehicle in transport	1646 (20.3%)			
	5-Pedal cycle/pedestrian	64 (0.7%)			
	6-Ran off road left/right	44 (0.5%)			
	7-Slow/stopped vehicle	251 (3.1%)			
	8-Other fixed/movable objects	17 (0.2%)			
	9-Other noncollisions	12 (0.1%)			
	10-No data base	6050 (74.6%)			
Road conditions	1-Dry	7887 (97.3%)			
	2-Wet	180 (2.2%)			
	3-Ice/snow	3 (0.03%)			
	4-Unknown base	34 (0.4%)			
Weather conditions	1-Clear	6809 (84.0%)			
	2-Cloudy	1107 (13.6%)			
	3-Rain	146 (1.8%)			
	4-Blowing sand, soil, dirt, and snow	7 (0.08%)			
	5-Others	8 (0.09%)			
	6-Unknown base	27 (0.3%)			
Lighting conditions	1-Daylight	5616 (69.2%)			
	2-Dark	2223 (27.4%)			
	3-Dawn	88 (1.0%)			
	4-Dusk	167 (2.0%)			
	5-Unknown base	10 (0.1%)			
Highway factor	1-Active work zone	95 (1.1%)			
	2-Inactive work zone	107 (1.3%)			
	3-Weather	154 (1.9%)			
	4-Others	2326 (28.7%)			
	5-None base	5421 (66.9%)			
	Mean	S.D.	Min.	Max.	
(iii) Continuous variables					
Total vehicle	Total vehicles involved	2.07	0.62	1	10

Note. Unknown category in the dataset has no actual data.

6. Conclusions

In this study, bivariate random-effects probit model was proposed initially to investigate the injury severity among novice and experienced drivers, in which both injury severity levels were addressed by bivariate (seemingly unrelated) probit simultaneously, and the interrelations between the unobservables (i.e., heterogeneity issue) were accommodated by random-effects model. The results showed that crash types, vehicle 2 types, pedestrians, and motorcyclists were potentially significant factors of injury severity for novice drivers, while crash types, vehicle 2 driver

condition, first harm, and highway factor were significant for experienced drivers.

Two main findings can be drawn from the results of the study. First, there indeed exists a correlation between novice drivers and experienced drivers in injury severity, although the correlation is not so strong. Second, bivariate random-effects probit model can address the injury severity levels simultaneously and accommodate the interrelations between the unobservables (i.e., heterogeneity issue), which extends the range of bivariate probit analysis.

Some drawbacks still exist in this study. One is that the division of novice and experienced drivers is conducted using the age difference as the dataset provides, and the preferred division should depend on the proposed criterion described, that is, the number of years with a valid driver's license or the number of miles driven, which may reflect the actual driving experience. Moreover, since the results of the study are based on the dataset from Las Vegas, it is worthwhile to try out different data sources to confirm the findings and transferability of this study in future studies. Further study may try other types of modeling, bivariate random-parameter probit model, or bivariate spatial probit model, so that spatial and temporal issues can be addressed efficiently.

Appendix

A. Summary of the Parameters for Novice Drivers

B. Summary of the Parameters for Experienced Drivers

Data Availability

The data that support the findings of this study are maintained by Nevada Department of Transportation, which can be accessed at the following website: https://data-ndot.opendata.arcgis.com/datasets/

Conflicts of Interest

The authors declare that they have no conflicts of interest.

Authors' Contributions

Yuan Q contributed to conceptualization and project administration; Xiao D and Xu X contributed to methodology, wrote the original draft , and were responsible for funding acquisition; Kang S. provided the software and performed validation and visualization; Xiao D performed formal analysis, investigation, , supervision, and data curation and provided the resources; Yuan Q. and Xu *X* reviewed and edited the article.

Acknowledgments

Thanks are due to the Nevada Department of Transportation (NDOT) for providing the dataset. This study was supported by the Fundamental Research Fund for the Central Universities (HUST: 2018KFYYXJJ001) and the National Natural Science Foundation of China (No. 71861023 & 52072214).

References

[1] T. Seacrist, A. Belwadi, A. Prabahar, S. Chamberlain, J. Megariotis, and H. Loeb, "Comparison of crash rates and rear-end striking crashes among novice teens and experienced adults using the SHRP2 Naturalistic Driving Study," *Traffic Injury Prevention*, vol. 17, no. 1, pp. 48–52, 2016.

[2] A. M. Ferrante, D. L. Rosman, and Y. Marom, "Novice drink drivers, recidivism and crash involvement," *Accident Analysis & Prevention*, vol. 33, no. 2, pp. 221–227, 2001.

[3] B. G. Simon-Morton, J. L. Hartos, W. A. Leaf, and D. F. Preusser, "The effects of the checkpoints program on parent-imposed driving limits and crash outcomes among Connecticut novice teen drivers at 6-monts post-licensure," *Journal of Safety Research*, vol. 37, pp. 9–15, 2006.

[4] K. A. Braitman, B. B. Kirley, A. T. McCartt, and N. K. Chaudhary, "Crashes of novice teenage drivers: characteristics and contributing factors," *Journal of Safety Research*, vol. 39, no. 1, pp. 47–54, 2008.

[5] R. Ivers, T. Senserrick, S. Boufous et al., "Novice drivers' risky driving behavior, risk perception, and crash risk: findings from the DRIVE study," *American Journal of Public Health*, vol. 99, no. 9, pp. 1638–1644, 2009.

[6] C. C. McDonald, J. B. Tanenbaum, Y.-C. Lee, D. L. Fisher, D. R. Mayhew, and F. K. Winston, "Using crash data to develop simulator scenarios for assessing novice driver performance," *Transportation Research Record: Journal of the Transportation Research Board*, vol. 2321, no. 1, pp. 73–78, 2012.

[7] E. A. Chapman, S. V. Masten, and K. K. Browning, "Crash and traffic violation rates before and after licensure for novice California drivers subject to different driver licensing requirements," *Journal of Safety Research*, vol. 50, pp. 125–138, 2014.

[8] A. E. Curry, K. B. Metzger, A. F. Williams, and B. C. Tefft, "Comparison of older and younger novice driver crash rates: informing the need for extended Graduated Driver Licensing restrictions," *Accident Analysis & Prevention*, vol. 108, pp. 66–73, 2017.

[9] G. Underwood, P. Chapman, N. Brocklehurst, J. Underwood, and D. Crundall, "Visual attention while driving: sequences of eye fixations made by experienced and novice drivers," *Ergonomics*, vol. 46, no. 6, pp. 629–646, 2003.

[10] S. De Craen, D. A. M. Twisk, M. P. Hagenzieker, H. Elffers, and K. A. Brookhuis, "Do young novice drivers overestimate their driving skills more than experienced drivers? Different methods lead to different conclusions," *Accident Analysis & Prevention*, vol. 43, no. 5, pp. 1660–1665, 2011.

[11] R. J. Mitchell, T. Senserrick, M. R. Bambach, and G. Mattos, "Comparison of novice and full-licenced driver common crash types in New South Wales, Australia, 2001-2011," *Accident Analysis & Prevention*, vol. 81, pp. 204–210, 2015.

[12] D. Crundall, "Hazard prediction discriminates between novice and experienced drivers," *Accident Analysis & Prevention*, vol. 86, pp. 47–58, 2016.

[13] S. E. Lee, S. G. Klauer, E. C. B. Olsen et al., "Detection of road hazards by novice teen and experienced adult drivers," *Transportation Research Record: Journal of the Transportation Research Board*, vol. 2078, no. 1, pp. 26–32, 2008.

[14] S. S. Smith, M. S. Horswill, B. Chambers, and M. Wetton, "Hazard perception in novice and experienced drivers: the effects of sleepiness," *Accident Analysis & Prevention*, vol. 41, no. 4, pp. 729–733, 2009.

[15] A. D. Ohlhauser, S. Milloy, and J. K. Caird, "Driver responses to motorcycle and lead vehicle braking events: the effects of motorcycling experience and novice versus experienced drivers," *Transportation Research Part F: Traffic Psychology and Behaviour*, vol. 14, no. 6, pp. 472–483, 2011.

[16] H. Scott, L. Hall, D. Litchfield, and D. Westwood, "Visual information search in simulated junction negotiation: gaze transitions of young novice, young experienced and older experienced drivers," *Journal of Safety Research*, vol. 45, pp. 111–116, 2013.

[17] C. F. Alberti, A. Shahar, and D. Crundall, "Are experienced drivers more likely than novice drivers to benefit from driving simulations with a wide field of view?" *Transportation Research Part F: Traffic Psychology and Behaviour*, vol. 27, pp. 124–132, 2014.

[18] B. G. Simon-Morton, Z. Zhang, P. S. Albert et al., "Crash and risky driving involvement among novice adolescent drivers and their parents," *American Journal of Public Health*, vol. 101, no. 12, pp. 2362–2366, 2011.

[19] D. Lord and F. Mannering, "The statistical analysis of crash-frequency data: a review and assessment of methodological alternatives," *Transportation Research Part A: Policy and Practice*, vol. 44, no. 5, pp. 291–305, 2010.

[20] P. T. Savolainen, F. L. Mannering, D. Lord, and M. A. Quddus, "The statistical analysis of highway crash-injury severities: a review and assessment of methodological alternatives," *Accident Analysis & Prevention*, vol. 43, no. 5, pp. 1666–1676, 2011.

[21] F. L. Mannering and C. R. Bhat, "Analytic methods in accident research: methodological frontier and future directions," *Analytic Methods in Accident Research*, vol. 1, pp. 1–22, 2014.

[22] F. Mannering, "Temporal instability and the analysis of highway accident data," *Analytic Methods in Accident Research*, vol. 17, pp. 1–13, 2018.

[23] T. Yamamoto and V. N. Shankar, "Bivariate ordered-response probit model of driver's and passenger's injury severities in collisions with fixed objects," *Accident Analysis & Prevention*, vol. 36, no. 5, pp. 869–876, 2004.

[24] C. Dong, D. B. Clarke, S. S. Nambisan, and B. Huang, "Analyzing injury crashes using random-parameter bivariate regression models," *Transportmetrica A: Transport Science*, vol. 12, no. 9, pp. 794–810, 2016.

[25] M. Ayuso, L. Bermúdez, and M. Santolino, "Copula-based regression modeling of bivariate severity of temporary disability and permanent motor injuries," *Accident Analysis & Prevention*, vol. 89, pp. 142–150, 2016.

[26] B. Wali, A. J. Khattak, and J. Xu, "Contributory fault and level of personal injury to drivers involved in head-on collisions: application of copula-based bivariate ordinal models," *Accident Analysis & Prevention*, vol. 110, pp. 101–114, 2018.

[27] F. Chen, M. Song, and X. Ma, "Investigation on the injury severity of drivers in rear-end collisions between cars using a random parameters bivariate ordered probit model," *International Journal of Environmental Research and Public Health*, vol. 16, no. 14, p. 2632, 2019.

[28] M. M. Besharati, A. Tavakoli Kashani, Z. Li, S. Washington, and C. G. Prato, "A bivariate random effects spatial model of traffic fatalities and injuries across Provinces of Iran," *Accident Analysis & Prevention*, vol. 136, Article ID 105394, 2020.

[29] P. C. Anastasopoulos, V. N. Shankar, J. E. Haddock, and F. L. Mannering, "A multivariate tobit analysis of highway accident-injury-severity rates," *Accident Analysis & Prevention*, vol. 45, pp. 110–119, 2012.

[30] P. C. Anastasopoulos, "Random parameters multivariate tobit and zero-inflated count data models: addressing unobserved and zero-state heterogeneity in accident injury-severity rate and frequency analysis," *Analytic Methods in Accident Research*, vol. 11, pp. 17–32, 2016.

[31] Q. Zeng, H. Wen, H. Huang, X. Pei, and S. C. Wong, "A multivariate random-parameters Tobit model for analyzing highway crash rates by injury severity," *Accident Analysis & Prevention*, vol. 99, pp. 184–191, 2017.

[32] H. Wen, J. Sun, Q. Zeng, X. Zhang, and Q. Yuan, "The effects of traffic composition on freeway crash frequency by injury severity: a Bayesian multivariate spatial modeling approach," *Journal of Advanced Transportation*, vol. 2018, Article ID 6964828, 2018.

[33] M. S. Shaheed, K. Gkritza, A. L. Carriquiry, and S. L. Hallmark, "Analysis of occupant injury severity in winter weather crashes: a fully Bayesian multivariate approach," *Analytic Methods in Accident Research*, vol. 11, pp. 33–47, 2016.

[34] W. Cheng, G. S. Gill, T. Sakrani, M. Dasu, and J. Zhou, "Predicting motorcycle crash injury severity using weather data and alternative Bayesian multivariate crash frequency models," *Accident Analysis & Prevention*, vol. 108, pp. 172–180, 2017.

[35] X. Ma, S. Chen, and F. Chen, "Multivariate space-time modeling of crash frequencies by injury severity levels," *Analytic Methods in Accident Research*, vol. 15, pp. 29–40, 2017.

[36] C. R. Bhat, S. Astroza, and P. S. Lavieri, "A new spatial and flexible multivariate random-coefficients model for the analysis of pedestrian injury counts by severity level," *Analytic Methods in Accident Research*, vol. 16, pp. 1–22, 2017.

[37] Q. Zeng, H. Wen, H. Huang, X. Pei, and S. C. Wong, "Incorporating temporal correlation into a multivariate random parameters Tobit model for modeling crash rate by injury severity," *Transportmetrica A: Transport Science*, vol. 14, no. 3, pp. 177–191, 2018.

[38] K. Xie, K. Ozbay, and H. Yang, "A multivariate spatial approach to model crash counts by injury severity," *Accident Analysis & Prevention*, vol. 122, pp. 189–198, 2019.

[39] K. Wang, T. Bhowmik, S. Yasmin, S. Zhao, N. Eluru, and E. Jackson, "Multivariate copula temporal modeling of intersection crash consequence metrics: a joint estimation of injury severity, crash type, vehicle damage and driver error," *Accident Analysis & Prevention*, vol. 125, pp. 188–197, 2019.

[40] J. Yildirim, N. Korucu, and S. Karasu, "Further education or Re-enlistment decision in Turkish armed forces: a seemingly unrelated probit analysis," *Defence and Peace Economics*, vol. 21, no. 1, pp. 89–103, 2010.

[41] W. H. Greene, *Econometric Analysis*, Prentice-Hall, Upper Saddle River, NJ, USA., 7th edition, 2012.

[42] A. Plum, "An estimator for bivariate random-effects probit models," *Stata the Journal*, vol. 16, no. 1, pp. 96–111, 2016.

[43] D. Xiao, X. Xu, and L. Duan, "Spatial-temporal analysis of injury severity with geographically weighted panel logistic

regression model," *Journal of Advanced Transportation*, vol. 2019, Article ID 8521649, 2019.

[44] X. Xu, J. Shao, and S. C. Wong, "Injury severity analysis in right-turn lanes at signalised intersections," *Proceedings of the Institution of Civil Engineers-Transport*, vol. 170, no. 1, pp. 26–37, 2017.

[45] M. Hosseinpour, S. Sahebi, Z. H. Zamzuri, A. S. Yahaya, and N. Ismail, "Predicting crash frequency for multi-vehicle collision types using multivariate Poisson-lognormal spatial model: a comparative analysis," *Accident Analysis & Prevention*, vol. 118, pp. 277–288, 2018.

[46] M. A. Quddus, R. B. Noland, and H. C. Chin, "An analysis of motorcycle injury and vehicle damage severity using ordered probit models," *Journal of Safety Research*, vol. 33, no. 4, pp. 445–462, 2002.

[47] F. Zmbon and M. Hasselberg, "Socioeconomic differences and motorcycle injuries: age at risk and injury severity among young drivers-A Swedish nationwide cohort study," *Accident Analysis & Prevention*, vol. 38, pp. 1183–1189, 2006.

[48] F. Chang, P. Xu, H. Zhou, A. H. S. Chan, and H. Huang, "Investigating injury severities of motorcycle riders: a two-step method integrating latent class cluster analysis and random parameters logit model," *Accident Analysis & Prevention*, vol. 131, pp. 316–326, 2019.

[49] C. Oh, "Factors affecting injury severity in pedestrian-vehicle crash by novice driver," *Journal of Korean Society of Transportation*, vol. 28, no. 4, pp. 43–51, 2011.

[50] M. Weber, J. Giacomin, A. Malizia, L. Skrypchuk, V. Gkatzidou, and A. Mouzakitis, "Investigation of the dependency of the drivers' emotional experience on different road types and driving conditions," *Transportation Research Part F: Traffic Psychology and Behaviour*, vol. 65, pp. 107–120, 2019.

[51] J. M. Wong, M. C. Arico, and B. Ravani, "Factors influencing injury severity to highway workers in work zone intrusion accidents," *Traffic Injury Prevention*, vol. 12, no. 1, pp. 31–38, 2011.

[52] N. N. Sze and Z. Song, "Factors contributing to injury severity in work zone related crashes in New Zealand," *International Journal of Sustainable Transportation*, vol. 13, no. 2, pp. 148–154, 2019.

Hindawi
Discrete Dynamics in Nature and Society
Volume 2021, Article ID 6640358, 16 pages
https://doi.org/10.1155/2021/6640358

Research Article

Multiobjective Optimization of Sustainable WCO for Biodiesel Supply Chain Network Design

Nana Geng[1] **and Yixiang Sun**[2]

[1]*Nanjing University of Posts and Telecommunications, Nanjing 210023, China*
[2]*Nanjing University of Aeronautics and Astronautics, Nanjing 211106, China*

Correspondence should be addressed to Yixiang Sun; sunyixiang@nuaa.edu.cn

Received 19 December 2020; Revised 18 February 2021; Accepted 26 February 2021; Published 9 March 2021

Academic Editor: Tingsong Wang

Bioenergy is attracting more attention worldwide due to its environmental and economic benefits. The design of a feasible biodiesel supply chain network can effectively improve the production and use of biodiesel and then further promote the development of the biodiesel industry. As an easy recyclable material with high yield, kitchen waste has a good prospect and can solve public health and safety problems. This paper takes the kitchen waste producing biodiesel as the object to design and optimize the biodiesel supply chain in order to improve the sustainable development of biodiesel industry and the operational efficiency of the biodiesel supply chain. By designing a sustainable biodiesel supply chain model under defined conditions, it proposes strategic and tactical decisions related to location, production, inventory, and distribution within multiple planning cycles. In order to effectively solve the model, a Pareto optimal NSGAII heuristic algorithm is proposed and applied to a practical case study of restaurants in Jiangsu Province. The efficiency of the method and the optimal solution are verified by a case study. The overall optimization of biodiesel supply can effectively improve the efficiency of supply chain, reduce system cost, improve the profit of biodiesel operators, and promote the sustainable development of biodiesel industry, which has important guiding significance and reference value for the practice of biodiesel supply chain network planning.

1. Introduction

Nowadays, food wasting is becoming a common problem of global resources and environment. Most countries, including the United Kingdom, the European Union, the United States, and some developing countries, face this challenge. In the UK, about 30% of the food in the market eventually becomes kitchen waste every year, with a total amount of about 6.7 million tons [1]. Figure 1 shows the fluctuation of China's kitchen waste productivity and growth rate during 2009–2019 [2]. With the economic growth and the improvement of residents' consumption level, people's consumption of food and beverage is increasing day by day, which brings about the rapid growth of kitchen waste. According to statistics, the annual output of kitchen waste in China was more than 120 million tons, with an average daily output of 27.4 t/day [3]. Among them, more than 60 million tons of kitchen waste is produced in major cities, especially in the Yangtze River Delta and other cities with developed catering industry [4]. The daily production of kitchen waste reaches more than 2000 tons.

The Chinese government highly supports the development of the biodiesel industry with kitchen waste as the raw material. In the development policy of the biodiesel industry (2015), it clearly states that kitchen waste should become the main raw material of biodiesel, and its supply chain needs effective design to improve the overall operational efficiency. The Chinese government promotes the centralized treatment and resource utilization of typical urban wastes, such as kitchen waste, construction waste, garden waste, and urban sludge. It is planned that the domestic kitchen waste recycling rate will reach 30% by 2020. Although the data for 2020 have not yet been released, according to the statistics from previous months, this indicator has almost reached.

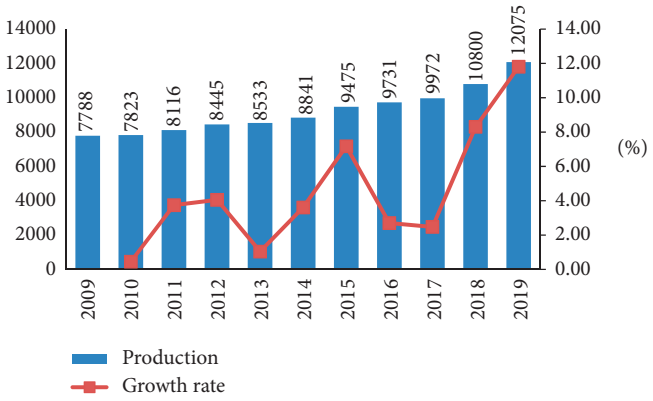

Figure 1: 2009–2019 annual production of kitchen waste in China.

Optimal design of the kitchen waste supply chain has great social significance. This paper is to study the modeling, solution, and application of biodiesel supply chain in the determination environment. Firstly, through the in-depth discussion of previous research papers, it is believed that, in the process of modeling, only the integration of effective biodiesel supply chain network system can improve efficiency. Therefore, it is necessary to consider the design of supply chain from the perspective of integration, specifically including the following: study the integration of facilities, propose inventory and distribution strategies, and make decisions on the location, capacity level of pretreatment facilities, and biodiesel refinery facilities in each period. Secondly, considering sustainability, a mixed integer linear programming model is constructed to solve three optimization problems of economic objectives, environmental objectives, and social objectives in the biodiesel supply chain. Thirdly, in terms of research methods, it is difficult to find accurate solutions by branching and delimitation for large-scale examples, and the algorithm based on group search mechanism has advantages for solving nondominant solution sets of multiobjective optimization problems. So, NSGAII, an improved multiobjective genetic algorithm, is adopted as the solving algorithm in this paper. Finally, in terms of application and analysis, this paper conducts a case study based on the actual data of Jiangsu Province in order to illustrate the potential use of the model and the decision-making solutions in the real environment.

2. Literature Review

2.1. Sustainability of Biofuel Supply Chain. Biofuel is known as a renewable alternative to traditional petroleum-based fuels for their low impact on ecosystems. Improving the sustainability performance of biofuel supply chain should be considered as a goal and standard for optimization of the biofuel supply chain. Energy sustainability requires that the needs of managing environment, achieving economic prosperity, and improving quality of life to be met artificially not only the present generation but also the future generations. At present, sustainable supply chain design and optimization has become an emerging method, which tries to take environmental, economic, and social decisions into full consideration [5]. Economic sustainability means the most important objective of the biofuel supply chain is to produce biofuel in an economically viable manner [6]. The research on economic sustainability includes the following contents: the debate between food and energy [7], the balance between efficiency and energy [8], the budget of the biofuel industry [9], the optimization of supply chain operating costs and profits [10], the evaluation of supply chain present value [11], and the avoidance of investment risks [12]. With the improvement of environmental awareness and the tightening of environmental policies, research on environmental sustainability has attracted more and more attention in the past few decades [13]. Early work tends to focus on some environmental aspects of the engineering process, such as waste management and net heat consumption [14]. Now, the study of environmental sustainability pays more attention on how to reduce the land, water, and energy consumption, reduce carbon emissions, and reduce pollutant discharge such as carbon emissions and its environmental impact on the global warming problem [15], the use of water resources [16], soil health problems [17], energy return [18], and chemical fertilizer problems [19]. Social sustainability reflected as the development of the bioenergy industry is likely to create new employment opportunities and bring greater economic vitality in rural areas [20–22]. Therefore, the social sustainability of the bioenergy industry emphasizes how to improve social welfare, including promoting employment, poverty reduction, and indirect effects on land crops, reducing impact on social public resources, product liability issues, safeguarding public health, and food safety issues.

2.2. Multiobjective Supply Chain Model and Solving Method. The multiobjective supply chain optimization model is mainly divided into linear model and nonlinear model. According to the current research, most multiobjective supply chain optimization models are biobjective linear models. Many authors considered economic goals as traditional objective functions, while environmental or social goals are seen as extensions of traditional single-objective models. A common modeling approach is to consider an economic goal and an environmental goal. Chaabane et al. [23] proposed a biobjective model for the supply chain design of aluminum products, which included the part of carbon credits in the economic target and took the minimization of greenhouse gas emissions as the second objective. The model also takes inventory control decision into account. Akgul et al. [24] proposed a multicycle, multiproduct mixed integer linear programming model to optimize the economic and environmental problems of biofuel supply chain. All phases of the biofuel life cycle, such as planting, transportation, and production, are included in the model. Quariguasi [25] proposed a two-objective model to assess the material flow and production capacity of each plant to select the most suitable terminal substitute for use. Gosalbe et al. [26] designed a biobjective mixed integer linear programming model for hydrogen supply chain to study the impact of hydrogen network operation on climate

change. In the chance constrained programming, the model is embedded with the probability that satisfies the uncertain constraint. Hugo et al. took into account the expansion of production capacity in their model also [27]. Govindan et al. [28] studied the two-stage multivehicle routing problem with time window to optimize the sustainable supply chain network of perishable food. They propose a deterministic model that incorporates two goals: an economic goal to minimize all costs and an environmental goal to minimize emissions from building facilities, distributing facilities, and transporting between facilities. Very few models have more than three objective functions. Erkut et al. [29] developed a multistandard facility site selection model for municipal solid waste management in northern Greece. Their mixed integer linear programming model includes five objective functions: one is the minimum total cost of facility implementation, and four are environmental impact targets (greenhouse gas effects, landfills, energy, and material recovery). Solutions to the model include technology sites, material recovery facilities, location selection of incinerators and sanitary landfills, and solid waste flows between these sites. Only a few two-objective models are nonlinear. Due to economies of scale, Zhang et al. [30] proposed a nonlinear model with CO_2 emission objective caused by transportation. The nonlinear model is usually linearized; for example, Yue et al. [31, 32] used Charnes–Cooper transform and Glover to linearly transform the nonlinear model.

The current methods to solve the multiobjective supply chain optimization model mainly include the following: (1) weighted summation. The most straightforward way to deal with multiobjective models is to weight each criterion and then minimize the weighted sum of all criteria. The main advantage of this method is that single-objective modeling can be used to solve multiobjective problems. The disadvantage is that this modeling may not represent the interest of decision makers and may modify the Pareto structure of the problem [33]. (2) Pareto optimization method. The Pareto optimization method is often achieved by ε-constraint; that is, while prioritizing the main goal, other goals are expressed as constraints [34]. By repairing various constraint values, the Pareto frontier is approximated. This method is very suitable for extending a single target economic value to a dual target model that integrates environmental or social standards. By using economic models as the main objective, this approach enables decision makers to measure the economic impact of environmental or social constraints [35]. (3) Multistandard decision analysis and interactive methods. Multicriteria decision analysis can handle more environmental and social standards. When the number of objective functions increases and decision makers want to participate in building solutions, interactive methods are usually preferred [36].

In general, the optimization of biofuel supply chain is extremely important in the development system of the bioenergy industry. Scholars at home and abroad have done extensive research on theories and methods of biofuel supply chain optimization, especially in the areas of biofuel supply chain site selection and vehicle routing (using straw as raw material) for in-depth analysis. However, it is insufficient to discuss the theory of supply chain optimization using kitchen waste as raw materials, especially the design of sustainable supply chain, the construction of multiobjective optimization model, and solutions of biofuel supply chain model.

3. Problem Description

The biofuel industry needs to design its supply chain to operate efficiently as the same as each production-distribution system. This paper considering the multistage biodiesel supply chain makes decisions on the supply, distribution, pretreatment facilities, and the location and capacity of biodiesel refineries with kitchen waste as the raw material. The structure of sustainable WCO for biodiesel supply chain is shown in Figure 2.

Figure 2 shows the operation processes of taking kitchen waste as raw material to produce biodiesel. Kitchen waste is provided by the restaurant, and biodiesel operator using garbage truck transport takes kitchen waste to pretreatment facility. After preprocessing, the waste cooking oil is transported to biodiesel refineries to produce biodiesel. Then, biodiesel is transported to distribution service to be blended with diesel oil. As mentioned earlier, the supply chain of biodiesel from kitchen waste is different from that of a traditional biofuel supply chain. Therefore, this research considers the four-level network structure of biodiesel supply chain composed of kitchen waste acquisition, kitchen waste pretreatment, biodiesel production, and biodiesel sales. The first level is the kitchen waste supply point, that is, the restaurant; the second level is the kitchen waste pretreatment facility, where the food and kitchen waste is stored and converted into waste cooking oil; the third stage is biodiesel refinery, which converts the pretreated waste cooking oil into biodiesel. The fourth level is the biodiesel demand point, where the petrochemical refinery is the blending facility of biodiesel and diesel. The diesel demand can cause the change in the biodiesel demand. Through the optimization of biodiesel supply chain in this mode, the objectives of the supply chain can be minimized.

Assuming the location and output of the supply point are known, it can be seen from Figure 2 that all the kitchen waste provided to biodiesel operators from the supply point is available. Then, kitchen waste is transported to the pretreatment facility, where kitchen waste is collected and stored. When the supply is high due to changes in the supply of kitchen waste caused by the environment, holidays, and other factors, the pretreatment facility can temporarily store the kitchen waste in these facilities waiting for demand. The pretreated waste cooking oil is transported to the biodiesel refinery. Biodiesel refineries convert it to biodiesel. Unlike pretreatment facilities, biodiesel refineries are larger and more complex, and it costs much money to build and operate the refineries. Biodiesel refineries produce, sell, and ship biodiesel to some large petrochemical refineries. Assuming a certain number of large biodiesel refinery blending facilities have already existed, in this condition, the location and demand for biodiesel are known. In biodiesel refineries, regular diesel is blended with biodiesel and then transported

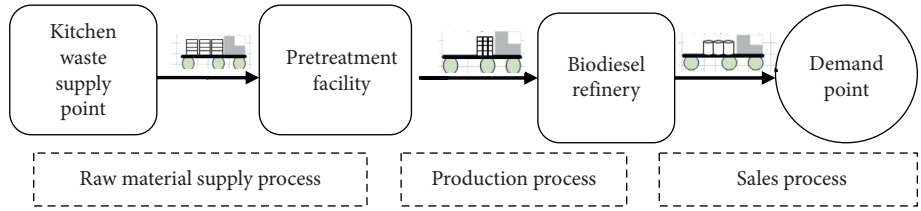

Figure 2: Sustainable WCO for biodiesel supply chain structure.

to petrol stations. Based on this information, the problems to be solved by designing the supply chain model include the following: the determination of the quantity, location, and capacity of kitchen waste pretreatment facilities; the location of the biodiesel refinery and its capacity to store the waste cooking oil and biodiesel; the amount of kitchen waste which the restaurant provides to each pretreatment facility; the quantity of waste cooking oil provided to the biodiesel refinery by each pretreatment facility; and the biodiesel production quantity. The network structure design and management plan of the supply chain affect each other. The location of pretreatment facilities and refineries determines the operation cost, which in turn affects the area and amount of kitchen waste collection. By establishing mixed integer linear programming (MILP) model and designing supply chain network, costs are reduced and overall profitability is improved.

3.1. Model Construction. The objectives of the mixed integer programming model for the optimization of the sustainable biofuels supply chain network using kitchen waste as raw materials include three parts: economic objectives, environmental objectives, and social objectives. The important assumptions in the model include the following: (1) the general annual operating cost is unchanged, which is not related to the processing and transferring of kitchen waste; (2) all final products are within the city, and the delivery time is not limited; (3) there are enough trucks to carry the collected kitchen waste; (4) urban traffic will not be affected by traffic jams, rush hours, etc.; (5) and the cost of facility construction is calculated at a specific annual interest rate. The symbols used in the model are shown in Table 1.

3.2. Objective 1: Economic Objective. The economic objective is to minimize the economic cost of the sustainable biodiesel supply chain system. Sustainable biodiesel supply chain economy target decision contains construction costs of pretreatment facilities and biodiesel refinery, pretreatment and storage cost of kitchen waste pretreatment facilities, production and storage costs of biodiesel refineries, and transportation cost between four facilities of supply point, pretreatment, refineries, and biodiesel demand point:

$$\begin{aligned} F_1 = \operatorname{Min} & \sum_{t\in T}\left[\sum_{i\in I}\sum_{j\in J} c^{f\,d}\times d_{ij}\times q_{ijt} + \sum_{j\in J}\sum_{k\in K} c^{w\,d}\times d_{jk}\times q_{jkt} + \sum_{k\in K}\sum_{o\in O} c^{b\,d}\times d_{ko}\times q_{kot}\right] \\ & + \sum_{j\in J} f_j \times Y_j + \sum_{k\in K}\sum_{l\in L} f_{kl}\times Z_{kl} \\ & + \sum_{j\in J}\sum_{t\in T} \mathrm{CPR}\times R_{jt} + \sum_{k\in K}\sum_{t\in T} \mathrm{CBP}\times R_{kt} \\ & + \sum_{t\in T}\left[\sum_{j\in J} \mathrm{CFS}\times S^f_{jt} + \sum_{k\in K} \mathrm{CWS}\times S^w_{kt} + \sum_{k\in K} CBS\times S^b_{kt}\right]. \end{aligned} \tag{1}$$

3.3. Objective 2: Environmental Objective. Objective 2 mainly takes carbon emissions as an environmental impact indicator and studies the minimization of carbon emissions in the supply chain of sustainable biodiesel from the perspective of life cycle. It considers carbon emissions in the process of kitchen waste collection, pretreatment, biodiesel production, and transportation. Transporting carbon emissions consist of three components: transporting kitchen waste from restaurants to pretreatment facilities, transporting waste cooking oil from pretreatment facilities to biodiesel refineries, and transporting biodiesel from refineries to demand point:

$$\begin{aligned} F_2 = \operatorname{Min} & \sum_{i\in I}\sum_{t\in T} \mathrm{EHV}\times \Phi_{it} + \sum_{t\in T}\sum_{i\in I}\sum_{j\in J} \mathrm{ECT}\times d_{ij}\times q_{ijt} \\ & + \sum_{t\in T}\sum_{j\in J}\sum_{k\in K} \mathrm{ECT}\times d_{jk}\times q_{jkt} + \sum_{t\in T}\sum_{k\in K}\sum_{o\in O} \mathrm{ECT}\times d_{ko}\times q_{kot} \\ & + \sum_{j\in J}\sum_{t\in T} \mathrm{EBD}\times R_{jt} + \sum_{k\in K}\sum_{t\in T} \mathrm{EPD}\times R_{kt}. \end{aligned} \tag{2}$$

3.4. Objective 3: Social Objective. On the one hand, kitchen waste can be used to produce biodiesel. On the other hand, it can also be illegally used to produce gutter oil, which will

Table 1: Notation.

Set	
I	Set of kitchen waste supply point i
J	Set of potential pretreatment facility locations j
K	Set of potential biodiesel refinery site k
O	Set of biodiesel demand location o
L	Set of biodiesel refinery size level l
T	The set of t in time
Parameter	
d_{ij}	Distance from kitchen waste supply point i to pretreatment facility j
d_{jk}	Distance from pretreatment facility j to biodiesel refinery k
d_{ko}	Distance from biodiesel refinery k to biodiesel demand point o
Φ_{it}	Supply of restaurant kitchen waste i at time t
D_{ot}	Demand of biodiesel demand point o at time t
M^c	Kitchen waste processing capacity of the pretreatment facility j
M_l^p	Waste oil processing capacity of a biodiesel refinery of size l
M^{cf}	Storage capacity of the pretreatment facility j
M_l^{pw}	Storage capacity of waste cooking oil from a biodiesel refinery of size l
M_l^{pb}	Storage capacity of biodiesel from a biodiesel refinery of size l
CPR	Pretreatment facility handles the cost of unit kitchen waste
CBP	Cost of process of waste cooking oil per unit at a biodiesel refinery
$c^{f\ d}$	Transportation cost of per unit kitchen waste
$c^{w\ d}$	Transportation cost of per unit waste cooking oil
$c^{b\ d}$	Distance transport cost of per unit biodiesel
CFS	Storage cost of per unit kitchen waste
CWS	Storage cost of per unit waste cooking oil
CBS	Storage cost of per unit biodiesel
f_j	Fixed construction cost of the pretreatment facility at j
f_{kl}	Fixed construction cost of a biodiesel refinery of size l at site k
EHV	Carbon emission of unit kitchen waste collection
EBD	Carbon emission of unit kitchen waste pretreatment
EPD	Carbon emission of unit waste cooking oil processing
ECT	Carbon emissions per kilometer transported by trucks
μ	Transformation factor of kitchen waste to waste cooking oil
β	Conversion factors of waste cooking oil to biodiesel
Decision variables	
q_{ijt}	Quantity of kitchen waste supply point transported to pretreatment facility j at time t
q_{jkt}	Quantity of pretreatment facility j delivered to biodiesel refinery k at time t
q_{kot}	Quantity of biodiesel refinery k transported to biodiesel demand point o at time t
Y_j	It is 1 when position j is used to build the pretreatment plant; otherwise, it is 0
Z_{kl}	It is 1 when location k is used to build a refinery of size l; otherwise, it is 0
R_{jt}	Quantity of kitchen waste processed by the pretreatment plant j at time t
R_{kt}	Quantity of waste oil treated by refinery k at time t
S_{jt}^f	Quantity of kitchen waste stored in the pretreatment facility j at time t
S_{kt}^w	Quantity of waste oil stored in biodiesel refinery k at time t
S_{kt}^b	Quantity of biodiesel stored in biodiesel refinery k at time t

have a negative impact on human health. Therefore, kitchen waste that is not recycled for production by biodiesel processing enterprises is likely to enter the supply chain of waste cooking oil production through various illegal means. The social goal of this paper is to minimize the amount of unused kitchen waste:

$$F_3 = \text{Min} \sum_{i\in I} \sum_{t\in T} \left(\Phi_{it} - \sum_{j\in J} q_{ijt} \right). \tag{3}$$

3.5. Constraint Set. The constraints on kitchen waste supply points, pretreatment facilities, biodiesel refineries, and biodiesel demand points are as follows.

Food and kitchen waste supply point constraints:

$$\sum_{j\in J} q_{ijt} \le \Phi_{it}, \quad \forall i \in I, t \in T. \tag{4}$$

Constraint (4) is that the total amount of kitchen waste transported by the restaurant cannot exceed the total supply.

Pretreatment facility constraints:

$$\sum_{i\in I} q_{ijt} \le M^{cf} \times Y_j, \quad \forall j \in J, t \in T, \tag{5}$$

$$S_{jt}^f \le M^{cf} \times Y_j, \quad \forall j \in J, t \in T, \tag{6}$$

$$\mu \times R_{jt} \le M^c \times Y_j, \quad \forall j \in J, t \in T, \tag{7}$$

$$\sum_{i\in I} q_{ijt} + S^f_{j(t-1)} = R_{jt} + S^f_{jt}, \quad \forall j \in J, t \in T, \tag{8}$$

$$\sum_{k\in K} q_{jkt} = \mu \times R_{jt}, \quad \forall j \in J, t \in T. \tag{9}$$

Constraint (5) ensures that kitchen waste is transported to the pretreatment facility only when the site is selected and specifies the capacity limits for opening the pretreatment facility at the site. Constraint (6) is the limit of the storage capacity of kitchen waste in the pretreatment facility. Constraint (7) is the limitation of the process capacity of the pretreatment facility. If the pretreatment facility is not selected, the constraint is also set to zero. Since the pretreatment facility can only store kitchen waste, constraints (8) and (9) ensure the balance between the amount of kitchen waste and waste cooking oil in and out of the pretreatment facility.

Biodiesel refinery constraints:

$$\sum_{j\in J} q_{jkt} \le \sum_{l\in L} M^{pw}_l \times Z_{kl}, \quad \forall k \in K, t \in T, \tag{10}$$

$$S^w_{kt} \le \sum_{l\in L} M^{pw}_l \times Z_{kl}, \quad \forall k \in K, t \in T, \tag{11}$$

$$S^b_{kt} \le \sum_{l\in L} M^{pb}_l \times Z_{kl}, \quad \forall k \in K, t \in T, \tag{12}$$

$$\beta \times R_{kt} \le \sum_{l\in L} M^{p}_l \times Z_{kl}, \quad \forall k \in K, t \in T, \tag{13}$$

$$\sum_{j\in J} q_{jkt} + S^w_{k(t-1)} = R_{kt} + S^W_{kt}, \quad \forall k \in K, t \in T, \tag{14}$$

$$\sum_{o\in O} q_{kot} + S^b_{kt} = \beta \times R_{kt} + S^b_{k(t-1)}, \quad \forall k \in K, t \in T. \tag{15}$$

Constraint (10) ensures that the pretreated waste cooking oil is transported to the biodiesel refinery only when the refinery is selected. At the same time, the capacity limits for the opening of the biodiesel refinery are limited. Constraint (11) has the limits on the inventory capacity of the pretreated waste cooking oil in the biodiesel refinery. Constraint (12) is the limit on biodiesel storage capacity of biodiesel refineries. Constraint (13) has limits on biodiesel production capacity of biodiesel refineries. If the biodiesel refinery is not selected, the constraint is also set to zero. Constraint (14) is to ensure the balance of the amount of pretreated waste cooking oil in and out of the biodiesel refinery. Constraint (15) is to ensure a balance of the amount of biodiesel in and out of a biodiesel refinery.

Biodiesel demand point constraint: constraint (16) is that the total amount of biodiesel transported from the biodiesel demand point is more than or equal to the total demand:

$$\sum_{k\in K} q_{kot} \ge D_{ot}, \quad \forall o \in O, t \in T. \tag{16}$$

Integer and nonnegative constraints: constraints (17) ~ (19) are nonnegative and integrity requirements for decision variables:

$$\sum_{l\in L} Z_{kl} \le 1, \quad \forall k \in K, \tag{17}$$

$$Z_{kl}, Y_j \in \{0, 1\}, \quad \forall j, k, l, \tag{18}$$

$$q_{ijt}, q_{jkt}, q_{kot}, R_{jt}, R_{kt}, S^f_{jt}, S^w_{kt}, S^b_{kt} \ge 0, \quad \forall i, j, k, o, t. \tag{19}$$

3.6. Solving Method. For optimization problems with multiple different goals, appropriate tradeoffs between different goals are often required. Multiobjective optimization problems have some common solving methods. For example, the double objective optimization problem, when solving method based on decision makers, prefers to choose a more important target as a single goal, first of all solving for obtaining a target and then taking the target value as a constraint of the original problem solving another single-objective optimization problem. Some scholars directly set the weights of different goals according to the preference of decision makers and then combine multiple goals into a composite goal for solving. Obviously, both methods require knowledge of decision makers' preferences, but in some cases, this is difficult to obtain, and the results are difficult to meet the needs of different decision makers at the same time. An effective way to solve multiobjective optimization problems is Pareto optimality based on the concept of nondominant solutions. Improving any objective function on the basis of the nondominant solution (Pareto solution) will inevitably weaken at least one other objective function [37]. As shown in Figure 3, the Pareto front composed of uniformly distributed Pareto solution sets can well express the solution space. The acquisition of Pareto front can provide decision makers with more cognition and awareness of the tradeoff between different objectives of the optimization problem [38].

The calculation amount involved in the optimization of biodiesel supply chain mainly depends on the number of network nodes. Here, we use N which represents the number of network nodes and G the number of construction levels of facilities. Therefore, the possible site selection scheme is $G \times 2^N$ in this paper. When the number of network nodes reaches dozens (in the case of this paper, the number of network nodes is close to 1500), the times of transportation distribution will be up to a million times. Because the cases in this paper cannot obtain exact solutions in an acceptable time, heuristic algorithms (such as genetic algorithms) must be used. For the multiobjective optimization problem, the best method is to use Pareto optimization. To find a set of solutions which can express the Pareto optimal frontier, we need to get a noninferior solution and the distribution of noninferior solution should be as uniform as possible. To solve the above two problems, this paper

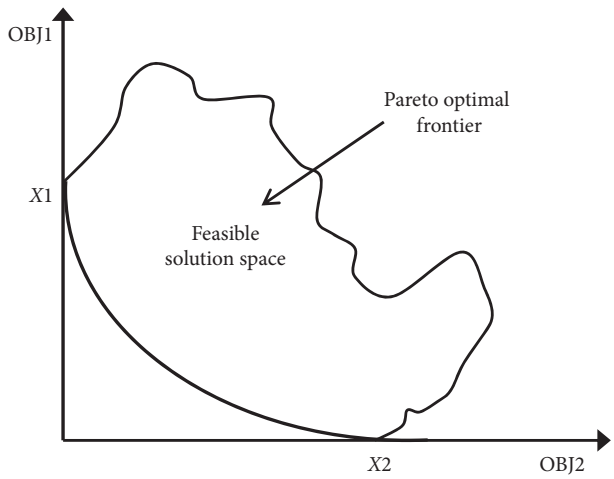

Figure 3: Schematic diagram of Pareto optimal frontier.

adopts the genetic (NSGAII) algorithm with elite strategy to solve the problem. The NSGAII algorithm can carry out the strategy design in the multiobjective genetic algorithm, which includes the fast noninferior sorting strategy, the fast-crowding distance estimation strategy, the selection strategy based on partial order, and the elite retention strategy. Because the NSGAII algorithm gives more noninferior solutions in a single calculation, it can better describe the Pareto front of the problem. In terms of the quality of the solution, the NSGAII algorithm can effectively solve the multicycle dynamic logistics network optimization problem, especially including the inventory and capacity decision in the multiphase plan.

4. Case Study

This paper takes the kitchen waste in Jiangsu Province as an example for analysis. In this case, the data of restaurant location, facility location, restaurant supply, and biodiesel demand are mainly used. Before analyzing the model results, the steps for processing the raw data to generate the input data used in the actual application are described. The locations of 104,922 restaurants and 748 municipal solid waste centers in Jiangsu Province were obtained through Baidu map. These restaurants and garbage stations were cleaned through SQL database, and 60,259 restaurants and 446 municipal solid waste collection and transfer centers were identified after screening and filtering. The data set includes the name, address, longitude, and latitude information of all data points. The restaurant serves as a source of kitchen waste, and the future kitchen waste pretreatment facility will be built on top of the existing MSW transfer center, with 56 prefecture-level cities selected as potential locations for biodiesel refineries. There is no comprehensive data set on kitchen waste production in China, and most kitchen waste statistics are based on random sampling rather than actual kitchen waste data from individual restaurants. Through GIS data, we can learn about the restaurant, but we do not know the size, so each restaurant food garbage cannot be calculated. So, this paper uses the K-means algorithm randomly sampling the data set to generate the typical database and then calculate the kitchen waste supply according to the clustering of database. Finally, the distance data in this paper are calculated by the matrix of ArcGIS starting point and destination.

4.1. Data Sources

4.1.1. Kitchen Waste Supply in Jiangsu Province. In this paper, all the restaurants (about 60,259 restaurants) in Jiangsu were selected as the kitchen waste suppliers. However, direct distribution of these restaurants is very difficult and time-consuming, so this paper uses the *k*-means clustering algorithm to divide them into several regions according to latitude and longitude (800 regions as shown in Figure 4).

In addition, it is reported that the average daily kitchen waste of the restaurant was set at 0.07 tons in 2017 [39]. At present, restaurants supply kitchen waste for biodiesel production accounting for about a quarter of all restaurants. Based on the calculation of all restaurants operating 365 days a year, the amount of kitchen waste that can be collected in the current period is calculated, as shown in Table 2 (only 10 points are shown due to space restrictions). The current period is set as the first period, and the supply in this period is the baseline supply of kitchen waste. Using some forecasting methods, the estimated supply value of the remaining 9 cycles within the planned scope is obtained based on the basic supply.

4.1.2. Biodiesel Demand in Jiangsu Province. The demand for biodiesel basically occurs when petrochemical refineries are blending biodiesel and diesel. Therefore, in order to calculate the biodiesel demand, this paper first determines the existing petrochemical refineries in Jiangsu Province. As of 2019, there are altogether 5 large-scale petrochemical refineries in Jiangsu Province producing diesel. It is assumed that these five facilities serve as the demand points for biodiesel, as shown in Figure 5. The diesel production capacity and the location of these refineries were obtained from the annual refinery report, and at the same time, 33% of the total capacity of these refineries is used to meet the production needs of B5 (5% biodiesel blend) diesel in Jiangsu Province. These values are used to obtain the basic biodiesel demand values for each blending facility. Based on the considered multicycle planning perspective, this paper obtained the demand for the remaining nine cycles through the prediction of the basic demand values, as shown in Table 3.

4.1.3. Parameters of the Alternative Pretreatment Facilities. In this research, 446 MSW transfer centers are selected as alternative pretreatment plants through data screening. It is assumed that the future kitchen waste pretreatment facility station will be built in the existing MSW transfer center, as shown in Figure 6. According to the literature, relevant parameters of the pretreatment facility are summarized in Table 4.

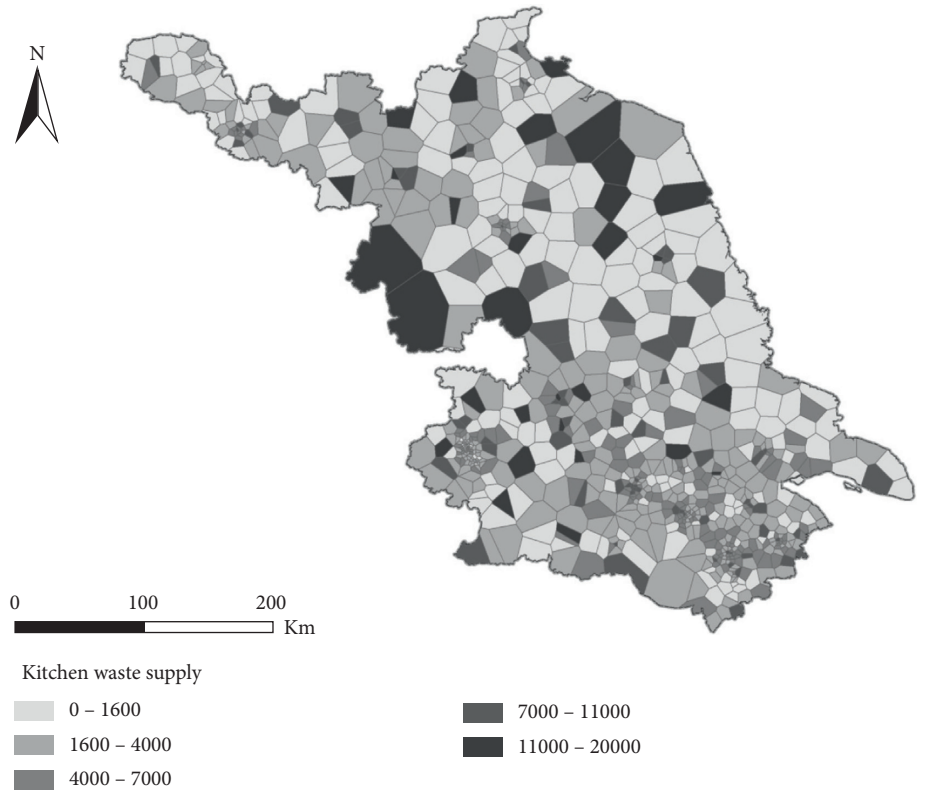

Figure 4: Food and beverage enterprises in Jiangsu Province kitchen waste supply situation.

Table 2: Regional basic information of catering enterprises in Jiangsu Province.

Category number	Number of catering enterprises (quantity)	Kitchen waste supply (tons)	Longitude mean	Latitude mean
1	58	1481.9	119.25	34.67
2	48	1226.4	120.18	31.72
3	39	996.45	117.32	34.19
4	36	919.8	121.10	31.66
5	13	332.15	118.57	32.13
6	55	1405.25	118.93	32.39
7	83	2120.65	120.64	31.17
8	59	1507.45	117.13	34.3
9	47	1200.85	119.10	33.60
10	48	1226.40	120.11	32.52

4.2. Parameters of the Crude Diesel Refinery. All the 56 counties and cities in Jiangsu Province will be potential candidates for biodiesel refineries, as shown in Figure 7. Zhang [40] estimates that the total investment cost of a biodiesel refinery in China producing 350 tons of biodiesel per day will exceed RMB 70 million. In consideration of the factory project life of 20 years and a 10% interest rate, the paper estimates the salvage value of biodiesel refineries with depreciation rate and calculates the further biological refinery current net fixed cost. We assume there are three alternative capacities (L1 (small), L2 (medium), and L3 (large)) of biodiesel refinery for biodiesel refining and then get the following relevant parameters of biodiesel refineries in Table 5.

4.2.1. Other Parameters. There are other parameters in this study, as shown in Table 6.

4.3. Effectiveness Analysis of the Algorithm. This case study takes into account the 10-year cycle of the development of the biodiesel industry, in which the first cycle starts from the development of kitchen waste as raw material to produce biodiesel in Jiangsu Province in 2019. The figure above shows the iterative curve of the sum of the target values of the 10 cycles. According to the addition requirement of B5, the biodiesel demand of kitchen waste production is calculated to be 25,700 tons with the diesel demand of Jiangsu oil refinery. From the perspective of supply, this paper believes

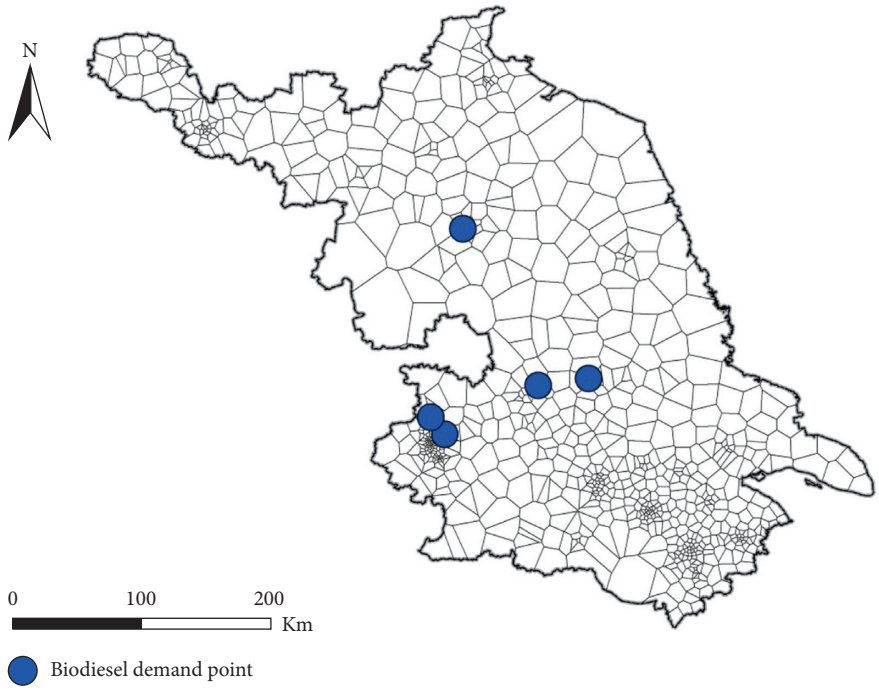

Figure 5: Biodiesel demand in Jiangsu Province.

Table 3: Biodiesel demand information of Jiangsu Province.

Cycle t	Demand point o				
	1	2	3	4	5
1	1250.00	11250.00	7916.67	958.33	41.67
2	1270.00	11187.50	8004.17	976.67	44.17
3	1365.00	11713.33	8184.17	995.00	49.17
4	1410.00	12240.83	8302.50	1013.33	52.50
5	1467.50	12472.50	8436.25	1031.67	56.25
6	1918.33	16396.78	11159.17	1363.33	72.50
7	2144.40	18278.52	12402.56	1515.95	81.61
8	2370.48	20160.25	13645.95	1668.57	90.71
9	2596.55	22041.99	14889.35	1821.19	99.82
10	2822.62	23923.73	16132.74	1973.81	108.93

that all kitchen waste from restaurants in the province could be converted into biodiesel after being treated. Therefore, there is great room for the future development of biodiesel production from kitchen waste. The multiobjective mixed integer linear programming problem calculated in this case study is solved by using Matlab on a desktop computer with Intel (*R*) Core (TM) i5-7500 CPU, using the optimization model as shown above.

To verify the distribution degree of the solution set of NSGAII algorithm, this paper takes three objective functions as fitness evaluation functions and obtains the iterative curves of the three objective functions, as shown in Figure 8. It can be seen that the curves converge after the iteration of 700 generations, and the objective function values are basically stable, indicating that the distribution degree of the noninferior solution of this algorithm is good. For this case, the whole solution process needs a total of 22012.24 seconds. The Pareto curve obtained is shown in Figure 8(d).

4.4. Result Analysis

4.4.1. Analysis of Target Value Results. The analysis of objective results is mainly based on comparison of the optimal objective value for each cycle. The paper taking the economic objective as the main target and measuring the relationship between the environmental objective and the economic objective or social objective and the economic objective obtains the curves in Figures 9 and 10, respectively.

First, consider the tradeoff between economic and social objective. All the best solutions for economic and social objective are on the Pareto optimal curve. The part above the curve in Figure 9 is a suboptimal solution, and any solution below the curve is not feasible. As can be seen from the figure, as the size of the company shrinks and the annual total cost decreases, the amount of unused kitchen waste increases. Specifically, when the optimal total annual cost was reduced from about RMB289 million yuan to RMB283

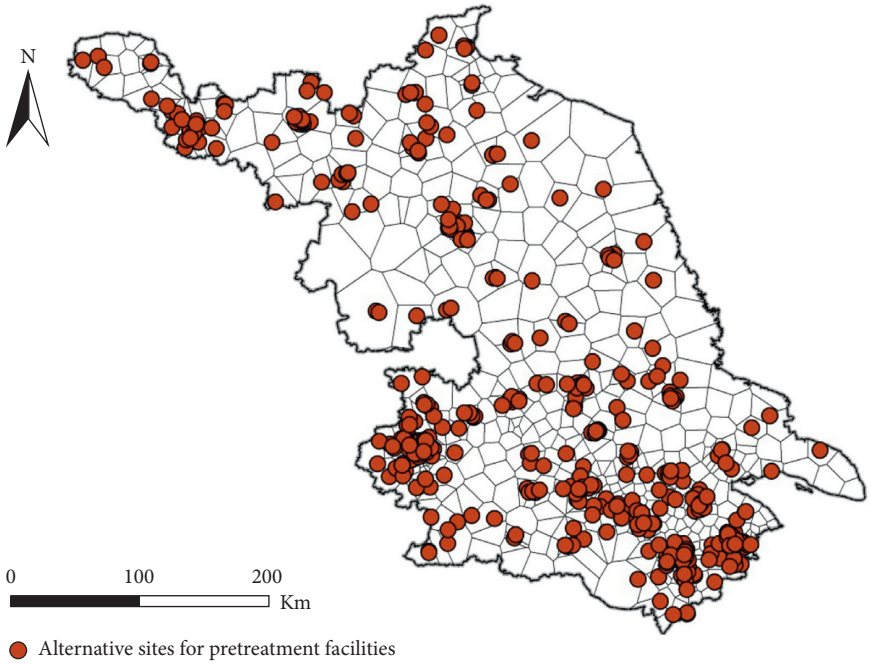

Figure 6: Alternative pretreatment facilities in Jiangsu Province.

Table 4: Parameters of the pretreatment facility.

Parameters of the pretreatment facility	Parameter value	Unit
Kitchen waste pretreatment capacity of the pretreatment facility is estimated according to the processing force of a single oil and water processor and a single unit from 5 to 100 m^3/hr	100000	Tons/year
Storage capacity of kitchen waste of the pretreatment facility M_l^{pw}	300000	Tons/year
Fixed construction cost of the pretreatment facility f_j	1400	Ten thousand yuan

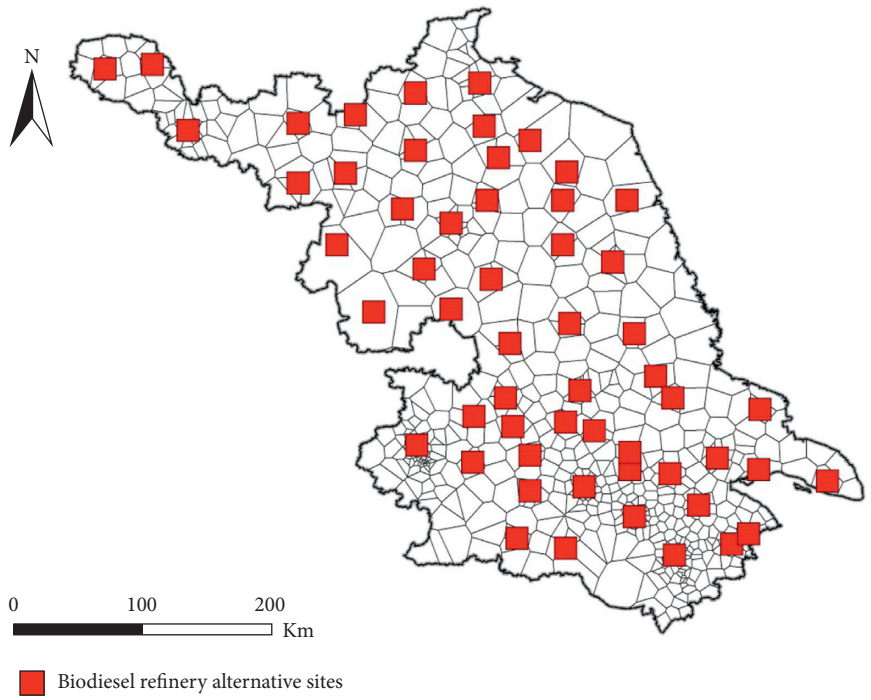

Figure 7: Alternative locations of biodiesel refineries in Jiangsu Province.

Table 5: Parameters of biodiesel refining plants.

Parameters of biodiesel refineries	Scale			Unit
	$L1$ (small)	$L2$ (medium)	$L3$ (large)	
Waste oil processing capacity of a biodiesel refinery of size l M_l^p	20000	40000	70000	Ton
Waste oil storage capacity of a biodiesel refinery of size l M_l^{pw}	7000	15000	25000	Ton
Biodiesel storage capacity of a biodiesel refinery of size l M_l^{pb}	7000	10000	20000	Ton
Fixed construction cost of a biorefinery at k of size l f_{kl}	4000	7000	10000	Ten thousand yuan

Table 6: Other parameters.

Other parameters	Parameter value
Conversion factor of kitchen waste to waste cooking oil is the separation rate of oil and water	6.32%
Conversion factor of waste cooking oil to biodiesel	85% [41]
Preprocessing facility preprocessing unit kitchen waste cost	15 yuan/ton [42]
Cost per unit of waste cooking oil treated by a refinery	1100 yuan/ton [43]
Cost of storing kitchen waste per unit	50 yuan/ton
Cost of storing a unit of waste cooking oil	80 yuan/ton
Cost of storing a unit of biodiesel	125 yuan/ton
Distance transportation cost of unit kitchen waste	0.20 yuan/ton/km [44]
Distance transportation cost per unit of waste oil	0.25 yuan/ton/km [44]
Distance transport cost per unit of biodiesel	0.35 yuan/ton/km [44]
Rate of greenhouse gas emissions from kitchen waste collection	5.6 kgCO_2eqv./ton
Carbon emission of unit kitchen waste pretreatment	12.6 kgCO_2eqv./ton [45]
Carbon emission of waste oil from processing unit	1465 kgCO_2eqv./ton [46]
Carbon emissions from transportation	0.1215 kgCO_2eqv./ton [46]

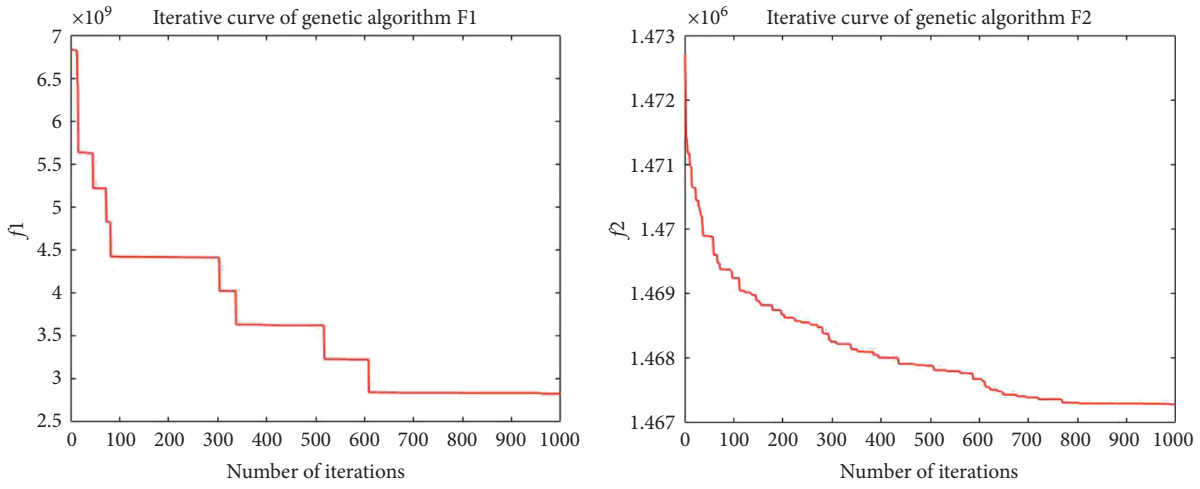

(a) (b)

Figure 8: Continued.

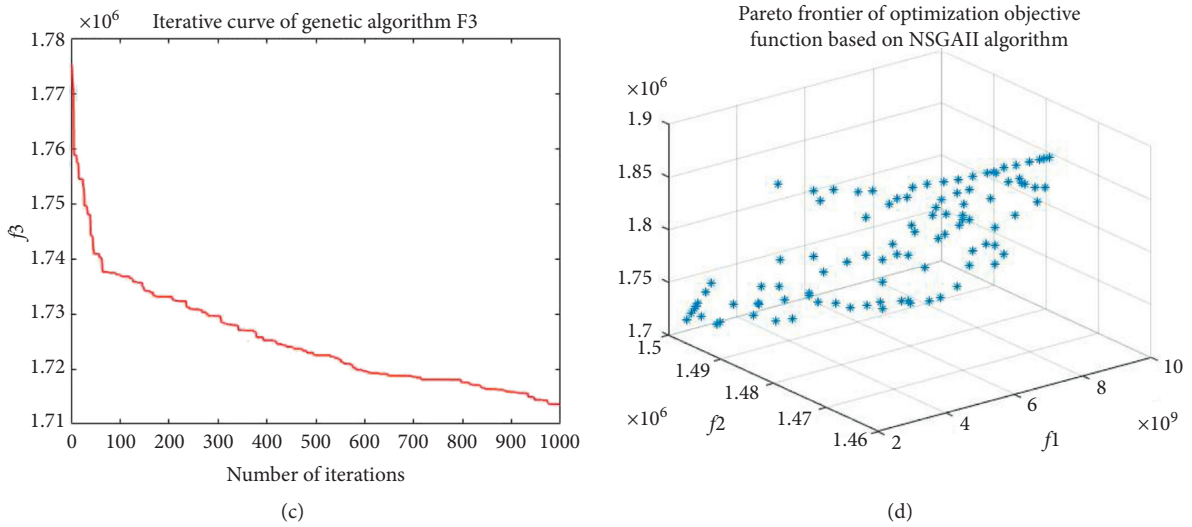

Figure 8: (a) Iterative curve of economic objectives. (b) Iterative curve of environmental objectives. (c) Iteration curve of social goals. (d) Pareto front diagram of the three objective functions.

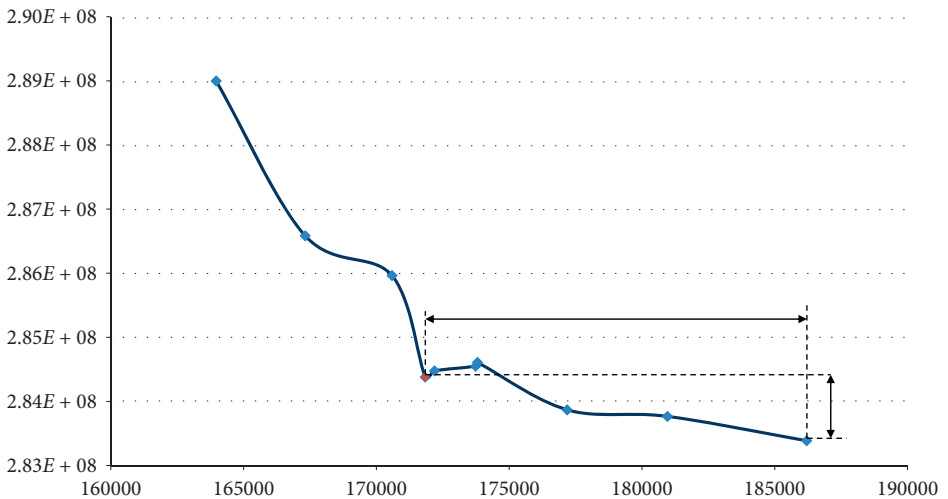

Figure 9: Pareto optimal curves of economic and social objectives.

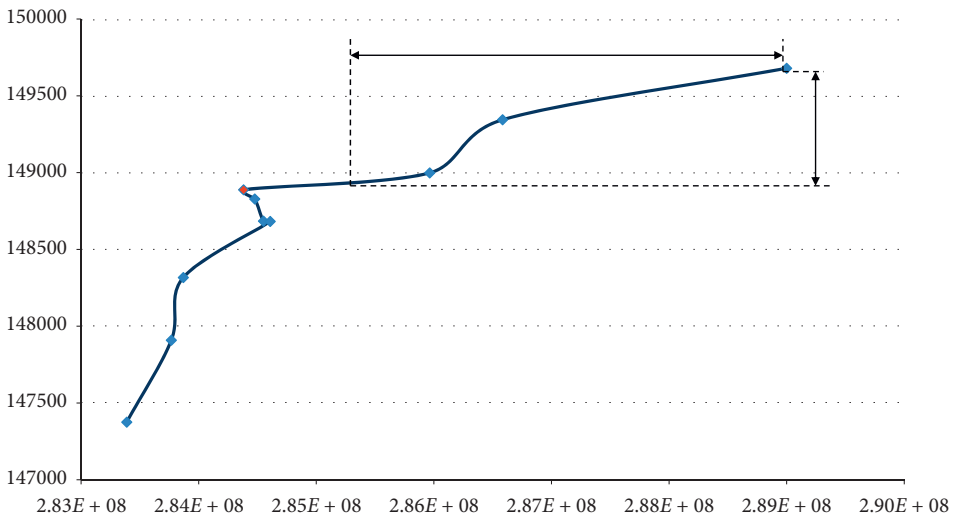

Figure 10: Pareto optimal curves of economic and environmental objectives.

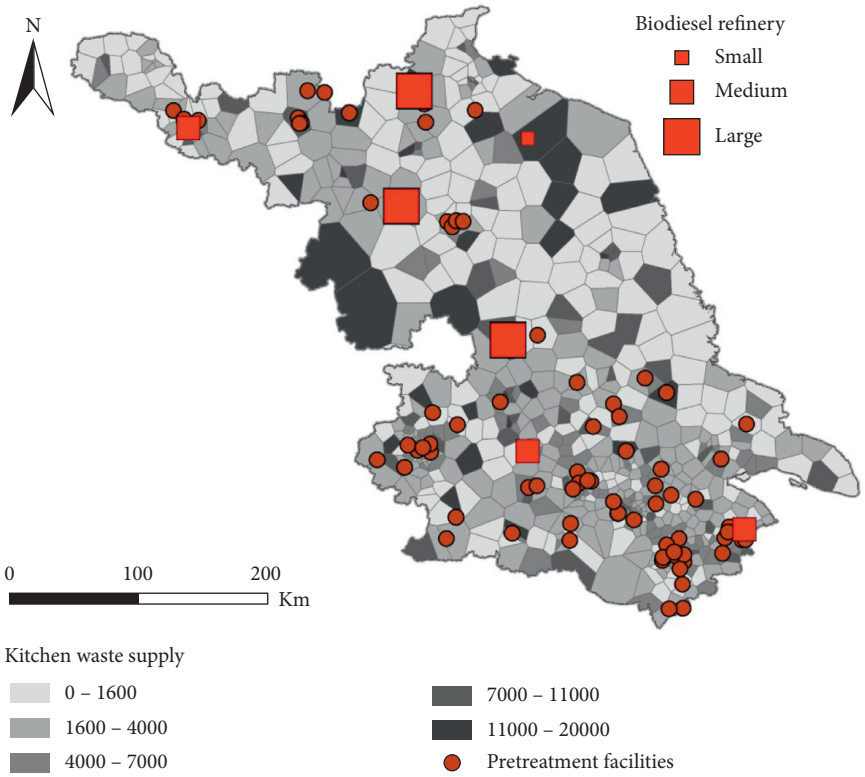

Figure 11: Results of biodiesel refineries and pretreatment facilities location.

million yuan, the social cost of running the biodiesel supply chain increased from about 165,000 tons of unused kitchen waste to about 185,000 tons. The trend of the Pareto curve reveals a tradeoff between economic and social effects. In particular, by comparing the two solutions with the red circle (phase 6 scale) in Figure 9, a well-chosen solution can be identified. Enterprises only do a small-scale expansion based on the lowest-cost solution, which makes a slight increase in economic cost and can significantly reduce the chaotic utilization of kitchen waste.

Then, consider the tradeoff between economic and environmental performance. According to the Pareto curve in Figure 10, with the expansion of the quantity and size of enterprise, the annual total cost increased from RMB283 million yuan to RMB289 million yuan, and the total carbon emissions increased from 147300 CO_2eqv to 149700 CO_2eqv. This is the same with other industries. When an enterprise's production capacity and its scale increases, due to production, transportation, and other reasons, more carbon emissions are bound to be caused. The trend of the Pareto curve reveals a tradeoff between economic and environmental effects. In particular, by putting the two solutions with the red circle in the figure (phase 6 scale), we can see, compared with the lowest-cost solution, the early stage of the small-scale expansion will increase a lot of carbon emission. This is not conducive to the development of the industry, but the scale expansion of the later stage can significantly reduce the carbon emissions increasing amplitude and the trend of the Pareto curve reveals the tradeoff between economy and environment objectives. Considering the economic, social, and environmental objectives comprehensively, the three-dimensional Pareto surface was obtained by solving the optimization problem, and the reasonable development scale and site selection of facilities were further calculated. Based on the three objectives, when the biodiesel enterprises reach the sixth cycle scale, the biodiesel operators will reach the optimal state, which is the optimal scale for enterprise expansion.

4.4.2. Analysis of Site Selection Results under the Optimal Scale. From Figure 11, we can see there are many pretreatment facilities in the south and central parts of the province, which mainly promote the transfer of biomass to the factories in the north by collecting the kitchen waste in the south of Jiangsu Province with a relatively large supply. In this case, a total of 7 biodiesel refineries were selected, including Taicang City, Xiangshui County, Donghai County, Gaoyou City, Danyang City, Siyang County, and Tongshan County. All three large-scale biodiesel refineries are located in the northern part of Jiangsu Province. The optimal location for these biodiesel refineries is the county where the production capacity and conversion technologies and biodiesel refineries are the lowest-cost solution. They are relatively close to the blending facilities or demand points. In addition, it can be seen from the figure that although the construction cost of biodiesel refineries in central and southern Jiangsu Province is relatively high, there are still

two medium-sized biodiesel refineries open in central and southeast Jiangsu Province due to the demand in these regions and the large supply of kitchen waste.

Pretreatment facilities are at the province of the three cities in the south of Jiangsu and Nanjing area which has more population. These cities produce more kitchen waste, and having pretreatment facility location in these cities can reduce transport costs. However, biodiesel refineries are located in areas with lower construction costs, which are relatively far from the demand point. The reason is that biodiesel has a higher density than the biomass materials, and the transportation costs are lower.

5. Conclusions

This paper presents a multiobjective biodiesel supply chain design model to optimize strategic decisions related to the biodiesel supply chain. In the construction of the model, the sustainable goals of economy, environment, and society are considered comprehensively. In the model solution, a heuristic algorithm based on Pareto optimality NSGAII is proposed to solve large-scale computational problems in supply chain, and it is applied to the case study of Jiangsu Province. The actual data were extracted by using the Baidu map, and the *K*-means clustering was used to preprocess the data. The objective value results show that the heuristic algorithm NSGAII based on Pareto optimality is suitable for large-scale biodiesel supply chain optimization research. With the expansion of biodiesel enterprises, the economic cost increases, the social target value (the amount of unused kitchen waste) is reduced, while the environmental target value (the cost of carbon emission) is increased. The design results of the supply chain network show that the pretreatment facilities are located in the places with large population and large supply of urban kitchen waste, so as to reduce the transportation cost of kitchen waste. Since biodiesel has a higher transport density than kitchen waste, biodiesel refineries are typically located in areas far from biodiesel demand and where construction costs are low. The paper has a reference for the study of biofuel supply chain in Jiangsu Province and the development of this industry in the future. Finally, although this study has comprehensively solved the biodiesel in different stages of the supply chain modeling and optimization, still some related works need further investigation, including the government's subsidy policy, different production technologies, design and operation of facilities of different priorities, and so on, which will become a biofuel supply chain research a development direction in the future.

Data Availability

The data used to support the findings of this study are available from the corresponding author upon request.

Conflicts of Interest

The authors declare that there are no conflicts of interest.

Authors' Contributions

Nana Geng and Yixiang Sun conceptualized the study and wrote the original draft. Nana Geng prepared methodology, analyzed using software, did formal analysis, investigated the study, and reviewed and edited the manuscript. Yixiang Sun was responsible for data curation.

Acknowledgments

This work was supported by the Nanjing University of Posts and Telecommunications research start-up fund (NY219168), Nature Foundation Incubation Fund of Nanjing University of Posts and Telecommunications (NY220214), and Project of Philosophy and Social Science Research in Colleges and Universities in Jiangsu Province (TJZ220011).

References

[1] E. Commission, *Preparatory Study on Food Waste across EU27*, European Commission, Brussels, Belgium, 2010.

[2] Report of Prospects and Investment Strategy Planning Analysis on China Food Waste Treatment Industry: 2017–2022.

[3] R. Chen, J. Jiang, R. Huang et al., "Review on recovery and reuse of waste oil," *Innovation and Application of Science and Technology*, vol. 9, no. 211, pp. 7–9, 2017.

[4] F. Zhou, Y. Xu, C. Tang et al., "Review on the development of food waste management policy in China," *Low-carbon Econo*, vol. 9, no. 2, p. 10, 2020.

[5] M. Eskandarpour, P. Dejax, J. Miemczyk, and O. Péton, "Sustainable supply chain network design: an optimization-oriented review," *Omega*, vol. 54, pp. 11–32, 2015.

[6] S. V. Mohan, G. Nikhil, P. Chiranjeevi et al., "Waste biorefinery models towards sustainable circular bioeconomy: critical review and future perspectives," *Bioresource Technology*, vol. 215, pp. 2–12, 2016.

[7] Y. Ge, L. Li, and L. Yun, "Modeling and economic optimization of cellulosic biofuel supply chain considering multiple conversion pathways," *Applied Energy*, vol. 281, 2021.

[8] H. Soleimaniankhezerlou, B. Vahdani, and M. Yazdani, "Designing a resilient and reliable biomass-to-biofuel supply chain under risk pooling and congestion effects and fleet management," *Journal of Cleaner Production*, vol. 281, Article ID 125101, 2020.

[9] G. Baudry, "How the cap limit for food-crop-based biofuels may affect France's stakeholders by 2030? a range-based multi-actor multi-criteria analysis," *Transportation Research Part D: Transport and Environment*, vol. 63, pp. 291–308, 2018.

[10] E. Gao, T. Sowlati, and S. Akhtari, "Profit allocation in collaborative bioenergy and biofuel supply chains," *Energy*, vol. 188, no. 1, pp. 116013.1–116013.13, 2019.

[11] G. Gosálbe, B. L. Montastruc, A. Stéphane Negny et al., "Optimal design and planning of biomass-to-biofuel supply chain considering economic dimension under strategic and tactical levels: a case study in Ethiopia," *Computer Aided Chemical Engineering*, vol. 48, pp. 1111–1116, 2020.

[12] E. Markel, C. Sims, and B. C. English, "Policy uncertainty and the optimal investment decisions of second-generation biofuel producers," *Energy Economics*, vol. 76, 2018.

[13] M. R. Anuar and A. Z. Abdullah, "Challenges in biodiesel industry with regards to feedstock, environmental, social and

sustainability issues: a critical review," *Renewable and Sustainable Energy Reviews*, vol. 58, pp. 208–223, 2016.

[14] B. D. Solomon, "Biofuels and sustainability," *Annals of the New York Academy of Sciences*, vol. 1185, no. 1, pp. 119–134, 2010.

[15] R. A. Efroymson, H. I. Jager, S. Mandal et al., "Better management practices for environmentally sustainable production of microalgae and algal biofuels," *Journal of Cleaner Production*, vol. 289, pp. 125–150, 2021.

[16] F. Javed, M. Aslam, N. Rashid et al., "Microalgae-based biofuels, resource recovery and wastewater treatment: a pathway towards sustainable biorefinery," *Fuel*, vol. 255, pp. 115826.1–115826.15, 2019.

[17] W. Ramakrishna, P. Rathore, R. Kumari et al., "Brown gold of marginal soil: plant growth promoting bacteria to overcome plant abiotic stress for agriculture, biofuels and carbon sequestration," *Science of the Total Environment*, vol. 711, pp. 135062, 2020.

[18] G. Chiriboga, Andrés De La Rosa, C. Molina et al., "Energy return on investment (EROI) and life cycle analysis (LCA) of biofuels in Ecuador," *Elsevier Public Health Emergency Collection*, vol. 6, no. 6, 2020.

[19] A. Kumar, C. Guria, and A. K. Pathak, "Optimal cultivation towards enhanced algae-biomass and lipid production using Dunaliella tertiolecta for biofuel application and potential CO2 bio-fixation: effect of nitrogen deficient fertilizer, light intensity, salinity and carbon supply strategy," *Energy*, vol. 148, pp. 1069–1086, 2018.

[20] F. You, L. Tao, D. J. Graziano, and S. W. Snyder, "Optimal design of sustainable cellulosic biofuel supply chains: multiobjective optimization coupled with life cycle assessment and input-output analysis," *AIChE Journal*, vol. 58, no. 4, pp. 1157–1180, 2012.

[21] L. F. Lira-Barragán, J. M. Ponce-Ortega, M. Serna-González, and M. M. El-Halwagi, "Synthesis of integrated absorption refrigeration systems involving economic and environmental objectives and quantifying social benefits," *Applied Thermal Engineering*, vol. 52, no. 2, pp. 402–419, 2013.

[22] H. S. Bamufleh, J. M. Ponce-Ortega, and M. M. El-Halwagi, "Multi-objective optimization of process cogeneration systems with economic, environmental, and social tradeoffs," *Clean Technologies and Environmental Policy*, vol. 15, no. 1, pp. 185–197, 2013.

[23] A. Chaabane, A. Ramudhin, and M. Paquet, "Design of sustainable supply chains under the emission trading scheme," *International Journal of Production Economics*, vol. 135, no. 1, pp. 37–49, 2012.

[24] O. Akgul, N. Shah, and L. G. Papageorgiou, "An optimisation framework for a hybrid first/second generation bioethanol supply chain," *Computers & Chemical Engineering*, vol. 42, pp. 101–114, 2012.

[25] J. Q. Neto, J. M. Bloemhof-Ruwaard, J. A. Van Nunen et al., *Designing and Evaluating Sustainable Logistics Networks*, University of Bath, Bath, UK, 2006.

[26] G. Guillén-Gosálbez, F. D. Mele, and I. E. Grossmann, "A bi-criterion optimization approach for the design and planning of hydrogen supply chains for vehicle use," *AIChE Journal*, vol. 56, no. 3, pp. 650–667, 2010.

[27] A. Hugo, P. Rutter, S. Pistikopoulos, A. Amorelli, and G. Zoia, "Hydrogen infrastructure strategic planning using multi-objective optimization," *International Journal of Hydrogen Energy*, vol. 30, no. 15, pp. 1523–1534, 2005.

[28] K. Govindan, R. Khodaverdi, and A. Jafarian, "A fuzzy multi criteria approach for measuring sustainability performance of a supplier based on triple bottom line approach," *Journal of Cleaner Production*, vol. 47, pp. 345–354, 2013.

[29] E. Erkut, A. Karagiannidis, G. Perkoulidis, and S. A. Tjandra, "A multicriteria facility location model for municipal solid waste management in North Greece," *European Journal of Operational Research*, vol. 187, no. 3, pp. 1402–1421, 2008.

[30] M. Zhang, B. Wiegmans, and L. Tavasszy, "Optimization of multimodal networks including environmental costs: a model and findings for transport policy," *Computers in Industry*, vol. 64, no. 2, pp. 136–145, 2013.

[31] D. Yue, M. A. Kim, and F. You, "Design of sustainable product systems and supply chains with life cycle optimization based on functional unit: general modeling framework, mixed-integer nonlinear programming algorithms and case study on hydrocarbon biofuels," *ACS Sustainable Chemistry & Engineering*, vol. 1, no. 8, pp. 1003–1014, 2013.

[32] D. Yue, M. Slivinsky, J. Sumpter, and F. You, "Sustainable design and operation of cellulosic bioelectricity supply chain networks with life cycle economic, environmental, and social optimization," *Industrial & Engineering Chemistry Research*, vol. 53, no. 10, pp. 4008–4029, 2014.

[33] C. Pozo, R. Ruíz-Femenia, J. Caballero, G. Guillén-Gosálbez, and L. Jiménez, "On the use of Principal Component Analysis for reducing the number of environmental objectives in multi-objective optimization: application to the design of chemical supply chains," *Chemical Engineering Science*, vol. 69, no. 1, pp. 146–158, 2012.

[34] M. Pérez-Fortes, J. M. Laínez-Aguirre, P. Arranz-Piera, E. Velo, and L. Puigjaner, "Design of regional and sustainable bio-based networks for electricity generation using a multi-objective MILP approach," *Energy*, vol. 44, no. 1, pp. 79–95, 2012.

[35] T. Xifeng, Z. Ji, and X. Peng, "A multi-objective optimization model for sustainable logistics facility location," *Transportation Research Part D: Transport and Environment*, vol. 22, pp. 45–48, 2013.

[36] G. Tuzkaya, B. Gülsün, and Ş. Önsel, "A methodology for the strategic design of reverse logistics networks and its application in the Turkish white goods industry," *International Journal of Production Research*, vol. 49, no. 15, pp. 4543–4571, 2011.

[37] A. Messac, A. Ismail-Yahaya, and C. A. Mattson, "The normalized normal constraint method for generating the Pareto frontier," *Structural and Multidisciplinary Optimization*, vol. 25, no. 2, pp. 86–98, 2003.

[38] C. Guo, X. Liu, M. Jin, and Z. Lv, "The research on optimization of auto supply chain network robust model under macroeconomic fluctuations," *Chaos, Solitons & Fractals*, vol. 89, pp. 105–114, 2016.

[39] R. Li, S. Wu, Z. Song et al., "The impact of restaurant's type on their kitchen waste production," *Environmental Engineering*, vol. 34, pp. 762–764, 2016.

[40] Y. Zhang, Y. Jiang, M. Zhong et al., "Robust optimization on regional WCO-for-Biodiesel supply chain under supply and demand uncertainties," *Scientific Programming*, vol. 2016, Article ID 1087845, 15 pages, 2016.

[41] L. Tan, "Research status and application prospect of biodiesel from waste cooking oil," *Chemical Production and Technology*, vol. 14, no. 1, pp. 30–33, 2007.

[42] Y. Qi, Z. Wang, and Y. Li, "Cost analysis of food waste collection and transportation in Shanghai," *Environmental Sanitation Engineering*, vol. 16, no. 3, pp. 47–49, 2008.

[43] Q. Lu, Q. Zhu, and Z. He, *Production Technology and Cost Analysis of Biodiesel at Home and Abroad*, 2011.

[44] Z. Liu, T. Qiu, and B. Chen, "A study of the LCA based biofuel supply chain multi-objective optimization model with multi-conversion paths in China," *Applied Energy*, vol. 126, pp. 221–234, 2014.

[45] H. Chen, J. Liu, H. Zhong et al., "Carbon emission reduction potential analysis of different treatment modes of kitchen waste," *Chinese Environmental Science*, vol. 33, no. 11, pp. 2102–2106, 2013.

[46] T. R. P. Ramos, M. I. Gomes, and A. P. Barbosa-Póvoa, "Planning waste cooking oil collection systems," *Waste Management*, vol. 33, no. 8, pp. 1691–1703, 2013.

Hindawi
Discrete Dynamics in Nature and Society
Volume 2021, Article ID 6683728, 11 pages
https://doi.org/10.1155/2021/6683728

Research Article

Evolutionary Game Analysis of Information Sharing in Fresh Product Supply Chain

Yanhui Li, He Xu, and Yan Zhao

School of Information Management, Central China Normal University, Wuhan 430079, China

Correspondence should be addressed to Yan Zhao; yanz@mails.ccnu.edu.cn

Received 19 November 2020; Revised 4 February 2021; Accepted 27 February 2021; Published 8 March 2021

Academic Editor: Tingsong Wang

Fresh produce has increasingly become an important part of people's diet. However, the loss of fresh produce in the supply chain has existed for a long time and is difficult to overcome. Some companies use their own information management systems or use information systems built by other companies to release and manage fresh agricultural product information in a timely manner, thereby reducing product loss caused by the "bullwhip effect." However, this will also bring pressure on construction costs and the risk of information leakage. Based on the evolutionary game model, this paper conducts process modeling and analysis on the behavior of enterprise groups participating in information sharing. It is concluded that the greater the difference between the income obtained through information sharing and the cost of building information system, the higher the likelihood of enterprises participating in information sharing. In addition, the greater the profit from the construction of information platform, the smaller the profit of "free rider," and the smaller the risk of information leakage, the greater the enthusiasm of enterprises to participate in information sharing. Finally, some suggestions are proposed from the perspective of maximizing supply chain benefits.

1. Introduction

Fresh produce refers to the primary products that are sold without deep processing such as cooking and making but need to be kept fresh and simply arranged on the shelves. Fresh produce generally needs to be refrigerated and frozen to keep fresh, and bulk commodities need to be sold by weighing and barcoding, with a relatively short shelf life. Fresh produce mainly includes fruits, vegetables, meat, and aquatic products. With the improvement of people's living standards, fresh produce has become an important part of people's diet. However, the loss of fresh produce in the supply chain has existed for a long time and is difficult to overcome. In 2019, the transaction volume of China's fresh food market reached 2.04 trillion, with a year-on-year increase of 6.8%. However, about 20%–30% of the fresh produce is wasted during different stages in the fresh product supply chain [1]. Compared with other commodities, such as daily necessities and household electrical appliances, the information asymmetry existing in the upstream and downstream of the fresh product supply chain has exacerbated the loss [2]. Therefore, information sharing behavior has a more profound impact on the business decisions of upstream suppliers and downstream retailers in the fresh product supply chain. Through information sharing, upstream and downstream companies can arrange production, sales, and inventory plans based on the shared information, which not only reduces operating costs of the supply chain but also is more flexible to market response; furthermore, it can reduce fresh produce loss of quantity and quality. According to Porter's competitive strategy theory [3], in order to gain advantages in negotiations, companies usually retain some private information. In the process of information sharing, information platform costs and risks of information leakage must also be considered. Once a company shares valuable private information with other companies, the company's control over the spread of this information in the supply chain will inevitably be weakened [4].

Therefore, how companies participate in the construction of information platforms and what form they use to share information has become a question worth exploring.

From the perspective of bounded rationality, this paper uses evolutionary game theory to study the dynamic evolution of information sharing between upstream suppliers and downstream retailers in the fresh product supply chain and discusses the evolution law of enterprise group information sharing strategy in supply chain.

2. Literature Review

Due to the special deterioration properties of fresh produce, the research on the supply chain of fresh produce is usually classified into the research on the supply chain of deteriorated products. In 1913, in the inventory control model based on the classical economic order quantity (EOQ) model proposed by Harris, the implicit assumption is that the inventory goods have an infinite shelf life and will not deteriorate or damage [5]. As early as 1953, Abad believed that fashion goods would deteriorate after the prescribed storage period [6]. Almost ten years later, Ghare and Schrader first proposed the use of a negative exponential decay function to simulate deteriorating product inventory [7]. About 50 years later, based on different assumptions, many researchers have discussed different issues about the supply chain with deterioration. Hau et al. believe that the information transmitted in the form of "orders" is easily distorted and may mislead upstream members' inventory and production decisions. In particular, the variance of orders may be greater than the variance of sales. From downstream to upstream, distortion will also increase. And they named this phenomenon "bullwhip effect" [8].

Some scholars have studied the factors that influence corporate information sharing behavior. Cachon and Fisher found that traditional inventory management and information exchange technologies enable companies to quickly exchange information with companies on the information chain. The author compared the traditional strategy of not using shared information with the complete information strategy of using shared information. The supply chain cost under the complete information strategy is on average 2.2% lower than that of the traditional information strategy, and the maximum difference is 12.1%. The authors believed that the implementation of information technology to accelerate and smooth the actual flow of goods in the supply chain is more valuable than the use of information technology to expand the flow of information [9]. Additionally, Huiping focused on analyzing the value created by information sharing, which reduced inventory levels in the three-level supply chain system. He discussed the coordination mechanism that upstream partners provide incentives for retailers through sharing profits and information sharing.

Some papers have explored the factors and mechanisms affecting information sharing. The author used the method of cooperative game to study the conflict of interest between the whole supply chain and a single partner and, finally, proposed a solution to how to effectively motivate partners to cooperate with each other to resolve the profit distribution between partners [10]. Luai et al. adopted a two-stage qualitative method. They conducted 40 interviews (4 in each case) through interviews with 7 experts and 10 comparative case studies on the relationship between producers and exporters. Supplemented by archival materials and non-participant observation, the author thought that specific affairs, relationships, and network drivers support information sharing in these relationships. This information sharing is linked to export performance. In the case of high performance, information sharing is triggered by integration-centric driving factors, and the focus is on long-term and joint planning on the basis of broader information sharing. In the case of poor performance, information sharing is triggered by more personalized driving factors [11]. Ye et al. [12] used CVaR criteria to measure risk and pointed out the influencing factors of demand information sharing from three different levels. Guo et al. studied the strategic information sharing behavior in two competitive channels: a decentralized supply chain and an integrated supply chain. The author believes that when competition in the retail market intensifies, retailers should reduce information sharing, but when their ability to obtain information improves, more information should be disclosed [13].

Many scholars have also used game theory to discuss the information sharing behavior in supply chain. In view of the asymmetry of supply and demand information between manufacturers and sellers, Wang Ying established a game model of information sharing, analyzed the changes in expected profits before and after sharing demand information and cost information, and eventually proposed an incentive mechanism for information sharing between manufacturers and distributors [14]. Esmaeili and Zeephongsekul proposed several seller-buyer supply chain models under the asymmetric information model and used the non-cooperative Stackelberg game model to study the incentive strategies when the buyer conceals the demand information and the seller conceals the cost information. The author also proposes a semi-cooperative model, which uses the sharing marketing expenditure as an incentive strategy to reveal information [15]. In traditional game theory, participants often participate in the game under complete information conditions, and they are often assumed to be completely rational. However, the complexity of the economic environment and the game problem itself causes incomplete information, which leads to the participants bounded rationally. Smith and Price have made contributions to the development of evolutionary game theory. Their evolutionary stability strategy has become the basic concept of evolutionary game theory [16, 17]. Furthermore, Bach, Helvikc, and Christiansen studied the divergence problem of the evolutionary stability strategy [18] and conducted related research on the cooperative evolutionary game problem in the case of one-party imitating [19].

In summary, to overcome the difficulties in information asymmetry in the supply chain and improve the level of information sharing, many studies have explored from the perspectives of technology applications, operation models, coordination mechanisms, incentive contracts, and competition forms. Different from supply chain of industrial products, the supply chain of fresh produce has the characteristics of short product cycle, volatile prices related to freshness, supply volume with a certain degree of

randomness, and more uncontrollable factors. Because of the particularity of its products, the "bullwhip effect" in the supply chain has a more profound impact on the supply chain. Since the evolutionary game theory is aimed at low-rational parties that only have simple imitating ability, the decision-making method is to follow the crowd and is greatly affected by random factors. In addition, most of the fresh product supply chain companies are small- and medium-sized enterprises. When making information sharing decisions, they often refer to the decision-making behavior of companies of the same type. Although evolutionary game has been used in many fields, it is seldom used in the study of information sharing behavior involving fresh supply chain. Based on the existing research and the evolutionary game model, this paper conducts a study on the behavior of information sharing in the fresh product supply chain.

3. Problem Description and Formulation

In this section, we discuss the information sharing behavior between upstream suppliers and downstream retailers in a two-level supply chain of fresh produce. In the process of information sharing, the upstream and downstream enterprises attach great importance to measure the profit and the loss. The profit and loss brought by the information sharing behavior will reverse affect the information sharing decision of the upstream and downstream enterprises.

The basic idea of evolutionary game is as follows: in the game group with a certain scale, the players carry out repeated game activities. Due to bounded rationality, it is impossible for players to find the optimal equilibrium point in every game. They will focus on the successful players to improve their game behavior. Therefore, their best strategy is to imitate and improve the most advantageous strategy of the past. The object of evolutionary game theory is a "population," which focuses on the change in population structure, rather than the effect analysis of individual behavior. When all participants in a system adopt the "evolutionary stability strategy," the individuals who adopt other strategies will not be able to invade the system. Or, individuals who adopt other strategies will change their strategies or exit the system under the pressure of natural selection. That is to say, the information sharing behavior of the upstream and downstream enterprises in the fresh product supply chain will eventually reach a stable state, and the income will be higher than that of the enterprises adopting other strategies, so as to reach a stable level.

In the process of this game, the behavior of upstream and downstream enterprises is not completely rational, and the strategic combination of both sides is {sharing, not sharing}. Moreover, in order to meet the needs of consumers and obtain profits, the relationship between the two sides is fixed. In the process of game, one member is chosen from each group. Each member will adjust his strategy according to the choice of other members. The assumptions and related variables are as follows.

Assumption 1. Regarding the two-level supply chain system of the upstream and downstream enterprises of agricultural products supply chain as a dynamic system, both sides of the cooperation are bounded rationality, and they pursue the maximization of interests and have learning ability and speculation behavior. In the process of learning and imitating, both sides of the game seek better strategies through trial and error and selection, so as to achieve a dynamic balance.

Assumption 2. When upstream suppliers and downstream retailers share information, the "bullwhip effect" will be eliminated to a certain extent, and then both sides will have information sharing benefits from responding flexibly to market and reducing fresh produce loss. When sharing unilaterally, the other side will get additional benefits, while the sharing party will have potential losses due to the risk of information leakage in addition to benefits and construction costs.

Assumption 3. Upstream supplier A (downstream retailer A) can make use of the information platform unilaterally constructed by downstream retailer B (upstream supplier b) and make use of the other party's information platform in a certain extent through "free rider," so as to obtain certain benefits. However, because the information platform is built according to the needs of enterprise B (upstream supplier B), the profit obtained by enterprise B through the construction of information platform is more than that of enterprise a by " free rider" ($\lambda > \beta$).

For ease of reference, the list of notations is shown in Table 1.

Based on the above assumptions, we can establish the payoff matrix U of both sides of the game.

4. Evolutionary Game Analysis

4.1. Equilibrium Analysis. According to the above payment matrix, the game is analyzed and solved by the bounded rationality game model.

According to Table 2, the expected payoff for upstream supplier sharing information is

$$\begin{aligned} u_{11} &= y\left(\pi_1 + \beta_1 l - \theta_1 - \alpha C\right) + (1-y)\pi_1 + \beta_1 l - \theta_1 - C \\ &= \pi_1 + \beta_1 l - \theta_1 - C + (1-\alpha) yC. \end{aligned} \tag{1}$$

The expected payoff for upstream supplier not sharing information is

$$u_{12} = y\left(\pi_1 + \lambda_1 l\right) + (1-y)\pi_1 = \pi_1 + y\lambda_1 l. \tag{2}$$

The average expected payoff for upstream supplier is

$$\begin{aligned} u_1 &= x u_{11} + (1-x) u_{12} = x\left[\pi_1 + \beta_1 l - \theta_1 - C + (1-\alpha) yC\right] \\ &\quad + (1-x)\left(\pi_1 + y\lambda_1 l\right) = \pi_1 + y\lambda_1 l \\ &\quad + x\left[\pi_1 + \beta_1 l - \theta_1 - C + (1-\alpha) yC - \pi_1 - y\lambda_1 l\right]. \end{aligned} \tag{3}$$

The replicator dynamics equation of upstream supplier is

Table 1: List of notations.

Symbol	Description
x	The proportion of upstream suppliers participating in information of fresh product sharing
$1-x$	The proportion of upstream suppliers not participating in information of fresh product sharing
y	The proportion of downstream retailers participating in information of fresh product sharing
$1-y$	The proportion of downstream retailers not participating in information of fresh product sharing
l	The additional revenue of two-echelon supply chain due to information sharing
C	The information of fresh product sharing cost
π_1	The upstream supplier's income, when the information is not shared
π_2	The downstream retailer's income, when the information is not shared
β_1	The percentage of the additional revenue of upstream supplier in the additional revenue of whole supply chain due to participation in information sharing
β_2	The percentage of the additional revenue of downstream retailer in the additional revenue of whole supply chain due to participation in information sharing
λ_1	The percentage of the additional revenue of upstream supplier in the additional revenue of whole supply chain due to unilateral use of shared information from downstream retailer
λ_2	The percentage of the additional revenue of downstream retailer in the additional revenue of whole supply chain due to unilateral use of shared information from upstream supplier
θ_1	The loss of information leakage caused by upstream supplier sharing information
θ_2	The loss of information leakage caused by downstream retailer sharing information
α	The proportion of the information sharing cost borne by the upstream supplier, when the supply chain participants are all involved in information sharing
$1-\alpha$	The proportion of the information sharing cost borne by the downstream retailer, when the supply chain participants are all involved in information sharing

Table 2: Information sharing evolutionary game payoff matrix.

		Downstream retailer	
		Sharing (y)	Not sharing ($1-y$)
Upstream supplier	Sharing (x)	$\pi_1+\beta_1 l-\theta_1-\alpha C$, $\pi_2+\beta_2 l-\theta_2-(1-\alpha)C$	$\pi_1+\beta_1 l-\theta_1-C$ $\pi_2+\lambda_2 l$
	Not sharing ($1-x$)	$\pi_1+\lambda_1 l$ $\pi_2+\beta_2 l-\theta_2-C$	π_1, π_2

$$F(x)=\frac{\mathrm{d}x(t)}{t}=x(u_{11}-u_1)=x(1-x)(u_{11}-u_{12}) = x(1-x)[\beta_1 l-\theta_1-C+(1-\alpha)yC-y\lambda_1 l]. \tag{4}$$

The expected payoff for downstream retailer sharing information is

$$u_{21}=x[\pi_2+\beta_2 l-\theta_2-(1-\alpha)C]+(1-x)(\pi_2+\beta_2 l-\theta_2-C)=\pi_2+\beta_2 l-\theta_2-C+x\alpha C. \tag{5}$$

The expected payoff for downstream retailer not sharing information is

$$u_{22}=x(\pi_2+\lambda_2 l)+(1-x)\pi_2=\pi_2+x\lambda_2 l. \tag{6}$$

The average expected payoff for downstream retailer is

$$\begin{aligned} u_2 &= yu_{21}+(1-y)\\ u_{22} &= y(\pi_2+\beta_2 l-\theta_2-C+x\alpha C)+(1-y)(\pi_2+x\lambda_2 l)\\ &= \pi_2+x\lambda_2 l+y(\pi_2+\beta_2 l-\theta_2-C+x\alpha C-\pi_2-x\lambda_2 l)\\ &= \pi_2+x\lambda_2 l+y(\beta_2 l-\theta_2-C+x\alpha C-x\lambda_2 l). \end{aligned} \tag{7}$$

The replicator dynamics equation of downstream retailer is

$$F(y)=\frac{\mathrm{d}y(t)}{t}=y(u_{11}-u_1)=y(1-y)(u_{21}-u_{22}) = y(1-y)(\beta_2 l-\theta_2-C+x\alpha C-x\lambda_2 l). \tag{8}$$

Let $F(x)=0$ and $F(y)=0$, then five singularities can be gained:
$O=(0,0), A=(1,0), B=(0,1), C=(1,1)$, and $D=(x^*, y^*)$, where $x^*=(C+\theta_2-\beta_2 l/\alpha C-\lambda_2 l)$ and $y^*=(C+\theta_1-\beta_1 l/(1-\alpha)C-\lambda_1 l)$. By solving$F\prime(x)$ and $F\prime(y)$ separately, we have $F\prime(x)=(1-2x)[\beta_1 l-\theta_1-C+(1-\alpha)yC-y\lambda_1 l]$ and $F\prime(y)=(1-2y)(\beta_2 l-\theta_2-C+x\alpha C-x\lambda_2 l)$. Then, let $F\prime(x)=0$ and $F\prime(y)=0$, we can get the solutions:$x_1=(1/2)$ and $y_1=(1/2)$, $x_2=(C+\theta_2-\beta_2 l/\alpha C-\lambda_2 l)$, and $y_2=(C+\theta_1-\beta_1 l/(1-\alpha)C-\lambda_1 l)$.

From the above results, when x^* and y^* exist, we get $\alpha C>\lambda_2 l, (1-\alpha)C>\lambda_1 l$, $C+\theta_2>\beta_2 l, C+\theta_1>\beta_1 l$. The cost shared by all parties in the cooperative construction of information platform is greater than the benefits brought by "free rider." And the total construction cost is greater than the difference between the profit brought by information

sharing minus the risk of information leakage when the two sides share information. The following is a detailed analysis.

When $\alpha C < \lambda_2 l < \beta_2 l - \theta_2$, $(1-\alpha)C < \lambda_1 l < \beta_1 l - \theta_1$, $C < \beta_2 l - \theta_2$, $C < \beta_1 l - \theta_1$, whether it is upstream or downstream, choosing information sharing is a dominant strategy. Choosing to share information always has more benefits than not sharing information. Then, the game will have the Nash equilibrium {sharing, sharing}. From this, we can also see that, with the development of information technology, when the cost of information construction is low to a certain extent, the two sides of the game will definitely choose to share information to maximize their own benefits.

4.2. Stability Analysis of Equilibrium. Use the local stability analysis of the Jacobian matrix to analyze the local stability of each point. The Jacobian matrix of the evolutionary game is $J = \begin{pmatrix} ((dx/dt)/dx) & ((dx/dt)/dy) \\ ((dy/dt)/dx) & ((dy/dt)/dy) \end{pmatrix}$. It can be obtained by substitution:

$$J = \begin{pmatrix} (1-2x)\left[\beta_1 l - \theta_1 - C + (1-\alpha)yC - y\lambda_1 l\right] & x(1-x)\left[(1-\alpha)C - \lambda_1 l\right] \\ y(1-y)\left(\alpha C - \lambda_2 l\right) & (1-2y)\left(\beta_2 l - \theta_2 - C + x\alpha C - x\lambda_2 l\right) \end{pmatrix}, \tag{9}$$

in which

$$\begin{aligned} \det J &= (1-2x)\left[\beta_1 l - \theta_1 - C + (1-\alpha)yC - y\lambda_1 l\right] * (1-2y)\left(\beta_2 l - \theta_2 - C + x\alpha C - x\lambda_2 l\right) - x(1-x)\left[(1-\alpha)C - \lambda_1 l\right] \\ &\quad * y(1-y)\left(\alpha C - \lambda_2 l\right), \\ \mathrm{tr} J &= (1-2x)\left[\beta_1 l - \theta_1 - C + (1-\alpha)yC - y\lambda_1 l\right] + (1-2y)\left(\beta_2 l - \theta_2 - C + x\alpha C - x\lambda_2 l\right). \end{aligned} \tag{10}$$

The equilibrium point satisfying the determinant $\det J > 0$ and the trace of matrix $\mathrm{tr} J < 0$ is the evolutionary stability strategy of the system. Calculating the expressions of determinant $\det J$ and trace $\mathrm{tr} J$ of the matrix at five equilibrium points, the results are shown in Table 3.

According to the above expression, the stability of the equilibrium point of the game is analyzed. The results are shown in Table 4.

4.3. Analysis of Evolutionary Game Results. According to the stability theorem of replicator equation and the properties of evolutionary stable strategy, when $F(y) = 0, F\prime(y) < 0, y^*$ is an evolutionary stable strategy. The following is discussion.

(1) When $x^* < (C + \theta_2 - \beta_2 l/\alpha C - \lambda_2 l)$, for $y^* = 0$, $F(y^*) = 0$, $F\prime(y^*) < 0$, $y^* = 0$ is asymptotically stable points. When the number of upstream suppliers participating in information sharing does not reach a certain amount or is relatively small, the proportion of downstream suppliers sharing information decreases. The changing trend of imitator dynamic evolution is shown in Figure 1.

(2) When $x^* = (C + \theta_2 - \beta_2 l/\alpha C - \lambda_2 l)$, for $F(y) = 0$, $F\prime(y) = 0$, all the values of the y are in a stable state. If the proportion of the upstream suppliers participating in information sharing reaches $(C + \theta_2 - \beta_2 l/\alpha C - \lambda_2 l)$, the dynamic evolution state of downstream retailers is relatively stable.

(3) When $x^* > (C + \theta_2 - \beta_2 l/\alpha C - \lambda_2 l)$, for $y^* = 1$, $F(y^*) = 0$, $F\prime(y^*) < 0$, $y^* = 1$ is asymptotically stable points. When the number of upstream suppliers participating in information sharing reaches a certain amount or relatively large, the proportion of downstream suppliers sharing information increases.

Same as above, when $F(x) = 0, F\prime(x) < 0, y^*$ is an evolutionary stable strategy. The following is discussion.

(1) When $y^* < ((C + \theta_1 - \beta_1 l)/((1-\alpha)C - \lambda_1 l))$, for $x^* = 0$, $F(x^*) = 0$, $F\prime(x^*) < 0$, $y^* = 0$ is asymptotically stable points. When the number of downstream retailers participating in information sharing does not reach a certain amount or is relatively small, the proportion of upstream suppliers sharing information decreases. The changing trend of imitator dynamic evolution is shown in Figure 2.

(2) When $y^* = ((C + \theta_1 - \beta_1 l)/((1-\alpha)C - \lambda_1 l))$, for $F(x) = 0$, $F\prime(x) = 0$, all the values of x are in a stable state. If the proportion of the downstream retailers participating in information sharing reaches $((C + \theta_1 - \beta_1 l)/((1-\alpha)C - \lambda_1 l))$, the dynamic evolution state of upstream suppliers is relatively stable.

(3) When $y^* > ((C + \theta_1 - \beta_1 l)/((1-\alpha)C - \lambda_1 l))$, for $y^* = 1$, $F(y^*) = 0$, $F\prime(y^*) < 0$, $y^* = 1$ is asymptotically stable points. When the number of downstream retailers participating in information sharing reaches a certain amount or is relatively large, the proportion of upstream suppliers sharing information increases.

As discussed above, if the cost is small enough, there will always be more additional benefits from sharing, and all companies will choose to share information. When

Table 3: The determinant det J and trace tr J of equilibrium point.

Equilibrium point	Determinant det J	Trace tr J
$(0,0)$	$(\beta_2 l-\theta_2-C)*(\beta_1 l-\theta_1-C)$	$(\beta_2 l-\theta_2-C)+(\beta_1 l-\theta_1-C)$
$(0,1)$	$(\beta_1 l-\theta_1-\alpha C-\lambda_1 l)*(-)(\beta_2 l-\theta_2-C)$	$[\beta_1 l-\theta_1-\alpha C-\lambda_1 l]-(\beta_2 l-\theta_2-C)$
$(1,0)$	$-(\beta_1 l-\theta_1-C)*(\beta_2 l-\theta_2-(1-\alpha)C-\lambda_2 l)$	$-(\beta_1 l-\theta_1-C)+(\beta_2 l-\theta_2-(1-\alpha)C-\lambda_2 l)$
$(1,1)$	$(\beta_1 l-\theta_1-\alpha C-\lambda_1 l)*[\beta_2 l-\theta_2-(1-\alpha)C-\lambda_2 l]$	$-(\beta_1 l-\theta_1-\alpha C-\lambda_1 l)-[\beta_2 l-\theta_2-(1-\alpha)C-\lambda_2 l]$
(x^*,y^*)	$-x^*(1-x^*)[(1-\alpha)C-\lambda_1 l]*y^*(1-y^*)(\alpha C-\lambda_2 l)$	0

Table 4: Stability analysis of equilibrium point.

Known conditions	Equilibrium point	Symbol of determinant	Symbol of trace	Result
Condition 1	$O(0,0)$	+	—	ESS
$\beta_1 l-\theta_1-C<0$	$A(0,1)$	—	Uncertain	Unstable
$\beta_2 l-\theta_2-C<0$	$B(1,0)$	—	Uncertain	Unstable
$\beta_1 l-\theta_1-\alpha C-\lambda_1 l<0$	$C(1,1)$	+	+	Unstable
$\beta_2 l-\theta_2-(1-\alpha)C-\lambda_2 l<0$	$D(x^*,y^*)$	—	0	Saddle point
Condition 2	$O(0,0)$	+	—	ESS
$\beta_1 l-\theta_1-C<0$	$A(0,1)$	+	+	Unstable
$\beta_2 l-\theta_2-C<0$	$B(1,0)$	—	Uncertain	Unstable
$\beta_1 l-\theta_1-\alpha C-\lambda_1 l>0$	$C(1,1)$	—	Uncertain	Unstable
$\beta_2 l-\theta_2-(1-\alpha)C-\lambda_2 l<0$	$D(x^*,y^*)$	—	0	Saddle point
Condition 3	$O(0,0)$	+	—	ESS
$\beta_1 l-\theta_1-C<0$	$A(0,1)$	—	Uncertain	Unstable
$\beta_2 l-\theta_2-C<0$	$B(1,0)$	+	+	Unstable
$\beta_1 l-\theta_1-\alpha C-\lambda_1 l<0$	$C(1,1)$	—	Uncertain	Unstable
$\beta_2 l-\theta_2-(1-\alpha)C-\lambda_2 l>0$	$D(x^*,y^*)$	—	0	Saddle point
Condition 4	$O(0,0)$	+	—	ESS
$\beta_1 l-\theta_1-C<0$	$A(0,1)$	—	Uncertain	Unstable
$\beta_2 l-\theta_2-C<0$	$B(1,0)$	—	Uncertain	Unstable
$\beta_1 l-\theta_1-\alpha C-\lambda_1 l>0$	$C(1,1)$	+	—	ESS
$\beta_2 l-\theta_2-(1-\alpha)C-\lambda_2 l>0$	$D(x^*,y^*)$	—	0	Saddle point

$1>x^*>0$ and $1>y^*>0$, for $y=((C+\theta_1-\beta_1 l)/((1-\alpha)C-\lambda_1 l))$, equation (4) is always be equal to 0, and x is stable. For $y>((C+\theta_1-\beta_1 l)/((1-\alpha)C-\lambda_1 l))$, equation (4) is positive and $x=0, x=1$ is a two-stable stage, where $x=1$ is an evolutionary stable strategy. For $y<((C+\theta_1-\beta_1 l)/((1-\alpha)C-\lambda_1 l))$, equation (4) is negative, and $x=0, x=1$ is a two-stable stage, where $x=0$ is an evolutionary stable strategy. The evolutionary stable strategy of y can be analyzed in the same way of x. The dynamic relationship between the above two groups is represented by a two-dimensional drawing, as shown in Figure 3.

Point O indicates that both upstream and downstream enterprises do not share information, while point C indicates that both upstream and downstream enterprises participate in information sharing. When the profit of information sharing is greater than that of building information system, both sides will adopt information sharing strategy after long-term game. Through the formula derivation, we can observe that the basic income π when information is not shared has no influence on the formation of decision equilibrium state.

With the improvement in people's living standards, the demand for fresh produce is also increasing. Information sharing in the supply chain of farm products is an effective means to improve the efficiency of the supply chain and reduce the consumption rate of fresh produce. This is also in line with the basic cognition. In fact, enterprises in fresh product supply chain may not be completely rational and often choose to follow others. Through the above model, it can be seen that the larger the S_{ADBC} area, the greater the possibility of enterprises to participate in information sharing. The area of S_{ADBC} is related to the difference in income from information sharing and cost of building information system. The greater the difference, the greater the probability of upstream and downstream enterprises participating in information sharing. We can observe that the closer point D is to point O, the larger area of S_{ADBC} is, the more likely enterprises are to share information. That is, $((C+\theta_2-\beta_2 l)/(\alpha C-\lambda_2 l))$, $((C+\theta_1-\beta_1 l)/((1-\alpha)C-\lambda_1 l))$ the smaller, the greater the possibility of information sharing. We can infer that the smaller the "free rider" revenue ratio (λ) is, the greater the proportion of construction income (β) is, the less loss caused by information leakage and the greater the possibility of enterprise information sharing is. The following text will use numerical simulation to verify this.

5. Numerical Simulation

In order to elaborate the evolution game more intuitively, we make some numerical analyses to simulate the dynamic evolution of its strategy select in different situations. We take initial point at 0.1 intervals and set the time step to 1. Referring to the research of Cai et al. [20–22], the parameter values are $\alpha=0.5$, $C=20$, and $l=100$.

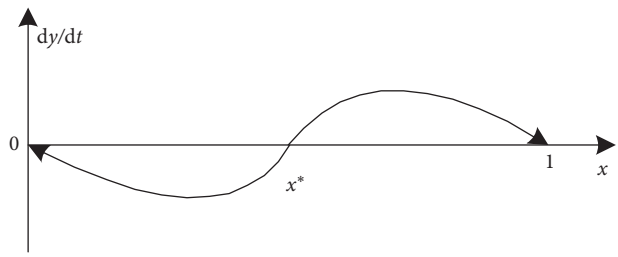

Figure 1: Changing trends of information sharing in evolutionary game $x^* = ((C + \theta_2 - \beta_2 l)/(\alpha C - \lambda_2 l))$.

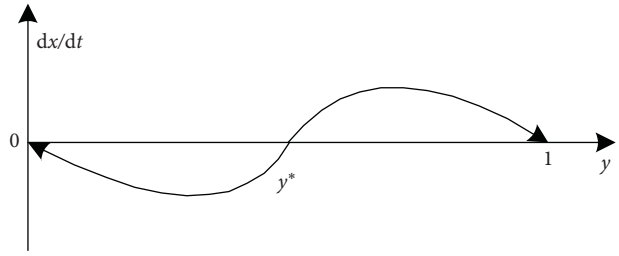

Figure 2: Changing trends of information sharing in evolutionary game $y^* = ((C + \theta_1 - \beta_1 l)/((1 - \alpha)C - \lambda_1 l))$.

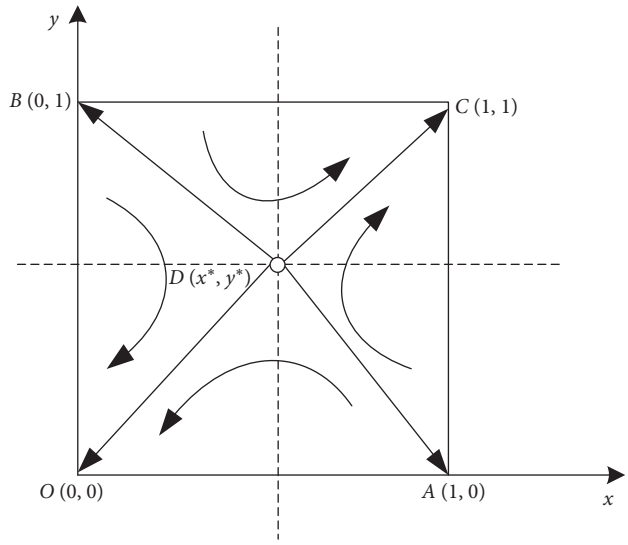

Figure 3: Schematic diagram of group replication dynamics and stability of both parties in the game.

(1) Assuming that $\lambda_1 = \lambda_2 = 0.05, \theta_1 = \theta_2 = 5$. The values of β are assumed to be 0.1, 0.2, 0.3, and 0.4. In the case of different β, the dynamic evolution process of enterprise's strategy is shown in Figure 4. When β is larger, enterprises gradually change from unwilling to share to willing to share. Because enterprises benefit more from information sharing, when β increases, the greater the percentage of the additional revenue (β), the faster the enterprises participate in information sharing.

(2) Assuming that $\theta_1 = \theta_2 = 5, \beta_1 = \beta_2 = 0.3$. The values of λ are assumed to be 0, 0.05, 0.075, and 0.1. In the case of different λ, the dynamic evolution process of enterprise's strategy is shown in Figure 5. The larger the percentage of the additional revenue (λ) due to unilateral use of shared information from others, the slower the enterprises participating in information sharing.

(3) Assuming that $\beta_1 = \beta_2 = 0.3, \lambda_1 = \lambda_2 = 0.05$. The values of θ are assumed to be 0, 5, 10, and 15. In the case of different θ, the dynamic evolution process of enterprise's strategy is shown in Figure 6. With the increase in information leakage loss, enterprises gradually change their strategies from information sharing to not sharing.

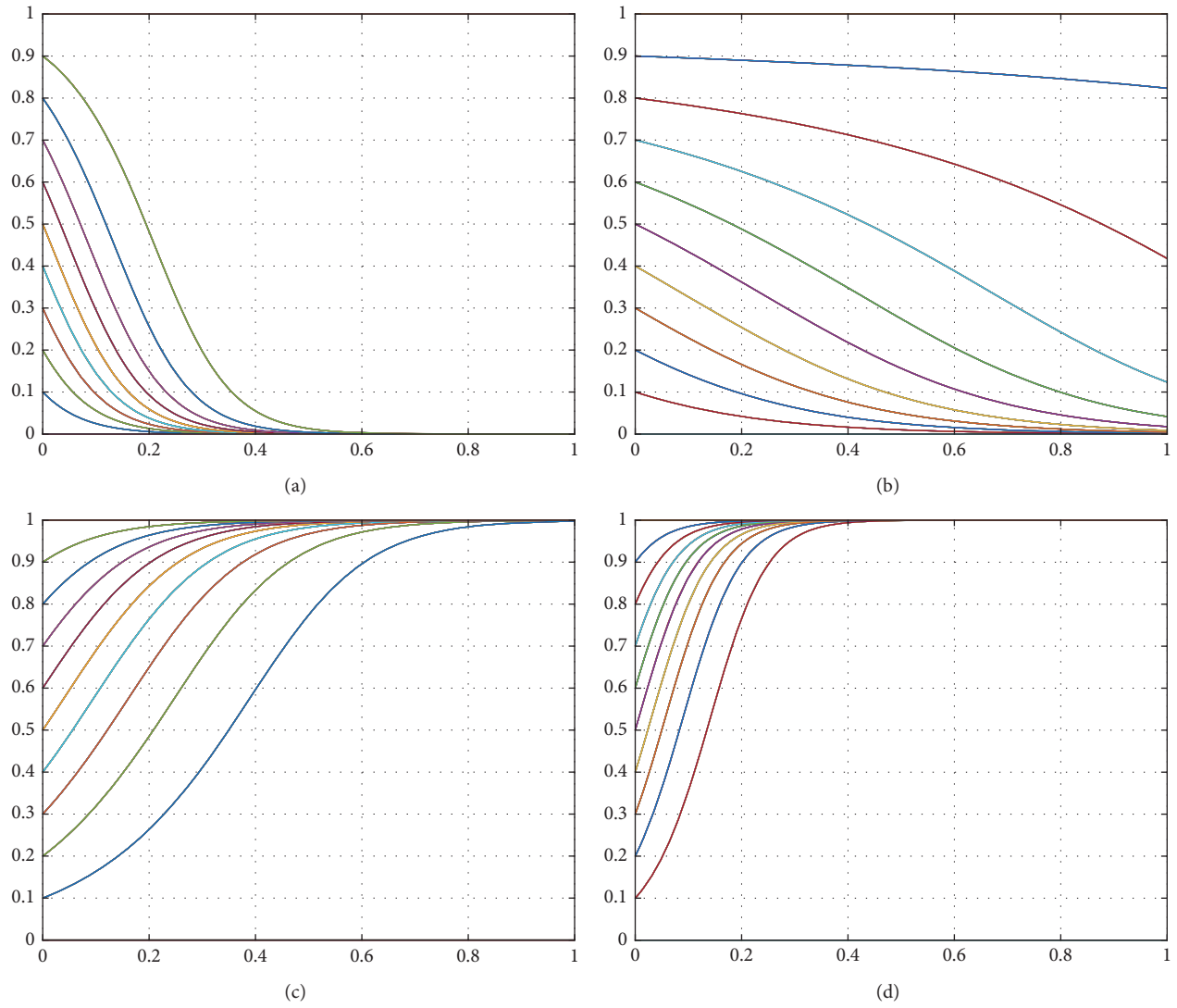

Figure 4: In the case of different β values, dynamic evolution process of information sharing: (a)$\beta_1 - \beta_2 = 0.1$; (b)$\beta_1 - \beta_2 = 0.2$; (c)$\beta_1 - \beta_2 = 0.3$; (d)$\beta_1 - \beta_2 = 0.4$.

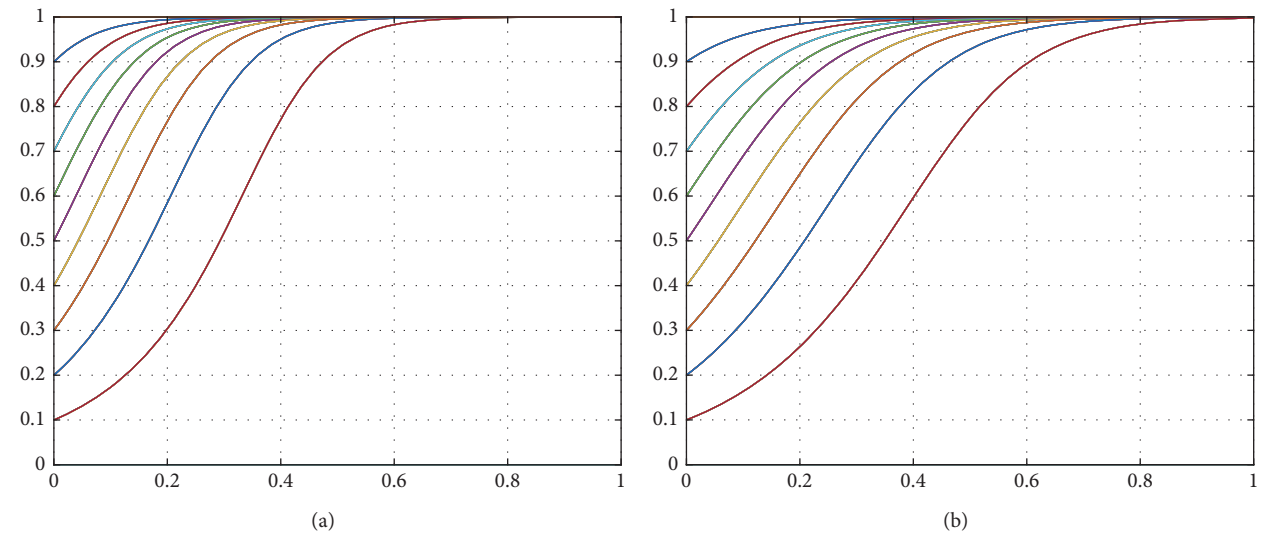

Figure 5: Continued.

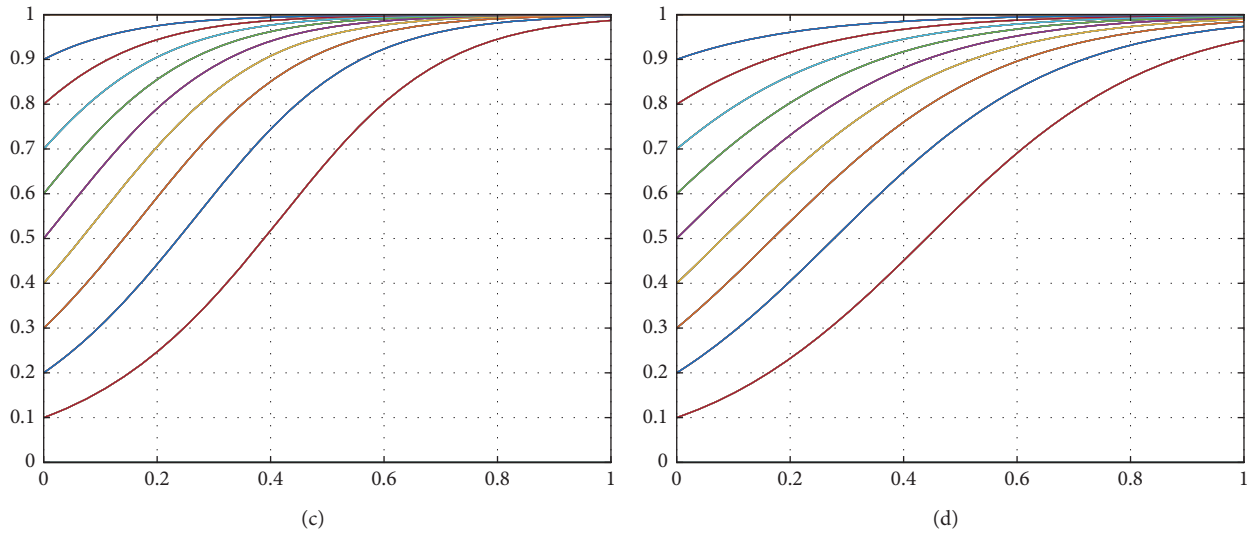

Figure 5: In the case of different λ values, dynamic evolution process of information sharing: (a)$\lambda_1 = \lambda_2 = 0$; (b) $\lambda_1 = \lambda_2 = 0.05$; (c) $\lambda_1 = \lambda_2 = 0.075$; (d)$\lambda_1 = \lambda_2 = 0.1$.

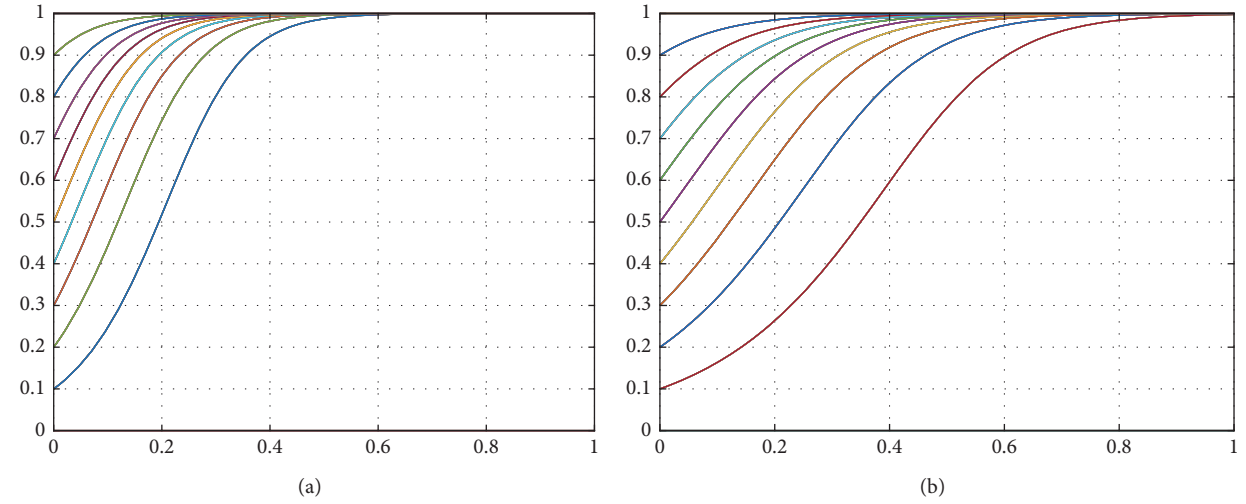

Figure 6: Continued.

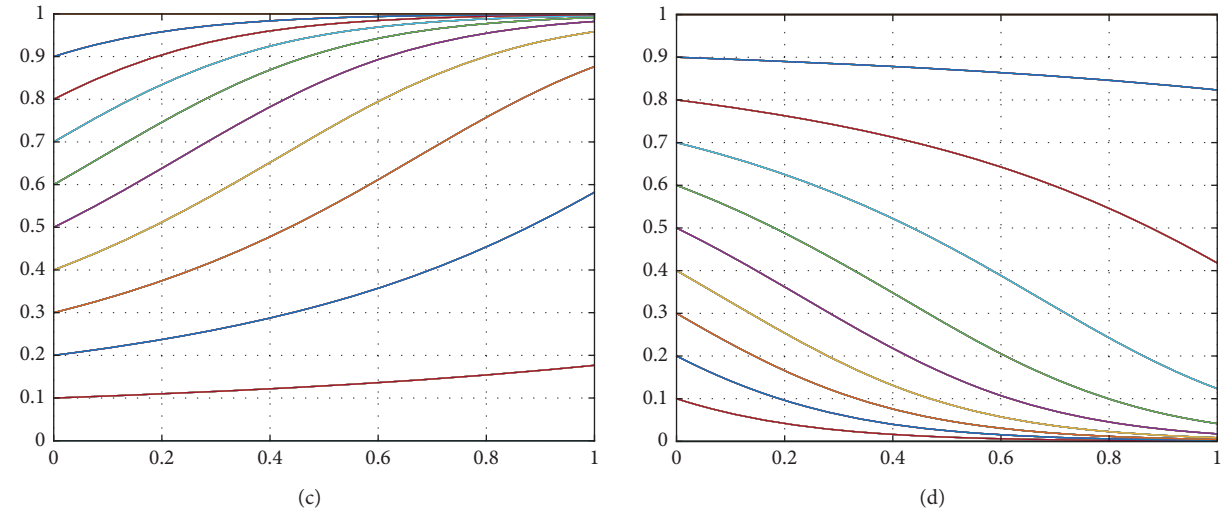

Figure 6: In the case of different θ values, dynamic evolution process of information sharing: (a)$\theta_1 = \theta_2 = 0$; (b) $\theta_1 = \theta_2 = 5$; (c)$\theta_1 = \theta_2 = 10$; (d)$\theta_1 = \theta_2 = 15$.

6. Conclusions

Information sharing in the fresh product supply chain is an effective means to improve the flexibility of the supply chain and reduce the consumption of fresh produce. To solve the loss of fresh produce in a two-echelon supply chain, some companies build their own information management systems or use information systems built by other companies to share and manage the information of fresh produce in a timely manner, thereby reducing product wastage brought by the "bullwhip effect." In practical situation, companies may not be completely rational and often follow suit. Based on the evolutionary game and the characteristics of fresh produce, this paper conducts process modeling and analysis on the behavior of upstream suppliers and downstream retailers participating in information sharing. Some conclusions are drawn as follows:

(1) The larger the difference between the profit obtained through information sharing and the cost of building information system, the greater the probability of upstream suppliers and downstream retailers participating in information sharing.

(2) When the proportion of construction revenue (β) is greater, "free rider" revenue ratio (λ) is smaller, and the loss (θ) of information leakage caused by information sharing is smaller, upstream suppliers and downstream retailers are more likely to participate in information sharing.

Based on the above findings, some management implications can be got as follows:

(1) For upstream wholesalers and downstream retailers, the loss and cost can be reduced effectively by building information sharing platforms, such as ERP, OMS, WMS, TMS, and DMS. At the same time, in order to improve the profit of supply chain members from information sharing, the government can give incentives and subsidies to the construction of information platform and launch farmers' information technology training, to encourage supply chain members to participate in information sharing more actively. In this way, the quality and the timeliness of fresh produce will be improved, and ultimately the efficiency of the whole fresh product supply chain also will be improved.

(2) When the supply chain members use the information sharing system that has been built by the other party, the platform builder can charge the management fee of the information platform or providing the system interface with compensation. By reducing the "free rider" income of the members who do not share information, the progress of their participation in information sharing speeds up. Furthermore, the members can obtain a certain proportion of extraprofits brought by information sharing by means of incentive contracts such as the revenue sharing contract, which can also encourage those who do not share information to change their strategies to participate in information sharing. At the same time, the loss caused by information leakage will reduce the information sharing willingness of supply chain participants, so it is necessary to formulate constraint mechanism and confidentiality agreement to reduce the risk of information leakage.

Although some useful conclusions and management implications have been obtained in this article, there is still a lot of research space in the future. Further research can consider increasing government subsidy variables to explore the impact of subsidy mechanism on upstream and downstream enterprises' participation in information sharing.

Data Availability

The corresponding data used to support the findings of this study are included within the article.

Conflicts of Interest

The authors declare that they have no conflicts of interest.

Acknowledgments

This research was supported by the National Natural Science Foundation of China (Grant no. 71471073) and Fundamental Research Funds for the Central Universities (Grant no. CCNU19TS078).

References

[1] C. Mena, L. A. Terry, A. Williams, and L. Ellram, "Causes of waste across multi-tier supply networks: cases in the UK food sector," *International Journal of Production Economics*, vol. 152, no. 6, pp. 144–158, 2014.

[2] Y. Yang, T.-J. Fan, and L. Zhang, "Coordination of fresh agricultural supply chain with asymmetric freshness information," *Chinese Journal of Management Science*, vol. 24, no. 9, pp. 147–155, 2016, in Chinese.

[3] M. E. Porter, "Competitive strategy," *Journal of Marketing*, vol. 1, no. 2, 1980.

[4] H. Fu and M. Jian, "Supply chain information management strategy under information leakage," *Computer Integrated Manufacturing Systems*, vol. 20, no. 8, pp. 2170–2178, 2015, in Chinese.

[5] F. W. Harris, "How many parts to make at once," *Operations Research*, vol. 38, no. 6, pp. 947–950, 1990.

[6] P. L. Abad, "Optimal price and order size for a reseller under partial backordering," *Computers & Operations Research*, vol. 28, no. 1, pp. 53–65, 2001.

[7] S. F. Schrader, "A model for exponentially decaying inventory," *The Journal of Industrial Engineering*, vol. 14, pp. 238–243, 1963.

[8] H. L. Lee, V. Padmanabhan, and S. Whang, "Information distortion in a supply chain: the bullwhip effect," *Management Science*, vol. 43, no. 4, pp. 546–558, 1997.

[9] G. P. Cachon and M. Fisher, "Supply chain inventory management and the value of shared information," *Management Science*, vol. 46, no. 8, pp. 1032–1048, 2000.
[10] H. Ding, B. Guo, and Z. Liu, "Information sharing and profit allotment based on supply chain cooperation," *International Journal of Production Economics*, vol. 133, no. 1, pp. 70–79, 2011.
[11] L. Jraisat, M. Gotsi, and M. Bourlakis, "Drivers of information sharing and export performance in the Jordanian agri-food export supply chain," *International Marketing Review*, vol. 30, no. 4, pp. 323–356, 2013.
[12] F. Ye, X.-M. Chen, and Q. Lin, "Analysis of supply chain's demand information sharing values based on decision-maker's risk aversion characteristics," *Journal of Industrial Engineering and Engineering Management*, vol. 26, no. 3, pp. 176–196, 2012, in Chinese.
[13] L. Guo, T. Li, and H. Zhang, "Strategic information sharing in competing channels," *Production and Operations Management*, vol. 23, no. 10, pp. 1719–1731, 2015.
[14] Y. Wang, "Game and incentives in the information sharing among supply chain members," *Chinese Journal of Management Science*, vol. 13, no. 5, pp. 61–66, 2005, in Chinese.
[15] M. Esmaeili and P. Zeephongsekul, "Seller-buyer models of supply chain management with an asymmetric information structure," *International Journal of Production Economics*, vol. 123, no. 1, pp. 146–154, 2010.
[16] J. M. Smith, "The theory of games and the evolution of animal conflict," *Journal of Theory Biology*, vol. 47, no. 1, pp. 209–221, 1973.
[17] J. M. Smith and G. R. Price, "The logic of animal conflicts," *Nature*, vol. 246, no. 1, pp. 15–18, 1974.
[18] L. A. Bach, T. Helvikc, and F. B. Christiansen, "The evolution of n-player cooperation-threshold games and ESS bifurcations," *Journal of Theoretical Biology*, vol. 238, no. 1, pp. 426–434, 2006.
[19] D. K. Levine and W. Pesendorfer, "The evolution of cooperation through imitation," *Games and Economic Behavior*, vol. 58, no. 2, pp. 293–315, 2007.
[20] X. Cai, J. Chen, Y. Xiao, X. Xu, and G. Yu, "Fresh-product supply chain management with logistics outsourcing," *Omega*, vol. 41, no. 4, pp. 752–765, 2013.
[21] B. H. Guo, Z. G. Fang, and Q. Liu, ""Study of regional energy-intensive industry's exit mechanism based on evolutionary game," *Chinese Journal of Management Science*, vol. 20, no. 4, pp. 79–85, 2012, in Chinese.
[22] B. Dan and J. Chen, "Coordinating Fresh Agricultural Supply Chain under the Valuable Loss," *Chinese Journal of Management Science*, vol. 16, no. 5, pp. 42–49, 2008, in Chinese.

Hindawi
Discrete Dynamics in Nature and Society
Volume 2021, Article ID 6690478, 12 pages
https://doi.org/10.1155/2021/6690478

Research Article

Sparse and Dense Mixed Grid Transit Accessible Network Based on Uneven Distribution of Travel Demand

Chen Guo,[1,2] **Jianjun Wang**,[1] **Yueying Huo**,[2,3] **and Meiying Jian**[2]

[1]*College of Transportation Engineering, Chang'an University, Xi'an 710064, China*
[2]*Transportation Institute, Inner Mongolia University, Huhhot 010070, China*
[3]*School of Mathematical Science, Inner Mongolia University, Huhhot 010021, China*

Correspondence should be addressed to Jianjun Wang; wjjun16@chd.edu.cn

Received 8 December 2020; Revised 22 January 2021; Accepted 2 February 2021; Published 18 February 2021

Academic Editor: Tingsong Wang

The uneven distribution of travel demand is incredibly commonplace in cities, but insufficient attention has been paid to this problem. In this paper, we explore the impact of the uneven distribution of travel demand on an accessible network. A model with a sparse and dense mixed grid transit network based on an uneven distribution of travel demand is proposed to provide a high-performance bus service. The transit network was composed of two parts: a dense grid network in the downtown area and a sparse grid network in the periphery. The objective function of the model included agency cost and passenger cost, where the decision variables were the downtown-to-city ratio, the downtown headway, stop spacing (line spacing), and ratio of the periphery headway to the downtown headway. This study validated the proposed model using the demands of San Francisco. The concentrated spatial demand resulted in a lower total cost, whereas the varying travel demand must be controlled within an appropriate range to maintain the bus performance. The stable bus lines and stops with a variable timetable of the proposed model are profitable for fast-growing cities.

1. Introduction

Public transportation is a key way to solve the low efficiency of traffic and serious environmental pollution caused by the proliferation of private vehicles. Increasing the competitiveness of the bus systems reduces private car travel. To attract more residents to travel by bus, transit agencies must provide a high-quality level of service. A bus network having good coverage in time and space is one of the main ways to improve the level of service for buses. Bus services with good coverage in time and space include the following elements: high spatial coverage of stops, accessible lines for passengers between any origin-destination (OD) pairs, high frequency of vehicles, and long service time [1]. A simple and robust bus network is helpful for optimizing these elements.

The bus network planning method can be divided into two categories: direct networks and accessible networks [1]. The direct network [2–11] aims to reduce passenger transfers by designing multidirectional lines based on the OD matrix. However, the following problems exist for direct networks: (1) The cost of bus agencies is high because of the high duplication of bus lines and the complexity of the network. (2) The frequency and service time of different lines are greatly affected by the OD matrix. Therefore, it is inconvenient for passengers to travel when there is less demand in the OD matrix. (3) With the development of the city, the bus lines need to be completely replanned, which would cause the bus system to have poor stability [12–17].

To overcome the above problems in direct networks, some researchers have developed an accessible network that minimizes the door-to-door travel time of passengers, although the transfers will increase. For an accessible network, the plans of the network are not based on the OD matrix. The design of the bus network is based on the geometry of the urban road structures and travel demand functions, such as direct-service everywhere [18], radial networks [19], grid networks [20], radial-ring networks [21], and mixed networks [12–17]. Compared with the direct network, the

accessible network has the following advantages: (1) The design of bus lines in the network is based on simplifications and reduces the duplication of the bus lines, which increases the frequency of all bus lines and is easy to understand. (2) An accessible network is human-oriented to passengers with flexible demands [22]. In the above studies, the grid-radial hybrid network with uniform demand proposed by Daganzo [12] is notable. The grid-radial hybrid network can substantially reduce the travel time of passengers without increasing the cost of bus agencies. Estrada et al. applied the results of Daganzo [12] to redesign the transit network of Barcelona [13]. By comparing the network of Barcelona before and after the transformation, it was proven that the mode share of transit greatly increased after the transformation [14]. Hugo et al. [15], Nocera et al. [16], and Chen et al. [17] transformed the network by Daganzo [12] for cities with different structures and travel demand functions.

In practice, travel demand is more concentrated in downtown areas, whereas, in the periphery, travel demand decreases. In other words, travel demand is always uneven in cities. The problem of uneven distribution of travel demand is more complex, but it is more accurate. Most current studies do not consider uneven travel demand when investigating the issue of accessible networks. In this paper, the impact of uneven travel demand on an accessible network is discussed. The grid-radial hybrid network was composed of a grid network in the downtown area and a radial network in the periphery, so the network would be less stable because of the development of the downtown area. Therefore, a sparse and dense mixed grid transit network is proposed, which transforms the grid-radial hybrid network to improve stability. The main purpose of this study is to provide a feasible method for bus line design and frequency allocation in transit planning. This is crucial for enhancing public transportation performance.

The structure of the paper is as follows: part 2 is the section introducing the sparse and dense mixed grid transit network, along with the objective function, constraints, and decision variables of the model; the results are presented in part 3 to validate the proposed model; part 4 analyzes the changes of spatial demands that were conducted, and the sparse and dense mixed grid transit network is compared with the grid-radial hybrid network; finally, part 5 presents the conclusions and considerations for future work.

2. Materials and Methods

2.1. Sparse and Dense Mixed Grid Network. The sparse and dense mixed grid network is used in cities with grid road networks and downtown areas at corners, such as San Francisco, Shanghai, Shantou, and Hohhot in China. The two adjacent cities of the downtown areas are close to the sides of the city. Cities are always limited by natural environmental factors or are developed according to their economy. The uneven distribution of urban structures has bigger impact on the transit planning. These types of sites are shown in Figure 1. The travel demand is unevenly distributed in space and time. The downtown demand is evenly distributed, and the peripheral travel demand decreases linearly with the distance from the edge of downtown. The travel demand downtown is f ($f \geq 1$) times that at the edge of the periphery. Let the downtown travel demand density function be 1, and let the periphery demand function be $(1 - kx)$, where x is the distance from the travel origin to the edge of the downtown area in the periphery and k is a function of f: $k = ((1 - (1/f))/((1 - \alpha)D))$. Passenger travel in a city is time-independent. The number of passengers traveling is Λ (pax/h) during peak hours and averages λ (pax/h) hourly during service time. λ is a constant.

According to the distribution of passenger demand, the layout of the bus network is a dense grid in the downtown area and a sparse grid in the periphery. The bus lines were designed in two directions. The model included four decision variables: spatial variables and time-related variables. Spatial variables are the bus stop spacing s (km) and α, which is the ratio of the downtown side length d (km) to the city side length D (km). The headway downtown H (h) and the ratio of headway in the periphery to the headway downtown are time-related variables. The bus stop spacing in the entire city is s. The headway downtown is H; in the periphery, one vehicle runs on n roads and the headway is nH. The spatial coverage of the transit is constant throughout the city, whereas the time coverage in the periphery is less than that in downtown areas. Compared to the even grid network, the distance traveled by vehicles and the number of vehicles are reduced, and the bus service maintains a high time and spatial coverage. For passengers, the maximum transfer is one, and the network is more convenient to read and remember.

2.2. Agency Cost. The objective function of the proposed model is to minimize the total cost of the network. To achieve this, agency and passenger costs are considered. The agency cost is composed of the lane construction cost L (km), cost of the total distance traveled by vehicles per hour V (veh.km/h), and cost of the total number of vehicles per hour M (veh/h). The lane construction cost is the fixed capital investment, whereas the others are flexible and belong to the operating costs. If bus lanes exist, the lane construction cost is zero. M is the ratio of V to the travel speed v_c (km/h) [12]. The full derivations of these parameters are presented in Appendix.

$$L = \frac{2D^2}{s},$$
$$V = \frac{4D^2\left(\alpha^2 n - \alpha^2 + 1\right)}{Hns}, \quad (1)$$
$$M = \frac{V}{v_c}.$$

2.3. Passenger Cost. The passenger cost includes the access and egress time A (h), waiting time W (h), in-vehicle time T (h), and transfer time. In-vehicle time is the ratio of the expected travel distance E (km) to v_c. The transfer time is

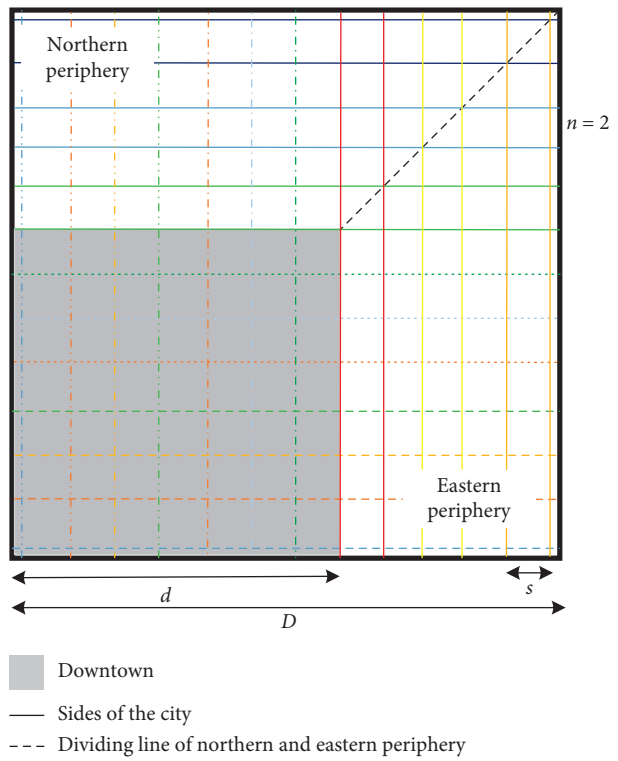

FIGURE 1: The sparse and dense mixed grid model. *Lines of the same line type and color are run by the same fleet.

calculated by the expected number of transfers per trip e_T, average transfer distance b (km), and walking speed v_w (km/h) [23]. The maximum occupancy in critical lines during peak hours O (pax/h) is also a key parameter to determine whether the bus capacity C (pax/h) can meet the travel demand [24]. Passengers are distributed based on an all-or-nothing basis. The assumptions are as follows: (1) passengers choose bus lines according to the minimum time, and (2) they choose the nearest bus stop. If two bus stops can be used and they are equidistant to the passenger, then they randomly choose a bus stop. According to this assumption, equations (2)–(8) are the expressions of the parameters related to passenger cost. Appendix includes the calculation procedure for each parameter.

$$v_c = \frac{1}{((1/v) + (\tau/s) + \Lambda\tau'(1 + e_T)/V)}, \tag{2}$$

$$e_T = 1 - \frac{9\alpha^2 fs(D + \alpha D + f D - 2fs - \alpha f D) - 3s\left(D - s + \alpha D + f D - fs - \alpha^2 f D\right)\left(2\alpha + f - 2\alpha f - 5\alpha^2 f + 2\alpha^2 + 2\right)}{2D^2\left(2\alpha + f - 2\alpha f - 2\alpha^2 f + 2\alpha^2 + 2\right)^2}, \tag{3}$$

$$A = \frac{s}{v_w}, \tag{4}$$

$$W = \frac{H\left(2n + 2\alpha n + fn + 3\alpha^2 f + 2\alpha^2 n - 2\alpha fn - 5\alpha^2 fn\right)}{2\left(2\alpha + f - 2\alpha f - 2\alpha^2 f + 2\alpha^2 + 2\right)} \times \left[2 - \frac{3s\left(2\alpha + f - 2\alpha f + 5\alpha^2 f + 2\alpha^2 + 2\right)(D - s + \alpha D + f D - fs - \alpha f D)}{2D^2\left(2\alpha + f - 2\alpha f - 2\alpha^2 f + 2\alpha^2 + 2\right)^2} - \frac{9\alpha^2 f(D + \alpha D + f D - 2fs - \alpha f D)}{2D^2\left(2\alpha + f - 2\alpha f - 2\alpha^2 f + 2\alpha^2 + 2\right)^2}\right], \tag{5}$$

$$E = \frac{3\,D\left(50\alpha^5 f^2 - 100\alpha^5 f + 50\alpha^5 - 124\alpha^4 f^2 + 24\alpha^4 f + 100\alpha^4 + 129\alpha^3 f^2 - 167\alpha^3 f + 38\alpha^3 - 3\alpha^2 f^2 - 183\alpha^2 f\right)}{70\left(2\alpha + f - 2\alpha f - 2\alpha^2 f + 2\alpha^2 + 2\right)^2} + \frac{3\,D\left(186\alpha^2 - 65\alpha f^2 - 59\alpha f + 124\alpha + 13 f^2 + 65 f + 62\right)}{70\left(2\alpha + f - 2\alpha f - 2\alpha^2 f + 2\alpha^2 + 2\right)^2}, \tag{6}$$

$$T = \frac{E}{v_c}, \tag{7}$$

$$O = \frac{2sH\Lambda}{\alpha\, D}\left(\frac{1}{2} - \frac{\alpha^4 (2\alpha + 3f - 5\alpha f)^2}{8(1-\alpha)^2\left(2\alpha + f - 2\alpha f - 2\alpha^2 f + 2\alpha^2 + 2\right)^2}\right), \tag{8}$$

where v (km/h) denotes the cruising speed, which is the same as private cars and is affected by traffic management and control measures; τ (h/stop) denotes the bus dwelling time at each stop; and τ' (h/p) denotes the average passengers' boarding time.

2.4. Objective Function. The objective function Z of the proposed model minimizes the total cost, which includes the cost of the passenger and the agent. Agency cost considers the fare of travel, and passenger cost considers the travel time. This study converts agency cost to the time of each passenger [12]. The three parts of agency costs are multiplied by the weight variables $\pi_V = (c_V/(\lambda\mu))$, $\pi_M = (c_M/(\lambda\mu))$, and $\pi_L = (c_L/(\lambda\mu))$, where μ is the time value of passengers. The four components of passenger costs are multiplied by weight variables, namely, w_A, w_w, w_T, and w_e [24]. The objective function and constraints are given in the two following equations, respectively:

$$\min Z = [\pi_V V + \pi_L L + \pi_M M] + \left[w_A A + w_w W + w_T T + w_e \frac{b}{v_w} e_T\right], \tag{9}$$

$$\text{s.t. } s > 0;\ H_{\min} \le H \le H_{\max};\ \frac{s}{D} \le \alpha \le 1;\ O \le C;\ M \in N^*. \tag{10}$$

The first bracket of the objective function is the agency cost Z_A, and the second is the passenger cost Z_U. The second constraint limits the minimum and maximum headway values. $H_{\min}$ denotes the minimum headway to avoid bunching [25], and $H_{\max}$ denotes the maximum headway to maintain the time coverage. The fourth constraint restricts the maximum occupancy O in vehicles and does not exceed the capacity of the vehicles C.

2.5. Results. This paper presents a numerical method to measure the effect of the proposed network. The city size and travel demand, in this case, are consistent with those of San Francisco [26, 27], in which μ is approximately \$20/h [12]. To achieve this, bus rapid transit (BRT) is the most adequate mode [12]. Therefore, BRT was chosen as the basic mode in this study. The values of parameters were taken from the literature originating from the United States, Europe, and China [12–17, 25, 28–31]. In those studies, factors such as the type of bus lanes, signal delays, bus bunching, and criteria of high-quality service were considered. The access and egress time, waiting time, and transfer time for passengers may cause discomfort and anxiety. Therefore, w_A, w_w, and w_e were set to 2.2, 2.1, and 2.5, respectively [24]. The weight of the in-vehicle time was 1. The walking speed of pedestrians was approximately 4.5 km/h, whereas v_w was 2 km/h owing to delays caused by signal control and detours. For ease of calculation, f was set to 1. The parameters used are listed in Table 1. The model can produce the global optimal solution using the Lingo software.

It took 37 minutes to obtain the global optimal solution, and the results are listed in Table 2. The solution time of the model was reasonable. Because f was 1, the travel demand was evenly distributed throughout the city. α was close to 1. The ratio of the downtown area to the entire city area was approximately 0.92. The headway was about four minutes in the downtown area and n was equal to 1, so the headway in the periphery was also approximately four minutes. The stop spacing was approximately 406 m. For the entire city, the space-time coverage was consistent. The total cost of each passenger was 1.22 h. The average passenger cost was 0.96 h, and the average passenger travel time Z_{UT} was 0.62 h. The agency cost for each passenger was 0.26 h. The maximum occupancy in critical lines during peak hours had not reached the capacity of the vehicle, so the passenger travels during peak hours could increase. The total costs were stable and less affected by the decision variables, according to the sensitivity analysis. This is similar to the results obtained by Daganzo [12] and Chen [17].

3. Discussion

3.1. Spatial Travel Distribution. The distribution of spatial demand has a greater impact on travel time and bus costs, and it is closely related to urban planning and land use. In

Table 1: Value of model parameters.

Parameter	D (km)	λ (p)	$\wedge$ (p)	μ (\$/h)	c_L (\$/km)	c_V (\$/veh·km)	c_M (\$/veh)	w_A	w_w	
Value	10	20,000	50,000	20	90	2	40	2.2	2.1	
Parameter	w_e	w_T	v_w (km/h)	C (p/veh)	τ (h/stop)	τ' (h/p)	v (km/h)	b (km)	$H_{\min}$ (h)	$H_{\max}$ (h)	f
Value	2.5	1	2	200	35/3600	1/3600	40	0.03	2/60	5/60	1

Table 2: Model results.

Parameter	α	H (min)	s (m)	n	L (km)	M (veh)	V (veh.km/h)		v_c (km/h)
Value	0.96	4.0	406	1	492.82	759	14 947.51		19.69
Parameter	A (h)	W (h)	T (h)	e_T	Z_U (h)	Z_{UT} (h)	Z_A (h)	Z (h)	O (p)
Value	0.20	0.06	0.34	0.96	0.96	0.62	0.26	1.22	138

this section, changes in the spatial demand are discussed. f changed from 1 to 1.9, whereas the other parameters remained unchanged. The larger the value of f was, the more concentrated the travels were downtown.

The changes in the objective function and the decision variables with spatial demand are shown in Figures 2 and 3. According to the results, when the travel demand was more concentrated in the downtown area, Z and Z_U significantly dropped, whereas Z_A slowly increased. For agents, resources were more concentrated in downtown areas to provide better service, where the demand was higher, and the average travel distance and time were reduced for passengers. The growth in agency costs was smaller than the decline in average travel time. Therefore, the total cost was reduced. When f increased, α and s decreased. H was between 4 and 5 min. n varied from 1 to 4 and was only one nonmonotonic decision variable. The stop spacing was changed from 406 to 309 m. In this case, the spatial coverage of the network increased. The ratio of the downtown area to that of the whole city and stop spacing were relatively stable, whereas the headway was more variable. As a result, the lines and stops of the network were stable and the timetable was flexible. Above all, the bus system is relatively stable in the proposed model.

Although the speed of vehicles will decrease with more concentrated demands, passengers still prefer to live in cities with dense demands. When f was 1.4, the total cost and maximum occupancy in the critical line during peak hours were minimal. When $f > 1.9$, the model had no solution, and the downtown area drastically changed. Therefore, based on the goals of reducing passenger travel time and maintaining the competitiveness of buses, the spatial density difference in cities should be bounded.

3.2. Comparison between Sparse and Dense Mixed Grid and Grid-Radial Hybrid Networks. In this section, the sparse and dense mixed grid network and the grid-radial hybrid network are compared. The hybrid network was composed of a grid network in the downtown area and a radial network in the northern and eastern periphery [17]. The two types of networks were compared when f was 1 and 1.6. When $f > 1.6$, the hybrid network collapsed [17]. The other parameters were the same as before.

As shown in Table 3, for the decision variables, the values for s in the two types of networks are close. However, the values for α significantly change from one network to another. The ratio of the downtown area to the city area in the mixed grid network was always larger than that in the hybrid network. The values for H are similar, and the headway in the grid network is always larger than that in the hybrid network.

For the objective functions, when f was 1, the total cost of the hybrid network was lower for the agent and passengers. In the grid network, the number of transfers was smaller and the travel speed was faster. When f was equal to 1.6, the grid network performed better. Although the agency cost increased, passenger costs decreased considerably. The total cost of the grid network decreased by 34% compared to that of the hybrid network. The agency cost was similar, whereas the passenger cost in the grid network was much lower. The significant decrease in in-vehicle time was a result of the simpler bus network. The average in-vehicle time was smaller in the grid network, which is more attractive to passengers. Under different circumstances, the length of bus lines in the periphery was longer in the grid network, but most cities do not need bus lane construction costs owing to the existing lanes. The greater the difference in space demand is, the more noticeable the advantages of the mixed grid network are.

Network stability was also compared. For the bus system, the bus lines and stops were relatively stable, whereas the timetable varied more. With the development of cities, the headway in the periphery of the grid network can only be reduced. Naturally, the stable bus lines and stops are much

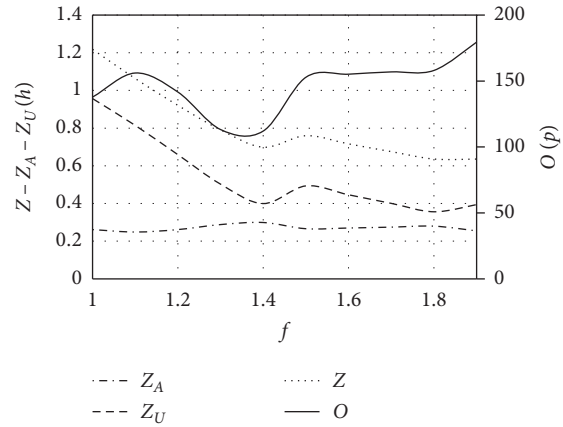

Figure 2: Change of the objective function with f.

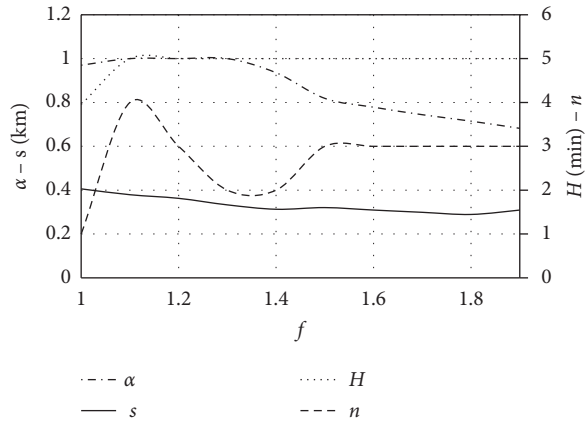

Figure 3: Change of the decision variables with f.

Table 3: Contrast of the sparse and dense mixed grid network and the grid-radial hybrid network.

		α	H (min)	s (m)	n	V (veh·km/h)	M (veh)	L (km)	v_c (km/h)
$f=1$	Hybrid	0.78	3	378	—	12 638.61	669.00	426.44	18.89
	Grid	0.97	4	406	1	14 947.51	759.00	492.82	19.69
$f=1.6$	Hybrid	0.68	3	334	—	11 058.20	625.00	438.52	17.69
	Grid	0.78	5	309	3	11 443.97	673.00	646.76	17.00
		A (h)	W (h)	e_T (h)	T (h)	Z_U (h)	Z_A (h)	Z (h)	O (pax/h)
$f=1$	Hybrid	0.19	0.05	1.01	0.34	0.91	0.23	1.14	76.00
	Grid	0.20	0.06	0.96	0.34	0.96	0.26	1.22	138.00
$f=1.6$	Hybrid	0.15	0.05	0.91	0.23	0.74	0.22	0.96	33.00
	Grid	0.17	0.06	0.95	0.10	0.45	0.27	0.72	155.00

more attractive to passengers with flexible travel demands. Therefore, the mixed grid network is more meaningful for developing cities because of the changes in urban planning and land use.

4. Conclusions

This paper proposes a sparse and dense mixed grid network based on the uneven travel demand facing cities with downtown areas at corners. The proposed model was tested by a numerical method in which the travel demand and urban structure are consistent with those in San Francisco. The global optimal solution was obtained within a satisfactory time using Lingo software. The impacts of uneven travel on an accessible network, such as bus line and frequency, are discussed. At present, few studies have focused on accessible bus networks, and the impacts of uneven travel demand on accessible networks have often been ignored.

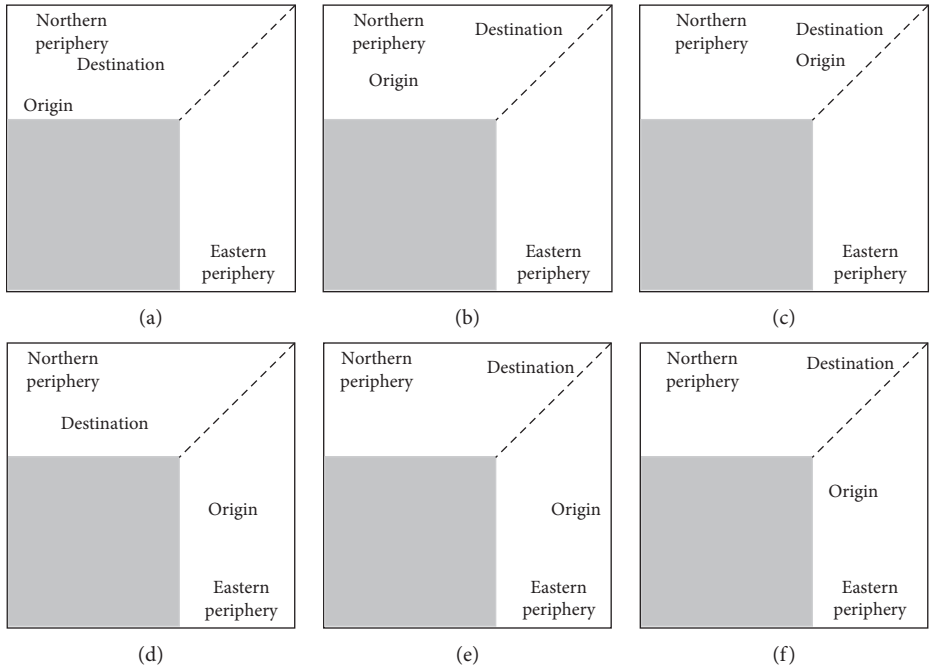

Figure 4: Different situations for case (b).

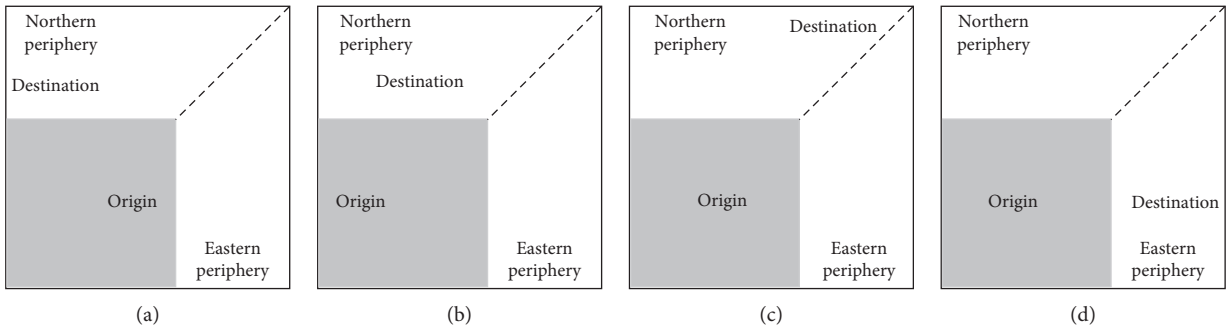

Figure 5: Four situations for case (c).

This type of network can be conducive to improving the stability of lines and stops and decreasing the in-vehicle time of passengers when compared with the grid-radial hybrid network. A sparse and dense mixed grid network is more beneficial for developing cities.

Analyses of the changes in spatial travel distribution were conducted. The results show that the model was consistent with real bus networks. Differences in spatial demand are critical for the sustainability and performance of transit. The concentrated spatial demand results in a lower total cost and better usage of buses by the public. Cities with concentrated demands are preferred by passengers because those cities have less access and egress time. However, if excessive travel is concentrated in downtown areas, it is not convenient for passengers in the periphery. As a result, bus competitiveness is weakened. Differences in land use should be planned within a reasonable range. The sparse and dense mixed grid network and grid-radial hybrid network were compared. The greater the difference in spatial demand is, the more noticeable the advantages of the sparse and dense mixed grid network are. The simple lines reduce the in-vehicle time of passengers and total costs. The stable bus lines and stops and the variable timetable of the sparse and dense mixed grid transit network are beneficial for fast-growing cities.

The bus design for cities with neighboring satellite cities, such as New York, Los Angeles, and Detroit, should be one of the focus points in future studies. The design problem of

clean energy buses, such as fleet size, lines, and stop locations, should also be considered, especially under stochastic charging demands [32].

Appendix

Result 1. The total length of the two-direction bus lane is given by $L = (2D^2/s)$.

Proof. Stops receiving double spatial coverage were associated with $2s$. The number of stops was $[D^2/s^2]$.

Result 2. The total distance traveled by vehicles per hour is given by $V = ((4D^2(\alpha^2 n - \alpha^2 + 1))/Hns)$.

The distance traveled by the vehicles is the ratio of the line length to the headway. The length of distance traveled is twice the length of the lines downtown: $2[2(D^2/s)\alpha^2] = ((4D^2\alpha^2)/s)$. The headway is H downtown, so the distance traveled per hour downtown V_d is $((4D^2\alpha^2)/(sH))$. The headway is nH in the periphery, and the length of distance traveled is $2[2(D^2/s)(1-\alpha)^2] = ((4D^2(1-\alpha^2))/s)$. Thus, the total distance traveled per hour in the periphery is $V_p = ((4D^2(1-\alpha^2))/(snH))$.
$V = V_d + V_p = ((4D^2(\alpha^2 n - \alpha^2 + 1))/(Hns))$.

Result 3. The expected number of transfers per trip is given by

$$e_T = P_1 = 1 - \frac{9\alpha^2 fs(D + \alpha D + fD - 2fs - \alpha fD) - 3s\left(D - s + \alpha D + fD - fs - \alpha^2 fD\right)\left(2\alpha + f - 2\alpha f - 5\alpha^2 f + 2\alpha^2 + 2\right)}{2D^2\left(2\alpha + f - 2\alpha f - 2\alpha^2 f + 2\alpha^2 + 2\right)^2}, \tag{A.1}$$

where e_T is equal to the probability of only doing one transfer.

Zero transfer: for a passenger, zero transfer occurred when both the origin and destination fell in the service area of one bus line. The probability may be calculated by the ratio of the travel demand satisfying that condition to the total travel demands. Thus, the origins in downtown areas or in the periphery are treated differently. Downtown, the following is true:

$$P_{0,d} = \frac{\int_0^{\alpha D}\int_0^{\alpha D} \mathrm{d}x\mathrm{d}y}{\int_0^{\alpha D}\int_0^{\alpha D} \mathrm{d}x\mathrm{d}y + 2\int_{\alpha D}^{D}\int_0^{x}(1-kx)\mathrm{d}x\mathrm{d}y} \frac{\alpha sD - s^2 + \int_{\alpha D}^{D} s(1-kx)\mathrm{d}x}{\int_0^{\alpha D}\int_0^{\alpha D} \mathrm{d}x\mathrm{d}y + 2\int_{\alpha D}^{D}\int_0^{x}(1-kx)\mathrm{d}x\mathrm{d}y}. \tag{A.2}$$

In the periphery, the following is true:

$$P_{0,p} = \frac{2\int_{\alpha D}^{D}\int_0^{x}(1-kx)\mathrm{d}x\mathrm{d}y}{\int_0^{\alpha D}\int_0^{\alpha D} \mathrm{d}x\mathrm{d}y + 2\int_{\alpha D}^{D}\int_0^{x}(1-kx)\mathrm{d}x\mathrm{d}y} \frac{\alpha sD + \int_{\alpha D}^{D} s(1-kx)\mathrm{d}x - \int_{(((1-\alpha)D)/2)-(s/2)}^{(((1-\alpha)D)/2)+(s/2)} s(1-kx)\mathrm{d}x}{\int_0^{\alpha D}\int_0^{\alpha D} \mathrm{d}x\mathrm{d}y + 2\int_{\alpha D}^{D}\int_0^{x}(1-kx)\mathrm{d}x\mathrm{d}y}, \tag{A.3}$$

$$P_0 = P_{0,d} + P_{0,p}.$$

One transfer: the probability of one transfer is one subtracting the probability of zero transfer. From this, the following is obtained: $e_T = P_1 = 1 - P_0$.

Result 4. The expected access and egress time are given by $A = (s/v_w)$.

The expected travel distance for one passenger at each stop was $s/2$. Thus, the expected access and egress distance is equal to s.

Result 5. The expected waiting time per passenger, including the origin and transfer stops, is

$$W = \frac{H\left(2n + 2\alpha n + fn + 3\alpha^2 f + 2\alpha^2 n - 2\alpha fn - 5\alpha^2 fn\right)}{2\left(2\alpha + f - 2\alpha f - 2\alpha^2 f + 2\alpha^2 + 2\right)} \times \left[2 - \frac{3s\left(2\alpha + f - 2\alpha f + 5\alpha^2 f + 2\alpha^2 + 2\right)(D - s + \alpha D + fD - fs - \alpha fD)}{2D^2\left(2\alpha + f - 2\alpha f - 2\alpha^2 f + 2\alpha^2 + 2\right)^2} - \frac{9\alpha^2 fs(D + \alpha D + fD - 2fs - \alpha fD)}{2D^2\left(2\alpha + f - 2\alpha f - 2\alpha^2 f + 2\alpha^2 + 2\right)^2}\right]. \tag{A.4}$$

Proof. Assume that passengers arrive independently of the timetable. The expected waiting time has two components: (i) W_O, at the origin stop, and (ii) W_T, at the transfer stop. W_O and W_T were identical.

W_O can be divided into waiting downtown $W_{O,d}$ and in the periphery $W_{O,p}$.

In downtown areas, the waiting time is $H/2$ and, when multiplied by the probability of being located downtown, the following is obtained:

$$W_{O,d} = \frac{H}{2} \cdot \frac{\int_0^{\alpha D} \mathrm{d}x \int_0^{\alpha D} \mathrm{d}y}{\int_0^{\alpha D} \int_0^{\alpha D} \mathrm{d}x\mathrm{d}y + 2\int_{\alpha D}^{D} \int_0^{x} (1 - kx)\mathrm{d}x\mathrm{d}y}. \tag{A.5}$$

In the periphery, the waiting time is $nH/2$. Multiplied by the probability of being located in the periphery, the following is obtained:

$$W_{O,p} = \frac{nH}{2} \cdot \frac{2\int_{\alpha D}^{D} \int_0^{x} (1 - kx)\mathrm{d}x\mathrm{d}y}{\int_0^{\alpha D} \int_0^{\alpha D} \mathrm{d}x\mathrm{d}y + 2\int_{\alpha D}^{D} \int_0^{x} (1 - kx)\mathrm{d}x\mathrm{d}y}. \tag{A.6}$$

Thus, $W_O = W_{O,d} + W_{O,p}$ and $W = W_O + P_1 \cdot W_O$.

Result 6. The expected in-vehicle travel distance per trip is given by

$$E = \frac{3D\left(50\alpha^5 f^2 - 100\alpha^5 f + 50\alpha^5 - 124\alpha^4 f^2 + 24\alpha^4 f + 100\alpha^4 + 129\alpha^3 f^2 - 167\alpha^3 f + 38\alpha^3 - 3\alpha^2 f^2 - 183\alpha^2 f\right)}{70\left(2\alpha + f - 2\alpha f - 2\alpha^2 f + 2\alpha^2 + 2\right)^2} + \frac{3D\left(186\alpha^2 - 65\alpha f^2 - 59\alpha f + 124\alpha + 13f^2 + 65f + 62\right)}{70\left(2\alpha + f - 2\alpha f - 2\alpha^2 f + 2\alpha^2 + 2\right)^2}. \tag{A.7}$$

Proof. According to the origin and destination location, travels can be divided into 3 cases: (a) both stops fall inside downtown; (b) both stops fall outside downtown; and (c) the rest. Let an XY coordinate system have as the origin the southwest corner of the city. Let the coordinates of the origin be (x_1, y_1) and the coordinates of the destination be (x_2, y_2).

For case (a), the travel distance between two random stops in downtown is $(2/3)\alpha D$ and the probability is

$$\left(\frac{\int_0^{\alpha D} \int_0^{\alpha D} \mathrm{d}x\mathrm{d}y}{\int_0^{\alpha D} \int_0^{\alpha D} \mathrm{d}x\mathrm{d}y + 2\int_{\alpha D}^{D} \int_0^{x} (1 - kx)\mathrm{d}x\mathrm{d}y}\right)^2. \tag{A.8}$$

Thus,

$$E_a = \frac{2}{3}\alpha D\left(\frac{\int_0^{\alpha D} \int_0^{\alpha D} \mathrm{d}x\mathrm{d}y}{\int_0^{\alpha D} \int_0^{\alpha D} \mathrm{d}x\mathrm{d}y + 2\int_{\alpha D}^{D} \int_0^{x} (1 - kx)\mathrm{d}x\mathrm{d}y}\right)^2. \tag{A.9}$$

For case (b), $E_b = (|x_1 - x_2| + |y_1 - y_2|)\, p(x_1)p(x_2)p(y_1)p(y_2) = 4(x_1 - x_2)p(x_1)p(x_2)(x_1 > x_2)$, according to the symmetry of the coordinate system. Case (b) includes three scenarios: (1) the origin and destination fall in the eastern periphery; (2) the origin and destination

fall in the northern periphery, as shown in Figures 4(a)–4(c); and (3) the rest, which is shown in Figures 4(d)–4(f).

$$
\begin{aligned}
E_{b_1} &= \frac{\int_{\alpha D}^{D}\int_{\alpha D}^{x_1}(x_1-x_2)(1-kx_2)x_2(1-kx_1)x_1\mathrm{d}x_2\mathrm{d}x_1}{\left(\int_0^{\alpha D}\int_0^{\alpha D}\mathrm{d}x\mathrm{d}y+2\int_{\alpha D}^{D}\int_0^{x}(1-kx)\mathrm{d}x\mathrm{d}y\right)^2},\\
E_{b_2} &= \frac{\int_0^{\alpha D}\int_{\alpha D}^{D}\int_0^{x_1}\int_{\alpha D}^{D}(x_1-x_2)(1-ky_2)\mathrm{d}y_2\mathrm{d}x_2(1-ky_1)\mathrm{d}y_1\mathrm{d}x_1}{\left(\int_0^{\alpha D}\int_0^{\alpha D}\mathrm{d}x\mathrm{d}y+2\int_{\alpha D}^{D}\int_0^{x}(1-kx)\mathrm{d}x\mathrm{d}y\right)^2}\\
&\quad+\frac{\int_{\alpha D}^{D}\int_{x_1}^{D}\int_0^{\alpha D}\int_{\alpha D}^{D}(x_1-x_2)(1-ky_2)\mathrm{d}y_2\mathrm{d}x_2(1-ky_1)\mathrm{d}y_1\mathrm{d}x_1}{\left(\int_0^{\alpha D}\int_0^{\alpha D}\mathrm{d}x\mathrm{d}y+2\int_{\alpha D}^{D}\int_0^{x}(1-kx)\mathrm{d}x\mathrm{d}y\right)^2}\\
&\quad+\frac{\int_{\alpha D}^{D}\int_{x_1}^{D}\int_{\alpha D}^{x_1}\int_{x_2}^{D}(x_1-x_2)(1-ky_2)(1-ky_1)\mathrm{d}y_2\mathrm{d}x_2\mathrm{d}y_1\mathrm{d}x_1}{\left(\int_0^{\alpha D}\int_0^{\alpha D}\mathrm{d}x\mathrm{d}y+2\int_{\alpha D}^{D}\int_0^{x}(1-kx)\mathrm{d}x\mathrm{d}y\right)^2},\\
E_{b_3} &= \frac{\int_{\alpha D}^{D}\int_{\alpha D}^{D}\int_0^{\alpha D}(x_1-x_2)(1-ky_2)\mathrm{d}x_2\mathrm{d}y_2(1-kx_1)x_1\mathrm{d}x_1}{\left(\int_0^{\alpha D}\int_0^{\alpha D}\mathrm{d}x\mathrm{d}y+2\int_{\alpha D}^{D}\int_0^{x}(1-kx)\mathrm{d}x\mathrm{d}y\right)^2}\\
&\quad+\frac{\int_{\alpha D}^{D}\int_{\alpha D}^{x_1}\int_{x_2}^{D}(x_1-x_2)(1-ky_2)\mathrm{d}y_2\mathrm{d}x_2(1-kx_1)x_1\mathrm{d}x_1}{\left(\int_0^{\alpha D}\int_0^{\alpha D}\mathrm{d}x\mathrm{d}y+2\int_{\alpha D}^{D}\int_0^{x}(1-kx)\mathrm{d}x\mathrm{d}y\right)^2}\\
&\quad\cdot\frac{\int_{\alpha D}^{D}\int_{x1}^{D}\int_{\alpha D}^{x_1}(x_1-x_2)(1-kx_2)x_2\mathrm{d}x_2(1-ky_1)\mathrm{d}y_1\mathrm{d}x_1}{\left(\int_0^{\alpha D}\int_0^{\alpha D}\mathrm{d}x\mathrm{d}y+2\int_{\alpha D}^{D}\int_0^{x}(1-kx)\mathrm{d}x\mathrm{d}y\right)^2},\\
E_b &= 4\left(E_{b_1}+E_{b_2}+E_{b_3}\right).
\end{aligned}
\tag{A.10}
$$

For case (c), $E_c = (|x_1-x_2|+|y_1-y_2|)p(x_1)p(x_2)p(y_1)\ p(y_2) = 2|x_1-x_2|p(x_1)p(x_2)$, according to the symmetry of the coordinate system. Let the origin be inside downtown and the destination be in the periphery, as shown in Figure 5, or vice versa.

$$
E_c = 4\left[\begin{array}{l}
\dfrac{\int_0^{\alpha D}\int_0^{x1}\int_{\alpha D}^{D}\alpha D(x_1-x_2)(1-ky_2)\mathrm{d}y_2\mathrm{d}x_2\mathrm{d}x_1}{\left(\int_0^{\alpha D}\int_0^{\alpha D}\mathrm{d}x\mathrm{d}y+2\int_{\alpha D}^{D}\int_0^{x}(1-kx)\mathrm{d}x\mathrm{d}y\right)^2}+\dfrac{\int_0^{\alpha D}\int_{\alpha D}^{D}\int_0^{x2}\alpha D(x_2-x_1)\mathrm{d}x_1(1-ky_2)\mathrm{d}y_2\mathrm{d}x_2}{\left(\int_0^{\alpha D}\int_0^{\alpha D}\mathrm{d}x\mathrm{d}y+2\int_{\alpha D}^{D}\int_0^{x}(1-kx)\mathrm{d}x\mathrm{d}y\right)^2}+\\
\dfrac{\int_{\alpha D}^{D}\int_{x2}^{D}\int_0^{\alpha D}\alpha D(x_2-x_1)\mathrm{d}x1(1-ky_2)\mathrm{d}y_2\mathrm{d}x_2}{\left(\int_0^{\alpha D}\int_0^{\alpha D}\mathrm{d}x\mathrm{d}y+2\int_{\alpha D}^{D}\int_0^{x}(1-kx)\mathrm{d}x\mathrm{d}y\right)^2}+\dfrac{\int_{\alpha D}^{D}\int_0^{\alpha D}\alpha D(x_2-x_1)\mathrm{d}x_1(1-kx_2)x_2\mathrm{d}x_2}{\left(\int_0^{\alpha D}\int_0^{\alpha D}\mathrm{d}x\mathrm{d}y+2\int_{\alpha D}^{D}\int_0^{x}(1-kx)\mathrm{d}x\mathrm{d}y\right)^2}
\end{array}\right],
\tag{A.11}
$$

$$E = E_a + E_b + E_c.$$

Result 7. The expected travel speed during the peak hour is given by

$$\frac{1}{v_c} \approx \frac{1}{v}+\frac{\tau}{s}-\tau'\frac{\Lambda\left(1+e_T\right)}{V}. \tag{A.12}$$

Proof. This proof can be found in Daganzo's work [12].

Result 8. The maximum occupancy on the critical load line during peak hours is approximately given by

$$O = \frac{2sH\Lambda}{\alpha D}\left(\frac{1}{2}-\frac{\alpha^4(2\alpha+3f-5\alpha f)^2}{8(1-\alpha)^2\left(2\alpha+f-2\alpha f-2\alpha^2 f+2\alpha^2+2\right)^2}\right). \tag{A.13}$$

Proof. These results can be seen by calculating the average passenger trips on the critical lines during peak hours and then multiplying the load factor by 2. Passengers traveling across the equatorial lines are the most. For the purpose of this proof, passengers traveling from north to south are taken as an example. The number of passengers traveling this way is $(\Lambda/4)$. Passengers traveling by east-west equatorial lines can be divided into two parts: (i) trips based on the peripheral lines and (ii) the rest. The number of trips belonging to (i) was

$$\Lambda\left[\frac{\int_{\alpha D}^{D}\int_{0}^{x}(1-kx)\mathrm{d}x\mathrm{d}y}{2\left(\int_{0}^{\alpha D}\int_{0}^{\alpha D}\mathrm{d}x\mathrm{d}y+2\int_{\alpha D}^{D}\int_{0}^{x}(1-kx)\mathrm{d}x\mathrm{d}y\right)}\right]. \tag{A.14}$$

Therefore, the average number of trips crossing the equatorial lines in downtown areas is

$$\frac{\Lambda}{4}-\Lambda\left[\frac{\int_{\alpha D}^{D}\int_{0}^{x}(1-kx)\mathrm{d}x\mathrm{d}y}{2\left(\int_{0}^{\alpha D}\int_{0}^{\alpha D}\mathrm{d}x\mathrm{d}y+2\int_{\alpha D}^{D}\int_{0}^{x}(1-kx)\mathrm{d}x\mathrm{d}y\right)}\right]. \tag{A.15}$$

Because there are αD/2s critical lines and the headway is H, the total number of vehicles per hour on these lines is $((\alpha D)/(2sH))$. On each equatorial line, an average of

$$\frac{\left\{(\Lambda/4)-\Lambda\left[\left(\int_{\alpha D}^{D}\int_{0}^{x}(1-kx)\mathrm{d}x\mathrm{d}y\right)/\left(2\left(\int_{0}^{\alpha D}\int_{0}^{\alpha D}\mathrm{d}x\mathrm{d}y+2\int_{\alpha D}^{D}\int_{0}^{x}(1-kx)\mathrm{d}x\mathrm{d}y\right)\right)\right]^{2}\right\}}{(\alpha D)/(2sH)}, \tag{A.16}$$

passengers are traveling.

Data Availability

The [DATA TYPE] data used to support the findings of this study are included within the article.

Conflicts of Interest

The authors declare that there are no conflicts of interest regarding the publication of this paper.

Acknowledgments

This work was supported by the National Natural Science Foundation of China (Grant no. 51668048), the Xi'an Special Funds for Urban Construction Program (Grant no. SZJJ2019-22), and the Natural Science Foundation of Inner Mongolia Autonomous Region (Grant no. 2020MS05060).

References

[1] J. Walker, *Human Transit*, Island Press/Center for Resource Economics, Washington, DC, USA, 2012.

[2] S. B. Jha, J. K. Jha, and M. K. Tiwari, "A multi-objective meta-heuristic approach for transit network design and frequency setting problem in a bus transit system," *Computers & Industrial Engineering*, vol. 130, no. 4, pp. 166–186, 2019.

[3] E. Cipriani, G. Fusco, S. M. Patella, M. Petrelli, and L. Quadrifoglio, "Transit network design for small-medium size cities," *Transportation Planning and Technology*, vol. 42, no. 1, pp. 84–97, 2019.

[4] X. Feng, X. Zhu, X. Qian, Y. Jie, F. Ma, and X. Niu, "A new transit network design study in consideration of transfer time composition," *Transportation Research Part D: Transport and Environment*, vol. 66, pp. 85–94, 2019.

[5] D. Zhu, Y. Gu, S. Wang, Z. Liu, and W. Zhang, "A two-phase optimization model for the demand-responsive customized bus network design," *Transportation Research Part C: Emerging Technologies*, vol. 111, pp. 1–21, 2020.

[6] N. Oliker and S. Bekhor, "An infeasible start heuristic for the transit route network design problem," *Transportmetrica A: Transport Science*, vol. 16, no. 3, pp. 388–408, 2020.

[7] M. Nikolić and D. A. Teodorović, "Transit network design by bee colony optimization," *Expert Systems with Applications*, vol. 40, no. 15, pp. 5945–5955, 2013.

[8] D. Huang, Z. Liu, X. Fu, and P. T. Blythe, "Multimodal transit network design in a hub-and-spoke network framework," *Transportmetrica A: Transport Science*, vol. 14, no. 8, pp. 706–735, 2018.

[9] F. Zhao and I. Ubaka, "Transit network optimization-minimizing transfers and optimizing route directness," *Journal of Public Transportation*, vol. 7, no. 7, pp. 67–82, 2004.

[10] F. Zhao and X. Zeng, "Simulated annealing-genetic algorithm for transit network optimization," *Journal of Computing in Civil Engineering*, vol. 20, no. 1, pp. 57–68, 2006.

[11] J. Boissière, F. Martin, N. Teypaz et al., "Using choquet-integral for guiding tabu search in multi-criteria public transport network design," *IFAC Proceedings, Volumes*, vol. 40, no. 18, pp. 617–622, 2007.

[12] C. F. Daganzo, "Structure of competitive transit networks," *Transportation Research Part B: Methodological*, vol. 44, no. 4, pp. 434–446, 2010.

[13] M. Estrada, M. Roca-Riu, H. Badia, F. Robusté, and C. F. Daganzo, "Design and implementation of efficient transit networks: procedure, case study and validity test," *Transportation Research Part A: Policy and Practice*, vol. 45, no. 9, pp. 935–950, 2011.

[14] H. Badia, A. C. Juan, and C. F. Daganzo, "How network structure can boost and shape the demand for bus transit," *Transportation Research Part A: Policy and Practice*, vol. 103, no. 9, pp. 83–94, 2017.

[15] H. Badia, M. Estrada, and F. Robusté, "Competitive transit network design in cities with radial street patterns,"

Transportation Research Part B: Methodological, vol. 59, pp. 161–181, 2014.

[16] S. Nocera, A. Fabio, F. Cavallaro et al., "The adoption of grid transit networks in non-metropolitan contexts," *Transportation Research Part A: Policy and Practice*, vol. 132, no. 2, pp. 256–272, 2020.

[17] G. Chen and J. H. Wang, "Research on radial and grid hybrid bus network model for square cities of downtown in the corner," *Journal of Transportation Systems Engineering and Information Technology*, vol. 21, pp. 1–8, 2021, accepted.

[18] G. L. Thompson, "Planning considerations for alternative transit route structures," *Journal of the American Institute of Planners*, vol. 43, no. 2, pp. 158–168, 1977.

[19] B. F. Byrne, "Public transportation line positions and headways for minimum user and system cost in a radial case," *Transportation Research*, vol. 9, no. 2-3, pp. 97–102, 1975.

[20] G. F. Newell, "Some issues relating to the optimal design of bus routes," *Transportation Science*, vol. 13, no. 1, pp. 20–35, 1979.

[21] R. Vaughan, "Optimum polar networks for an urban bus system with a many-to-many travel demand," *Transportation Research Part B: Methodological*, vol. 20, no. 3, pp. 215–224, 1986.

[22] H. Badia, M. Estrada, and F. Robusté, "Bus network structure and mobility pattern: a monocentric analytical approach on a grid street layout," *Transportation Research Part B: Methodological*, vol. 93, no. 11, pp. 37–56, 2016.

[23] H. Pan and Y. Xiaoguang, "Probability distribution of per capita travel speed in urban road," *Journal of Transportation Systems Engineering and Information Technology*, vol. 16, no. 5, pp. 149–156, 2016.

[24] J. Zhang, "A real-time bus transfer scheme recommendation systems," in *Proceedings of the International Conference on Advanced Cloud and Big Data*, pp. 206–212, Shanghai, China, August 2017.

[25] D. Huang, Z. Liu, P. Liu, and J. Chen, "Optimal transit fare and service frequency of a nonlinear origin-destination based fare structure," *Transportation Research Part E: Logistics and Transportation Review*, vol. 96, no. 12, pp. 1–19, 2016.

[26] SFMTA Municipal Transportation Agency, *SFMTA Ar18 Final Online 2*, SFMTA, San Francisco, CA, USA, 2018.

[27] SFMTA Municipal Transportation Agency, *Commuter Shuttle Program Annual Status Report*, SFMTA, San Francisco, CA, USA, 2018.

[28] J. Zhao, J. Yu, X. Xia, J. Ye, and Y. Yuan, "Exclusive bus lane network design: a perspective from intersection operational dynamics," *Networks and Spatial Economics*, vol. 19, no. 4, pp. 1143–1171, 2019.

[29] Transportation Research Board, *Transit Capacity and Quality of Service Manual*, Transportation Research Board, Washington, DC, USA, 3rd edition, 2013.

[30] O. Heddebaut, B. Finn, S. Rabuel, and F. Rambaud, "The European bus with a high level of service (BHLS): concept and practice," *Built Environment*, vol. 36, no. 6, pp. 307–316, 2010.

[31] B. Finn, "Buses with high level of service: fundamental characteristics and recommendations for decision making and research," *Cost action TU0603*, Final report, European Cooperation in Science and Technology, Brussels, Belgium, 2011.

[32] K. An, "Battery electric bus infrastructure planning under demand uncertainty," *Transportation Research Part C: Emerging Technologies*, vol. 111, pp. 572–587, 2020.

Hindawi
Discrete Dynamics in Nature and Society
Volume 2021, Article ID 6688236, 14 pages
https://doi.org/10.1155/2021/6688236

Research Article

Reliability Analysis of Bus Timetabling Strategy during the COVID-19 Epidemic: A Case Study of Yixing, China

Liangpeng Gao,[1] **Yue Zheng**,[2] **Yanjie Ji**,[3] **Chenghong Fu**,[1] **and Lihai Zhang**[4]

[1]*Institute of Transportation, Fujian University of Technology, Fuzhou, Fujian, China*
[2]*School of Modern Posts and Institute of Modern Posts, Nanjing University of Posts and Telecommunications, Nanjing, Jiangsu, China*
[3]*School of Transportation, Southeast University, Nanjing, Jiangsu, China*
[4]*Department of Infrastructure Engineering, University of Melbourne, VIC, Australia*

Correspondence should be addressed to Yue Zheng; zhengyue_seu@163.com

Received 13 December 2020; Revised 15 January 2021; Accepted 22 January 2021; Published 15 February 2021

Academic Editor: Tingsong Wang

How to meet the daily demand for resident transport while limiting the transmission of infectious diseases is a problem of social responsibility of urban transport systems during major public health emergencies. Considering the novel coronavirus pneumonia epidemic (COVID-19), a bus timetable system based on the "if early, wait, and if late, leave soon" strategy is proposed. Based on public transport vehicle constraints in this system, the concept of reliability is introduced to evaluate public transport timetable systems, and a model based on an event tree is built to calculate the failure rate of urban bus timetables. Then, the public transport situation in Yixing city is used as an example to perform confirmatory analysis, and the fluctuations in the reliability of the bus timetable during the novel coronavirus pneumonia epidemic are discussed. The research results show that the method proposed in this paper can obtain the overall failure rate of urban bus timetable by traversing the calculation of each round-trip interval and achieve an accurate evaluation of the reliability of bus timetables. During the early, middle, and more recent stages of the COVID-19 outbreak, the failure rate of bus timetables in Yixing city initially decreased and then increased. In the early stage of the outbreak, the failure rate of the Yixing bus timetable was 7.8142. However, the failure rate decreased to 4.3306 and 5.0160 in the middle and late stages of the epidemic, respectively. In other words, the failure rate of the public transport network in the middle and late stages decreased by 44.58% and 35.81%, respectively, compared with that in the early stage. Thus, during major health emergencies, such as the novel coronavirus pneumonia outbreak, the reliability of the urban bus timetable system can be improved by at least 35%, and cross-infection at bus stations can be prevented. The research results verify the feasibility and reliability of the implementation of bus timetabling strategies during major health emergencies.

1. Introduction

Major epidemics involving infectious diseases are serious public health events that can lead to the spread of infection sources across regions and borders and pose a threat to the safety of all human beings [1, 2]. Taking effective measures to prevent, control, and eliminate the outbreak of major infectious diseases can not only reduce the degree of social harm caused and ensure the safety of individuals and property but also help maintain regional public order and promote harmonious social communication.

Since novel coronavirus pneumonia emerged in late December 2019, the COVID-19 epidemic has spread to many countries and regions around the world and has had a critical impact on individuals' daily life, security stability, and socioeconomic status. Through early June 2020, the COVID-19 disease, which has been reported in 188 countries/regions, had led to 420,000 deaths, and over 7.5 million

cases were confirmed [3]. To delay and reduce the onset of peak infection effects, governments and public health authorities adopted a variety of social distancing interventions and policies to avoid overloading the health care system before a vaccine is available. Notably, a series of measures implemented by the Chinese government to block the spread of COVID-19 achieved an ideal health outcome [4].

From January 23 to 29, 2020, 31 provinces, cities, and regions in China successively launched the first level of national response to the major public health emergency. Specifically, prevention and control measures, such as complete travel bans, travel quarantines, and entry screening for incoming travellers, were mainly implemented [5]. In regard to urban transport systems, dual social responsibility, including providing basic traffic functions and blocking the spread of epidemics in the process of citizen travel, should be considered. Taking public transport as an example, in addition to regular epidemic prevention measures such as real-name boarding, passenger temperature monitoring, scattered seating, and the all-weather disinfection of vehicles, developing an operation mechanism to reduce the risk of cross-infection in bus travel and meet the rigid needs of passengers has become an urgent issue for scholars to consider.

Novel coronavirus pneumonia is mainly spread through droplets, contact, aerosols, faecal orifices, etc. [6]. Because of the rapid spreading and high morbidity characteristics of the virus, the urban public transport system needs to avoid mass gatherings of passengers in public places in the process of epidemic prevention. If virus-carrying passengers enter the public transport system, other people face a huge risk of infection, especially during rush-hour periods. An epidemic can quickly spread to every corner of a city due to the connectivity of bus lines among stations in different areas. If a bus timetabling system is used in conventional public transport, passengers can arrange their own itinerary and effectively reduce the waiting time at bus stations [7, 8]. Thus, while meeting the rigid demands of residents for bus travel, the probability of contracting a virus while using public transport systems can be reduced. Moreover, the personal travel demand for leisure and social interaction has been greatly reduced, and the urban traffic situation has been significantly improved during the execution of social distancing policies. Therefore, it is possible for buses to travel smoothly through transportation networks, and the accuracy of the bus timetable is high.

We design a time control point method based on the "a vehicle would wait if it arrives early and leave quickly if it arrives late" scheme for a bus timetabling strategy to assess bus travel time performance. The aim of this study is to provide an evaluation method for analysing the characteristics of bus arrival with inbound and outbound information. By treating the upstream or downstream operation processes of a bus line as a single event, we construct an event tree model to explore the overall reliability of the public transport network. Finally, the public transport system in Yixing city, which is a county-level city with a population of one million in Southeast China, is studied to verify the feasibility and reliability of bus timetabling in the context of the COVID-19 epidemic.

2. Literature Review

As the fundamental dimension of passenger service, the reliability of urban public transport systems has been defined from several perspectives. According to the Transit Capacity and Quality of Service Manual [9], various factors that influence bus service reliability have been explored, such as the traffic conditions, road construction, maintenance quality, staff availability, schedule achievability, and passenger demand. Some achievements have been widely considered in bus system planning and design in many countries and regions, thereby providing a powerful scientific basis for the application of transit priority policies [10]. Specifically, many studies have focused on bus timetables. Therefore, this section focuses on the following three interrelated issues: timetable generation and optimization, vehicle and crew scheduling, and the operational strategy of bus system services.

2.1. Timetable Generation and Optimization. Timetable generation is one of the major tasks in the urban bus system [11]. A suitable bus timetable not only allows passengers to reach their destination quickly with as few bus routes as possible but also provides transfers with a short waiting time, which can greatly affect the service attractiveness of public transport systems [12]. The earliest research in this field can be traced to Newell and Potts's study of bus schedule maintenance, which identified the factors that influence the practical operation of bus systems [13]. Subsequently, an increasing number of scholars have explored the mechanisms of the associated phenomena, such as bus bunching [14–16], bus-specific holding [17–20], and dispatching control [21–24]. Although the focus of these studies varied, there is a certain correlation among each approach and the corresponding findings. For example, one purpose of dispatching control is to reduce the frequency of bus punching with a regularity-based or punctuality-based service strategy [25]. Compared with the regularity-based strategy, which minimizes the deviation in bus headways, the punctuality-based strategy focuses on the adherence to scheduled arrival times at stops, although some studies have found that passengers may ignore the exact arrival time when the schedule headway is less than 12 min [26–30]. Table 1 summarizes the recent research on the scheduling of bus timetable (including the train timetable) under the constraints of external factors.

Generally, there are two main research directions in the existing research: improving the performance of model algorithms and relaxing the modelling hypothesis to improve the representation of the objective world [45, 52–54]. The corresponding results of these studies include complex mathematical descriptions and rigorous derivation processes; therefore, the time costs of these methods can be high, but accurate calculation and evaluation results can be obtained.

2.2. Vehicle and Crew Scheduling. The vehicle and crew scheduling problem in bus systems is of practical importance because efficient schedules can reduce operational costs and

Table 1: Recent research on the scheduling of bus timetable.

Authors	Factors considered in the study	Notes
Gkiotsalitis et al. [31–34]	Rolling horizons bus fleet allocation, holding control, and transit rescheduling strategies	The purpose is to increase the coordination among running buses, avoid vehicle bunching, and obtain the accurate evaluation of bus timetable
Salicru et al. [35]; Steiner and Irnich [36]; Zhang et al. [37]; Ma et al. [38]	Passenger travel demands extracted from multisource traffic datasets	Smarter computational methods were provided to reduce operational costs and improve the server level of bus timetable
Domschke [39]; Ceder et al. [40]; Eranki [41]; Liu et al. [42]; Ibarra-Rojas et al. [43–45]	Bus line network, route choices of passengers, waiting time at nodes, and the operational costs	They developed a series of models to represent the route choice behaviours of various passengers and minimize the operational cost of bus timetables
Wong et al. [46]; Shafahi and Khani [47]; Kang et al. [48]; Guo et al. [49, 50]; Chu et al. [12]; Abdolmaleki et al. [51]	Trains' run times, station dwell times, interchange waiting times of all passengers, transfer redundant time, and the network accessibility	A series of nonlinear programming models were provided to achieve the synchronize timetables in the transit network and improve the transfer efficiency of passengers

increase the capacity of transit services [55]. Related studies can be traced back to the 1940s when some scholars in developed countries introduced a series of approaches to maximize the scheduling profit [56, 57]. Notably, in addition to minimizing the internal and external operating costs and synchronizing departure times, previous studies focused on the following aspects of timetable systems.

2.2.1. Timetabling considering the Vehicle Scheduling Efficiency. The research field of traditional bus scheduling covers all trips with fixed travel times and locations for the starting and ending points in a timetable [58]. Some studies mainly focused on minimizing the fleet size for a conventional bus service, which is a fixed timetable service with a single depot or single vehicle type [59–64]. Referring to the review of Ibrra-Rojas et al. [65], other studies were presented to solve multidepot vehicle scheduling problems [66, 67] and assess the robustness, network topology, and flexibility of different methods [44, 68]. Subsequent studies further improved the integration of vehicle timing and scheduling strategies [53, 69, 70], and other studies considered various practical factors, such as bus ridership, new vehicle types, skip-stop strategies, and functional planning periods, to make the mathematical model as similar to the actual daily bus travel situation as possible [36, 71–73].

2.2.2. Timetabling Integrated with Vehicle and Crew Scheduling. Early studies of vehicle scheduling and crew scheduling were formulated as network flow problems or sets of coverage or partitioning problems [74]. The integration of these two scheduling tasks can be regarded as a particular case of the vehicle scheduling problem that was first discussed by Gaffi and Nonato [75]. The following scholars applied various algorithms to relax the relevant constraints, such as duty flow, bus itinerary, overall operating cost, and multicommodity network constraints, to obtain satisfactory results [76–80]. These studies provided a functional framework for people to explore efficient timetables. For example, based on the achievements of Gintner et al. [81] and Steinzen et al. [82], Kliewer et al. [83] proposed a flexible timetable to reduce the operational costs and maintain the service quality by addressing the vehicle and driver scheduling problem with the possibility of shifting trips within defined time windows. Petersen et al. [84] proposed a model that integrated the bus network timetable and multidepot vehicle scheduling to minimize the usage costs of stocks and the transfer waiting times of passengers. The results indicated that flexibility in the bus timetables can reduce transfer waiting times by 20%.

2.3. Operational Strategy for Bus System Services. As discussed above, bus holding, dispatching control, and vehicle and crew scheduling can be used as operational strategies to improve the service level of urban public transit. The Transit Capacity and Quality of Service Manual [9] also discusses some other measures, such as transit development plans, transit signal priority, park-and-ride schemes, and ticket pricing adjustment, that involve modern technical methods. However, not all technical measures can provide stable transit services because passenger behaviour influences the service quality of bus systems [85]. Therefore, scholars have considered a series of instances when exploring on-time performance, which has a strong relationship with bus timetables [86]. As a case of bus holding control, time control point rules that were applied in a previous study to evaluate network reliability were also used to solve dynamic engineering problems [23, 87–90]. For example, in recent studies, Van Oort et al. [91] introduced a method to increase the reliability of bus timetables by using the holding point strategy. The on-time arrival and departure characteristics of a bus station timetable were used to measure reliability. Dou et al. [92] developed a novel time control point strategy to obtain the optimal slack time scheme and applied an MINLP model to improve schedule adherence and reduce transfer waiting time. Wang et al. [93] proposed a joint strategy with bus holding and timetabling slack to optimize the locations of control points and formulate a bus timetable considering the uncertainty in the operational process. Other external

factors, including the headway in a rolling horizon scheme, greenhouse gas emission policy, and bus line capacity, were also considered to integrate the vehicle procurement scheme and timetabling for urban transport [37, 94, 95].

In our previous work, we proposed a slack arrival strategy in which transit vehicles are allowed to reach checkpoints somewhat later than the scheduled departure time and delayed vehicles must leave the checkpoints immediately after serving the boarding and alighting passengers [96]. In this paper, we extended this strategy of time control points to the environment of the COVID-19 epidemic and proposed a reliability evaluation model to quickly acquire and identify which intervals in the bus network would have large arrival delays or transfer synchronization problems in the operational process. The contributions of this paper are listed as follows:

(1) A system analysis framework for estimating the overall reliability of the time control point strategy is provided considering the spread of the COVID-19 epidemic in the bus network

(2) A first-order reliability method and Ditlevsen's bounds theory are integrated to simplify the reliability calculation and improve the operating speed of the bus network

(3) The event tree approach is applied to analyse the real case of Yixing city during the epidemic considering vehicle arrival delays for multiple bus lines

The remainder of this paper is structured as follows. Section 3 presents the methodology for calculating the reliability of the bus network, and a first-order reliability method and Ditlevsen's bounds theory are integrated. Section 4 introduces the case study and provides an analysis of the results. Section 5 presents a summary of the study and gives suggestions for future studies.

3. Methodology

3.1. Problem Description. Generally, the public recognition of major public health emergencies is a gradual process, especially for the transmission route, transmission mechanism, vaccine research, and development cycle, which are difficult to constrain; as a result, the requirements for the formulation of epidemic prevention measures are extensive. In this outbreak of COVID-19, the Chinese government took a series of active social distancing measures to prevent the spread of the virus and achieved good results. These measures not only reduced human contact but also significantly improved urban traffic conditions, which made it possible for bus stations to adopt operational strategies based on bus timetabling.

Under this timetable system, buses that arrive earlier than the planned arrival time need to wait until the departure time is reached based on the time control points established for the bus station, and buses that arrive late leave as soon as possible on the basis of ensuring the service of passengers. The arrival time at each bus station is often accurate to the minute. From the perspective of reliability, if a bus arrives at a station before the expected time, it is considered an on-time arrival, and the bus service is in a "reliable" state. Otherwise, if a bus fails to meet the time point condition, it will be considered late. To determine the overall reliability rate of the system, we must first calculate the reliability of each station interval and then estimate the overall reliability of the bus route. Finally, the event tree analysis method is applied to determine the reliability of the whole public transport network. In the following subsection, we introduce a three-stage reliability calculation framework for the bus timetabling strategy.

3.2. Stage 1: Reliability of the Arrival Interval. According to the previous description, when a bus starts from an upstream station and reaches a downstream station before the specified time point, the bus is considered "reliable." Therefore, under normal conditions, each interval between two adjacent stations has a planned arrival time Tr_{ij} and an actual arrival time Ar_{ij}. The performance of the punctuality index Gr_{ij} refers to the difference between these two arrival time points and can be computed from the following formula:

$$Gr_{ij} = Tr_{ij} - Ar_{ij}\,\forall, \quad i \in (1, n-1),\ j \in (2, n),\ i \neq j, \quad (1)$$

where i and j refer to the corresponding values at two adjacent stations along the same route.

Based on the punctuality index Gr_{ij}, we can determine whether vehicles can reach the downstream station according to the bus timetable. If the value of this index is larger than zero, i.e., the vehicle arrives at the downstream station on time, the timetable status is reliable. Otherwise, the time requirements are not met, and the timetable is invalid. We assume that during the epidemic period, passengers can obtain the bus timetable through various information channels in real time. Additionally, to shorten the waiting time of passengers at a bus station, which may lead to the spread of coronavirus, bus companies will adjust the timetables of subsequent bus stations according to the real-time arrival of each bus, and these changes are announced in real time. In the actual operation of a bus timetable, a vehicle often shuttles forward and backward between bus stations, so the travel time difference in each interval can be regarded as a set. By using a mathematical method, we can quantify the reliability and failure characteristics of the timetable for each interval. Therefore, when the bus timetable is dynamically updated, we can assume that the planned time point and actual time point of bus arrival both satisfy the normal distribution, e.g., $Tr_{ij} \sim (\mu_{Tij}, \sigma^2_{Tij})$ and $Ar_{ij} \sim (\mu_{Aij}, \sigma^2_{Aij})$. Therefore, the punctuality index Gr_{ij} also satisfies the normal distribution, e.g., $Gr_{ij} \sim (\mu_{Tij} - \mu_{Aij}, \sigma^2_{Tij} + \sigma^2_{Aij})$. We can obtain the following result after the standard normal transformation:

$$\frac{Gr_{ij} - \left(\mu_{Tij} - \mu_{Aij}\right)}{\sqrt{\sigma^2_{Tij} + \sigma^2_{Aij}}} \sim (0, 1). \quad (2)$$

By setting $W = Gr_{ij} - (\mu_{Tij} - \mu_{Aij})/\sqrt{\sigma^2_{Tij} + \sigma^2_{Aij}}$, we can obtain $Gr_{ij} = W \cdot \sqrt{\sigma^2_{Tij} + \sigma^2_{Aij}} + (\mu_{Tij} - \mu_{Aij})$. If the timetable of a bus line fails, e.g., $Gr_{ij} < 0$, $W < -(\mu_{Tij} - \mu_{Aij})/$

$\sqrt{\sigma_{Tij}^2 + \sigma_{Aij}^2}$. Therefore, the reliability index r_{ij} of each interval can be calculated using the following formula:

$$r_{ij} = \frac{\mu_{Tij} - \mu_{Aij}}{\sqrt{\sigma_{Tij}^2 + \sigma_{Aij}^2}}. \tag{3}$$

According to the first-order reliability method [97, 98], the probability of an arrival delay between two adjacent stations due to various factors can be determined by the following formula:

$$P\left(Gr_{ij} < 0\right) = P\left(W < \frac{-\left(\mu_{Tij} - \mu_{Aij}\right)}{\sqrt{\sigma_{Tij}^2 + \sigma_{Aij}^2}}\right), \tag{4}$$

where $P(Gr_{ij} < 0)$ refers to the failure probability at the downstream station and the corresponding reliability for a given interval can be calculated according to $1 - P(Gr_{ij} < 0)$.

3.3. Stage 2: Reliability of Bus Route. In an actual transit network, a bus route contains several subroutes and often covers multiple intervals. Considering the operational mechanism of a bus timetable, the reliability of a bus route depends on whether the bus can reach stations on time. If the bus is delayed in any interval, it may lead to the failure to reach the downstream bus station according to the timetable; as a result, the subsequent timetable for the bus trip will be in a "nonreliable" state. Therefore, when assessing the overall reliability of the timetable of a bus line, the operational state of the timetable should be considered in each interval of the bus route.

Figure 1 is the operation status diagram for a bus timetable. The solid line in the figure shows that the travel time difference between two adjacent stations is greater than 0 or equal to 0, e.g., $Gr_{ij} \geq 0$, and the dotted line represents a value less than 0, e.g., $Gr_{ij} < 0$. For example, in scenario (a) in Figure 1, the bus is delayed in interval 1, and the subsequent timetable of the route is invalid. The failure probability can be obtained from the following formula:

$$P_f = P(F_1). \tag{5}$$

In scenario (b) in Figure 1, part of the arrival delay shifts from interval 1 to interval 2. According to set theory, the failure probability for this situation can be calculated by

$$P_f = P(F_2 \cap S_1). \tag{6}$$

Similarly, as shown in scenario (c) in Figure 1, when an arrival delay occurs in interval 3, the corresponding probability is

$$P_f = P(F_3 \cap S_2 \cap S_1). \tag{7}$$

Analogously, when the timetable fails in interval n, the formula for the probability is as follows:

$$P_f = P(F_n \cap S_{n-1} \cap S_{n-2} \cdots \cap S_2 \cap S_1). \tag{8}$$

According to set theory, the failure probability of a timetable for a bus route is as follows:

$$\begin{aligned} P_f = {} & P(F_1)) + P(F_2 \cap S_1) + P(F_3 \cap S_2 \cap S_1) \cdots \\ & + P(F_n \cap S_{n-1} \cap S_{n-2} \cdots \cap S_2 \cap S_1). \end{aligned} \tag{9}$$

If the timetable state of each interval on the bus route is regarded as a set R, two subsets can be obtained accordingly: the reliable subset S and failure subset F. The arrivals delays that occur in intervals 2 and 3 in scenarios (b) and (c) in Figure 1 can be expressed as follows:

$$\begin{aligned} P_f &= P(F_2 \cap S_1) = P\{F_2 \cap (R - F_1)\} \\ &= P(F_2 \cap R) - P(F_2 \cap F_1) \\ &= P(F_2) - P(F_2 \cap F_1), \\ P_f &= P\{F_3 \cap (R - F_2) \cap (R - F_1)\} \\ &= P\{(F_3 - F_2 \cap F_3) \cap (R - F_1)\} \\ &= P(F_3) - P(F_2 \cap F_3) - P(F_3 \cap F_1) + P(F_3 \cap F_2 \cap F_1). \end{aligned} \tag{10}$$

Moreover, the formula for calculating the failure probability of a bus route can be deduced as follows:

$$\begin{aligned} P_f &= P(F_1) + P(F_2) - P(F_2 \cap F_1) + P(F_3) - P(F_3 \cap F)_1 - P(F_3 \cap F_2) + P(F_3 \cap F_2 \cap F_1) + \cdots \\ &= \sum_{g=1}^{n} P(F_g) - \sum \sum_{g<h}^{n} P(F_g \cap F_h) + \sum \sum \sum_{g<h<k}^{n} P(F_g \cap F_h \cap F_k) - \cdots. \end{aligned} \tag{11}$$

Formula (11) shows that the number of calculations required to determine the failure probability for the timetable of a bus route will increase with the number of intervals, which is not conducive to the rapid evaluation of reliability based on the time control point strategy. Therefore, this paper considers using the upper and lower boundary values of the failure probability to simplify the calculation process and improve the computational efficiency. According to the narrow bound theory, the following relationship exists for any adjacent stations along a bus route:

$$P(S_{n-1} \cap S_{n-2} \cdots \cap S_1) \leq P(S_n) = P(1 - F_n). \tag{12}$$

By applying formulas (11) and (12), we can obtain

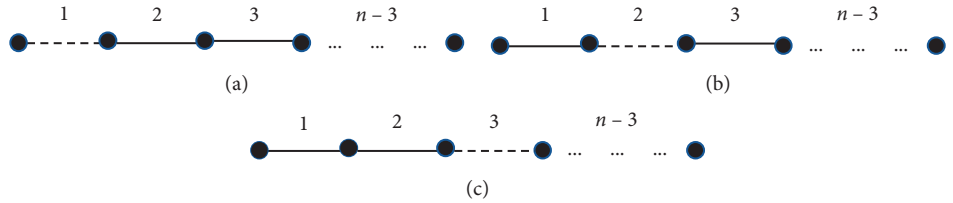

Figure 1: Operational state diagram for a bus timetable.

$$P_f \le \sum_{g=1}^{n} P\left(F_g\right) - \sum_{h=2}^{n} \max_{h<k}\{P\left(F_h \cap F_k\right)\}. \tag{13}$$

In addition, for any interval, the following relationships can be established:

$$\begin{aligned} P\left(S_{n-1} \cap S_{n-2} \cdots \cap S_1\right) &\ge 1 - \{P\left(F_1\right) + P\left(F_2\right) + \cdots + P\left(F_{n-1}\right)\}, \\ P\left(F_1 \cap S_{n-1} \cap S_{n-2} \cdots \cap S_1\right) &\ge P\left(F_1\right) - \sum_{g=1}^{n-1} P\left(F_1 \cap F_g\right), \\ P_f &\ge P\left(F_1\right) + \sum_{g=2}^{n} \max\left\{P\left(F_g\right) - \sum_{h=1}^{g-1} P\left(F_g \cap F_h\right), 0\right\}. \end{aligned} \tag{14}$$

According to the Ditlevsen bounds theory, the upper and lower limits of the failure probability of timetables for bus routes can be obtained as follows:

$$\begin{aligned} P_{\text{upper}} &= \sum_{g=1}^{n} P\left(F_g\right) - \sum_{h=2}^{n} \max_{h<k}\{P\left(F_h \cap F_k\right)\}, \\ P_{\text{lower}} &= P\left(F_1\right) + \sum_{g=2}^{n} \max\left\{P\left(F_g\right) - \sum_{h=1}^{g-1} P\left(F_g \cap F_h\right), 0\right\}, \end{aligned} \tag{15}$$

where P_{upper} refers to the upper limit of the failure probability and P_{lower} refers to the lower limit of the failure probability. To facilitate the calculation, the failure rate is taken as the mean value of the upper and lower limits:

$$P_f \approx \frac{1}{2}\left(P_{\text{upper}} + P_{\text{lower}}\right). \tag{16}$$

3.4. Stage 3: Reliability of a Transit Network. A transit network is composed of bus lines and stations. Bus stations can be regarded as nodes in a network diagram that are connected by the route intervals mentioned above. The overall structure of an urban transit network influences the convenience and timetable reliability of residents' bus trips and directly affects the operation efficiency of the public transport system. In daily life, residents often expect to be able to transfer through adjacent bus stations or the same station in a short time to conveniently complete their bus trips. Therefore, we assume that if residents transfer more than two times in a single bus trip, they will consider the travel experience poor. Since the novel coronavirus pneumonia outbreak, people have focused on reasonable travel planning and become aware of the risk of transit transfer.

When analysing the reliability of a transit network, under the background of an epidemic situation, it is assumed that the daily bus trips of residents will not include more than 2 transfers. If the residents that travel via bus during the epidemic period are regarded as independent events without mutual interference, the network reliability can be calculated by analysing the travel structure chart with event tree traversal based on the above research results.

Figure 2 shows the event tree structure for passenger bus trips with no more than 2 transfers. Event tree analysis is an analysis method in which a tree view is applied to obtain the entire occurrence process for a series of events. The tree starts from the event occurrence, and the various development directions can be individually assessed. Each development direction is completely independent and has a corresponding event consequence [99]. For bus trips in the context of the COVID-19 epidemic, each branch in the event tree structure diagram represents a bus route that residents may choose when travelling. The output results of the event tree represent various bus routes. The occurrence probability of each failure mode (FM_m) in Figure 2 can be obtained by traversing all output results, and the bottleneck areas of the transit network can be identified. Among all the failure modes, those with the highest failure rates are the most likely to fail in the timetable. Additionally, the failure conditions of each bus route are independent, and the failure rate of each output in the event tree must satisfy the following relationship:

$$P\left(\text{FM}_r\right) = P\left(F_o \cap F_p \cap F_q\right), \tag{17}$$

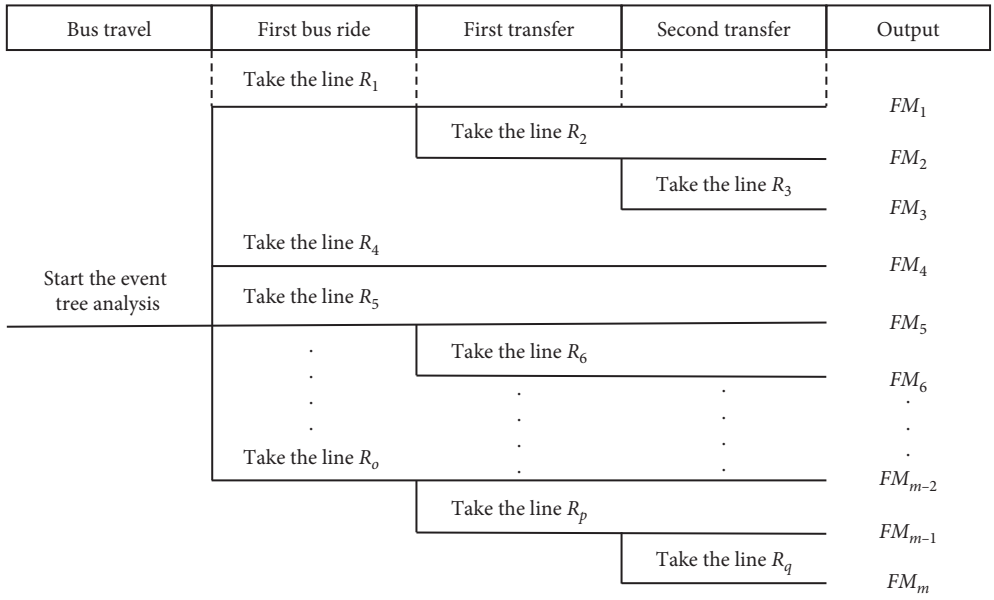

Figure 2: The structure of the event tree based on bus trips.

where FM_r refers to a failed bus timetable and the overall failure rate of the transit network should be the maximum value for all event results. The higher this value is, the lower the reliability of the timetable in the transit network is; conversely, the smaller the value is, the more reliable the timetable is.

4. Results

4.1. Case Study. To test the feasibility and effectiveness of the proposed method, Yixing city is selected as a case study. Yixing is a county-level city managed by Wuxi city, which is located in the southwestern part of Jiangsu province. The city is situated in the centre of the Shanghai–Nanjing–Hangzhou triangle (three large cities in Southeast China) and includes 5 blocks and 13 towns. At present, there are 51 bus lines in Yixing city, with a total length of 246.4 km, an average daily departure frequency of 5400, and an average daily traffic volume of 166,000 persons. The overall density of the public transport network in the city is 1.48 km/km^2, and the sharing rate of bus travel in the urban traffic structure reaches 26%. Urban public transport has become an important mode of daily travel for Yixing citizens. Figure 3 shows the location of Yixing city.

Figure 3: The location map of Yixing city.

Yixing Public Transport Co., Ltd., is the only urban public transport enterprise in Yixing city. Since the outbreak of the COVID-19 epidemic in January 2020, rapid and effective adjustments to the bus operation lines in Yixing city have been made. To smooth the operation of the urban public transport system during the Spring Festival and try to reduce the waste of transit capacity resources, the number of bus lines in Yixing city was adjusted on January 20th. Then, the number of bus trips was reduced by two-thirds on January 27th (according to the original plan, one shift was implemented, and then a pause occurred for two shifts) to promote epidemic prevention and control while meeting the basic bus travel needs of residents. When the novel coronavirus pneumonia epidemic entered the severe stage on February 8th, the bus operation schedule in Yixing was adjusted again, and the departure frequency of the 26 main bus routes was further reduced to 2 per day. In the context of the COVID-19 epidemic, Yixing city adopted a timetabling strategy with time control points, and this strategy was implemented through March 25th. Thus, in the process of epidemic prevention and control, Yixing applied a public transport operation control scheme that gradually increased in strictness according to the actual situation, and a bus timetable similar to a time control point strategy was used

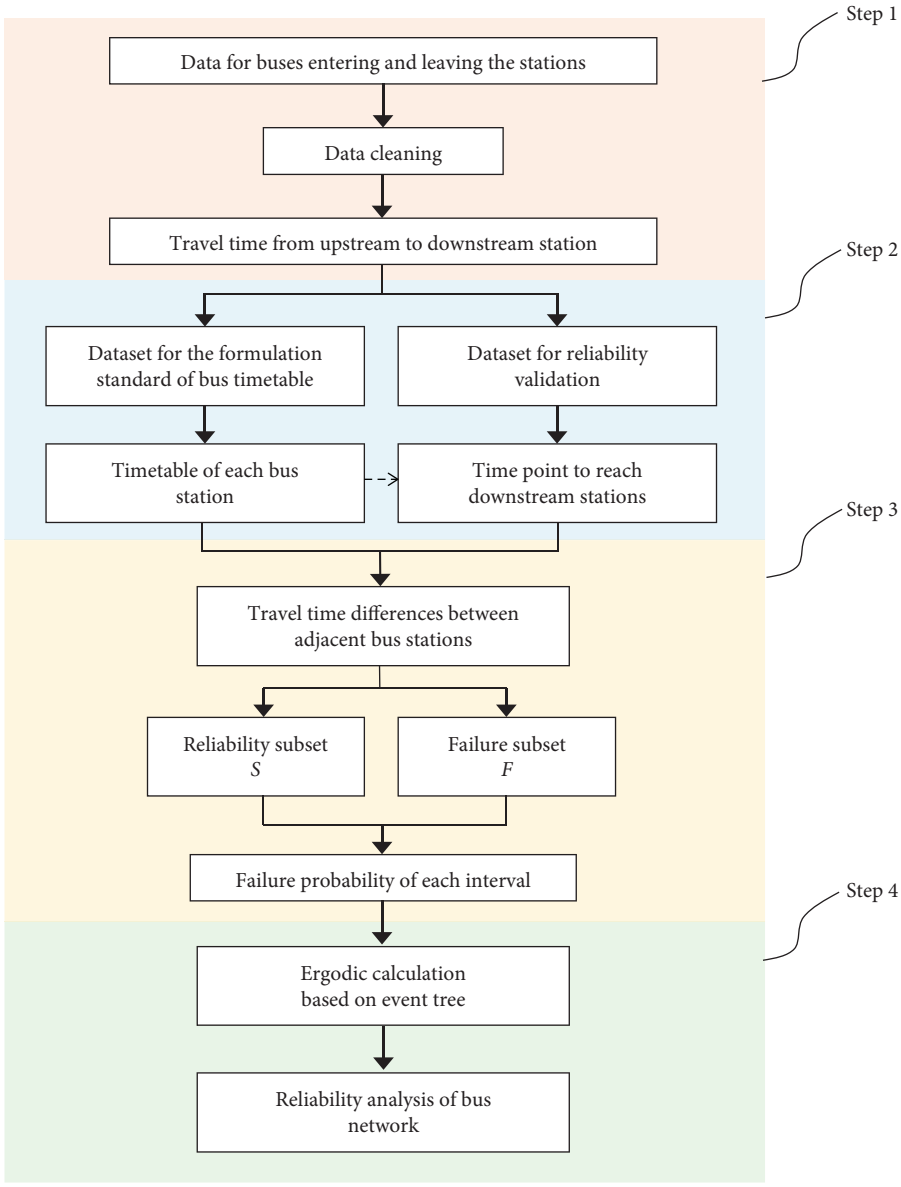

Figure 4: Flowchart for the reliability assessment of the bus timetable.

for up to two months. Therefore, the analysis data from Yixing city collected between December 1, 2019, and March 31, 2020, are used to evaluate the reliability of the bus timetable system during a major health emergency.

4.2. Data Analysis and Results. Figure 4 shows the flowchart of our study, which uses Yixing data to evaluate the reliability of the bus timetable. As mentioned above, the reliability of the overall system depends on the total number of bus routes and the on-time performance in each interval. The specific process steps are as follows.

(i) *Step 1*. We cleaned the data for buses entering and leaving the stations and eliminated missing and abnormal bus records.

(ii) *Step 2*. We divided the extracted punctuality index of the interval travel time into two parts. The first part was the interval travel time in December 2019, which was used to formulate the timetables of bus routes. The second part was the interval travel time between January and March 2020, which was used to verify the reliability of bus timetables during a major public health emergency.

(iii) *Step 3*. According to the bus timetables, we extracted the planned travel times from upstream to downstream stations. Then, we calculated the travel time differences based on the actual arrival time and made appropriate comparisons. If the travel time difference was larger than 0, we considered the bus timetable "reliable"; otherwise, the bus timetable was "nonreliable."

(iv) *Step 4*. We calculated the failure probability of each bus route and constructed the event tree for resident bus travel during the epidemic period. The overall

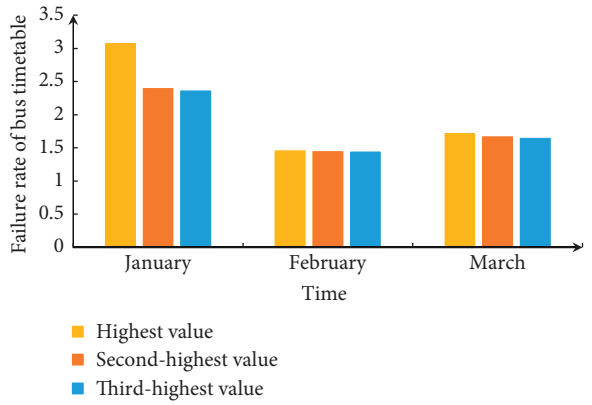

Figure 5: Peak diagram of timetable failure rate.

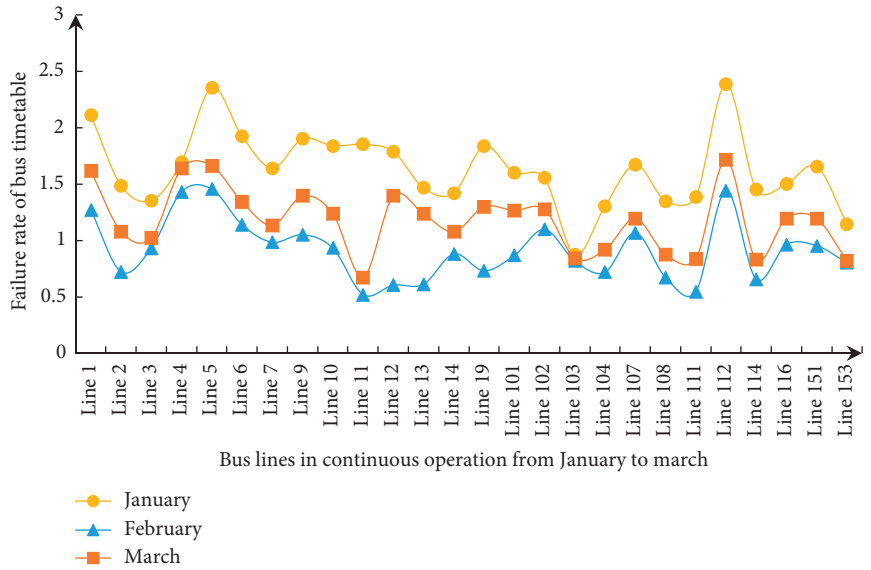

Figure 6: Timetable failure rate of each bus line under epidemic.

reliability of the timetable for the urban transit network was calculated and analysed.

To verify the reliability of the bus timetable, the 75% quantiles of the bus travel time in each interval before the outbreak of the epidemic were used as part of the failure criterion in Step 2. If a bus arrives at the downstream station prior to a given time, the timetable is considered reliable. The bus timetable is set in minutes, and the travel times are rounded up to the nearest minute for ease of understanding by residents. Moreover, this study eliminates the data for bus routes used less than 30 times in the same month to avoid the statistical bias caused by data collection.

Figure 5 shows the highest, second-highest, and third-highest failure rates for bus timetables in Yixing from January to March. Under the time control point strategy, the failure rate in January was significantly higher than that in February or March because of the arrival of the Spring Festival and the outbreak of the COVID-19 epidemic. Additionally, the urban traffic conditions significantly improved in late January, and the reliability of the bus timetabling strategy also improved; this improvement lasted until late March.

Figure 6 shows the bus lines that operated steadily in Yixing during the epidemic period and the corresponding failure rate under the time control point strategy. Notably, in the actual operation process, the failure rate of various lines displays certain volatility, but overall, the failure rate in January is higher than that in February or March. Moreover, the failure rate of most bus lines in February was lower than that in March because the residents of Yixing gradually returned to work and school during the later stage of the COVID-19 epidemic; in addition, the bus lines in Yixing resumed normal operation based on the original schedule. In the epidemic prevention process, the reliability of bus timetables gradually improved due to the lack of urban traffic. Furthermore, we used event tree analysis to traverse the timetable failure rate in Yixing city from January to March and found that the failure rate of the transit network was 7.8142 in the early stage of the COVID-19

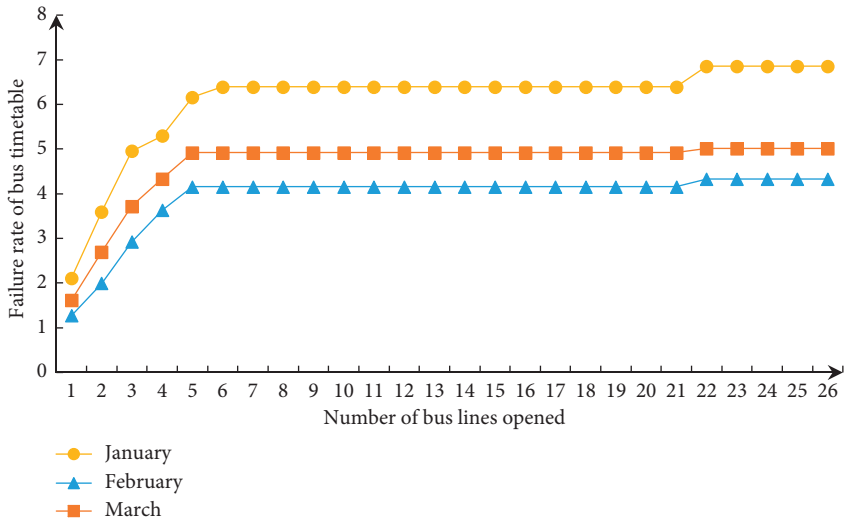

Figure 7: Timetable failure rate for each bus line during the pandemic.

epidemic outbreak and 4.3306 and 5.0160 in the middle and late stages, respectively. The failure rates of the timetables in the middle and late stages of the epidemic decreased by 44.58% and 35.81% compared with that in the early stage, respectively (Figure 7).

In regard to the evolution of the failure rate, we can see that as the number of bus lines opened increases from 1 to 26, the COVID-19 pandemic has a gradually increasing negative impact on the reliability of bus timetables. However, from the perspective of increment, the failure rate of bus timetables increases and tends to be stable when the bus network has a growing scale of operation. This shows that the negative influence of the bus line number follows the principle of diminishing marginal utility to affect the reliability of the timetable. If the number of bus lines is small, the failure rate of the bus timetable shows a significant increasing trend, and when the number of timetables exceeds 6, the reliability enters a step-by-step decline stage. Thus, when planning the bus timetable, policy makers should pay attention to the relationship between the difficulty of pandemic transmission and the number of bus lines to avoid a high risk of epidemic spread caused by insufficient bus capacity or too many bus lines.

5. Conclusions

In this paper, we proposed a reliability analysis framework to evaluate the bus timetabling strategy for a transit network during the COVID-19 epidemic period. By integrating the first-order reliability method and Ditlevsen's bounds theory, a detailed formula derivation process and calculation steps were included in the analysis framework. Three scenarios, e.g., the early, middle, and late stages of the epidemic outbreak, were considered to verify the validity of the model. The failure rate of the bus timetabling strategy, an important indicator used to reflect the operational reliability of the transit network, can be obtained quickly from statistical computations involving the model output.

The reliability analysis framework developed here can be used to determine how to apply data for buses entering and leaving stations to dynamically determine the punctuality characteristics of the time control point strategy. Event tree analysis was used in this study to compute the timetable failure rate considering the transfer and waiting times of residents at bus stations. Each bus trip in the model was regarded as an independence event, and the events did not affect each other in the probability calculation. Because of the bottleneck effect, the highest value of failure probability for all events was the final rate for the entire transit network. The model calibration results illustrate that, in the context of major health emergencies, it is not only feasible but also important to implement the time control point strategy of "if a bus arrives early, it must wait, and if a bus arrives late, it should leave as quickly as possible." According to the case study of Yixing city, the failure rate of the bus timetable initially decreased and then increased based on the analysis framework. Compared with that in the early stage of the epidemic, the failure rate in the middle and late stages decreased by 44.58% and 35.81%, respectively. This finding suggests that the reliability of the timetabling strategy increased by at least 35% during the epidemic period.

Overall, the notable innovation of this paper is to provide a refined reliability measurement method based on the failure rate of bus timetables. The calculation framework is a convenient and easily applicable evaluation model which does not consider the topology of bus line network. Compared with the previous studies, the final result can be ideally obtained by traversing the calculation of the failure probability of each round-trip interval. The decision makers could quickly find out the weak point of bus timetable in the network and work out the corresponding solutions. However, because the evaluation process does not consider the influence of the network topology fully, the results may be insufficient in some situation, such as under the environment of extreme congestion. Further research should explore a refined reliability measurement

method and combine such a method with real-time bus travel data to build a dynamic evaluation model for considering the special environments. And the functional requirements of synchronous multistation evaluation and reliable early warnings for various bus scheduling operation schemes should also be in view in the further reliability framework of bus timetable.

Data Availability

The data used to support the findings of this study are available from the corresponding author upon request.

Conflicts of Interest

The authors declare that they have no conflicts of interest regarding the publication of this paper.

Acknowledgments

The financial support from the National Key R&D Program of China (no. 2018YFE0120100), the Natural Science Foundation of Fujian Province (2020J05194), the Education and Scientific Research Foundation of Fujian Finance Department (GY-Z21001), and the Technology Program of Fujian University of Technology (GY-Z19094 and GY-Z17155) is gratefully acknowledged.

References

[1] R. Anderson and R. May, *Infectious Diseases of Humans: Dynamics and Control*, Oxford University Press, Oxford, England, 1995.

[2] J. Mossong, N. Hens, P. Beutels et al., "Social contacts and mixing patterns relevant to the spread of infectious diseases," *PLoS Medicine*, vol. 5, no. 3, pp. 381–391, 2008.

[3] "Johns Hopkins University, Coronavirus Resource Center," http://coronvirus.jhu.edu/(2020-06-01).

[4] M. U. G. KraemerC.-H. Yang et al., "The effect of human mobility and control measures on the COVID-19 epidemic in China," *Science*, vol. 368, no. 6490, pp. 493–497, 2020.

[5] A. AnzaiT. Kobayashi et al., "Assessing the impact of reduced travel on exportation dynamics of novel coronavirus infection (COVID-19)," *Journal of Clinical Medicine*, vol. 9, no. 2, p. 601, 2020.

[6] G.-Q. SunS.-F. Wang et al., "Transmission dynamics of COVID-19 in Wuhan, China: effects of lockdown and medical resources," *Nonlinear Dynamics*, vol. 101, no. 3, p. 1981, 2020.

[7] I. Kaddoura, B. Kickhöfer, and A. Neumann, A. Tirachini, "Agent-based optimisation of public transport supply and pricing: impacts of activity scheduling decisions and simulation randomness," *Transportation*, vol. 42, no. 6, pp. 1039–1061, 2015.

[8] G. K. D. Saharidis, C. Dimitropoulos, and E. Skordilis, "Minimizing waiting times at transitional nodes for public bus transportation in Greece," *Operational Research*, vol. 14, no. 3, pp. 341–359, 2013.

[9] Trasportation Research Board, Transit Capacity and Quality of Service Manual, Third Edition, The National Academies Press, Washington, DC, USA, 2013.

[10] National Academies of Sciences, "Engineering, and medicine". Using Archived AVL-APC Data to Improve Transit Performance and Management. The National Academies Press, Washington, DC, USA, 2006.

[11] A. Ceder, Public Transit Planning and Opertaion: Theory, Modeling and Practice. Routledge & CRC Press, Boca Raton, FL, USA, 2007.

[12] J. C. Ho, K. Korsesthakarn, and Y.-T. Hsu, H.-Y. Wu, "Models and a solution algorithm for planning transfer synchronization of bus timetables," *Transportation Research Part E: Logistics and Transportation Review*, vol. 131, pp. 247–266, 2019.

[13] G. F. Newell and R. B. Potts, "Maintaining a bus schedule," in *Proceedings of the 2nd Australian Road Research Board Conference*, Perth, Australia, August 1964.

[14] D. Helbing and B. Tilch, "Generalized force model of traffic dynamics," *Physical Review E*, vol. 58, no. 1, pp. 133–138, 1998.

[15] M. D. Hickman, "An analytic stochastic model for the transit vehicle holding problem," *Transportation Science*, vol. 35, no. 3, pp. 215–237, 2001.

[16] E. E. Osuna and G. F. Newell, "Control strategies for an idealized public transportation system," *Transportation Science*, vol. 6, no. 1, pp. 52–72, 1972.

[17] X. J. Eberlein, N. H. M. Wilson, and D. Bernstein, "Modeling real-time control strategies in public transit operations," *Lecture Notes in Economic and Mathematical Systems*, Springer, Berlin, Germany, 1999.

[18] L. Fu and X. Yang, "Design and implementation of bus-holding control strategies with real-time information," *Journal of the Transportation Research Board*, vol. 1791, pp. 6–12, 2001.

[19] P. Marguier, *Bus route performance evaluation under stochastic conditions*, Ph.D. thesis, Massachusetts Institute of Technology, Combridge, MA, USA, 1985.

[20] G. F. Newell, "Control of pairing of vehicles on a public transportation route, two vehicles, one control point," *Transportation Science*, vol. 8, no. 3, pp. 248–264, 1974.

[21] A. Adamski and A. Turnau, "Simulation support tool for real-time dispatching control in public transport," *Transportation Research Part A: Policy and Practice*, vol. 32, no. 2, pp. 73–87, 1998.

[22] A. Kinoshita, "On controlling randomness in transit operations," *Transportation Science*, vol. 8, no. 2, pp. 102–116, 1974.

[23] J. G. StrathmanK. J. Dueker et al., "Automated bus dispatching, operations control, and service reliability: baseline analysis," *Transportation Research Record: Journal of the Transportation Research Board*, vol. 1666, no. 1, pp. 28–36, 1999.

[24] A. Sun and M. Hickman, "The real-time stop-skipping problem," *Journal of Intelligent Transportation Systems*, vol. 9, no. 2, pp. 91–109, 2005.

[25] M. Trompet, X. Liu, and D. Graham, "Development of Key performance indicator to compare regularity of service between urban bus operators," *Transportation Research Record: Journal of the Transportation Research Board*, vol. 1791, pp. 6–12, 2001.

[26] J. J. Bartholdi and D. D. Eisenstein, "A self-coördinating bus route to resist bus bunching," *Transportation Research Part B: Methodological*, vol. 46, no. 4, pp. 481–491, 2012.

[27] X. Chen, L. Yu, and Y. Zhang, J. Guo, "Analyzing urban bus service reliability at the stop, route, and network levels," *Transportation Research Part A: Policy and Practice*, vol. 43, no. 8, pp. 722–734, 2009.

[28] M. Dessouky, R. Hall, and L. Zhang, A. Singh, "Real-time control of buses for schedule coordination at a terminal,"

Transportation Research Part A: Policy and Practice, vol. 37, no. 2, pp. 145–164, 2003.

[29] X. J. Eberlein, N. H. M. Wilson, and D. Bernstein, "The holding problem with real-time information available," *Transportation Science*, vol. 35, no. 1, pp. 1–18, 2001.

[30] J. G. Gerhart, T. J. Kimpel, and K. J. Dueker, R. L. Gerhart, S. Callas, "Evaluation of transit operations: data applications of tri-met's automated," *Transportation*, vol. 29, no. 3, pp. 321–345, 2002.

[31] K. Gkiotsalitis and A. Stathopoulos, "Demand-responsive public transportation Re-scheduling for adjusting to the joint leisure activity demand," *International Journal of Transportation Science and Technology*, vol. 5, no. 2, pp. 68–82, 2016.

[32] K. Gkiotsalitis and E. C. van Berkum, "An exact method for the bus dispatching problem in rolling horizons," *Transportation Research Part C: Emerging Technologies*, vol. 110, pp. 143–165, 2020.

[33] K. Gkiotsalitis and O. Cats, "Reliable frequency determination: incorporating information on service uncertainty when setting dispatching headways," *Transportation Research Part C: Emerging Technologies*, vol. 88, pp. 187–207, 2018.

[34] K. Gkiotsalitis, Z. Wu, and O. Cats, "A cost-minimization model for bus fleet allocation featuring the tactical generation of short-turning and interlining options," *Transportation Research Part C: Emerging Technologies*, vol. 98, pp. 14–36, 2019.

[35] M. Salicrú, C. Fleurent, and J. M. Armengol, "Timetable-based operation in urban transport: run-time optimisation and improvements in the operating process," *Transportation Research Part A: Policy and Practice*, vol. 45, no. 8, pp. 721–740, 2011.

[36] K. Steiner and S. Irnich, "Schedule-based integrated intercity bus line planning via branch-and-cut," *Transportation Science*, vol. 52, no. 4, pp. 882–897, 2018.

[37] S. Zhang, A. A. Ceder, and Z. Cao, "Integrated optimization for feeder bus timetabling and procurement scheme with consideration of evironmental impact," *Computers and Industrial Engineering*, vol. 145, Article ID 106501, 2020.

[38] H. Ma, X. Li, and H. Yu, "Single bus line timetable optimization with big data: a case study in beijing," *Information Sciences*, vol. 536, pp. 53–66, 2020.

[39] W. Domschke, "Schedule synchronization for public transit networks," *OR Spektrum*, vol. 11, no. 1, pp. 17–24, 1989.

[40] A. Ceder, B. Golany, and O. Tal, "Creating bus timetables with maximal synchronization," *Transportation Research Part A: Policy and Practice*, vol. 35, no. 10, pp. 913–928, 2001.

[41] A. Gong, "A model to create bus timetables to attain maximum synchronization considering waiting times at transfer stops," Master's Thesis, University of South Florida, Tampa, FL, USA, 2004.

[42] Z. Liu, J. Shen, and H. Wang, W. Yang, "Regional bus timetabling model with synchronization," *Journal of Transportation Systems Engineering and Information Technology*, vol. 7, no. 2, pp. 109–112, 2007.

[43] O. J. Ibarra-Rojas, F. López-Irarragorri, and Y. A. Rios-Solis, "Multiperiod bus timetabling," *Transportation Science*, vol. 50, no. 3, pp. 805–822, 2016.

[44] O. J. Ibarra-Rojas, R. Giesen, and Y. A. Rios-Solis, "An integrated approach for timetabling and vehicle scheduling problems to analyze the trade-off between level of service and operating costs of transit networks," *Transportation Research Part B: Methodological*, vol. 70, pp. 35–46, 2014.

[45] O. J. Ibarra-Rojas and Y. A. Rios-Solis, "Synchronization of bus timetabling," *Transportation Research Part B: Methodological*, vol. 46, no. 5, pp. 599–614, 2012.

[46] R. C. W. Wong, T. W. Y. Yuen, and K. W. Fung, J. M. Y. Leung, "Optimizing timetable synchronization for rail mass transit," *Transportation Science*, vol. 42, no. 1, pp. 57–69, 2008.

[47] Y. Shafahi and A. Khani, "A practical model for transfer optimization in a transit network: model formulations and solutions," *Transportation Research Part A: Policy and Practice*, vol. 44, no. 6, pp. 377–389, 2010.

[48] L. Kang, J. Wu, and H. Sun, X. Zhu, B. Wang, "A practical model for last train rescheduling with train delay in urban railway transit networks," *Omega*, vol. 50, pp. 29–42, 2015.

[49] X. Guo, H. Sun, and J. Wu, J. Jin, J. Zhou, Z. Gao, "Multi-period-based timetable optimization for metro transit networks," *Transportation Research Part B: Methodological*, vol. 96, pp. 46–67, 2017.

[50] X. Jin, J. Wu, and J. Zhou, X. Yang, D. Wu, Z. Gao, "First-train timing synchronisation using multi-objective optimisation in urban transit networks," *International Journal of Production Research*, vol. 57, no. 11, pp. 3522–3537, 2019.

[51] M. Abdolmaleki, N. Masoud, and Y. Yin, "Transit timetable synchronization for transfer time minimization," *Transportation Research Part B: Methodological*, vol. 131, pp. 143–159, 2020.

[52] Y. Guo, B. Mao, and Y. Bai, T. K. Ho, Z. Li, "Timetable synchronization of last trains for urban rail networks with maximum" accessibility," *Transportation Research Part C: Emerging Technologies*, vol. 99, pp. 110–129, 2019.

[53] J. P. Fonseca, E. Van Der Hurk, and R. Roberti, A. Larsen, "A matheuristic for transfer synchronization through integrated timetabling and vehicle scheduling," *Transportation Research Part B: Methodological*, vol. 109, pp. 128–149, 2018.

[54] P. Fouilhoux, O. J. Ibarra-Rojas, and S. Kedad-Sidhoum, Y. A. Rios-Solis, "Valid inequalities for the synchronization bus timetabling problem," *European Journal of Operational Research*, vol. 251, no. 2, pp. 442–450, 2016.

[55] Y. Shen and J. Xia, "Integrated bus transit scheduling for the Beijing bus group based on a unified mode of operation," *International Transactions in Operational Research*, vol. 16, no. 2, pp. 227–242, 2009.

[56] M. Hickman, P. Mirchandani, and S. Vob, *Computed-aided Systems in Public Transport. Lecture Notes In Economics & Mathematical Systems*, Springer, Berlin, Heidelberg, 2008.

[57] D. PeñaA. Tchernykh et al., "Operating cost and quality of service optimization for multi-vehicle-type timetabling for urban bus systems," *Journal of Parallel and Distributed Computing*, vol. 133, pp. 272–285, 2019.

[58] L. Wu, H. K. Lo, and F. Xiao, "Mixed bus fleet scheduling under range and refueling constraints," *Transportation Research Part C: Emerging Technologies*, vol. 104, pp. 443–462, 2019.

[59] L. Bodin and B. Golden, "Classification in vehicle routing and scheduling," *Network*, vol. 11, no. 1, pp. 97–108, 1981.

[60] L. Bodin, B. Golden, A. Assad et al., "Routing and scheduling of vehicles and crews: the state of the art," *Computers and Operations Research*, vol. 10, no. 1, pp. 63–212, 1983.

[61] S. Bunte and N. Kliewer, "An overview on vehicle scheduling models," *Public Transport*, vol. 1, no. 4, pp. 299–317, 2009.

[62] R. Freling, A. P. M. Wagelmans, and J. M. P. Paixão, "Models and algorithms for single-depot vehicle scheduling," *Transportation Science*, vol. 35, no. 2, pp. 165–180, 2001.

[63] L. J. J. Van Der Bruggen, J. K. Lenstra, and P. C. Schuur, "Variable-depth search for the single-vehicle pickup and delivery problem with time windows," *Transportation Science*, vol. 27, no. 3, pp. 298–311, 1993.

[64] J. Zhang, W. Li, and F. Qiu, "Optimizing single-depot vehicle scheduling problem: fixed-interval model and algorithm," *Journal of Intelligent Transportation Systems*, vol. 19, no. 3, pp. 215–224, 2015.

[65] O. J. Ibarra-Rojas, F. Delgado, and R. Giesen, J. C. Muñoz, Planning, "operation, and control of bus transport systems: a literature review," *Transportation Research Part B: Methodological*, vol. 77, pp. 38–75, 2015.

[66] N. Kliewer, T. Mellouli, and L. Suhl, "A time-space network based exact optimization model for multi-depot bus scheduling," *European Journal of Operational Research*, vol. 175, no. 3, pp. 1616–1627, 2006.

[67] M. Michaelis and A. Schobel, "Integrating line planning, timetabling, and vehicle scheduling: a customer-oriented heuristic," *Public Transportation*, vol. 1, no. 4, pp. 211–232, 2009.

[68] S. Hassold and A. Ceder, "Public transport vehicle scheduling featuring multiple vehicle types," *Transportation Research Part B: Methodological*, vol. 67, pp. 129–143, 2014.

[69] V. Schmid and J. F. Ehmke, "Integrated timetabling and vehicle scheduling with balanced departure times," *OR Spectrum*, vol. 37, no. 4, pp. 903–928, 2015.

[70] J. Li, T. Chen, W. D. Fan et al., "Integrated approach to vehicle scheduling and bus timetabling for an electric bus line," *Journal Of Transportation Engineering, Part A: Systems*, vol. 146, Article ID 4019073, 2020.

[71] Z. Cao and A. Ceder, "Autonomous shuttle bus service timetabling and vehicle scheduling using skip-stop tactic," *Transportation Research Part C: Emerging Technologies*, vol. 102, pp. 370–395, 2019.

[72] B. David, M. Kresz, "Multi-depot bus schedule assignment with parking and maintenance constrains for intercity transportation over a planning period," *Transportation Letters: The International Journal of Transportation Research*, vol. 12, pp. 66–75, 2020.

[73] P. C. Guedes, D. Borenstein, and M. Sâmara Visentini, O. C. B. De Araújo and A. F. Kummer Neto, "Vehicle scheduling problem with loss in bus ridership," *Computers & Operations Research*, vol. 111, pp. 230–242, 2019.

[74] R. Freling, D. Huisman, and A. P. M. Wagelmans, "Models and algorithms for integration of vehicle and crew scheduling," *Journal of Scheduling*, vol. 6, no. 1, pp. 63–85, 2003.

[75] A. Graffi and M. Nonato, "An integrated approach to ex-urban crew and vehicle scheduling," *Lecture Notes in Economic & Mathematical Systems*, Springer, Berlin, Heidelberg, 1999.

[76] R. Borndorfer, A. Lobel, and S. Weider, "A bundle method for integrated multi-depot vehicle and duty scheduling in public transit," *Computer-aided Systems in Public Transport.*vol. 600, pp. 3–24, 2008.

[77] M. A. Boschetti, A. Mingozzi, and S. Ricciardelli, "An exact algorithm for the simplified multiple depot crew scheduling problem," *Annals of Operations Research*, vol. 127, no. 1-4, pp. 177–201, 2004.

[78] S. Singh and D. Huisman, "Vehicle and crew scheduling: solving large real-world instances with integrated approach," in *Proceedings of the Presented at the 9th International Conference on Computer-Aided Scheduling of Public Transport*, San Diego, CA USA, August 2004.

[79] K. Haase, G. Desaulniers, and J. Desrosiers, "Simultaneous vehicle and crew scheduling in urban mass transit systems," *Transportation Science*, vol. 35, no. 3, pp. 286–303, 2001.

[80] M. Mesquita and A. Paias, "Set partitioning/covering-based approaches for the integrated vehicle and crew scheduling problem," *Computers & Operations Research*, vol. 35, no. 5, pp. 1562–1575, 2008.

[81] V. Gintner, I. Steinzen, and L. Suhl, "A time-space network based approach for integrated vehicle and crew scheduling in public transport," in *the Proceedings of the EURO World Group on Transportation Joint Conference*, Delft, Netherlands, June 2006.

[82] I. Steinzen, V. Gintner, and L. Suhl, N. Kliewer, "A time-space network approach for the integrated vehicle- and crew-scheduling problem with multiple depots," *Transportation Science*, vol. 44, no. 3, pp. 367–382, 2010.

[83] N. Kliewer, B. Amberg, and B. Amberg, "Multiple depot vehicle and crew scheduling with time windows for scheduled trips," *Public Transport*, vol. 3, no. 3, pp. 213–244, 2012.

[84] H. L. Petersen, A. Larsen, and O. B. G. Madsen, B. Petersen, S. Ropke, "The simultaneous vehicle scheduling and passenger service problem," *Transportation Science*, vol. 47, no. 4, pp. 603–616, 2013.

[85] C. Gershenson and L. A. Pineda, "Why does public transport not arrive on time? The pervasiveness of equal headway instability," *Plos One*, vol. 4, no. 10, Article ID e7292, 2009.

[86] S. M. Moosavi, A. Ismail, and C. W. Yuen, "Using simulation model as a tool for analyzing bus service reliability and implementing improvement strategies," *PLoS One*, vol. 15, no. 5, Article ID e0232799, 2020.

[87] G. Liu and S. C. Wirasinghe, "A simulation model of reliable schedule design for a fixed transit route," *Journal of Advanced Transportation*, vol. 35, no. 2, pp. 145–174, 2001.

[88] S. C. Wirasinghe and G. Liu, "Optimal schedule design for a transit route with one intermediate time point," *Transportation Planning and Technology*, vol. 19, no. 2, pp. 121–145, 1995.

[89] Y. Wu, J. Tang, and X. Luo, "Comparative analysis of operation strategies in schedule design for a fixed bus route," *International Transactions in Operational Research*, vol. 22, no. 3, pp. 545–562, 2015.

[90] Y. Yan, Q. Meng, and S. Wang, X. Guo, "Robust optimization model of schedule design for a fixed bus route," *Transportation Research Part C: Emerging Technologies*, vol. 25, pp. 113–121, 2012.

[91] N. Van Oort, J. W. Boterman, and R. Van Nes, "The impact of scheduling on service reliability: trip-time determination and holding points in long-headway services," *Public Transport*, vol. 4, no. 1, pp. 39–56, 2012.

[92] X. Dou, Y. Yan, and X. Guo, "Time control point strategy coupled with transfer coordination in bus schedule design," *Journal of Advanced Transportation*, vol. 50, no. 7, pp. 1336–1351, 2016.

[93] Y. Wang, Y. Bie, and L. Zhang, "Joint optimization for the locations of time control points and corresponding slack times for a bus route," *KSCE Journal of Civil Engineering*, vol. 23, no. 1, pp. 411–419, 2019.

[94] B. Varga, T. Kulcsár, and B. Kulcsar, "Optimally combined headway and timetable reliable public transport system," *Transportation Research Part C: Emerging Technologies*, vol. 92, pp. 1–26, 2018.

[95] Y. Zhu, B. Mao, and Y. Bai, S. Chen, "A bi-level model for single-line rail timetable design with consideration of demand and capacity," *Transportation Research Part C: Emerging Technologies*, vol. 85, pp. 211–233, 2017.

[96] Y. Zheng, W. Li, and F. Qiu, "A slack arrival strategy to promote flex-route transit services," *Transportation Research Part C: Emerging Technologies*, vol. 92, pp. 442–455, 2018.

[97] J. Zhang and X. Du, "A second-order reliability method with first-order efficiency," *Journal of Mechanical Design*, vol. 132, pp. 973–984, 2010.

[98] Y.-G. Zhao and T. Ono, "A general procedure for first/second-order reliability method (FORM/SORM)," *Structural Safety*, vol. 21, no. 2, pp. 95–112, 1999.

[99] C. Cheng, L. Zhang, R. G. Thompson, "Reliability analysis of road networks in disaster waste management," *Waste Management*, vol. 84, pp. 383–393, 2019.

Hindawi
Discrete Dynamics in Nature and Society
Volume 2021, Article ID 6622291, 11 pages
https://doi.org/10.1155/2021/6622291

Research Article

Container Slot Allocation for Time-Sensitive Cargo in Maritime Transportation: A One-Phase Model with consideration of Port Congestion

Qi Yao,[1] **Lu Xu**,[2] **and Qin Zhang**[1]

[1]*School of Management, Wuhan College, Wuhan 430212, China*
[2]*School of Information Management, Central China Normal University, Wuhan 430079, China*

Correspondence should be addressed to Qin Zhang; 9231@whxy.edu.cn

Received 17 October 2020; Revised 18 November 2020; Accepted 19 January 2021; Published 12 February 2021

Academic Editor: Fabio Tramontana

This paper studies a container slot allocation problem with dynamic pricing for time-sensitive cargo considering port congestion. Time-sensitive cargo calls for express delivery as soon as possible, and hence a new pricing pattern is proposed considering port congestion. To solve the slot allocation with dynamic pricing issue, a one-phase allocation model which is from different points of view on slot allocation strategy is proposed to formulate this problem. Finally, numerical examples are carried out to test the applicability of the proposed model and solution algorithm.

1. Introduction

In recent years, with the rapid development of economic globalization, the maritime industry has got steady growth [1], among which the container transportation gets the most rapid growth for its large scale, security, convenience for multimodal transport, and so on [2, 3]. In 2015, the total container trade volume amounted in 175 million twenty-foot equivalent units (TEUs) [4]. Containerized cargoes from different shippers are transported by container shipping lines from their origin port to destination port (simply noted as O-D pair). With the fierce competition in market, it is significantly vital for shipping lines to assign its finite ship capacity resource measured by TEUs to container slot demand in different O-D pairs so as to complete customer's demand efficiently as well as to maximize the transportation benefits. Therefore, the slot allocation is an issue for the shipping lines to be concerned about, and it also attracts the attention of researchers.

Another issue which should be concerned by the shipping line is the cargo's call for transit time, and we call this category of cargo as time-sensitive cargo. With the improvement of people's living standard, more attention is put on products' quality, especially for perishable products like fruits, fish, flowers, crabs, and meat. In order to keep the quality of the time-sensitive cargoes, customers expect to obtain them as soon as possible, which indicates that the time-sensitive cargoes are expected to be express delivered and even the payment for such express delivery is high. The high payment motivates a shipping company to receive the delivery of time-sensitive cargoes. Moreover, if the cargoes are delivered to shippers before the due date of shipping, the shippers can have more time to deliver the product to customers before expiration with high quality so as to obtain extra reward; accordingly, the actual freight rate should increase, which is another motivation as well. Of course, if the cargoes are arrived at their destination after the negotiated date, the shipping company has to be penalized. Hence, whether the time-sensitive cargoes can be delivered on time or not is a key issue to be considered by the shipping company. The delivery time for a cargo consists of the shipping time on sailing and staying time in port which mainly includes the waiting time and service time for loading/unloading at port. From the point of shipping line, the sailing time can be controlled by adjusting the vessel's sailing speed without considering the influence of extreme

conditions. However, the staying time in port is not easy to predict by the shipping line due to some uncontrollable common factors in terminal operations. The most common uncontrollable factor is port congestion, caused by schedule unreliability in terminals [5], source limitation such as berths, quay cranes, and internal transport trucks [6, 7], ship collisions or ship groundings [8], and so on, all of which make the ships to wait on anchor point. Therefore, when the shipping line intends to sign a contract of shipping time-sensitive cargoes with the shippers, the port congestion is an issue that cannot be ignored in the estimation of delivery time because the shipping line needs to leave enough suffer time for the delay at port.

Therefore, the container slot allocation problem of time-sensitive cargoes proposed in this paper is different from that for general cargoes, which indicates that the methodologies in the existing researchers studied for general cargoes cannot be directly applied for the proposed problem in this paper. We need to develop a new one for our problem, which is the work we intend to take effort in this paper.

The remainder of this paper is organized as follows. Section 2 is a review of previous research. Section 3 elaborates the container slot allocation of time-sensitive cargo considering time limit and port congestion. Section 4 develops the two models for the proposed problem, which are one-phase allocation model and two-phase allocation model, respectively. Solution algorithm is proposed in section 5, in which the chance constrained programming (CCP) method is introduced to solve the models. Section 6 uses a numerical example to evaluate the models and solution algorithm proposed in the study. Finally, section 7 concludes the study and provides recommendations for future work.

2. Literature Review

Many researches have been studied on the slot allocation problem in container shipping, and most of the studies focused on network planning and path optimization, dynamic pricing based on revenue management, multimodal transportation, and so on. While few literatures focus on the particularity of shipping cargo, such as the special requirements of goods on the due time.

2.1. Literature on Slot Allocation, Dynamic Pricing, and Time-Sensitive Cargo. Slot allocation issue has been widely studied for decades. Maragos [9] made the first step to analyze the feature of liner shipping and considered the problem of the dynamic slot allocation and pricing in both single-segment and multisegment container shipping, while a very important problem in shipping operation management, i.e., the empty container repositioning problem caused by region trade imbalance was, not considered. Feng and Chang [10] and Song and Carter [11] solved the empty container repositioning problem within seaborne shipping networks, while no laden container routing was done explicitly. Feng and Chang [12] studied the optimal slot allocation problem serving a specific shipping service route for ocean carriers and took into account the empty and laden containers allocation. But in their papers, the demand has been assumed to be known and deterministic, while in reality, the demand generally fluctuates and the unknown and uncertain demand is more practical. Considering the demand uncertainty, Bu et al. [13] developed two stochastic programming models on capacity allocation with and without empty containers transportation involved, which were solved by the method of robust optimization. Wang [14] considered the stochastic resource allocation problem for containerized cargo transportation with uncertain capacities and network effects and provided theoretical results about the proposed constrained stochastic programming model. There still exist some studies which discussed the issue of containership slot management from different perspectives. Song and Dong [15], Wang et al. [16], and Guericke and Tierney [17] studied the container routing problem by path-based in operational level, tactical-level, and strategic level, respectively, or by link-based such as Wang [18] and Wang et al. [19], which are all formulated as multicommodity flow problems and can be used to assess the rationalization of slot utilization.

Considering the dynamic pricing problem, Feng and Xiao [20] addressed the integrated dynamic pricing and capacity allocation problem for perishable products, in which they assumed that the supplier sells the same products to different micromarkets at distinct prices. Taudes and Rudloff [21] proposed a pricing and inventory control model with a two-period linear demand model, proving that the optimal joint pricing/inventory policy for the replenishment opportunity after the first period is a base-stock list-price policy. Zhu [22] studied a single-item periodic-review model for dynamic pricing problem with returns and expediting. Lee [23] studied a periodic-review pricing and inventory replenishment problem with stochastic demands in multiple periods. Liu and Yang [24] proposed a joint slot allocation and dynamic pricing model with demand uncertainties in the container sea-rail multimodal transport system. It can be seen that the dynamic pricing problem are usually multi-phase issue with distinct prices.

It is noted that the existing literature made most effort on slot allocation and dynamic pricing of ordinary cargo, mainly about method improvement of the slot allocation. Few studies can be found about slot allocation for time-sensitive which has a specific delivery requirement especially for delivery time. According to Panayides and Song [25] and Wang and Meng [26], the "time factor" is a fundamental requirement of practical liner shipping networks, in which port congestion plays an important role. Meng and Wang [27], Wang et al. [16], Wang and Meng [26], and Meng et al. [28] considered transit time to solve the container paths and network design problem. Wang and Meng [29] proposed a mixed-integer nonlinear stochastic model to hedge against uncertain container handling times and port congestion. Wang et al. [30] took port time windows in their nonlinear model to deal with ship route schedule design problem. Readers can refer to [31] for further information on the cargo allocation and scheduling problem. While all of them pay more attention on network design, rather than container slot allocation problem. As for time-sensitive cargo shipping

demand, Wang et al. [32] and Wang et al. [33] considered the transit-time-sensitive demand which was assumed to be a decreasing continuous function of transit time, to optimal containership schedule as well as the total profit. Also, the path schedule is the main concern in those papers. However, we intend to pay more attention on slot allocation with dynamic pricing problem, which is distinct to the previous studies. Recently, Wang and Li [34] reported the dynamic pricing model for container slot allocation at an international conference.

In conclusion, to the best of our knowledge, the container slot allocation problem with dynamic pricing for time-sensitive cargoes has been hardly studied yet. For time-sensitive cargoes, the design of new pricing pattern for freight rate is the main issue we are concerned about, thus we make a correlation between freight rate and delivery time, in which port congestion is taken into account as the major influence factor to delivery time. In addition, most existing researches take the uncertainty of demand of cargo into account and regard the market of cargo as two categories: contract cargo and spot cargo, but rarely take the contract market and spot market of cargoes as a whole system. So, this paper will study the container allocation problem for time-sensitive cargoes in which the demand uncertainty and empty transportation caused by imbalanced region trade are two key issues to be involved in our considerations, and a new pricing pattern is designed considering port congestion. This paper will formulate the proposed problem as two different models based on two different points of view and will analyze and discuss the solutions of the two developed models.

2.2. Objectives and Contributions. Through the research reviewed above, we can find that the proposed container slot allocation with dynamic pricing problem for time-sensitive cargo considering port congestion remaining an interesting research issue and is deserved to be taken effort. This paper focuses on this issue and takes time limit of shipping cargo and port congestion into consideration, namely, constructing a correlation between freight rate and delivery time, in which port congestion is one of the main influence factors. The objective is to maximize the total revenue of container shipping company in both contract and spot markets, considering empty containers and demand uncertainties.

The contribution of this paper has four aspects. First, it contributes to the literature of container slot allocation for time-sensitive cargoes, which is of practical significance. Second, it develops a new pricing pattern for a shipping company in which the freight rate is determined based on the service efficiency of the shipping company, namely, the pricing pattern is dynamic not static. Such a pricing pattern motivates the shipping company to provide efficient delivery service and benefits the customers as well. Third, port congestion, which cannot be ignored in nowadays for more and more booming global seaborne trade leading to crowded for ports, is taken into consideration as one of the main influence factors for cargoes' delivery time, and it is of importance for it will further impact the service efficiency as well as the revenue of the shipping company. Fourth, this paper develops a model based on different points of view to contrast the optimal solutions and demonstrates which one is more efficient for the container slot allocation problem, which has not been studied in the existing literature. Finally, the proposed methodology and solution algorithm could also be applied to other similar problem with time limit requirement, such as air transportation planning problem and railway transporting with perishable cargo.

3. Problem Statement

This section firstly addresses the shipping route and the container shipment flow and then presents the proposed container slot allocation and dynamic pricing problem for time-sensitive cargo with demand uncertainty in detail, including the slot allocation scheme, the proposed new price mechanism, and two different allocation strategies, and finally describes the notations used in this paper.

3.1. Shipping Route and Container Shipment Flow. The existing studies on container slot allocation problem generally assume the shipping route as a back and forth route separately [13, 24], and obviously it is not consistence with the actual situation, in which the shipping route is an itinerary of shipping sailing with the ports of call on the sail. Assume a target container shipping company operates a shipping line which serves a group of ports denoted by the set Ω. The port rotation in the line can be expressed as

$$p^1 \longrightarrow p^2 \longrightarrow p^3 \longrightarrow \cdots \longrightarrow p^m \longrightarrow p^1, \quad (1)$$

where $p^i \in \Omega\,(i = 1, 2, \ldots, m)$ is the ith port of call on the shipping route and m is the number of ports of call.

Let $\Omega = \{p^1, \ldots, p^i, \ldots p^m\}$ be the set of ports called at the shipping line, and let (p^i, p^j) denote the port pair from port p^i to port p^j. The set of O-D port pairs having container slot demand can be expressed by $M = \{(p^i, p^j) | i, j = 1, 2, \ldots, m; p^i \neq p^j\}$. The container slot demand between O-D port pair (p^i, p^j) is uncertain and denoted by a random variable $\xi^{(p^i, p^j)}$. A leg i is defined as the voyage from port p^i to port $p^{i+1} i = 1, 2, \ldots, m-1$, and leg m stands for the voyage from port p^m to port p^1. When a ship sails on leg $l\,(l = 1, 2, \ldots, m)$ of the itinerary shipping line, the container on the ship includes the newly loaded at port p^l and those loaded at previous ports but still remained on ship, which is referred to as container shipment flow on leg l, denoted by η_l. Generally, we can express the container shipment flow for a leg l as follows [32]:

$$\eta_l = \sum_{(p^i, p^j) \in M} \rho_l^{(p^i, p^j)} \xi^{(p^i, p^j)}, \quad l = 1, 2, \ldots, m. \quad (2)$$

3.2. Problem Description. The shipping line operates a shipping route which calls at a total of m ports in sequence in an itinerary line, with slot capacity denoted by Q. The

cargoes transported by the shipping company are all time-sensitive ones which call for express delivery as soon as possible. Meanwhile, this study assumes that the transported time-sensitive cargoes are the same one type and have the same requirement to delivery time. Slots are then sold to different kinds of shippers so as to maximize the revenue for the shipping company.

We divide the market into two groups: contract sale market and free sale market (or spot market). It is assumed that the market is relatively stable, that is to say the price in same condition is steady and there exists no risk for contract shipper's transfer to spot market. On one hand in the contract sale market, there are large shippers who have a regular, steady, and high amount of demand and have the bargaining power to acquire the slots with a low price. To ensure stable income, the container shipping company should reserve a large portion of slots for the contract customers. It is important to note that the shipping company determines allocation scheme according its prejudgment on the market referring historical data, and thus the amount of contract sale demand is uncertain. While on the other hand, in the free sale market, scattered shippers do not have bargaining power, and hence they must attain the slots with a series relatively high price associated with booking period. The scattered shippers can book slots during t periods of the whole freight solicitation time T, and the price will always go up over time. It is assumed that the demand of free sale in different booking periods' changes with price fluctuations, and the form of demand function is a linear function. The shipping company can divide the freight solicitation time T into t periods, the greater the t, the closer it to canvassing deadline, and the less the sensitive of shippers' demand to price changes. With the growth of the price, free sale demand varies inversely with changes which are assumed to be a simple linear relationship. The container slot demand in contract and spot market is assumed to be sufficient, namely, the market is seller's market. With this assumption, the container shipping company has the priority to decide the slot allocation scheme and dynamic pricing with the limited slot resources among shippers. In addition, considering the trade imbalance among ports, there may be empty container demand in some ports, resulting in empty container reposition, which produces cost for the shipping company and is also an issue we must considered when making slot allocation determination.

Without considering the demand that exceeds the capacity of the ship, here we assumed that the container slot capacity Q is big enough for contract cargoes and empty containers, so that there are left slots for scattered shippers. Therefore, the shipping company allocates the Q slots in three aspects. Firstly, a great proportion of the slots are sold in advance with a lower price as a series contract sale negotiated with large shippers in contract sale market. Secondly, considering empty container demand caused by trade imbalance among ports, shipping company must set aside some slots to fulfill the empty container demand of some ports. Third, the remaining slots are sold to the scattered shippers who have no bargaining power in the spot market freely with a series of relatively high price associated with booking period. The container shipping company has to decide the optimal price according to the forecast demand in each booking period and the reallocation of residual slots on each loaded container O-D pair.

3.3. New Price Mechanism for Time-Sensitive Cargo considering Port Congestion. Considering the delivery requirement of time-sensitive cargo on due time, a new price mechanism is designed, in which we make a correlation between freight rate and delivery time, and a penalty/incentive factor is introduced for delivered delay or advance each one day, respectively. Hence, a basis price is set up for time-sensitive cargo delivered just on the agreed delivery time $U^{(p^i,p^j)}$ for each loaded container O-D pair (p^i, p^j); however, when cargo is delivered in advance, the shipping company will charge an extra fee; on the contrary, if cargo delivered exceeds the time limit, the company should pay certain penalty for the overdue time. Thus, the actual freight rate in final will be the basis price minus a penalty price which equals the penalty factor multiplied by the overdue time, or plus an incentive price which equals the incentive factor multiplied by the advance delivery time.

As to the actual delivery time (or we can say due time), it is mainly concerned with sailing time on board, and the waiting and loading/unloading time on loaded port considering port congestion. As mentioned before, the most common uncontrollable factor is port congestion, which further impacts the total delivery time as well as the actual freight rate. Given that the complexity of influence factors on port congestion, this paper takes queuing theory into account, regarding the port system as an M/M/c system to construct slot allocation models. Suppose that there is finite number of cargo handling equipment in each port, which have independent service time which follows negative exponential distribution, and the ships' arrival with the Poisson process and the time interval between two successive arrivals follows negative exponential distribution. Although in reality, the arrival time of ships are given at least one week in advance, while the information is unknown to the shipping line. Thus, when the shipping line predicts the waiting time at port so as to determine the negotiated delivery time with shippers, the service system can be regarded as an M/M/c queuing system. According to the queuing theory, ship's dwell time in a port, including waiting to be served and service time and also follows a negative exponential distribution.

3.4. Strategies for Slot Allocation. Traditional studies on slot allocation problem usually divide the allocation process into two stages and assign as many as possible container slots to large shippers on contract market to obtain a steady income. However, scattered shippers on spot market are the ones that can provide higher freight rate to get instant service, and certainly high yield means high risk for shipping line. So, it indicates that we need to determine a proper proportion in the allocation scheme, other than giving an absolute preference to contract shippers or determining a proportion artificially. Accordingly, this paper proposes a method based on

the strategy to deal with the issue of container slot allocation and dynamic pricing process. The method is to take the three parts as a whole system, consider the contract container slots, scattered container slots, and empty container slots together to make the total expected revenue maximize. This paper will construct an optimization model accordingly.

For the expression convenient, the notations used in this paper are listed as follows:

Sets:

Parameters:

Decision variables:

Ω: set of all ports indexed by i, $\Omega = \{p^i | i = 1, 2, \ldots, m\}$.

M: set of the O-D pairs from port i to port j, $M = \{(p^i, p^j) | p^i \in \Omega, p^j \in \Omega, i \neq j\}$.

$p_{a^0}^{(p^i,p^j)}$: the negotiated basis price for contract shippers when cargo delivered on time.

$p_a^{(p^i,p^j)}$: the actual price for contract shippers, which equals the basis price minus a penalty price when cargo delivery postponed or plus an award price when cargo delivery advanced.

$U^{(p^i,p^j)}$: the expected delivery time for the time-sensitive cargo on O-D pair (p^i, p^j), the cargo freight will be basis price when cargo is delivered just in time $U^{(p^i,p^j)}$.

e: the penalty or incentive factor for delivered delay or advance one day for each container.

$c^{(p^i,p^j)}$: the cost of transporting an empty container on O-D pair (p^i, p^j).

$\Delta t^{(p^i,p^j)}$: sailing time of ship between O-D pair (p^i, p^j).

w^{p^j}: the waiting time caused by port congestion in p^j, which indicates the dwell time of ship in queuing system including the time waiting for service and the service time, i.e., loading or unloading time. The waiting time follows negative exponential distribution with parameter λ^{p^j}.

$t^{(p^i,p^j)}$: the actual delivery time for cargo from p^i to p^j, which equals $\Delta t^{(p^i,p^j)}$ plus w^{p^j}.

Q: the slot capacity of ship.

$D_a^{(p^i,p^j)}$: the random demand of contract shippers on O-D pair (p^i, p^j).

E^{p^j}: the empty container demand in p^j.

ES^{p^i}: the empty container stock in p^i.

$P_U^{(p^i,p^j)}$: the upper limit of basis price for free sale on O-D pair (p^i, p^j).

T: the freight solicitation time of free sale.

t: the booking period of free sale.

$\alpha_t^{(p^i,p^j)}$, $\beta_t^{(p^i,p^j)}$: the coefficients in demand function $x_{bt}^{(p^i,p^j)}(p_{b^0t}^{(p^i,p^j)})$, which can be estimated using statistical historical data.

$x_a^{(p^i,p^j)}$: the numbers of slots allocated to contract shippers for contract sale on O-D pair (p^i, p^j).

$x_c^{(p^i,p^j)}$: the number of slots allocated to empty containers allocation on O-D pair (p^i, p^j).

$p_{bt}^{(p^i,p^j)}$: the actual price in the booking period t of free sale on O-D pair (p^i, p^j).

$p_{b^0t}^{(p^i,p^j)}$: the basis price for free sale in the booking period t on O-D pair (p^i, p^j) when cargo delivered on time.

$x_{bt}^{(p^i,p^j)}$: the slot demand in the booking period t of free sale on O-D pair (p^i, p^j), which can be expressed as the function of the basis price $p_{b^0t}^{(p^i,p^j)}$.

$\rho_{al}^{(p^i,p^j)}$: binary variable, which equals 1 if the contract sale journey of containers of port pair (p^i, p^j) contains leg l ($l = 1, 2, \cdots, \mathrm{m}$) and 0 otherwise.

$\rho_{bl}^{(p^i,p^j)}$: binary variable, which equals 1 if the free sale journey of containers of port pair (p^i, p^j) contains leg l ($l = 1, 2, \cdots, \mathrm{m}$) and 0 otherwise.

$\rho_{cl}^{(p^i,p^j)}$: binary variable, which equals 1 if the journey of empty containers of port pair (p^i, p^j) contains leg l ($l = 1, 2, \cdots, \mathrm{m}$) and 0 otherwise.

η_{al}: slots allocated for contract containers on leg l. As mentioned before, it can be expressed as $\eta_{al} = \sum_{(p^i,p^j)\in M} \rho_{al}^{(p^i,p^j)} x_a^{(p^i,p^j)}$, $l = 1, 2, \ldots, m$.

η_{btl}: slots allocated for free sale containers on leg l in the booking period t. Thus it can be expressed as $\eta_{btl} = \sum_{(p^i,p^j)\in M} \rho_{bl}^{(p^i,p^j)} x_{bt}^{(p^i,p^j)}$, $l = 1, 2, \ldots, m$.

η_{cl}: slots allocated for empty containers on leg l. As described before, it can be expressed as $\eta_{cl} = \sum_{(p^i,p^j)\in M} \rho_{cl}^{(p^i,p^j)} x_c^{(p^i,p^j)}$, $l = 1, 2, \ldots, m$.

4. Model Development

4.1. Chance Constraints for Container Demand Uncertainty. In this paper, the uncertainty of container slot demand is taken into consideration, which makes the slot allocation problem more complex and more realistic due to the existence of random demand variables $D_a^{(p^i,p^j)}$, whereas results no decisions would definitely exclude later constraint violation caused by unexpected random effects. Since decisions derived under adverse conditions may not fully meet the requirement for its customers, it makes sense for container shipping company to control the possibility of the case at a low level, namely, only a low percentage of realizations of the random parameter of shipment demand leads to constrain violation under the determined and fixed decision. Therefore, the chance constrained programming (CCP) method, proposed by Charnes and Cooper [35], is utilized in this paper to formulate the constraint violation.

In the chance constrained programming model, given the confidence parameter $\alpha \in (0, 1)$, the container shipping company can satisfy the customers' demand with a possibility of $1 - \alpha$, which can be formulated in the following probabilistic form:

$$\Pr\left(x_a^{(p^i,p^j)} \leq D_a^{(p^i,p^j)}\right) \geq 1 - \alpha, \quad \forall \left(p^i, p^j\right) \in M. \tag{3}$$

Equation (3) is a chance constraint. By taking into account the demand uncertainty, the shipping company can guarantee decision-making feasibility. And also, the shipping company can control its chance facing the risk resulting from uncontrollable and unpredicted factors with the range of α.

4.2. Model I: One-Phase Allocation Model (1PAM). With the consideration of container slot demand uncertainty and the new price mechanism caused by the attribute of time-sensitive cargo, there is a need to build a mathematical model for the container shipping company to handle the issue so as to maximum the revenue. Through the new price mechanism, the actual price of time-sensitive cargo for contract and scattered shippers can be expressed by equations (4) and (5), respectively, in which the items in parentheses represent the difference between actual delivery time (the sum of sailing time and service time) and negotiated time for cargo from p^i to p^j:

$$p_a^{(p^i,p^j)} = p_{a^0}^{(p^i,p^j)} - \left(\Delta t^{(p^i,p^j)} + w^{p^j} - U^{(p^i,p^j)}\right) \times e, \quad \forall \left(p^i, p^j\right) \in M, \tag{4}$$

$$p_{bt}^{(p^i,p^j)} = p_{b^0t}^{(p^i,p^j)} - \left(\Delta t^{(p^i,p^j)} + w^{p^j} - U^{(p^i,p^j)}\right) \times e, \quad \forall \left(p^i, p^j\right) \in M, \forall t. \tag{5}$$

According to the description of the first method, we consider the slot allocation as a whole to construct model I. The model I is a one-phase allocation model, in which the slot allocation system is taken as an entirety, and the objective is to maximize the whole revenue. The model is formulated as a chance constrained stochastic integer programming with dynamic pricing:

$$\max Z = \sum_{(p^i,p^j)\in M} p_a^{(p^i,p^j)} x_a^{(p^i,p^j)} + \sum_{t=1}^{T} \sum_{(p^i,p^j)\in M} p_{bt}^{(p^i,p^j)} x_{bt}^{(p^i,p^j)} - \sum_{(p^i,p^j)\in M} c^{(p^i,p^j)} x_c^{(p^i,p^j)}, \tag{6}$$

subject to

$$x_{bt}^{(p^i,p^j)} = \alpha_t^{(p^i,p^j)} - \beta_t^{(p^i,p^j)} p_{b^0t}^{(p^i,p^j)}, \quad \forall \left(p^i, p^j\right) \in M, \forall t, \tag{7}$$

$$p_{a^0}^{(p^i,p^j)} \le p_{b^0t}^{(p^i,p^j)} \le P_U^{(p^i,p^j)}, \quad \forall \left(p^i, p^j\right) \in M, \forall t, \tag{8}$$

$$\eta_{al} + \sum_{t=1}^{T} \eta_{btl} + \eta_{cl} \le Q, \quad \forall l = 1, 2, \ldots, m, \tag{9}$$

$$\Pr\left(x_a^{(p^i,p^j)} \le D_a^{(p^i,p^j)}\right) \ge 1 - \alpha, \quad \forall \left(p^i, p^j\right) \in M, \tag{10}$$

$$\sum_{(p^i,p^j)\in M} x_c^{(p^i,p^j)} \ge E^{p^j}, \quad \forall p^j \in \Omega, \tag{11}$$

$$x_c^{(p^i,p^j)} \le \mathrm{ES}^{p^i}, \quad \forall p^i \in \Omega, \tag{12}$$

$$x_c^{(p^j,p^k)} = 0, \text{ when } E^{p^j} > 0, \quad \forall p^j, p^k \in \Omega, \tag{13}$$

$$x_a^{(p^i,p^j)}, x_{bt}^{(p^i,p^j)}, x_c^{(p^i,p^j)} \in N \cup \{0\}, \quad \forall \left(p^i, p^j\right) \in M. \tag{14}$$

Equation (6) is the objective function of this model, in which the first term is the profit of shipping contract cargoes, and the second term is the revenue of cargos from scattered shippers in all booking periods of free sale; finally, the last term is the cost of empty containers transportation, which must be deducted from the company's total revenue. The set of constraints (7) indicates the linear relation between price and demand in free market. The set of constraints (8) ensures that the basis price in free market is in any period and cannot be less than the basis price of contract sale and cannot be more than a price upper limit on each O-D pair. The set of constraints (9) requires that the total number of slot allocated to the contract shippers, the scattered shippers, and the empty containers cannot exceed the capacity of the ship. The set of constraints (10) is a chance constraint to define that the slots reserved for contract shippers can be efficiently used, namely, the probability of the slots allocated to contract shippers exceed the actual demand, the situation in which the shipping company suffers opportunity loss, is less than α. Constraint set (11) presents the empty container slot allocation from each p^i to p^j cannot be less than the empty container demand of p^j. Constraint set (12) presents the empty containers transporting from p^i to p^j cannot be more than the available empty containers in port p^i. While constraint set (13) indicates that the empty container cannot be transported from p^j to the other ports when p^j has an empty container demand. Constraint (14) is an integer constraint of the decision variables.

5. Two Key Challenges in Solving the Stochastic Optimization Model

There are mainly two key difficulties in solving the proposed stochastic optimization model. Due to the existence of uncertain demand in contract market and the random variables of waiting time caused by port congestion, the proposed models are nondeterministic optimization problems and intractable to deal with. In this section, the chance constraint programming and Jensen's inequality are introduced, respectively, to make a transformation of the models.

5.1. Solving the Chance Constraints in Model. The most difficulty in the model is how to deal with the chance constraints. Here, we assume that the demand of contract sale is a random value following log-normal distribution and the demand on each O-D pair is independent. Previous studies mostly assumed that the demand follows normal distribution, which inevitably leads to some negative values when use the normal distribution to generate a sample; obviously, the negative demand is unrealistic. Whereas the log-normal assumption effectively overcomes this shortcoming of normal distribution, and it is proved by Kamath and Pakkala [36] that the log-normal distribution is well suited for modeling economic stochastic variables such as demand. Therefore, we assume the demand in each O-D pair follows log-normal distribution, i.e.,$D_a^{(p^i,p^j)} \sim \ln N(\mu^{(p^i,p^j)}, \sigma^{(p^i,p^j)})$, and they are independent from each other.

Under the precondition of this hypothesis, we can express the set of chance constraints given by equation (11) with the equivalence deterministic constraints, where $(\Phi^{(p^i,p^j)})^{-1}$ is the inverse function of the distribution function $\Phi^{(p^i,p^j)}$ of $D_a^{(p^i,p^j)}$:

$$x_a^{(p^i,p^j)} \le Z_{1-\alpha} = \sup\left\{Z | Z = \left(\Phi^{(p^i,p^j)}\right)^{-1}(1-\alpha)\right\}, \quad \forall\left(p^i, p^j\right) \in M. \tag{15}$$

Thus, the chance constraints (10) can be replaced by equation (15), and then the model can be transformed into quadratic programming problem with linear constraints and can be solved efficiently by the program solver.

5.2. Solving the Random Variables of Waiting Time in Model. Another difficult problem encountered by the model is how to deal with the random variables of waiting time, which makes the model become a nondeterministic optimization problem. To solve this problem, two aspects of the measures are taken as follows.

Firstly, considering the randomness of the waiting time, N tests are implemented to get the general tendency of the model, so as to compare their robustness. In each test, the only optimal solution is obtained under the deterministic value of waiting time. After N tests, the model which gets relatively stable results has higher robustness than the other one.

Secondly, to get the exact optimal solution for the proposed model, we can use the Jensen's inequality proposed by Wallace and Fleten [37] to transfer the model into deterministic optimization models. They proved that for any x, if $F(x, W)$ is concave in W, where W is a random variable with its mean $\lambda = E[W]$, then the following Jensen's inequality holds:

$$F(x, \lambda) \ge E[F(x, W)]. \tag{16}$$

Hence

$$\max_{x\ge 0} F(x, \lambda) \ge \max_{x\ge 0} E[F(x, W)]. \tag{17}$$

Thus, the optimal value of the deterministic optimization problem is biased upward relative to the optimal value of the stochastic optimization problem. In our model, the waiting time w^{p^j} is a random variable with its mean λ^{p^j}. In both objective functions (6) and (16), $p_a^{(p^i,p^j)}$ is concave with w^{p^j}. Thus the two functions are both concave in w^{p^j}, which is a random variable with its mean λ^{p^j}. Therefore, we can replace the random variable w^{p^j} with its mean λ^{p^j}, and then the models can be solved by deterministic optimization problem.

As a consequence, when the two key difficulties are treated by the methods described in Section 4.1 and Section 4.2, the proposed model is transformed into a model with deterministic forms, which can be efficiently solved by any optimization solver provided by Matlab. Hence, the optimal slot allocation strategy can be obtained by solving the model.

6. Numerical Experiment and Computational Results

Here, an example is implemented to assess the model of slot allocation for time-sensitive cargo and the solution algorithm developed for solving the slot allocation problem with uncertain demand.

6.1. Numerical Experiment. In the case, the container ship route calls at three ports clockwise with order $p^1 \longrightarrow p^2 \longrightarrow p^3 \longrightarrow p^1$ and serves six O-D port pairs, with the slot capacity $Q = 5000$ TEUs. It is assumed that slot demand of contract shippers for each port pair has been obtained through historical data, which is a random variable following log-normal distribution, i.e., $D_a^{(p^i,p^j)} \sim \ln N(\mu^{(p^i,p^j)}, \sigma^{(p^i,p^j)})$, with parameters shown in Table 1. It is noted that previous studies mostly assumed that the demand follows normal distribution, which inevitably leads to some negative values when use the normal distribution to generate a sample, and obviously the negative demand is unrealistic. Whereas the log-normal assumption effectively overcomes this shortcoming of normal distribution and it is proved by Kamath and Pakkala [36] that the log-normal distribution is well suited for modeling economic stochastic variables such as demand.

The data of the basis price of contract sale on each loaded container O-D pair (p^i, p^j) and the cost of transporting an

Table 1: Basis price and demand of contract sale and cost and demand of empty container transportation.

O-D pair (p^i, p^j)		(p^1, p^2)	(p^1, p^3)	(p^2, p^1)	(p^2, p^3)	(p^3, p^1)	(p^3, p^2)
Contract sale	$p_{a^0}^{(p^i,p^j)}$	1250	2820	2680	1970	1130	1860
	$\mu^{(p^i,p^j)}$	1870	1100	990	2052	1918	1285
	$\sigma^{(p^i,p^j)}$	120	115	78	110	109	130
	$c^{(p^i,p^j)}$	155	360	345	250	135	275
Empty container	E^{p^j}	$E_1 = 0$		$E_2 = 380$		$E_3 = 0$	
	ES^{p^i}	$\mathrm{ES}_1 = 400$		$\mathrm{ES}_2 = 0$		$\mathrm{ES}_3 = 200$	

Table 2: Data about delivery time.

O-D pair (p^i, p^j)		(p^1, p^2)	(p^1, p^3)	(p^2, p^1)	(p^2, p^3)	(p^3, p^1)	(p^3, p^2)
Delivery time	$\Delta t^{(p^i,p^j)}$(day)	5.5	13	11.5	7	4	10
	$U^{(p^i,p^j)}$	6	15	13.5	8.5	4.5	11.5
	λ^{p^j} (hour)	5		16		12	

Table 3: Estimation and variation of demand function coefficients and price limit in free market.

O-D pair (p^i, p^j)		(p^1, p^2)	(p^1, p^3)	(p^2, p^1)	(p^2, p^3)	(p^3, p^1)	(p^3, p^2)
$t = 1$	$\alpha_t^{(p^i,p^j)}$	750	675	695	620	675	550
	$\beta_t^{(p^i,p^j)}$	0.36	0.19	0.20	0.25	0.4	0.25
$t = 2$	$\alpha_t^{(p^i,p^j)}$	770	655	705	630	680	560
	$\beta_t^{(p^i,p^j)}$	0.37	0.18	0.19	0.25	0.38	0.24
$P_U^{(p^i,p^j)}$		2080	3550	3470	2475	1685	2195

The confidence parameter $\alpha = 0.05$.

empty container on each O-D pair (p^i, p^j) are presented in Table 1.

Here, we set the penalty or incentive factor $e = 500$ dollars per day for each TEU. The sailing time between O-D port pair is obtained from the schedule. And, $U^{(p^i,p^j)}$ is given according to cargo's property and distance of O-D port pair. Waiting time is given based on port service efficiency, and the arrival rate of the ship. The data are shown in Table 2.

It is assumed that freight solicitation time of free sale is divided into 2 periods, $t = 1$ represents that the slots are reserved two weeks in advance; $t = 2$ represents that the slots are reserved one weeks in advance. The greater the t, the closer it is to canvassing deadline, and less sensitive the shippers' demand to price changes. Through statistical analysis of relevant data, the estimation and variation of demand function coefficients in different periods on each loaded container O-D pair are presented in Table 3.

6.2. Result Analysis. According to Jensen's inequality, we transfer the model into a deterministic optimization model. We use the average of the waiting time to replace the random waiting time; therefore, we can obtain the result of the model in detail. The optimal solutions are shown in Table 4:

Based on the results, first, we can have a look on the whole, and the optimal total revenue in our model is 2.3797×10^7. Thus, the results are close in the model and the result obtained from the model is good. Obviously, we can see that the slot allocation revenue gained from the contract market and empty container in the model is lower than that benefited from the free market income. A reasonable explanation behind such a result is that the container demand in contract and spot market is assumed to be sufficient, namely, the market is seller's market. Therefore, our model takes the market system as a whole, all shippers including contract shippers and spot ones compete freely, and the higher-price-offer ones can be allocated container slots. No matter how the actual price changes mainly caused by waiting time, our model will preferentially assign the slots to the higher-price-offer ones.

To demonstrate the efficiency of the price mechanism proposed in this paper, we will compare the results in Tables 4 and 5 with the results obtained from the general slot allocation models without considering the time limit of cargo and port congestion, namely, take the basis price in this paper as the actual price in objective functions.

Furthermore, we can extrapolate that the longer the waiting time is, the higher probability that the revenue acquired in new price mechanism is lower than the one attained in basis price. Because with the increase of the waiting time in discharging port, the shipping company will face a higher risk of delays in delivery for time-sensitive cargo, and a penalty will incur for delivered delay. As a consequence, the shipping company must determine under which circumstances should this new pricing strategybe adopted. For example, when the port of call is much congested, it is obviously unwise to consider the new pricing mechanism, which will result heavy loss for shipping company in this condition.

Table 4: Results of slot allocation and actual price for Model I.

O-D pair (p^i, p^j)			(p^1, p^2)	(p^1, p^3)	(p^2, p^1)	(p^2, p^3)	(p^3, p^1)	(p^3, p^2)	Revenue
Contract market	Actual price		1167	3570	3576	2470	1276	2277	1.9929×10^7
	Number of slots (TEU)		1538	1118	1005	2069	1935	1304	
Free market	$t = 1$	Basis price	1666	2930	2750	1970	1286	1990	1.8746×10^6
		Actual price	1583	3680	3646	2470	1432	2407	
		Slots (TEU)	150	118	145	128	161	53	
	$t = 2$	Basis price	1666	2973	2868	1970	1337	2057	2.0520×10^6
		Actual price	1583	3723	3764	2470	1483	2474	
		Slots (TEU)	153	120	160	138	172	66	
Empty container	Slots (TEU)	380	0	0	0	0	0	0	
Total revenue: 2.3797×10^7									

Table 5: Results of slot allocation just considering basis price in Model I.

O-D pair (p^i, p^j)			(p^1, p^2)	(p^1, p^3)	(p^2, p^1)	(p^2, p^3)	(p^3, p^1)	(p^3, p^2)	Revenue
Contract market	Slots (TEU)		1708	1118	1005	2069	1935	1184	1.6446×10^7
Free market	$t = 1$	Price	1666	3016	2680	1970	1149	2030	1.5701×10^6
		Slots (TEU)	150	102	159	128	215	43	
	$t = 2$	Price	1666	3059	2774	1970	1200	2097	1.7287×10^6
		Slots (TEU)	154	104	178	138	224	57	
Empty container	Slots (TEU)	380	0	0	0	0	0	0	-5.8900×10^4
Total revenue: $1.9686 * 10^7$									

7. Conclusions

This paper focuses on time-sensitive cargo transportation, and a new price mechanism is proposed considering the time limit of time-sensitive cargo and port congestion of O-D port pairs to make a correlation between freight charge and delivery time when determining cargo freight. Then, a one-phase allocation model is proposed to solve the container slot allocation with dynamic pricing problem for time-sensitive cargo considering port congestion.

The model considers the revenue in a whole system, namely, considering the contract container slots, scattered container slots and empty container slots demand together to make the total expected revenue maximize. The chance constrained programming method is used to deal with the demand uncertainty issue, and Jensen's inequality proposed by Wallace S W et al. (2003) is introduced to solve the random variable waiting time.

Then, a numerical example of slot allocation for time-sensitive cargo is carried out to test the applicability of the proposed models and solution algorithm. Additionally, it is proved that the new price mechanism is efficient by comparing with the general slot allocation model without considering the time limit of cargo and port congestion, and the result indicates that the proposed pricing pattern can significantly increase the revenue of shipping company and enhance customer satisfaction.

However, the conclusions are based on the assumption that the container demand in contract and spot market is sufficient, thus the model performance show good robustness. Hence, the shipping company needs to select container slot allocation model according to the market condition or uses Model I to determine the slots proportion reserved for contract shippers who have steady demand.

This study is a preliminary exploration on the pricing pattern of time-sensitive cargo shipping freight in container slot allocation. Although muck work has been done, there still exist some limitations in this paper. Firstly, the time-sensitive cargo studied in this paper limits to one kind of cargo with the same time limit demand during the same O-D pair, while there usually exist several different kinds of cargo to deliver in the same ship in reality, which have different time limit demands during the same O-D pair. Thus, the future research direction is suggested to take different categories of cargoes into account, so as to make the study more practical. Secondly, container slot allocation for complex transport routes based on network needs to be further studied. Thirdly, another extension study can focus on pricing mechanism parameter design, such as how to determine a reasonable penalty or incentive factor to make revenue maximization and the effects that the extent of port congestion made on the efficiency of the new pricing mechanism. These aspects are the future study directions which are deserved to take effort on.

Data Availability

The data used to support the study are available from the corresponding author upon request.

Conflicts of Interest

The authors declare that they have no conflicts of interest.

Acknowledgments

The authors thank Dr. Wang from Wuhan University for his suggestions. This study was supported by the Research and

Innovation Platform Construction Plan of Wuhan College (Grant no. KYP201901) and Fundamental Research Funds for the Central Universities (Grant no. CCNU19TS078).

References

[1] L. Song, D. Yang, A. T. H. Chin et al., "A game-theoretical approach for modeling competitions in a maritime supply chain," *Maritime Policy & Management*, vol. 43, no. 8, pp. 976–991, 2016.

[2] D. Mao and A. T. H. Chin, "Impact of politics, economic events and port policies on the evolution of maritime traffic in Chinese ports," *Maritime Policy & Management*, vol. 41, no. 4, pp. 346–366, 2014.

[3] D. Chen, G. P. Ong, and A. T. H. Chin, "An exploratory study on the effect of trade data aggregation on international freight mode choice," *Maritime Policy & Management*, vol. 41, no. 3, pp. 212–223, 2014.

[4] UNCTAD, *Review of Maritime Transportation: Paper Presented at the United Nations Conference on Trade and Development*, UNCTAD, New York, NY, USA, 2016, http://unctad.org/en/PublicationsLibrary/rmt2016_en.pdf.

[5] M. R. Brooks and T. Schellinck, "Measuring port effectiveness: what really determines cargo interests' evaluations of port service delivery?" *Maritime Policy & Management*, vol. 42, no. 7, pp. 699–711, 2015.

[6] Y. Wan, C. L. Yuen, and A. Zhang, "Effects of hinterland accessibility on us container port efficiency," *International Journal of Shipping & Transport Logistics*, vol. 6, no. 4, 2014.

[7] X. T. Shang, J. X. Cao, and J. Ren, "A robust optimization approach to the integrated berth allocation and quay crane assignment problem," *Transportation Research Part E: Logistics and Transportation Review*, vol. 94, pp. 44–65, 2016.

[8] C. Jiang, Y. Wan, and A. Zhang, "Internalization of port congestion: strategic effect behind shipping line delays and implications for terminal charges and investment," *Maritime Policy & Management*, pp. 1–19, 2016.

[9] S. A. Maragos, *Yield Management for the Maritime Industry*, Massachusetts Institute of Technology, Cambridge, MA, USA, 1994.

[10] C.-M. Feng and C.-H. Chang, "Empty container reposition planning for intra-asia liner shipping," *Maritime Policy & Management*, vol. 35, no. 5, pp. 469–489, 2008.

[11] D.-P. Song and J. Carter, "Empty container repositioning in liner shipping1," *Maritime Policy & Management*, vol. 36, no. 4, pp. 291–307, 2009.

[12] C. M. Feng and C. H. Chang, "Optimal slot allocation with empty container reposition problem for Asia ocean carriers," *International Journal of Shipping and Transport Logistics*, vol. 2, no. 1, pp. 22–43, 2010.

[13] X. Z. Bu, Q. W. Zhao, Q. Huang et al., "Optimal capacity allocation model of ocean shipping container revenue management considering empty container transportation," *Chinese Journal of Management Science*, vol. 13, no. 1, pp. 71–75, 2005.

[14] X. Wang, "Stochastic resource allocation for containerized cargo transportation networks when capacities are uncertain," *Transportation Research Part E: Logistics and Transportation Review*, vol. 93, pp. 334–357, 2016.

[15] D.-P. Song and J.-X. Dong, "Cargo routing and empty container repositioning in multiple shipping service routes," *Transportation Research Part B: Methodological*, vol. 46, no. 10, pp. 1556–1575, 2012.

[16] S. Wang, Q. Meng, and Z. Sun, "Container routing in liner shipping," *Transportation Research Part E: Logistics and Transportation Review*, vol. 49, no. 1, pp. 1–7, 2013b.

[17] S. Guericke and K. Tierney, "Liner shipping cargo allocation with service levels and speed optimization," *Transportation Research Part E: Logistics and Transportation Review*, vol. 84, pp. 40–60, 2015.

[18] S. Wang, "A novel hybrid-link-based container routing model," *Transportation Research Part E: Logistics and Transportation Review*, vol. 61, no. 1, pp. 165–175, 2014.

[19] T. Wang, Z. Xing, H. Hu, and X. Qu, "Overbooking and delivery-delay-allowed strategies for container slot allocation," *Transportation Research Part E: Logistics and Transportation Review*, vol. 122, pp. 433–447, 2019.

[20] Y. Feng and B. Xiao, "Integration of pricing and capacity allocation for perishable products," *European Journal of Operational Research*, vol. 168, no. 1, pp. 17–34, 2006.

[21] A. Taudes and C. Rudloff, "Integrating inventory control and a price change in the presence of reference price effects: a two-period model," *Mathematical Methods of Operations Research*, vol. 75, no. 1, pp. 29–65, 2012.

[22] S. X. Zhu, "Joint pricing and inventory replenishment decisions with returns and expediting," *European Journal of Operational Research*, vol. 216, no. 1, pp. 105–112, 2012.

[23] J. Lee, "Dynamic pricing inventory control under fixed cost and lost sales," *Applied Mathematical Modelling*, vol. 38, no. 2, pp. 712–721, 2014.

[24] D. Liu and H. Yang, "Joint slot allocation and dynamic pricing of container sea-rail multimodal transportation," *Journal of Traffic and Transportation Engineering (English Edition)*, vol. 2, no. 3, pp. 198–208, 2015.

[25] P. M. Panayides and D.-W. Song, "Maritime logistics as an emerging discipline," *Maritime Policy & Management*, vol. 40, no. 3, pp. 295–308, 2013.

[26] S. Wang and Q. Meng, "Liner shipping network design with deadlines," *Computers & Operations Research*, vol. 41, pp. 140–149, 2014.

[27] Q. Meng and S. Wang, "Optimal operating strategy for a long-haul liner service route," *European Journal of Operational Research*, vol. 215, no. 1, pp. 105–114, 2011.

[28] Q. Meng, T. Wang, and S. Wang, "Multi-period liner ship fleet planning with dependent uncertain container shipment demand," *Maritime Policy & Management*, vol. 42, no. 1, pp. 43–67, 2015.

[29] S. Wang and Q. Meng, "Robust schedule design for liner shipping services," *Transportation Research Part E: Logistics and Transportation Review*, vol. 48, no. 6, pp. 1093–1106, 2012.

[30] S. Wang, A. Alharbi, and P. Davy, "Liner ship route schedule design with port time windows," *Transportation Research Part C: Emerging Technologies*, vol. 41, pp. 1–17, 2014.

[31] Q. Meng, S. Wang, H. Andersson, and K. Thun, "Containership routing and scheduling in liner shipping: overview and future research directions," *Transportation Science*, vol. 48, no. 2, p. 265, 2014.

[32] S. Wang, Q. Meng, and Z. Liu, "Containership scheduling with transit-time-sensitive container shipment demand," *Transportation Research Part B: Methodological*, vol. 54, no. 3, pp. 68–83, 2013a.

[33] S. Wang, Q. Meng, and C.-Y. Lee, "Liner container assignment model with transit-time-sensitive container shipment demand and its applications," *Transportation Research Part B: Methodological*, vol. 90, pp. 135–155, 2016.

[34] T. Wang and M. Li, "Dynamic pricing model for container slot allocation considering port congestion," *Smart Innovation, Systems and Technologies*, vol. 149, pp. 243–250, 2019.
[35] A. Charnes and W. W. Cooper, "Chance-constrained programming," *Management Science*, vol. 6, no. 1, pp. 73–79, 1959.
[36] K. R. Kamath and T. P. M. Pakkala, "A Bayesian approach to a dynamic inventory model under an unknown demand distribution," *Computers & Operations Research*, vol. 29, no. 4, pp. 403–422, 2002.
[37] S. W. Wallace and S.-E. Fleten, "Stochastic programming models in energy," *Handbooks in Operations Research and Management Science*, vol. 10, pp. 637–677, 2003.

Hindawi
Discrete Dynamics in Nature and Society
Volume 2021, Article ID 6690213, 10 pages
https://doi.org/10.1155/2021/6690213

Research Article

Research on the Construction of Supply Chain Management for Undergraduate Programs at Chinese Applied Universities

Yanhui Li,[1,2] **Yating Wei**,[2] **Qi Yao**,[1] **and Mengsiying Li**[1]

[1]*School of Management, Wuhan College, Wuhan 430212, China*
[2]*School of Information Management, Central China Normal University, Wuhan 430079, China*

Correspondence should be addressed to Qi Yao; 8427@whxy.edu.cn

Received 20 November 2020; Revised 21 December 2020; Accepted 19 January 2021; Published 30 January 2021

Academic Editor: Tingsong Wang

At present, China regards supply chain innovation and application as a new national strategy, which leads to a large demand for applied supply chain professionals. In order to provide useful references for applied universities that have already set up the supply chain management (SCM) program and promote the healthy development of China's application-oriented SCM for undergraduates, this paper discussed the necessity and feasibility of setting up the SCM program in Chinese universities. In addition, it analyzes the current situation of SCM programs from three aspects involving approval, type of universities, and issues of application-oriented undergraduate. Based on practical experience in specialty development, in this paper, specific measures were shown from three dimensions: requirements of knowledge, ability, and quality, curriculum setting, and teaching material design.

1. Introduction

The General Office of the State Council of China issued "the Guidance on Actively Promoting Supply Chain Innovation and Application" in 2017, which sent a clear and strong message to the whole society that China's industrial development will enter a new stage of "supply chain +." The following year, the Chinese Ministry of Education approved the establishment of supply chain management (SCM) of undergraduate programs in mainland universities, which started a great trend of talent training for undergraduates. Due to the program is new in China without reference and experience, colleges and universities are constantly exploring how to embody the application-oriented characteristics of SCM talents. Therefore, it is significant to explore the way to build application-oriented SCM undergraduate major in China.

By analyzing the progress of higher education from elitism to popularization, researchers realized that application-oriented talents who were more practical and meet social requirements would be increasingly valued in the 1990s. Robbins [1] believes that the key point of undergraduate education is to build a curriculum system with application ability as the main point while doing talent training. Greiner [2] holds the view that the training in colleges and universities cannot be separated from the orientation of employment demand; that is, in order to meet the diversified needs of market and individual enterprise, we should strengthen the communication between colleges and enterprises through active school enterprise cooperation and improve their professional quality. In terms of teaching modes, the main methods are case teaching mode, resource-based teaching mode, task-driven teaching mode, group cooperation teaching mode, and project teaching mode. There are generous relevant empirical research results. Bilgin et al. [3] found that compared with group learning based on traditional learning methods, undergraduate students that based on project-based learning have more self-efficacy beliefs in learning through comparative analysis of experiments. Rogers and Braziotis [4] believed that some commonly used methods (such as case studies, classroom discussions, and individual and group work) do not seem to be the most important methods in the future, while commercial games/simulations and competitions seem to be the preferred teaching methods. Similar to Helen's research, Chuang [5] helps students think logically and systematically

through scenarios of uncertainty and complexity, so as to cope with the challenges of responsive supply chains. Nguyen [6] showed that although the traditional teaching methods (such as the inductive method, active learning method, the participatory teaching method, and inquiry teaching strategy) are effective, nowadays, most of the teaching makes a mixture of traditional and nontraditional methods.

The study of the higher education system focuses more on how to train students to meet social needs from the perspective of curriculum setting. Elliott and Paton [7] believe that as the world continues to follow the path of specialization, the flexibility of students' educational should to be improved constantly. The flexible course selection system will enhance the adaptability and responsiveness of undergraduate education to meet the changing social demand. SCM is a discipline that requires students to make decisions and invent new solutions, which forces students to understand the tactical and strategic decisions of enterprises [8]. In recent years, with more breakthrough technologies enter the market, enterprises should change the job requirements. And it increases the academic pressure of undergraduates in SCM [9]. Sodhi et al. [10] studied some of the top 50 business school postgraduate courses in the US, including 37 SCM optional course and 36 core courses in operation management. Their analysis shows that there is a gap between industry demand and SCM courses, while Western Michigan University (WMU) offers the integrated supply management (ISM) program to focus on creating value for students while meeting the needs of the professionals through its experiential learning program. Because students learn technology and soft skills in an interactive environment, SCM education integrates more experiential learning courses [11]. Curkovic and Fernandez [12] proved that the ISM program at WMU successfully narrowed the gap between graduates' abilities and employers' expectations through continuous collaboration with the industry.

2. The Necessity and Feasibility of Establishing the SCM Program in China

2.1. Meeting the Needs of Economic Development. As the second largest economy in the world, China has actively integrated into the development trend of the global economy. "One belt, one road," and "Internet+" have effectively promoted the free operation of market and economic factors, and it promoted the formation of global industrial chains, global value chains, and global supply chains. Blanchard, a senior researcher at the Peterson Institute of International Economics (PIIE) said that China has been deeply involved in the global supply chain [13, 14]. A report by HIS Markit, a British market research organization, shows that while China continues to be a purchasing destination, it is no longer "a target country for low-cost outsourcing business" but "a center of the global supply chain that it has leapt to" [15].

Most of the traditional management and operation modes of Chinese enterprises are self-contained and relatively closed, and they pay little attention to open SCM. In this case, manufacturers, suppliers, and distributors lack long-term strategic partnership. They lack a value chain and mutual trust, so it is difficult to get the profits effectively and meet the requirements of customers in the aspects of cost, quality, delivery time, and experience. It is also difficult to form a sensitive pattern of business flow, logistics, capital flow, and information flow. It is necessary to speed up the promotion of enterprises to take market demand as the guidance and to be market demand oriented, which will creative a win-win situation with upstream and downstream enterprises and final consumers. It can also effectively connect business flow, logistics, information flow, capital flow, and business flow to achieve seamless integration between enterprises, and improve the response speed of the entire supply chain, form the optimization of the logistics of the entire supply chain. It is one of the main trends of modern economic development to improve the internal supply chain architecture of enterprises, improve the operation efficiency of the overall supply chain, and reduce the operation cost of the supply chain by making use of efficient external supply chain service platform and relying on the services provided by professional SCM companies.

2.2. Huge Market Demand. With the continuous influence of economic globalization and Internet, the flow of goods, information, and capital in the supply chain will all be connected to the Internet. And with the help of the latest information technologies such as big data and cloud computing, traditional industries are seamlessly integrated with the new economy, ushering in a new cycle of development. According to the China Logistics Development Report [16], the compound growth rate of China's logistics and supply chain in the next five years will reach 15%, and the market value will reach 3.2 trillion US dollars in 2020. 70% of the supply chain outsourcing providers have experienced annual business growth of more than 20% over the past three years. In addition, according to the forecast of the Qianzhan Industry Research Institute [17], the market size of China's SCM services will reach 3.1 trillion US dollars in 2020, as shown in Figure 1. And the compound growth rate of the market value of China's logistics and supply chain services in the next five years will remain at about 15%.

The rapid development of SCM service market has put forward urgent demand for SCM talents. According to the latest statistics of China Employment Training Technical Guidance Center (CETTIC), there are more than 5 million logistics and SCM employees in China, and only 50% of the graduates majored in business administration, logistics management, and SCM (2019). Among them, the interdisciplinary supply chain talents who can cope with the challenges of globalization have Internet thinking and are familiar with the knowledge and operation of various subdivisions of the supply chain are rare and scarce that are about 50,000 people, accounting for only 1%. So, cross-border talents who can adapt to the complex environment of global supply chain (familiar with procurement, logistics, trade, information technology, e-commerce, law, and other fields at the same time) will become the focus of competition for all enterprises.

Figure 1: Market size and forecast of SCM services in China from 2010 to 2020. Source: Qianzhan database.

2.3. International Experience for Reference. According to our survey of relevant universities in the US, Hong Kong, and mainland China, the SCM program is generally located in the school of management or business school, while some universities offer the major under Industry Engineering. There are three main directions for this program: First, research on SCM methods; second, supply chain model analysis and research; and the third one is a branch of the MBA. The graduates are mainly engaged in logistics planning, global procurement, supply management analysis, and other professions. Their work fields involve manufacturing, service, health, retail, and other industries.

2.3.1. SCM Programs in American Universities. As companies operate across borders, manufacturing, retail, and technology companies, as well as the consulting firms, are in desperate need of talent in SCM. World-renowned universities, including Michigan State University (MSU) and the Massachusetts Institute of Technology (MIT), have set up the SCM program. From 2011 to 2014, eight US universities have set up undergraduate program, MBA, and even all degree courses on purchasing, inventory management, and international supply chain strategy (see Table 1).

In the United States, SCM graduates are in great demand, and their income level is considerable. At Arizona State University (ASU), the average starting salary for a supply chain undergraduate in 2012 was $56,410, while that for a business undergraduate was $50,098. As for the MBA level, the starting salary for students who are in charge of operations or supply chain work is $97,481, while the average MBA salary is $92,556.

2.3.2. SCM Programs in Hong Kong. Hong Kong has always been a global logistics and trade hub, maintaining its status as the world's busiest container port and international air cargo center for many years. Due to the vigorous promotion of the Hong Kong government and the influence of a number of cooperation policies between China and Hong Kong, the development of the trade and logistics industry in Hong Kong is more vigorous, and there is a great demand for SCM professionals in the market.

The Hong Kong Polytechnic University (PolyU) offers the Bachelor of Business Administration (Honours) in Global SCM for the school of business administration. The course focuses on operation management, information technology, cross-departmental management, global trade, and transportation processes and provides students with comprehensive and professional industry knowledge, so that they can prepare for the logistics industry. In addition to the diversity of subjects, the most important feature of the course is interaction and activity teaching. Through different case analysis, role playing, and simulation exercises, students can be exposed to more practical cases and train their thinking. The course will arrange students to visit enterprises and organizations in the industry and invite experienced staff to share their experiences, so as to broaden students' international vision. Due to the wide coverage of the courses, graduates can gain in-depth understanding of transportation logistics, supply chain logistics, and enterprise management. Therefore, there are a lot of options for employment, and they can be engaged in SCM in procurement, shipping, transportation, retail and wholesale, and other industries.

The School of Business at Hang Seng University of Hong Kong (HSUHK) launched the Bachelor of Business Administration (Honours) in SCM (BBA-SCM) in 2010. And the course was invited by the Education Bureau to join the "designated professional/sector course funding scheme" of the Education Bureau of the Hong Kong Special Administrative Region in 2015. The following year, it was awarded the subject scope certification by the Hong Kong Council of Academic and Vocational Qualifications. At present, it is recognized as one of the largest supply chain and logistics management courses in Greater China.

BBA-SCM is a four-year program in the school of decision science, with two semesters (15 weeks) per year. Each project module of BBA-SCM contains three credits, and each credit has at least 15 face-to-face class hours. In the four-year system, students are required to complete at least 43 modules with a total of 129 credits. The BBA-SCM project has designed two professional directions. The first direction is designed for those students who want to continue to study in the supply chain and logistics related fields, while the second direction is designed for those students who want to

Table 1: New SCM program in some American universities.

Universities	Location	Course	Beginning year
Bauer School of Business, University of Houston	Houston	SCM, MBA	2011
Rutgers Business School	New Jersey	Bachelor of SCM	2011
Business School, Bryant University	Smithfield, Rhode Island	Bachelor degree and MBA in international SCM	2012
School of Business and Public Administration, Governor State University	University Park, Illinois	SCM MBA online course	2013
Business School, Portland State University	Portland, Oregon	Master of Science in international SCM	2013
Nylie School of Business, Texas Christian University	Fort Worth, Texas	MSc SCM	2013
Marshall School of Business, University of Southern California	Los Angeles	MSc international SCM online course	2013
W. P. Carey School of Business, Arizona State University	Tempe, Arizona	Bachelor of Science in SCM Bachelor of SCM and operations	2014

carry out professional training in related practical work. Both of the directions provide students with a foundation to seek development opportunities in the field of business and SCM. The BBA-SCM project works closely with industrial institutions and enterprises, and it provides students with opportunities for vocational training and professional qualification examinations.

3. The Construction of SCM Programs in China

3.1. SCM Programs Approved to Be Constructed. In 2017, Wuhan College (WHXY), an application-oriented private university in mainland China, applied to the Ministry of Education of China to establish the undergraduate program of "global supply chain and the informationization." After the evaluation of the Teaching Guidance Committee in Higher Educational Institutions of Chinese universities, the Ministry of Education approved the request, which made WHXY the only one institution qualified to open this major. Since then, as a formal undergraduate major, SCM has been listed in the subclass of "logistics management and engineering" in the Catalogue of Undergraduate Majors in Higher Education (CUMHE) and has been given professional code, 120604T. After finishing their four-year studies, the students receive the management degree. From 2018, WHXY began to recruit undergraduate students majoring in SCM, marking the beginning of undergraduate education in SCM in mainland China.

In China, it will be relatively easy for Chinese universities to set up a program when it is included in the CUMHE and has a unique code. This is because the follow-up application process adopts the filing system, and the universities that meet the requirements apply to the Ministry of Education and can be approved after the reviews and records. Many Chinese universities are actively applying for an SCM undergraduate program, especially those that already offer logistics management and engineering. Following to Wuhan College initiative, in 2019 other seven universities, as well as, in 2020, 17 universities, also have been approved by the Ministry of Education to offer the undergraduate SCM program. Therefore, there are in total 25 universities in China that offer this program, as shown in Table 2.

3.2. Analysis of School Types. Universities are mainly classified from two perspectives inside the Chinese classification system: (1) from the perspective of the school running system, it can be divided into three categories: public university, private university, and independent college; (2) from the perspective of research strength, it can be divided into research-oriented universities and application-oriented universities. The 25 universities mentioned in this paper cover five types of two dimensions. Next, it will analyze from these two dimensions.

In terms of the school running system, 4 of the 25 universities are private universities. They are WHXY, XJTLU, BCU, and HXXY, accounting for 16% of the total, while CUC, GCU, and CQYTI are independent colleges, accounting for 12% of all. The rest are public universities, accounting for 72% of all. From this point of view, public universities still account for the main share.

As for research strength, 8 universities are research-oriented universities, and they are CUFE, SMU, SDU, SWUFE, DMU, BTBU, AHNU, and HAUT, accounting for 32% of the 25 universities. And all of them are all public universities. The remaining 17 universities, whether public, private, or independent, are all applied universities, accounting for 68%. It can be seen that the SCM program in China is mainly application-oriented university and covers three different school running systems. Therefore, it is of great significance to focus on application-oriented universities.

3.3. Some Issues at Application-Oriented Universities. At present, there are two dilemmas in developing competencies of SCM students. One dilemma is about training SCM professionals in China, because it mainly relies on postgraduate programs of Management Science and Engineering, as well as, Logistics Engineering, which mainly focused on the mastery and application of students' basic theoretical knowledge and the cultivation of scientific research as well as innovation ability. In this case, students' ability to solve practical problems and their hands-on ability is relatively insufficient, so it is difficult to meet the needs of social application-oriented talents.

Table 2: List of universities that are specialized in SCM.

School name	Year
Wuhan College (WHXY)	2017
Central University of Finance and Economics (CUFE)	2018
Beijing Wuzi University (BWU)	2018
Baoding University (BDU)	2018
Yingkou Institute of Technology (YKU)	2018
Shanghai Maritime University (SMU)	2018
Xi'an Jiaotong-Liverpool University (XJTLU)	2018
Hefei University (HFUU)	2018
Shandong University (SDU)	2019
Southwestern University of Finance and Economics (SWUFE)	2019
Dalian Maritime University (DMU)	2019
Beijing Technology and Business University (BTBU)	2019
Beijing City University (BCU)	2019
Zhejiang Wanli University (ZWU)	2019
Anhui Normal University (AHNU)	2019
Bengbu University (BBC)	2019
Xiamen Huaxia University (HXXY)	2019
Chengyi College of Jimei University (CUC)	2019
Henan University of Technology (HAUT)	2019
Hunan Business University (HUTB)	2019
Guangzhou College of South China University of Technology (GCU)	2019
Chongqing University of Science and Technology (CQUST)	2019
College of Mobile Telecommunications, Chongqing University of Posts and Telecommunications (CQYTI)	2019
Chongqing University of Education (CQUE)	2019
Chengdu University of Information Technology (CUIT)	2019

The second dilemma is that some universities are over emphasis research and neglect practice education. There is a trend that colleges and universities generally attach great importance to the vocational skills training based on logistics management and technology, overemphasizing the cultivation of students' operation skills, while ignoring the mastery of the necessary basic theoretical knowledge, which is similar to the mode of secondary and higher vocational education. As a result, it does not help students' career development after their graduation.

4. Measures

The directions of the above two modes of personnel training are opposite, and it cannot be consistent with the training objectives of application-oriented universities. The cultivation of talents in application-oriented universities should be different from both research universities and vocational education. The graduates should not only master the basic theories, but also the professional skills in the field of SCM, and have strong practical ability. Based on the idea, we have taken the following measures to achieve this goal.

4.1. Ability, Knowledge, and Diathesis of Students

4.1.1. Ability of Students. Through the study of various courses, the graduation of the SCM program should achieve the following expected abilities:

(1) The ability to make correct value judgment and behavior choice from the perspective of Marxism. The ability of thinking, expressing, and writing; the ability of innovation and independent work (A1)

(2) Effective communication, teamwork skills, and basic social skills (A2)

(3) IT ability to quickly access and act on digital data; engage in lifelong learning to meet future career challenges (A3)

(4) Understanding big data processing and analytics; ability to analyze and optimize the supply chain with tools, technologies, and frameworks (A4)

(5) To meet the needs of customers and improve supply chain efficiency, achieve cross-functional and cross-organizational boundary management (A5)

(6) With system thinking and innovative spirit, ability to think and act in different ways to solve problems in an ever-changing environment (A6)

4.1.2. Knowledge of Students. Through the study of various courses in SCM, the graduates should have the following knowledge:

(1) Mastering the true spirit of Marxism and grasping the combining of Marxism and China's reality (K1)

(2) Understand the relevant technical standards, advanced technology, and development trend of SCM (K2)

(3) Have basic knowledge of natural sciences such as humanities and social sciences, computer science, and advanced mathematics (K3)

(4) Master the basic theory and knowledge of economics, management, financial management, accounting, production and operation management, and marketing (K4)

(5) Know well the theory and application method of supply chain planning and design, such as business data analysis, supply chain analysis method, supply chain planning, and simulation (K5)

(6) Master the core theories and application methods of logistics management, procurement and supply management, supply chain strategic management, supply chain finance, supply chain information system, supply chain financial analysis, and performance management (K6)

(7) Familiar with the practice process of proprietary trading and pop operation in Jingdong supply chain management (K7)

4.1.3. Diathesis of Students. The program focuses on cultivating applied talents and their value-added in the future with the concept of "Whole Person Development," and it has four core qualities: ideal ambition, governance capacity, excellent morals and academic skills, and overall situation. After studying professional courses, graduates should have the following 12 diathesis: keep the world in view (D1); social responsibility (D2); lifelong learning (D3); innovation and entrepreneurship ability (D4); leadership (D5); critical thinking (D6); individual self-restraint (D7); noble virtues (D8); professionalism (D9); resolve difficulties (D10); self-esteem and confidence (D11); geniality (D12). The details are as follows:

(1) Have good political quality, ideological and moral quality, cultural quality, physical quality, psychological quality, and the spirit of cooperation (D2, D7, and D12)

(2) Have the ability and attitude of self-reliance and self-improvement, have ideals and aspirations, and have a sense of responsibility (D5, D9, and D11)

(3) Have a sense of social responsibility and critical spirit (D2 and D6)

(4) Have a rigorous and positive attitude at work and attach importance to the awareness of innovation and entrepreneurship (D4 and D5)

(5) Have noble morality, stay in good mental and physical health, and pay attention to scientific spirit with humanistic touch (D8 and D10)

(6) Have a sense of responsibility and develop self-directed learning and lifelong learning (D1 and D3)

4.2. Curriculum System Setting. Table 3 shows the corresponding relationship between ability, knowledge, diathesis, and curriculum [18]. It puts requirement of ability, knowledge, and accomplishment into the specific teaching course, so as to achieve the expected training objectives in these aspects and form a complete curriculum system. Table 4 shows the course credit distribution, and Table 5 shows the practice credit distribution.

As shown in the table, practical credits account for 31.51%. Through open experimental teaching, students can participate in a series of activities such as market analysis, strategy formulation, production organization, overall marketing, and financial settlement, so as to realize the supply chain integrity, understand the interoperability of logistics, capital flow, and information flow in the supply chain, and make them become skilled talents to meet social needs.

4.3. Creating Effective Teaching Materials. The core knowledge system of the SCM program includes supply chain strategic management, supply chain planning and design, and supply chain operation management. The authoritative materials in this field are mainly in Europe and America. "Purchasing and Supply Chain Management" by Lysons and Farrington [19] is the textbook of the Chartered Institute of Procurement and Supply (CIPS) in the UK which comprehensively explains various supply chain-related concepts. Martin [20] introduces the main professional ideas and the development direction of supply chain in "logistics and supply chain management." The famous teaching material of SCM subdivision field is Purchasing and Supply Chain Management [21]. The author integrates many elements into one definition, which is highly professional. And "The Handbook of Logistics and Distribution Management: Understanding the Supply Chain" by Alan is the representative CIPS textbook in warehousing logistics. After actively participating in the discussion of the state education commission and organizing many domestic experts and scholars' symposiums in the field of SCM, this paper discussed and determined the following 10 textbooks, such as "Basis of Supply Chain Management," "Supply Chain Strategic Management," "Supply Chain Risk Management," "Supply Chain Finance," "Supply Chain Planning and Design," "Purchasing and Supply Management," "Jingdong Supply Chain Management Experimental Teaching Guide," "Supply Chain Operation Management," "Supply Chain Case Analysis," and "Supplier Performance and Contract Management."

In order to meet the social needs in the field of supply chain, this series of teaching materials draw lessons from excellent teaching materials' writing ideas and methods in the world and focus on the professional knowledge as well as skills. In addition, the future industry development trend and cutting-edge materials will be shown to students in the form of reading materials. The theoretical knowledge of this teaching materials attaches great importance to the systematicness and foundation, while the skill modules focus on the practicability and effectiveness, especially the application of methods, techniques, charts, and tools. It is organically integrated with a large number of the latest cases for systematic analysis, or to give a large number of calculation examples that are combined with practical application scenarios. In brief, the aim is to emphasize the inspiration and exercise of students' thinking and improve the comprehensive ability of students to solve practical problems.

Table 3: Corresponding relation of knowledge, ability, diathesis, and curriculum.

Expected results / Course	Knowledge							Ability						Diathesis											
	K1	K2	K3	K4	K5	K6	K7	A1	A2	A3	A4	A5	A6	D1	D2	D3	D4	D5	D6	D7	D8	D9	D10	D11	D12
Basic Principle of Marxism	●							●								●			●						
Mao Zedong Thought and the theoretical system of socialism with Chinese characteristics	●							●						●	●								●		
Ideological and moral cultivation and legal basis	●							●												●	●				
Outline of modern Chinese history	●							●							●										
College Writing		●							●													●			
Psychology and life	●							●												●					●
College English (1–4)		●							●													●		●	
College physical education (1–4)																				●			●	●	
Situation and policy (1–4)	●							●						●	●				●						
Fundamentals of computer application		●							●							●						●			
Career planning	●							●								●	●							●	●
employment guidance	●							●									●			●				●	

Expected results / Course	Knowledge							Ability						Diathesis											
	K1	K2	K3	K4	K5	K6	K7	A1	A2	A3	A4	A5	A6	D1	D2	D3	D4	D5	D6	D7	D8	D9	D10	D11	D12
Calculus (1)		●								●					●				●						
Calculus (2)		●								●					●				●						
Linear algebra		●								●					●				●						
Probability and statistics			●							●					●				●						
Database application			●							●					●				●						
Principles of economics				●								●			●					●					●
management				●								●					●	●							
Marketing			●									●						●				●			
Principles of accounting				●								●						●				●		●	
Financial management				●											●				●						
Production and operation management						●						●	●					●				●	●		
Logistics management						●					●					●			●						
Operations research				●						●							●	●							
Procurement and supply management						●						●						●	●						

Table 3: Continued.

Expected results / Course	Knowledge							Ability						Diathesis											
	K1	K2	K3	K4	K5	K6	K7	A1	A2	A3	A4	A5	A6	D1	D2	D3	D4	D5	D6	D7	D8	D9	D10	D11	D12
Introduction to supply chain management						●						●					●	●							
Strategic management of supply chain				●				●	●									●				●		●	
Financial analysis and performance management of supply chain						●						●						●	●						
Supply chain finance					●							●					●	●							
Teaching module of Jingdong supply chain management							●					●	●					●				●			●
Business data analysis					●						●	●					●	●							
Supply chain information system						●					●	●					●	●							
Business negotiation				●					●							●					●				●
Supply chain analysis method			●								●						●	●							
Supply chain case study		●										●										●		●	
Supplier performance and contract management						●						●			●					●					●
International business environment				●									●	●		●									
Data mining and analysis			●		●				●	●							●	●							
Business process reengineering and change management					●							●	●				●	●							
International logistics						●						●						●				●		●	
Introduction to e-commerce				●								●					●	●							
Big data visualization					●					●	●	●							●				●		
Market Research and prediction				●					●	●							●	●							
Enterprise tax and practice				●				●				●						●				●		●	
Graduation practice							●				●			●		●									
Graduation thesis (design)							●					●		●		●									

Table 4: Credit distribution.

Course category			Class hour	Proportion of total class hours (%)	
Class instructions	Compulsory course	General education curriculum	44	26.67	76.98
		Basic courses	33	20.00	
		Professional courses	39	23.64	
		Modular practice course	11	6.67	
	Optional course	General education curriculum	10	6.06	23.02
		Professional courses	14	8.48	
		Modular practice course	4	2.42	
		Whole person development education	10	6.06	
Total			**165**		100

Table 5: Practice credit distribution.

Category	Credits	Proportion of total credits (%)
Independent setting experiment	3	1.2
Modular practice course	12	727
Whole person development education	10	606
Practice and experiment in class	27	1636
Total	**52**	**3151**

4.4. Teaching Method

4.4.1. Comprehensive Application of Different Teaching Methods. Teachers should focus on using different teaching methods, widening the breadth of knowledge and classroom space, to improve students' class participation. The teaching methods that can be used are case studies, game-based learning, watching videos, and enterprise training. The case study requires teachers to provide related cases for students and lead them to analyze and solve the practical problems of the enterprise by using the knowledge they have learned; game-based learning is a teaching method that allows teachers to design a series of attractive scenarios for the students as a form of learning; in the enterprise training method, teachers always organize students to study or research in enterprises, so that students can deepen their understanding of various theoretical knowledge. In brief, during the teaching, the teacher mobilizes and stimulates the students' learning interest, enthusiasm, and initiative fully by adopting variety of teaching methods.

4.4.2. Construction of Training Base. Teachers should realize the importance of practice teaching in the course of supply chain management. An important evaluation standard of high-quality talents is practical operation ability; in other words, students need to quickly adapt to the needs of work and apply theoretical knowledge to practical activities, which is also the quality of applied talents. In order to enable students to adapt to the requirements of the job as soon as possible, universities should set up relevant training bases for supply chain management and provide a good environment for the growth of applied talents. For example, schools can sign student training agreements with supermarkets, high-quality logistics enterprises, and manufacturing enterprises. Through effective communication between schools and enterprises, students can get more practical learning.

4.4.3. Reform of Student Assessment Method. Different assessment methods of teaching effect need to be adopted. Universities should reform the traditional way of assessing students' performance in the form of written examination, and teachers should pay more attention to the assessment of professional ability. For example, students can be assessed through the group work, case lectures, class discussions, classroom performance, and homework. Teachers can also combine theory examination with practical training skill assessment according to the content of training report. The students trained in this way will not only master the theoretical knowledge but also pay more attention to the cultivation of practical ability.

5. Conclusion

Supply chain innovation and application has reached the national strategic level for China. In this case, Chinese government departments, enterprises, and industries attach great importance to SCM, which constitutes a huge demand for SCM application-oriented talents. Therefore, Chinese universities should comply with the trend to build the SCM program and especially pay attention to the characteristics of application-oriented talents. At present, many application-oriented universities have set up the SCM undergraduate program. However, this is a brand-new major, and there are still many issues to be explored due to the lack of replicable experience. Through the research, this paper attempts to put forward some reasonable suggestions.

This paper introduces the practical background of the SCM undergraduate program in Chinese universities, analyzes the necessity and feasibility of setting up this program, and discusses the present SCM programs in Chinese universities. Based on practical experience, it gives a series of corresponding construction measures, which is of great significance for the development of SCM program in China's application-oriented universities.

Due to the limited time of setting up this program in China and our insufficient experience, there are some limitations in this study. For example, whether the teaching materials can meet the needs of students and whether graduates can meet the social requirements need to be verified. In the future, the research can be carried out from the following aspects: (1) research on teaching methods for application-oriented SCM undergraduate talents training; (2) research on teaching applicability of application-oriented SCM teaching materials; (3) empirical research on the satisfaction of applied SCM talents to social requirements.

Data Availability

The data used to support the findings of the study are available from the corresponding author upon request.

Conflicts of Interest

The authors declare that they have no conflicts of interest.

Acknowledgments

This study was supported by the Research and Innovation Platform Construction Plan of Wuhan College (grant no. KYP201901), National Natural Science Foundation of China (grant no. 71471073), and Fundamental Research Funds for the Central Universities (grant no. CCNU19TS078).

References

[1] S. P. Robbins, *Organiazation Behavior*, Prentice-Hall International, Inc, London, UK, 7 edition, 1997.

[2] A. Greiner, "On the dynamics of an endogenous with Learning by doing," *Economic Theory*, vol. 21, no. 1, pp. 201–214, 2003.

[3] I. Bilgin, Y. Karakuyu, and Y. Ay, "The effects of project based learning on undergraduate students' achievement and self-efficacy beliefs towards science teaching," *Eurasia Journal of Mathematics, Science & Technology Education*, vol. 11, no. 3, pp. 469–477, 2015.

[4] H. Rogers and C. Braziotis, "Current issues in teaching logistics management," in *Proceedings of the 4th International Conference LDIC*, pp. 553–563, Bremen, Germany, 2014.

[5] M.-L. Chuang, "A web-based simulation game for teaching supply chain management," *Management Teaching Review*, vol. 5, no. 3, p. 265, 2019.

[6] K. Nguyen, R. DeMonbrun, M. Borrego et al., "The variation of nontraditional teaching methods across 17 undergraduate engineering classrooms," in *Proceedings of the 2017 ASEE Annual Conference & Exposition*, Columbus, OH, USA, June 2017.

[7] R. W. Elliott and V. O. Paton, "U.S. higher education reform: Origins and impact of student curricular choice," *International Journal of Educational Development*, vol. 61, no. 61, pp. 1–4, 2018.

[8] K. Cottrill, *Are You Prepared for the Supply Chain Talent Crisis?*, MIT Center for Transportation Logistics, Cambridge, MA, USA, 2010.

[9] MHI, *The 2016 MHI Annual Industry Report*, MHI Report, 2017, https://www.mhi.org/publications/report.

[10] M. S. Sodhi, B.-G. Son, and C. S. Tang, "ASP, the art and science of practice: what employers demand from applicants for MBA-level supply chain jobs and the coverage of supply chain topics in MBA courses," *Interfaces*, vol. 38, no. 6, pp. 469–484, 2008.

[11] E. Stuba, S. Curkovic, and B. Wagner, "The benefits of simulated coursework in Western Michigan University's undergraduate supply chain program," *Creative Education*, vol. 08, no. 12, pp. 1821–1832, 2017.

[12] S. Curkovic and N. Fernandez, "Closing the gap in undergraduate supply chain education through live experiential learning," *American Journal of Industrial and Business Management*, vol. 6, no. 6, pp. 697–708, 2016.

[13] People's Daily: China becomes center of global supply chain [DB/OL], 2017, http://english.www.gov.cn/news/top_news/2017/02/10/content_281475564088064.htm.

[14] O. Blanchard, *Light of the Elections: Recession, Expansion, and Inequality*, Peterson Institute for International Economics, Washington, DC, USA, 2016.

[15] IHS Markit, "Survey on New Trends of Global Procurement," IHS Markit, London, UK, 2017.

[16] CFLP and CLA, *China Logistics Development Report*, China Fortune Publishing House, Beijing, China, 2016.

[17] Qianzhan Industry Research Institute, *Report on China Supply Chain Management Service Industry*, FORWARD Business Information Co., Ltd., New Taipei City, Taiwan, 2016, in Chinese.

[18] WHXY Talent, *Training Program of Supply Chain Management*, Wuhan College, Wuhan, China, 2019, in Chinese.

[19] K. Lysons and B. Farrington, *Purchasing and Supply Chain Management*, Trans-Atlantic Publications, Philadelphia, PA, USA, 2004.

[20] C. Martin, *Logistics & Supply Chain Management*, Pearson Education, Edinburgh, Scotland, 3 edition, 1998.

[21] J. V. W. Arjan, *Purchasing and Supply Chain Management*, Cengage Learning, London, UK, 7 edition, 2009.

Hindawi
Discrete Dynamics in Nature and Society
Volume 2021, Article ID 6669567, 10 pages
https://doi.org/10.1155/2021/6669567

Research Article

Vehicle Routing and Scheduling of Flex-Route Transit under a Dynamic Operating Environment

Yue Zheng,[1] **Liangpeng Gao**,[2] **and Wenquan Li**[3]

[1]*School of Modern Posts & Institute of Modern Posts, Nanjing University of Posts and Telecommunications, Nanjing, China*
[2]*Institute of Transportation, Fujian University of Technology, Fuzhou, China*
[3]*School of Transportation, Southeast University, Nanjing, China*

Correspondence should be addressed to Liangpeng Gao; liangpenggao.acad@gmail.com

Received 7 December 2020; Revised 20 December 2020; Accepted 31 December 2020; Published 18 January 2021

Academic Editor: Tingsong Wang

To improve the reliability, responsiveness, and productivity of the flex-route transit service, this paper investigates the vehicle scheduling and routing problem under a dynamic operating environment. First, we discuss the new operating polices after the introduction of intelligent transportation systems (ITSs), including automatic vehicle location (AVL) system, mobile data terminal (MDT), and computer-aided dispatch (CAD) system. Second, a mixed integer programming (MIP) formulation is employed to solve the offline routing problem. Third, an online scheduling scheme is presented to tackle different dynamic events, such as dynamic requests, travel time fluctuations, cancellations of requests, and customer no-shows. Finally, simulation experiments based on a real-life flex-route transit service are conducted to assess the influence of different dynamic events. The results demonstrate that the proposed scheduling scheme is reliable for coping with various dynamic events, and our findings can be used to guide the policy making of flex-route transit services.

1. Introduction

Currently, public transit systems play an indispensable role in people's daily life. High volume transit modes such as subway and conventional bus lines can provide convenient, rapid, and efficient service in high-density urban areas. However, in many low-density suburban and rural areas, these traditional fixed-route transit services are considered to be inefficient and inconvenient due to the rigid itineraries and infrequent intervals. Unsurprisingly, the dependency on private cars is reinforced, which poses severe challenges to environmental sustainability and social equity.

To address these challenges, many efforts have been focused on providing new mobility solutions in these low demand regions (e.g., sprawling suburban areas) to not only meet the diverse demands of passengers but also improve the quality of service. Among the many types of flexible transit services, flex-route transit (also referred to as route deviation [1]), mobility allowance shuttle transit [2], and demand adaptive transit system [3]) is the most popular operating polic [4]. This innovative service is a hybrid public transportation mode that combines the low-cost operability of fixed-route transit with the flexibility of demand-responsive transit. Similar to the conventional fixed-route service, flex-route transit has a base route with several mandatory checkpoints located in high-density demand zones. Typically, these checkpoints are assigned with fixed departure times to serve regular customers and are synchronized with other public transportation lines. On the other hand, flex-route transit shares some common features with demand-responsive transit because the vehicles are allowed to deviate from the base route for a certain distance (usually between 0.25 and 0.75 miles) to serve curb-to-curb requests. Practical operation experiences have shown that ridership and passenger satisfaction remarkably increased after implementing flex-route transit service [5, 6].

In practice, the passengers who need deviation service are required to make reservations at least two hours ahead of time. Therefore, most studies focus on fully static systems in

which all the requests are known in advance and all the unforeseeable events that may happen during the flex-route transit operation are neglected [7–11]. However, real-life situations could be more complex, and the distributions of some accidents cannot be clearly identified. The predetermined schedule is likely to be modified in real time due to dynamic events such as travel time fluctuations [12–14], cancellations of requests, customer no-shows [15, 16], and dynamic requests [17, 18]. All these unpredictable events severely influence the on-time performance of the flex-route transit and inevitably degrade the system reliability [19]. That may be the one reason why the application of this innovative transit service is quite limited and far behind prior expectations. Therefore, a flexible and efficient real-time scheduling scheme is needed to tackle these practical problems.

Recent developments in intelligent transportation system (ITS) technologies, such as automatic vehicle location (AVL) systems and digital communications, provide solid technical support for real-time fleet management. In particular, these technologies allow a dispatching center to constantly track the real-time positions of the vehicles, traffic information, and up-to-date information about customer requests. In addition, advances in computing power have accelerated the data-processing abilities so that any schedule modifications can be processed and transmitted to the drivers in real time. With the help of these ITS technologies, the dispatcher is now able to quickly track these dynamic events and adjust the schedule of the flex-route transit in real time. A case study on real-life ITS-assisted flex-route transit [5, 20] showed that the schedule reliability was greatly enhanced after the implementation of several ITS projects.

In this paper, we study the vehicle routing and scheduling problem of flex-route transit under a dynamic operation environment. As an extension of our previous research [21], an online scheduling model is developed to deal with the various dynamic events, including customer travel time fluctuations, no-shows, cancellations, and dynamic requests. To the best of our knowledge, the dynamic scheduling problem of flex-route transit has not been examined in past studies. The structure of this paper is organized as follows. The system structure and operating policy of the flex-route transit system are described in detail in Section 2. Then, an offline routing mode and an online scheduling model are proposed in Section 3. In Section 4, we evaluate the system performance under different dynamic events through simulation experiments. A summary of the findings and future works is presented in Section 5.

2. System Description

2.1. Service Area and Demand. To simplify the modeling process, the flex-route transit system is assumed to operate within a rectangular service area of width W and length L (see Figure 1). All the reserved pick-up/drop-off points should be located within the scope of the service area. There are C checkpoints along the base route (denoted by $c = 1, 2, \ldots, C-1, C$), which are located at major connection points or high-density demand zones (see Figure 1). The departure times of the checkpoints are fixed, which can be regarded as hard constraints for vehicle operations.

The flex-route transit service can respond to four different types of requests: type I—the pick-up and drop-off points are both at checkpoints; type II—the pick-up point is at a checkpoint, but the drop-off point is not at a checkpoint; type III—the pick-up point is not at a checkpoint, but the drop-off point is at a checkpoint; type IV—neither the pick-up point nor the drop-off point is at a checkpoint. Type I requests use flex-route transit as a traditional fixed-route transit service. Therefore, they do not need to book the service in advance. The other three types of requests are required to make a reservation by calling or using the Internet to schedule their non-checkpoint stops.

To accommodate possible deviation requests, the scheduled running time between adjacent checkpoints must be greater than the direct running time. The difference between them is called slack time. In flex-route transit, the slack time allocated for the deviation service in each route segment is predetermined based on the expected demand level. If the slack time between the checkpoints is not used up, the vehicles must wait and experience additional idle time until the scheduled departure time. In contrast, when the predetermined slack time is not sufficient to accommodate the unexpected higher demand, some passengers may be rejected (see Figure 1).

2.2. Operating Policy. In real-life operation, due to the low demand level of suburban areas, the headways of flex-route transit systems are usually more than half an hour [1]. Hence, unlike other demand-responsive shared-ride systems [22, 23], passengers are more likely to reserve a specific trip based on the timetables rather than specify a pick-up time window. As shown in Figure 2, each passenger (except type I) needs to specify a desired trip, a pick-up location, and a drop-off location with the reservation center before the reservation deadline. The reservation center provides the connection between the customers and the dispatching center. It is responsible for recording the demand information and dealing with some dynamic events such as service cancellations, updating demand information, and dynamic requests. Generally, the reservation should be made between two days beforehand to one hour earlier than the departure time of the trip. The requests are processed on a first-come, first-serve basis. Once the request is received, the dispatching center immediately informs the customer whether or not the request can be accommodated. After the reservation deadline, all accepted passenger requests collected for a given trip are used as inputs for the offline routing model to calculate the optimal routing plan. After finishing the calculation process, the planned pick-up times are sent to the accepted customers before the trip begins.

There are two common categories of data that need to be treated differently. The first category of data, called static data, consists of data that are relatively stable and do not need to be updated frequently. Examples include the road

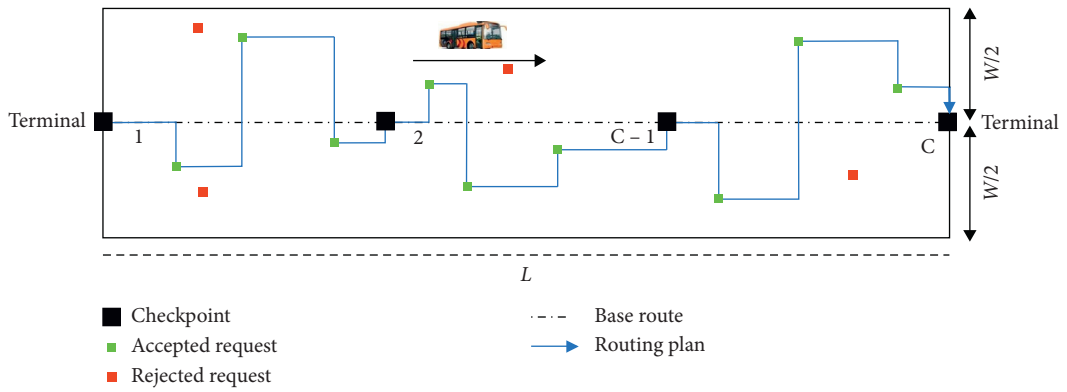

Figure 1: Flex-route transit service.

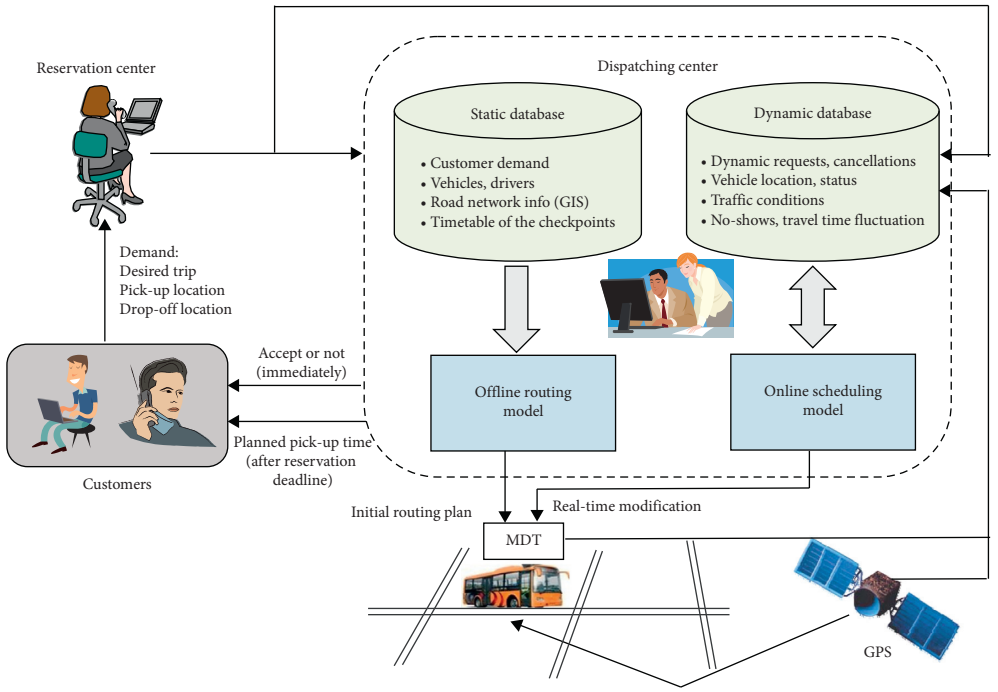

Figure 2: System structure of the flex-route transit system.

network topology, customer demand, and information of fleet, drivers, and timetables. Before the actual operation of the service, the initial routing plan of the vehicle is calculated by the offline routing model using the static database. The second category is a dynamic database that includes vehicle location, traffic conditions, and dynamic events. During the operation, the AVL system provides the dispatcher with up-to-date location information for each vehicle via the global positioning system (GPS) equipment. The dispatcher continuously monitors any operational changes in the system and updates them in real time. Once a dynamic event occurs, the dispatcher calls on the online scheduling model to reschedule the planned route, and the modified routing plan is transmitted to the drivers through a mobile data terminal (MDT). Both the offline and online models can be calculated using the computer-aided dispatch (CAD) system installed in the dispatching center to obtain the initial routing plans and responses to dynamic events in real time.

3. Vehicle Scheduling Model

3.1. Offline Routing Model. A mixed integer programming (MIP) formulation is proposed for the offline routing problem. We define a directed graph $G = (N, A, T)$ to describe the vehicle routing network, where N represents all the stops for a trip, $A = N^2$ is the set of arcs, and $T = (t_{ij})$ is the matrix of the travel time associated with A. The objective of the problem is to determine the optimal path without violating the constraints.

The system parameters are defined as follows:

C = number of checkpoints

Q = maximum vehicle capacity

$N_0 = \{1, 2, \ldots, C\}$ = set of stops at the checkpoints

δ_i = scheduled departure time of checkpoint i $\forall i \in N_0$

$K = K_{\text{Type I}} \cup K_{\text{Type II}} \cup K_{\text{Type III}} \cup K_{\text{Type IV}}$ = set of all accepted requests

$TS = C + |K_{\text{Type II}}| + |K_{\text{Type III}}| + 2 \times |K_{\text{Type IV}}|$ = total number of visiting stops in a trip

$N_n = \{C+1, \ldots, TS\}$ = set of non-checkpoint stops reserved by passengers

$N = N_0 \cup N_n$ = set of all stops

A = set of all arcs in the network

q_i = number of passengers boarding ($q_i > 0$) or alighting ($q_i < 0$) at stop i

t_{ij} = rectilinear travel time from node i to node j $\forall i, j \in N$

$dwell\_n$ = dwelling time at every non-checkpoint stop

$dwell\_c = dwell\_n$ dwelling time at every checkpoint

$ps(k)$ = pick-up stop of each request k $\forall k \in K$

$ds(k)$ = drop-off stop of each request k $\forall k \in K$

The decision variables of the model are as follows:

$x_{ij} = \{0, 1\}$ $\forall (i, j) \in A$ = indicating an arc (i, j) is chosen ($x_{ij} = 1$) or not ($x_{ij} = 0$)

t_dep_i = departure time of stop i, $i = 1, 2, \ldots, TS$

t_arr_i = arrival time of stop i, $i = 1, 2, \ldots, TS$

w_i = vehicle's passenger load at node i, $i = 1, 2, \ldots, TS$

p_k = pick-up time of request k $\forall k \in K$

d_k = drop-off time of request k $\forall k \in K$

Given the above definitions, the problem can be formulated as a mixed integer linear program in which ω_R and ω_V are the costs of the passengers' in-vehicle time and the operating cost of the service vehicle.

$$\min \omega_R \left(\sum_{k \in K} (d_k - p_k) \right) + \omega_V \left(\sum_{i,j \in A} t_{ij} x_{i,j} \right), \tag{1}$$

subject to

$$\sum_{i=1}^{TS} x_{1i} = 1, \qquad \sum_{i=1}^{TS} x_{i1} = 0, \tag{2}$$

$$\sum_{i=1}^{TS} x_{Ci} = 0, \qquad \sum_{i=1}^{TS} x_{iC} = 1, \tag{3}$$

$$\sum_{j=1}^{TS} x_{ji} = \sum_{j=1}^{TS} x_{ij} = 1, \quad i = N/\{1, C\}, \tag{4}$$

$$x_{ii} = 0, \quad \forall i \in N, \tag{5}$$

$$\sum_{i,j \in V} x_{ij} \le |V| - 1, \quad \forall V \subset N, \tag{6}$$

$$t\_dep_i = \delta_i, \quad \forall i \in N_0, \tag{7}$$

$$w_1 = q_1, \tag{8}$$

$$w_j \ge w_i + x_{ij} q_j - MQ\left(1 - x_{ij}\right), \quad \forall (i, j) = A, \tag{9}$$

$$t\_arr_j \ge t\_dep_i + x_{ij} t_{ij} - MT\left(1 - x_{ij}\right), \quad \forall (i, j) = A, \tag{10}$$

$$t\_dep_i = t\_arr_i + dwell\_n, \quad \forall i \in N_n, \tag{11}$$

$$t\_dep_i \ge t\_arr_i + dwell\_c, \quad \forall i \in N_0/\{1\}, \tag{12}$$

$$0 \le w_i \le Q, \quad \forall i \in N, \tag{13}$$

$$p_k = t\_dep_{ps(k)}, \quad \forall k \in K, \tag{14}$$

$$d_k = t\_arr_{ds(k)}, \quad \forall k \in K, \tag{15}$$

$$d_k > p_k, \quad \forall k \in K. \tag{16}$$

The objective function (1) minimizes the total cost of two factors, namely, the in-vehicle time cost of all passengers and the driving cost of the vehicle; this definition incorporates the costs associated with the transit operators as well as the service quality of the system. Constraints (2) and (3) address the special case of the incoming and outgoing degree of the first stop and last stop, respectively. For the first terminal checkpoint, there is no incoming arc and one outgoing arc; for the last terminal checkpoint, only one incoming arc is allowed, and there is no outgoing arc. For other intermediate nodes, constraint (4) indicates that the incoming/outgoing degree of each node is equal to 1. Constraint (5) forbids the self-connection of each node. Constraint (6) ensures that no illegal subtours are contained in the optimal solution by eliminating all the loops that make the other points disjointed. Constraint (7) guarantees that the scheduled departure times of the checkpoints are fixed. Constraint (8) ensures that for the first terminal checkpoint, the vehicle's passenger load is equal to the number of boarding passengers. Constraint (9) defines the vehicle's passenger load at each node as the passenger occupancy at the preceding node plus or minus the number of passengers boarding or alighting (depending on the sign of q_j). Constraint (10) defines that for any two nodes that have a connection, the arrival time of node j should be no later than

the departure time of node i plus the travel time between the two nodes. We let MQ and MT be a sufficiently large number to ensure that constraints (9) and (10) are irrelevant when there is no connection between the two nodes. Constraint (11) makes sure that the departure time of every non-checkpoint stop is always equal to the arrival time plus the dwelling time. Since there may be some idle time at each checkpoint, constraint (12) guarantees that the departure time of the checkpoint is always later than the arrival time plus the dwelling time. Constraint (13) ensures that the vehicle capacity is not violated during the operation. Constraint (14) establishes the equality for each request between the pick-up time and the departure time of its corresponding node. Similarly, constraint (15) establishes for each request the equality between the drop-off time and the arrival time of its corresponding node. Constraint (16) ensures that the pick-up time of each request should be scheduled before the corresponding drop-off time.

3.2. Dynamic Events. In reality, some dynamic events may happen during the operation of the flex-route transit service. In our study, we consider four kinds of uncertain events which are summarized as follows. Other rare events, such as vehicle breakdown or traffic jam, are not considered in our research.

(1) Dynamic requests: customers call for service after the reservation deadline of the trip. The pick-up or drop-off points are randomly distributed over the service area.

(2) No-shows: customers do not show up at their pick-up points.

(3) Cancellations: customers cancel requests before or during their reserved trip.

(4) Travel time fluctuation: the travel time between two sites varies due to the changing travel speed.

3.3. Online Scheduling Model. Recent advances in information and communication have facilitated real-time fleet management. In our assumed flex-route transit system, the real-time location information for each vehicle can be provided by the AVL system. The up-to-date status of customers (such as before service time, on board, serviced, and no-show) can be transmitted through the MDT. Customers' dynamic requests and cancellations can also be accommodated by the reservation center via telephone or through the Internet. The offline and online models can be executed using the CAD system. With these technologies, the vehicle routing and scheduling can now be performed dynamically, introducing greater opportunities to reduce operational costs and improve customer service.

Figure 3 shows the framework of the online scheduling model. In this model, all the events are also sent to the event queue and are processed based on the first-come, first-serve policy. During the operation, the dispatcher continuously fetches one event from the event queue and processes it based on the event type. After finishing the online calculation, the dispatcher sends the updated routing plan to the driver through the MDT and informs the reservation center on how to respond to the customers. The specific scheduling schemes for the corresponding dynamic events are described in the following sections.

3.3.1. Dynamic Request Events. In a partially dynamic environment, a number of real-time requests, which are not known to the dispatcher at the time of planning, are revealed gradually after the reservation deadline. All the dynamic requests are assumed to be immediate requests that wish to be served instantly. To accommodate these dynamic requests, an insertion heuristic algorithm was adopted to insert these requests into the initial routing plan determined by the offline routing model. The dynamic requests are processed in time order, and the routing plan is updated immediately when a dynamic request is accepted.

Specifically, once a dynamic request is received, the algorithm first checks the feasibility of the insertion. Assume that the requested new stop q is located between checkpoints n and $n+1$. The algorithm tries to insert the stop into any two consecutive stops a and b that are scheduled within checkpoint n and $n+1$. If any of these insertions can meet the slack time constraints and vehicle capacity constraints mentioned in equations (7) and (13), the requested new stop is accepted; otherwise, the requested new stop is rejected. It is worth mentioning that type IV passengers need to check the feasibility of both the pick-up point and drop-off point, and only when both stops are inserted successfully can the request be accepted. Since there is likely to be more than one feasible position, the next step is to determine the best insertion position with the minimum incremental costs. The incremental costs of inserting the new stop q between any two consecutive stops a and b can be calculated by the following equation:

$$\Delta F = \omega_V \times \Delta t + \omega_R \times \Delta R + \omega_A \times \Delta A, \tag{17}$$

where Δt is the extra travel time of the vehicle after the insertion (calculated by equation (18)), ΔR is the sum of the extra in-vehicle time of the passengers caused by the insertion, ΔA is the sum of the extra waiting time of the passengers caused by the insertion, and ω_V, ω_R, and ω_A are the corresponding weights.

$$\Delta t = t_{a,q} + t_{q,b} - t_{a,b} + dwell\_n. \tag{18}$$

Once the best insertion with the minimum incremental costs is determined, the new stop is inserted into the route, and the updated vehicle routing plan and schedule will be sent to the driver immediately. Meanwhile, the decision regarding the acceptance and the scheduled pick-up time of the dynamic request is also sent to the customer.

3.3.2. No-Show Events. In practice, some customers may be absent without giving any advanced notice when a vehicle arrives at their reserved pick-up points. A previous study [5] indicated that customer no-shows are frequently observed during the actual operation of flex-route transit services. Therefore, it is necessary to consider no-show events and update the route dynamically.

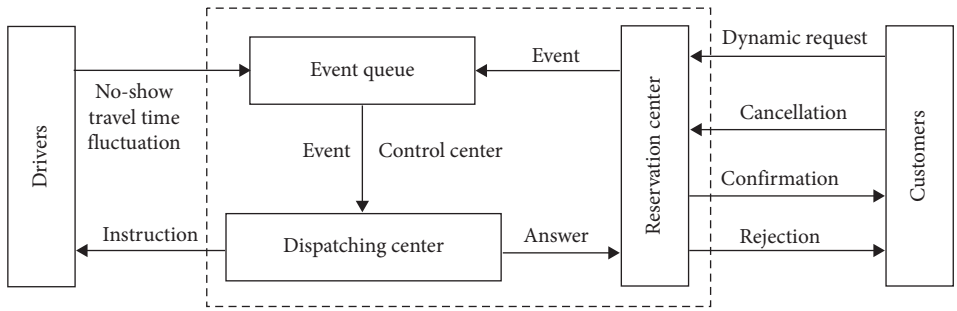

Figure 3: The framework of online scheduling model.

During the operation of the flex-route transit service, once a no-show event is detected, the driver sends a data message (for example: "no-show") to the dispatching center through the MDT. The dispatcher checks the drop-off point of the absent customer in the route. If the drop-off point is at a checkpoint (i.e., type III passengers), the current routing plan remains unchanged. Otherwise, the drop-off point is deleted in the current routing plan without changing the visiting sequence of the other stops. After determining the visiting sequence, the next step is to update the time schedule of the vehicle. More specifically, the schedule of stops before the deleted drop-off point remains unchanged. For the stops after the deleted drop-off point, if it is a drop-off point, the vehicle departs immediately after the customer is dropped off. If it is a pick-up point, the vehicle has to wait at the stop until the planned pick-up time of the customer. This scheme can save the unnecessary travel distance of the vehicle and the in-vehicle time of the passengers onboard. Meanwhile, the on-time performance of the service is also guaranteed.

3.3.3. Cancellation Events. There are two kinds of cancellations that should be treated differently. If the customer cancels the trip before the reservation deadline of the trip, the request is removed from the static database, and the optimal initial routing plan is calculated using the rest of the demand. In contrast, if the cancellation is made after the reservation deadline (i.e., a real-time cancellation), it may affect the scheduling and routing of the vehicle. In particular, once a cancellation event is received by the reservation center, the dispatcher first removes the non-checkpoint pick-up and drop-off stops in the initial routing plan and then reconnects the remaining stops with the shortest distance. Similar to the scheme of no-show events, the vehicle departs immediately after serving the drop-off passengers and waits until the previously notified pick-up times at the pick-up points.

3.3.4. Travel Time Fluctuation. In the offline routing model, the travel time between any two stops is calculated based on the location coordinates, average travel speed, and road networks. However, travel speeds are rarely constant in reality but are instead subject to many stochastic variations, such as random fluctuations in travel demands, frequent interruptions of traffic controls, and unpredictable occurrences of traffic incidents. These travel time fluctuations inevitably affect the on-time performance of the flex-route transit system, but it can only be known to the dispatching center when the vehicle arrives at the stops. In our study, we assume that the vehicles are operated based on the following schemes.

(i) For the non-checkpoint pick-up points, if the vehicle arrives earlier than expected, the vehicle has to wait for the customers until the planned arrive time. If the vehicle arrives late, passengers would experience a waiting time and the vehicle would depart immediately after picking them up.

(ii) For the non-checkpoint drop-off points, regardless of whether running ahead of or behind schedule, the vehicle departs immediately after dropping off the passengers.

(iii) For the checkpoints, if the vehicle arrives early, it needs to spend additional idle time at the checkpoint until the scheduled departure time. If the vehicle arrives late, passengers who need to get off may experience excessive in-vehicle time and the passengers waiting at the checkpoints also experience a delay. After serving the passengers, the vehicle departs immediately.

Although excessive in-vehicle time and waiting time due to travel time fluctuations have a negative effect on perceived service quality, a workable balance between on-time performance and serving route-deviation requests is difficult to achieve. In our study, the service time fluctuation is not taken into account because it can be considered as part of the travel time between two stops.

4. Result Analysis

4.1. Simulation Settings. In this section, numerical experiments are conducted based on the MTA Line 646, which operates under a flex-route policy in Los Angeles County. This line has been widely regarded as a benchmark and testbed of flex-route transit for comparing and evaluating different system settings, models, and solution methods [2, 8, 10, 11, 24, 25]. The default parameter values are shown in Table 1. Line 646 has three checkpoints that are evenly distributed along the base route. A constant vehicle speed of 25 miles/h and Manhattan distances are assumed in calculating the travel times between the stops. The

Table 1: Parameter values.

Parameter	Value
L	10 miles
W	1 miles
C	3
θ	12 passenger/trip
V_b	25 miles/h
ω_V	\$60/vehicle/h
ω_R	\$20/passenger/h
ω_A	\$15/passenger/h
ω_I	\$30/passenger/h
$dwell\_n$	0.3 min
$dwell\_c$	1 min
T_r	40 min
$\eta_1/\eta_2/\eta_3/\eta_4$	0.1/0.4/0.4/0.1

operating cost of the service vehicles and the values of the customer cost indicators are set based on the National Database of the US (2010) and [26]. The cost of the idle time at checkpoints is assumed to be twice the cost of the waiting time. The system is designed with an expected demand level of $\theta = 12$ passengers/trip. For each trip, the requests are generated based on the expected demand level and predefined type proportion. The non-checkpoint pick-up or drop-off points are uniformly distributed throughout the service area. In the simulation model, each request is assigned a sequence number in each trip to indicate the order of the reservation time. Based on the theoretical model proposed in [11], we can derive the single-trip time of the flex-route transit T_r as 40 min. Therefore, the scheduled departure times of the three checkpoints are 0, 20, and 40 min.

4.2. Simulation Results. To average out the effects of randomness in the request generation, 1000 replications of a single-trip operation were run to provide statistical estimates of the system performance for each kind of dynamic event. The offline routing model was solved by GRUOBI (version 9.0) through the YALMIP platform to achieve the optimal results [27].

The system performance of the flex-route transit service is evaluated using the following indicators: (1) the riding time (R), i.e., the average riding time per passenger, including the vehicle running time and service time at each stop (also equal to the in-vehicle time minus the idle time); (2) the waiting time (A), i.e., the average waiting time per passenger at stops; (3) the idle time (I), i.e., the extra waiting time on-board per passenger if the vehicle arrives before the scheduled departure times; (4) the rejection rate (Rej), i.e., the fraction of passengers rejected by the system; (5) operating cost (O_p), i.e., the operating cost per passenger for a trip (it can be calculated by equation (19), where T is the average operation time in one trip and θ_{accept} is the average number of accepted passengers per trip); and (6) system cost (F), i.e., the sum of the operating cost per customer and the average customer cost, which can be calculated by equation (20).

$$O_p = \frac{\omega_V \times T}{\theta_{\text{accept}}}, \tag{19}$$

$$F = O_p + \omega_R \times R + \omega_A \times A + \omega_I \times I. \tag{20}$$

4.2.1. Dynamic Requests. To explore the effect of dynamic requests on the operating efficiency, the degree of dynamism (DOD) is used as an index in our experiments. The degree of dynamism is defined as the ratio between the number of dynamic requests N_d and the total number of requests N_{tot}:

$$\text{DOD} = \frac{N_d}{N_{\text{tot}}}. \tag{21}$$

For a fixed number of total requests received per trip, we vary the DOD from 0% (pure static scenario) to 100% (pure dynamic scenario) to generate different numbers of static and dynamic requests. The simulation results in Table 2 illustrate that with the increasing DOD, the riding time R decreases from 15.76 min to 15.60 min and then stabilizes after DOD = 75%. This trend is mainly caused by the decreased number of accepted passengers and the fewer detours that are taken by the vehicles. For the same reason, the idle time I is also considerably increased. In contrast, the waiting time A increases dramatically with the increasing DOD. This is because in scenarios with a high DOD, the dynamic requests may be frequently inserted before the prebooking requests or even before some dynamic requests that have already received the scheduled pick-up time. This unexpected delay inevitably deteriorates the reliability of the service and degrades the service level of flex-route transit systems. It is interesting to see that the rejection rate first experiences a gradual increase and then deceases after DOD is higher than 50%. This finding is not in accord with our common intuition that "better routing can be achieved when more information is known." When the system is highly (but not fully) dynamic, there are some advanced requests assigned to the routes. Hence, the route with assigned stops is less flexible for rerouting, and the detour to the accept dynamic requests is constrained by these determined visiting sequences. The same phenomenon was also observed in scheduling demand-responsive transport services [17]. In general, the system cost F increases with the increasing DOD. The system performance can be improved by 1.2% when all the online requests turn into static requests. This suggests that the insertion heuristic is myopic compared to that of the offline routing model, which can provide an optimal solution with all the requests information available. Hence, lowering the DOD may be a more attractive policy for transit operators to improve the system efficiency.

4.2.2. No-Shows. When a vehicle arrives at the pick-up site and finds that the customer did not show up, the schedule must be quickly adjusted and some wasted costs may be incurred. In our study, the simulations were carried out by varying the no-show rate from 0 to 20% with a random distribution. Table 3 shows that with an increasing no-show

Table 2: Simulation results under different DOD values.

DOD (%)	R (min)	A (min)	I (min)	Rej (%)	O_p ($)	F ($)
0	15.76	0	0.46	11.55	3.53	9.01
25	15.69	0.13	0.49	12.20	3.54	9.05
50	15.61	0.30	0.52	12.76	3.55	9.08
75	15.60	0.44	0.53	12.70	3.54	9.11
100	15.60	0.47	0.53	12.64	3.54	9.12

Table 3: Simulation results with different no-show rates.

No-show (%)	R (min)	A (min)	I (min)	Rej (%)	O_p ($)	F ($)
0	15.76	0	0.46	11.55	3.53	9.01
5	15.70	0	0.50	11.55	3.67	9.15
10	15.66	0	0.56	11.55	3.82	9.32
15	15.60	0	0.59	11.55	3.99	9.49
20	15.55	0	0.65	11.55	4.19	9.69

rate, the riding time R declines constantly. However, the idle time I gradually increases. In general, the passengers' in-vehicle time, which is equal to the sum of the riding time and the idle time, remains stable. This finding shows that although the rerouting could save the travel distance for not serving the drop-off points of the no-show customers, it could not significantly reduce the in-vehicle time of the passengers. Even worse, passengers who experience a prolonged idle time may develop a negative perception towards the flex-route transit service. We also observe that the operating cost O_p increases with the growing number of no-show passengers. This is because the salvaged operation time could not compensate for the decreased ridership. As a consequence, the system cost gradually increases with an increasing no-show rate.

4.2.3. Cancellations. In this study, only a real-time cancellation is considered. Unlike cancelling requests in advance, this kind of cancellation affects the scheduling and routing of vehicles and needs to be adjusted in real time. Table 4 indicates that the system performance indicators show a similar trend to the no-show events. The difference is that a real-time cancellation has a more significant impact on the riding time R and idle time I. This is because both the pick-up and drop-off points could be skipped when the cancellation happens while the vehicle can only skip the drop-off stops when the passengers are absent. The saved travel distance also leads to a lower operating cost O_p than their counterparts of no-show events. Overall, both the no-show and cancellation events have a great impact on the system performance, and some extra cost is incurred for both the customers and transit operators. Therefore, customers who have a poor record of no-shows or cancellations should be identified and added onto a blacklist in practice to prevent the frequent occurrence of such events.

In Figure 4, we compare the system cost without a dynamic intervention and those with a dynamic rerouting

Table 4: Simulation results with different cancellation rates.

Cancellation (%)	R (min)	A (min)	I (min)	Rej (%)	O_p ($)	F ($)
0	15.76	0	0.46	11.55	3.53	9.01
5	15.60	0	0.56	11.55	3.64	9.13
10	15.47	0	0.68	11.55	3.77	9.27
15	15.31	0	0.77	11.55	3.91	9.41
20	15.16	0	0.87	11.55	4.07	9.56

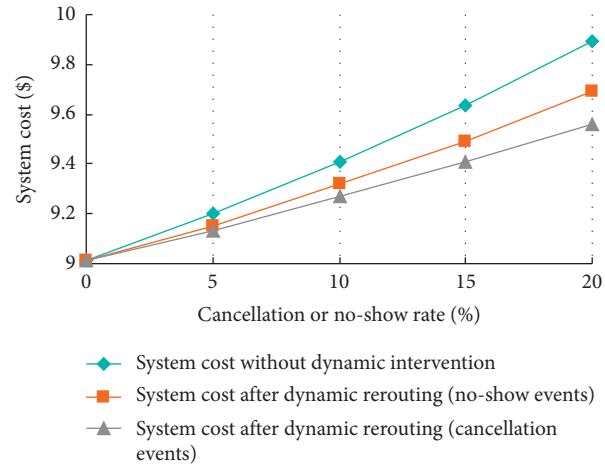

Figure 4: System cost with and without dynamic intervention.

scheme. We can see that our proposed rerouting scheme could save the system cost F for both no-show and cancellation events. This is because after the dynamic intervention, the unnecessary travel distance to reach the voided pick-up or drop-off points is eliminated, which leads to a lower operating cost O_p. This finding confirms that more high quality schedules can be generated under real-time adjustment.

4.2.4. Travel Time Fluctuation. The travel time that is estimated based on the average travel speed of the road segment is very likely to fluctuate in practice. Therefore, in our simulation, we assume that the travel time t_{ij} between point i and point j is normally distributed with its mean $\overline{t_{ij}}$ calculated based on the average vehicle speed, and its standard deviation σ_{ij} is defined as

$$\sigma_{ij} = \eta \overline{t_{ij}}. \tag{22}$$

We vary η from 0 to 0.2, and simulation results are shown in Table 5. It reveals that the riding time R and operating cost O_p are almost unaffected by the travel time fluctuation. However, due to the frequent early arrival and delay at both the requested stops and checkpoints, the passengers may have to bear some unwanted waiting time and idle time. These unexpected time costs can also be reflected in the system cost F. In our experiments, we assume that the time constraints of the checkpoints can be violated in the dynamic operation environment. This is not a problem for most cases, except when the checkpoint is synchronized with other transit lines. In this case, some

Table 5: Simulation results with different travel time standard deviations.

η	R (min)	A (min)	I (min)	Rej (%)	O_p ($)	F ($)
0	15.76	0	0.46	11.55	3.53	9.01
0.05	15.78	0.06	0.50	11.55	3.53	9.06
0.10	15.76	0.14	0.56	11.55	3.53	9.10
0.15	15.74	0.22	0.64	11.55	3.53	9.16
0.20	15.78	0.33	0.70	11.55	3.53	9.22

passengers who are not served may have to be abandoned by the designated vehicles to save the insufficient slack time. To remedy the inconvenience, the transit operator should arrange another vehicle or give some financial compensation to these passengers.

5. Conclusions

As the most widely used flexible transit services, flex-route transit is a promising option to meet the diversified travel needs in low-density areas and cover the first/last mile of a trip. Most studies have focused on fully static systems in which all the input is known beforehand and the vehicle routes do not change once they are being executed. This idealized assumption is fragile in real-life cases because some dynamic events occur during the execution of the plan and the predetermined schedule and route need to be adjusted via online manipulations.

In this article, we study the vehicle routing and scheduling problem of flex-route transit under a dynamic operating environment. A two-stage scheduling model is designed to address the prebooking requests and dynamic events. In the first stage, an offline routing model formulated as a mixed integer program is employed to build the initial routing plan. In the second stage, an online scheduling scheme is proposed to cope with the different dynamic events.

Simulation experiments were carried out to evaluate the influences of different dynamic events. The simulation results reveal that although allowing real-time requests can improve the reservation flexibility of the system, more prebooking requests can improve the system performance. This finding suggests that the transit operator should encourage more passengers to reserve their trip in advance. A possible incentive mechanism for stimulating the riders' willingness to prebook is to reduce the transit fare for advanced requests or increase the transit fare for dynamic requests. In addition, mobile-based applications can be developed to provide real-time vehicle location of the vehicles and the updated estimated arrival times.

We also find that although the dynamic intervention could reduce unnecessary travel distances, the no-show and cancellation events still have a substantial negative impact on the operating cost of the transit operators. Frequent occurrence of these events not only leads to revenue loss but also wastes the slack time, by which some rejected passengers could have been served by the transit service. Therefore, we suggest that the transit operator should identify the customers who have a poor record of no-shows or cancellations and add them onto a blacklist. In the near future, with the widespread use of mobile payment technologies, deducting the transit fare in advance may be a more efficient way to prevent these events.

Moreover, the results show that the travel time fluctuations lead to an increase in the waiting and idle time for passengers. The influence is minor compared to other dynamic events. However, it is noteworthy that punctuality at the checkpoints that are synchronized with other transit lines should be guaranteed; otherwise, the delay at these time points may result in missed connections for the passengers.

To the best of our knowledge, this is the first work that addresses the dynamic scheduling problem of the flex-route transit service. Future work will investigate the stochastic vehicle routing problems of the flex-route transit service. The inherent uncertainty of the inputs, such as demands and travel times, will be considered in the planning phase.

Data Availability

All data generated or analyzed during this study are included within this article.

Conflicts of Interest

The authors declare that they have no conflicts of interest.

Acknowledgments

This study was supported by the National Natural Science Foundation of China (grant no. 61573098) and NUPTSF (grant no. NY220170).

References

[1] J. F. Potts, M. A. Marshall, E. C. Crockett, and J. Washington, *A Guide for Planning and Operating Flexible Public Transportation Services: TCRP Report 140*, Transportation Research Board, Washington, DC, USA, 2010.

[2] L. Quadrifoglio, R. W. Hall, and M. M. Dessouky, "Performance and design of mobility allowance shuttle transit services: bounds on the maximum longitudinal velocity," *Transportation Science*, vol. 40, no. 3, pp. 351–363, 2006.

[3] T. G. Crainic, F. Errico, F. Malucelli, and M. Nonato, "Designing the master schedule for demand-adaptive transit systems," *Annals of Operations Research*, vol. 194, no. 1, pp. 151–166, 2012.

[4] D. Koffman, *Operational Experiences with Flexible Transit Services: a Synthesis of Transit Practice. TCRP Synthesis*, Transportation Research Board, Washington, DC, USA, 2004.

[5] E. Bruun and E. Marx, "OmniLink," *Transportation Research Record: Journal of the Transportation Research Board*, vol. 1971, no. 1, pp. 91–98, 2006.

[6] S. R. Fittante and A. Lubin, "Adapting the Swedish service route model to suburban transit in the United States," *Journal of the Transportation Research Board*, vol. 2536, pp. 52–59, 2015.

[7] F. Malucelli, M. Nonato, and S. Pallottino, "Demand adaptive systems: some proposals on flexible transit 1," in Operations Research in Industry, T. Ciriania, E. Johnson, and R. Tadei Eds., pp.157–182, McMillan Press, London, UK, 1999.

[8] L. Quadrifoglio, M. M. Dessouky, and F. Ordóñez, "Mobility allowance shuttle transit (MAST) services: MIP formulation and strengthening with logic constraints," *European Journal of Operational Research*, vol. 185, no. 2, pp. 481–494, 2008.

[9] B. Alshalalfah and A. Shalaby, "Feasibility of flex-route as a feeder transit service to rail stations in the suburbs: case study in Toronto," *Journal of Urban Planning and Development*, vol. 138, no. 1, pp. 90–100, 2012.

[10] F. Qiu, W. Li, and J. Zhang, "A dynamic station strategy to improve the performance of flex-route transit services," *Transportation Research Part C: Emerging Technologies*, vol. 48, pp. 229–240, 2014.

[11] Y. Zheng, W. Li, and F. Qiu, "A slack arrival strategy to promote flex-route transit services," *Transportation Research Part C: Emerging Technologies*, vol. 92, pp. 442–455, 2018.

[12] L. Fu, "Improving paratransit scheduling by accounting for dynamic and stochastic variations in travel time," *Transportation Research Record: Journal of the Transportation Research Board*, vol. 1666, no. 1, pp. 74–81, 1999.

[13] L. Fu, "Scheduling dial-a-ride paratransit under time-varying, stochastic congestion," *Transportation Research Part B: Methodological*, vol. 36, no. 6, pp. 485–506, 2002.

[14] M. Schilde, K. F. Doerner, and R. F. Hartl, "Integrating stochastic time-dependent travel speed in solution methods for the dynamic dial-a-ride problem," *European Journal of Operational Research*, vol. 238, no. 1, pp. 18–30, 2014.

[15] Z. Xiang, C. Chu, and H. Chen, "The study of a dynamic dial-a-ride problem under time-dependent and stochastic environments," *European Journal of Operational Research*, vol. 185, no. 2, pp. 534–551, 2008.

[16] T. Kim, *Model and Algorithm for Solving Real Time Dial-A-Ride Problem*, Ph. D. thesis, University of Maryland, College Park, MD, USA, 2011.

[17] K. I. Wong, A. F. Han, and C. W. Yuen, "On dynamic demand responsive transport services with degree of dynamism," *Transportmetrica A: Transport Science*, vol. 10, no. 1, pp. 55–73, 2014.

[18] J. Shen, S. Yang, X. Gao, and F. Qiu, "Vehicle routing and scheduling of demand-responsive connector with on-demand stations," *Advances in Mechanical Engineering*, vol. 9, no. 6, Article ID 1687814017706433, 2017.

[19] R. G. Farwell and E. Marx, "Planning, implementation, and evaluation of omniride demand-driven transit operations: feeder and flex-route services," *Transportation Research Record: Journal of the Transportation Research Board*, vol. 1557, no. 1, pp. 1–9, 1996.

[20] J. A. Lee, *Evaluating its Investments in Public Transportation: A Proposed Framework and Plan for the Omnilink Route Deviation Service*, Virginia Polytechnic Institute and State University, Blacksburg, VI, USA, 2002.

[21] Y. Zheng and W. Li, "Flex-route transit service with different degree of dynamism," in *Proceedings of the 19th COTA International Conference of Transportation Professionals*, pp. 4369–4380, Nanjing, China, 2019.

[22] S. C. Ho, W. Y. Szeto, Y.-H. Kuo, J. M. Y. Leung, M. Petering, and T. W. H. Tou, "A survey of dial-a-ride problems: literature review and recent developments," *Transportation Research Part B: Methodological*, vol. 111, pp. 395–421, 2018.

[23] D. Huang, Y. Gu, S. Wang, Z. Liu, and W. Zhang, "A two-phase optimization model for the demand-responsive customized bus network design," *Transportation Research Part C: Emerging Technologies*, vol. 111, pp. 1–21, 2020a.

[24] L. Quadrifoglio, M. M. Dessouky, and K. Palmer, "An insertion heuristic for scheduling mobility allowance shuttle transit (mast) services," *Journal of Scheduling*, vol. 10, no. 1, pp. 25–40, 2007.

[25] F. Qiu, W. Li, and A. Haghani, "A methodology for choosing between fixed-route and flex-route policies for transit services," *Journal of Advanced Transportation*, vol. 49, no. 3, pp. 496–509, 2015.

[26] M. Wardman, "Public transport values of time," *Transport Policy*, vol. 11, no. 4, pp. 363–377, 2004.

[27] D. Huang, X. Chen, Z. Liu, C. Lyu, S. Wang, and X. Chen, "A static bike repositioning model in a hub-and-spoke network framework," *Transportation Research Part E: Logistics and Transportation Review*, vol. 141, Article ID 102031, 2020.

Hindawi
Discrete Dynamics in Nature and Society
Volume 2020, Article ID 8816314, 9 pages
https://doi.org/10.1155/2020/8816314

Research Article

The Dark Side of Ridesharing in China: A Case Study of Qiangsheng Taxi

Tian Meng, Songyi Cai, You Qu, Evelyn Ng, Barney Tan, and Bo Zhu

Shanghai Sci-Tech Finance Institute, Shanghai University, Shanghai 200072, China

Correspondence should be addressed to Bo Zhu; zhubo@staff.shu.edu.cn

Received 9 September 2020; Revised 9 October 2020; Accepted 2 December 2020; Published 16 December 2020

Academic Editor: Tingsong Wang

Our understanding of the negative implications of the sharing economy is limited, particularly from the perspective of the traditional businesses that are being displaced. To address this knowledge gap, this paper documents our ongoing study of Qiangsheng Taxi, the oldest and largest taxi company based in Shanghai, China. Our aim is to develop a preliminary process model based on the data collected to date that sheds light on the negative implications of ridesharing, one of the most recognized forms of the sharing economy. More specifically, our process model suggests that there are contextual conditions that are particularly conducive to the growth of ridesharing platforms in China and how they accumulate resources, which give rise to four negative outcomes for the traditional taxi business. These negative outcomes, in turn, reinforce the prevailing contextual conditions to form a vicious cycle that exacerbates the negative influence of the ridesharing platforms even further.

1. Introduction

In recent years, a new consumption paradigm known as the sharing economy has been on rapid rise all over the world as it generates many benefits and allows people to access idle goods and resources without having to own them [1]. The sharing economy is defined as the "peer-to-peer-based activity of obtaining, giving, or sharing the access to goods and services, coordinated through community-based online services" ([2], p. 2047). It is predicated that the global sharing economy will reach $335 billion by 2025 [3]. In the transportation sector, for example, ridesharing has become a very popular form of the sharing economy, with large number of ridesharing platforms, such as Uber, Lyft, and DiDi, operating all over the world [4]. With ridesharing, people can use their smartphones to access the ridesharing platform to request transportation service and the platforms match the requests with available private cars in real time. As it is more convenient than street-hailing and their prices tend to be lower, the ridesharing platforms have grown rapidly to become a popular mode of travel. This has caused disruption to the existing taxi industry and resulted in competition and regulatory concerns [5]. In particular, there is a growing realization that ridesharing may lead to the exploitation of labor (e.g., unsafe working conditions and lower than minimum wages) and fares poorly in checking undesirable provider behaviors (e.g., sexual harassment by Uber drivers), and its ecological impact may be overstated [6].

Reflecting the growing awareness of these issues, a number of researchers within academia have now turned their attention to examining the impact of the sharing economy and offering prescriptions on mitigating its potential negative implications (e.g., [7]). And yet, these emerging works tend to be conceptual in nature and not corroborated by empirical evidence. In addition, the sharing economy may have a negative impact on the incumbent industries that it is attempting to displace as well, precipitating the loss of revenue and jobs or even the exit of traditional businesses [8]. However, there have been only a handful of studies undertaken from the perspective of these traditional businesses, and the mechanisms that underlie the negative influence of the sharing economy on these businesses have not been adequately studied. Addressing these knowledge gaps is important if we are to understand the real impact of the sharing economy more fully, which may be

important for policy makers to formulate effective legislation to regulate the sector, and for traditional businesses to develop countermeasures to the challenges and threats that they are facing.

This paper documents an ongoing study aimed at addressing these knowledge gaps. More specifically, based on a case study of Qiangsheng Taxi, the oldest and largest taxi company based in Shanghai, China, our aim is to develop a preliminary process model that sheds light on the negative implications of ridesharing (i.e., one of the most widely recognized forms of the sharing economy represented by platforms such as Uber and Didi—see [9]) from the perspective of a traditional taxi business. Accordingly, our research question is as follows: How does the sharing economy influence the business of a traditional company?

2. Literature Review

2.1. Existing Research on the Sharing Economy. The sharing economy is based on the principle of sharing access to products and services in peer-to-peer (P2P) markets [10]. This principle of sharing in itself is not new [11]: the sharing of forestry machinery and the services of public libraries, for example, are manifestations of the principle in the business-to-business (B2B) and business-to-consumer (B2C) domains, respectively [12]. The extension of the principle of sharing into the P2P domain, however, is a relatively recent development that is driven by economic crises and an increasing awareness of the importance of protecting the environment [10]. This development is made possible by advances in information and communications technology (ICT), changing consumer preferences, the proliferation of collaborative web communities, and the emergence of social commerce [2].

Sharing economy businesses tend to be digital platforms that are based on an online website and/or a mobile app [13]. These platforms can be classified into four categories arranged in a 2×2 matrix depending on whether they are for-profit or not-for profit, and whether they have a P2P or B2C business model [1]. Of the four categories, the for-profit/P2P platforms have arguably been the most visible with the greatest economic impact: platforms such as Uber and Airbnb that fall under this category have become multi-billion-dollar businesses that are operating in numerous countries across the globe (i.e., 60 and 191 countries, respectively). As a result, this category of platforms has been the most extensively studied to date (e.g., [8, 14]). The majority of the existing research on the sharing economy, in particular, can be classified into three main streams.

The first is centered on the *adoption* of collaborative consumption. Studies aligned with this stream are typically seeking to identify the antecedent factors that promote participation on a sharing economy platform, as either a supplier or a consumer of a product/service. For instance, Hamari et al. [2] found that sustainability (i.e., a preference for greener consumption), enjoyment of the activity, and economic gains were the primary participation drivers for the sharing economy. However, the influence of sustainability is only significant if it is also associated with a positive disposition toward this new mode of consumption, which suggests that the factor may only be important for those who are environmentally conscious. In a similar vein, Zhu et al. [15] found that the functional, emotional, and social value of a sharing economy platform will have a positive influence on the attitude of its users, which will translate to the intention to adopt.

The second research stream focuses on the *nature and development* of sharing economy platforms. Studies belonging to this research stream are generally attempting to explain the components and functions of these platforms, as well as the strategies and activities that facilitate their development. Puschmann and Alt [12], for example, described the components of the strategies, processes, and systems that constitute a sharing economy platform, and suggested that the platform as an intermediary has to perform the roles of listing, contracting, billing, fulfillment, and rating. On the other hand, Tan et al. [16] described the developmental trajectory of a sharing economy platform and argued that a platform should first emphasize its pro-social objectives before ensuring business viability and, finally, striking a balance between the market and social logics.

The third research stream is centered on the *implications* of sharing economy platforms. Studies of this stream are mainly aimed at investigating the economic, environmental, and social impact of these platforms. For instance, Martin [17] examined the existing discourse surrounding the sharing economy and found that the phenomenon is typically framed as a combination of (1) an economic opportunity, (2) a more sustainable form of consumption, and (3) a pathway to a decentralized, equitable, and sustainable economy. But at the same time, the sharing economy may also be criticized for (4) creating unregulated marketplaces, (5) reinforcing the neoliberal paradigm, and (6) being an incoherent field of innovation. Adopting a more specific focus, Zervas et al. [8] investigated the impact of Airbnb on the incumbent hotel industry and found that the sharing economy platform reduced the revenue of traditional hotels by 8–10%, with lower-priced hotels and hotels that do not cater to business travelers the most affected. This impact is mostly due to lower prices on Airbnb and is most pronounced when there is a spike in demand, suggesting that sharing economy platforms have an advantage in terms of its ability to flexibly scale its supply to meet demand.

2.2. The Potential Negative Implications of the Sharing Economy. Within the third research stream (refer to Table 1), our review of the literature reveals at least two research gaps in relation to our research question. First, although the emerging works in this area are demonstrating an awareness of the potential negative implications of the sharing economy, much of the present discourse is anecdotal in nature (e.g., [1, 18]). The potential negative implications that have been raised in the existing literature include a lack of concern for the interests of related stakeholders, the creation of shortages for long-term asset owners, the amplification of social biases, the perpetuation of unfair regulatory regimes, the exploitation of labor, and a

Table 1: Literature review.

Author/year	Article/title	Source	Results
Hart et al. (2016)	Do We Need Rules for "What's Mine Is Yours"?	Journal of Business Research	The sharing economy is based on the principle of sharing access to products and services in peer-to-peer (P2P) markets. The extension of the principle of sharing into the P2P domain, however, is a relatively recent development that is driven by economic crises and an increasing awareness of the importance of protecting the environment.
Belk (2014)	You Are What You Can Access: Sharing and Collaborative Consumption Online	Journal of Business Research	The principle of sharing is not new.
Hamari et al. (2016)	The Sharing Economy: Why People Participate in Collaborative Consumption	Journal of the Association for Information Science and Technology	The development is made possible by advances in information and communications technology (ICT), changing consumer preferences, the proliferation of collaborative web communities, and the emergence of social commerce. Sustainability (i.e., a preference for greener consumption), enjoyment of the activity, and economic gains were the primary participation drivers for the sharing economy. However, the influence of sustainability is only significant if it is also associated with a positive disposition toward this new mode of consumption, which suggests that the factor may only be important for those who are environmentally conscious.
Barann et al. (2017)	An Open-Data Approach for Quantifying the Potential of Taxi Ridesharing	American Journal of Sociology	Sharing economy businesses tend to be digital platforms that are based on an online website and/or a mobile app.
Schor (2016)	Debating the Sharing Economy	Journal of Self-Governance and Management Economics	The platforms can be classified into four categories arranged in a 2×2 matrix depending on whether they are for-profit or not-for profit, and whether they have a P2P or B2C business model.
Cramer and Krueger (2016)	Disruptive Change in the Taxi Business: The Case of Uber	American Economic Review	The category of platforms has been the most extensively studied to date.
Zhu et al. (2017)	Inside the Sharing Economy: Understanding Consumer Motivations behind the Adoption of Mobile Applications	International Journal of Contemporary Hospitality Management	The functional, emotional, and social value of a sharing economy platform will have a positive influence on the attitude of its users, which will translate to the intention to adopt. The developmental trajectory of a sharing economy platform, and it argues that a platform should first emphasize its pro-social objectives before ensuring business viability and, finally, striking a balance between the market and social logics.
Puschmann and Alt (2016)	Sharing Economy	Business & Information Systems Engineering	The sharing of forestry machinery and the services of public libraries, for example, are manifestations of the principle in the business-to-business (B2B) and business-to-consumer (B2C) domains, respectively.
Tan et al. (2017)	How GoGet Carshare's Product-Service System Is Facilitating Collaborative Consumption	MIS Quarterly Executive (16 : 4)	The developmental trajectory of a sharing economy platform and it argues that a platform should first emphasize its pro-social objectives before ensuring business viability and, finally, striking a balance between the market and social logics.

lack of control over undesirable provider and consumer behaviors, among others (see [7]). However, few of them have been corroborated or verified by empirical investigation. Without empirical support, the arguments presented in these works can only remain in the realm of guesswork and assumptions, from which it is difficult to derive theories and insights for the advancement of knowledge in this area.

Second, of the existing works on the negative implications of the sharing economy, there are only a handful that have been conducted from the perspective of the traditional firms that the sharing economy platforms are displacing. One exception is the aforementioned study by Zervas et al. [8]; but even though the impact of Airbnb on traditional hotels has been ascertained, the relationship uncovered remains a "black box" because the precise mechanisms through which the platform affects the hotels fall beyond the scope of the paper. Similarly, Chang [19] discovered that the entry of Uber in Taiwan reduced taxi revenues by approximately 12% in its initial year and 18% by the third year of its entry, but once again the underlying reason proffered for this effect is merely speculative in nature (i.e., a substitution effect) and has been contradicted in other studies (see [20]). To address these research gaps, our aim is to conduct an in-depth investigation into the underlying mechanisms through which the negative implications of the sharing economy manifest from the perspective of a traditional business. In the following sections, we will describe our research approach and the preliminary findings from our ongoing study.

3. Research Method

The case research method is especially appropriate for our study because its strengths lie in exploring 'how' research questions [21], understudied and multi-faceted phenomena, and processes that cannot be separated from their contexts [22]—all conditions that are relevant to our study. To address our research question, we identified two criteria for case selection. First, the selected organization should be a traditional firm whose business has been severely affected by a sharing economy platform. The extent of severity is important because our study is aiming to capture the potential magnitude of the negative implications of the sharing economy. Second, the selected organization should be a commercially successful business and a market leader within the industry prior to the inception of the sharing economy. This is to rule out possible alternative explanations for the negative effects that we may uncover (e.g., sub-par organizational performance may be attributed to a general lack of competitiveness instead). The case of Qiangsheng Taxi is particularly appropriate for our study because not only is the firm the oldest and largest taxi company in Shanghai, China, but its historically viable taxi business has seen its revenue drastically diminished since the inception of ridesharing in 2012. This makes Qiangsheng a revelatory or extreme case [23] for the purpose of our study.

Qiangsheng Taxi was founded in Shanghai as Xiangsheng Automobile in 1919. In 1954, Xiangsheng was renamed the Shanghai Taxi Company, and within a short span of 2 years, it acquired and merged with 16 other car dealers in the city to become the market leader within the local taxi industry, a position that it has held for over 60 years. The firm became publicly listed on the Shanghai Stock Exchange in 1992 and acquired its present name in 2001. Qiangsheng Taxi is currently a state-owned holding company under the corporate umbrella of the Shanghai Jiushi Group. It currently has an asset base valued at approximately US$868 million, 35,000 employees, and a fleet of over 13,000 vehicles (including taxis and rental cars). Qiangsheng is known as a technology leader within the industry as well, pursuing an array of cutting-edge technological innovations such as establishing an intelligent dispatching center, installing location tracking and speed monitoring devices in all of its vehicles, and developing a traffic management system that intelligently routes its vehicles based on traffic and road conditions. Qiangsheng currently has five main lines of business, including its taxi, car rental, automobile servicing, travel, and property investment divisions. The first two, in particular, have felt the brunt of the market revolution brought about by the sharing economy.

3.1. Data Collection and Analysis. Case access was granted in May 2018 and the study has been ongoing for the past 12 months. The study was designed with two main phases: a preparatory phase and a fieldwork phase. The focus of the preparatory phase was to collect and analyze data from a variety of secondary sources so as to gain an overview of the case organization as well as the industry in which it operates. The emphasis of the ongoing fieldwork phase, on the other hand, is to collect primary data that are specific to our research question and explore the implications of ridesharing on Qiangsheng in depth [24]. Interviews are the primary means of data collection [25] during the fieldwork phase and a total of 19 informants were identified via chain referral sampling [26]. The informants included representatives from Qiangsheng's top management, organizational IT function, and various business units (e.g., Asset Management and Human Resource (HR) departments). In addition, we interviewed two taxi drivers, five taxi/ridesharing users, and two industry insiders who were intimately familiar with the contextual conditions surrounding the taxi industry as well. Each interview took an average of 45 minutes and was conducted with the help of a semi-structured interview guide [25] that had a set of standard questions with respect to the development and performance of Qiangsheng since the inception of ridesharing. There were also specific questions for each informant that were tailored based on their role (e.g., the taxi drivers interviewed were asked questions in relation to why they were also driving for ridesharing platforms and, hence, their dual identity) within the organization as well [24]. All the interviews were recorded, transcribed in mandarin, and subsequently translated for data analysis.

Data analysis is being performed concurrently with data collection to take full advantage of the flexibility that the case research method affords [27]. A set of second-order themes

were first derived from the literature on the sharing economy to serve as a theoretical lens to guide our data collection. These themes consisted of the potential negative implications of the sharing economy that have been raised in the existing literature, which were then conceptually abstracted (i.e., firm-specific, economic, and social implications) into three aggregate dimensions (see [28]). The data collected was then coded using a mix of open, axial, and selective coding [29]. More specifically, open coding was used to assign conceptual labels to our interview data to create a number of first-order concepts. Axial coding was then used to classify the first-order concepts around our existing second-order themes (e.g., "unbalanced regulatory regime"), with new themes created (e.g., "unfulfilled societal role") if the first-order concepts did not fit with our existing schema. Selective coding was then used to group the second-order themes into the existing aggregate dimensions, which were similarly modified if the second-order themes did not fit with our initial theoretical lens (e.g., social implications was reclassified as "contextual conditions" because the external environment did not merely reflect the influence of ridesharing, but served as a driver of its development as well). Coding was restarted whenever new second-order themes or aggregate dimensions were created. The study is still currently ongoing, but this process of iterating between data, analysis, and theory development will continue until the state of theoretical saturation is reached [27].

4. Negative Influence of Ridesharing

Our ongoing study of Qiangsheng suggests that there are contextual conditions that are particularly conducive to the growth of ridesharing platforms in China and the accumulation of resources by these platforms, which give rise to a number of negative outcomes for the traditional taxi company (refer to Figure 1). These negative outcomes, in turn, reinforce the prevailing contextual conditions to form a vicious cycle that exacerbates the negative influence of the ridesharing platforms even further. We describe and explain our findings in detail in the stream of reporting that follows.

4.1. Contextual Conditions Favorable to the Growth of Ridesharing in China. The taxi industry in Shanghai is an established and mature sector with a history of over 100 years. And because taxis are largely seen as a means of public transportation that plays an important societal role, the industry is subject to stringent government oversight and regulatory control. For instance, the Shanghai government has a cap on taxi fares that has remained unchanged for around a decade, and like most other cities in China, it is both expensive and difficult to obtain a taxi license (see [30]). In contrast, the Chinese government tends to adopt a permissive attitude toward new technology-enabled businesses so as to avoid stifling innovation (see [31]). This has resulted in an *unbalanced regulatory regime* that is highly favorable to the ridesharing platforms. The HR Manager of Qiangsheng provided an example: *"the government regulations are not helping. For example, drivers from other provinces cannot drive taxis, but the rule does not apply to Didi (China's de facto ridesharing platform). Because of this, our business is like stagnant water. We do not have new people joining this profession. This affects the viability of our business."*

At the same time, the high smartphone penetration in China has induced a shift in *consumer preferences*, as the convenience of hailing a ride in real time with just a few swipes and finger taps via a ridesharing app presents a compelling value proposition for the majority of the country's smartphone users. As a result, there is a substitution effect (see [19]) at work in relation to the public's choice of transportation, and the fact that China now also has a sophisticated transportation network in place is preventing traditional taxi businesses like Qiangsheng from taking steps to ameliorate the situation (i.e., in contrast to the findings of [20]). The Vice-President (VP) of Operations at Qiangsheng explained: "*people tend to take the trains if the distance is more than 10 km. For distances around 4-5 km, people tend to use Didi, and for distances below 3 km, people tend to use bicycles or bike shares (e.g., Mobike). Therefore, you can see that the demand for taxis is not very high.*"

The shifting consumer preferences, in tandem with the unbalanced regulatory regime, presented conditions that were highly conducive to the emergence and *business growth* of ridesharing platforms such as Didi. In addition, these factors facilitated *resource accumulation* on the part of the platforms as well because they presented better opportunities for income generation, and there was a lack of participatory barriers (e.g., few regulations preventing anyone from becoming a Didi driver, echoing [7]). The VP of Operations provided an illustration: *"Didi drivers are able to earn about CNY$20k monthly, compared to just CNY$7-8k for taxi drivers. Not only that, Didi has flexible working hours, while for taxi drivers, you work very long hours. Because of these (differences), many drivers are preferring to drive for Didi than taxi companies."* Consequently, the ridesharing platforms in Shanghai were able to proliferate and grow rapidly, which had severe implications for the business of Qiangsheng.

4.2. The Negative Implications of Ridesharing on Qiangsheng. More specifically, our informants indicated that the rise of ridesharing platforms gave rise to at least four negative outcomes for Qiangsheng. First, it resulted in *business stagnation*, due to increased business competition and the loss of revenue. This finding is in line with previous studies on the impact of the sharing economy on incumbent firms (e.g., [8, 19]) and may be attributed to the enhanced value proposition and lower prices of the ridesharing platforms. The Communist Party Secretary of Qiangsheng described the current situation: *"since 2015, our business has not been earning profits and now we have a net loss. This is because we use our (taxi) business revenue to subsidize our drivers... Competition is unfair because these ridesharing platforms are using their massive capital base (from venture capital investments) to keep their prices low... They are burning money*

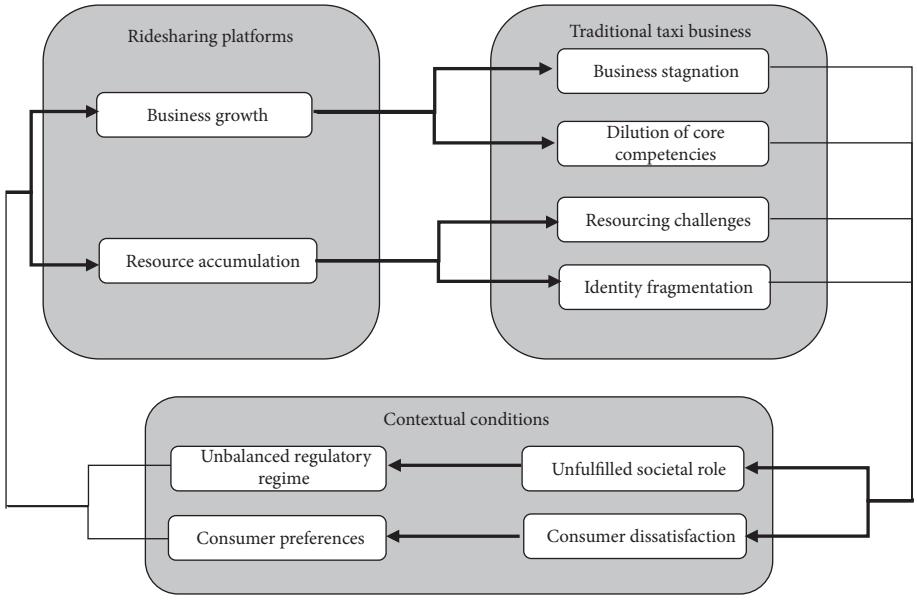

Figure 1: The negative economic and social implications of ridesharing.

and operating at a loss to acquire customers and there is no way we can compete with that!"

Second, with the stagnation of its taxi business, Qiangsheng was forced to diversify into a variety of unrelated businesses to maintain its profitability, which resulted in the *dilution of core competencies*. In particular, as both a market and technology leader within the industry, Qiangsheng has acquired and maintained a number of critical organizational and technological capabilities over the years. However, because its corporate attention is now focused on the development of its other business divisions (e.g., its travel and property businesses), the development of those capabilities has been curtailed, if not neglected. One of the industry insiders we interviewed described this development: *"because of low profits and stagnation, there is a need to reform their business or their (taxi) business will not be able to survive in the next 5 years. They are diversifying into other businesses. For example, they are aiming to be a high-end commercial travel service provider, integrating transport, meeting facilities, advertising, and travel services together"*. This finding resonates with Helfat and Peteraf's [32] assertion that while related diversification can allow for the renewal or redeployment of core competencies, unrelated diversification can lead to their retirement or retrenchment (i.e., gradual decline). In other words, the dilution of its core competencies may affect Qiangsheng's ability to operate and compete with the ridesharing platforms even further.

Third, because Qiangsheng and the ridesharing platforms operate within the same organizational niche, defined as a multi-dimensional space where organizations with the same productive capacities and resource requirements compete [33], when the latter is finding it easier to accumulate resources, it naturally follows that Qiangsheng would be confronted with *resourcing challenges*. As indicated in the evidence presented previously, ridesharing drivers not only enjoy flexible working hours but also have the potential to make an income that is twice that of a traditional taxi driver. Coupled with the fact that Qiangsheng is prevented by regulations from hiring drivers from other provinces to replenish or renew its existing labor pool, these factors make it very difficult for the firm to acquire the resources it needs, which will become more of a problem in the future as the average age of Qiangsheng's drivers is high (over 50 years of age), with many close to retirement. A taxi driver we interviewed explained: *"nobody wants to be a taxi driver anymore. The younger generation, most of them are technology-savvy, and they know how to use Didi well. . . It is hard to find someone like me who just drives a taxi and is not on Didi (at the same time). . . Most of the people like me are close to retiring."*

Fourth, not only is Qiangsheng finding it challenging to acquire the resources it needs, but it is facing difficulties in retaining its resources as well as its business stagnates and there are no viable means of stemming the outflow of resources. The Deputy General Manager of Qiangsheng explained: *"we cannot tell our drivers to stop using Didi. We can only offer incentives like long service awards. . . and make house visits. . . to let the drivers know that their services are valued. . . But the effectiveness of these incentives is limited. . . I think it is natural to be drawn to where the material rewards are."* As a result, particularly in relation to their pool of drivers, most of their drivers are now not only driving for Qiangsheng but also operating on ridesharing platforms as well. This has caused the issue of *identity fragmentation*, which we define as the breakdown of the original professional identity as the result of taking on a new occupational role. Identity fragmentation is especially problematic for Qiangsheng because it may result in conflicted loyalties and

the prioritization of objectives beyond that of the firm [34], which may limit the options of Qiangsheng for competing with the ridesharing platforms even further.

4.3. The Formation of a Vicious Cycle. The four negative outcomes for Qiangsheng, in turn, affected the broader environment in which the firm operates. In particular, beyond their economic contributions, taxi businesses tend to have important social responsibilities as well [35]. The Manager of the Asset Management Department of Qiangsheng provided an example: "*during Chinese New Year, Didi drivers who come from other provinces are not working because they are back home for the holidays. Because of this, many customers are unable to get a Didi, and there is only us, the state-owned taxi business, that is reliable and able to provide taxi services for customers. During the time, we even have to subsidize our drivers out of our own pockets to encourage them to work.*" However, due to the stagnation of its business, the dilution of its core competencies, and its inability to acquire and retain resources, Qiangsheng's ability to fulfil those responsibilities has been curtailed.

In other words, with fewer drivers and taxis on the road, there is an *unfulfilled societal role* that was once taken on by traditional taxi businesses like Qiangsheng. And when societal needs have to be met, the government will be forced to intervene, which will tend to further reinforce the unbalanced regulatory regime that is in place. For example, at present in Shanghai, only taxi businesses are required by law to put vehicles out on the roads during the major public holidays. Moreover, if there are fewer taxis because traditional taxi companies are forced to scale back their business, it may cause *consumer dissatisfaction* because their ability to access the service is reduced, especially among the digitally excluded (e.g., elderly and disabled passengers). One of the taxi/ridesharing users we interviewed explained: *"my elderly parents who do not know how to use the Didi app are now finding it very difficult to catch a taxi. I have to book a taxi on their behalf, which can be very frustrating for them because I may not always be by their side."* And because taxis are both a taken-for-granted institution and a clearly marked sight on the road, the negative responses toward an inability to catch a ride may be especially targeted at the traditional taxi businesses (as opposed to unmarked ridesharing cars or a distant ridesharing platform), which may increase the consumer preferences for ridesharing even further. These effects close a loop on a vicious cycle that will exacerbate the negative influence of the ridesharing platforms.

5. Discussion and Concluding Remarks

The sharing economy is constrained by whimsical ideas about decentralized social markets. Any fair assessment of the sharing economy should recognize a series of specific benefits that are also emphasized by economists and regulators, including but not limited to maximizing the utility of personal assets, flexible work schedules, (some) income security, increasing the quality and quantity of available goods and services through greater competition, and local access to new infrastructure resources [36]. Therefore, at one level, we should regard the sharing economy as a new form of technology-driven business. In fact, sharing does have many advantages implied by its supporters. However, at another level, we must also remain vigilant about the negative impact of sharing economy.

While our study is still in progress, our work to date already hints at a number of potential theoretical contributions. First, the process model developed based on our preliminary data not only is a conceptual innovation but also presents an overview of the negative economic and social implications of ridesharing in China. More specifically, our model suggests that the ascendency of ridesharing platforms can lead to (1) business stagnation, (2) the dilution of core competencies, (3) resourcing challenges, and (4) identity fragmentation for a traditional taxi business, which may reinforce the prevailing contextual conditions that favor the growth of ridesharing even further. In addition, none of the factors and relationships identified in our study appear to be specific to ridesharing or China, which suggests that our process model can potentially advance our understanding of the dark side of the sharing economy [7] beyond its specific context as well. Second, our study not only corroborates the findings of previous studies (e.g., [8, 19]) but also presents an empirically supported explanation "to tell the story of how (the outcome) occurs whenever it does occur" ([37], p. 37). With an understanding of the links of the vicious cycle uncovered, it is hoped that policy makers and leaders of the traditional businesses that are being displaced by the sharing economy can use our research to identify ways of breaking the cycle, so that the traditional businesses can survive, or even thrive, in spite of the growth of ridesharing, and continue to fulfill their important economic and societal roles. In addition, it is hoped that our process model would be a useful reference for the owners and managers of traditional businesses that are being affected by the emergence of the sharing economy as well. For instance, our process model suggests that while diversifying into other potentially more profitable lines of businesses may be a short-term solution to mitigate the negative financial impact of the sharing economy (see [8, 19]), it may in fact cause the dilution of core competencies for a traditional business. As such, we contend that diversification decisions should be carefully considered even if they present a quick fix, and perhaps resources would be more optimally leveraged in the long run if they were invested in reinforcing the core competencies of a traditional business instead [38].

This study is not without its limitations. In particular, although the single case research method adopted in this study is a *"typical and legitimate endeavor"* ([39], p. 231) in qualitative information systems research, the generalizability of our findings and process model may be an issue that is associated with the singular context of our study [40]. As such, our future research will be centered on extending and validating our process model with the collection and analysis of additional data from Qiangsheng, as well as a variety of stakeholders (e.g., passengers, taxi drivers, and representatives of ridesharing platforms) from contexts beyond the one studied here (e.g., the taxi industry in Singapore, which

appears to have reached an ideal equilibrium where a dominant ridesharing platform is thriving alongside a thriving traditional taxi industry). The boundary conditions and implications of our model will also be explored in greater depth through an ongoing literature review and further analyses of our data. By collecting and incorporating further data, and subjecting the data to more in-depth analyses, we hope to refine our process model further so that a more holistic understanding of the negative implications of the sharing economy can emerge.

Data Availability

The data used to support the findings of this study are available from the corresponding author upon request.

Disclosure

An earlier version of this work was presented as an abstract at the International Conference on Information Systems (ICIS), 2019.

Conflicts of Interest

The authors declare that they have no conflicts of interest.

References

[1] J. Schor, "Debating the sharing economy," *Journal of Self-Governance and Management Economics*, vol. 4, no. 3, pp. 7–22, 2016.

[2] J. Hamari, M. Sjöklint, and A. Ukkonen, "The sharing economy: why people participate in collaborative consumption," *Journal of the Association for Information Science and Technology*, vol. 67, no. 9, pp. 2047–2059, 2016.

[3] M. A. Cusumano, "The sharing economy meets reality," *Communications of the ACM*, vol. 61, no. 1, pp. 26–28, 2018.

[4] A. Witt, N. Suzor, and P. Wikström, "Regulating ride-sharing in the peer economy," *Communication Research and Practice*, vol. 1, no. 2, pp. 174–190, 2015.

[5] The Economist, "The rise of the sharing economy," The Economist, London, UK, 2013, https://www.economist.com/leaders/2013/03/09/the-rise-of-the-sharing-economy.

[6] A. Rinne, *The Dark Side of the Sharing Economy*, World Economic Forum, Cologny, Switzerland, 2018, https://www.weforum.org/agenda/2018/01/the-dark-side-of-the-sharing-economy/.

[7] A. Malhotra and M. Van Alstyne, "The dark side of the sharing economy . . . and how to lighten it," *Communications of the ACM*, vol. 57, no. 11, pp. 24–27, 2014.

[8] G. Zervas, D. Proserpio, and J. W. Byers, "The rise of the sharing economy: estimating the impact of Airbnb on the hotel industry," *Journal of Marketing Research*, vol. 54, no. 5, pp. 687–705, 2017.

[9] B. Cohen and J. Kietzmann, "Ride on! Mobility business models for the sharing economy," *Organization & Environment*, vol. 27, no. 3, pp. 279–296, 2014.

[10] B. Hartl, E. Hofmann, and E. Kirchler, "Do we need rules for "what's mine is yours"? Governance in collaborative consumption communities," *Journal of Business Research*, vol. 69, no. 8, pp. 2756–2763, 2016.

[11] R. Belk, "You are what you can access: sharing and collaborative consumption online," *Journal of Business Research*, vol. 67, no. 8, pp. 1595–1600, 2014.

[12] T. Puschmann and R. Alt, "Sharing economy," *Business & Information Systems Engineering*, vol. 58, no. 1, pp. 93–99, 2016.

[13] B. Barann, D. Beverungen, and O. Müller, "An open-data approach for quantifying the potential of taxi ridesharing," *Decision Support Systems*, vol. 99, no. 1, pp. 86–95, 2017.

[14] J. Cramer and A. B. Krueger, "Disruptive change in the taxi business: the case of Uber," *American Economic Review*, vol. 106, no. 5, pp. 177–182, 2016.

[15] G. Zhu, K. K. F. So, and S. Hudson, "Inside the sharing economy," *International Journal of Contemporary Hospitality Management*, vol. 29, no. 9, pp. 2218–2239, 2017.

[16] F. T. C. Tan, M. Cahalane, B. Tan, and J. Engelert, "How GoGet carshare's product-service system is facilitating collaborative consumption," *MIS Quarterly Executive*, vol. 16, no. 4, pp. 265–277, 2017.

[17] C. J. Martin, "The sharing economy: a pathway to sustainability or a nightmarish form of neoliberal capitalism?" *Ecological Economics*, vol. 121, no. 1, pp. 149–159, 2016.

[18] W. Kathan, K. Matzler, and V. Veider, "The sharing economy: your business model's friend or foe?" *Business Horizons*, vol. 59, no. 6, pp. 663–672, 2016.

[19] H.-H. Chang, "The economic effects of Uber on taxi drivers in Taiwan," *Journal of Competition Law & Economics*, vol. 13, no. 3, pp. 475–500, 2017.

[20] K. Kim, C. Baek, and J.-D. Lee, "Creative destruction of the sharing economy in action: the case of Uber," *Transportation Research Part A: Policy and Practice*, vol. 110, no. 110, pp. 118–127, 2018.

[21] G. Walsham, "Interpretive case studies in IS research: nature and method," *European Journal of Information Systems*, vol. 4, no. 2, pp. 74–81, 1995.

[22] S. Rynes and R. P. Gephart Jr., "From the editors: qualitative research and the academy of management journal," *Academy of Management Journal*, vol. 47, no. 4, pp. 454–462, 2004.

[23] J. Gerring, "Case selection for case-study analysis: qualitative and quantitative techniques," in *The Oxford Handbook of Political Methodology*Oxford University Press, Oxford, UK, 2009, http://www.oxfordhandbooks.com/view/10.1093/oxfordhb/9780199286546.001.0001/oxfordhb-9780199286546-e-28.

[24] S. L. Pan and B. Tan, "Demystifying case research: a structured-pragmatic-situational (SPS) approach to conducting case studies," *Information and Organization*, vol. 21, no. 3, pp. 161–176, 2011.

[25] M. D. Myers and M. Newman, "The qualitative interview in IS research: examining the craft," *Information and Organization*, vol. 17, no. 1, pp. 2–26, 2007.

[26] P. Biernacki and D. Waldorf, "Snowball sampling: problems and techniques of chain referral sampling," *Sociological Methods & Research*, vol. 10, no. 2, pp. 141–163, 1981.

[27] K. M. Eisenhardt, "Building theories from case study research," *Academy of Management Review*, vol. 14, no. 4, pp. 532–550, 1989.

[28] D. A. Gioia, K. G. Corley, and A. L. Hamilton, "Seeking qualitative rigor in inductive research," *Organizational Research Methods*, vol. 16, no. 1, pp. 15–31, 2013.

[29] A. Strauss and J. Corbin, *Basics of Qualitative Research: Techniques and Procedures for Developing Grounded Theory*, Sage, Thousand Oaks, CA, USA, 2nd edition, 1998.

[30] L. Kuo, *Chinese Taxi Drivers Attempt Suicide to Protest the Government's Heavy-Handed Cab Monopoly*, Quartz, New

York City, NY, USA, 2015, https://qz.com/377047/chinese-taxi-drivers-attempt-suicide-to-protest-the-governments-heavy-handed-cab-monopoly/.

[31] E. Wilson, "China takes a swipe at the fintech sector,"*Euromoney*, 2018, https://www.euromoney.com/article/b18ws9x3trz4gz/china-takes-a-swipe-at-the-fintech-sector?copyrightInfo=true.

[32] C. E. Helfat and M. A. Peteraf, "The dynamic resource-based view: capability lifecycles," *Strategic Management Journal*, vol. 24, no. 10, pp. 997–1010, 2003.

[33] J. A. C. Baum and J. V. Singh, "Organizational niches and the dynamics of organizational mortality," *American Journal of Sociology*, vol. 100, no. 2, pp. 346–380, 1994.

[34] C. M. Fiol, M. G. Pratt, and E. J. O'Connor, "Managing intractable identity conflicts," *Academy of Management Review*, vol. 34, no. 1, pp. 32–55, 2009.

[35] Deloitte Access Economics, *The Economic and Social Contribution of the NSW Taxi Industry*, Deloitte Access Economics Pty Ltd, London, UK, 2013, https://www2.deloitte.com/content/dam/Deloitte/au/Documents/Economics/deloitte-au-economics-economic-social-contribution-nsw-taxi-industry-121213.pdf.

[36] C. Ryan and A. Rosenblat, "The taking economy: uber, information, and power," *Columbia Law Review*, vol. 117, no. 6, pp. 1623–1690, 2017.

[37] L. B. Mohr, *Explaining Organizational Behavior*, Jossey-Bass, San Francisco, CA, USA, 1982.

[38] V. Abhishek, J. Guajardo, and Z. Zhang, "Business models in the sharing economy: manufacturing durable goods in the presence of peer-to-peer rental markets," SSRN Working Papers, https://papers.ssrn.com/sol3/papers.cfm?abstract_id=2891908, 2019.

[39] A. S. Lee and R. L. Baskerville, "Generalizing generalizability in information systems research," *Information Systems Research*, vol. 14, no. 3, pp. 221–243, 2003.

[40] G. Walsham, "Doing interpretive research," *European Journal of Information Systems*, vol. 15, no. 3, pp. 320–330, 2006.

Hindawi
Discrete Dynamics in Nature and Society
Volume 2020, Article ID 6621752, 13 pages
https://doi.org/10.1155/2020/6621752

Research Article

Random-Parameter Multivariate Negative Binomial Regression for Modeling Impacts of Contributing Factors on the Crash Frequency by Crash Types

Chenzhu Wang,[1] Fei Chen,[1] Jianchuan Cheng,[1] Wu Bo,[2] Ping Zhang,[2] Mingyu Hou,[1] and Feng Xiao[1]

[1]*School of Transportation, Southeast Univ.2 Sipailou, Nanjing, Jiangsu 210096, China*
[2]*Tibet University, No. 36 Jiangsu, Lhasa, Tibet 850000, China*

Correspondence should be addressed to Fei Chen; cf@seu.edu.cn

Received 11 October 2020; Revised 6 November 2020; Accepted 12 November 2020; Published 28 November 2020

Academic Editor: Tingsong Wang

Highways provide the basis for safe and efficient driving. Road geometry plays a critical role in dynamic driving systems. Contributing factors such as plane, longitudinal alignment, and traffic volume, as well as drivers' sight characteristics, determine the safe operating speed of cars and trucks. In turn, the operating speed influences the frequency and type of crashes on the highways. *Methods*. Independent negative binomial and Poisson models are considered as the base approaches to modeling in this study. However, random-parameter models reduce unobserved heterogeneity and obtain higher dimensions. Therefore, we propose the random-parameter multivariate negative binomial (RPMNB) model to analyze the influence of the traffic, speed, road geometry, and sight characteristics on the rear-end, bumping-guardrail, other, noncasualty, and casualty crashes. Subsequently, we compute the goodness-of-fit and predictive measures to confirm the superiority of the proposed model. Finally, we also calculate the elasticity effects to augment the comparison. *Results*. Among the significant variables, black spots, average annual daily traffic volume (AADT), operating speed of cars, speed difference of cars, and length of the present plane curve positively influence the crash risk, whereas the speed difference of trucks, length of the longitudinal slope corresponding to the minimum grade, and stopping sight distance negatively influence the crash risk. Based on the results, several practical and efficient measures can be taken to promote safety during the road design and operating processes. Moreover, the goodness-of-fit and predictive measures clearly highlight the greater performance of the RPMNB model compared to standard models. The elasticity effects across all the models show comparable performance with the RPMNB model. Thus, the RPMNB model reduces the unobserved heterogeneity and yields better performance in terms of precision, with more consistent explanatory power compared to the traditional models.

1. Introduction

The highway is a dynamic system that includes drivers, vehicles, roads, and environment. Drivers play important roles, and inattention, distraction, and misjudgment are the main causes of highway crashes. Nowadays, research studies mainly focus on drivers. Meanwhile, the road characteristics, which serve as an important basis of the dynamic system and influence safety, are often neglected [1–3]. As the basis of driving, road geometry has a very important impact on safety. Almost 40% of all crashes attributed to driver mistake or vehicle failure are fundamentally caused by road geometry [4]. Babukov et al. studied the internal relationship between plane, profile parameters, and road safety in the design of highways and made significant suggestions for improving safety [4–7]. McGee et al. established statistical models between the curve length, curvature, traffic volume, and the crash frequency [8].

After studying 141,812 crashes, Pei and Ma focused on the relationship between road design factors (plane, vertical,

cross section, and intersection) and crashes and put forward corresponding countermeasures [9]. Many types of research have evaluated the safety of road geometry by visualization and computer simulation. Hassan et al. simulated the influence of the 3D environment on driver vision and analyzed the influence of a combination of the horizontal and vertical curve on road safety [10–14]. Then, the Federal Highway Administration developed the Interactive Highway Safety Design Model (IHSDM). Software used the lane width, lane number, horizontal alignment, vertical alignment, cross section, and superelevation as the evaluation parameters to check the consistency of the design [15–17]. Drivers often attempt to improve the efficiency of transportation when road and traffic conditions allow speeding, which causes many crashes on the highway. The Solomon and the Monash University Accident Research Center modeled the relationship between crash rate and vehicle speed and found that the higher the difference between the operating speed and the average speed, the higher the crash rate [18, 19]. The average speed is often exceeded because of the favorable geometry and environmental conditions of modern highways. Meanwhile, the speed difference between cars and trucks increases owing to the relatively poor power and braking performance of trucks, which lead to frequent rear-end crashes.

The initial road alignment design was based on the design speed, which was first proposed by the American Association of State Highway and Transportation Officials (AASHTO) as the key factor in road design. At the same time, designers and researchers also used design speed to evaluate the consistency of horizontal and longitudinal profiles. The expected speed would greatly exceed the design speed during favorable road conditions, and the traditional design method based on the design speed led to poor continuity and imbalance in actual driving. In addition, the drivers' visual perception expressed poor consistency with actual vehicle control [20]. Due to these limitations, AASHTO later adopted the operating speed to dominate the design, which is defined as the driving speed at the 85th percentile selected by the actual measurement of medium-skilled drivers under a free-flow state with good weather and road conditions [21]. Lamm et al. studied the influence of curve on the operating speed based on the design data, vehicle speed, traffic volume, and crash data of 261 intercontinental highway sections and determined the model of the curve radius and operating speed [22, 23]. Anderson et al. investigated the influence of curve radius on the operating speed according to the speed attenuation while passing the curve [24, 25]. Krammes et al. established the operation speed model by collecting the operating speed and design data of 138 plane curve sections based on 1,126 curve sections as samples for a preliminary evaluation to determine the causes of accidents in curve sections and select improvement methods [26]. Collins et al. evaluated the free-flow condition by measuring the actual driving speed at the midpoint of the curve [27–33]. Sil and Maji measured the operating speed through the curve on three sections and established a model between the speed at the curve and the combined curves on the four-lane highway [34]. Based on the existing research abroad, the operating speed model of different vehicle types has been adopted in research in China. In 2004, the Guidelines for Safety Evaluation of Highway Projects proposed the highway speed model based on many research datasets. Specifications for the Highway Safety Audit published in 2015 optimized and improved the speed model of low-grade highways [35]. The evaluated sections are divided into tangent sections, longitudinal slope sections, horizontal curve sections, curved slope combination sections, tunnel sections, interchange sections, and other sections for calculation according to the radius of the horizontal curve and the slope of the profile. A sufficient driving sight distance is directly related to the safety and speed on the highway and is an important index of evaluation. The stopping sight distance enables drivers to stop, meet, and overtake smoothly, and the transverse clear distance measures the safe zone allowed for lateral offset during driving. Both distances are measurable representations of sight characteristics [35].

In summary, previous research studies focused on the contributing factors of road geometry or operating speed characteristics separately, and the sight characteristics determined by the road geometry alignments were rarely studied. This study takes the geometric, speed, and sight characteristics into consideration simultaneously under a single condition and then adopts the random-parameter approach to reduce the interactions between various variables to acquire a higher dimension and discover the contributing factors. The traditional negative binomial and Poisson models used in previous research studies become complicated when analyzing crash types. In contrast, this random-parameter multivariate negative binomial (RPMNB) model allows for a more simplified framework and reduces the unobserved heterogeneity with higher accuracy. In this study, we collect three-year (2009–2011) statistical crash data of the Beijing-Shanghai Highway as a sample to analyze whether the road geometry, operating speed, traffic volume, and sight characteristics affect the crash types (rear-end, bumping-guardrail, roll-over, etc.).

2. Methodology

Many methodological approaches, such as the multivariate Poisson (lognormal) model, zero-inflated negative binomial model, and Poisson lognormal spatial and/or temporal model typically address the crash rate considering the number of crashes occurring over a roadway segment or at an intersection [36–38].

Generally, some of the significant factors affecting the crash rate are missed in the collected data or difficult to analyze. These factors (called unobserved heterogeneity) make a variation in the influence on the observed factors, which may lead to misspecified parameters and erroneous inferences. To reduce the influence of the unobserved

heterogeneity, random parameters, latent-class (finite-mixture) models, and Markov switching models are considered in the multivariate models [39].

2.1. Poisson (Negative Binomial) Regression Model. In statistics researches on crash frequency, Poisson regression is a generalized linear model analysis used to model crash data. The response variable Y is assumed yielding to Poisson distribution, with the expected value modeled by a linear combination of unknown parameters. In Poisson regression, the Poisson incidence rate μ is determined by X_k (the regressor variables) [40–42]:

$$\mu = te^{(\beta_1 X_1 + \beta_2 X_2 + \cdots + \beta_k X_k)}. \tag{1}$$

The fundamental Poisson regression model (PRM) for an observation i is written as

$$\Pr(Y_i = y_i|\mu_i, t_i) = \frac{e^{-\mu_i, t_i}(\mu_i, t_i)^{y_i}}{y_i!},$$
$$\mu_i = t_i\mu(x_i'\beta) = t_i e^{(\beta_1 X_{1i} + \beta_2 X_{2i} + \cdots + \beta_k X_{ki})}, \tag{2}$$

where t is the exposure of a period of time and $\beta_1, \beta_2, \ldots, \beta_k$ are coefficients estimated as unknown parameters.

Negative binomial (NB) regression is a common generalization of Poisson regression including a gamma noise variable [43]. This model is very popular because it models the Poisson heterogeneity with a gamma distribution, and the variance is not equal to the mean restrictively. The negative binomial regression model (NBRM) meets the equation

$$\Pr(Y = y_i|\mu_i, \alpha) = \frac{\Gamma(y_i + \alpha^{-1})}{\Gamma(y_i + 1)\Gamma(\alpha^{-1})}\left(\frac{1}{1 + \alpha\mu_i}\right)^{\alpha^{-1}}\left(\frac{\alpha\mu_i}{1 + \alpha\mu_i}\right)^{y_i}, \tag{3}$$

$$\mu_i = e^{(\ln(t_i) + \beta_1 X_{1i} + \beta_2 X_{2i} + \cdots + \beta_k X_{ki})}. \tag{4}$$

When α is significantly different from 0, the negative binomial regression is appropriate. Otherwise, the Poisson model is better.

2.2. Zero-Inflated Poisson Model. When the crash data contain excess zero-count values in the model, the well-known zero-inflated Poisson model is adopted.

$$\Pr(Y = 0) = \pi + (1 - \pi)e^{-\lambda},$$
$$\Pr(Y = y_i) = (1 - \pi)\frac{\lambda^{y_i}e^{-\lambda}}{y_i!}, \quad y_i = 1, 2, 3, \ldots, \tag{5}$$

where y_i is the nonnegative integer value; λ is the i_{th} expected Poisson count; and π is the probability of extra zeros.

2.3. Random-Parameter Multivariate Negative Binomial Model

2.3.1. Random Parameters for Unobserved Heterogeneity. The PRM restricts the mean to be equal to the variance ($E = \text{VAR}$), and the PRM model does not fit well in some cases. When the model does not hold the equality, the data may be overdispersed ($E < \text{VAR}$) or underdispersed ($E > \text{VAR}$), and the standard errors of the estimated parameter of the PRM will be incorrect. To account for overdispersion in the crash count data, PRM is promoted and derived.

$$\lambda_{ik} = e^{(b'\mathbf{x_i} + \varepsilon_{ik})}, \tag{6}$$

where $e^{\varepsilon_{ik}}$ are error terms following the gamma distribution with mean 1 and variance α.

In response to the nonconstant explanatory variables in the models, we developed the random parameters in each estimated parameter to account for unobserved heterogeneity [39].

$$\beta_{lk} = b_k + \varphi_{lk}, \tag{7}$$

where β_{lk} denotes the l_{th} explanatory variable for observation l; b_k are the mean parameter estimates; and φ_{lk} is a randomly distributed term capturing unobserved heterogeneity.

2.3.2. Multivariate Negative Binomial Model. In recent research studies, the general framework of the random-parameter multivariate negative binomial (RPMNB) model is mostly proposed with the expected number of crashes [44, 45], λ, in the i_{th} road segment and k_{th} crash types (in this paper, these types are rear-end, bumping-guardrail, and crash):

$$\lambda_{ik} = e^{(\beta_{lk}X_{ik}' + \varepsilon_{ik})}, \quad k = 1, 2, 3, \tag{8}$$

where $X_{ik} = (1, X_{1k}, X_{2k}, \ldots, X_{Nk})$ is the independent variable vector; $\beta_{lk} = (\beta_{0k}, \beta_{1k}, \ldots, \beta_{Nk})$ is the coefficient vector; and ε_{ik} is the multivariate error term distributed with zero mean and variance θ^2.

In the RPMNB model, the correlation ρ follows the unstructured correlation covariance matrix, which represents the correlation between ε_{ik} of models for crash type a and b:

$$\mathbf{M} = \begin{bmatrix} \theta_1^2 & \theta_1\theta_2\rho_{12} & \theta_1\theta_2\rho_{13} \\ \theta_2\theta_1\rho_{21} & \theta_2^2 & \theta_2\theta_3\rho_{23} \\ \theta_3\theta_1\rho_{31} & \theta_3\theta_2\rho_{32} & \theta_3^2 \end{bmatrix}. \quad (9)$$

2.4. Model Comparison and Evaluation

2.4.1. Goodness of Fit. When analyzing the structure of the crash data model across different crash types, it is important and necessary to confirm the structure of the unobserved parameters. The likelihood ratio test is used to assess the models [46].

$$\chi^2 = -2\left[LL(\beta_R) - LL(\beta_U)\right], \quad (10)$$

where β_R and β_U denote the log-likelihood at the convergence of the restricted and unrestricted model, respectively.

Bayesian information criterion (BIC) is also used for model comparison, which is a generalized version of the Akaike information criterion (AIC) considering the Bayesian equivalent [47]:

$$\begin{aligned} \mathrm{BIC} &= k\ln(n) - 2\ln(L), \\ \mathrm{AIC} &= 2k - 2\ln(L), \end{aligned} \quad (11)$$

where k and L denote the number of model parameters and the likelihood function, respectively.

AIC introduces the penalty term to minimize the parameters of the model, which helps to reduce the possibility of overfitting and promote the degree of model fitting (maximum likelihood). BIC considers the number of samples, leading to a larger penalty term than AIC. When the number of samples is too large, BIC can effectively prevent the excessively high complexity caused by the precision of the model. So, the models with smaller AIC and BIC values perform better.

2.4.2. Prediction Accuracy. Other than BIC, we used root mean square error (RMSE) to evaluate the accuracy of the models. Similar to BIC, smaller RMSE values mean the model predicts more accurately.

$$\mathrm{RMSE} = \sqrt{\frac{1}{n_0}\sum_{j=1}^{n_0}\left(O_j - P_j\right)^2}. \quad (12)$$

At the same time, the mean absolute error (MAE) and mean absolute percentage error (MAPE) are also used to estimate the accuracy of models:

$$\begin{aligned} \mathrm{MAE} &= \frac{1}{n_0}\sum_{j=1}^{n_0}\left(O_j - P_j\right), \\ \mathrm{MAPE} &= \frac{100\%}{n_0}\sum_{j=1}^{n_0}\left|\frac{O_j - P_j}{O_j}\right|, \end{aligned} \quad (13)$$

where O_j is the j_{th} observation value; P_j is the j_{th} predicted value; and n_0 is the number of observations.

3. Data Description

Yearly crash data from the Beijing-Shanghai Highway from Xinyi to Jiangdu, from 2009 to 2011, were collected from the traffic management department. Originally, the data were used to record the emergency vehicle on the highway. The crash data contained 3,293 crashes in detail, including crash type, location, time, vehicle type, climate, road surface condition, and casualty condition. Rear-end and bumping-guardrail crashes made up 52.9% and 30.3% of the crash data, respectively. The rear-end and bumping-guardrail crash type are the focus of this research, but the other crash types (roll-over, fire, scrub, and others) are also utilized in the models to better explore the correlations to the first two crash types. Table 1 summarizes descriptive statistics of the five crash types in each section on the highway.

Besides, roadway geometric data are collected by road design and construction drawings, which include road geometric features. The undivided four-lane highway from Xinyi to Jiangdu in this study is 259.5 km in total, with the design speed of 120 km/h, and includes 27 interchanges and rest areas. We divide the road into 426 different sections according to different horizontal alignment, vertical alignment, and interchange both-way. We obtain the AADT of 426 sections reported by roadway management agencies.

We adopt the modified crash frequency method to identify the crash black spots and calculate the average crash number of each section:

$$\lambda = \frac{\sum m_i}{n}. \quad (14)$$

The critical value of the crash number is determined with the confidence level of 95%:

$$R = \lambda + 1.96\lambda, \quad i = 1, 2, \ldots, n, \quad (15)$$

where λ is the average crash number; m_i is the crash number in the i_{th} section; n is the total number of sections; and R is the critical value of the crash number.

The actual crash number of each section is compared with the critical value, and the section is identified as crash black spots if the actual number is greater than R.

Based on the models in the Specifications for Highway Safety Audit published in 2015, we calculated the operating speeds of cars and trucks by segments according to different geometric features [35].

The stopping sight distance means the shortest distance required for one ordinary driver to react and slow down or stop when encountering obstacles while driving at a certain speed. Based on the Guidelines for Design of Highway Grade-separated Intersections [48], the stopping sight distances of the car and truck are equations (16) and (17), respectively.

$$S_{\mathrm{car}} = \frac{v_{85}t}{3.6} + \frac{\left(v_{85}/3.6\right)^2}{2gf}. \quad (16)$$

The truck drivers can see the vertical plane of the obstacles at a considerable distance from the point of view with the low speed, but this advantage is not enough to make up

Table 1: Descriptive statistics of dependent variables.

Variable names	Definitions	Minimum	Maximum	Mean	SD
Rear-end crash	Rear-end crash occurs when a vehicle strikes the one in front of it	1	27	4.58	3.93
Bumping-guardrail crash	A vehicle strikes the guardrails in the middle of or outside the highways	1	14	3.08	2.23
Other crash	This type includes roll-over (a vehicle tips over onto its side or roof), fire (a vehicle caught fire due to mechanical failure), scrub (crashes caused by side scrub between vehicles), and other crashes	0	14	1.18	1.59
Noncasualty crash	Crashes leading to property damage only	0	42	6.70	6.41
Casualty crash	Crashes resulted in injury, disability, or fatality	0	5	0.39	0.75

for the poor braking performance. Despite the high viewpoint, truck drivers also lose their sight in places with limited lateral line of sight, especially

$$S_{\text{truck}} = \frac{v_{85}t}{3.6} + \frac{(v_{85}/3.6)^2}{2g(f+i)}, \tag{17}$$

where S_{car} and S_{truck} are the stopping sight distance of the car and truck, respectively; v_{85} is the the operating speed (km/h); t is the reaction time, takes 2.5 s generally (judging time as 1.5 s and running time as 1.0 s); g is the gravitational acceleration, takes 9.8 m/s^2; i is the longitudinal grade; and f is the longitudinal friction coefficient between truck tires and the road surface which takes 0.17 generally.

Corrugated beam guardrails are set in the middle and beside the road across all sections, which affect the drivers` sight. We consider the biggest transverse clear distance to confirm the sight safety, which means the distance between the curve of sight and the track. When the plane curve is sharp, the transverse clear distance should be judged on the inside lane. We calculate the required stopping sight distance of each section for safety following the equation

$$H = R_s\left(1 - \cos\frac{\gamma}{2}\right), \tag{18}$$

where H is the biggest transverse clear distance; R_s is the radius of the inside lane; and γ is the central angle of line of sight.

As shown in Table 2, we summarize the traffic, speed, geometric, and sight characteristics as the independent variables.

4. Results and Discussion

4.1. Model Specification. Estimation of traditional and proposed models is involved in the empirical analysis: (1) traditional model: independent (separate model for 5 different crash types) NB model and independent Poisson model are adopted as bases. Meanwhile, two models are estimated including the zero-inflated multivariate NB (ZIMNB) model and zero-inflated multivariate Poisson (ZIMP) model considering the excess zero-count data; (2) proposed model: random-parameter multivariate NB (RPMNB) model and random-parameter multivariate Poisson (RPMP) model are proposed to estimate. The results of the proposed models are shown in Tables 3 and 4, and Appendix provides the results of corresponding traditional models.

Subsequently, each base effect is estimated for common exogenous variables across five crash types, and we estimate the deviation of variables versus the base for each crash type. The corresponding t-statistic will present statistically significant if the deviation term offers a difference from the base effect. Based on the t-statistic, the parameter does not reveal differential sensitivity for the base crash type if the variable is statistically insignificant.

4.2. Model Estimation Results. In this section, we conduct a detailed discussion of the significant factors affecting crash count components on different crash types. The model estimation results for the RPMP model and RPMNB model are shown in Tables 3 and 4, respectively.

Similar to the traditional approach, we presented the individual effect of each exogenous variable accommodating to the crash propensity. Taken the constants estimated in various crash type propensity equations as an example, the effect of the casualty crash in Table 3 can be computed as 1.867 (base of the rear-end crash) ±1.000 (casualty crash deviation) = 0.867. At the same time, we identify the number of significant parameters estimated across the five crash types and estimate one individual parameter across 5 crash types. The positive value of the variable in Table 3 indicates there will be more crashes with the increase of the variable, and less crashes, otherwise. As shown in Tables 3 and 4, the significant factors in the two models are not exactly the same. Then, we focus on the results of the RPMNB model while analyzing the effects of factors, and the differences in the RPMP model are appended.

4.2.1. Constant. The constant represents the intercept of the crash type with exogenous variables, without any substantive interpretation.

4.2.2. Traffic Characteristics. Whether there is an interchange in the section is found to negatively influence other, noncasualty, and casualty crashes indicating a lower likelihood of crash propensity for these three crash types in interchange sections. Compared with the general sections, more vehicles accelerate, decelerate, and change lanes leading to more interweaving areas in the interchange sections, getting more attention from drivers and causing fewer crashes to some extent. The results are consistent with the earlier research on the highway interchange [48]. And the impact is also found not significantly different for rear-

Table 2: Summary statistics of independent variables.

Variable names	Definition	Min.	Max.	Mean	SD
Traffic characteristics					
Interchange	1, interchange in the section (25.8%); 0, otherwise (74.2%)	0.00	1.00	0.25	0.44
Black spots	1, the crash number is higher than 18 (7.0%); 0, otherwise (93.0%)	0.00	1.00	0.07	0.26
AADT	Average annual daily traffic volume	31158	68836	46685.94	11969.59
Speed characteristics					
$V_{O-\text{car}}$	Operating speed of cars	88.92	134.37	121.91	21.70
$\Delta V_{O-\text{car}}$	Speed difference of cars with the adjacent segment	−85.93	78.03	0.00	34.07
$V_{O-\text{truck}}$	Operating speed of trucks	60.38	104.86	78.80	12.34
$\Delta V_{O-\text{truck}}$	Speed difference of trucks with the adjacent segment	−34.01	25.72	0.01	19.89
ΔV_O	Speed difference between cars and trucks	12.64	73.99	43.11	16.99
Geometric characteristics					
R_{front}	Radius of the plane curve of the front section	5597.0	1000000.0	370713.6	478894.40
L_{front}	Length of the plane curve of the front section	45.0	3677.0	1218.48	703.48
R_{present}	Radius of the present plane curve	5597.0	1000000.0	370717.10	478891.70
L_{present}	Length of the present plane curve	45.0	3677.0	1218.48	703.48
R_{back}	Radius of the plane curve of the back section	5597.0	1000000.0	373043.70	479536.80
L_{back}	Length of the plane curve of the back section	45.0	3677.0	1218.48	703.48
$i_{\min}$	Minimum longitudinal grade of the current section	−1.63	1.63	0.00	0.47
$Ls_{\min}$	Length of the longitudinal slope corresponding to the minimum grade	240.00	1740.00	773.33	296.03
$i_{\max}$	Maximum longitudinal grade of the current section	−2.50	2.50	0.00	0.97
$Ls_{\max}$	Length of the longitudinal slope corresponding to the maximum grade	362.00	1740.00	652.63	248.00
Sight characteristics					
S_{car}	Stopping sight distance of cars	244.00	1009.90	439.06	142.23
S_{truck}	Stopping sight distance of trucks	52.00	279.50	87.48	29.92
H_{car}	Transverse clear distance of cars	0.02	6.59	1.66	1.71
H_{truck}	Transverse clear distance of trucks	0.00	0.47	0.06	0.06

Table 3: Random-parameter multivariate Poisson model estimation results.

Variables[1]	No.[2]	Rear-end estimate (t-stat)	Bumping-guardrail estimate (t-stat)	Other estimate (t-stat)	Noncasualty estimate (t-stat)	Casualty estimate (t-stat)
Constant	5	0.0432 (0.27)	0.501 (3.17)	−0.527 (−2.11)	−0.0332 (−0.21)	−0.430 (−1.13)
Traffic characteristics						
Interchange	3	—[3]	—	−0.422 (−2.91)	−0.164 (−1.95)	−0.601 (−2.55)
Black spots	5	0.0986 (1.24)	0.859 (9.77)	1.276 (7.17)	1.196 (9.54)	1.322 (4.88)
AADT	4	1.057 (11.06)	0.00000936 (3.00)	0.0000126 (2.52)	0.0000365 (11.55)	—
Speed characteristics						
$V_{O-\text{car}}$	5	−0.0131 (−3.63)	−0.00812 (−2.38)	−0.0140 (−2.63)	−0.0177 (−4.58)	−0.016 (−1.85)
$\Delta V_{O-\text{car}}$	5	0.0114 (3.31)	0.00828 (2.45)	0.0109 (2.09)	0.0119 (3.25)	0.0237 (2.45)
$V_{O-\text{truck}}$	2	0.0210 (3.14)	—	—	−0.0272 (3.82)	—
$\Delta V_{O-\text{truck}}$	4	−0.0190 (−4.09)	−0.00148 (0.22)	−0.0182 (−2.67)	−0.0221 (−4.40)	—
Geometric characteristics						
L_{front}	1	—	—	—	—	0.000251 (2.13)
R_{present}	2	0.000000361 (3.69)	—	—	0.000000375 (3.63)	—
L_{present}	5	0.000588 (10.32)	0.000468 (8.12)	0.000755 (8.09)	0.000753 (11.64)	0.000748 (6.25)
L_{back}	1	—	−0.000133 (−2.48)	—	—	—
$Ls_{\min}$	2	−0.000357 (−2.51)	—	—	−0.000423 (−2.83)	—
Sight characteristics						
S_{truck}	5	−0.00540 (−2.78)	−0.00633 (−2.86)	−0.0111 (−3.20)	−0.00706 (−3.44)	−0.0135 (−2.51)
H_{car}	3	−0.0860 (−2.13)	−0.105 (−2.57)	—	−0.0878 (−2.06)	—

Note: variables not shown here attribute to insignificant. [1]Variable definitions and units can be seen in Table 2. [2]Number of parameters estimated. [3]Insignificant at the 95% significance level. Total number of parameters: 52; log-likelihood: −14353.079; AIC: 28996.159; BIC: 29567.814; χ^2: 21264.957.

Table 4: Random-parameter multivariate negative binomial model estimation results.

Variables[1]	No.[2]	Rear-end estimate (t-stat)	Bumping-guardrail estimate (t-stat)	Other estimate (t-stat)	Noncasualty estimate (t-stat)	Casualty estimate (t-stat)
Constant	5	1.867 (1.77)	15.393 (15.21)	11.763 (0.02)	−0.604 (−3.49)	0.867 (0.85)
Traffic characteristics						
Interchange	3	—[3]	—	−0.422 (−2.91)	−0.165 (−2.05)	−0.636 (−2.58)
Black spots	5	1.048 (11.25)	0.859 (9.77)	1.276 (7.17)	1.052 (12.37)	1.274 (4.97)
AADT	5	0.0000254 (7.90)	0.00000936 (3.00)	0.0000126 (2.52)	0.0000322 (11.11)	−0.0000128 (−1.63)
Speed characteristics						
V_{O-car}	5	−0.0120 (−3.37)	−0.00795 (−2.32)	−0.0161 (−3.10)	−0.0180 (−5.34)	−0.0165 (−1.89)
ΔV_{O-car}	5	0.00999 (2.76)	0.00788 (2.29)	0.0120 (2.22)	0.0103 (3.07)	0.0231 (2.30)
$V_{O-truck}$	2	0.0200 (2.92)	—	—	−0.0326 (4.93)	—
$\Delta V_{O-truck}$	4	−0.0189 (−4.02)	−0.00948 (−2.12)	−0.020 (−3.18)	−0.0243 (−5.44)	—
Geometric characteristics						
R_{front}	2	0.000000173 (1.98)	—	—	0.00000017 (1.91)	—
L_{front}	1	—	—	—	—	0.000278 (2.44)
$R_{present}$	2	0.000000359 (3.72)	—	—	0.000000365 (3.75)	—
$L_{present}$	5	0.000557 (9.86)	0.000468 (8.12)	0.000672 (7.32)	0.000685 (11.07)	0.000747 (6.44)
L_{back}	1	—	−0.000133 (−2.48)	—	—	—
Ls_{min}	3	−0.000319 (−2.34)	—	—	−0.000453 (−3.19)	−0.000608 (−1.85)
Ls_{max}	1	—	—	—	−0.000420 (−2.17)	—
Sight characteristics						
S_{truck}	5	−0.00493 (−2.29)	−0.0059 (−2.61)	−0.0107 (−3.01)	−0.00706 (−3.44)	−0.0135 (−2.51)
H_{car}	2	—	−0.100 (−2.40)	—	−0.0878 (−2.06)	—

Total number of parameters: 56; log-likelihood: −14326.558; AIC: 28985.114; BIC: 29610.316; χ^2:23043.735.

end and bumping-guardrail crashes, which shows that these two crash types are not associated with the interchange areas.

The corresponding parameter of black spots offers a positive impact on crash occurrence for rear-end, bumping-guardrail, other, noncasualty, and casualty crashes revealing a higher likelihood of crashes with the increased proportion of black spots. More crashes across all the crash types occurred in the black spots than other sections. Similarly, the AADT offers a positive influence across the five crash types in the RPMNB model indicating more crashes occur with more traffic. Greater traffic volume results in higher crash risk [49]. Then, the AADT indicates no significance on the casualty crashes in the RPMP model.

4.2.3. Speed Characteristics. In terms of operating speed, the estimated results of both RPMP model and RPMNB model show that the higher operating speed of cars is likely to result in less crash risk across five crash types. The finding is expected because drivers of cars are likely to drive at a higher speed under good traffic conditions in the sections with great geometric alignment.

The estimated results show that the speed difference of cars with the adjacent segment shows the same positive effect on all the crash types. The higher speed difference of cars between adjacent segments leads to higher crash risk, and this finding is corresponding to the Solomon curve [18]. Oppositely, the speed difference of trucks with the adjacent segment shows the same negative effect on all the crash types except the casualty crash.

The result of trucks is contrary, and the estimated variable of the speed difference of trucks shows a negative influence on the rear-end, bumping-guardrail, other, and noncasualty crashes and an insignificant effect on the casualty crashes. The reasonable explanation is that the poor power and braking performance of trucks limit the operating speed. When the design speed reaches a certain value, the operating speed will not increase with the improvement of the geometric alignment. And the operating speed restricted by the poor geometric alignment of the sections reduces the crash risk. The operating speed of trucks has a positive influence on the risk of rear-end crashes and a negative influence on the noncasualty crashes. The higher operating speed of trucks leads to more rear-end crashes and less casualty in the crashes.

Relative to the cars, the trucks show poor power and braking performance. The greater operating speed results in a higher propensity of rear-end crashes and a smaller difference between cars and trucks, which lead to less collision impact and damage in the crashes.

4.2.4. Geometric Characteristics. The length of the present plane curve presents a positive effect on the five crash types, which is perhaps indicating that the longer length of the plane curve results in more crash risk propensity. The reasonable explanation for this result is that the drivers will adapt to the curvature of the curve gradually, causing the fatigue or distraction of drivers. Otherwise, this adaption causes the drivers to accelerate to the speed not suitable for the geometric alignment, leading to more crashes. The

positive effect of the radius of the present plane curve on the rear-end and casualty crashes shows the same tendency.

Concerning the radius of the plane curve of the front section, the variable is found to have a positive influence on the rear-end and noncasualty crashes with relatively little influence coefficients (0.000000359 and 0.000000365) in the RPMNB model. However, the estimated results are not found in the RPMP model. The vehicles will run at an uncoordinated speed when transiting to a smaller radius and increasing the rear-end crash propensity. Similarly, the coefficient of the length of the plane curve of the front section shows a positive influence on the casualty crashes. The length of the longitudinal slope corresponding to the minimum grade is also found to have a negative influence on the probability of rear-end, noncasualty, and casualty crashes in the RPMNB model. And in the RPMP model, only the rear-end and noncasualty crashes show significance. Among the road sections with the small longitudinal grade, the trucks show greater speed with less speed difference from cars, which promotes safety. In the RPMNB model, the length of the longitudinal slope corresponding to the maximum grade also presents a negative influence on the noncasualty crashes. However, the results are not present in the RPMP model.

4.2.5. Visibility Characteristics. As expected, the coefficient associated with the stopping sight distance of trucks offers a negative effect on the crash risk of all the crash types. The likelihood of all single-vehicle crashes will reduce with higher stopping sight distance of trucks.

The visibility field and distance in front of the vehicle are important for safe and effective driving on the highway. The speed and direction of the vehicles depend on the visibility of the ahead road and surrounding environment. Therefore, the higher stopping sight distance of the truck facilitates the drivers to control the direction more accurately, leading to fewer crashes. Meanwhile, the transverse clear distance of cars indicates negative effects on the rear-end, bumping-guardrail, and noncasualty crashes in the RPMP model. And the transverse clear distance of cars only shows a negative influence on bumping-guardrail and noncasualty crashes in the RPMNB model. The more transverse safe zone allows for a higher tolerance for vehicles, which leads to fewer crashes.

4.3. Model Comparisons. Statistical measures such as log-likelihood, AIC, and BIC values are calculated to measure the goodness of fit in the estimated models, and the results are shown in Table 5.

Based on the comparison of AIC and BIC values, we firstly find the models with zero-inflated effects are not suitable for the crash data in this study. Secondly, the models considering effects caused by unobserved heterogeneity perform better than the independent models. Finally, the proposed models estimate efficient and accurate parameters in the parsimonious model systems. To assess the predictive accuracy of the estimated models, we used RMSE (root mean square error), MAE (mean absolute error), and MAPE (mean absolute percentage error) for discussion. Table 6 presents the values of these measures.

Despite the difference in the total number of parameters between the two models (56 vs. 52), the performance of the two models across five crash types is quite similar. From the total values of the three measures, we can observe that the RPMNB model performs better than the RPMP model. From the perspective of different crash types, the RPMP model performs marginally better than the RPMNB model for the measures with respect to bumping-guardrail and noncasualty crashes, and RPMNB performs better in terms of rear-end, other, noncasualty, and casualty crashes. The difference in the number of parameters across the two models makes no effects on the deviation measures.

4.4. Elasticity Effects. To provide more insight and explain the marginal effects of the exogenous variables, the elasticity effect is computed for RPMNB and RPMNB across all the crash types. Elasticity effect denotes an estimate of the effect of a variable on the expected frequency assuming all the other variables take the average values. The elasticity effect is the effect on the expected frequency λ_i of a 1% change in the variable, which is as follows:

$$E_{x_{ik}}^{\lambda_i} = \frac{\partial \lambda_i}{\lambda_i} \times \frac{x_{ik}}{\partial x_{ik}} = \beta_k x_{ik}, \tag{19}$$

where x_{ik} is the value of the k_{th} independent variable for observation i; β_k is the estimated parameter for the k_{th} independent variable; and λ_i is the expected frequency for observation i.

As shown in Figure 1, there is not any large difference in the elasticity effects of the two models across five crash types. And almost half of the number of the variables make very little effects (41 out of 79).

We observe that there are significant differences in the elasticity effects for different crash types across different models. With respect to the length of the present plane curve for the rear-end crashes, the RPMNB model predicts a 27.4% increase, while a 52.7% increase from the RPMP. Most likely, the nonlinearity of the two models results in such differences.

5. Conclusions

The empirical analysis was based on the traffic crash data from the Beijing-Shanghai Highway for the year 2009–2011 and the road design and construction drawings including the road geometric features. The road geometric alignment, operating speed, traffic volume, and sight distance are considered as the exogenous variables across the traditional and proposed models.

The traditional negative binomial and Poisson models are commonly adopted in the analysis on crash count frequency to analyze the impacts of various factors. To reduce the influence of the unobserved heterogeneity and get higher dimensions, we adopt the random-parameter multivariate NB (RPMNB) model and random-parameter multivariate Poisson (RPMP) model to analyze the impacts on different

Table 5: Goodness-of-fit measure of six models.

Model	Total no.	Log-likelihood	AIC	BIC
Independent NB model	55	−14,352.787	29,007.581	29,602.802
Independent Poisson model	61	−16,595.848	33,441.697	33,934.501
ZIMNB model	53	−14,352.888	29,131.770	29,674.168
ZIMP model	53	−16,194.117	32,662.229	33,203.686
RPMNB model	52	−14,326.558	28,985.114	29,610.316
RPMP model	56	−14,353.079	28,996.159	29,567.814

Table 6: Predictive performance measure of two models (RPMNB and RPMP).

Crash type	RMSE		MAE		MAPE	
	RPMNB	RPMP	RPMNB	RPMP	RPMNB	RPMP
Rear-end	7.413	8.374	6.551	6.941	1.433	1.638
Bumping-guardrail	11.070	10.833∗	9.781	9.551∗	3.639	2.919∗
Other crash	12.222	12.983	10.661	11.051	5.349	5.989
Noncasualty crash	1.643	1.597∗	1.253	1.252∗	0.136	0.128∗
Casualty crash	14.351	15.105	12.811	13.298	10.372	11.116
Total	46.699	48.892	41.055	42.092	20.929	21.789

Note: RPMNB = random-parameter multivariate negative binomial model. RPMP = random-parameter multivariate Poisson model. ∗Measures where the RPMP model performs better.

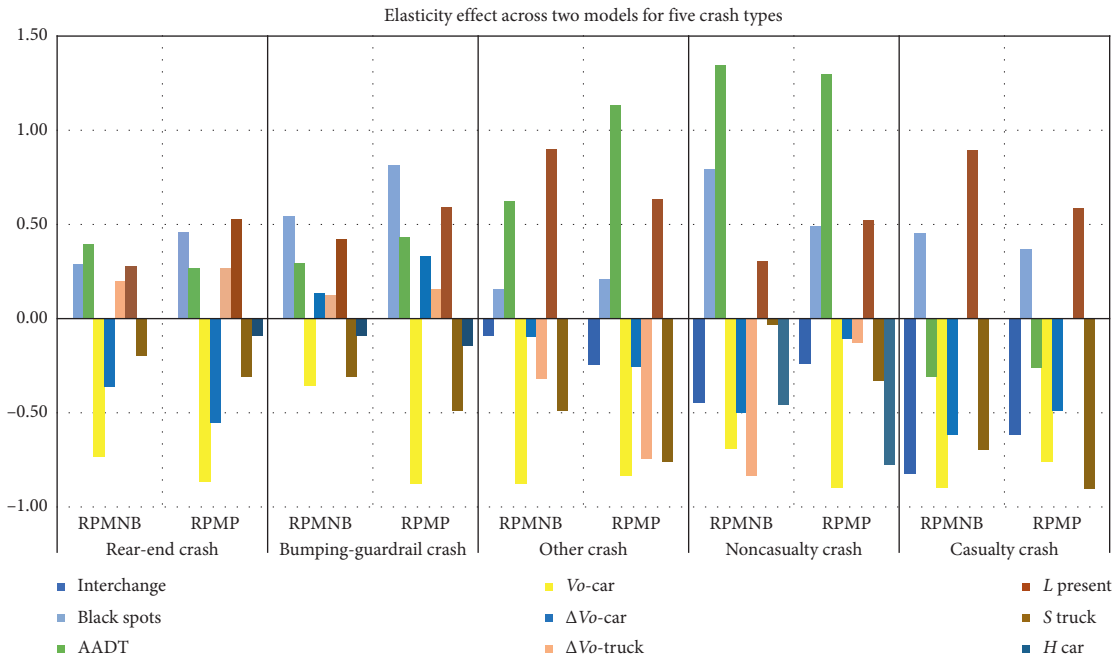

Figure 1: Elasticity effects across two models (RPMNB and RPMP) for 5 crash types.

crash types including rear-end, bumping-guardrails, noncasualty, and casualty crashes, with the traditional models as the base.

Viewing on the traffic characteristic, more rear-end, bumping-guardrail, other, and noncasualty crashes occurred with more black spots and AADT, while other, noncasualty, and casualty crashes happened in interchange sections less likely. For speed characteristics, the crash risk of five types is greater with the higher operating speed of cars, while greater speed difference of cars results in more crashes across five types. Oppositely, the greater speed difference of trucks results in less rear-end, bumping-guardrail, other, and noncasualty crashes. As for the road geometry, more crashes occurred on the longer length of the present plane curve, while the greater length of the longitudinal slope corresponding to the minimum grade reduces the crash propensity. Considering the sight characteristics, truck drivers with greater stopping sight distance perform safer on the highways.

From the perspective of road design, to avoid the long length of a plane curve with big curvature and reduce the length of the longitudinal slope with large grade are

Table 7: Independent negative binomial model estimation results.

Variables[1]	No.[2]	Rear-end estimate (t-stat)	Bumping-guardrail estimate (t-stat)	Other estimate (t-stat)	Noncasualty estimate (t-stat)	Casualty estimate (t-stat)
Constant	5	0.043 (0.27)	0.502 (3.07)	−0.528 (−2.11)	−0.033 (−0.21)	−0.431 (−1.13)
Traffic characteristics						
Interchange	3	—[3]	—	−0.422 (−2.91)	−0.165 (−1.95)	−0.601 (−2.55)
Black spots	5	1.057 (11.06)	0.859 (9.77)	1.276 (7.17)	1.196 (9.54)	1.322 (4.88)
AADT		0.00003 (8.66)	0.00001 (3.00)	0.00001 (2.52)	0.00004 (11.55)	—
Speed characteristics						
V_{O-car}	5	−0.013 (−3.63)	−0.008 (−2.38)	−0.014 (−2.63)	−0.017 (−4.58)	−0.016 (−1.85)
ΔV_{O-car}	5	0.011 (3.31)	0.008 (2.45)	0.010 (2.09)	0.011 (3.25)	0.023 (0.014)
$V_{O-truck}$	2	0.021 (3.14)	—	—	0.027 (3.82)	—
$\Delta V_{O-truck}$	4	−0.019 (−4.09)	−0.009 (−2.11)	−0.018 (−2.67)	−0.022 (−4.40)	—
Geometric characteristics						
L_{front}	1	—	—	—	—	0.000251 (2.13)
$R_{present}$	2	0.00000036 (3.63)	—	—	0.000000379 (3.60)	—
$L_{present}$	5	0.0005888 (10.28)	0.0004658 (8.04)	0.0007505 (8.02)	0.0007521 (11.57)	0.000750 (6.23)
L_{back}	1	—	−0.0001341 (−2.49)	—	—	—
Ls_{min}	4	−0.000356 (−2.5)	—	−0.0004069 (−1.88)	−0.0004248 (−2.83)	−0.000586 (−1.76)
Sight characteristics						
S_{truck}	5	−0.054 (−2.78)	−0.006 (−2.86)	−0.011 (−3.20)	−0.007 (−3.44)	−0.013 (−2.51)
H_{car}	3	−0.086 (−2.13)	−0.105 (−2.57)	—	−0.087 (−2.06)	—

Note: [1]variable definitions and units can be seen in Table 2. Variables not shown here attribute to insignificant. [2]Number of parameters estimated. [3]Insignificant at the 95% significance level. Total number of parameters: 55; log-likelihood: −14352.787; AIC: 29007.581; BIC: 29602.802; χ^2:21274.146.

Table 8: Independent Poisson model estimation results.

Variables[1]	No.[2]	Rear-end estimate (t-stat)	Bumping-guardrail estimate (t-stat)	Other estimate (t-stat)	Noncasualty estimate (t-stat)	Casualty estimate (t-stat)
Constant	5	0.177 (1.41)	0.515 (3.27)	−0.460 (−2.31)	0.228 (2.51)	−0.348 (−1.07)
Traffic characteristics						
Interchange	3	—[3]	—	−0.3482 (−3.01)	−0.088 (−1.93)	−0.529 (−2.54)
Black spots	5	1.020 (16.68)	0.859 (10.40)	1.227 (10.68)	1.083 (23.20)	1.316 (6.10)
AADT	5	0.0000236 (10.04)	0.00000909 (3.03)	0.000011 (2.77)	0.0000312 (18.14)	−0.000014 (0.047)
Speed characteristics						
V_{O-car}	5	−0.0134 (−5.96)	−0.00807 (−2.81)	−0.0144 (−3.73)	−0.0181 (−10.98)	−0.0154 (−2.05)
V_{O-car}	5	0.0119 (5.27)	0.00829 (2.85)	0.0112 (2.80)	0.0124 (7.53)	0.0219 (2.70)
$V_{O-truck}$	2	0.0209 (4.86)	—	—	0.0285 (8.90)	—
$\Delta V_{O-truck}$	4	−0.0196 (−6.81)	−0.00939 (−2.54)	−0.0190 (−3.90)	−0.0234 (−11.05)	—
Geometric characteristics						
R_{front}	2	0.000000154 (2.54)	—	—	0.000000148 (3.36)	—
L_{front}	3	—	—	—	0.0000506 (1.94)	0.000272 (2.62)
$R_{present}$	2	0.000000410 (6.12)	—	—	0.000000375 (7.71)	—
$L_{present}$	5	0.000567 (15.62)	0.000460 (9.02)	0.000659 (10.59)	0.000630 (24.12)	0.00075 (7.16)
L_{back}	1	—	−0.000131 (−2.71)	—	—	—
i_{min}	1	—	—	—	−0.108 (−2.44)	—
Ls_{min}	4	−0.0003483 (−3.67)	—	−0.0004866 (−2.91)	−0.000437 (−6.18)	−0.000644 (−2.12)
Sight characteristics						
S_{truck}	5	−0.00644 (−4.78)	−0.00641 (−3.35)	−0.0118 (−4.28)	−0.00847 (−8.14)	−0.0142 (−3.03)
H_{car}	4	−0.104 (−3.93)	−0.106 (−3.06)	−0.110 (−2.37)	−0.1232 (−6.11)	—

Total number of parameters: 61; log-likelihood: −16595.848; AIC: 33441.697; BIC: 33934.501; χ^2:50507.432.

beneficial for highway safety. To reduce the interference between cars and trucks, it is suggested to adopt the lane distribution mode of different vehicle types. Set up door-frame traffic signs along with pavement markings to remind the drivers of trucks to drive in the outside lane and the ones of cars to drive in the inside lane.

With respect to the data fit, the comparison exercise including log-likelihood, AIC, and BIC value highlights the superiority of the multivariate models over the traditional models. Based on the exercise, the RPMNB model shows identical performance even with more numbers of significant parameters compared with the RPMP model (56 vs. 52).

Table 9: Zero-inflated multivariate negative binomial model estimation results.

Variables[1]	No.[2]	Rear-end estimate (t-stat)	Bumping-guardrail estimate (t-stat)	Other estimate (t-stat)	Noncasualty estimate (t-stat)	Casualty estimate (t-stat)
Constant	5	0.0433 (0.27)	0.501 (3.07)	−0.527 (−2.11)	−0.0191 (−0.12)	−0.430 (−1.13)
Traffic characteristics						
Interchange	3	—[3]	—	−0.422 (−2.91)	−0.164 (−1.95)	−0.601 (−2.55)
Black spots	5	1.057 (11.06)	0.859 (9.77)	1.276 (7.17)	1.196 (9.54)	1.322 (4.88)
AADT	4	0.0000263 (8.66)	0.00000936 (3.00)	0.0000126 (2.52)	0.0000365 (11.55)	—
Speed characteristics						
V_{O-car}	5	−0.0131 (−3.63)	−0.00812 (−2.38)	−0.0140 (−2.63)	−0.0177 (−4.58)	−0.0161 (−1.85)
ΔV_{O-car}	5	0.0114 (3.31)	0.00828 (2.45)	0.0109 (2.09)	0.0119 (3.25)	0.0237 (2.45)
$V_{O-truck}$	2	0.0210 (3.14)	—	—	0.0272 (3.82)	—
$\Delta V_{O-truck}$	4	−0.0190 (−4.09)	−0.00934 (−2.11)	−0.0182 (−2.67)	−0.0221 (−4.40)	—
Geometric characteristics						
L_{front}	1	—	—	—	—	0.000251 (2.13)
$R_{present}$	2	0.000000361 (3.69)	—	—	0.000000375 (3.63)	—
$L_{present}$	5	0.000588 (10.32)	0.000468 (8.12)	0.000755 (8.09)	0.000753 (11.64)	0.000748 (6.25)
L_{back}	1	—	−0.000133 (−2.48)	—	—	—
Ls_{min}	3	−0.000357 (−2.51)	—	—	−0.000423 (−2.83)	−0.000588 (−1.76)
Sight characteristics						
S_{truck}	5	−0.00540 (−2.78)	−0.00633 (−2.86)	−0.0111 (−3.20)	−0.00706 (−3.44)	−0.0135 (−2.51)
H_{car}	3	−0.0860 (−2.13)	−0.105 (−2.57)	—	−0.0878 (−2.06)	—

Total number of parameters: 53; log-likelihood: −14352.888; AIC: 29131.777; BIC: 29674.168; χ^2:19426.561.

Table 10: Zero-inflated multivariate Poisson model estimation results.

Variables[1]	No.[2]	Rear-end estimate (t-stat)	Bumping-guardrail estimate (t-stat)	Other estimate (t-stat)	Noncasualty estimate (t-stat)	Casualty estimate (t-stat)
Constant	5	0.177 (1.41)	0.515 (3.27)	−0.228 (−1.02)	0.426 (4.48)	−0.0568 (−0.16)
Traffic characteristics						
Interchange	2	—[3]	—	−0.314 (−2.48)	—	−0.552 (−2.46)
Black spots	5	1.020 (16.68)	0.859 (10.40)	1.004 (7.92)	1.050 (22.56)	1.230 (5.18)
AADT	4	0.0000236 (10.04)	0.00000909 (3.03)	0.0000114 (2.62)	0.0000282 (15.83)	—
Speed characteristics						
V_{O-car}	4	−0.0134 (−5.96)	−0.00807 (−2.81)	−0.00999 (−2.21)	−0.0155 (−9.21)	—
ΔV_{O-car}	4	0.0119 (5.27)	0.00829 (2.85)	—	0.0113 (6.76)	0.0235 (2.48)
$V_{O-truck}$	2	0.0209 (4.86)	—	—	0.0228 (6.93)	—
$\Delta V_{O-truck}$	4	−0.0196 (−6.81)	−0.00939 (−2.54)	−0.0142 (−2.62)	−0.202 (−9.33)	—
Geometric characteristics						
R_{front}	2	0.000000154 (2.54)	—	—	0.000000110 (2.45)	—
L_{front}	1	—	—	—	—	0.000239 (2.13)
$R_{present}$	2	0.00000041 (6.12)	—	—	0.000000336 (6.75)	—
$L_{present}$	5	0.000567 (15.62)	0.000460 (9.02)	0.000606 (8.71)	0.000595 (21.66)	0.000735 (6.54)
R_{back}	1	—	—	—	0.000000093 (2.08)	—
L_{back}	1	—	−0.000131 (−2.71)	—	—	—
Ls_{min}	3	−0.000348 (−3.67)	—	−0.000545 (−3.07)	−0.000423 (−2.83)	—
Sight characteristics						
S_{truck}	5	−0.00644 (−4.78)	−0.00641 (−3.35)	−0.0106 (−3.51)	−0.00696 (−6.65)	−0.0137 (−2.61)
H_{car}	3	−0.104 (−3.93)	−0.106 (−3.06)	—	−0.107 (−5.39)	—

Total number of parameters: 53; log-likelihood: −16194.117; AIC: 32662.229; BIC: 33203.686; χ^2:41460.088.

To quantify the predictive performance measure, we calculate the elasticity effects of significant variables including interchange, black spots, AADT, V_{O-car}, ΔV_{O-car}, $\Delta V_{O-truck}$, $L_{present}$, S_{truck}, and H_{car} for both RPMNB and RPMP models. Significant differences in the elasticity effects exist for different crash types across the two models, which are attributed to the nonlinearity of the two models.

Really, more efforts can be done on further research. With the respect to the variables, more detailed information can be added to reduce the parameter explosion, such as the proportion of trucks in each section and distinguishing the rear-end crash between different vehicle types. Otherwise, the spatial and temporal terms of the crashes are beneficial for the models to reduce the potential unobserved effects,

which can be considered in the future. Furthermore, the other methodological approaches such as latent-class, finite-mixture, and Markov switching models can be used to confirm the finding of this study.

Appendix

The estimation results of the independent negative binomial (INB) model, independent Poisson (IP) model, zero-inflated multivariate negative binomial (ZIMNB) model, and zero-inflated multivariate Poisson (ZIMP) model are shown in Tables 7–10. And the goodness-of-fit measure of the four models is shown in Table 5.

Based on the comparison in Table 5, the ZIMNB model has higher AIC and BIC values than the independent NB model and RPMNB model. The length of the longitudinal slope corresponding to the minimum grade indicates a negative influence on the casualty crashes in the ZIMNB model, while the same result is not shown in the RPMNB model.

As shown in Table 8, the number of parameters estimated in the ZIMP model is 53, which is the least in the three Poisson models. For example, the common significant factors such as interchange show no significance on the noncasualty crashes in the ZIMP model. However, the bigger AIC and BIC values indicate that the ZIMP model performs worse than the RPMP model, even with fewer parameters.

Data Availability

Yearly crash data and roadway geometric data from the Beijing-Shanghai Highway from Xinyi to Jiangdu, from 2009 to 2011, were collected from the traffic management department in this article.

Conflicts of Interest

The authors declare no conflicts of interest.

Authors' Contributions

All authors reviewed the results and approved the final version of the manuscript.

Acknowledgments

This study was supported by the Project of the National Natural Science Foundation of China (Grant nos. 51768063 and 51868068).

References

[1] M. A. Rupp, M. D. Gentzler, and J. A. Smither, "Driving under the influence of distraction: examining dissociations between risk perception and engagement in distracted driving," *Accident Analysis & Prevention*, vol. 97, pp. 220–230, 2016.

[2] M. A. Regan, C. Hallett, and C. P. Gordon, "Driver distraction and driver inattention: definition, relationship and taxonomy," *Accident Analysis and Prevention*, vol. 43, no. 5, pp. 1771–1781, 2011.

[3] T. Horberry, J. Anderson, M. A. Regan, T. J. Triggs, and J. Brown, "Driver distraction: the effects of concurrent in-vehicle tasks, road environment complexity and age on driving performance," *Accident Analysis & Prevention*, vol. 38, no. 1, pp. 185–191, 2006.

[4] T. J. Babukov, *Road Condition and Traffic Safety*, Tongji University Press, Shanghai, China, 1990.

[5] C. V. Zegeer, D. Reinfurt, T. Neuman et al., "Safety improvements on horizontal curves for two-lane rural roads-informational guide (FHWA-RD-90-074)," *Curves*, 1991.

[6] C. V. Zegeer, J. R. Stewart, F. M. Council, D. W. Reinfurt, and E. Hamilton, "Safety effects of geometric improvements on horizontal curves," *Transportation Research Record*, vol. 1356, 1992.

[7] J. McFadden and L. Elefteriadou, "Evaluating horizontal alignment design consistency of two-lane rural highways: development of new procedure," *Transportation Research Record: Journal of the Transportation Research Board*, vol. 1737, no. 1, pp. 9–17, 2000.

[8] H. W. McGee, W. E. Hughes, and K. Daily, *Effect of Highway Standards on Safety*, Transportation Research Board, Washington, DC, USA, 1995.

[9] Y. L. Pei and J. Ma, "Research on countermeasures for road condition causes of traffic accidents," *China Journal of Highways*, vol. 16, no. 4, pp. 77–82, 2003.

[10] Y. Hassan, S. M. Easa, and A. El Halim, "Analytical model for sight distance analysis on three-dimensional highway alignments," *Transportation Research Record: Journal of the Transportation Research Board*, vol. 1523, no. 1, pp. 1–10, 1996.

[11] S. M. Easa, T. R. Strauss, Y. Hassan, and R. R. Souleyrette, "Three-dimensional transportation analysis: planning and design," *Journal of Transportation Engineering*, vol. 128, no. 3, pp. 250–258, 2002.

[12] S. M. Easa, Y. Hassan, and Z. A. Karim, "Establishing highway vertical alignment using profile field data," *ITE Journal*, vol. 68, no. 8, pp. 81–86, 1998.

[13] Y. Hassan, S. M. Easa, and A. O. Abd El Halim, "State-of-the-art of three-dimensional highway geometric design," *Canadian Journal of Civil Engineering*, vol. 25, no. 3, pp. 500–511, 1998.

[14] M. Hasan, T. Sayed, and Y. Hassan, "Influence of vertical alignment on horizontal curve perception: effect of spirals and position of vertical curve," *Canadian Journal of Civil Engineering*, vol. 32, no. 1, pp. 204–212, 2005.

[15] J. A. Reagan, "The interactive highway safety design model: designing for safety by analyzing road geometrics," *Public Roads*, vol. 58, no. 1, 1994.

[16] W. Levison, ""Interactive highway safety design model: issues related to driver modeling," *Transportation Research Record: Journal of the Transportation Research Board*, vol. 1631, no. 1, pp. 20–27, 1998.

[17] FHWA, *Interactive Highway Safety Design Model*, IHSDM, Chicago, IL, USA, 2017.

[18] D. Solomon, *Accidents on Main Rural Highways Related to Speed, Driver, and Vehicle*, Bureau of Public Roads, U.S. Department of Transportation, Washington, DC, USA, 1964.

[19] R. Elvik, P. Christensen, and A. H. Amundsen, "Speed and road accidents: an evaluation of the power model," Report 740, Institute of Transport Economics, Oslo, Norway, 2004.

[20] X. S. Fu, *Study on Theoretical Speed and Highway Alignment Design and Evaluation Method*, Chang'an University, Xi'an, China, 2008.

[21] AASHTO, *A Police on Geometric Design of Highways and Streets*, American Association of State Highway and Transportation Officials, Washington, DC, USA, 2011.

[22] R. Lamm and E. M. Choueiri, *Recommendations for Evaluating Horizontal Design Consistency Based on Investigations in the State of New York*, Transportation Research Board, Washington, DC, USA, 1987.

[23] R. Lamm, B. Psarianos, and T. Mailaender, *Highway Design and Traffic Safety Engineering Handbook*, McGraw-Hill, New York, NY, USA, 1999.

[24] I. Anderson and R. Krammes, "Speed reduction as a surrogate for accident experience at horizontal curves on rural two-lane highways," *Transportation Research Record: Journal of the Transportation Research Board*, vol. 1701, no. 1, pp. 86–94, 2000.

[25] R. A. Krammes, K. D. Tyer, D. R. Middleton et al., "An alternative to post-mounted delineators at horizontal curves on two-lane highways (FHWA/TX-90/1145-1F)," *Geometric Design*, 1990.

[26] R. A. Krammes, R. Q. Brackett, M. A. Shafer et al., "Horizontal alignment design consistency for rural two-lane highways," *Geometric Design (FHWA-RD-94-034)*, 1995.

[27] J. Collins, K. Fitzpatrick, K. Bauer et al., "Speed variability on rural two-lane highways," *Transportation Research Record: Journal of the Transportation Research Board*, vol. 1658, no. 1, pp. 60–69, 1999.

[28] K. Fitzpatrick, "Speed prediction for two-lane rural highway," Federal Highway Administration, US Department of Transportation, Washington, DC, USA, FHWA-RD-99-171, 2000.

[29] R. Lamm, E. M. Choueiri, and T. Mailaender, "Comparison of operating speeds on dry and wet pavements of two-lane rural highways," *Transportation Research Record*, vol. 1280, no. 1, pp. 199–207, 1990.

[30] R. Lamm, B. Psarianos, E. M. Chourieri, and G. Soilemezoglou, "A practical safety approach to highway geometric design. International case studies: Germany, Greece, Lebanon and the United States," in *Proceedings of the International Symposium on Highway. Geometric Design Practices*, Transportation Research Board, Boston, MA, USA, August 1995.

[31] A. Jacob and M. V. L. R. Anjaneyulu, "Operating speed of different classes of vehicles at horizontal curves on two-lane rural highways," *Journal of Transportation Engineering*, vol. 139, no. 3, pp. 287–294, 2012.

[32] A. Maji, G. Sil, and A. Tyagi, "85th and 98th percentile speed prediction models of car, light, and heavy commercial vehicles for four-lane divided rural highways," *Journal of Transportation Engineering, Part A: Systems*, vol. 144, no. 5, Article ID 04018009, 2018.

[33] A. Maji and A. Tyagi, "Speed prediction models for car and sports utility vehicle at locations along four-lane median divided horizontal curves," *Journal of Modern Transportation*, vol. 26, no. 4, pp. 278–284, 2018.

[34] G. Sil and A. Maji, "Video based data collection process for geometric design consistency evaluation of four-lane median divided horizontal curves," *Transportation Research Procedia*, vol. 27, pp. 672–679, 2017.

[35] The Ministry of Transportation of the People's Republic of China, *Specifications for Highway Safety Audit: JTG B05-2015*, People's Communications Press, Beijing, China, 2016.

[36] M. A. Mohammadi, V. A. Samaranayake, and G. H. Bham, "Crash frequency modeling using negative binomial models: an application of generalized estimating equation to longitudinal data," *Analytic Methods in Accident Research*, vol. 2, pp. 52–69, 2014.

[37] X. Wang and M. Abdel-Aty, "Temporal and spatial analyses of rear-end crashes at signalized intersections," *Accident Analysis & Prevention*, vol. 38, no. 6, pp. 1137–1150, 2006.

[38] E. Chen and A. P. Tarko, "Modeling safety of highway work zones with random parameters and random effects models," *Analytic Methods in Accident Research*, vol. 1, pp. 86–95, 2014.

[39] F. L. Mannering, V. Shankar, and C. R. Bhat, "Unobserved heterogeneity and the statistical analysis of highway accident data," *Analytic Methods in Accident Research*, vol. 11, pp. 1–16, 2016.

[40] D. Lambert, "Zero-inflated Poisson regression, with an application to defects in manufacturing," *Technometrics*, vol. 34, no. 1, pp. 1–14, 1992.

[41] C. Gouriéroux, "The econometrics of discrete positive variables: the Poisson model," *Econometrics Of Qualitative Dependent Variables*, pp. 270–283, Cambridge University Press, New York, NY, USA, 2000.

[42] R. Winkelmann, "Seemingly unrelated negative binomial regression," *Oxford Bulletin of Economics and Statistics*, vol. 62, no. 4, pp. 553–560, 2000.

[43] J. M. Hilbe, *Negative Binomial Regression*, Cambridge University Press, Cambridge, UK, 2007.

[44] R. Winkelmann, *Econometric Analysis of Count Data*, Springer, Berlin, Germany, 2008.

[45] P. C. Anastasopoulos, V. N. Shankar, J. E. Haddock, and F. L. Mannering, "A multivariate Tobit analysis of highway accident-injury-severity rates," *Accident Analysis & Prevention*, vol. 45, pp. 110–119, 2012.

[46] P. W. Simon, G. K. Matthew, and L. M. Fred, *Statistical and Econometric Methods for Transportation Data Analysis*, CRC Press, Boca Raton, FL, USA, 2004.

[47] D. J. Spiegelhalter, N. G. Best, B. P. Carlin, and A. van der Linde, "Bayesian measures of model complexity and fit," *Journal of the Royal Statistical Society: Series B (Statistical Methodology)*, vol. 64, no. 4, pp. 583–639, 2002.

[48] B. H. Pang, B. Liu, H. Y. Zhou, Y. F. Hou, and S. Q. Wu, "Design index of transition section of ramp lane number change," *Journal of Chang'an University (Natural Edition)*, vol. 38, no. 1, pp. 82–88, 2018.

[49] J. B. Hu, L. C. He, and R. H. Wang, "Review of Safety evaluation of freeway interchange," *China Journal of Highway Transportation*, vol. 33, no. 7, pp. 17–27, 2020.

[50] Y. Zhang, Y. Xie, and L. Li, "Crash frequency analysis of different types of urban roadway segments using generalized additive model," *Journal of Safety Research*, vol. 43, no. 2, pp. 107–114, 2012.

Hindawi
Discrete Dynamics in Nature and Society
Volume 2020, Article ID 4760862, 15 pages
https://doi.org/10.1155/2020/4760862

Research Article

A Comparative Analysis of Strategic Values of Four Silk-Road International Transport Corridors Based on a Fuzzy Integral Method with Comprehensive Weights

Chengfu Wang,[1,2] Chengfeng Huang ,[1] Haichang Guan,[1] and Tao Zeng[1]

[1]*School of Economics and Management, Chongqing Jiaotong University, Chongqing 400074, China*
[2]*School of Management, Chongqing University of Technology, Chongqing 400054, China*

Correspondence should be addressed to Chengfeng Huang; 981327204@qq.com

Received 27 July 2020; Revised 31 October 2020; Accepted 6 November 2020; Published 24 November 2020

Academic Editor: Tingsong Wang

This paper carries out a comparative analysis of the strategic values of four silk-road international transport corridors, "China-Pakistan-Iran-Turkey" (CPIT), "China-Mongolia-Russia" (CMR), "Bangladesh-China-India-Myanmar" (BCIM), and "China-Singapore-Egypt-Greece" (CSEG). These corridors aim to reactivate the Northwest, North, South, and Marine Silk Road during the period of the "Belt and Road" (B&R), reflect China's overarching strategic goal of "furnishing land-sea internal and external linkage and achieving east-west mutual aid," and possess important strategic values. To facilitate the comparison, this paper constructs a hierarchical model and evaluation index system for assessing the strategic value of international transport corridors (SVITC). From China's perspective, this paper uses a fuzzy integral method with comprehensive weights to evaluate and compare the SVITC of the four international corridors as fuzzy integrals can handle interdependent indices and comprehensive weights can accommodate both subjective and objective weights. In the evaluation process, we first clarify the strategic attributes and characteristics of each corridor and identify its corresponding missions so that the overseas infrastructure projects along the four corridors can be carried out smoothly. By assessing their strategic values and ranking them accordingly, we offer the policy maker with useful information to prioritize investment opportunities and deploy limited resources in the construction of these corridors. Finally, this comparative study identifies the weaknesses and strengths in different corridors, which allow them to learn from each other, make joint progress, and strengthen linkages and integrations, thereby providing a set of feasible solutions for the construction of B&R international corridors.

1. Introduction

As an extension of China's long maritime and land borders, its historical Silk Road consists of four international transport corridors, including the Northwest Oasis, Northern Grassland, South (Southwest), and Maritime Silk Road. These four corridors correspond to four exit routes located in Xinjiang, Inner Mongolia, Yunnan, and Tibet, and the eastern coastline as well as their extension lines, respectively. Stretching for thousands of miles and lasting for thousands of years, the Silk Road carries out China's trade and cultural interactions with different regions, countries, nations, and districts, which has important strategic value since ancient times. Under the current "Belt and Road" (B&R) initiative, the conception or construction of the four international transport corridors, "China-Mongolia-Russia" (CMR), "Bangladesh-China-India-Myanmar" (BCIM), "China-Pakistan-Iran-Turkey" (CPIT), and "China-Singapore-Egypt-Greece" (CSEG), aims to reinvigorate the historical Silk Road in the north, southwest, northwest, and sea, respectively. They constitute an important core of the B&R international transport corridors and embody the grand strategic goal of "furnishing land-sea internal and external linkages and achieving east-west mutual aids." In the era of combating deglobalization, trade friction, and rampant populism, China proposes its own solution to promote globalization and free trade. By providing the public goods of international infrastructure, China lays out the foundation for the world to maintain interactions and communications, which has great

strategic values for both China and partner nations along the corridors. Moreover, megainfrastructure projects are a Chinese tradition; ranging from the Great Wall as an ancient defense structure to Grand Canal as a significant water highway connecting Beijing and Hangzhou and the more recent Three-Gorge Dam on the Yangtze River. The aforesaid megaprojects were constructed on Chinese territory. On the contrary, most of the infrastructure construction along the Silk Road will take place beyond China's borders and, thus, will bring additional challenges outside its control [1]. At the same time, despite the establishment of the Silk Road Fund and the proposal of the Asian Infrastructure Investment Bank, there remains a huge financial gap in international infrastructure construction projects, which often requires enormous investments. For example, the Asian Development Bank (ADB) estimated Asia's infrastructure funding gap at a massive $8 trillion through 2020 [2]. Given the aforesaid challenges, firstly, we clarify the strategic attributes and characteristics of the four corridors and identify their corresponding missions so that concrete suggestions can be offered to facilitate the smooth construction of overseas infrastructure along these corridors. Secondly, we put forward an effective evaluation framework to assess the strategic value of the four corridors, thereby obtaining their relative ranking. Given the huge funding gap in B&R infrastructure investments, this research contributes to long-term overall planning and prioritization of different investment opportunities, thereby allowing the policy makers to make more informed decisions in funding allocation. Finally, the comparison among the corridors allows them to learn from each other, make joint progress, and strengthen linkages and integrations, thereby providing a set of feasible solutions for the construction of B&R international corridors.

In recent years, research on transportation corridors has been carried out from different angles such as economy, risk, and security. In particular, the studies on the economic impact of corridors are the primary concern. From the perspective of user benefits, Regmi and Hanaoka utilized a time-cost-distance approach to assess and compare the performance of transport corridors [3]. This is a direct economic result. Berechman et al., Vinokurov and Tsukarev, and Donaldson evaluated not only direct but also indirect economic results such as the general economic development, including trade flows, economic welfare, and other issues [4–6]. Berg et al. and Roberts et al. studied the impact of large transport infrastructure projects from a wider perspective covering economic performance, social benefits, environmental quality, and other issues [7–11]. Hahm and Raihan suggested maximizing a wider economic impact of the B&R economic belt by accounting for social and environmental risks [12]. Chang and Khan considered other issues such as maritime cooperation and security [13].

To the best of the authors' knowledge, limited research is conducted on assessing the SVITC. Wang and Zhu characterized strategic values from different angles such as political diplomacy, security, and economy and assessed the SVITC of the CMR international corridor from the perspectives of China, Mongolia, and Russia, respectively [14]. From a qualitative perspective, Lin examined the impact of the China-Nepal-India economic corridor on China's internal affairs, diplomacy, economy, energy, and so on, thereby illuminating the necessity and feasibility of the construction as well as its content and path [15]. In essence, this transport corridor is the Tibet exit route in addition to the Yunnan exit route of the Southern Silk Road. From the perspectives of China and Pakistan, Li and Sun qualitatively described the strategic value of the China-Pakistan Economic Corridor (CPEC) by considering geopolitics, economy, and security [16]. Zubir and Malik analyzed the strategic value of key nodes from military and economic value perspectives from the standpoint of the Strait of Malacca and the Gwadar Port, respectively [17, 18]. Yang et al. quantitatively evaluated the strategic value of the Ryukyu Island, oil and gas resources in the South China Sea, islands and reefs in the South China Sea and other key nodes, and regions or specific resources in the marine international transport corridor. Their research takes a nonnational angle to conduct strategic value assessment [19–21]. Yang et al. carried out a qualitative analysis from the perspective of geopolitics and route trend of BCIM, which is a particular aspect of SVITC [22, 23].

In summary, current studies about transport corridors have gradually extended from a purely economic perspective to a wider economic perspective including society, environment, and security. Firstly, following this idea, research can be further extended from the broader perspective to a systematic level of the strategic value that accounts for political, military, and cultural aspects. Secondly, current studies on the SVITC are mostly carried out from a single channel or focus on a key node in a qualitative manner. In contrast, this research takes the whole network of the Silk Road as our subject and considers the four international corridors in a much bigger scope. When assessing their SVITC and carrying out the comparative analysis, we rely on a quantitative framework. This research helps us to obtain an overall assessment of B&R projects along the four corridors.

2. An Evaluation Index System and Hierarchy Theory of Assessing SVITCs

2.1. Construction of an Evaluation Index System of SVITCs. A narrow definition of international transport corridors is a route network that crosses the borders of two or more sovereign countries, including roads, railways, air transport, waterways, and pipelines. An international corridor provides an infrastructure and platform for the relevant nations to maintain interactions and communications. Moreover, as an international public product, it often has the characteristics of national interest [24]. Therefore, the research subjects of international transport corridors are actually the sovereign countries along the route, which is a scope of a national perspective. From this point of view, the "first existence" of strategies is national interests [25]. The key to success or failure of a grand strategy is the attempt by different powers to integrate their overall political, economic, and military objectives and, thus to preserve their long-term national interests [26]. It is clear that national interests are the essence and key of a strategy. In addition, a value is a degree to which an object meets the needs of the

subject through their interaction. Therefore, the SVITC is the degree to which a sovereign state along the route meets its national interests via interaction with other countries along or around the route with the aid of the route network of the international transport corridor.

As Waltz put it, "national interests are a small number of big and important things" [27]. More specifically, national interests refer to the main benefits and rights pursued by a nation, which reflect the collective needs and interests of its citizens and various interest groups. National interests are essentially a comprehensive weighted value that accounts for both objective benefits (such as territorial integrity, economic strength, and military power) and subjective interests (such as image and self-esteem) [28]. From the perspective of needs and desires, national interests can be defined from both a material and spiritual angle. Materially, a country needs security and development; spiritually, it needs respect and recognition from the international community [29]. According to Kortunov's holistic approach to identifying sources of national interests, each country has to fulfill a historical mission. Typically, a mission is deeply rooted in the culture, history, and geopolitical position of a particular country, which cannot be freely chosen, changed, or rejected. A country that cannot follow its mission is doomed to decline and eventually collapse [30]. Different cultural traits can influence a country's subjective definition of its objective national interests [31]. Based on the aforesaid viewpoints, one can see that national interests, as a comprehensive weighted value, are related to national sovereignty, economy, military, security, society, culture, political diplomacy, and so on. At the same time, it needs to make trade-offs for the overlapped and partially overlapped indices. For instance, national sovereignty is also a comprehensive and overlapping concept covering security, military, economy, politics, culture, and society, among others, where national security can be roughly gauged by national military. Moreover, an international corridor has to consider its geographical limits, but a well-connected network helps to reduce travel time and expand the scope. As such, this paper confines politics to a geopolitical consideration.

Given the aforesaid analysis, this research first defines an evaluation index system to evaluate SVITC as a comprehensive weight of cultural, geopolitical, social, military, and economic values, denoted by C (Culture), P (Politics), S (Society), M (Military), and E (Economy) in Figure 1 below.

2.2. A Hierarchy Theory of SVITC. SVITC research on a corridor considers it as an interactive carrier system to meet national interests of sovereign countries along the corridor. As mentioned earlier, national interests reflect the collective needs and desires of its citizens and various interest groups. From a micropoint of view, countries are made up of people. State behavior is bounded rational behavior of a group, and state needs can be regarded as demands from the vast majority of citizens in a country [32]. Therefore, to decompose national interests into a citizen level, one can see that they presumably integrate individual demands and desires and, hence, the underlying logic conforms to Maslow's theory of hierarchy needs, which, from the bottom to the top, covers physiological (survival) (seeking basic necessities of life), safety (seeking security through order and law), belongingness and love needs (seeking affiliation with a group), esteem (seeking esteem through recognition or achievement), and self-actualization needs (seeking fulfillment of personal potentials) [33]. In parallel, this paper models the demands and desires of the national interests as the five levels of economy, military, society, geopolitics, and culture following Maslow's theory. This mapping matches the survival, safety, belongingness, respect, and self-realization needs at a national level. To project national interests into SVITC, we thus construct a hierarchical model of SVITC as shown in Figure 2. At the same time, as the right of Figure 2 indicates, national development can be divided into three stages, the subsistence stage (covering economy and military values), the well-off stage (including social and geopolitical values), and the wealthy stage (corresponding to cultural value).

Figure 2 clearly shows that the relationship between the values in the evaluation index system of SVITC is not a parallel but a hierarchical structure. The general idea of Maslow's theory is that the needs of the lower level should be satisfied prior to those of the higher levels. This is not only true at an individual level but also at a national level though exceptions exist as needs are also related to the characteristics of the endowment rooted in national cultural genes. Lower level needs are foundational and subsistent, which offer guarantees for higher-level needs. Among them, national security is generally regarded as a red line and is inviolable. When a country's territorial integrity is threatened, it will normally vow to defend at any expense. Furthermore, the foundations must be strong to furnish solid support for upper-level needs. At a national level, its economy and military determine the stability of the upper structure. At the same time, higher-level needs often set up a framework for lower-level needs, especially the tradition of culture, which is deeply rooted in the collective subconsciousness of different countries and has strong inertia. The needs across different levels or at the same level can promote or contain each other. In short-term emergencies, a certain value may be sacrificed in exchange for another value. For example, during the COVID-19 pandemic, China took the initiatives to lock down Wuhan and the whole country for an extended period of time. This extraordinary measure is to sacrifice short-term economic value for social value, namely, to contain the virus spread and protect the lives, health, and well-being of all its citizens. At the same development stage, such as the economy and the military value (subsistence stage), without sacrificing the red line of national security, a dynamic balance should be struck by balancing their mutual restraints and promotion. In other words, the economy cannot be damaged by an unconstrained arms race, but strategic military deterrence can safeguard national security and create a stable and secure environment for economic development. However, no matter how to promote and restrain each other across different levels or at the same development stage, these values collectively serve national interests of sovereign states and aim to achieve overall utility maximization of national interests in a dynamic environment.

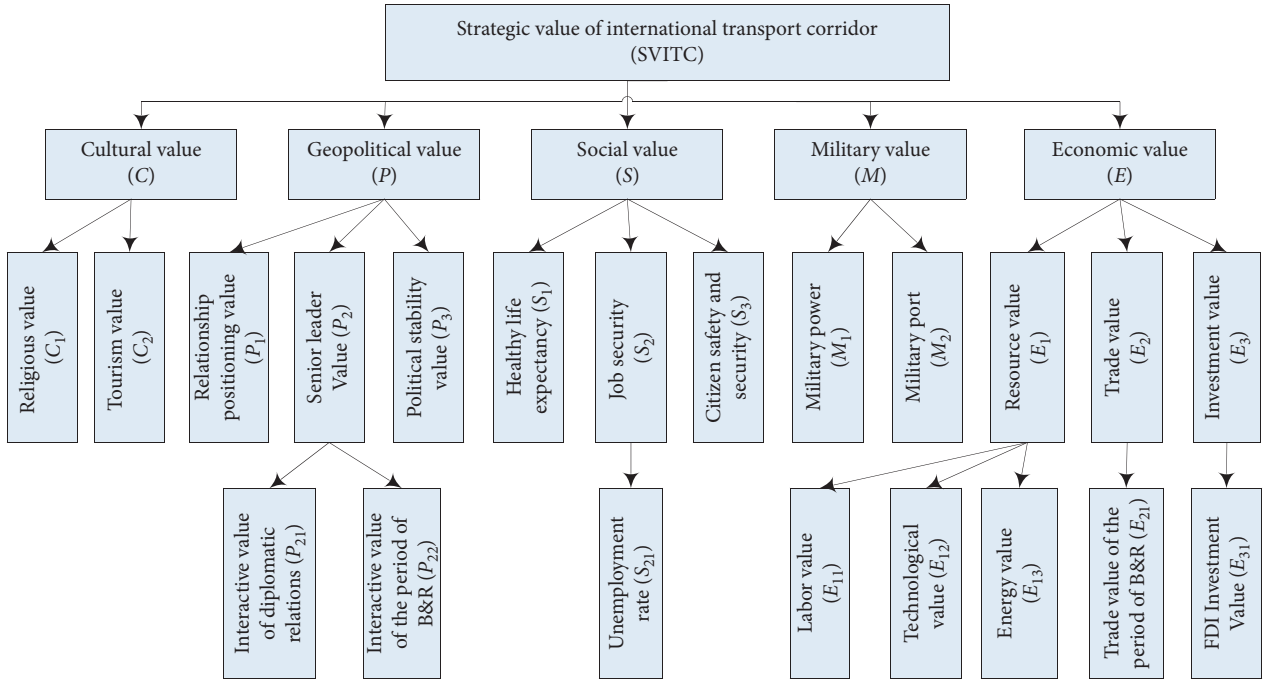

Figure 1: An evaluation index system of SVITC.

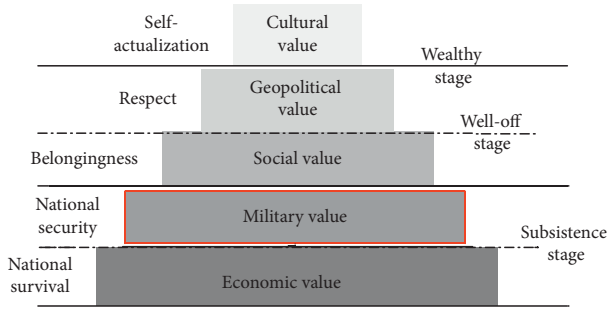

Figure 2: A hierarchical model of SVITC.

Different development stages of the same country have different utilities across the five value needs, which require the evaluation system to be adjusted dynamically. This means that different weights are to be assigned to the five values as per distinct development stages. Moreover, in the same period, different countries usually have different preferences to the five values due to their distinct stages of development and unique needs. Even at the same stage of development, different countries may still assign different weights to these values due to their diverse cultures and development modes. For example, the aforesaid national security is generally sacred and inviolable and regarded as the red line. However, Satmar Jews would argue that the establishment of a modern secular Zionism state is inconsistent with their religious doctrine. They believe that the fate of the Jews lies in the Jewish diaspora and, hence, strongly opposes Zionism. Therefore, in a comprehensive evaluation of SVITC, it is necessary to assess the development stage and cultural tradition of the sovereign states associated with a corridor and assign proper weights to the five values accordingly.

3. Background Information of the Four Silk-Road International Transport Corridors

3.1. The Four Corridors Connecting Ancient and Modern Times. The four international transport corridors studied in this research connects China with the rest of the world along with four directions, which correspond to the four exits of the ancient Silk Road.

The CPIT, which takes a land exit in Xinjiang located in northwest China, inherits and aims to reinvigorate the Northwest Oasis Silk Road, which was the most influential one in history among the ancient Silk Roads. The key countries involved in this corridor are China, Pakistan, Iran, and Turkey. About two thousand years ago, they were connected by the Northwest Oasis Silk Road, corresponding to the four major historical empires of Han-Kushan-Parthian-Roman [34]. By

capitalizing on Turkey's unique geographical location of Eurasian crossroads, the future CPIT can be either retracted or extended to the northwest through Bulgaria to Serbia, where it joins the transport artery of the China-Europe land-sea express line in Belgrade (Serbia). In this case, it forms a closed loop with the CSEG of the Maritime Silk Road.

The CMR aims to revive the Northern Grassland Silk Road, which is a grassland zone stretching between the 40th–50th parallel north and the earliest communication channel for Eurasian nations. The terrain is wide and flat, and the route is largely natural. Unlike the other three routes that need to cross mountains or over the sea, this route is unimpeded. The natural corridor had witnessed the three western expeditions of the Mongolian army under Genghis Khan, Badu, and Hulagu. Moreover, the Treaty of Kiakhta between China and Russia in 1728 established trading cities along the border and engendered the Kiakhta Tea Road. The CMR corresponds to the exit route of Inner Mongolia in north China, which goes through Mongolia and, then to Russia. Reviving this corridor will allow China, Mongolia, and Russia to better collaborate with each other and pave the road for continued prosperity in the new era.

The BCIM, as a representative of the Southern Silk Road, takes the south exit route via Yunnan. The scope of the Southern Silk Road also includes the China-Nepal -India International corridor, corresponding to the Tibet exit. These two routes are the main connections between the south (southwest) China and the outside world for many years in history. In ancient times, Yunnan was locked by high mountains and deep valleys and was beyond the reach of the Central Plains Dynasties in China owing to limited traffic routes. Dali was conquered by Mongolia forces in 1253, and Yunnan was integrated into the Central Plains Dynasty since then. Before its integration into the Yuan Dynasty, Yunnan used shell currency, which was consistent with the source, type, and counting unit of shell coins in South and Southeast Asia. This coincidence clearly shows that Yunnan had been sharing a common regional market with South and Southeast Asia for a long historical period [35]. During World War II, Japan tried to completely cut off China's material supply lines by blocking the coastline in southeast China with an extension to the Indochina Peninsula and destroying the Yunnan-Vietnam Railway. To counter this effort, the Yunnan-Burma Road completed in 1939 and the Stilwell Road started in 1945 became China's "anti-Japanese lifeline" in times of crisis. These historical clues are of great reference values for the resurrection and planning of the BCIM.

The CSEG, as a star passageway on the Maritime Silk Road, is the exit route for China's eastern coastline. It departs from the Yangshan Port of Shanghai and reaches the Piraeus Port in Greece. The countries along the route include China, Singapore, Egypt, and Greece, as well as surrounding nations. The starting and ending points of the ancient land-based Silk Roads are connected by the Maritime Silk Road. The three ancient civilizations of China, Egypt, and Greece and the rising star of Singapore have learned from each other. As the southern gateway of Europe, the Piraeus port is conceived to be the bridgehead of sea-land multimodal transport in the construction of the China-Europe land-sea express line. Upon its completion, the CSEG, after arriving at the Piraeus port, will be connected to the "Iron Silk Road," part of the China-Europe land-sea express line, and pass through Skopje (Macedonia), Belgrade (Serbia) in succession, and then, head north to Budapest (Hungary). This route will quickly connect to the hinterland of Europe and be integrated with the other "Iron Silk Road" of CPIT in Serbia with the potential of directly benefiting over 32 million people.

3.2. Comparative Spatial Structures of Orientation and Transportation Indexes of the Four Corridors. The approximate spatial structures of orientations for the four international transport corridors (labelled as T1, T2, T3, and T4) are shown in Figure 3. Table 1 displays the comparative transportation metrics of the four corridors along with their acronyms and labels T1, T2, T3, and T4. Due to the vast territory of China, if a starting point is selected at a different location, the total transportation distance will change dramatically. For example, if the starting point of Urumqi (T1) is moved to Shanghai (T4), the distance of T1 will increase by more than 4,000 kilometers and become 11,500 kilometers. Therefore, the transportation distance of the four corridors will be calculated in such a way that the starting point is chosen as the provincial capital city of the corresponding exit of a particular corridor. This is also in line with the open-up reality of inland borders and coastal areas of China. First, the border areas should not only be opened to the outside world but also integrated into the comprehensive domestic transport network to promote the overall integration process.

3.2.1. The Spatial Structures of Orientations. As shown in Figure 3, the four corridors represent the Northwest, North, Southwest, and East exit passageways starting from Urumqi, Hohhot, Kunming, and Shanghai, respectively. Here, T3 is worth further explanations. At present, several plans have been proposed for the route of T3. Figure 3 selects the China-Myanmar railway plan based on the former Yunnan-Burma Road and chooses the west line of the China-Myanmar "herringbone" railway, namely, Kunming-Dali-Ruili-Lashio-Mandalay-Marqui-Kyaukpyu Port (about 1,549 km). Then, the Kyaukpyu Port is connected to the Chittagong (Bangladesh) and the Kolkata Port (India) by a waterway. The Kyaukpyu Port on the west line has an absolute advantage in water depth than the Yangon Port on the east line. At present, China and Bangladesh are not connected by land. Furthermore, trades between China and Bangladesh are mainly transported by waterways, and 90% of cargo shipment between China and India goes through waterways at the Kolkata Port and the Mumbai Port. Therefore, we select the "railway + waterway" intermodal transportation route for T3 in this paper. The railway stretches 1,549 kilometers and the waterway extends for 1,074 kilometers, totaling about 2,623 kilometers.

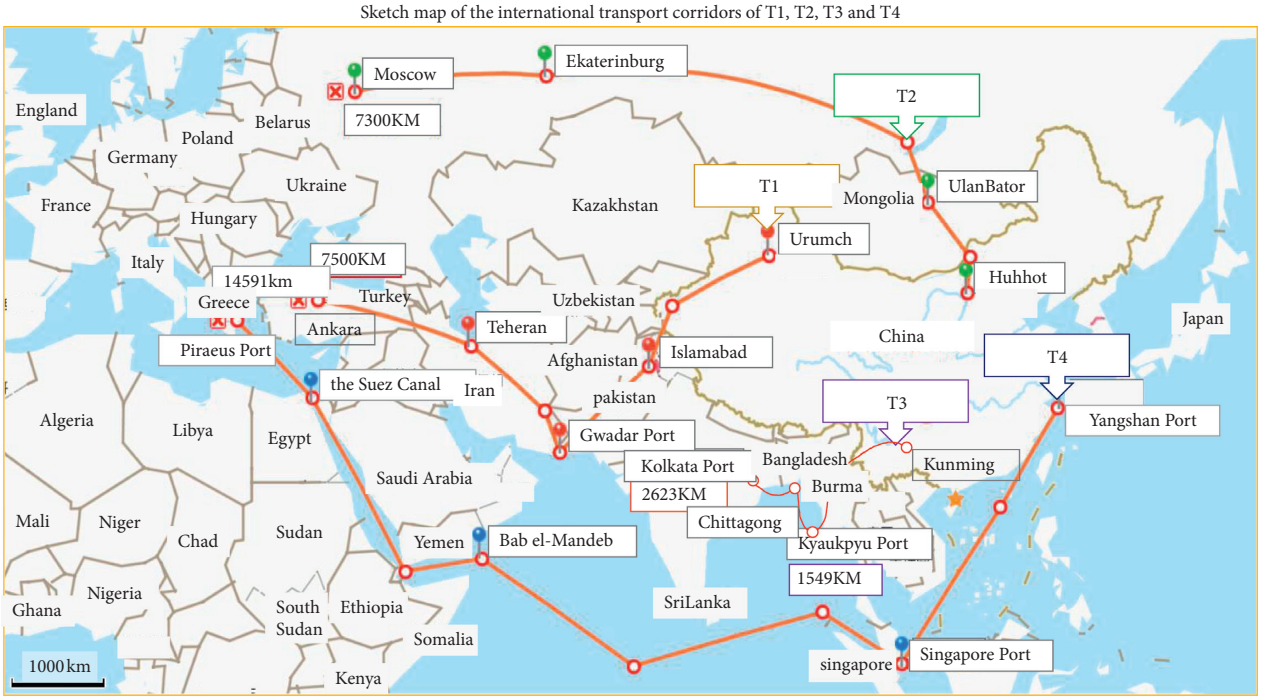

Figure 3: Corridors orientation roadmap of T1, T2, T3, and T4.

Table 1: Comparative metrics of T1, T2, T3, and T4.

Routes	Name	Shipment distance (km)	Shipment time (day)	Border Clearance efficiency①	Cost (USD/40 ft)②	Transport infrastructure③	The exit region	Corridor form
CPIT	T1	7500	11④	37	4125	54.36	Xinjiang	Railway
CMR	T2	7300	10⑤	33	4105	46.6	Nei Mongol	Railway
BCIM	T3	2623	4⑥	41	955⑦	54.25	Yunnan	Railway + waterway
CSEG	T4	14591	21⑧	53	1400⑨	70.46	Shanghai	Sea lane

①Data source: index 7.07 of "Global Competition Report 2019" from World Economic Forum. The countries along each route take the average after summarizing, and the higher scores indicate the higher efficiency of border clearance. ②Data source: China Ministry of Commerce, "Yuxinou's freight rate dropped to sea level," http://www.mofcom.gov.cn/article/resume/n/201505/20150500961358.html, accessed on Feb. 20, 2020. Assuming that T1 and T2 will be high-speed rail channels in the future, the unit price of the Yuxinou high-speed rail in this article is USD 0.55/km/40 ft. Therefore, according to the distance, the costs of T1 and T2 are, respectively, estimated as USD 4125/40 ft and USD 4105/40 ft. ③Data source: average weighting of indexes 1.01–1.04 of "Global Competition Report 2019" from World Economic Forum. The countries along each route take the average after summarizing, and the higher scores indicate the higher connectivity of transport infrastructure. ④We assume that T1 is planned as high-speed rail channel, and the train speed and customs clearance time are similar to those of Yuxinou (11000 km, 15 days), the estimated transport time of T1 is $7500/11000 \times 15 = 10.2$ days, and the estimated transport time is 11 days. ⑤The same as above, $7300/11000 \times 15 = 9.95$ days, the estimated transportation time of T2 is about 10 days. ⑥Because T3 selects the "railway + waterway" intermodal transportation route, the estimated transportation time is divided into two sections, that is, the railway section is the same as Yuxinou's standard. The waterway transport section is estimated based on T4 as the reference value, $1549/11000 \times 15 + 1074/14591 \times 21 = 3.65$ days, the valuation is 4 days. ⑦The same as above, the transportation costs of T3 are estimated in two sections, that is, the railway section is estimated based on Yuxinou's standard, and the waterway section is estimated based on the T4. $1549 \times 0.55 + 1074/14591 \times 1400 =$ USD 955/40 ft. ⑧This data is calculated based on the Cosco Shipping Group's operating routes on this channel, which is calculated by tracking its regular routes in the trans-Pacific-Indian Ocean route (Asia-Europe).⑨ Data source: "the shipping cost from Shanghai to Piraeus Port is USD1 400/40 ft," http://www.daili56.com/hyunfeix/?9-2070.html, accessed on Feb. 20, 2020.

3.2.2. Comparison of Key Transportation Metrics. Referring to Table 1 and Figure 3, we can see that there are three passages for China to go south into the Indian Ocean. The fastest passage is T3. Kunming-Kyaukpyu Port is only 1549 km on land. Following the east line of the China-Myanmar "herringbone" railway, China may lift the barrier to build a high-speed rail along the west line with Myanmar and restart the "Memorandum of Understanding on the Muse-Kyaukphyu Railway Transportation System Project" signed earlier in 2011 to support the Kyaukpyu Port which is under construction. Obviously, this helps to convert it into an integrated "railway + water + pipe" hub. The natural water depth of the Kyaukpyu Port is 24 meters and can accommodate cargo ships in the range of 250,000–300,000 tons, surpassing the Gwadar Port (100,000–200,000 tons) on T1, the Suez Canal (250,000 tons), and the Malacca Strait (200,000 tons) on T4. If the port and the feeding infrastructure projects are completed, it will not only be able to

easily meet the docking needs of cargo ships on the Suez Canal route but also satisfy the berthing needs of large or super-large cruise ships (between 200,000 and 300,000 tons) detouring the Cape of Good Hope route, In this case, these vessels will be able to land directly in the Indian Ocean without continuing eastbound through the Strait of Malacca or bypassing the Sunda Strait. This can not only shorten the transportation distance but also hedge the risk of relying heavily on the Strait of Malacca, thereby seamlessly connecting to the existing Sino-Burmese oil and gas pipelines. This move will greatly change China's energy supply landscape. Since 2014, Japan offered to spend 7.8 billion yen (about 472 million yuan) to assist Myanmar in building a railway for free, which effectively obstructed the construction of the west line of the China-Myanmar "herringbone" railway, resulting in the suspension of the project till now. Therefore, this development, on the flip side, proves the strategic significance of this west line to China. T1 is the second fastest way to the Indian Ocean. The distance from Xinjiang to the Gwadar Port is about 3,000 km, namely, the CPEC. As a flagship B&R project, its overall progress is smooth and moves the fastest. The Gwadar Port has already started sailing in 2016, and the regular container liner route was opened in 2018. Clearly, it has changed from a blueprint to reality in contrast to the stagnation and on-and-off of the Kyaukphyu Port.

From the perspective of the travel distance of the four corridors, T3 is the shortest about 2,623 km, but the west line of the China-Myanmar "herringbone" railway remains at the planning stage. Because of its importance, it can be predicted that more obstacles may arise in the future. The distances of T1 and T2 are both more than 7000 km, and T4 is the traditional maritime channel which is the longest, but with the most mature and complete supporting facilities. In addition, the key nodes are typically well-connected and coordinated.

From the perspective of transportation time and costs, T3 has significant advantages. The estimated transportation time is 4 days, and the transportation costs are only USD 955/40 ft. The longest distance of T4 is 14,590 km, but the freight is only USD 1400/40 ft, ranking the second at a unit price of USD 0.096/km/40 ft. However, the freight rate along Yuxinou (Chongqing-Xinjiang-Europe Railway) is USD 0.55/km/40 ft, which is about 5.7 times the marine route. It is clear that T4 has the lowest unit transport rate but takes the longest time. The estimated speeds of marine transportation and Yuxinou high-speed railway are 695 km/day and 733 km/day, respectively, which do not make much difference, indicating that the land-based high-speed railway transport is significantly delayed by customs clearance, loading, and other factors. In contrast, mature T4 has the advantage of efficient customs clearance. In the future, T1, T2, and T3 have significant room for improvement in customs clearance efficiency and other supporting facilities to tap into the speed advantage of high-speed railway.

From the perspective of domestic infrastructure of each corridor, T2 has the lowest score, and the infrastructure of Mongolia and the Far East of Russia are relatively poor, especially the Mongolian infrastructure ranks the lowest among the 12 countries in the four corridors.

4. Methodology

In the proposed hierarchical evaluation model of SVITC in this paper, the indicators at each level may not be completely independent. Therefore, this paper adopts a fuzzy integral method that can handle interrelated indicators at each level. In addition, the important index of fuzzy density in fuzzy integral is related to the weight of each index. Based on the hierarchical model, this article conceives that different countries at different stages of development have distinct preferences for their national interests and specific national conditions must be considered in the assessment process. Although the overall idea can be grasped relatively easily, the specific weights at different levels are hard to obtain and subjective human judgments are often inevitable. At the same time, this paper also uses an entropy weight method to evaluate objective weights. By integrating subjective and objective weights to obtain comprehensive weights, the approach in this paper can properly handle human judgment embedded in the subjective weights and bridge data to objective weights.

4.1. Fuzzy Integral Method

4.1.1. λ-Fuzzy Measure. Fuzzy measures are a prerequisite and key element of using a fuzzy integral method. Among different measures, a λ-fuzzy measure is a typical and widely used one. Its definition is as follows.

Definition 1. If a fuzzy measure g satisfies the following properties: if $A \cap B = \phi$, then $g(A \cup B) = g(A) + g(B) + \lambda g(A)g(B)$, where $\lambda \in [-1, \infty)$, then g is called a λ-fuzzy measure or g_λ measure. Let $X = \{x_1, x_2, \ldots, x_n\}$ be a finite set, and the fuzzy density function of each variable x_i is $g(x_i)$, then g_λ can be written as follows:

$$\begin{aligned} g_\lambda = (\{x_1, x_2, \ldots, x_n\}) &= \sum_{i=1}^{n} g(x_i) + \lambda \sum_{i1=1}^{n-1} \sum_{i2=i1+1}^{n} g(x_{i1}) \\ &+ g(x_{i2}) + \cdots + \lambda^{n-1} g(x_1)g(x_2), \ldots, g(x_n) \\ &= \frac{1}{\lambda}\left|\prod_{i=1}^{n}(1 + \lambda g(x_i)) - 1\right|, \quad \lambda \in [-1, \infty), \lambda \neq 0. \end{aligned} \tag{1}$$

4.1.2. Fuzzy Integral. A fuzzy integral is a nonlinear function defined based on a fuzzy measure. It does not require mutual independence of evaluation indicators. Different fuzzy integrals have been proposed in the literature such as Suggeon fuzzy integral [36], Weber fuzzy integral [37], and Choquet fuzzy integral [38]. This paper will use the most widely used Choquet fuzzy integral as defined below.

Definition 2. Let $f(x_1) \geq f(x_2) \geq \cdots \geq f(x_i) \geq \cdots \geq f(x_n)$, the Choquet fuzzy integral of the fuzzy measure g of f on X is

$$\int f \mathrm{d}_g = f(x_n)g(X_n) + [f(x_{n-1}) - f(x_n)]g(X_{n-1}) + \cdots + [f(x_1) - f(x_2)]g(X_1), \tag{2}$$

where $f(x_i)$ is the standardized ith index value of the evaluation object; $g(X_i)$ indicates the importance of simultaneously considering attributes $x_1, x_2, \ldots, x_i$. $g(X_1) = g(\{X_1\})$, $g(X_n) = g(\{X_1, X_2, \ldots, X_n\})$.

4.2. Entropy Weight Method. Assuming that there are m evaluation objects and n evaluation indexes, the standardized dimensionless matrix of the original data is

$$\begin{aligned} p &= \left(p_{ij}\right)_{m\times n}, \quad 0 \leq p_{ij} \leq 1, \\ \sum_{i=1}^{m} p_{ij} &= 1, \quad i = 1, 2, \ldots, m,\ j = 1, 2, \ldots, n. \end{aligned} \tag{3}$$

For the index x_j, its information entropy is given as

$$E_j = -k \sum_{i=1}^{m} p_{ij} \ln\left(p_{ij}\right), \tag{4}$$

where $k = (1/\ln m)$.

The entropy weight for the jth index is defined as follows:

$$W_j = \frac{1 - E_j}{n - \sum_{i=1}^{n} E_j}. \tag{5}$$

4.3. Comprehensive Weight

$$\beta_j = \frac{\alpha_{j*W_j}}{\sum_{j=1}^{n} \alpha_{j*W_j}}. \tag{6}$$

Here, a_j is the subjective weight and W_j is the objective weight calculated by the entropy weight method (equation (5)). Furthermore, by combining these two weights, we obtain a comprehensive weight β_j, which will be used as the fuzzy density in the fuzzy integral. According to the transfer function between the evaluation indexes, we can calculate the abovementioned correlation weights and the $g(X_i)$ value of each evaluation index.

5. Evaluation of SVITC for the Four Corridors

As discussed above, because different countries are often at different stages of development and have distinct preferences for the five values, they usually assign different weights as per their specific considerations. In addition, this paper analyzes and compares the strategic values of the four corridors from China's perspective.

5.1. Data Sources for the Index of SVITC for the Four Corridors

5.1.1. A Description of the Indexes in Assessing SVITC. Following Figure 1 in Section 2, we collect data for the following indexes from different sources based on their representativeness, authority, and availability. Table 2 describes the indicators and data selection.

In Table 2, the index P_1 needs further explanations: it represents how close the bilateral relationship between China and Ti, and the qualitative assessment will be converted into the quantitative evaluation. Because of China's foreign policy of nonalignment, its bilateral relations have always been defined as different levels of "partnership" with other nations. According to the closeness of the bilateral relationship and the level of cooperation, different semantic rhetorics are employed to China's relations with other nations. By collecting the semantic differences between China and different countries since the establishment of diplomatic relations, the semantic differences are categorized into 9 levels, and the 11 countries in the four corridors are scored accordingly. The specific scores are shown in Table 4.

5.1.2. Original and Standardized Data of SVITC Indexes. The original and normalized data of SVITC indexes are shown in Table 5. Because the raw data are different in magnitudes and units, to facilitate a fair comparison and further processing, equation (3) is employed to standardize them. The three indexes, C_1, C_2, and M_2, require further explanations as follows.

C_1 represents the ability of cultural diffusion. At present, most scholars take Confucius Institutes as a representative of Chinese traditional culture, whose output represents the influence and diffusion power of Chinese culture [39–41]. C_2 stands for the value of tourism, measured by the number of tourists from Ti to China (in ten thousand). Because culture is the soul of tourism, the number of inbound tourists can thus represent the cultural attractiveness of a country, measured by C_2 here. However, because the national statistical data source only shows information on the top countries of inbound tourists to China, data are missing for seven of the eleven countries, especially no information is available for any country on the T1 corridor, meaning that the numbers of tourists from these nations are relatively low and below the threshold to be included in our statistical source. While each of the other three corridors has data for at least one nation, it is sensible to infer that T1 ranks the lowest in this metric among the four corridors. To handle missing original data in this dimension, we use the deduced ranking of T2, T4, T3, and T1 to obtain normalized data in this row.

Table 2: Description of the indexes and data collection for assessing SVITC.

Index			Measurement index data selection and units	Contribution	Data sources	Remarks
C		C_1	Number of Confucius Institutes and Confucius Classrooms in Ti (unit)	Positive	Information on the Headquarters of the Confucius Institute	Confucius Institutes represent Chinese Confucian culture
		C_2	Number of tourists from Ti to China (10,000 people)	Positive	Data of the National Bureau of Statistics of China in 2018	The number of inbound tourists symbolizes cultural attractiveness
P		P_1	Positioning of relations between China and Ti (0–9 points)	Positive	https://www.fmprc.gov.cn/web/ and http://www.mofcom.gov.cn/	Ratings are given based on whether a bilateral relationship is established and the closeness of the relationship
	P_2	P_{21}	Number of high-level interactions between China and Ti after the establishment of diplomatic ties (times)	Positive	https://www.fmprc.gov.cn/web/	Total since establishment of diplomatic relations up to 2019
		P_{22}	Number of high-level interactions between China and Ti during the period of B&R (times)	Positive	https://www.fmprc.gov.cn/web/	Total from 2013 to 2019
		P_3	Political stability (0–100 points)	Positive	World Economic Forum: "Global Competitiveness Report 2019"	Index 1.20
S		S_1	National Health (0–100 points): healthy life expectancy	Positive	World Economic Forum: "Global Competitiveness Report 2019"	Index 5.01
	S_2	S_{21}	Job security is characterized by the unemployment rate (%)	Negative	World Economic Forum: "Global Competitiveness Report 2019"	Statistics data on the unemployment rate in 2018
		S_3	National security (0–100 points) Measured from four aspects: organized crime, homicide rate, terrorism incidence, and reliability of police services	Positive	World Economic Forum: "Global Competitiveness Report 2019"	Average weighting of indexes 1.01–1.04
M		M_1	Military strength (the larger the number, the stronger the strength)	Uncertain	https://www.globalfirepower.com/	Value, which can be positive or negative, should be modified after incorporating the P_1 index
		M_2	The key nodes of the corridor are used as the score of the military port	Positive	Analysis carried out by the authors	See the corresponding explanations in Section 5.1.2
E	E_1	E_{11}	Labor Force size in Ti (ten thousand people)	Positive	International data from the National Bureau of Statistics of China	Use data from the most recent year of 2015
		E_{12}	T_i technology (0–100 points)	Positive	World Economic Forum: "Global Competitiveness Report 2019"	The innovation capability of index 12.0 represents the technology level of Ti
		E_{13}	T_i state energy: to measure the total production of primary energy	Positive	https://cn.knoema.com	Use data in 2017
	E_2	E_{21}	Total value of import and export trade during the period of B&R (USD 100 million)	Positive	Data from the National Bureau of Statistics of China	Reflecting the economic and trade reality between China and Ti after implementing the B&R initiative
	E_3	E_{31}	Total of net FDI inflows in Ti over 2014–2017 years (USD millions)	Positive	UNCTAD: "World Investment Report 2018"	Reflect expected economic growth in Ti

T_i stands for country i along the four corridors other than China.

M_2 is the logistics support capability of military stations at key nodes. The Gwadar Port in T1 has taken root and is regarded as a model of political mutual trust, thanks to the high-level relationship between China and Pakistan (8 points). Therefore, it can be considered as China's navy base and logistics supply base in the future, and we assign it a value of 1 point. At the same time, the Kyaukpyu Port in T3, after being delayed for three years, a framework agreement was signed in 2018. As China accounts for 70% of the shares and the relationship between China and Myanmar is at a relatively high level (7 points), it can also be considered as a military port and logistics supply point in the future. On the contrary, the Kyaukphyu Port in T3 is of great significance to China as analyzed earlier, but it remains at the blueprint stage and has to overcome significant extraterritorial resistance before coming to fruition, so it is assigned 0.5 points. The Straits of Malacca and the Piraeus Port in T4 are, respectively, assigned −1 and 1 for their contributions to M_2. In the context of the current Sino-US trade friction, given the close military cooperation between Singapore and US, the

Table 3: Subjective weights' assignment.

Index weight distribution (%)		
$C\ (20) = C_1\ (15) + C_2\ (5)$		
$P\ (25) = P_1\ (10) + P_2\ (7.5) + P_3\ (7.5)$;	$P_2\ (7.5) = P_{21}\ (3.5) + P_{22}\ (4)$	
$S\ (25) = S_1\ (25/3) + S_2\ (25/3) + S_3\ (25/3)$;	$S_2\ (25/3) = S_{21}\ (25/3)$	
$M\ (15) = P_1{\cdot}M_1\ (7.5) + M_2\ (7.5)$		
$E\ (15) = E_1\ (5) + E_2\ (5) + E_3\ (5)$;	$E_1\ (5) = E_{11}\ (1) + E_{12}\ (2) + E_{13}\ (2)$; $E_2\ (5) = E_{21}\ (5)$	$E_3\ (5) = E_{31}\ (5)$
SVITC = $C\ (20) + P\ (25) + S\ (25) + M\ (15) + E\ (15)$		

Strait of Malacca has actually served as a military port for the US Navy and is assigned a value of −1 point owing to its significant negative value for China. As for the Piraeus Port, as a China-Greece joint venture, COSCO Group won the bid to obtain 35-year franchise rights of its Pier 2 and Pier 3 in 2008 and acquired 67% equity in 2016. In the future, the Piraeus Port in Greece has well positioned a logistics supply base of Chinese naval ships, which will help to improve China's security and escort capability for cargo ships sailing to the Mediterranean, so it is assigned a value of 1 point.

Judging from the original data of the 11 countries in the four corridors, Russia ranks first most frequently and takes the first place for eight indicators. The next is Singapore, ranking the first for five indicators, especially in the social value dimension: healthy life expectancy (S_1) and citizen safety and security (S_3). Singapore's welfare of the people's livelihood has obvious advantages, consistent with its characteristics of the wealthy phase and its FDI inflow in 2014–2017 also ranks the first (E_{31}), indicating that Singapore is also a hot spot for foreign investment. India has scored first twice, with the lowest unemployment rate and the most abundant labor force, and Pakistan and Greece, respectively, rank the first once in terms of military port security. In terms of the lowest ranking indicators, each of Bangladesh and Greece ranks at the bottom three times, followed by Singapore, Mongolia, Iran, and Pakistan with two lowest-ranking indicators each. Singapore ranks the lowest in military port (M_2) and energy value (E_{13}). Mongolia has the lowest score in labor value (E_{11}) and FDI investment value (E_{31}). Iran has the lowest score in the number of Confucius Institutes (C_1) and high-level interactions (P_{21}), where the low score in P_{21} is partly due to the absence of statistical data prior to 2013 as noted in the footnote in Table 5. Pakistan scores the lowest in S_1 and S_3.

5.2. Evaluation Steps and Results

5.2.1. Subjective Weights Based on SVITC Hierarchy Theory. Without accounting for the development stage of a country, it is sensible to assign equal weights to the five criterion-level indexes with 20% each. However, according to the hierarchy theory, China is now at a well-off stage with social and geopolitical value taking more prominent positions. China's President Xi Jinping reported to the 19th National People's Congress: "as socialism with Chinese characteristics has entered a new era, the principal contradiction facing Chinese society has evolved. What we now face is the contradiction between unbalanced and inadequate development and the people's ever-growing needs for a better life [42]." Domestically, China's current focus is to improve people's livelihoods, so the weight of social value is set at 25%; Internationally, China's B&R initiative aims to promote collective development with partner nations, thereby gaining more recognition and respect from the international community. Therefore, a weight of 25% is assigned to the geopolitical value. Correspondingly, the weights of economic value and military value are adjusted to 15%, and the weight of cultural value remains unchanged at 20%. For the cultural value weight, due to lack of data for index C_2, we assign to it a lighter weight of 5%, leaving the weight to C_1 at 15% and the ratio between them as $C_1 : C_2 = 0.750 : 0.250$. In the subsequent calculation, we divide the overall weight for the main indicators into the subindexes in the lower levels in a similar fashion. In geopolitics, P_1 is a principal indicator of the relationship between two countries, so it takes 10% of the 25% total weight allocated to P with the remaining 15% weight equally split between the other two indicators, P_2 and P_3. For P_2, we assign 3.5% weight to P_{21} and 4% to P_{22}. The key rationale behind this allocation is due to the consideration that bilateral relations are more closely related to changes in the current world situation and better characterized by the number of interactions during the period of B&R, which are more representative and up to date. Several secondary and tertiary indicators of S and M are all equally weighted. The resource value of E is equally divided into three indicators: labor, technology, and energy. For the secondary indicator E_{11}, as it only considers the number of labor without accounting for quality, its weight is reduced to 1% while the remaining two secondary indicators E_{12} and E_{13} are set at 2% each. The specific subjective weights assigned to all levels of indicators are shown in Table 3.

5.2.2. Objective Weights by the Entropy Method, Comprehensive Weights, λ-Value, and Calculation Steps. Using equations (4) and (5) of the entropy weight method, objective weights are calculated based on a bottom-up approach. For example, the lowest level indicators (P_{21}, P_{22}) are calculated as follows: their objective weights are determined as (0.501, 0.499), and subjective weights are normalized as ($0.467 = 3.5/7.5$, $0.533 = 4/7.5$). According to equation (6), the comprehensive weights are calculated as (0.467, 0.533) by combining subjective and objective weights. Its value is the fuzzy integral of fuzzy density. Next, we use equation (1) to compute the fuzzy measure, which requires us to determine the critical λ-value first. Existing research shows that when λ is positive, the evaluation focuses on balancing the

Table 4: Evaluating the relationship positioning between China and Ti.

Positioning of bilateral relations	Point	Countries along the corridors
No diplomatic relations	0	NA
Partnerships	1	NA
Cooperative partnership	2	NA
Partnership of cooperation in all respects	3	Bangladesh
Comprehensive partnership of cooperation	4	Singapore
Strategic cooperative partnership	5	Indian, Turkey
Comprehensive strategic partnership	6	Greece, Egypt, Mongolia, Iran
Comprehensive strategic cooperative partnership	7	Myanmar
All-weather strategic cooperative partnership	8	Pakistan
Comprehensive strategic partnership of coordination	9	Russia

Data source: according to the information on the websites of the Ministry of Foreign Affairs and the Ministry of Commerce, PRC, the authors create this table.

Table 5: Raw and normalized data of SVITC for the four corridors and 11 countries.

Index			T1			T2			T3			T4	
			Pakistan	Iran	Turkey	Mon-golia	Russia	Bangla-desh	India	Myan-mar	Singa-pore	Egypt	Greece
C		C_1	7	2	4	5	17	3	7	3	3	5	3
		$\mathbf{C_1}$①	**0.119**	**0.034**	**0.068**	**0.085**	**0.288**	**0.051**	**0.119**	**0.051**	**0.051**	**0.085**	**0.051**
		C_2	NA	NA	NA	149.4	241.6	NA	86.3	NA	97.8	NA	NA
		$\mathbf{C_2}$②		**0.121**			**0.481**			**0.160**			**0.24**
P		P_1	8	6	5	6	9	3	5	7	4	6	6
		$\mathbf{P_1}$	**0.123**	**0.092**	**0.077**	**0.138**	**0.092**	**0.046**	**0.077**	**0.108**	**0.062**	**0.092**	**0.092**
	P_2	P_{21}	88	18③	19	38	103	56	64	43	46	75	25
		$\mathbf{P_{21}}$	**0.153**	**0.031**	**0.033**	**0.066**	**0.179**	**0.097**	**0.111**	**0.075**	**0.08**	**0.13**	**0.043**
		P_{22}	35	18	14	20	58	17	35	39	18	37	16
		$\mathbf{P_{22}}$	**0.114**	**0.059**	**0.046**	**0.065**	**0.189**	**0.055**	**0.114**	**0.127**	**0.059**	**0.121**	**0.052**
		P_3	46.7	23.6	46.1	32.3	44.9	44.4	58.6	NA	89.1	50.4	19
		$\mathbf{P_3}$	**0.103**	**0.052**	**0.101**	**0.071**	**0.099**	**0.098**	**0.129**	**0.0**	**0.196**	**0.111**	**0.042**
S		S_1	45.5	72.8	61	74.1	68.6	67.9	56.4	NA	96.1	67.8	77.5
		$\mathbf{S_1}$	**0.075**	**0.108**	**0.117**	**0.085**	**0.093**	**0.096**	**0.081**	**0.0**	**0.134**	**0.087**	**0.125**
	S_2	S_{21}	3	12	10.9	6.3	4.7	4.3	2.6	NA	3.8	11.4	19.2
	$\mathbf{S_2}$	$\mathbf{S_{21}}$	**0.175**	**0.044**	**0.048**	**0.084**	**0.112**	**0.122**	**0.202**	**0.0**	**0.139**	**0.046**	**0.027**
		S_3	56.3	80.4	87.1	63.3	69.2	72.1	60.5	NA	100	65	93.5
		$\mathbf{S_3}$	**0.066**	**0.106**	**0.089**	**0.108**	**0.10**	**0.099**	**0.082**	**0.0**	**0.14**	**0.099**	**0.113**
M		M_1	4.2	4.6	4.8	0.5	14.7	1.4	10.5	1.8	1.3	5.3	1.9
		$P_1{\cdot}M_1$④	33.8	27.4	23.8	3.0	132.2	4.2	52.5	12.3	5.0	32.1	11.3
		$\mathbf{P_1{\cdot}M_1}$	**0.10**	**0.081**	**0.071**	**0.009**	**0.391**	**0.013**	**0.155**	**0.036**	**0.015**	**0.095**	**0.033**
		M_2	1	0	0	0	0	0	0	0.5	−1	0	1
		$\mathbf{M_2}$	**0.667**	**0.0**	**0.0**	**0.0**	**0.0**	**0.0**	**0.0**	**0.333**	**−0.667**	**0.0**	**0.667**
E		E_{11}	6618	2691	2940	132	7615	7059	50160	3045	313	3024	478
		$\mathbf{E_{11}}$	**0.079**	**0.032**	**0.035**	**0.002**	**0.091**	**0.084**	**0.597**	**3.6**	**0.4**	**3.6**	**0.6**
	E_1	E_{12}	35.8	30.4	44.5	32.3	52.9	30.7	50.9	NA	75.2	39.6	45.1
		$\mathbf{E_{12}}$	**0.082**	**0.070**	**0.102**	**0.074**	**0.121**	**0.07**	**0.116**	**NA**	**0.172**	**0.091**	**0.103**
		E_{13}	1.86	18.21	1.57	1.33	61.59	1.13	17.68	0.84	0.01	3.44	0.33
		$\mathbf{E_{13}}$	**0.017**	**0.169**	**0.015**	**0.012**	**0.570**	**0.01**	**0.164**	**0.008**	**0.0**	**0.032**	**0.003**
	E_2	E_{21}	933	1891	1075	314	4242	772	3120	811	3918	601	252
		$\mathbf{E_{21}}$	**0.052**	**0.105**	**0.060**	**0.018**	**0.237**	**0.043**	**0.174**	**0.045**	**0.219**	**0.034**	**0.014**
	E_3	E_{31}	8744	12636	54262	−2231	103470	8271	11100	163043	275671	27036	11075
		$\mathbf{E_{31}}$	**0.013**	**0.019**	**0.081**	**− 0.003**	**0.154**	**0.012**	**0.016**	**0.242**	**0.41**	**0.04**	**0.016**

①The normalized value is represented by the index label in italics. The remaining indexes are similarly labelled in italic in this table. ②Due to lack of inbound tourism data for seven countries, normalized data on this index are obtained by using the corridor ranking, (4, 1, 3, 2). ③Iran and China established diplomatic relations in 1971, but the Ministry of Foreign Affairs of China recorded data on high-level exchanges between the two countries only since 2013. ④The positioning relationship of P_1 is used to modify M, that is, a stronger military strength of Ti does not necessarily translate into a larger positive value as its relationship with China has to be considered.

indicators; when λ is a small negative number, the evaluation takes into account some special indicators while balancing the indicators [43]. In this index system, the emphasis differs from the index layer to the criterion layer (such as P_1, P_2, and $P_3 \Longrightarrow P$) and the criterion layer as well as the target layer (C, P, S, M, and $E \Longrightarrow$ SVITC). The former considers the balanced development of all indicators, while the latter considers both balancing the relevant indicators and certain

Table 6: Comparison of SVITC of the four corridors.

Index	Objective weights	Subjective weights	Comprehensive weights	λ	Upper index	Fuzzy integral value			
						T1	T2	T3	T4
P_{21}	0.501	0.467	0.467	**0.5**	P_2	**0.217**	**0.249**	**0.289**	**0.240**
P_{22}	0.499	0.533	0.533						
E_{11}	0.055	0.200	0.028						
E_{12}	0.649	0.400	0.668	**0.5**	E_1	**0.228**	**0.299**	**0.200**	**0.238**
E_{13}	0.296	0.400	0.304						
C_1	0.530	0.750	0.772	**0.5**	C	**0.185**	**0.397**	**0.214**	**0.192**
C_2	0.470	0.250	0.228						
P_1	0.336	0.400	0.403						
P_2	0.336	0.300	0.302	**0.5**	P	**0.256**	**0.214**	**0.245**	**0.271**
P_3	0.329	0.300	0.296						
S_1	0.330	0.333	0.332						
S_2	0.336	0.330	0.334	**0.5**	S	**0.275**	**0.195**	**0.223**	**0.296**
S_3	0.333	0.333	0.334						
M_1	0.992	0.500	0.992	**0.5**	M	**0.253**	**0.396**	**0.201**	**0.139**
M_2	0.008	0.500	0.008						
E_1	0.346	0.033	0.347						
E_2	0.348	0.033	0.348	**0.5**	E	**0.183**	**0.229**	**0.239**	**0.309**
E_3	0.306	0.033	0.306						
C	0.196	0.200	**0.195**						
P	0.205	0.250	**0.255**						
S	0.203	0.250	**0.253**	**–0.5**	SVITC	**0.241**	**0.285**	**0.228**	**0.257**
M	0.194	0.150	**0.145**						
E	0.203	0.150	**0.151**						

special preferences due to different countries with diverse preferences for distinct values at various development stages.

Given these considerations, λ is set at 0.5 below the criterion level to accommodate the balancing effect. While λ takes a value of −0.5 to account for both "balance" and "particularity" in the criterion layer to the target layer. Therefore, for the index layer (P_{21}, P_{22}), $\lambda = 0.5$, the fuzzy measure is calculated and normalized; then, the upper index value P_2 (0.217, 0.249, 0.289, 0.240) is calculated based on equation (2). Following this procedure, the index weights and main results are shown in Table 6. The comparison of each subindex of the four corridors is shown in Figure 4, and the comparison of SVITC of the four corridors is illustrated in Figure 5.

① Comparison of subindicators:

In the cultural value, T2 is far ahead (0.397) of the other three corridors whose scores are quite close to each other. This indicates that Chinese Confucian culture is the most influential in T2, but still needs more diffusion in the other three corridors. Especially in T1, the number of inbound tourists does not even show up in the statistical data source, indicating that China's cultural diffusion there is insignificant to attract tourists. In T3 and T4, China's cultural influence in Southeast and South Asia also need to be further strengthened along the corridors. In terms of social value, T4 leads the way, mainly thanks to Singapore's wealthy stage and high level of people's well-being. Especially, its values of S_1 and S_3 are outstanding even on a global scale and set up a model for China to learn. In terms of the military value, T2 has a significant advantage (0.396) owing to Russia's huge contribution, and T1 ranks the second with a comparative advantage, especially in the key node, the military port, the Gwadar Port has obvious strength. The Kyaukpyu Port of T3 is also likely to become a logistics depot in the future. T4 has the lowest military value mainly due to the negative impact of the Malacca Strait, but we should not overlook the positive contribution of the Piraeus Port in this corridor. In terms of economic value, T4 has a clear advantage, while T1 is the weakest. The four corridors are basically equal in geopolitical value, indicating that, during the period of B&R, China equally values the political contributions from the four corridors and aims to expand its circle of friends.

② Comparison of overall indicators:

From the criterion level in Table 6, the calculated comprehensive weights for C, P, S, M, and E (0.195, 0.255, 0.253, 0.145, 0.151) are basically consistent with their subjective weights (0.20, 0.25, 0.25, 0.15, 0.15). As mentioned earlier, we assign subjective weights according to the SVITC hierarchy theory. This confirms the rationality of setting weights based on this theory in combination with specific national conditions.

As Figure 5 indicates, the annular ratio of the strategic value of the four corridors is basically in the mean distribution state. The overall strategic values of

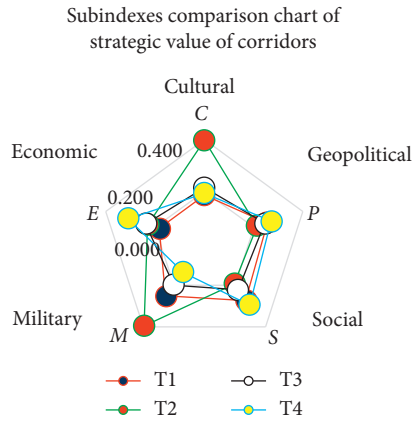

Figure 4: Comparison of SVITC for T1, T2, T3, and T4 by subindexes.

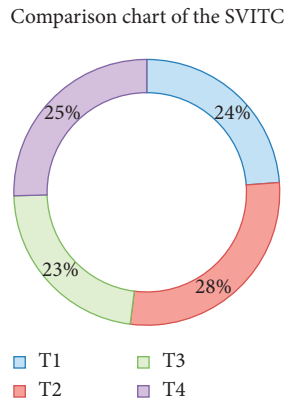

Figure 5: Loop comparison chart of SVITC for T1, T2, T3, and T4.

the four corridors are as follows: T2 (0.285) takes a slight lead, followed by T4 (0.257), T1 (0.241), and finally T3 (0.228). This can be used as the basis for our strategic decisions. In addition, T2 and T4 are currently in operation and can be upgraded at a later stage. So, further investment in these two corridors is not as urgent as the current work-in-progress T1 and T3 lines. Since T1 and T3 are also of strategic importance and need more urgent funding to bring them online. So, if sufficient financial resource is available, they should both be prioritized in receiving investment. Otherwise, if limited is available for B&R construction, T1 should be invested first.

6. Discussion and Conclusions

① The calculated comprehensive weights are consistent with the subjective weights, which shows the rationality of setting weights according to the hierarchy model and the specific national development stage, indicating that SVITC does have preferences at five levels. At present, China's emphases are indeed on the geopolitical and social values.

② From the perspective of reinvigorating the ancient Silk Road, the Northern and Maritime Silk Roads have been completely restarted and in operation as the T2 and T4 corridors. In addition, the "China-Pakistan" part of T1 has also been restarted and its demonstration and model effects are significant. Nevertheless, the "Iran-Turkey" part of T1 still has to be further pushed. The overall progress of T3 is very slow with 90% of the corridor remaining at the blueprint stage. This development is consistent with the ranking result of the strategic values of the four corridors in this study.

③ The strategic value of T2 ranks at the top, which is largely attributed to the model relations between China and Russia. Russia has the largest number of Confucius Institutes, the highest level of relationship positioning (9 points), the largest number of high-level interactions, the largest bilateral trade scale, and the strongest military strength. The positioning of a comprehensive strategic cooperative partnership is indeed the best annotation for this important bilateral relationship. It is apparent that Russia is the key factor to ensure smooth operations of T2, but the role of Mongolia as another neighboring country cannot be ignored, either. Mongolia's economy is under pressure with the lowest infrastructure index among the 12 countries in the four corridors. Due to China's apparent infrastructure strengths, abundant

opportunities exist for the two nations to cooperate to improve Mongolia's infrastructure and combat its economic depression, thereby embracing breakthroughs to bridging geopolitical gaps and promoting communications between the peoples.

④ T4 ranks second in the strategic value thanks to its superb performance in economic and social values as well as slight outperformance in geopolitical value. As a traditional corridor with mature supporting systems, it has the highest customs clearance efficiency, which sets up a model for other corridors. In the future, more investment is needed to transform and upgrade its aging infrastructure. Moreover, its negative value can be further mitigated by promoting the common mainstream Confucian culture between China and Singapore. A sensible strategy for China to accomplish this goal is to increase cultural exchanges and cooperation with Singapore, thereby enhancing mutual trust and promoting mutual understanding between the peoples.

⑤ Although T1 ranks third, it is actually the leading corridor under construction. Its strategic value is basically equal to the T2 and T4 that are currently in operations. One can see that it is strongly supported by Pakistan and the Gwadar Port has great potential in military and economic value. In the future, T1 can be integrated into multimodal transport of "railway + waterway" or "Iron Silk Road." If the standard gauge is adopted in the planed China-Pakistan Railway, it can be conveniently integrated into T1 and T4 in Serbia upon its completion. If this grand blueprint is accomplished, it can unleash the great potential of the high-speed corridor connecting the Far East to the European hinterland.

⑥ T3 is divided into two steps, which is highly feasible and can be an operational solution. The China-Myanmar channel will lead first, followed by the Bangladesh-India channel. Firstly, the relationship positioning between China and Myanmar is ranked third (7.0). Secondly, the Kyaukpyu Port is the most dazzling pearl in the four corridors. Moreover, the China-Myanmar oil and gas pipelines can serve as foreshadowing of what a successful Kyaukpyu Port may benefit the economy and people in Myanmar. Finally, it seems that the east line of China-Myanmar "herringbone" railway will motivate the construction of the west line of China-Myanmar "herringbone" railway in the future. Distinctly, the China-Myanmar channel has a solid foundation owing to the good bilateral relations. However, it should be noted that the diplomatic relations between United States and Myanmar have been resumed since the US announcing its "Asia-Pacific Strategy" in 2012. Furthermore, due to the disruption caused by Japan's involvement in 2014, it is important to pay attention to potential external influences from other sources.

⑦ At the same time, the second half of T1, T3, and T4 can be integrated in the future. Only the Gwadar port is insufficient to satisfy the supply demand of China's ocean-going military ports and more port infrastructure is needed to provide adequate supports. Therefore, it is necessary to build more military ports at other key nodes. Upon their full operations, the Gwadar Port, the Kyaukpyu Port, and the Piraeus Port can form a conglomerate to fulfill this task by capitalizing on their complementary support to each other and ensure corridor and national security.

⑧ Upon the completion of the four corridors, the Northwest, North, South, and Maritime Silk Roads will be reinvigorated and in full operations, which will presumably facilitate each country along the B&R to tap on its potentials and achieve the third stage of development, leading to these countries' self-realization with a strengthened sense of mission and calling rooted in the national blood. This vision also presents a valuable window of opportunity for a grand integration of different national cultures. Above the level of self-realization of the SVITC hierarchy model, there should be a superego that transcends self-realization, that is, a superego that breaks through the boundaries of ethnic groups, countries, and cultures, thereby bridging across the borders of different national interests and facilitating realization of the common interests of all mankind or building of the "community of human destiny."

Data Availability

The data used to support the findings of this study are included in the article.

Conflicts of Interest

The authors declare that there are no conflicts of interest.

Acknowledgments

This paper was supported by the National Social Science Foundation of China (no. 16AGJ007) and Humanities and Social Science Planning Project of Education Commission of Chongqing, China (no. 19SKGH134).

References

[1] T. Fallon, "The new silk road: Xi Jinping's grand strategy for Eurasia," *American Foreign Policy Interests*, vol. 37, no. 3, pp. 140–147, 2015.

[2] World Economic Forum, "US $8 trillion needed to bridge ASEAN's infrastructure gap," 2020, https://www.weforum.org/press/2014/05/us-8-trillion-needed-to-bridge-aseans-infrastructure-gap/.

[3] M. B. Regmi and S. Hanaoka, "Assessment of intermodal transport corridors: cases from north-east and central Asia," *Research in Transportation Business & Management*, vol. 5, pp. 27–37, 2012.

[4] J. Berechman, D. Ozmen, and K. Ozbay, "Empirical analysis of transportation investment and economic development at

state, county and municipality levels," *Transportation*, vol. 33, no. 6, pp. 537–551, 2006.

[5] E. Vinokurov and T. Tsukarev, "The belt and road initiative and the transit countries: an economic assessment of land transport corridors," *Area Development and Policy*, vol. 3, no. 1, pp. 93–113, 2018.

[6] D. Donaldson, "Railroads of the Raj: estimating the impact of transportation infrastructure," *American Economic Review*, vol. 108, no. 4-5, pp. 899–934, 2018.

[7] C. N. Berg, U. Deichmann, Y. Liu, and H. Selod, "Transport policies and development," *The Journal of Development Studies*, vol. 53, no. 4, pp. 465–480, 2017.

[8] J. J. Laird and A. J. Venables, "Transport investment and economic performance: a framework for project appraisal," *Transport Policy*, vol. 56, pp. 1–11, 2017.

[9] A. Quium, "Transport corridors for wider socio-economic development," *Sustainability*, vol. 11, no. 19, p. 5248, 2019.

[10] M. Alam, M. H. Dappe, M. Melecky et al., *Wider Economic Benefits of Transport Corridors: Evidence from International Development Organizations*, The World Bank, Washington, DC, USA, 2019.

[11] M. Roberts, M. Melecky, T. Bougna, and Y. Xu, "Transport corridors and their wider economic benefits: a quantitative review of the literature," *Journal of Regional Science*, vol. 60, no. 2, pp. 207–248, 2020.

[12] H. Hahm and S. Raihan, "The belt and road initiative: maximizing benefits, managing risks—a computable general equilibrium approach," *Journal of Infrastructure, Policy and Development*, vol. 2, no. 1, pp. 97–115, 2018.

[13] Y.-C. Chang and M. I. Khan, "China-Pakistan economic corridor and maritime security collaboration: a growing bilateral interests," *Maritime Business Review*, vol. 4, no. 2, pp. 217–235, 2019.

[14] H. S. Wang and Y. Q. Zhu, "A comparative study on the orientation of strategic values in the construction of China-Mongolia-Russia economic corridor," *Northern Economy*, vol. 9, pp. 54–57, 2015.

[15] M. W. Lin, "China-Nepal-India economic corridor: its strategic significance and developing model," *Modern International Relations*, vol. 2, pp. 31–39, 2017.

[16] X. G. Li and L. Z. Sun, "The strategic value and security situation of the China-Pakistan economic corridor," *People's Forum. Academic Frontiers*, vol. 12, pp. 32–50, 2015.

[17] M. Zubir, *The Strategic Value of the Strait of Malacca, Analysis Paper*, Maritime Institute of Malaysia, Kuala Lumpur, Malaysia, 2004.

[18] H. Y. Malik, "Strategic importance of Gwadar port," *Journal of Political Studies*, vol. 19, no. 2, 2012.

[19] X. T. Yang, B. H. Jiao, S. H. Li et al., "Strategic value evaluation of sea lanes based on remote sensing and GIS method," *Geography and Geographic Information Science*, vol. 1, pp. 47–52, 2018.

[20] H. X. Zhang, Y. X. Liu, M. C. Li et al., "Strategic value assessment of oil and gas exploitation in the central and southern South China sea," *Resources Science*, vol. 11, pp. 2142–2149, 2013.

[21] W. Y. Cheng, Y. X. Liu, M. C. Li et al., "Strategic value evaluation of the atolls in the eastern Nansha islands based on AHP and fuzzy comprehensive evaluation method," *Tropical Geography*, vol. 33, no. 4, pp. 381–386, 2013.

[22] S. L. Yang and H. P. Gao, "BCIM economic cooperation and the forging of geopolitical reality of China," *Indian Ocean Economy Research*, vol. 2, pp. 70–83, 2014.

[23] Y. L. Yin, "Route Research of BCIM economic corridor," *Yunnan Social Sciences*, vol. 1, pp. 73–77, 2016.

[24] C. R. Smit and D. Snidal, *The Oxford Handbook of International Relations*, Oxford University Press, Oxford, UK, 2010.

[25] H. W. Li, "Four-dimensional perspective of strategic value," *Technical Economics and Management Research*, vol. 2, p. 42, 2014.

[26] P. Kennedy, *The Great Strategy of War and Peace*, World Knowledge Press, Boston, MA, USA, 2005.

[27] K. N. Waltz, "Reflections on theory of international politics: a response to my critics," in *R. O. Keohane (ed.), Neorealism and its Critics, Columbia University Press*, pp. 322–345, New York, NY, USA, 1986.

[28] Y. Z. Wang, *World Politics—Views from China: National Interests*, New World Press, Generation Sequence, Beijing, China, 2007.

[29] X. T. Yan, *An Analysis of China's National Interests*, Tianjin People Press, Tiajin, China, 1997.

[30] A. Kortunov, *Russian National Interests: The State of Discussion, Russia's Place in Europe: a Security Debate*, Peter Lang, Bern, Switzerland, 1999.

[31] T. Sun and C. M. Liu, "Culture attributes in shaping the vision of international order-on the cultural origin of "the building of a community with a shared future for mankind," *Journal of Pacific Science*, vol. 2, p. 17, 2019.

[32] F. Gao and X. Ma, "What we can learn from the hierarchy of needs in studying foreign policy making," *International Forum*, vol. 12, no. 1, pp. 51–56, 2010.

[33] A. H. Maslow, "A theory of human motivation," *Psychological Review*, vol. 50, no. 4, pp. 370–396, 1943.

[34] C. F. Wang and C. F. Huang, "Research on the cultural value of the CPIT international transportation corridor," *Pacific Journal*, vol. 26, no. 5, pp. 40–50, 2018.

[35] W. X. Lin, "The Road of "shellfish coin" and its significance in the study of Yunnan frontier history," *The Study of Frontier History and Geography in China*, vol. 23, no. 1, pp. 1–9, 2013.

[36] M. Sugeno, *Fuzzy Measurement and Fuzzy Integrals: A Survey in Fuzzy Automata and Decision Processes*, North-Holland Publishing, Amsterdam, Netherlands, 1977.

[37] S. Weber, "Decomposable measures and integrals for Archimedean t-conorm," *Journal of Mathematical Analysis and Applications*, vol. 101, no. 1, pp. 114–138, 1984.

[38] T. Murofushi and M. Sugeno, "An interpretation of fuzzy measures and the Choquet integral as an integral with respect to a fuzzy measure," *Fuzzy Sets and Systems*, vol. 29, no. 2, pp. 201–227, 1989.

[39] M. J. Xie, T. S. Wang, and R. M. Cui, "Does China's cultural output promote outward foreign direct investment?—An empirical test based on the development of Confucius Institute," *Economics (Quarterly)*, vol. 16, no. 4, pp. 167–188, 2017.

[40] Y. M. Chen, Q. K. Sun, and X. Y. Zhang, "Will Confucius Institute promote outward foreign direct investment?—Based on the panel data of the countries along "The Belt and Road," *International Trade Issues*, vol. 8, pp. 84–95, 2017.

[41] B. J. Wang and Y. M. Chen, "Overview of international investment in 2017," *World Economic Yearbook*, vol. 1, pp. 402–421, 2018.

[42] China Daily, "Full text of Xi Jinping's report at 19th CPC National Congress," 2020, https://www.chinadaily.com.cn/china/19thcpcnationalcongress/2017-11/04/content_34115212.htm.

[43] J. H. Sun, J. Hu, and Z. Liu, "A new criterion for λ-fuzzy measure and its application," *Computer Engineering and Applications*, vol. 19, pp. 249–255, 2014.

Hindawi
Discrete Dynamics in Nature and Society
Volume 2020, Article ID 4318182, 13 pages
https://doi.org/10.1155/2020/4318182

Research Article

Public Acceptance of Driverless Buses in China: An Empirical Analysis Based on an Extended UTAUT Model

Jian Chen,[1] **Rui Li**,[1] **Mi Gan**,[2] **Zhiyan Fu**,[3] **and Fatao Yuan**[1]

[1]*College of Traffic and Transportation, Chongqing Jiaotong University, Chongqing 400074, China*
[2]*School of Transportation and Logistics, Southwest Jiaotong University, Chengdu, Sichuan 610031, China*
[3]*School of Economics and Business Administration, Chongqing University of Education, Chongqing 400067, China*

Correspondence should be addressed to Mi Gan; migan@swjtu.edu.cn

Received 5 August 2020; Revised 17 October 2020; Accepted 25 October 2020; Published 11 November 2020

Academic Editor: Tingsong Wang

Driverless buses are expected to play a vital role in the future, and better public acceptance will provide a social foundation for its development. In this study, two new variables, personal innovativeness (PI) and perceived risk (PR), were incorporated into the integrated technology acceptance model (UTAUT, unified theory of acceptance and use of technology) to construct an extended model, which was then applied to explore the influencing factors for the public acceptance of driverless buses. The quality of this extended model was verified through survey data collected in Chongqing, China. The structural equation modeling (SEM) method was adopted to quantitatively describe the impact of each factor on acceptance intention (AI) as well as the mutual influence relationships between the factors. The moderating effects of demographic attributes (gender, age, and education level) on each factor in the model were also analyzed. The results showed that PI and PR are the most critical factors that affect the public's acceptance intention; effort expectancy (EE), performance expectancy (PE), social influence (SI), and facilitating condition (FC) can also determine the acceptance intention to a certain extent; gender, age, and education level have exhibited significantly different moderating effects on the influencing factors. The explanatory power of the current research model for acceptance intention has reached 48%. This study has confirmed the applicability of the extended UTAUT model to the research of driverless bus acceptance and the research outcomes can serve as a reference basis for improving the service quality of driverless buses in China.

1. Introduction

Autonomous or self-driving technology has received unprecedented attention since its inception. At present, as the relevant technology development is becoming mature, autonomous vehicles (AVs) are gradually coming out of the laboratory and making their debut in the market. This will bring brand-new travel experiences to consumers and alter future traffic patterns. The American Society of Automotive Engineers (SAE) classifies AVs into six levels according to their level of automation [1]; among them, Level 5 (full driving automation) represents the true "unmanned driving." The autonomous driving technology can be expected to effectively reduce traffic accidents caused by fatigued drivers and other violation behaviors, alleviate traffic congestion resulting from differences in driving behaviors, and reduce fuel consumption through optimal trajectory planning and automatic operations [2].

Major automobile and Internet companies worldwide (such as Tesla, EasyMile, Google, and IBM) are now racing to deploy autonomous driving technology and striving to influence the transportation industry. Nevertheless, the urban public transportation field—where the operating lines are relatively fixed, and the road traffic conditions are relatively regular—may be given priority for applying autonomous driving technology. The driverless bus is a new type of intelligent bus that can learn the surrounding road environment through numerous on-board sensors, as well as automatically control the vehicle steering and driving speed through the automated driving system. Road tests of

driverless buses have already been initiated in many countries, such as Olli launched jointly by IBM and Local Motors (a vehicle manufacturing company) in the United States (USA), EZ10 developed by EasyMile, Arma from Navya in France, and the Alphabus in Shenzhen, and Baidu's Apolong in China. However, due to the comprehensiveness and complexity of transportation systems, there are still many constraints for officially launching large-scale operations of driverless public transportation to the public. Such constraints are mainly manifested in terms of software technology, regulatory mechanisms, and public acceptance. A series of accidents—such as the world's first AV-related fatal accident during a highway collision of a Tesla Model S in 2016, the collision between a Navya driverless bus and a truck in 2017, and the death of a pedestrian caused by one of the Uber's driverless vehicles in 2018—have triggered the public to question the technology readiness level (TRL) of autonomous driving and the regulatory system.

In addition to the inherent technical reasons, public acceptance is also a factor that affects the official introduction and application of autonomous driving technology in the market [3, 4]. In recent years, many scholars have investigated public acceptance for autonomous vehicles. Schoettle and Sivak [5] conducted a public opinion survey based on 1,533 respondents from the USA, the United Kingdom, and Australia; most of the respondents expressed a reluctance to pay additional fees for the autonomous driving technology. Kyriakidis et al. [6] surveyed 4,886 respondents in 109 countries or regions and revealed that fully automated driving is more acceptable than manual driving, but respondents are particularly concerned about software abuse by hackers, legal issues, and security problems. Tennant et al. [7] surveyed 11,827 drivers in 11 European countries and regions; they found that the respondents' acceptances are correlated with their optimism as well as knowledge of autonomous driving technology. Other studies have pointed out the acceptance of autonomous driving technology is significantly affected by demographic attributes (such as age, gender, and education level) as well as personality heterogeneity [8–10].

Many projects of autonomous driving technology in the public transportation sector (such as EUREF in Berlin, Germany; CityMobil2 funded by the European Union (EU); and SmartShuttle in Switzerland) are in the process of performing acceptance assessments. The questionnaire study by Nordhoff et al. [11] found that the functional design (such as spaciousness and comfort) of automated shuttles and the service characteristics (such as travel cost, time en route, and waiting time) are the key factors influencing public acceptance. The study of Salonen et al. [12] points out that Finnish respondents of different ages, genders, and education levels have significantly different subjective perceptions of traffic safety, in-vehicle security, and emergency management in driverless shuttle buses. Bernhard et al. [13] conducted a survey in Mainz, Germany, and found that public acceptance of Elektro-Mobilität Mainz Autonom (EMMA) is mainly affected by ease of using the buses and performance expectancy of the buses.

Although many studies have begun to investigate the acceptance of autonomous driving technology, the influencing factors being considered in these studies are still limited. Some of the psychological determinants of public acceptance remain unclear, and the psychological decision-making process of the public cannot be described comprehensively. There are some studies on the acceptance of autonomous driving in China [4, 14–16]; however, the research is still in its infancy, and there are few studies on the acceptance of driverless buses. Thus, in this study, the driverless bus is the research object, and a corresponding acceptance analysis model is established to quantitatively describe the public's psychological feelings about driverless buses and to reveal the influence mechanism of various factors on the acceptance intention (AI). The research outcomes are expected to provide decision-making references for technical developers, policymakers, and operations managers of driverless buses in China, thereby facilitating the ability to provide better products and service quality.

The rest of this paper is organized as follows: in Section 2, the research hypotheses of this study are proposed after reviewing the literature related to autonomous driving technology; in Section 3, the research survey design, variable measurement, and data analysis methods are introduced; in Section 4, the data analysis results of the research model are presented; in Section 5, the impacts of model variables on the acceptance intention of driverless buses are compared and analyzed against the research findings of other studies; in Section 6, the theoretical and practical significance of this study is summarized and the limitations of the current study and the future research directions are also noted.

2. Literature Review and Research Hypothesis

2.1. Previous Theoretical Model Research. In sociology and psychology research, many theoretical models have been developed to analyze and explain the public acceptance of a certain technology. The most widely used models are technology acceptance model (TAM) and unified theory of acceptance and use of technology (UTAUT). In 1989, Davis proposed TAM while studying the acceptance of information systems; he argued that behavioral intention (BI) plays an important role in affecting people's actual use behavior (UB), and BI is influenced by the combined effect of three determinant factors, namely, perceived usefulness (PU), perceived ease of use (PEOU), and attitude toward using (ATU) [17]. The corresponding model framework is illustrated in Figure 1(a). PU in the model reflects the degree to which an individual believes that using the information system would enhance his/her job performance; PEOU reflects the degree of ease/difficulty an individual believes is involved in using the information system; ATU refers to the positive or negative subjective feeling of an individual when using the information system. The TAM adopted the theory of reasoned action (TRA) [19] and theory of planned behavior (TPB) [20] as the theoretical basis and applied the behavioral theories to the field of technology acceptance research for the first time. Some variables in the model (such as attitude, use intention, and UB) are along the same line as

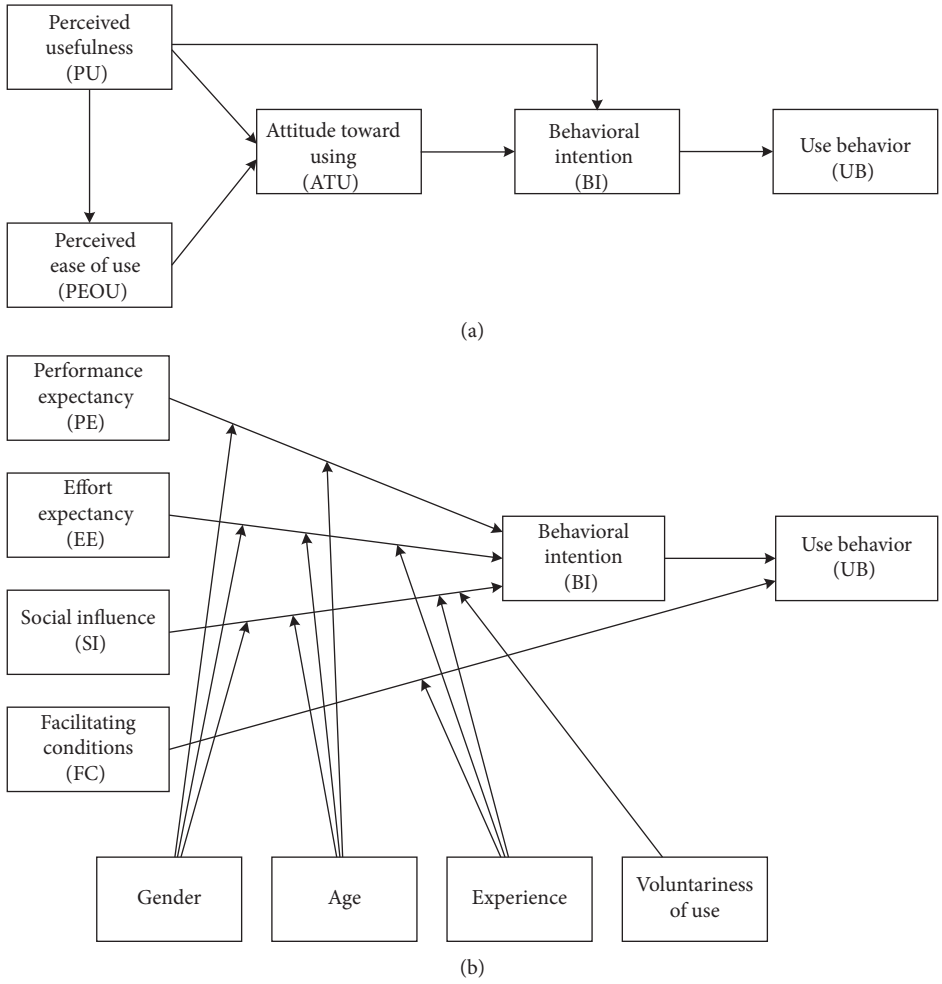

Figure 1: (a) Original TAM proposed in Davis [17]. (b) Original UTAUT proposed in Venkatesh et al. [18].

TRA and TPB; also, external factors—such as system design features, user characteristics, and policy environment—are permitted to impose a moderating effect on model variables [21]. There have been many studies that applied TAM to the research field of acceptance for AVs or automated road transportation systems (ARTS). However, researchers have gradually noticed that the influencing factors for acceptance intention are not only limited to the typical PU and PEOU in TAM, but also include trust, perceived risk (PR), social influence (SI) [16, 22, 23] and hedonic motivation (HM), psychological ownership, personality traits, and external environment [24–26]. Therefore, researchers have extended the original TAM by incorporating these new variables, the impacts of which on the acceptance behaviors have also been confirmed through investigations and research.

In order to further extend the influencing factors for acceptance of information systems and enhance the explanatory power of the model, Venkatesh et al. [18] proposed an integrated technology acceptance model (UTAUT) by combining eight behavioral theories, including TRA, TRB, diffusion of innovations (DIT) theory, social cognitive theory, and others. The UTAUT model regards effort expectancy (EE), performance expectancy (PE), SI, and facilitating condition (FC) as the core variables and considers that gender, age, experience, and voluntariness of use (VOU) have significant moderating effects on these core variables. The model framework is illustrated in Figure 1(b). The UTAUT model is a powerful theoretical tool for predicting and explaining the acceptance of information technology by individuals or organizations. It has been widely applied in research of social behavior, learning behavior, business behavior, and many other fields [27–31]. However, because its initial variables are mainly designed to study the acceptance of information systems, it has certain limitations for research in other fields. Therefore, it is usually necessary to incorporate new variables—that can reflect the characteristics of the research object—to extend and improve the UTAUT model, thereby enhancing its explanatory power. The most representative application of the UTAUT model in the research field of acceptance for ARTS is the study by Madigan et al. At first, they used the original UTAUT model to explore the impacts of the existing variables on the acceptance of ARTS in the CityMobil2 project [32]; then, in a later study, they added a new variable HM to the original model [33]. Their studies found that EE, PE, SI, FC, and HM all have a significant impact on acceptance

intention, but the explanatory power of their model needs further improvement. Rahman et al. [34] applied the UTAUT framework to investigate the acceptance intentions of American drivers for advanced driver assistance systems (ADAS) and pointed out that PE has the greatest impact on acceptance intention compared to other variables. Based on UTAUT, Kaur and Rampersad [35] discussed the impacts of trust, PE, safety, reliability, and other factors on the acceptance of driverless cars for Australian respondents. In a study of acceptance for driverless buses, Bernhard et al. [13] initiated an intention survey on an autonomous minibus, EMMA, in Mainz, Germany, and found that PE in the UTAUT model is an important predictor of acceptance intention, while the role of EE is less effective.

Recent studies that have applied TAM or UTAUT to explore the public acceptance of autonomous driving are summarized in Table 1. The literature review showed that the applications of TAM and UTAUT in the research of the acceptance behavior for autonomous driving technology are still in the early development stage. Researchers are constantly exploring new influencing factors to extend the TAM or UTAUT model and thereby better analyze the psychological decision-making process of the acceptance behavior for autonomous driving technology. The adopted research methods include descriptive statistics, multiple regression analysis (MRA), and structural equation modeling (SEM). In addition, it has been confirmed that UTAUT has a stronger explanatory power than TAM [18]. Therefore, this study aims to extend the UTAUT framework to explore the public acceptance of driverless buses in China.

2.2. Research Hypothesis. To better explain the public acceptance intention for driverless buses and explore the corresponding influencing factors, a UTAUT-based acceptance analysis model for driverless buses is established in this study. In this model, the five variables of AI, EE, PE, SI, and FC are from the original UTAUT model, while the other two variables of personal innovativeness (PI) and perceived risk (PR) are newly added in the current study after referring to relevant theories, to enhance the applicability of UTAUT model for the analysis of public acceptance intention for driverless buses. The research hypothesis and overall architecture of the model is illustrated in Figure 2.

2.2.1. Acceptance Intention (AI). The idea of using BI to reflect actual behaviors originated from the TRA and TPB theories. In later TAMs, this idea continues to apply, and its effectiveness has been extensively studied and demonstrated. In the UTAUT model, BI is usually used as the dependent variable of influencing factors for the research [17, 36]. Acceptance intention is a BI that reflects the willingness of people to accept driverless buses. Therefore, acceptance intention can be used as the dependent variable of each influencing factor in the study to explore public acceptance.

2.2.2. Effort Expectancy (EE) and Performance Expectancy (PE). EE and PE are both from the UTAUT model [18], and their definitions are similar to those by Venkatesh et al. EE here refers to the public's subjective feelings about the ease/difficulty of using driverless bus services or the degree of effort. The public believes that the more accessible the facilities and equipment of driverless buses are, and the easier the system is to use, their acceptance intentions will be more positive. PE here refers to the public's subjective feelings about the level of satisfaction of their traveling requirements, the degree of enhancement of their work efficiency, and the level of improvement in their life quality when using driverless buses. The stronger these subjective feelings are, the more likely the public will accept driverless buses. Moreover, many studies have agreed that both EE and PE have a positive impact on BI [18, 33]. Therefore, the following hypotheses are formulated:

H1: EE has a positive impact on the public's acceptance intention of driverless buses

H2: PE has a positive impact on the public's acceptance intention of driverless buses

2.2.3. Social Influence (SI) and Facilitating Conditions (FC). SI refers to the degree to which the public's personal thoughts, cognitions, and behaviors are influenced by social groups (family, friends, colleagues, etc.) in their living environment. Similar to the concept of subjective norm in TRA, TPB, and TAM [18–20], the acceptance intention of driverless public transportation by the surrounding social groups will directly affect an individual's acceptance intention. In some studies, SI has already been explored as an influencing factor for the acceptance intention of autonomous driving technology [23, 25, 37]. FC represents the extent to which existing organizations or infrastructures have promoted the development of driverless public transportation. They are mainly used to characterize the impacts of external environmental factors, such as management policies that promote the use intention. FC was initially used to examine employees' use intentions of personal computers [38]. After the empirical research by Venkatesh, it was incorporated into the UTAUT model as an important influencing factor in the research field of technology acceptance. According to the roles of these two variables in the UTAUT model, the following hypotheses are formulated:

H3: SI has a positive impact on the public's acceptance intention of driverless buses

H4: FC has a positive impact on the public's acceptance intention of driverless buses

2.2.4. Personal Innovativeness (PI) and Perceived Risk (PR). The concept of PI originates from the DIT theory [39]. It describes personality traits; more specifically, here it refers to the personal interest in and acceptance of innovative technologies. Individuals with stronger PI tend to have higher expectations for the applicability of emerging technologies and also pay closer attention to the innovative development of technologies. They often aspire to stay ahead

Table 1: Research exploring the public acceptance of autonomous driving technology using the TAM or UTAUT model.

Lead Author (year)	Country	Theoretical model	Analytical method	Main influencing factors	References
Choi (2015)	Korea	TAM	Partial least-squares (PLS) regression analysis	Trust, PEOU	Choi and Ji [22]
Madigan (2016)	France and Switzerland	UTAUT	MRA	EE, PE, SI	Madigan et al. [32]
Madigan (2017)	Greece	UTAUT	MRA	PE, SI, FC, HM	Madigan et al. [33]
Rahman (2017)	USA	UTAUT	Confirmatory factor analysis (CFA)	EE, PE	Rahman et al. [34]
Winter (2018)	USA	TAM	Descriptive statistics	Personality traits, external environment	Winter et al. [24]
Kaur (2018)	Australia	UTAUT	SEM	PE, trust, reliability	Kaur and Rampersad [35]
Panagiotopoulos (2018)	Greece	TAM	MRA	Perceived trust, SI	Panagiotopoulos and Dimitrakopoulos [25]
Lee et al., 2019	Korea	TAM	SEM	PR, self-efficacy, psychological ownership	Lee et al. [26]
Zhang (2019)	China	TAM	SEM	Initial trust, PR	Zhang et al. [16]
Zhang (2020)	China	TAM	SEM	Initial trust, SI	Zhang et al. [23]
Bernhard (2020)	Austria	UTAUT	SEM	EE, PE, environmental awareness, use experience	Bernhard et al. [13]

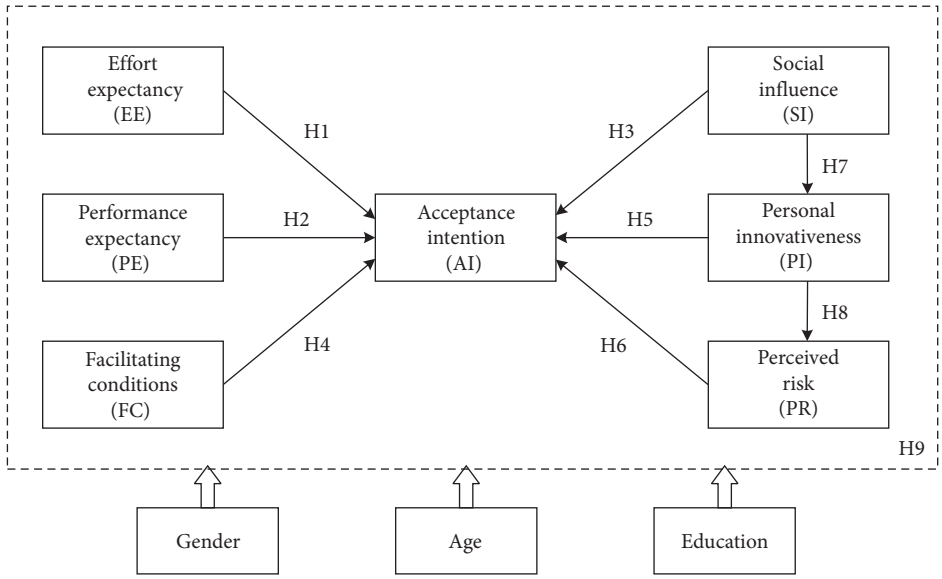

Figure 2: Research hypothesis and overall architecture of the model.

of their peers and act as the earliest adopters of the latest products. PI can also trigger continuous personal attention to emerging technologies, thereby affecting their acceptance intention. The higher the PI is, the stronger the acceptance intention will be for emerging technologies.

PR refers to an individual's perceived uncertainty about the outcome of a decision [40]. Some studies have further subdivided PR into the six aspects of time risk, financial risk, functional risk, physical risk, psychological risk, and social risk [41]. PR has also found preliminary applications in the research field of technology acceptance for autonomous driving [14, 42]. In this study, it is believed that PR has a direct impact on the acceptance of emerging driverless bus technology. When individuals are exposed to emerging technologies, they may assess the potential risks subconsciously. If the PR reaches a certain level, it will result in a negative acceptance intention; on the contrary, if an individual feels that the technology is safe and reliable, he/she will be more willing to accept and use it.

In addition, we believe that the innovation behavior and consciousness of relatives and friends of an individual will stimulate the development of his/her innovative thinking; that is, SI can have a positive impact on PI. Also, a person with stronger PI will possess more courage to try new things and assume corresponding risks and thereby unconsciously ignore potential risks, resulting in a relatively low PR level. Therefore, the following hypotheses are formulated:

H5: PI has a positive impact on the public's acceptance intention of driverless buses

H6: PR has a negative impact on the public's acceptance intention of driverless buses

H7: SI has a positive impact on PI

H8: PI has a negative impact on PR

2.2.5. Controlled Variables. In a use intention study of information technology, Venkatesh et al. analyzed the moderating effects of personal attributes—such as age, gender, experience, and VoU—on the core variables in the UTAUT model [18]. The driverless bus is an emerging technology, and relevant use experience is still lacking; also, the public has sufficient freedom to determine their acceptance of the technology, and there is no forced acceptance due to pressure from the government or organizations at the moment. Therefore, the effects of experience and VoU on the model are not addressed in the current study. Additionally, considering that individuals with higher education levels may have a better understanding of the pros and cons of driverless buses, they could be more likely to accept the technology. To explore whether personal attribute variables (age, gender, and education level) have significantly different effects on the acceptance intention of driverless buses, the following hypothesis is formulated:

H9: there are significant differences in the effects of controlled variables—such as age, gender, and education level—on the core variables of the model

3. Methods

3.1. Survey Design. Chongqing is the third demonstration zone of smart vehicles and intelligent transport, but also one of the first cities to carry out road testing for autonomous driving in China. Its automobile industry (the city's pillar industry) has certain advantages throughout the country. In addition, compared with other cities, Chongqing's road traffic situation is more complicated, and the traffic behavior of citizens is more special because Chongqing is a typical mountainous city. Therefore, exploring the public acceptance of autonomous driving or unmanned driving in Chongqing has a certain representative. In this study, residents of Chongqing were selected as the survey object, and a combination of online and offline questionnaires was distributed to investigate the public acceptance intention of driverless buses. A brief textual introduction of the driverless bus was given at the beginning of the questionnaires in the survey, accompanied by relevant pictures of its appearance, internal space, and actual operating status. The online survey also included related operating videos of driverless buses. This was expected to create a more intuitive feeling of driverless buses for the respondents and increase their understanding of the item descriptions in the questionnaires. And the survey contained two parts: the first part gathered the demographic characteristics, including gender, age, and education level; the second part was a measurement scale for the public's subjective perceptions of driverless buses, covering the measurement of seven variables, namely, EE, PE, SI, FC, PI, PR, and AI. The measurement scales used in the past research of technology acceptance were analyzed and adapted accordingly, so as to obtain the measured scale applicable for this study. Based on the designed measurement scale, the reliability and validity of the questionnaires were examined by the data collected through a small sample pretest. The measurement items that failed in the test were removed to obtain the final and formal questionnaires. After testing, it took approximately 5 to 10 minutes to complete one questionnaire.

The survey was conducted in August 2019 and October 2020 in Chongqing, where 1000 copies of the formal questionnaire were issued within two weeks totally. After eliminating invalid questionnaires—that were not filled in carefully, had more than three missing values, and selected more than five extreme values consecutively—a total of 913 valid questionnaires were recovered, with an effective recovery rate of 91.30%. The number of online and offline questionnaires was 262 and 651, respectively, with a ratio of approximately 1.0 : 2.5. The number of valid samples was more than ten times the number of questions in the questionnaire (26 questions), which conforms to the empirical criteria proposed by Hoogland and Boomsma as well as Kline [43, 44], and it was sufficient in terms of theoretical research and could be used to verify the theoretical model. The basic information of the recovered 913 valid questionnaires was categorized, and the specific personal attributes data are detailed in Table 2. In order to ensure that the influence of control variables (gender, age, and education level) on the acceptance intention is not interfered by the diversity of samples, this survey intentionally controlled the selection of respondents and the sampling area in the process of offline questionnaires distribution, so as to make the total number of samples was evenly distributed in age, gender, and education level.

3.2. Research Measurement. The 7-point Likert scale was adopted in this study to measure the latent variables that cannot be directly observed in the model. A 7-point score—from "strongly disagree (=1)" to "strongly agree (=7)"—was used to rank the respondent's degree of approval towards the relevant description given in each questionnaire measurement item, so as to reflect the public's psychological feelings about driverless buses. The measurement items for each variable were adapted accordingly based on previous research in the field of technology acceptance, mainly from Davis [17], Venkatesh et al. [18], and Thompson et al. [38]. The specific measurement items are detailed in Table 3.

3.3. Data Analysis. To simultaneously explore the influence relationships between latent variables—that are relatively abstract in concept and cannot be measured directly—the method of SEM, a multivariate statistical analysis technique, was applied to analyze the data. SEM can be divided into measurement modeling (MM) and structural modeling (SM), where MM is used to describe the relationship between the observable variables and the latent variables, and

Table 2: Description of questionnaire statistics ($N = 913$).

Personal attribute	Classification	Sample size (N)	Percentage (%)
Gender	Male	468	51.24
	Female	445	48.76
Age (years)	<18	167	18.27
	18–25	198	21.68
	26–40	184	20.15
	41–60	185	20.31
	>60	179	19.59
Education level	High school and below	218	23.87
	College degree	235	25.73
	Bachelor's degree	242	26.49
	Master's degree and above	218	23.91

Table 3: Measurement items for model variables.

Latent variable	Item no.	Measurement item	Adapted source/reference
EE	EE1	Test ride locations for driverless buses will be easy to find	Venkatesh et al. [18]
	EE2	The payment methods for taking driverless buses will be straightforward	
	EE3	I will soon become familiar with and accustomed to taking driverless buses	
PE	PE1	Driverless buses can reduce traffic congestion, thereby shortening the riding time	Davis [17] and Venkatesh et al. [18]
	PE2	Driverless buses can reduce traffic accidents	
	PE3	Driverless buses can improve the efficiency and quality of my study, work, and life	
SI	SI1	If relatives and friends around me are taking driverless buses, I will follow along	Thompson et al. [38] and Ajzen [20]
	SI2	If colleagues around me are taking driverless buses, I will follow along	
	SI3	Propaganda and guidance from the media will convince me to take the driverless bus	
	SI4	Taking the driverless bus will give me more conversation starters in social activities, thereby enhancing my social image	
FC	FC1	Driverless buses have received much policy support	Thompson et al. [38]
	FC2	Related management technologies can support driverless bus operations	
	FC3	I already have the knowledge needed to ride a driverless bus	
PI	PI1	I often pay attention to the development trend of driverless buses	Rogers [39]
	PI2	I am willing to try new technology products and services	
	PI3	I am often the first to use emerging technology products or services among my acquaintances	
	PI4	I am good at exploring and trying new things	
PR	PR1	I think the speed of driverless buses is not fast enough, which will affect my travel time	Zhang et al. [16] and Zmud et al. [45]
	PR2	I am concerned that driverless buses will cost more than traditional buses	
	PR3	I am concerned that the functional design of driverless buses is still not perfect today	
	PR4	I am concerned about being persecuted by others in the driverless buses	
	PR5	I am concerned that the safety performance of driverless buses is not guaranteed	
	PR6	I am concerned that driverless buses will conflict and interfere with human-driven vehicles	
AI	AI1	I will take the driverless bus when the technology is mature in the future	Davis [17]
	AI2	I will take driverless buses often in the future	
	AI3	I would highly recommend taking driverless buses to my relatives and friends	

SM is used to describe the relationships between each latent variable. The SEM method has been widely applied in psychology, pedagogy, sociology, and other research fields [46–48]. At the same time, to ensure the validity of the questionnaire design and the adaptability of the constructed model, the reliability and validity of the model, as well as its overall goodness of fit, need to be tested through the data obtained from the questionnaire survey. Related calculations were performed using Mplus 7.4 software.

The reliability and validity of the questionnaires were tested using the confirmatory factor analysis (CFA) method. The reliability test generally examines the internal consistency of the questionnaire measurement items, which is usually evaluated by the construct reliability (CR). The evaluation criteria (threshold) adopted by Kline and many other researchers [44, 49, 50] are as follows: a CR value of above 0.9 is the best; 0.8-0.9 is very good; 0.7-0.8 is moderate; 0.5–0.7 is acceptable. The validity test generally examines the two aspects of convergent validity and discriminant validity.

If the factor loading coefficient of each measurement variable exceeds 0.6, and the average variance extracted (AVE) is greater than 0.5, the model has a good convergent validity [51]. According to the evaluation criteria proposed by Fomell and Larcker [52], if the square root of AVE of each latent variable is greater than the Pearson correlation coefficient (PCC) between this variable and the other variables, the model has good discriminant validity.

The covariance matrix of measurement variables generated by quantitative parameter estimation was tested for its closeness to the sample covariance matrix. The better the model fits, the more accurate the parameter estimation is. The model's overall goodness-of-fit indices include chi-square degree of freedom ratio (χ^2/df, also known as standard chi-square), root mean square error of approximation (RMSEA), comparative fit index (CFI), nonnormed fit index (NNFI, also known as the Tucker–Lewis Index, TLI), and standardized root mean square residual (SRMR). Kline et al. pointed out that for a good model fit, the goodness-of-fit indices should meet the following criteria: χ^2/df is in the range of 1–3, CFI and TLI are greater than 0.90, and RMSEA and SRMR are less than 0.08 [44, 53].

Since the core variables in the current model are all latent variables, which are difficult to observe directly, the average score of each measurement variable corresponding to the latent variable in each data sample was taken as the observed value of the latent variable. With these observed values as the dependent variable, and with age, gender, and education as the independent variables, a multivariate analysis of variance (ANOVA) was conducted to test whether these controlled variables had significantly different effects on the latent variables in the model ($P < 0.05$ was used as the significance criterion).

4. Results

4.1. Measurement Model Evaluation. The CFA results of the measurement model are listed in Tables 4 and 5. The CR values of all latent variables are greater than 0.8, indicating that the internal consistency or isomorphism between the measurement variables of the same latent variable is good. As reflected by the measurement variables, the construct (latent trait) has a good consistency, and the reliability is at the "very good" level. The factor loading coefficients of all measurement variables are greater than 0.7, and the AVE values are greater than 0.5, indicating that the measurement variables have a high degree of internal correlation, which can effectively reflect the latent traits of the latent variables. Also, the proportion of variance explained by the latent variable is much higher than that explained by the measurement error, thus indicating that the measurement model has good convergent validity. The square root of AVE value of each latent variable is all greater than the PCC value between this latent variable and the other ones, indicating that there are significant differences between the constructs of different latent variables, and the model has good discriminant validity. It can be seen that both the reliability and validity of the model have passed the test, thereby showing that the model has good internal quality.

4.2. Structural Model Evaluation. The overall goodness-of-fit test results of the model are listed in Table 6. All the goodness-of-fit evaluation indices reached the test criteria, indicating that the model has good adaptability and external quality. The standardized path coefficient β can reflect the magnitude of the interaction between variables. The square multiple correlation (SMC) of endogenous latent variables, namely, R^2, can reflect the explanatory power of the model.

Table 4: Analysis results of reliability and convergent validity.

Latent variable	Item no.	Factor loading coefficient	CR	AVE
EE	EE1	0.857	0.858	0.669
	EE2	0.811		
	EE3	0.784		
PE	PE1	0.719	0.817	0.599
	PE2	0.767		
	PE3	0.832		
SI	SI1	0.769	0.850	0.586
	SI2	0.775		
	SI3	0.781		
	SI4	0.736		
FC	FC1	0.722	0.802	0.575
	FC2	0.797		
	FC3	0.753		
PI	PI1	0.781	0.872	0.631
	PI2	0.802		
	PI3	0.730		
	PI4	0.859		
PR	PR1	0.845	0.924	0.672
	PR2	0.762		
	PR3	0.873		
	PR4	0.767		
	PR5	0.835		
	PR6	0.829		
AI	AI1	0.847	0.874	0.698
	AI2	0.782		
	AI3	0.875		

Table 5: Analysis results of discriminant validity.

	EE	PE	SI	FC	PI	PR	AI
EE	**0.818**						
PE	0.523	**0.774**					
SI	0.719	0.716	**0.766**				
FC	0.431	0.682	0.373	**0.758**			
PI	0.447	0.640	0.605	0.634	**0.794**		
PR	0.390	0.531	0.433	0.420	−0.622	**0.820**	
AI	0.535	0.549	0.468	0.653	0.715	−0.731	**0.835**
CR	0.858	0.817	0.850	0.802	0.872	0.924	0.874
AVE	0.669	0.599	0.586	0.575	0.631	0.672	0.698

Note: values on the diagonal of the coefficient matrix in the table are the square roots of the AVE values, and values in the lower triangular matrix are the PCCs between variables.

Table 6: Test results of goodness of fit.

Evaluation Index	χ^2/df	CFI	TLI	RMSEA	SRMR
Criterion	(1, 3)	>0.90	>0.90	<0.08	<0.08
Test value	2.49	0.95	0.93	0.04	0.05

The standardized path analysis results of the structural model are given in Table 7 and Figure 3.

The impact of each latent variable on acceptance intention is ranked from the highest to lowest as follows: PR ($\beta = -0.82$, $P < 0.001$), PI ($\beta = 0.71$, $P < 0.001$), SI ($\beta = 0.65$, $P < 0.001$), PE ($\beta = 0.59$, $P < 0.001$), EE ($\beta = 0.43$, $P < 0.01$), and FC ($\beta = 0.30$, $P < 0.05$). All latent variables have shown a significant impact on the acceptance intention with a confidence interval of 95% (corresponding to $P < 0.05$). PI has also exhibited a significant impact on PR ($\beta = -0.62$, $P < 0.001$). The only exception is that SI did not present a significant impact on PI ($\beta = 0.33$, $P > 0.05$). Therefore, among the research hypotheses about the latent variables, H1–H6 and H8 are valid, but H7 is invalid. In the model, the proportion of variance in PI that can be explained by SI is 11% ($R^2 = 0.11$); the proportion of variance in PR that can be explained by PI is 35% ($R^2 = 0.35$); the proportion of variance in acceptance intention (AI) that can be explained by all the other variables is 48% ($R^2 = 0.48$). The evaluation criteria of R^2 pointed out by Marcoulides [54] are as follows: R^2 lower than 0.19 indicates that the explanatory power is unacceptable; 0.19–0.33 indicates that the explanatory power is weak; 0.33–0.67 indicates that the explanatory power is moderate; above 0.67 indicates that the explanatory power is good. In addition, the evaluation criteria proposed by Cohen et al. [55] point out that when R^2 reaches 0.40, the theoretical model is considered as having good explanatory power. Following the evaluation criteria proposed by Marcoulides [54] and Cohen et al. [55], it can be inferred that the theoretical model has good explanatory power for acceptance intention.

4.3. Controlled Variable Analysis. The results of ANOVA for the moderating effect of controlled variables on each latent variable are given in Table 8. It can be seen that gender has a significant moderating effect on the three influencing factors of EE, SI, and PR; age has a significant moderating effect on the four influencing factors of EE, SI, FC, PI, PR, and AI; education level has a significant moderating effect on the four influencing factors of PE, FC, PI, PR and AI. Overall, the three controlled variables of gender, age, and education level have significantly different effects on the latent variables of the model; thus, the research hypothesis about controlled variables (H9) is valid.

5. Discussion

According to the empirical analysis results, except for research hypothesis H7, the other research hypotheses have all been verified as valid. The PI and PR variables newly added in this study are shown to have a significant impact on the acceptance intention, even greater than the impacts of the other variables in UTAUT. Also, the impacts of model variables on the acceptance intention are similar to those observed in other countries or regions in the field of technology acceptance and, even more specifically, in the field of autonomous driving technology acceptance; however, there are also some differences.

5.1. Impacts of EE and PE on Acceptance Intention. It is found from the empirical study that both EE and PE have a significantly positive impact on acceptance intention. However, in some studies on the acceptance behavior of automated driving in other countries or regions, such as Germany and France, EE showed no decisive impact on acceptance intention [33, 56]. In the current study, although the impact of EE on acceptance intention is found to be small, it cannot be ignored. Only when the public believes that it is convenient to travel with driverless buses, and the facilities and equipment in the buses are easy to operate and effortless, will they be willing to accept the use of driverless buses. In fact, a concept similar to EE is PEOU in TAM. In a survey conducted by Zhang et al. [16] in Shenzhen, China, the impact of PEOU on AV acceptance has also been demonstrated, indicating that the Chinese public might be more concerned about the ease/difficulty of using driverless buses. On the other hand, PE is equivalent to PU in TAM. Only when the public believes that driverless buses have significant benefits in improving their work efficiency and quality of life, will they be willing to accept driverless buses. The impact of PE on acceptance intention observed in this study can be mutually supported by the results of relevant investigations and research conducted in Australia and Greece by Kaur and Rampersad [35] and Panagiotopoulos and Dimitrakopoulos [25], respectively.

5.2. Impacts of SI and FC on Acceptance Intention. Similar to the results obtained in other countries or regions [25, 57], SI has a significantly positive impact on acceptance intention. That is, when there is someone (influencer) who can significantly influence an individual's decision-making process, he/she will present a stronger acceptance intention if the influencer thinks that he/she should use driverless buses. In China, the composition of personal social relations is relatively complex, and an individual's behaviors are often susceptible to the influences of people or organizations closely related to them. If the information and messages about driverless buses passed around by acquaintances or organizations are positive, the possibility that he/she will understand and accept driverless buses will increase; otherwise, he/she will be likely to develop a negative stereotype towards driverless buses and believe that traveling by driverless buses is not worth considering or choosing. The impact of FC on acceptance intention is the weakest but does exist, which is similar to the research result of technology acceptance behavior reported by Venkatesh et al. [58]. Since the driverless bus is an emerging technology and has not been widely used in China, the public has little understanding of the relevant policy support, which could be the main reason for the relatively weak impact of FC on acceptance intention.

5.3. Impacts of PI and PR on Acceptance Intention. The newly added variable PI showed the second greatest impact on the acceptance intention of driverless buses, only lower than PR. This observation indicates that PI plays a vital role in affecting acceptance intention; that is, the stronger the PI is,

Table 7: Standardized path analysis results of the structural model.

Hypotheses	Standardized path coefficients	CR	P	Significance	Hypothesis test result	R^2
H1: EE ⟶ AI	0.43	5.19	**	Significant	H1 valid	AI: 0.48
H2: PE ⟶ AI	0.59	6.61	***	Significant	H2 valid	
H3: SI ⟶ AI	0.65	7.36	***	Significant	H3 valid	
H4: FC ⟶ AI	0.30	4.71	*	Significant	H4 valid	
H5: PI ⟶ AI	0.71	10.05	***	Significant	H5 valid	
H6: PR ⟶ AI	−0.82	−12.38	***	Significant	H6 valid	
H7: SI ⟶ PI	0.33	1.52	0.11	Insignificant	H7 invalid	PI: 0.11
H8: PI ⟶ PR	−0.62	−6.97	***	Significant	H8 valid	PR: 0.35

Note: CR is the critical ratio, and a CR value greater than 1.96 indicates a significance level of 0.05 has been reached. $^{***}P < 0.001$, $^{**}P < 0.01$, and $^{*}P < 0.05$.

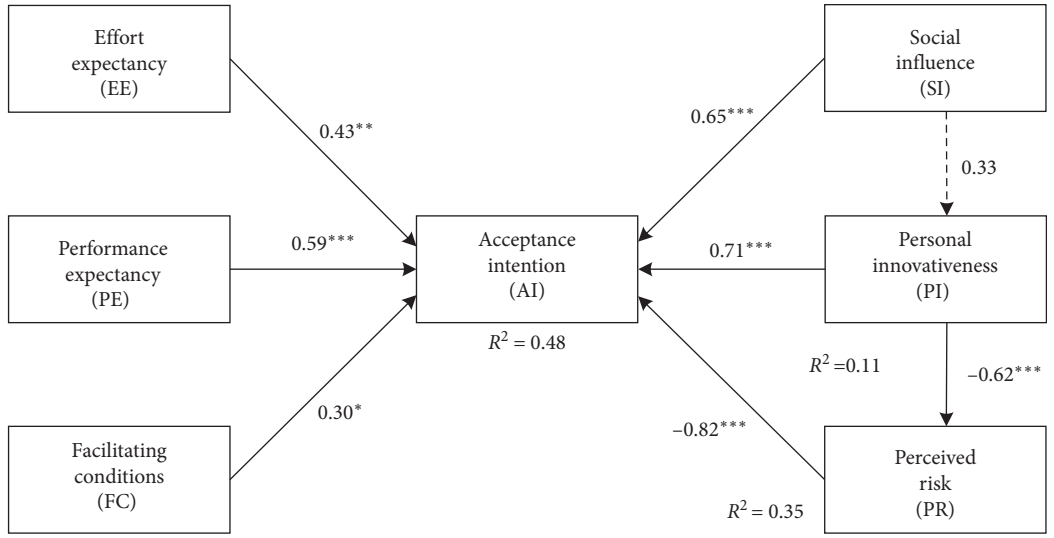

Figure 3: Analysis results of the structural model. Note: the solid arrows represent the paths with significant impacts, and the dotted arrow represents the path with insignificant impact. *** $P < 0.001$, $^{**}P < 0.01$, and $^{*}P < 0.05$.

Table 8: Results of ANOVA (P value).

Controlled variables	EE	PE	SI	FC	PI	PR	AI
Gender	0.039*	—	0.043*	—	—	0.004**	—
Age	0.045*	—	0.036*	0.022*	0.000***	0.000***	0.001**
Education level	—	0.008**	—	0.043*	0.002**	0.020*	0.036*

Note: if the test P value is greater than 0.05, the moderating effect is not significant; if the P value is lower than 0.05, the moderating effect is significant. $^{***}P < 0.001$, $^{**}P < 0.01$, and $^{*}P < 0.05$.

the stronger the acceptance and sensitivity to emerging technologies an individual would possess, and the stronger his/her acceptance intention will be. In the studies of Jackson et al. [59] and Turan et al. [60], it has also been pointed out that PI should be regarded as one of the core influencing factors for technology acceptance in combination with the DIT theory. The impact of PR on acceptance intention ranks first in this study, indicating that respondents in Chongqing, China, are especially concerned about the safety of driverless buses. The greater an individual's PR is, the more likely he/she will express a negative acceptance intention. This observation could be related to the more conservative and cautious personality traits of some Chinese people. In the studies of Piao et al. [61] and Nazari et al. [62], it has also been emphasized that perception of lower risk is a critical factor affecting the public acceptance of AVs. In the investigations and research conducted by Zmud et al. [45] and Menon et al. [63] in Texas and Florida in the USA, it has also been found that PR has a negative impact on the acceptance intention of AVs. In the study conducted by Liu et al. [14] in Tianjin, China, it was pointed out that the impact of PR on the acceptance intention of AVs does exist but is not strong. It is explained that this phenomenon could be due to the public's insufficient awareness about the risks of AVs. At the same time, in the current study, PI was also found to have a relatively significant negative impact on PR; that is, the stronger an individual's PI is, the more optimistic he/she will be in considering the risk factors in the environment, thereby presenting a relatively weaker ability to perceive risks.

5.4. Effects of Age, Gender, and Education Level on the Model Variables. Through the ANOVA, it is concluded that the effects of demographic attributes—such as age, gender, and education level—on the core latent variables in the constructed model are significantly different; that is, they have a moderating effect on the influence relationships in the model. Many studies have argued that the effects of these demographic attribute variables on the UTAUT model are not obvious or have been weakening gradually [16, 32]. However, the current study finds that the effects of these demographic attribute variables on the model variables cannot be ignored. This conclusion coincides with the findings of Venkatesh et al. [58] and Bansal et al. [37] in their studies in Arkansas and Texas, USA. Among the demographic attributes, age and education level have exhibited an especially obvious effect on the public's acceptance intention of driverless buses.

6. Conclusions

The purpose of this study is to explore the influencing factors that affect the public's acceptance intention of driverless buses as well as the relationships between the various factors. The research results can be expected to provide preliminary references for research in this field. A driverless bus acceptance analysis model was constructed by extending the UTAUT model. The SEM method was applied to describe the measurement relationship between latent variables and measurement variables, as well as the structural relationships between the latent variables. The data obtained from the actual survey of respondents in Chongqing, China, were used to verify the mutual influence relationships in the model quantitatively. In the current study, it is found that EE, PE, SI, FC, PI, and PR all have a significant impact on acceptance intention; also, the impacts of the two newly added variables—PR and PI—on the acceptance intention for driverless buses are especially prominent. It can be considered that this extended model has good applicability for the research of acceptance intention for driverless buses.

This study has two levels of significance in terms of theoretical enlightenment and practical application reference. At the theoretical level, this study extends the integrated technology acceptance model and incorporates new variables that can characterize the features of driverless buses. An empirical basis has been provided for the effective combination of the DIT theory, perceived risk theory, and UTAUT model. The theoretical analysis methods have been enriched in the research field of technology acceptance. At the practical application level, this study explored the influencing factors that could affect the public's acceptance intention of driverless buses. An understanding of these factors will be beneficial for analyzing the market, thereby providing directions for driverless bus manufacturers and policymakers in future technology research and development as well as functional design. The research outcomes can also provide objective reference opinions for the government to issue management policies for driverless buses. For example, it is found in this study that PR is the most important influencing factor for acceptance intention, so the functional design of driverless buses should improve their safety performance to reduce the public's concerns about the riding time, cost, and personal safety en route.

However, this study inevitably has limitations that need to be resolved. First, this study analyzed the acceptance BIs for driverless buses, which could not represent actual behaviors completely because driverless public transportation has not yet been widely put into market application in China, and most respondents did not have actual use experience. Therefore, their acceptance behaviors can only be explored indirectly through BIs, which will more or less lead to some deviations. Once driverless bus technology has become more mature, further research can be carried out according to the actual use behaviors of the public. Second, the explanatory power of the current research model for the acceptance intention of driverless buses is 48%, which indicates that the model has not fully captured the influencing factors for the public acceptance intention. Whether other influencing factors in the research field of technology acceptance (such as HM, trust level, and environmental awareness) would significantly affect acceptance intention still requires further exploration. Third, the effects of demographic attributes (such as gender, age, and education level) of respondents on acceptance intention are found to be significantly different in this study, but many other studies suggest the opposite; therefore, more follow-up research should be conducted to verify this observation.

Data Availability

The data used to support the findings of this study are available from the corresponding author upon request.

Conflicts of Interest

The authors declare that there are no conflicts of interest regarding the publication of this paper.

Acknowledgments

This research was funded by the Western Project of the National Social Science Fund of China (grant no. 17XGL009).

Supplementary Materials

Questionnaire on public acceptance of driverless buses. Part 1: personal information. Part 2: a measurement scale for public's subjective perceptions of driverless buses. (*Supplementary Materials*)

References

[1] SAE International, "Taxonomy and definitions for terms related to on-road motor vehicle automated driving systems," Report No, J3016_201806, SAE International, Warrendale, PA, USA, 2018.

[2] D. J. Fagnant and K. Kockelman, "Preparing a nation for autonomous vehicles: opportunities, barriers and policy recommendations," *Transportation Research Part A: Policy and Practice*, vol. 77, pp. 167–181, 2015.

[3] I. Y. Noy, D. Shinar, and W. J. Horrey, "Automated driving: safety blind spots," *Safety Science*, vol. 102, pp. 68–78, 2018.

[4] Z. Xu, K. Zhang, H. Min, Z. Wang, X. Zhao, and P. Liu, "What drives people to accept automated vehicles? findings from a field experiment," *Transportation Research Part C: Emerging Technologies*, vol. 95, pp. 320–334, 2018.

[5] B. Schoettle and M. Sivak, *A Survey of Public Opinion about Autonomous and Self-Driving Vehicles in the U.S., the U.K., and Australia*, Transportation Research Institute: University of Michigan, Ann Arbor, MI, USA, 2014.

[6] M. Kyriakidis, R. Happee, and J. C. F. De Winter, "Public opinion on automated driving: results of an international questionnaire among 5000 respondents," *Transportation Research Part F: Traffic Psychology and Behaviour*, vol. 32, pp. 127–140, 2015.

[7] C. Tennant, S. Stares, and S. Howard, "Public discomfort at the prospect of autonomous vehicles: building on previous surveys to measure attitudes in 11 countries," *Transportation Research Part F: Traffic Psychology and Behaviour*, vol. 64, pp. 98–118, 2019.

[8] W. Payre, J. Cestac, and P. Delhomme, "Intention to use a fully automated car: attitudes and a priori acceptability," *Transportation Research Part F: Traffic Psychology and Behaviour*, vol. 27, pp. 252–263, 2014.

[9] C. Hohenberger, M. Spörrle, and I. M. Welpe, "How and why do men and women differ in their willingness to use automated cars? the influence of emotions across different age groups," *Transportation Research Part A: Policy and Practice*, vol. 94, pp. 374–385, 2016.

[10] C. J. Haboucha, R. Ishaq, and Y. Shiftan, "User preferences regarding autonomous vehicles," *Transportation Research Part C: Emerging Technologies*, vol. 78, pp. 37–49, 2017.

[11] S. Nordhoff, J. de Winter, R. Madigan, N. Merat, B. van Arem, and R. Happee, "User acceptance of automated shuttles in Berlin-Schöneberg: a questionnaire study," *Transportation Research Part F: Traffic Psychology and Behaviour*, vol. 58, pp. 843–854, 2018.

[12] A. O. Salonen, "Passenger's subjective traffic safety, in-vehicle security and emergency management in the driverless shuttle bus in Finland," *Transport Policy*, vol. 61, no. 1, pp. 106–110, 2018.

[13] C. Bernhard, D. Oberfeld, C. Hoffmann, D. Weismüller, and H. Hecht, "User acceptance of automated public transport: valence of an autonomous minibus experience," *Transportation Research Part F: Traffic Psychology and Behaviour*, vol. 70, pp. 109–123, 2020.

[14] P. Liu, R. Yang, and Z. Xu, "Public acceptance of fully automated driving: effects of social trust and risk/benefit perceptionsffects of social trust and risk/benefit perceptions," *Risk Analysis*, vol. 39, no. 2, pp. 326–341, 2019.

[15] J. Wu, H. Liao, J.-W. Wang, and T. Chen, "The role of environmental concern in the public acceptance of autonomous electric vehicles: a survey from China," *Transportation Research Part F: Traffic Psychology and Behaviour*, vol. 60, pp. 37–46, 2019.

[16] T. Zhang, D. Tao, X. Qu, X. Zhang, R. Lin, and W. Zhang, "The roles of initial trust and perceived risk in public's acceptance of automated vehicles," *Transportation Research Part C: Emerging Technologies*, vol. 98, pp. 207–220, 2019.

[17] F. D. Davis, "Perceived usefulness, perceived ease of use, and user acceptance of information technology," *MIS Quarterly*, vol. 13, no. 3, pp. 319–340, 1989.

[18] V. Venkatesh, M. G. Morris, G. B. Davis, and F. D. Davis, "User acceptance of information technology: toward a unified view," *MIS Quarterly*, vol. 27, no. 3, pp. 425–478, 2003.

[19] M. Fishbein and I. Ajzen, "Belief, attitude, intention and behaviour: an introduction to theory and research," *Philosophy & Rhetoric*, vol. 41, no. 4, pp. 842–844, 1980.

[20] I. Ajzen, "The theory of planned behavior," *Organizational Behavior and Human Decision Processes*, vol. 50, no. 2, pp. 179–211, 1991.

[21] V. Venkatesh and F. D. Davis, "A theoretical extension of the technology acceptance model: four longitudinal field studies," *Management Science*, vol. 46, no. 2, pp. 186–204, 2000.

[22] J. K. Choi and Y. G. Ji, "Investigating the importance of trust on adopting an autonomous vehicle," *International Journal of Human-Computer Interaction*, vol. 31, no. 10, pp. 692–702, 2015.

[23] T. Zhang, D. Tao, X. Qu et al., "Automated vehicle acceptance in China: social influence and initial trust are key determinants," *Transportation Research Part C: Emerging Technologies*, vol. 112, pp. 220–233, 2020.

[24] S. R. Winter, S. Rice, R. Mehta et al., "Do Americans differ in their willingness to ride in a driverless bus?," *Journal of Unmanned Vehicle Systems*, vol. 6, no. 4, pp. 267–278, 2018.

[25] I. Panagiotopoulos and G. Dimitrakopoulos, "An empirical investigation on consumers' intentions towards autonomous driving," *Transportation Research Part C: Emerging Technologies*, vol. 95, pp. 773–784, 2018.

[26] J. Lee, D. Lee, Y. Park, S. Lee, and T. Ha, "Autonomous vehicles can be shared, but a feeling of ownership is important: examination of the influential factors for intention to use autonomous vehicles," *Transportation Research Part C: Emerging Technologies*, vol. 107, pp. 411–422, 2019.

[27] N. Puspitasari, M. B. Firdaus, C. A. Haris, and H. J. Setyadi, "An application of the UTAUT model for analysis of adoption of integrated license service information system," *Procedia Computer Science*, vol. 161, pp. 57–65, 2019.

[28] R. Hoque and G. Sorwar, "Understanding factors influencing the adoption of mHealth by the elderly: an extension of the UTAUT model," *International Journal of Medical Informatics*, vol. 101, pp. 75–84, 2017.

[29] S. Chauhan and M. Jaiswal, "Determinants of acceptance of ERP software training in business schools: empirical investigation using UTAUT model," *The International Journal of Management Education*, vol. 14, no. 3, pp. 248–262, 2016.

[30] J. Khalilzadeh, A. B. Ozturk, and A. Bilgihan, "Security-related factors in extended UTAUT model for NFC based mobile payment in the restaurant industry," *Computers in Human Behavior*, vol. 70, pp. 460–474, 2017.

[31] S. Sarosa, "The role of brand reputation and perceived enjoyment in accepting compulsory device's usage: extending UTAUT," *Procedia Computer Science*, vol. 161, pp. 115–122, 2019.

[32] R. Madigan, T. Louw, M. Dziennus et al., "Acceptance of automated road transport systems (ARTS): an adaptation of the UTAUT model," *Transportation Research Procedia*, vol. 14, pp. 2217–2226, 2016.

[33] R. Madigan, T. Louw, M. Wilbrink, A. Schieben, and N. Merat, "What influences the decision to use automated public transport? using UTAUT to understand public acceptance of automated road transport systems," *Transportation Research Part F: Traffic Psychology and Behaviour*, vol. 50, pp. 55–64, 2017.

[34] M. M. Rahman, M. F. Lesch, W. J. Horrey, and L. Strawderman, "Assessing the utility of TAM, TPB, and UTAUT for advanced driver assistance systems," *Accident Analysis & Prevention*, vol. 108, pp. 361–373, 2017.

[35] K. Kaur and G. Rampersad, "Trust in driverless cars: investigating key factors influencing the adoption of driverless cars," *Journal of Engineering and Technology Management*, vol. 48, pp. 87–96, 2018.

[36] R. J. Holden and B.-T. Karsh, "The technology acceptance model: its past and its future in health care," *Journal of Biomedical Informatics*, vol. 43, no. 1, pp. 159–172, 2010.

[37] P. Bansal, K. M. Kockelman, and A. Singh, "Assessing public opinions of and interest in new vehicle technologies: an Austin perspective," *Transportation Research Part C: Emerging Technologies*, vol. 67, pp. 1–14, 2016.

[38] R. L. Thompson, C. A. Higgins, and J. M. Howell, "Personal computing: toward a conceptual model of utilization," *MIS Quarterly*, vol. 15, no. 1, pp. 125–143, 1991.

[39] E. M. Rogers, *Diffusion of Innovations*, The Free Press, New York, NY, USA, 1983.

[40] R. A. Bauer, "Consumer behavior as risk taking," in *Proceedings of the 43rd American Marketing Association Conference*, R. S. Hancock, Ed., American Marketing Association: CHI, Chicago, IL, USA, pp. 389–398, June 1960.

[41] J. Jacoby and L. B. Kaplan, "The components of perceived risk," *Advances in Consumer Research*, vol. 3, pp. 382-383, 1972.

[42] P. Bansal and K. M. Kockelman, "Forecasting Americans' long-term adoption of connected and autonomous vehicle technologies," *Transportation Research Part A: Policy and Practice*, vol. 95, pp. 49–63, 2017.

[43] J. J. Hoogland and A. Boomsma, "Robustness studies in covariance structure modeling," *Sociological Methods & Research*, vol. 26, no. 3, pp. 329–367, 1998.

[44] R. B. Kline, *Principles and Practice of Structural Equation Modeling*, Guilford Press, New York, NY, USA, 2nd edition, 2005.

[45] J. P. Zmud, I. N. Sener, and J. Wagner, *Consumer Acceptance and Travel Behavior Impacts of Automated Vehicles (PRC15-49F)*, Texas A&M Transportation Institute, Bryan, TX, USA, 2016.

[46] J. R. Priester, "The use of structural equation models in consumer psychology: a methodological dialogue on its contributions, cautions, and concerns," *Journal of Consumer Psychology*, vol. 20, no. 2, pp. 205–207, 2010.

[47] H. Camgoz-Akdag and S. Zaim, "Education: a comparative structural equation modeling study," *Procedia—Social and Behavioral Sciences*, vol. 47, pp. 874–880, 2012.

[48] F. Boccia and P. Sarnacchiaro, "Structural equation model for the evaluation of social initiatives on customer behaviour," *Procedia Economics and Finance*, vol. 17, pp. 211–220, 2014.

[49] R. P. Bagozzi and Y. Yi, "On the evaluation of structural equation models," *Journal of the Academy of Marketing Science*, vol. 16, no. 1, pp. 74–94, 1988.

[50] J. F. J. Hair, R. E. J. Anderson, R. L. Tatham, and W. C. Black, *Multivariate Data Analysis*, Prentice Hall, Upper Saddle River, NJ, USA, 5th edition, 1998.

[51] M. R. A. Hamid, W. Saml, and M. H. Mohmad-Sldek, "Discriminant validity assessment: use of Fornell & Larcker criterion versus HIMT criterion," *Journal of Physics: Conference Series*, vol. 890, Article ID 012163, 2017.

[52] C. Fomell and D. F. Larcker, "Evaluating structural equation models with unobservable variables and measurement error," *Journal of Marketing Research*, vol. 18, no. 1, pp. 39–50, 1981.

[53] L. T. Hu and P. M. Bentler, "Cutoff criteria for fit indexes in covariance structure analysis: conventional criteria versus new alternatives," *Structural Equation Modeling: A Multidisciplinary Journal*, vol. 6, no. 1, pp. 1–55, 1999.

[54] G. Marcoulides, *Modern Methods for Business Research*, Psychology Press, New York, NY, USA, 1998.

[55] P. Cohen, S. G. West, and L. S. Aiken, *Applied Multiple Regression/Correlation Analysis for the Behavioral Sciences*, Psychology Press, London, UK, 2014.

[56] E. Adell, "Acceptance of driver support systems," in *Proceedings of the European Conference on Human Centred Design for Intelligent Transport Systems*, J. Krems, T. Petzoldt, and M. Henning, Eds., Humanist VCE: Ifsttar—Lyon-Bron, Berlin, Germany, pp. 475–486, April 2010.

[57] J. P. Zmud and I. N. Sener, "Towards an understanding of the travel behavior impact of autonomous vehicles," *Transportation Research Procedia*, vol. 25, pp. 2500–2519, 2017.

[58] V. Venkatesh, J. Y. L. Thong, and X. Xu, "Consumer acceptance and use of information technology: extending the unified theory of acceptance and use of technology," *MIS Quarterly*, vol. 36, no. 1, pp. 157–178, 2012.

[59] J. D. Jackson, M. Y. Yi, and J. S. Park, "An empirical test of three mediation models for the relationship between personal innovativeness and user acceptance of technology," *Information & Management*, vol. 50, no. 4, pp. 154–161, 2013.

[60] A. Turan, A. Ö. Tunç, and C. Zehir, "A theoretical model proposal: personal innovativeness and user involvement as antecedents of unified theory of acceptance and use of technology," *Procedia—Social and Behavioral Sciences*, vol. 210, pp. 43–51, 2015.

[61] J. Piao, M. Mcdonald, N. Hounsell, M. Graindorge, T. Graindorge, and N. Malhene, "Public views towards implementation of automated vehicles in urban areas," *Transportation Research Procedia*, vol. 14, pp. 2168–2177, 2016.

[62] F. Nazari, M. Noruzoliaee, and A. Mohammadian, "Shared versus private mobility: modeling public interest in autonomous vehicles accounting for latent attitudes," *Transportation Research Part C: Emerging Technologies*, vol. 97, pp. 456–477, 2018.

[63] N. Menon, A. R. Pinjari, Y. Zhang, and L. Zou, *Consumer Perception and Intended Adoption of Autonomous Vehicle Technology—Findings from a University Population Survey*, Transportation Research Board: WDC, Washington, DC, USA, 2016.